VIRGINIA ELECTRIC AND POWER COMPANY
RICHMOND, VIRGINIA 23261

August 15, 2022

10 CFR 50.90

United States Nuclear Regulatory Commission
Attention: Document Control Desk
Washington, DC 20555-0001

Serial No.: 22-018
NRA/GDM: R0
Docket Nos.: 50-280/281
License Nos.: DPR-32/37

VIRGINIA ELECTRIC AND POWER COMPANY
SURRY POWER STATION UNITS 1 AND 2
LICENSE AMENDMENT REQUEST - PROPOSED TECHNICAL SPECIFICATIONS CHANGE FOR NEW FUEL AND SPENT FUEL STORAGE AREAS

Pursuant to 10 CFR 50.90, Virginia Electric and Power Company (Dominion Energy Virginia) requests an amendment to Facility Subsequent Renewed Operating License Numbers DPR-32 and DPR 37 in the form of a change to the Technical Specifications (TS) for Surry Power Station (SPS) Units 1 and 2. The proposed change revises the following TS:

- TS 5.3.1.1: Spent Fuel Pool Storage Racks
- TS 5.3.1.2: New Fuel Storage Racks
- TS 5.3.1.3: Two Region Spent Fuel Pool Layout
- Adds new Figure 5.3-1: New Fuel Storage Racks Empty Cells
- Figure 5.3-2: Region 1 Burnup Curve

Dominion Energy Virginia performed a criticality safety analysis (CSA) for fuel assembly storage in the SPS Spent Fuel Pool (SFP) storage racks and New Fuel Storage Racks (NFSR), which is common for Units 1 and 2, to support the proposed TS change. The CSA credits soluble boron for the purposes of meeting the SFP k-effective (k_{eff}) limits of 10 CFR 50.68. Therefore, a SFP dilution analysis was also performed to support the proposed TS change.

This proposed amendment implements the following conditions associated with fuel assembly storage at SPS:

- Increases the TS allowed maximum U-235 enrichment for the SFP storage racks.
- Increases the TS allowed maximum U-235 enrichment for the NFSR.
- Adds allowed storage patterns for initial enrichments for new fuel assemblies in the NFSR to meet k_{eff} requirements under normal and accident conditions as follows:
    - IF the NFSR exclusively contains fuel having a maximum U-235 enrichment of 4.35 weight percent, THEN all NFSR fuel cells may be used.
    - IF the NFSR contains any fuel having a maximum U-235 enrichment greater than 4.35 weight percent, THEN the NFSR fuel cells shown in Figure 5.3-1 must remain vacant.

- Provides a new Region 1 burnup vs. initial U-235 enrichment curve.
- Credits SFP soluble boron in the SFP CSA. SPS already has a minimum TS SFP boron concentration that was used in the safety evaluation; therefore, no change to TS 5.3.2 is necessary.

Information provided in the attachments to this letter is summarized below:

- Attachment 1 provides an evaluation of the proposed TS changes.
- Attachment 2 provides marked-up TS pages.
- Attachment 3 provides proposed TS pages.
- Attachment 4 contains the CSA Checklist.
- Attachment 5 contains the CSA Report (Proprietary).
- Attachment 6 contains the CSA Report (Non-proprietary).
- Attachment 7 contains the SPS SFP Boron Dilution Analysis.
- Attachment 8 provides marked-up Updated Final Safety Analysis Report (UFSAR) pages.
- Attachment 9 contains the Framatome Inc. (Framatome) application for withholding proprietary information from public disclosure.
- Attachment 10 contains the Westinghouse Electric Company LLC (Westinghouse) application for withholding proprietary information from public disclosure.

Attachment 5 contains information proprietary to Framatome and Westinghouse; therefore, it is supported by affidavits signed by the owners of the information, which are provided in Attachments 9 and 10, respectively. The affidavits set forth the basis on which the information may be withheld from public disclosure by the Commission and addresses with specificity the considerations listed in paragraph (b)(4) of 10 CFR 2.390. Accordingly, it is respectfully requested that the proprietary information be withheld from public disclosure in accordance with 10 CFR 2.390. Correspondence with respect to the Westinghouse copyright or proprietary aspects or the supporting Westinghouse affidavit should reference letter CAW-22-029 and should be addressed to Camille T. Zozula, Manager, Regulatory Compliance & Corporate Licensing.

Dominion Energy Virginia has evaluated the proposed amendment and determined that it does not involve a significant hazards consideration as defined in 10 CFR 50.92. The basis for this determination is included in Attachment 1. Dominion Energy Virginia has also determined that operation with the proposed change will not result in any significant increase in the amount of effluents that may be released offsite or any significant increase in individual or cumulative occupational radiation exposure. Therefore, the proposed amendment is eligible for categorical exclusion from an environmental assessment as set forth in 10 CFR 51.22(c)(9). Pursuant to 10 CFR 51.22(b), no environmental impact statement or environmental assessment is needed in connection with the approval of the proposed change.

Dominion requests approval of the proposed amendment by December 31, 2023. SPS

plans to fully implement the revised TS within ninety (90) days after NRC approval of the proposed license amendment.

Should you have any questions in regard to this submittal, please contact Gary D. Miller at (804) 273-2771.

Sincerely,

James E. Holloway
Vice President – Nuclear Engineering and Fleet Support

Commitments made in this letter: None

Attachments:
1. Discussion of Change
2. Proposed Technical Specifications Pages (Mark-up)
3. Proposed Technical Specifications Pages (Typed)
4. Criticality Safety Analysis Checklist
5. Criticality Safety Analysis Report - (**Proprietary**)
6. Criticality Safety Analysis Report - (Non-proprietary)
7. Spent Fuel Pool Boron Dilution Analysis
8. Planned UFSAR Changes (Mark-up)
9. Framatome Inc. Application for Withholding Proprietary Information from Public Disclosure
10. Westinghouse Electric Company LLC Application for Withholding Proprietary Information from Public Disclosure

COMMONWEALTH OF VIRGINIA)
)
COUNTY OF HENRICO)

The foregoing document was acknowledged before me, in and for the County and Commonwealth aforesaid, today by James E. Holloway, who is Vice President – Nuclear Engineering and Fleet Support of Virginia Electric and Power Company. He has affirmed before me that he is duly authorized to execute and file the foregoing document in behalf of that Company, and that the statements in the document are true to the best of his knowledge and belief.

Acknowledged before me this 15th day of August, 2022.

My Commission Expires: 12/31/24

CRAIG D SLY
Notary Public
Commonwealth of Virginia
Reg. # 7518653
My Commission Expires December 31, 2024

Notary Public

cc: U.S. Nuclear Regulatory Commission – Region II
Marquis One Tower
245 Peachtree Center Avenue, NE Suite 1200
Atlanta, GA 30303-1257

Mr. L. John Klos
NRC Project Manager - Surry
U.S. Nuclear Regulatory Commission
One White Flint North, Mail Stop 09 E-3
11555 Rockville Pike
Rockville, MD 20852-2738

Mr. G. Edward Miller
NRC Senior Project Manager - North Anna
U.S. Nuclear Regulatory Commission
One White Flint North, Mail Stop 09 E-3
11555 Rockville Pike
Rockville, MD 20852-2738

NRC Senior Resident Inspector
Surry Power Station

State Health Commissioner
Virginia Department of Health
James Madison Building – 7th floor
109 Governor Street
Suite 730
Richmond, VA 23219

Attachment 1

DISCUSSION OF CHANGE

VIRGINIA ELECTRIC AND POWER COMPANY
(DOMINION ENERGY VIRGINIA)
SURRY POWER STATION UNITS 1 AND 2

DISCUSSION OF CHANGE

Table of Contents

1.0 Summary Description 2
2.0 Detailed Description of Change 2
2.1 TS 5.3.1.1 – Spent Fuel Storage Racks 2
2.2 TS 5.3.1.2 – New Fuel Storage Racks 3
2.3 TS 5.3.1.3 – Two Region Spent Fuel Pool Layout 3
2.4 TS Figure 5.3-1 – New Fuel Storage Racks Required Vacant Cells 3
2.5 TS Figure 5.3-2 – Spent Fuel Pool Region 1 Burnup Curve 3
3.0 Discussion 4
3.1 Current Surry Fuel Storage Configuration 4
4.0 Technical Evaluation Summary 4
4.1 Introduction 4
4.2 Fuel Storage Criticality Analysis - General 5
4.3 New Fuel Storage Racks Criticality Analysis – Normal Storage and Accident Conditions 5
4.4 Spent Fuel Pool Criticality Safety Analysis - Normal Storage Conditions 6
4.5 Spent Fuel Pool Criticality Safety Analysis - Accident Conditions 6
4.6 Boron Dilution 7
4.7 Storage of Non-fuel Components and Non-standard Fuel Assemblies 7
4.8 Spent Fuel Pool Storage – Other Items 8
4.9 Implementation Considerations 11
4.10 Conclusions 11
5.0 Regulatory Evaluation 12
5.1 Applicable Regulatory Requirements and Criteria 12
5.2 No Significant Hazards Consideration 12
5.3 Precedents 16
5.4 Conclusion 17
6.0 Environmental Considerations 17
7.0 References 18

1.0 SUMMARY DESCRIPTION

In accordance with 10 CFR 50.90 Virginia Electric and Power Company (Dominion Energy Virginia) requests an amendment to Subsequent Renewed Facility Operating License Nos. DPR-32 and DPR-37, in the form of the Technical Specifications (TS) for Surry Power Station (SPS) Units 1 and 2. Dominion Energy Virginia is proposing to change the following TS:

- TS 5.3.1.1: Spent Fuel Pool Storage Racks
- TS 5.3.1.2: New Fuel Storage Racks
- TS 5.3.1.3: Two Region Spent Fuel Pool Layout
- Add Figure 5.3-1: New Fuel Storage Racks Empty Cells
- Figure 5.3-2: Region 1 Burnup Curve

A summary of the changes that are being proposed:

- Increase the TS allowed maximum U-235 enrichment for the Spent Fuel Pool (SFP) storage racks.
- Increase the TS allowed maximum U-235 enrichment for the New Fuel Storage Racks (NFSR).
- Add allowed storage patterns for initial enrichments for new fuel assemblies in the NFSR to meet k_{eff} requirements under normal and accident conditions as follows:
    - IF the NFSR exclusively contains fuel having a maximum U-235 enrichment of 4.35 weight percent, THEN all NFSR fuel cells may be used.
    - IF the NFSR contains any fuel having a maximum U-235 enrichment greater than 4.35 weight percent, THEN the NFSR fuel cells shown in Figure 5.3-1 must remain vacant.
- Region 1 will have a new burnup vs. initial U-235 enrichment curve.
- The SFP criticality safety analysis will credit SFP soluble boron. Surry TS 5.3.2 already sets a minimum TS SFP boron concentration which was used in the criticality safety analysis. Therefore, no change to TS 5.3.2 is necessary.

The proposed change has been reviewed and confirmed to accommodate all fuel currently in the SFP, NFSR, and fuel assembly designs anticipated in the future.

2.0 DETAILED DESCRIPTION OF CHANGE

2.1 TS 5.3.1.1 – Spent Fuel Storage Racks

In part (a), the maximum U-235 enrichment will increase from 4.3 weight percent to 5.0 weight percent.

In part (b), the word “unborated” will be changed to “borated”. This change occurs because this analysis takes credit for soluble boron. 10 CFR 50.68(b)(4) states that the

k-effective must not exceed 0.95 when flooded with borated water. The attached Spent Fuel Pool dilution accident analysis and criticality analysis shows that a dilution event will be identified and arrested before the k-effective increases above 0.95.

Add a new part after part (b) which will state that the k-eff will remain ≤ 1.0 if fully flooded with unborated water. 10 CFR 50.68(b)(4) states that the k-effective must remain below 1.0 when flooded with unborated water. The attached criticality safety analysis demonstrates that the k-eff limit is met with 0 ppm of boron.

2.2 TS 5.3.1.2 – New Fuel Storage Racks

In part (a), the maximum U-235 enrichment will increase from 4.3 weight percent to 5.0 weight percent.

In part (b), the storage geometry will be a function of the maximum U-235 enrichment. All cells can be used if the maximum U-235 enrichment of all assemblies in the New Fuel Storage Racks is ≤4.35 weight percent. If any assembly in the New Fuel Storage Racks has a U-235 enrichment >4.35 weight percent, then specific cells are required to remain vacant. These vacant cell locations are shown in TS Figure 5.3-1. The attached criticality safety analysis demonstrates that the k-eff limits are met at these storage configurations.

In parts (c) and (d), the reference to the methodology in the VEPCO 1997 letter is removed and replaced with Appendix 9A of the UFSAR which will describe and reference this criticality safety analysis.

2.3 TS 5.3.1.3 – Two Region Spent Fuel Pool Layout

The only change to the text of TS 5.3.1.3 is administrative. Since a figure is being added to TS 5.3.1.2, the current Figure 5.3-1 in the TS will be renamed to Figure 5.3-2. Note that this figure is being updated (and described in Section 2.5 below), but no other changes are needed to the text of TS 5.3.1.3.

2.4 TS Figure 5.3-1 – New Fuel Storage Racks Required Empty Cells

The New Fuel Storage Racks will have two storage configurations. The required configuration depends on the U-235 enrichment of the stored fuel assemblies (described in proposed TS 5.3.1.2). Figure 5.3-1 shows which cells must remain vacant if the NFSR contains any fuel assemblies that have a U-235 enrichment >4.35 weight percent.

2.5 TS Figure 5.3-2 – Spent Fuel Pool Region 1 Burnup Curve

The burnup curve is being updated to (i) extend its applicability range out to a U-235 enrichment of 5.0 weight percent and (ii) update it for the methodology described in the attached criticality safety analysis. Fuel assemblies that are above the curve can be stored in Region 1 after 150 days of cooling. The equation of the curve is a polynomial and is displayed at the bottom of the figure. Note that this figure is an updated version of Figure 5.3-1 currently in the TS. It has been renamed to Figure 5.3-2 to accommodate

the proposed 'New Fuel Storage Racks Required Empty Cells' figure.

3.0 DISCUSSION

Dominion Energy Virginia proposes to amend the Operating Licenses by incorporating the attached proposed changes into the SPS TS. A summary of the proposed changes is provided in Section 1.0 above. The supporting criticality safety analysis report is included as Attachment 5 (Proprietary) and Attachment 6 (Non-proprietary), and the supporting SFP dilution analysis is included as Attachment 7.

Two Regions have been analyzed for the SFP. Both regions have the same rack design with 14 inch nominal pitch spacing and do not have neutron absorbing material. Both regions require no vacant cells. Region 1 is susceptible to damage from a dropped cask accident. Therefore, the fuel in Region 1 is required to have a minimum amount of burnup which is a function of U-235 enrichment. Region 2 has no burnup requirements. The rack and fuel assembly design and the modeling thereof are discussed in the criticality safety analysis.

There are 1044 storage locations currently in the Surry SFP as follows:

- Region 1: 324 storage locations
  - Nine 6 x 6 racks
- Region 2: 720 storage locations
  - Twenty 6 x 6 racks

The criticality safety analysis was performed for each Region and verified that no adverse boundary effects occur at Regions' interface. The analysis includes soluble boron credit. The present TS SFP boron concentration requirement of the SFP is 2300 ppm of soluble boron which is not being changed.

3.1 Current Surry Fuel Storage Configuration

The changes to the SFP configuration are minimal. The proposed Surry SFP Region layout is the same as the current configuration. Region 1 contains 324 storage locations and Region 2 contains 720 storage locations for a total of 1044 fuel storage locations. However, the proposed changes could impact the configuration of the New Fuel Storage Racks. Currently, the New Fuel Storage Racks only allow fuel with a maximum U-235 enrichment of 4.30 weight percent and do not require any vacant cells.

4.0 TECHNICAL EVALUATION SUMMARY

4.1 Introduction

The analysis and results in this section are summarized from the criticality safety analysis report (Attachment 5 [Proprietary] / Attachment 6 [Non-proprietary]). The topics presented here have the most significant impact with regard to the proposed license

amendment.

The proposed license amendment does not result in any equipment modifications to the plant or any changes regarding how equipment is operated and maintained. There are no changes in how fuel assemblies are handled and moved, nor are there any changes in how they are inserted into or removed from a SFP or NFSR storage location. There are no changes to how rod cluster control assemblies (RCCAs) are handled and moved, nor are there any changes in how they are inserted into or removed from a fuel assembly.

The existing two regions in the pool are being maintained. Region 2 has no restrictions other than the maximum U-235 enrichment must be less than or equal to 5 weight percent. Region 1 has a minimum amount of burnup required, and this burnup curve is being modified. There is no change to how personnel qualify and verify fuel assembly storage in the SFP.

There are two storage configurations proposed for the NFSR. All cells can be used if the maximum U-235 enrichment of all assemblies in the New Fuel Storage Racks is ≤4.35 weight percent. If any assembly in the New Fuel Storage Racks is >4.35 and ≤5.00 weight percent, then specific cells are required to remain vacant. These vacant cell locations are shown in TS Figure 5.3-1. This storage pattern is analogous to a 3-out-of-4 loading configuration.

Note that the administrative process for verifying proper fuel assembly loading using the new 3-out-of-4 storage arrangement in the NFSR and the new burnup curve in Region 1 will be the same as the process used for the present burnup curve and fuel qualification.

From an operational perspective, the proposed license amendment is transparent. SFP soluble boron concentration requirements will not change. The proposed change takes credit for the soluble boron currently in place for postulated accident scenarios. However, there are no changes regarding how fuel assemblies are handled and moved, how RCCAs are inserted into and removed from a fuel assembly, or in the administrative means used to ensure that fuel assemblies are not dropped or misloaded.

4.2 Fuel Storage Criticality Analysis - General

For each normal operational and postulated accident scenario (both in the NFSR and the SFP) the criticality safety analysis conservatively assumes that each fuel assembly is of a design to maximize fuel reactivity. The limiting design is a bounding composite of current and historical fuel designs and is expected to remain bounding for future fuel designs. The analyses assume bounding conservative depletion conditions for depleted fuel and account for biases and uncertainties as described in the criticality safety analysis.

4.3 New Fuel Storage Racks Criticality Analysis – Normal Storage and Accident Conditions

The NFSR was analyzed under both storage configurations (4-out-of-4 and 3-out-of-4 with higher enriched fuel). Results of the criticality safety analysis show that the NFSR

maintains $k_{eff} \leq 0.95$ under normal storage conditions, accounting for biases and uncertainties. The following postulated accident conditions were limiting:

- NFSR area fully flooded (with water)
- NFSR area with optimum moderation (fully flooded with foam).

The accident analysis results show that the SFP maintains $k_{eff} \leq 0.95$ for the area fully flooded scenario and maintains $k_{eff} \leq 0.98$ for the optimum moderation scenario after accounting for biases and uncertainties.

4.4 Spent Fuel Pool Criticality Safety Analysis - Normal Storage Conditions

Under normal storage conditions, the only difference between Region 1 and Region 2 is that Region 1 contains less reactive fuel. This is because both regions have the same rack design while Region 1 requires fuel burnup and Region 2 has no restrictions other than a maximum U-235 enrichment limit. Specific requirements for each region are listed below:

- Region 1:
  - Exceed the minimum amount of required burnup which is a function of initial U-235 enrichment (proposed TS Figure 5.3-2)
  - Decay at least 150 days after discharge (current TS 5.3.1.3)
- Region 2: Have a U-235 enrichment ≤5.0 weight percent.

Results of the SFP criticality safety analysis show that the proposed SFP storage Technical Specifications will maintain $k_{eff} < 1.0$ with 0 ppm of soluble boron in the SFP water, and $k_{eff} \leq 0.95$ with the SFP filled with 350 ppm soluble boron for normal fuel assembly storage conditions after accounting for biases and uncertainties.

4.5 Spent Fuel Pool Criticality Safety Analysis - Accident Conditions

The SFP criticality safety analysis has analyzed the following postulated accident conditions:

- cask drop damaging the fuel racks
- single fuel assembly misload in the spent fuel racks
- multiple fuel assembly misload in the spent fuel racks
- loss of SFP cooling including partial voiding
- dropped assembly into the racks with grid damage (optimum fuel pin pitch)
- misload of an assembly between fuel racks
- fuel handling error (two fresh fuel assemblies out of rack in close proximity)
- seismic event
- boron dilution event.

The bounding accident is the cask drop damaging the spent fuel racks accident. This scenario assumes a dry storage cask tips over in the direction of the fuel racks due to a crane accident, which then comes into contact and damages the fuel racks. All the fuel rack cells and assemblies in Region 1 are assumed to be consequentially damaged and deformed. Three plausible damage scenarios were analyzed. The three scenarios are (i) when all the fuel stays in the fuel cells, (ii) when fuel pellets fall to the SFP floor, and (iii) when fuel pellets are between the fuel cells. In all scenarios, the fuel pins and stacks of fuel pellets are modeled at optimum pitch for all Region 1 fuel. These scenarios are not meant to simulate how the SFP would actually look after a cask drop accident. Instead, they are meant to be extremely conservative scenarios that bound what the actual configuration could be. Each of these scenarios were modeled and tested. The limiting scenario was then used to calculate the bias, uncertainties, and maximum k-eff for each analyzed burnup state point.

The criticality safety analysis shows that 2250 ppm of soluble boron along with a minimum amount of burnup maintains $k_{eff} \leq 0.95$ for this bounding scenario, accounting for biases and uncertainties. Note the current SFP TS boron concentration limit is 2300 ppm and will not be changing.

4.6 Boron Dilution

The current criticality safety analysis of record did not include a SFP boron dilution analysis because it met the regulatory limit of $k_{eff} < 0.95$ with 0 ppm of boron. However, the proposed change will require 350 ppm of boron to meet that same regulatory limit. No equipment that could contribute to or mitigate a boron dilution event will be changed as part of this proposed change. Thus, no new avenues for a boron dilution event will be created. There are no proposed changes regarding boron concentration maintenance or response to a boron dilution event.

A SFP boron dilution analysis was performed that assumes a dilution from 2300 ppm to 400 ppm soluble boron (summarized in Attachment 7 of this submittal). The systems that could dilute SFP boron, either by direct connection to the SFP or by a potential crack/break of a pipe adjacent to the SFP, were analyzed via a bleed and feed methodology. The analysis demonstrates that sufficient time is available to detect and mitigate a boron dilution event prior to reaching a concentration of 400 ppm.

4.7 Storage of Non-fuel Components and Non-standard Fuel Assemblies

The criticality safety analysis found that non-fuel components may be placed in any spent fuel rack storage location since these components are less reactive than fuel and since the SFP has no required vacant cells. Non-fuel components can also be placed in the guide tubes of any fuel assembly because the fuel lattice is under moderated.

The criticality safety analysis evaluated each existing Non-standard Fuel Assembly currently stored in the SPS SFP using the same methods used for standard fuel. The reactivity of Non-standard Fuel Assemblies in the SFP is bounded by the limiting

assembly design under nominal conditions. However, due to the complexity of modeling a deformed Fuel Rod Storage Canister during a cask drop accident, it will be restricted to being stored only in Region 2.

4.8 Spent Fuel Pool Storage – Other Items

Seismic Response:

The criticality safety analysis considered the reactivity impact of a postulated seismic event under the proposed storage requirements for both the SFP and the NFSR. The evaluation found that the spent fuel racks and the NFSR met their respective k_{eff} limits. The evaluation considered fuel assembly motion within the storage cell, but it did not consider fuel rack movement since they cannot slide during any design-basis seismic event. The reactivity impact of the seismic event is bounded by the cask drop accident.

The proposed change will not change the number of fuel storage locations or physically change any of the spent fuel racks or NFSR. Additionally, the number of assemblies allowed to be stored will remain the same in the SFP and will either remain the same or decrease in the NFSR. Thus, the SFP and NFSR seismic/structural loading requirements for the proposed change are bounded by the existing TS.

Fuel Handling Event:

The criticality safety analysis analyzed a postulated fuel handling event that brings two fresh 5.0 weight percent U-235 fuel assemblies, not stored in a spent fuel rack or dry cask container, within 12 inches (30.48 cm) from each other. The analysis shows the assembly is effectively neutronically isolated with 0 ppm of soluble boron in the SFP water at a distance of $\geq$12 inches. With credit for soluble boron the criticality safety analysis shows that k_{eff} is maintained $\leq$0.95 for any distance, including less than 12 inches apart.

Radiological Consequences of Accidents:

The radiological consequences of accident scenarios described in the Surry UFSAR will not increase as a result of the proposed increase in fuel enrichment. Assessments of the impact of increasing the fuel burnup by the NRC and fuel vendors demonstrated that radionuclide concentrations in the fuel are largely a function of fuel burnup and power rather than fuel enrichment (References 6 and 7). Surry Units 1 and 2 burnup (lead rod burnup of 62,000 MWD/MTU) (Reference 4) and power limits (rated thermal power of 2587 MWt) (Reference 2) will not change as a result of the increase in maximum initial fuel enrichment. Thus, the proposed license amendment does not increase the radiological consequences of postulated accidents.

Safety Analysis Limits:

Other than the proposed changes to the TS identified and described above, there are no changes to any other TS or operating or safety-related setpoints associated with the

proposed increase in the maximum U-235 enrichment. No changes are being made to the core power level, operating temperature or pressure, or any peaking factors. Additionally, there will be no change to existing limits on the primary system coolant activity.

SFP Heat Load:

The proposed license amendment makes no changes to the core power level, operating temperature or pressure, or any peaking factors. The maximum allowable SFP heat load will remain the same, and future reload designs shall continue to meet the present maximum SFP heat load requirement.

Environmental Effects:

The environmental effects of higher enrichment fuel and SFP criticality calculation changes are analyzed in terms of the radiological impacts, concerning both normal and accident conditions. Radiological impacts are only indirectly affected by increasing fuel enrichment. The radiological impacts are primarily a function of operating power and burnup. Assemblies with higher enrichments could be utilized for an additional cycle of operation, but the power level will remain the same. Therefore, increased fuel enrichments will result in the same power level but could increase burnups.

The environmental impact of operation of the Surry units with high burnup fuel was previously addressed in References 1 through 4 and 14. Westinghouse has generically addressed the impact of extended burnup on the design and operation of Westinghouse fuel (Reference 5). In addition, the NRC had an independent assessment conducted (Reference 6 and 7) of the environmental and economic impacts of the use of extended burnup fuels in light water power reactors.

The overall findings of these assessments were that no significant adverse effects would be generated by increasing the lead rod burnup to 62,000 MWD/MTU (Reference 14). These evaluations concerning the impact of extended burnup fuel are valid for an enrichment of 5.0 weight percent U-235 since the NRC generic environmental effects study included fuel enrichments up to 5.0 weight percent (Reference 7). In 2007, the NRC approved operation of Surry fuel to burnup levels consistent with these findings (References 3 and 4).

Increasing burnup has limited effect on the short-lived isotope inventory in the fuel due to the development of an equilibrium condition between production and decay. Instead, extended burnups increase the fraction of the short-lived isotopes that migrate into the fuel-clad gap region (Reference 6). With increasing burnup there is no decrease in fuel rod integrity or the leakage probability of a fuel rod. However, with the increased activity in the clad-gap region, increased burnup can result in increased activity being released into the reactor coolant under normal operations. The increase is small enough to be easily accommodated by the reactor coolant clean-up system.

Finally, the proposed license amendment will not change the operating power or lead rod and other fuel burnup limits. Thus, it is concluded that the increase in the maximum fuel enrichment to 5.0 weight percent U-235 for SPS Units 1 and 2 will not have a significant adverse environmental effect.

Fuel Rod Integrity:

Fuel rod integrity is not directly affected by the initial fuel enrichment. Fuel rod integrity is more sensitive to operating power, radial peaking factors, and operating temperature of the cladding than to fuel enrichment or burnup. Extensive studies have been conducted that show there is no loss in fuel integrity for fuel rod average burnups reaching 62,000 MWD/MTU as long as the operating power remains normal (Reference 7 and 14).

The fuel melt temperature for UO_2 is assumed to be 5080°F (Reference 5). Although this property of UO_2 is not a function of enrichment, the fuel melt temperature decreases with burnup (Reference 5). The Surry overpower limits are set to ensure no fuel melting occurs, and this is verified each cycle as part of the reload safety analysis.

The current generation Surry fuel uses advanced zirconium alloys for fuel cladding, guide thimbles, instrumentation thimbles, and mixing vane grids. Advanced zirconium alloys replaced Zircaloy for the purpose of enhancing the reliability of the clad and extending fuel burnup levels. However, References 5 and 6 analyzed fuel assemblies whose cladding is constructed from Zircaloy.

The SPS operating power, radial peaking factors, operating temperatures, and maximum burnup limits will not be changed when the fuel enrichment is increased. Therefore, it is concluded that the increase in the maximum fuel enrichment to 5.0 weight percent U-235 for SPS Units 1 and 2 will not have a significant adverse effect on the integrity or performance of the fuel rods. These factors also indicate that the probability of leakage from the fuel rods will not be affected by the increased fuel enrichment.

Control Rod Insertion:

Concerns have been raised about the possible effects of fuel burnup on the fuel assembly structure, potentially leading to conditions that could interfere with control rod insertion and thus the safe shutdown of the reactor. It has been postulated that such conditions could develop at higher fuel burnups as a result of the mechanical design of the fuel assembly guide thimble tubes, the material used to fabricate the fuel assembly skeleton, and irradiation induced changes to the fuel assembly such as growth and corrosion. No changes to the TS SFP boron concentrations are proposed. Therefore, the fuel assembly storage environment will not significantly change.

The irradiation induced factors that could conceivably affect the guide thimble geometry and thus the ability to insert the control rods as designed are burnup, rather than enrichment, related. Use of a higher initial U-235 enrichment, with no increase in the fuel burnup limits, will not adversely affect fuel performance in a manner that would affect the

ability of the control rods to fully insert.

Dominion Energy Virginia continues to perform cycle specific calculations to verify that SPS core designs incorporate sufficient shutdown margin to ensure safe shutdown if the most reactive control rod fails to insert. An increase in the initial fuel enrichment from 4.3 to 5.0 weight percent of U-235 will not affect the nature of such shutdown margin calculations for SPS 1 and 2.

4.9 Implementation Considerations

Following NRC approval of the proposed license amendment, Dominion Energy Virginia will rearrange fuel assemblies in the SFP so that each fuel assembly will be in compliance with the current cooling time requirement and the new enrichment/burnup curve.

Given the planning and effort needed to perform this campaign, SPS plans to complete this work and fully implement the revised TS within ninety (90) days after NRC approval of the proposed license amendment.

4.10 Conclusions

Implementation of the proposed license amendment is safe and will not negatively affect plant operation. The proposed change will make no modifications to equipment or how equipment is operated or maintained. In particular, there are no changes to how fuel is handled, including how fuel is moved, inserted into, and removed from SFP and NFSR storage locations. There are no changes to how RCCAs are handled, including how they are moved, inserted into, and removed from a fuel assembly. There are no changes to qualifying and verifying fuel storage in the SFP. Also, since the proposed license amendment does not modify plant equipment or its operation and maintenance, including equipment used to maintain SFP soluble boron levels, the proposed license amendment will not impact a boron dilution event or plant response to it.

SFP fuel storage requirements will continue to be maintained by administrative means to ensure compliance with the proposed Region 1 burnup curve and Region 2 fresh fuel enrichment requirements. Additionally, these same administrative means will continue to be used to ensure compliance with the fresh fuel enrichment and vacant cell requirements of the NFSR.

The criticality safety analysis shows that the NFSR will maintain $k_{eff} \leq 0.95$ in the fully flooded condition and $k_{eff} \leq 0.98$ in the optimum moderation condition. Furthermore, the criticality safety analysis shows that the SFP will maintain $k_{eff} \leq 0.95$ under normal and all postulated accident conditions with credit for soluble boron. The SFP will also maintain $k_{eff} < 1.0$ with no soluble boron under normal conditions under the most reactive fuel storage configuration allowed by the proposed change.

5.0 REGULATORY EVALUATION

5.1 Applicable Regulatory Requirements and Criteria

Appendix A to Title 10 of the *Code of Federal Regulations,* Part 50 (10 CFR 50), General Design Criterion (GDC) 62, "Prevention of criticality in fuel storage and handling," states that "criticality in the fuel storage and handling system shall be prevented by physical systems or processes, preferably by use of geometrically safe configurations." The NRC has established a 5% subcriticality margin (i.e., k-effective (k_{eff}) less than or equal to 0.95) for nuclear power plant licensees to comply with GDC 62.

10 CFR 50.68 subpart (b), regarding New Fuel Storage Racks specifies the following:

> (2) The estimated ratio of neutron production to neutron absorption and leakage (k-effective) of the fresh fuel in the fresh fuel storage racks shall be calculated assuming the racks are loaded with fuel of the maximum fuel assembly reactivity and flooded with unborated water and must not exceed 0.95, at a 95 percent probability, 95 percent confidence level. This evaluation need not be performed if administrative controls and/or design features prevent such flooding or if fresh fuel storage racks are not used.
>
> (3) If optimum moderation of fresh fuel in the fresh fuel storage racks occurs when the racks are assumed to be loaded with fuel of the maximum fuel assembly reactivity and filled with low-density hydrogenous fluid, the k-effective corresponding to this optimum moderation must not exceed 0.98, at a 95 percent probability, 95 percent confidence level. This evaluation need not be performed if administrative controls and/or design features prevent such moderation or if fresh fuel storage racks are not used”

Also, Subpart (b)(4) of 10 CFR 50.68, "Criticality accident requirements," specifies:

> If credit is taken for soluble boron, the k-effective of the SFP storage racks loaded with fuel of the maximum fuel assembly reactivity must not exceed 0.95, at a 95 percent probability, 95 percent confidence level, if flooded with borated water, and the k-effective must remain below 1.0 (subcritical), at a 95 percent probability, 95 percent confidence level, if flooded with unborated water.

5.2 No Significant Hazards Consideration

Dominion Energy Virginia has performed the significant hazards consideration for the proposed license amendment by addressing the three standards set forth in 10 CFR 50.92, “Issuance of Amendment,” as discussed below:

1. Does the proposed change involve a significant increase in the probability or consequences of an accident previously evaluated?

   Response: *No*.

The proposed change does not involve a significant increase in the probability or consequences of an accident previously evaluated**.**

The proposed change will not affect plant equipment or structure, including the SFP, NFSR, or fuel handling equipment, including how the equipment is operated and maintained. There are no changes to the equipment for fuel handling or how fuel assemblies are handled, including how fuel assemblies are inserted into and removed from SFP and NFSR storage locations. There is no change to administrative means for verifying correct fuel assembly storage in the SFP. There are no changes to how RCCAs will be handled, including how RCCAs are inserted into or removed from a fuel assembly or other location such as a SFP storage location. Also, since the proposed change does not modify plant equipment or its operation and maintenance, including equipment used to maintain SFP soluble boron levels, the proposed change will not impact a boron dilution event or plant response to it.

The criticality safety analysis concluded that the NFSR limiting accident is the optimum moderation condition with each allowed storage location loaded with a maximum reactivity fuel assembly. The NFSR maintains $k_{eff} \leq 0.98$ for this postulated scenario including all uncertainties and biases. The NFSR also maintains $k_{eff} \leq 0.95$ for the fully flooded scenario including all uncertainties and biases. Thus, the consequences of a previously evaluated NFSR related accident is not significantly increased. There is no change to plant equipment or its operation and maintenance due to the proposed change. Thus, the probability of a flooding accident that could impact the NFSR is not significantly increased.

Regarding the SFP, the storage geometry for both regions will stay the same. The Region 1 burnup curves will be updated but the process of choosing fuel assembly storage locations and qualifying fuel assemblies will not change. The physical handling, insertion, removal, and storage of fuel assemblies in SFP racks will not change. The SPS program for choosing fuel assembly storage locations, for fuel handling, and for assuring that the fuel assemblies are placed into correct locations will remain in place. Thus, the probability of a fuel assembly misloading or a fuel assembly drop in the SFP will not significantly increase due to the proposed change.

Regarding the SFP cask drop accident, the proposed change does not impact the physical handling, cask design, insertion, or removal of the dry storage cask from SFP. Additionally, the SFP layout and fuel storage racks are not changing. The only change is that the minimum amount of burnup required for fuel adjacent to the cask loading area will increase, which decreases the chances for a criticality accident. Thus, the probability of a cask drop accident in the SFP will not significantly increase due to the proposed change.

Several postulated accidents for the SFP were reviewed for the proposed change including postulated fuel assembly misload, assembly drop scenarios, and the cask drop accident. The criticality safety analysis for the SFP concluded that the limiting accident, which bounds all other scenarios, is the dry storage cask drop accident. The

criticality safety analysis concluded that a SFP soluble boron concentration of 2250 ppm and a minimum amount of burnup will maintain $k_{eff} \leq 0.95$, including all uncertainties and biases, for this postulated scenario. The minimum TS soluble boron concentration will be maintained at 2300 ppm, so the proposed change will not affect the routine activities associated with maintaining boron concentration.

There are no changes to plant equipment or its operation and maintenance, including equipment associated with maintaining SFP soluble boron concentration or possible flow paths that could contribute to a boron dilution event. Thus, no new avenues for a boron dilution event will be created. There is no change regarding how the plant maintains boron concentration or responds to a boron dilution event. The criticality safety analysis for the postulated boron dilution event shows the SFP maintains $k_{eff} \leq 0.95$ at 350 ppm soluble boron. Thus, there is no significant increase in the probability or consequences of a boron dilution accident.

The SPS SFP is currently licensed to store 1044 fuel assemblies (TS 5.3.4), which is not changing as a result of the proposed changes. Additionally, the maximum number of assemblies that can be stored in the NFSR remains unchanged. Thus, the SFP and NFSR seismic/structural loading requirements for the proposed change are bounded by the existing analysis. The criticality safety analysis shows that SFP and NFSR k_{eff} will be maintained below their respective limits during a postulated seismic event. Thus, there is no increase in the consequences of a seismic event.

The proposed license amendment makes no changes to any safety analysis limits, including core power level, operating temperature or pressure, or peaking factors. There are no changes being made to any fuel burnup limits. Thus, it is concluded that:

- there is no increase in the radiological consequences in response to postulated accidents
- there is no change to the maximum allowable SFP heat load
- there is no impact on fuel rod integrity during normal or accident conditions
- there is no impact on the ability of RCCAs to fully insert during normal or accident conditions.

In each of the above scenarios the proposed change does not significantly increase the probability of an accident previously evaluated and maintains required k_{eff} margin. Therefore, it is concluded that the probability or consequences of a previously evaluated accident do not significantly increase.

2. Does the proposed change create the possibility of a new or different kind of accident from any accident previously evaluated?

   Response: *No*

   The proposed change does not create the possibility of a new or different kind of accident from any accident previously evaluated.

There is no change to any plant equipment, including how equipment is operated and maintained. There will be no changes to equipment used to handle fuel assemblies (or any heavy load) over the NFSR or the SFP. There is no change regarding how the fuel assemblies are stored, inserted into, and removed from fuel storage locations.

The criticality safety analysis for the first time at SPS specifically analyzes a SFP boron dilution event. However, the overall accident analyzed is the potential for a SFP criticality event, and the boron dilution event is another potential initiator of the postulated SFP criticality accident. Also, the possibility of a SFP boron dilution event has always existed at SPS and the proposed change does not create or change the possibility of such an event occurring.

Similarly, the criticality safety analysis discusses misloaded fuel assemblies in the NFSR for the first time since the NFSR could require vacant storage cells. However, the overall accident analyzed is the potential for a NFSR criticality event, and the NFSR misload event is another potential initiator of the postulated SFP criticality accident. Also, the possibility of a NFSR event has always existed at SPS by loading fuel >4.3 weight percent U-235, and the proposed change does not create or change the possibility of such an event occurring.

Thus, there are no new accidents created over and above the existing postulated accidents in the SFP or in the NFSR area. Also, since there is no change to the plant equipment or how equipment is operated and maintained, the probability of a new or different type of accident that could impact the SFP or NFSR is not significantly increased.

3. Does the proposed change involve a significant reduction in a margin of safety?

   Response: *No*.

   The proposed change does not involve a significant reduction in a margin of safety.

   The licensing requirement for the SFP is that k_{eff} remain $\leq$ 0.95 under normal and all postulated accident conditions with credit for soluble boron. The criticality safety analysis concludes this requirement is met for the bounding postulated accident of a cask drop accident damaging the fuel racks in Region 1. The analysis applies to all fuel assembly designs currently stored in the SPS SFP and to future anticipated fuel designs.

   In addition, the criticality safety analysis concludes that the SFP will maintain $k_{eff} < 1.0$ with 0 ppm soluble boron in the SFP under normal conditions with the maximum allowed reactivity fuel assembly stored in each fuel storage location.

   The criticality safety analysis also allows the following storage configurations. In each case the storage configuration does not increase reactivity assuring that k_{eff} margin is maintained:

- Storing non-fuel components in any spent fuel rack storage location where fuel assemblies are allowed
- Storing non-fuel components in the guide tubes of any fuel assembly.

The criticality safety analysis evaluated Non-standard Fuel to determine where they can be stored in the SFP. This information is used to maintain k_{eff} margin when storing Non-standard Fuel Assemblies.

The licensing requirement for the NFSR is that k_{eff} remain $\leq$ 0.95 for the fully flooded scenario, and $\leq$ 0.98 for the optimum moderation scenario. The criticality safety analysis concludes that these requirements are met assuming the maximum allowed enriched fuel assembly in each allowed fuel storage location.

Therefore, the margins of safety are maintained, and the proposed change does not involve a significant reduction in a margin of safety.

Based on the above information, Dominion Energy Virginia concludes that the proposed license amendment involves no significant hazards consideration under the criteria set forth in 10 CFR 50.92(c) and, accordingly, a finding of no significant hazards consideration is justified.

5.3 Precedents

The proposed change to the SPS TS is similar in fundamental aspects to those referenced in the following NRC Safety Evaluation Reports (SER) (References 9 and 10):

- NRC License Amendment and associated SER under cover letter "North Anna Power Station, Unit Nos. 1 and 2 - Issuance of Amendments to Revise Technical Specifications Regarding New and Spent Fuel Storage (CAC NOS. MF9712 AND MF9713, EPID L-2017-LLA-0240)," from J. R. Hall (NRC) to D. G. Stoddard (Dominion Energy, Inc.), July 27, 2018 (ADAMS Accession No. ML18180A197).

- NRC License Amendment and associated SER under cover letter "Millstone Power Station, Unit No. 3 - Issuance of Amendment No. 273 Regarding Technical Specification Changes for Spent Fuel Storage and New Fuel Storage (EPID L-2018-LLA-0126)," from R. V. Guzman (NRC) to D. G. Stoddard (Dominion Energy, Inc), May 28, 2019 (ADAMS Accession No. ML19126A000).

Additionally, the method of the criticality safety analysis closely follows the current industry guidance (References 11 and 12). A checklist, Attachment 4, shows and explains any deviations from this guidance.

- Nuclear Energy Institute, NEI 12-16, "Guidance for Performing Criticality Analyses of Fuel Storage at Light-Water Reactor Power Plants," Revision 4, Washington, DC (ADAMS Accession No. ML19269E069).

- NRC, RG 1.240, "Regulatory Guide RG 1.240, Fresh and Spent Fuel Pool Criticality Analyses," March 2021 (ADAMS Accession No. ML20356A127).

The current SPS application includes unique aspects that reflect Dominion's understanding of NRC staff expectations for the content and supporting analyses of spent fuel criticality submittals. The enclosed submittal content was developed based on insights and discussion between Dominion Energy Virginia and the NRC staff which occurred during a pre-submittal meeting (Reference 13):

- NRC, "Surry Units 1 And 2 - May 13, 2021, Summary Regarding Pre-application Meeting To Discuss Planned License Amendment Requests," June 11, 2021.

5.4 Conclusion

Based on the considerations discussed above, there is reasonable assurance that (1) the health and safety of the public will not be endangered by the proposed changes, (2) such activities will be conducted in compliance with the Commission's regulations, and (3) the issuance of the requested license amendments will not be inimical to the common defense and security or to the health and safety of the public.

6.0 ENVIRONMENTAL CONSIDERATIONS

Dominion Energy Virginia has reviewed the proposed license amendment for environmental considerations. The proposed license amendment does not involve (i) a significant hazards consideration, (ii) a significant change in the types or significant increase in the amounts of any effluent that may be released offsite, or (iii) a significant increase in individual or cumulative occupational radiation exposure. Accordingly, the proposed amendment meets the eligibility criterion for categorical exclusion from an environmental assessment as set forth in 10 CFR 51.22(c)(9). Therefore, pursuant to 10 CFR 51.22(b), no environmental impact statement or environmental assessment needs to be prepared in connection with the proposed amendment.

7.0 REFERENCES

1. Letter from J. P. O'Hanlon (Virginia Electric and Power Company) to U.S. Nuclear Regulatory Commission, "Virginia Electric and Power Company; Surry Power Station Units No. 1 and 2; Proposed Technical Specifications Change for Increased Enrichment of Reload Fuel," Serial Number 97-614, November 5, 1997.

2. Letter from L. N. Hartz (Virginia Electric and Power Company, Dominion) to the U.S. Nuclear Regulatory Commission, "Surry Power Station, Units 1 and 2 - License Amendment Request, Measurement Uncertainty Recapture Power Uprate," January 27, 2010 (ADAMS Accession No. ML100320264).

3. Letter from Leon B. Engle and Bart C. Buckley (U.S. Nuclear Regulatory Commission) to W. L. Stewart (Virginia Electric and Power), "Surry, Units 1 and 2, and North Anna, Units 1 and 2 - Removal of 45,000 MWD/MTU Batch Average Burnup Restriction," December 14, 1993 (ADAMS Accession No. ML18153B396).

4. Letter from S. P. Lingam (U.S. Nuclear Regulatory Commission) to D. A. Christian (Virginia Electric and Power), "Surry, Units, 1 and 2, Issuance of Amendments 257 and 256 Regarding Increase in Lead Rod Average Burnup Limit," December 19, 2007 (ADAMS Accession No. ML073230074).

5. NRC Safety Evaluation Report, "Safety Evaluation Report on Westinghouse Electric Corporation, Extended Burnup Topical Report – WCAP-10125 (Proprietary)", May 1985 (Adams Accession No. ML20135G151).

6. D. A. Baker, et al., "Assessment of the Use of Extended Burnup Fuel in Light Water Power Reactors," NUREG/CR-5009, PNL-6258, February 1988.

7. J. V. Ramsdell Jr., et al., "Environmental Effects of Extending Fuel Burnup Above 60 Gwd/MTU," NUREG/CR 6703, PNNL-13257, January 2001.

8. Addendum 1 to WCAP-12610-P-A, "Addendum 1 to WCAP-14342-P-A and CENPD-404-P-A Optimized ZIRLO," February 2003.

9. NRC License Amendment and associated SER under cover letter "North Anna Power Station, Unit Nos. 1 and 2 - Issuance of Amendments to Revise Technical Specifications Regarding New and Spent Fuel Storage (CAC NOS. MF9712 AND MF9713, EPID L-2017-LLA-0240)," from J. R. Hall (NRC) to D. G. Stoddard (Dominion Energy, Inc.), July 27, 2018 (ADAMS Accession No. ML18180A197).

10. NRC License Amendment and associated SER under cover letter "Millstone Power Station, Unit No. 3 - Issuance of Amendment No. 273 Regarding Technical Specification Changes for Spent Fuel Storage and New Fuel Storage (EPID L-2018-LLA-0126)," from R. V. Guzman (NRC) to D. G. Stoddard (Dominion Energy, Inc), May 28, 2019 (ADAMS Accession No. ML19126A000).

11. Nuclear Energy Institute, NEI 12-16, “Guidance for Performing Criticality Analyses of Fuel Storage at Light-Water Reactor Power Plants,” Revision 4, Washington, DC (ADAMS Accession No. ML19269E069).

12. NRC, RG 1.240, “Regulatory Guide RG 1.240, Fresh and Spent Fuel Pool Criticality Analyses,” March 2021 (ADAMS Accession No. ML20356A127).

13. NRC, “Surry Units 1 and 2 - May 13, 2021, Summary Regarding Pre-application Meeting To Discuss Planned License Amendment Requests,” June 11, 2021.

14. Letter from G. T. Bischof (Virginia Electric and Power) to U.S. Nuclear Regulatory Commission, “Surry, Units 1 & 2, License Amendment Request re Proposed Increase in the Lead Rod Average Burnup Limit,” March 06, 2007 (ADAMS Accession No. ML070720620).

Attachment 2

PROPOSED TECHNICAL SPECIFICATIONS PAGES (MARK-UP)

VIRGINIA ELECTRIC AND POWER COMPANY
(DOMINION ENERGY VIRGINIA)
SURRY POWER STATION UNITS 1 AND 2

5.3 FUEL STORAGE

5.3.1 Criticality

5.3.1.1 The spent fuel storage racks are designed and shall be maintained with:

a. Fuel assemblies having a maximum U-235 enrichment of ~~4.3~~ 5.0 weight percent; to 350 ppm,

b. $k_{eff} \leq 0.95$ if fully flooded with ~~un~~borated water, and biases which includes an allowance for uncertainties as described in Appendix 9A of the UFSAR; ~~and~~

c. $k_{eff} < 1.0$ if fully flooded with unborated water, which includes an allowance for uncertainties and biases as described in Appendix 9A of the UFSAR, and;

~~c.~~ d. A nominal 14 inch center to center distance between fuel assemblies placed in the storage racks.

5.3.1.2 The new fuel storage racks are designed and shall be maintained with:

a. Fuel assemblies having a maximum U-235 enrichment of ~~4.3~~ 5.0 weight percent;

b. Required empty cells in accordance with Figure 5.3-1, when any stored fuel has an enrichment greater than 4.35 weight percent;

~~b.~~ c. $k_{eff} \leq 0.95$ if fully flooded with ~~un~~borated water, and biases which includes an allowance for uncertainties calculated in accordance with the methodology described in ~~Virginia Electric and Power Company letter dated November 5, 1997 (Serial No. 97-614)~~ Appendix 9A of the UFSAR;

~~c.~~ d. $k_{eff} \leq 0.98$ if moderated by aqueous foam, which includes an allowance for uncertainties calculated in accordance with the methodology described in ~~Virginia Electric and Power Company letter dated November 5, 1997 (Serial No. 97-614)~~ Appendix 9A of the UFSAR; and

~~d.~~ e. A nominal 21 inch center to center distance between fuel assemblies placed in the storage racks.

5.3.1.3 The spent fuel pool is divided into a two-region storage pool. Region 1 comprises the first three rows of fuel racks (324 storage locations) adjacent to the Fuel Building Trolley Load Block. Region 2 comprises the remainder of the fuel racks in the fuel pool. During spent fuel cask handling, Region 1 is limited to storage of spent fuel assemblies which have decayed at least 150 days after discharge and shall be restricted to those assemblies in the "acceptable" domain of Figure ~~5.3-1~~ 5.3-2. Administrative controls with written procedures will be employed in the selection and placement of these assemblies.

DELETE

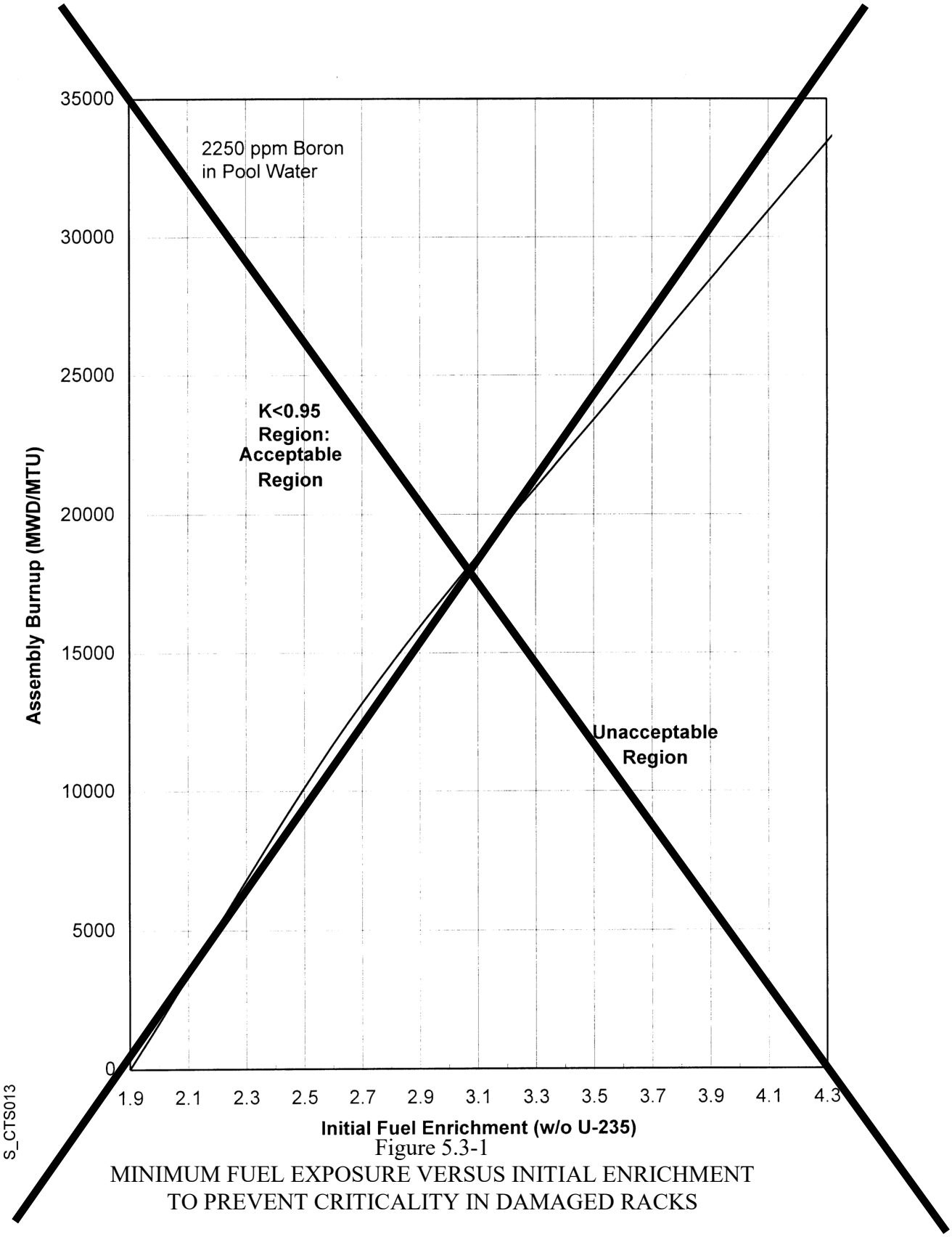

Figure 5.3-1
MINIMUM FUEL EXPOSURE VERSUS INITIAL ENRICHMENT
TO PREVENT CRITICALITY IN DAMAGED RACKS

INSERT

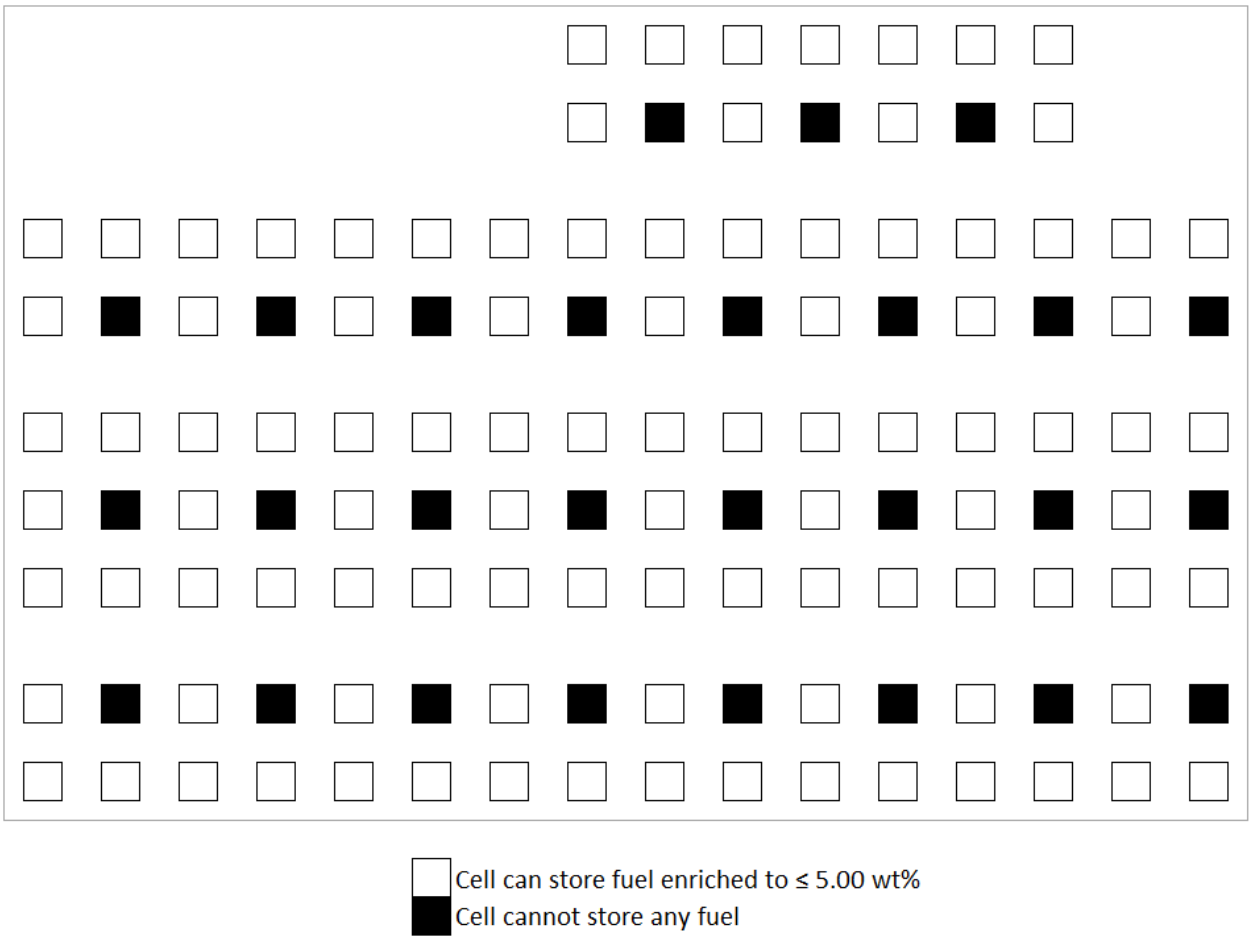

Figure 5.3-1
NEW FUEL STORAGE RACKS
REQUIRED EMPTY CELLS WHEN ANY STORED FUEL IS > 4.35 WT% U-235

INSERT

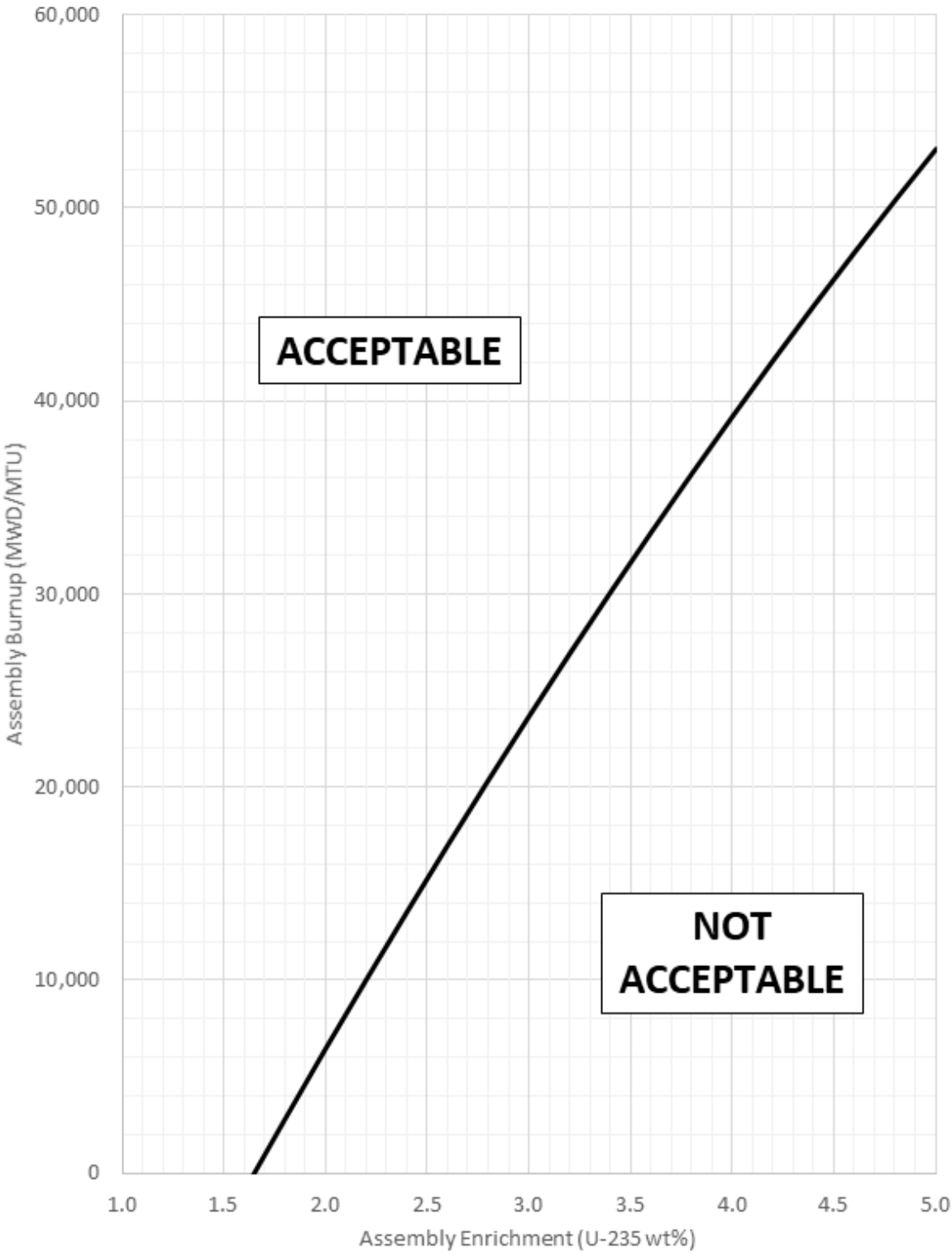

Figure 5.3-2
MINIMUM FUEL EXPOSURE VERSUS INITIAL ENRICHMENT TO PREVENT CRITICALITY IN DAMAGED RACKS

$$Required\ Burnup\ (MWD/MTU) = -849x^2 + 21470x - 33110$$

where "x" is the U-235 enrichment in wt%.

Attachment 3

PROPOSED TECHNICAL SPECIFICATIONS PAGES (TYPED)

VIRGINIA ELECTRIC AND POWER COMPANY
(DOMINION ENERGY VIRGINIA)
SURRY POWER STATION UNITS 1 AND 2

5.3 FUEL STORAGE

5.3.1 Criticality

5.3.1.1 The spent fuel storage racks are designed and shall be maintained with:

a. Fuel assemblies having a maximum U-235 enrichment of 5.0 weight percent;

b. $k_{eff} \leq 0.95$ if fully flooded with borated water to 350 ppm, which includes an allowance for uncertainties and biases as described in Appendix 9A of the UFSAR;

c. $k_{eff} < 1.0$ if fully flooded with unborated water, which includes an allowance for uncertainties and biases as described in Appendix 9A of the UFSAR, and;

d. A nominal 14 inch center to center distance between fuel assemblies placed in the storage racks.

5.3.1.2 The new fuel storage racks are designed and shall be maintained with:

a. Fuel assemblies having a maximum U-235 enrichment of 5.0 weight percent;

b. Required empty cells in accordance with Figure 5.3-1, when any stored fuel has an enrichment greater than 4.35 weight percent;

c. $k_{eff} \leq 0.95$ if fully flooded with unborated water, which includes an allowance for uncertainties and biases calculated in accordance with the methodology described in Appendix 9A of the UFSAR;

d. $k_{eff} \leq 0.98$ if moderated by aqueous foam, which includes an allowance for uncertainties and biases calculated in accordance with the methodology described in Appendix 9A of the UFSAR; and

e. A nominal 21 inch center to center distance between fuel assemblies placed in the storage racks.

5.3.1.3 The spent fuel pool is divided into a two-region storage pool. Region 1 comprises the first three rows of fuel racks (324 storage locations) adjacent to the Fuel Building Trolley Load Block. Region 2 comprises the remainder of the fuel racks in the fuel pool. During spent fuel cask handling, Region 1 is limited to storage of spent fuel assemblies which have decayed at least 150 days after discharge and shall be restricted to those assemblies in the “acceptable” domain of Figure 5.3-2. Administrative controls with written procedures will be employed in the selection and placement of these assemblies.

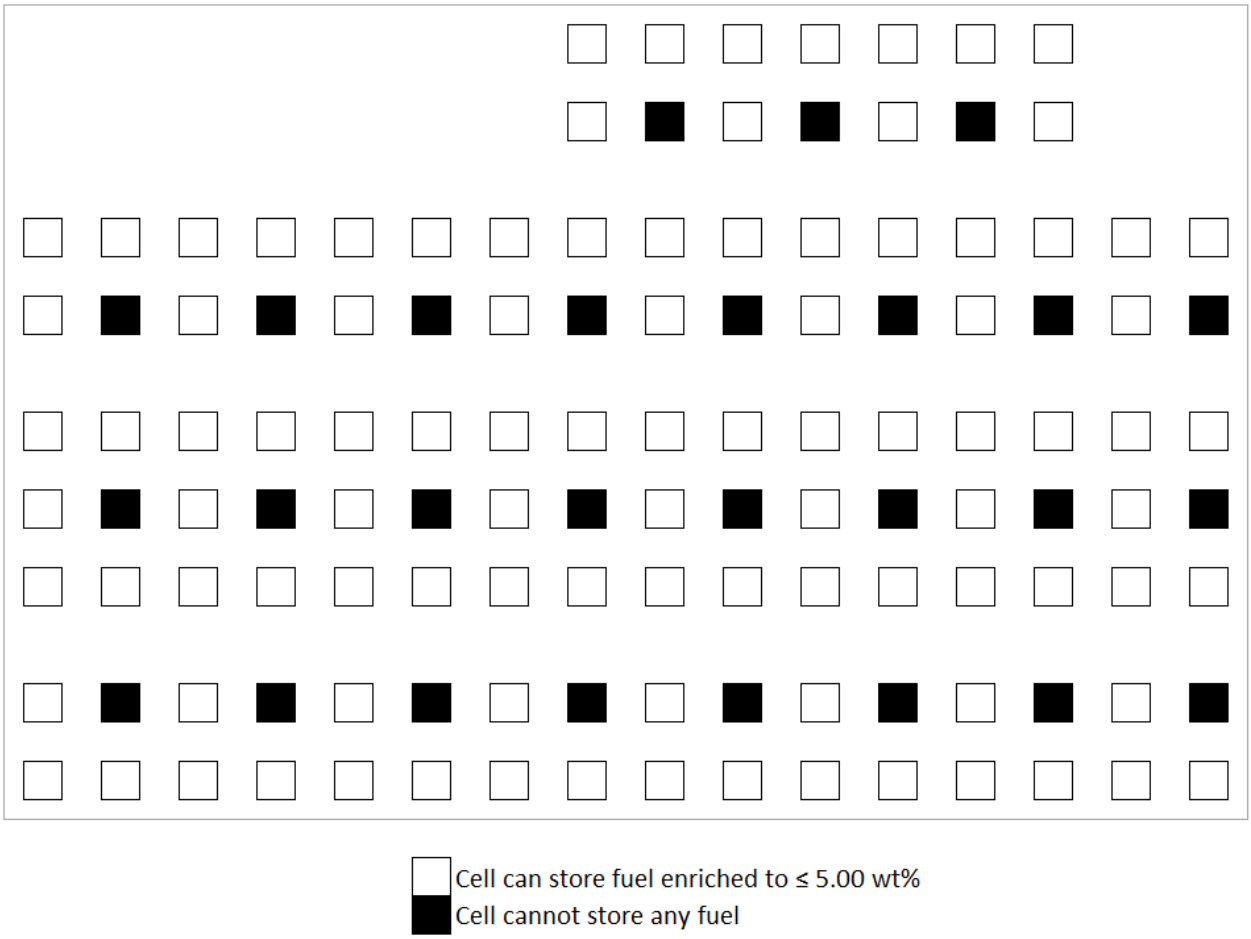

Figure 5.3-1
NEW FUEL STORAGE RACKS
REQUIRED EMPTY CELLS WHEN ANY STORED FUEL IS > 4.35 WT% U-235

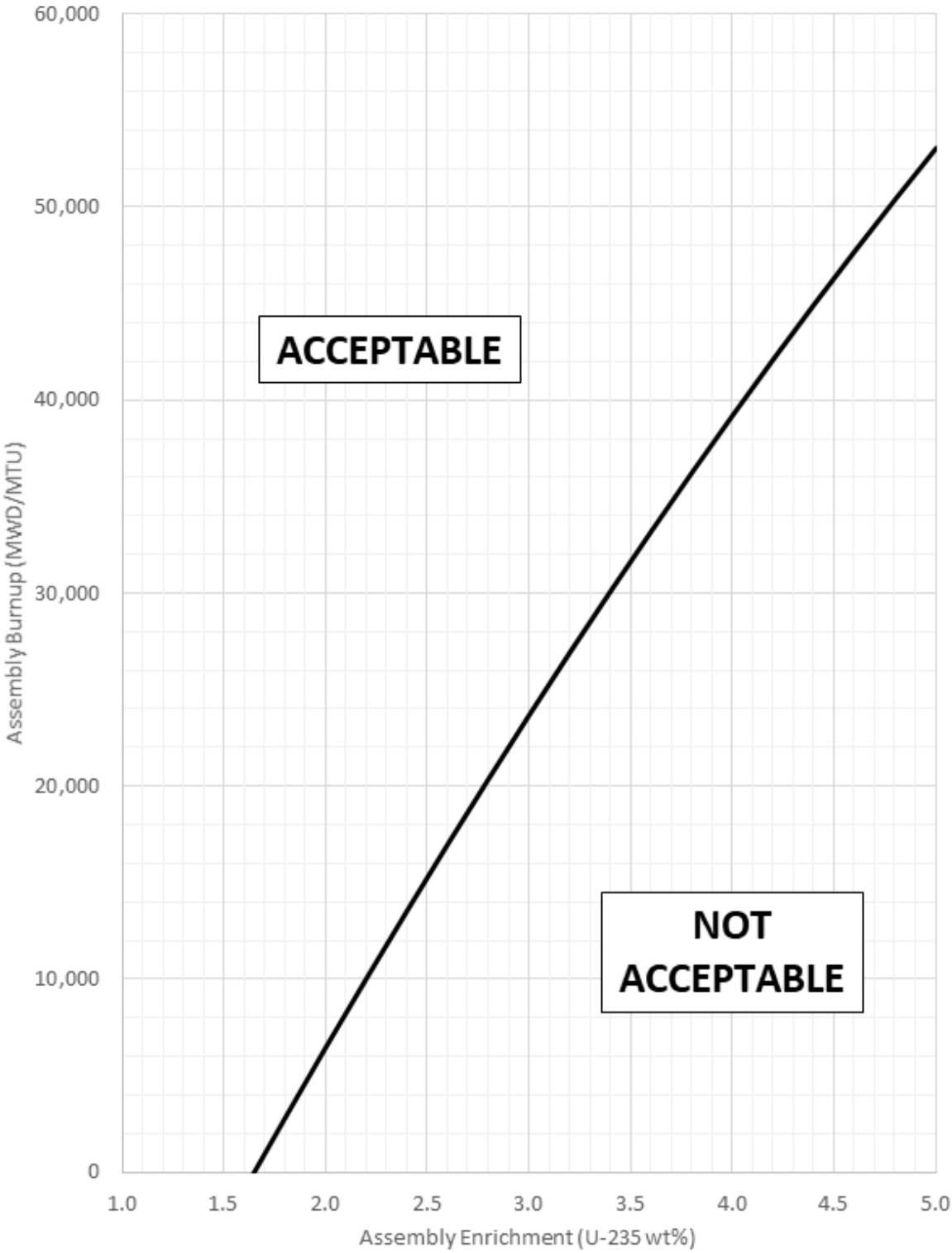

Figure 5.3-2
MINIMUM FUEL EXPOSURE VERSUS INITIAL ENRICHMENT TO PREVENT CRITICALITY IN DAMAGED RACKS

$$Required\ Burnup\ (MWD/MTU) = -849x^2 + 21470x - 33110$$

where "x" is the U-235 enrichment in wt%.

Attachment 4

CRITICALITY SAFETY ANALYSIS CHECKLIST

VIRGINIA ELECTRIC AND POWER COMPANY
(DOMINION ENERGY VIRGINIA)
SURRY POWER STATION UNITS 1 AND 2

Criticality Safety Analysis Checklist

The purpose of this checklist is to assist the NRC reviewer in identifying areas of the analysis that conform or do not conform to the guidance in NEI 12-16 (endorsed in RG 1.240). Unless otherwise stated, the sections listed in the "Notes / Explanation" column refer to the sections in Attachment 5 (Proprietary Version) or Attachment 6 (Non-Proprietary Version) of this LBDCR.

Subject	Included	Notes / Explanation
1.0 Introduction and Overview		
Purpose of submittal	YES	Increase enrichment, update methods & codes, include gadolinium. (Section 1)
Changes requested	YES	Change Tech. Spec. burnup curve, change maximum enrichment, add empty cell requirement to NFSA (Section 1)
Summary of physical changes	NO	No physical changes
Summary of Tech Spec changes	YES	Change burnup curve, change maximum enrichment, add empty cell loading pattern (Attachments 1 & 2 of the LBDCR)
Summary of analytical scope	YES	SFP and new fuel storage criticality safety analysis including normal storage and fuel handling, abnormal conditions, boron dilution analysis, an accompanying code benchmarking analysis, and a SFP dilution analysis. (Section 1)
2.0 Acceptance Criteria and Regulatory Guidance		
Summary of requirements and guidance	YES	(Section 2)
Requirements documents referenced	YES	
Guidance documents referenced	YES	
Acceptance criteria described	YES	
3.0 Reactor and Fuel Design Description		
Describe reactor operating parameters	YES	(Section 8)
Describe all fuel in pool	YES	(Section 3.1 & 3.3)
Geometric dimensions (Nominal and Tolerances)	YES	(Section 3.1)
Schematic of guide tube patterns	YES	15x15 PWR fuel (Section 3.1) four old 17x17 demonstration assemblies (Section 3.3)
Material compositions	YES	(Section 3.1 & 3.3)
Describe future fuel to be covered	NO	None proposed. Using composite bounding fuel design
Geometric dimensions (Nominal and Tolerances)	NO	None proposed.
Schematic of guide tube patterns	NO	None proposed.

Subject	Included	Notes / Explanation
Material compositions	NO	None proposed.
Describe all fuel inserts	YES	Burnable poisons, control rods, and source rods, flux suppression inserts, and In-core flux detector thimbles (Section 3.2)
Geometric Dimensions (Nominal and Tolerances)	YES	(Section 3.2)
Schematic (axial/cross-section)	NO	Geometry of inserts are explained. Their geometry is common and simple.
Material compositions	YES	(Section 3.2)
Describe non-standard fuel	YES	Fuel Rod Canister and old 17x17 Demonstration Assemblies (Section 3.3)
Geometric dimensions	YES	(Section 3.3)
Describe non-fuel items in fuel cells	NO	(Section 11.5)
Nominal and tolerance dimensions	NO	
4.0 Spent Fuel Pool/Storage Rack Description		
New fuel vault & Storage rack description	YES	(Section 4.1)
Nominal and tolerance dimensions	YES	(Section 4.1)
Schematic (axial/cross-section)	YES	Rack diagrams (Section 4.1)
Material compositions	YES	(Section 4.1)
Spent fuel pool, Storage rack description	YES	(Section 4.2)
Nominal and tolerance dimensions	YES	(Section 4.2)
Schematic (axial/cross-section)	YES	Rack diagrams (Section 4.2)
Material compositions	YES	(Section 4.2)
Other Reactivity Control Devices (Inserts)	NO	No installed rack inserts. No neutron absorbing material.
Nominal and tolerance dimensions	NO	
Schematic (axial/cross-section)	NO	
Material compositions	NO	
5.0 Overview of the Method of Analysis		
New fuel rack analysis description	YES	(Section 5.1)
Storage geometries	YES	Two storage options: -4 out of 4 for enrichments ≤4.35% -3 out of 4 for enrichments >4.35% (Section 5.1)
Bounding assembly design(s)	YES	(Sections 3.1 & 7.2)
Integral absorber credit	NO	No absorber material credited
Accident analysis	YES	- Flooded with water - Flooded with optimum density water - Dropped/misplaced assembly - Seismic event (Sections 5.1 & 7.7)
Spent fuel storage rack analysis description	YES	(Section 5.2)

Subject	Included	Notes / Explanation
Storage geometries	NO	All regions are 4 out of 4. No empty cells are required. (Section 5.2.1)
Bounding assembly design(s)	YES	(Section 5.2.2)
Soluble boron credit	YES	(Section 5.2.3)
Boron dilution analysis	YES	(Attachment 7 of this LBDCR)
Burnup credit	YES	Region 1 credits burnup Region 2 does not credit burnup (Section 5.2.4)
Decay/Cooling time credit	NO	The criticality analysis does not credit cooling time (Decays to 100 hours for all cases to maximize reactivity).
Integral absorber credit	NO	
Other credit	YES	Small amount of leakage is credited in the Region 1 cask drop analysis (Section 5.2.5)
Fixed neutron absorbers	NO	No neutron absorber material installed (Section 5.2.6)
Aging management program	NO	No neutron absorber material installed (Section 5.2.6)
Accident analysis	YES	(Section 5.2.7)
Temperature increase	YES	(Sections 5.2.7 & 12.2)
Assembly drop	YES	Into racks and outside of racks (Sections 5.2.7 & 12.5)
Single assembly misload	YES	No empty cells required. Fresh, 5.0wt% assemblies in all cells meet regulatory limits with normally spaced cells. (Sections 5.2.7 & 12.4)
Multiple misload	YES	No empty cells required. Fresh, 5.0wt% assemblies in all cells meet regulatory limits with normally spaced cells. (Sections 5.2.7 & 12.4)
Boron dilution	YES	(Sections 5.2.7 & 12.1)
Other	YES	Cask drop analysis (Section 9.1) Seismic Event (Section 12.8)
Fuel out of rack analysis	YES	(Sections 5.2.8, 11, and 12)
Handling	YES	(Sections 11.2 & 12.6)
Movement	YES	(Sections 11.2 & 12.6)
Inspection	YES	(Section 11.3)
6.0 Computer Codes, Cross Sections and Validation Overview		
Code/Modules Used for Calculation of k_{eff}	YES	SCALE 6.2.3 / CSAS5 - KENO V.a (Section 6.1.1)
Cross section library	YES	238 group ENDF/B-VII

Subject	Included	Notes / Explanation
		(Section 6.1)
Description of nuclides used	YES	233 isotopes used (Section 6.1.2)
Convergence checks	YES	Convergence tests run on all cases (Section 6.1.1)
Code/Module Used for Depletion Calculation	YES	SCALE 6.2.3 / Depletion: Triton t5-depl (Section 6.1.3) Decay: ORIGAMI (Section 6.1.4)
Cross section library	YES	238 group ENDF/B-VII (Section 6.1)
Description of nuclides used	YES	233 isotopes used (Section 6.1.2)
Convergence checks	YES	Test cases displayed convergence (Section 6.1.3)
Validation of Code and Library	YES	(Section 6.3) CSAS5 (Appendix A) TRITON/ORIGAMI (Appendix B)
Major Actinides and Structural Materials	YES	(Section 6.3.1)
Minor Actinides and Fission Products	YES	1.5% bias (Section 6.3.2)
Absorbers Credited	YES	(Section 6.3.4)
7.0 Criticality Safety Analysis of the New Fuel Rack		
Rack model	YES	Full storage area with structure and concrete. (Section 7.1)
Boundary conditions	YES	Void (Section 7.1)
Source distribution	YES	Uniform in fissile material (Section 7.1)
Geometry restrictions	YES	Two storage options: -4 out of 4 for enrichments ≤4.35% -3 out of 4 for enrichments >4.35% (Section 7.1)
Limiting fuel design	YES	(Section 7.2)
Fuel density	YES	Bounding high (Section 7.2.5)
Burnable Poisons	NO	No credit taken (Section 7.2.6)
Fuel dimensions	YES	Composite bounding design (Sections 7.2.1 – 7.2.4)
Axial blankets	NO	No credit taken (Section 7.2.6)
Limiting rack model	YES	(Section 7.3)
Storage vault dimensions and materials	YES	(Section 4.1)
Temperature	YES	(Section 7.3.2)
Multiple regions/configurations	YES	Only one type of rack. Two storage configurations. (Section 7.4)
Flooded	YES	(Section 7.6)
Low density moderator	YES	(Section 7.6)

Subject	Included	Notes / Explanation
Eccentric fuel placement	YES	(Section 7.3.3)
Tolerances	YES	(Section 7.5)
Fuel geometry	YES	(Section 7.5.1)
Fuel pin pitch	YES	(Section 7.5.1)
Fuel pellet OD	YES	(Section 7.5.1)
Fuel clad OD	YES	(Section 7.5.1)
Fuel content	YES	(Section 7.5.1)
Enrichment	YES	(Section 7.5.1)
Density	YES	(Section 7.5.1)
Integral absorber	NO	No credit (Section 7.2.6)
Rack geometry	YES	(Section 7.5.1)
Rack pitch	YES	(Section 7.5.1)
Cell wall thickness	YES	(Section 7.5.1)
Storage vault dimensions/materials	YES	(Section 7.5.1)
Code uncertainty	YES	(Section 7.5.3)
Biases	YES	(Section 7.5)
Temperature	YES	(Section 7.5.4)
Code bias	YES	(Section 7.5.3)
Moderator Conditions	YES	(Section 7.6)
Fully flooded and optimum density moderator	YES	(Section 7.6)
8.0 Depletion Analysis for Spent Fuel		
Depletion Model Considerations	YES	(Section 6.1.3 & 8)
Time step verification	YES	(Section 6.1.3)
Convergence verification	YES	(Section 6.1.3)
Simplifications	YES	(Section 8.1)
Non-uniform enrichments	NO	No credit taken for axial blankets
Post Depletion Nuclide Adjustment	YES	Reduced volatile fission product content (Section 6.1.2)
Cooling Time	YES	Only peak reactivity 100 hour decay used (Section 8.14)
Depletion Parameters	YES	(Section 8)
Burnable Absorbers	YES	(Section 8.7)
Integral Absorbers	YES	(Section 8.7)
Soluble Boron	YES	Bounding high soluble boron (Section 8.3)
Fuel and Moderator Temperature	YES	Calculated using bounding high fuel assembly power history and bounding high core moderator exit temperature (Sections 8.4 & 8.5)
Power	YES	Bounding high power (Section 8.2) Reduced power at end of depletion (Section 8.10)
Control rod insertion	YES	Bounded by bounding burnable poison

Subject	Included	Notes / Explanation
		(Section 8.8)
Atypical Cycle Operating History	YES	Bounded or justified. (Section 9.3)
9.0 Criticality Safety Analysis of Spent Fuel Pool Storage Racks		
Rack model	YES	Region 1 models the entire region (Section 9.1.2) Region 2 is an infinite array (Section 9.2.2)
Boundary conditions	YES	Region 1: Reflective with large amount of water and concrete between fuel and boundary. (Section 9.1.2) Region 2: Reflective (Section 9.2.2)
Source distribution	YES	Uniform in fissile material (Sections 9.1.3 & 9.2.3)
Geometry restrictions	NO	No required empty cells or low reactivity cells
Design Basis Fuel Description	YES	Composite bounding design. (Section 3.1)
Fuel density	YES	Bounds all fuel assemblies. (Section 3.1)
Burnable Poisons	NO	Burnable poison credit not utilized
Fuel assembly inserts	NO	Control rod credit not utilized
Fuel dimensions	YES	Present, past, and anticipated future designs bounded (Section 3.1)
Axial blankets	NO	Axial blanket credit not utilized.
Configurations considered	YES	Evaluated with and without boron. (Section 9 & 12.1)
Borated	YES	(Section 9.1 & 12.1)
Unborated	YES	(Section 9.2)
Multiple rack designs	NO	Only one rack type present in SFP
Alternate storage geometry	NO	No required empty cells or low reactivity cells
Reactivity Control Devices	NO	
Fuel Assembly Inserts	NO	Control rod credit not utilized
Storage Cell Inserts	NO	No storage cell inserts installed
Storage Cell Blocking Devices	NO	No empty cells required
Axial burnup shapes	YES	(Sections 8.6 & 9.1.6)
Uniform/Distributed	YES	NUREG/CR-6801 shapes and uniform. Justified with Surry shapes. (Sections 8.6 & 9.1.6)
Nodalization	YES	NUREG/CR-6801 - 18 nodes. (Section 8.6)
Blankets modeled	NO	No credit.
Tolerances/Uncertainties	YES	(Sections 9.1 & 9.2)
Fuel geometry	YES	(Sections 9.1.7 & 9.2.7)

Subject	Included	Notes / Explanation
Fuel rod pin pitch	YES	(Region 1 modeled at optimum pin pitch Section 9.2.7 for Region 2)
Fuel pellet OD	YES	(Sections 9.1.7 & 9.2.7)
Cladding OD	YES	(Sections 9.1.7 & 9.2.7)
Axial fuel position	YES	(Section 9.1.2.2 for Region 1 Not important for Region 2)
Fuel content	YES	(Sections 9.1.7 & 9.2.7)
Enrichment	YES	(Sections 9.1.7 & 9.2.7)
Density	YES	(Sections 9.1.7 & 9.2.7)
Assembly insert dimensions and materials	NO	No inserts used
Rack geometry	YES	(Sections 9.1.7 & 9.2.7)
Flux-trap size (width)	NO	No flux trap racks
Rack cell pitch	YES	(Region 1 modeled at optimum cell pitch Section 9.2.7 for Region 2)
Rack wall thickness	YES	(Sections 9.1.7 & 9.2.7)
Neutron Absorber Dimensions	NO	No neutron absorber material
Rack insert dimensions and materials	NO	No rack inserts used
Code validation uncertainty	YES	(Sections 9.1.13 & 9.2.9)
Criticality case uncertainty	YES	(Sections 9.1.16 & 9.2.10)
Depletion Uncertainty	YES	EPRI Benchmark method used (Section 9.1.11 & Appendix B)
Burnup Uncertainty	YES	5% of measured burnup. (Section 9.1.14)
Biases	YES	(Section 9)
Design Basis Fuel design	YES	(Section 3.1)
Code bias	YES	(Sections 9.1.11, 9.1.13 & 9.2.9)
Temperature	YES	(Section 9.1.12 & 9.2.8)
Eccentric fuel placement	YES	(Region 1 cells are deformed so that there is no space for eccentric fuel placement Region 2: Section 9.2.5)
Incore thimble depletion effect	YES	Incore thimble included in fuel depletion model. (Section 8.9)
NRC administrative margin	YES	(Sections 9.1.16 & 9.2.10)
Modeling simplifications	YES	(Sections 9.1.2 & 9.2.2)
Identified and described	YES	(Sections 9.1.2 & 9.2.2)
10.0 Interface Analysis		
Interface configurations analyzed	YES	(Section 10)
Between dissimilar racks	NO	Only one type of rack in SFP
Between storage configurations within a rack	YES	Region 1 (burned fuel) – Region 2 (fresh fuel) interface analyzed (Sections 10.1 & 10.2)
Interface restrictions	NO	Benign interface (Section 10.3)

Subject	Included	Notes / Explanation
11.0 Normal Conditions		
Fuel handling equipment	YES	(Section 11.2)
Administrative controls	YES	(Section 11.2)
Fuel inspection equipment or processes	YES	(Section 11.3)
Fuel reconstitution	YES	Evaluated and limitations applied (Section 11.4)
12.0 Accident Analysis		
Boron dilution	YES	350 ppm: $k_{eff} < 0.95$ (Section 12.1)
Normal conditions	YES	0 ppm: $k_{eff} < 1.00$ (Section 9.2)
Accident conditions	YES	2250 ppm: $k_{eff} < 0.95$ (Sections 9.1 & 12)
Single assembly misload	YES	(Section 12.3)
Fuel assembly misplacement	YES	(Section 12.3)
Neutron Absorber Insert Misload	NO	No neutron absorbing material
Multiple fuel misload	YES	(Section 12.4)
Dropped assembly	YES	(Section 12.5)
Temperature	YES	(Section 12.2)
Seismic event/other natural phenomena	YES	(Section 12.7)
13.0 Analysis Results and Conclusions		
Summary of results	YES	(Section 13)
Burnup curve(s)	YES	Bounding polynomial coefficients (Section 13.5)
Intermediate Decay time treatment	NO	No decay credit utilized.
New administrative controls	YES	(Section 13.5)
Technical Specification markups	YES	Attached to this LBDCR
14.0 References	YES	(Section 14)
Appendix A: Criticality Computer Code Validation:		
Code validation methodology and bases	YES	(Section A.1)
New Fuel	YES	(Section A.3)
Depleted Fuel	YES	(Section A.3)
MOX	YES	(Section A.3)
HTC	YES	(Section A.3)
Convergence	YES	(Section A.4.1)
Trends	YES	(Section A.5)
Bias and uncertainty	YES	(Section A.5)
Range of applicability	YES	(Section A.7)
Analysis of Area of Applicability coverage	YES	(Section A.7)

Subject	Included	Notes / Explanation
Appendix B: Depletion Computer Code Validation:		
Code validation methodology and bases	YES	(Section B.2)
Convergence	YES	(Section B.3)
Trends	YES	(Section B.4)
Bias and uncertainty	YES	(Section B.4)
Range of applicability	YES	(Section B.5)

Serial No. 22-018
Docket Nos. 50-280/281

NON-PROPRIETARY

Attachment 6

CRITICALITY SAFETY ANALYSIS REPORT

VIRGINIA ELECTRIC AND POWER COMPANY
(DOMINION ENERGY VIRGINIA)
SURRY POWER STATION UNITS 1 AND 2

CRITICALITY SAFETY ANALYSIS REPORT
VIRGINIA ELECTRIC AND POWER COMPANY
SURRY POWER STATION UNITS 1 AND 2

Table of Contents

1 Introduction 14
2 Acceptance Criteria and Regulatory Guidance 15
3 Reactor and Fuel Design Description 18
3.1 Fuel Description 18
3.2 Fuel Inserts Description 22
3.2.1 Burnable Absorbers 22
3.2.2 Control Rods 24
3.2.3 Sources and Other Inserts 25
3.3 Non-Standard Fuel in the Pool 26
4 Storage Rack Description 29
4.1 New Fuel Storage Area 29
4.2 Spent Fuel Pool 32
5 Overview of the Method of Analysis 37
5.1 New Fuel Storage Area 37
5.2 Spent Fuel Storage Racks 38
5.2.1 Storage Requirements 38
5.2.2 Bounding Fuel Design 39
5.2.3 Soluble Boron Credit 40
5.2.4 Burnup Credit 40
5.2.5 Other Credit 43
5.2.6 Neutron Absorbers 43
5.2.7 Accident Analysis 44
5.2.8 Normal Operations 45
6 Cross Sections, Computer Codes, and Validation 46
6.1 Cross Sections and Computer Codes 46
6.1.1 CSAS5 46
6.1.2 Isotopes Used 47
6.1.3 TRITON 51
6.1.4 ORIGAMI 52
6.2 Uncertainty and Bias in Depleted Fuel Isotopic Content 52
6.3 Validation of Criticality Analysis 54

6.3.1 Major Actinides and Structural Materials 54
6.3.2 Minor Actinides and Fission Products 57
6.3.3 Temperature Dependence 57
6.3.4 Absorbers Credited 58
7 Criticality Safety Analysis of the New Fuel Storage Area 59
7.1 New Fuel Storage Area Overview and KENO Model 59
7.2 Limiting Fuel Design 63
7.2.1 Fuel Cladding Materials 63
7.2.2 Instrument and Guide Tubes 65
7.2.3 Top and Bottom Assembly Reflectors 67
7.2.4 Assembly Grids 69
7.2.5 Fuel Density 70
7.2.6 Burnable Poisons and Axial Blankets 70
7.3 Limiting Rack Model 71
7.3.1 Concrete 71
7.3.2 Temperature and Water Density 73
7.3.3 Asymmetric Fuel Placement 76
7.3.4 Credited Structural Beams 78
7.4 Summary of the Base Case for the NFSA Analysis 80
7.5 Biases and Uncertainties for the New Fuel Storage Area Analysis 81
7.5.1 Manufacturing Uncertainties 81
7.5.2 Nominal Model Uncertainty 82
7.5.3 Code Benchmark Bias and Uncertainty 83
7.5.4 Code Temperature Bias 84
7.5.5 NRC Administrative Margin 84
7.6 NFSA Maximum k-eff 85
7.7 Accident Conditions 87
7.7.1 Optimum Moderation 87
7.7.2 Dropped and Misloaded Assembly 87
7.7.3 Seismic Event 87
8 Depletion Modeling and Burnup Effects 88
8.1 Depletion Method Overview 88
8.2 Bounding Fuel Assembly Depletion Power 89
8.3 Bounding Depletion Boron 92
8.4 Bounding RCS Temperature 94
8.5 Bounding Fuel Temperature 98

8.6 Bounding Axial Burnup Profiles 100
8.7 Burnable Absorbers 107
8.8 Control Rod History 111
8.9 In-core Thimble in the Instrument Tube 114
8.10 Reduced Power before Storage 115
8.11 Planar Burnup Tilt 116
8.12 Grids 118
8.13 Clad Volume 120
8.14 Common Depletion Elements Not Modeled/Credited 121
8.15 TRITON Depletion Model Summary 122
9 Spent Fuel Rack Analysis 124
9.1 Damaged Rack Analysis (Cask Drop Accident) – Region 1 125
9.1.1 Region 1 Fuel Storage Requirements 125
9.1.2 Cask Drop Accident Description and Assumptions 126
9.1.3 Region 1 Infinite Lattice KENO Model 144
9.1.4 Optimum Pitch Calculation and Bias 146
9.1.5 SFP Normal Operation Water Temperature and Density 150
9.1.6 Axial Burnup Shapes 151
9.1.7 Manufacturing Uncertainties 152
9.1.8 Planar Burnup Tilt Bias 155
9.1.9 Reduced Power Coastdown Bias 159
9.1.10 Minor Actinides and Fission Product Bias 160
9.1.11 Depletion Benchmark Bias and Uncertainty 161
9.1.12 Code Temperature Bias 162
9.1.13 Code Validation Bias and Uncertainty 163
9.1.14 Measured Burnup Uncertainty 164
9.1.15 Common Depletion Biases Not Applicable for Surry 166
9.1.16 Region 1 Damaged Rack Analysis Results 167
9.2 Nominal Rack Analysis (Unborated) – Region 2 171
9.2.1 Region 2 Fuel Storage Requirements 171
9.2.2 Region 2 Modeling Assumptions 171
9.2.3 Region 2 Infinite Lattice Model 172
9.2.4 SFP Normal Operation Water Temperature and Density 174
9.2.5 Asymmetric or Eccentric Fuel Positioning 175
9.2.6 Wall Boundary and Wall-to-Rack Gap 176
9.2.7 Manufacturing Uncertainties 177

9.2.8 Code Temperature Bias 178
9.2.9 Code Validation Bias and Uncertainty 179
9.2.10 Region 2 Nominal Rack Analysis Results 180
9.3 Unbounded Fuel Assemblies 182
9.3.1 Unbounded Depletion Boron (Assembly 4G7) 183
9.3.2 17x17 Fuel Assemblies 184
10 Interface Analysis 186
10.1 Interface Analysis – Average k-eff vs. Generation Trend 188
10.2 Interface Analysis – Interface Only Models 191
10.3 Interface Analysis Summary 193
11 Normal Conditions 194
11.1 Fuel Inserts 194
11.2 Fuel Handling 197
11.3 Fuel Inspection 199
11.4 Non-standard Fuel 199
11.4.1 Fuel Rod Storage Canister 199
11.4.2 Reconstituted Fuel 203
11.5 Trash Cans 206
12 Accident Analysis 206
12.1 Boron Dilution Accident 206
12.2 Loss of Cooling 208
12.3 Single Assembly Mis-placement 211
12.4 Assembly Misload 214
12.5 Dropped Assembly 215
12.6 Fuel Handling Error 216
12.7 Seismic Event 218
12.8 Accident Analysis Summary 218
13 Summary and Conclusions 219
13.1 New Fuel Storage Area 219
13.2 Spent Fuel Pool 219
13.3 Bounding Fuel Design Inputs 220
13.4 Bounding Depletion Condition Inputs 221
13.5 Summary of Loading Constraints 222
14 References 226

List of Tables

Table 3-1: Fuel Design Dimensions 19
Table 3-2: Fuel Design Tolerances 19
Table 3-3: Assembly Model Dimensions in SFP and NFSA 20
Table 3-4: Description of Discrete Burnable Poisons 23
Table 3-5: Description of Integral Burnable Poisons....23
Table 3-6: Description of Control Rods 24
Table 3-7: Dimensions of In-core Thimble....25
Table 3-8: Fuel Rod Storage Container 26
Table 3-9: 17x17 Demonstration Assemblies....26
Table 4-1: New Fuel Storage Area Rack Dimensions 29
Table 4-2: New Fuel Storage Area Rack Positions 29
Table 4-3: Surry Power Station Spent Fuel Racks....34
Table 5-1: Storage Requirements 37
Table 5-2: Storage Restrictions....38
Table 6-1: Isotopes Used in the Criticality Analysis 48
Table 6-2: Fission Product Gases and Volatiles 49
Table 6-3: Fission Gas Release Fractions....50
Table 6-4: Application-Specific Calculated Bias....53
Table 6-5: Depletion Code Additional Bias and Uncertainty....53
Table 6-6: Maximum k-eff with Kopp Uncertainty vs EPRI Benchmarks....53
Table 6-7: Validation Code Bias and Uncertainty 56
Table 7-1: k-eff of Zirconium Alloys in Optimum Moderation 63
Table 7-2: k-eff of Zirconium Alloys in Flooded Conditions....63
Table 7-3: Instrument and Guide Tube Inner and Outer Diameter....65
Table 7-4a: k-eff of Instrument and Guide Tubes in Optimum Moderation....65
Table 7-4b: k-eff of Instrument and Guide Tubes in Full Density Water....65
Table 7-5a: NFSA k-eff with Varying Reflector in Optimum Moderation 67
Table 7-5b: NFSA k-eff with Varying Reflector in Full Density Water....67
Table 7-6a: NFSA k-eff with Varying Height Above Floor in Optimum Moderation 68
Table 7-6b: NFSA k-eff with Varying Height Above Floor in Full Density Water....68
Table 7-7: Grid Volume in Active Fuel Region for Historical Fuel Designs....69
Table 7-8: Grid Volume Fractions 69

Table 7-9: Concrete Composition 71
Table 7-10a: k-eff of Various Concrete Types in Optimum Moderation 72
Table 7-10b: k-eff of Various Concrete Types in Full Density Water 72
Table 7-11: Water Density Sensitivity Cases for All Enrichment Combinations....74
Table 7-12a: k-eff of NFSA with Asymmetry in Optimum Moderation 76
Table 7-12b: k-eff of NFSA with Asymmetry in Full Density Water....76
Table 7-13: Manufacturing Tolerance in Optimum Moderation....81
Table 7-14: Manufacturing Tolerance in Full Density Water 82
Table 7-15: Code Benchmarking Bias and Uncertainty (Appendix A)....83
Table 7-16: Code Uncertainty for Nominal Cases 83
Table 7-17: Maximum k-eff of New Fuel Storage Area, Optimum Moderation Scenario ...85
Table 7-18: Maximum k-eff of New Fuel Storage Area, Full Water Density 86
Table 8-1: Bounding BARAP versus Burnup 91
Table 8-2: Sensitivity Cases with Increased Depletion Power 91
Table 8-3: Sensitivity Cases with Increased Depletion Boron 93
Table 8-4: RCS Thermal Hydraulic History for Surry 95
Table 8-4: RCS Thermal Hydraulic History for Surry (cont.) 96
Table 8-5: RCS Thermal Hydraulic History for Surry 97
Table 8-6: Sensitivity Cases with Increased Moderator Temperature 97
Table 8-7: Example Calculations for Fuel Temperature 99
Table 8-8: Sensitivity Cases with Increased Moderator Temperature 99
Table 8-9: Depletion with Different Burnable Absorbers....108
Table 8-10: Mixed Burnable Poison Loadings During Depletion 108
Table 8-11: Secondary Sources Dimensions 109
Table 8-12: Control Rod Model....111
Table 8-13: Control Rod Use Sensitivity Cases 113
Table 8-14: In-Core Thimble and Instrument Tube Dimensions 114
Table 8-15: In-Core Thimble Material Parameters....114
Table 8-16: Low Power EOC Effect on SFP Reactivity 115
Table 8-17: Modeled Planar Burnup Tilt 117
Table 8-18: Grid Volume in Active Fuel Region for Historical Fuel Designs....118
Table 8-19: Grid Volume Fractions 119
Table 8-20: Varying Methods for Modeling Grids Cases 119
Table 8-21: Bounding Assembly Parameters....120

Table 8-22: Varying Clad Volume Fractions Cases....120
Table 8-23: Depletion Inputs for TRITON Depletion Model....122
Table 8-24: Assembly Inputs for TRITON Models....123
Table 9-1: Region 1 Reactivity Under Various Cask Drop Scenarios....129
Table 9-2: Optimum Pellet Stack Pitch....136
Table 9-3: Region 1 k-eff at Varying Degrees of Rack Deformation....148
Table 9-4: Optimum Pitch Bias....149
Table 9-5: Region 1 k-eff at Varying Spent Fuel Pool Temperatures....150
Table 9-6: Bounding Burnup Shape Cases....151
Table 9-7: Uncertainty Cases....152
Table 9-7: Uncertainty Cases (cont.)....153
Table 9-7: Uncertainty Cases (cont.)....154
Table 9-8: Radial Burnup Tilt Burnup....157
Table 9-9: Radial Burnup Tilt Bias....157
Table 9-10: Low Power Coastdown Bias....159
Table 9-11: Minor Actinides Bias....160
Table 9-12: Depletion Application Code Bias (Δk)....161
Table 9-13: Additional Depletion Bias and Uncertainty Terms....162
Table 9-14: Code Benchmarking Bias and Uncertainty (Appendix A)....163
Table 9-15: Cask Drop Code Benchmarking Bias and Uncertainty....163
Table 9-16: Measured Burnup Uncertainty....165
Table 9-17: Cask Drop Accident Maximum k-eff and Margin to the Limit....168
Table 9-18: Region 2 k-eff at Varying Spent Fuel Pool Temperatures....174
Table 9-19: Region 2 k-eff at with Varying Fuel Placements....175
Table 9-20: Rack Wall Proximity Case....176
Table 9-21: Region 2 Manufacturing Uncertainty Cases....177
Table 9-22: Code Benchmarking Bias and Uncertainty (Appendix A)....179
Table 9-23: Cask Drop Code Benchmarking Bias and Uncertainty....179
Table 9-24: Region 2 Summary of Biases, Uncertainties and Margins....181
Table 9-25: Depletion Boron Effect on SFP Reactivity....183
Table 9-26: 17 x 17 Demonstration Assemblies....184
Table 9-27: 17 x 17 Assembly Enrichment and Burnup....184
Table 9-28: Depletion Worth Comparison of 15x15 and 17x17 Fuel, Node 16....185
Table 10-1: Interface-Only Model Results....192

Table 11-1: Optimum Pitch k-eff for Assemblies With and Without Inserts 195
Table 11-2: Fresh Water Separation Cases 197
Table 11-3: Fuel Rod Canister Dimensions 200
Table 11-4: Reactivity of the Fuel Rod Canister 200
Table 11-5: Reactivity Change from Removing One Fuel Pin 203
Table 12-1: k-eff of Boron Dilution Accident 207
Table 12-2: k-eff of Boron Dilution Accident 207
Table 12-3: Temperature Increase Accident Cases 208
Table 12-4: Misplaced Assembly Case Results 213
Table 12-5: Fresh 5.00 wt% Fuel in All Cells with 2250 ppm 214
Table 12-6: Dropped Assembly Case Results 215
Table 12-7: Borated Water Separation Cases 216
Table 13-1: Bounding Fuel Design Inputs 220
Table 13-2: Bounding Depletion Conditions for Burnup Credit 221
Table 13-3: Surry SFP Storage Constraint Summary 222

List of Figures

Figure 3-1: 15x15 Fuel Design....21
Figure 3-2: Fuel Rod Storage Container....27
Figure 3-3: 17x17 Fuel Design....28
Figure 4-1: Surry Power Station New Fuel Storage Area (Radial View) 30
Figure 4-2: Surry Power Station New Fuel Storage Area (Axial View)....31
Figure 4-3: Surry SFP Rack Orientation 33
Figure 4-4: Surry Power Station Spent Fuel Racks (Radial View) 35
Figure 4-5: Surry Power Station Spent Fuel Racks (Axial View)....36
Figure 7-1: Planar View of the New Fuel Storage Area Model....60
Figure 7-2: Axial Representation of the New Fuel Storage Area Model 61
Figure 7-3: Empty Cells Required New Fuel Storage Area....62
Figure 7-4: k-eff of NFSA vs. Zirconium Volume Fraction in Lattice 66
Figure 7-5: k-eff of NFSA vs. Water Density....75
Figure 7-6: k-eff of NFSA vs. Water Density....75
Figure 7-7: Asymmetric Skewing of Assemblies 77
Figure 7-8: Drawing of NFSA Lower Structural Beams 78
Figure 7-9: KENO Model of NFSA Lower Structural Beams....79
Figure 8-1: Bounding Burnup Averaged Relative Assembly Power....91
Figure 8-2: Surry Bounding Cycle Average Soluble Boron 93
Figure 8-3: NUREG vs. Surry Axial Burnup Shapes, 14-18 GWD/T Burnup Bin 102
Figure 8-4: NUREG vs. Surry Axial Burnup Shapes, 18-22 GWD/T Burnup Bin 102
Figure 8-5: NUREG vs. Surry Axial Burnup Shapes, 22-26 GWD/T Burnup Bin 103
Figure 8-6: NUREG vs. Surry Axial Burnup Shapes, 26-30 GWD/T Burnup Bin 103
Figure 8-7: NUREG vs. Surry Axial Burnup Shapes, 30-34 GWD/T Burnup Bin 104
Figure 8-8: NUREG vs. Surry Axial Burnup Shapes, 34-38 GWD/T Burnup Bin 104
Figure 8-9: NUREG vs. Surry Axial Burnup Shapes, 38-42 GWD/T Burnup Bin 105
Figure 8-10: NUREG vs. Surry Axial Burnup Shapes, 42-46 GWD/T Burnup Bin 105
Figure 8-11: NUREG vs. Surry Axial Burnup Shapes, 46-62 GWD/T Burnup Bin 106
Figure 8-12: Assembly Map with 12 Discrete BP Rods 110
Figure 8-13: Assembly Map with 148 IFBA Rods....110
Figure 8-14: Cycle Average Control Rod Insertion....112
Figure 8-15: Planar Tilt vs. Burnup for Surry Assemblies....117

Figure 9-1: Cask Drop Accident Model (x-y Profile) 131
Figure 9-2: Cask Drop Accident Model, Zoomed In (x-y Profile).....132
Figure 9-3: Cask Drop Accident Model (y-z Profile).....133
Figure 9-4: Cask Drop Accident Model, Zoomed In, x-y Profile, In-Fuel Racks 137
Figure 9-5: Cask Drop Accident Model, Zoomed In, x-y Profile, Beneath Fuel Racks....138
Figure 9-6: Cask Drop Accident Model, Zoomed In, y-z Profile 139
Figure 9-7: Cask Drop Accident Model, Zoomed In, x-y Profile 141
Figure 9-8: Cask Drop Accident Model, Zoomed In, y-z Profile 142
Figure 9-9: Cask Drop Accident Model, Zoomed In, y-z Profile, Pellet Stacks Reversed Axially 143
Figure 9-10: Region 1 Model, Nominal Pitch 145
Figure 9-11: Example of Optimum Pitch Bias Regression Curve (53 GWD/MTU).....149
Figure 9-12: Radial Tilt KENO Model (zoomed out) 158
Figure 9-13: Radial Tilt KENO Model (zoomed in).....158
Figure 9-14: Region 1 Burnup Curve and Relevant Data.....169
Figure 9-15: Burnup Curve for Region 1 170
Figure 9-16: Planar View of the Region 2 KENO Model.....173
Figure 9-17: Rack Wall Proximity Case 176
Figure 4-3: Surry SFP Rack Orientation 187
Figure 10-1: Initial Neutron Source Location 188
Figure 10-2: Full Pool Model 189
Figure 10-3a: Generation Average k-eff, Fresh Fuel in Regions 1 & 2 190
Figure 10-3b: Generation Average k-eff, Burned in Region 1 – Fresh in Region 2.....190
Figure 10-4: Interface Only Model.....191
Figure 11-1: Optimum Pitch k-eff for Assemblies With and Without Inserts 196
Figure 11-2: Fuel Handling Model 198
Figure 11-3: Reactivity of Two Assemblies in Fresh Water 198
Figure 11-4: Drawing of Fuel Rod Storage Canister.....201
Figure 11-5: Picture of Fuel Rod Storage Canister.....201
Figure 11-6: SCALE Model of Fuel Rod Storage Canister.....202
Figure 11-7: Location of Open Water Hole 205
Figure 12-1: Temperature Increase Model with Boiling.....209
Figure 12-2: Temperature Increase Model with Boiling (zoomed in).....210
Figure 12-3: Location of Misplaced Assembly.....211

Figure 12-4: Misplaced Assembly SCALE Model.....213
Figure 12-5: Reactivity of Two Assemblies in Fresh Water 217
Figure 13-1: Surry SFP Region Orientation.....223
Figure 13-2: Region 1 Burnup Credit Curve.....224
Figure 13-3: Empty Cells Required New Fuel Storage Area.....225

Annotation of proprietary information herein corresponds to the following companies. Specific reason(s) for claiming the information as proprietary is delineated in the respective Affidavit executed by the owners of the information.

1) Framatome proprietary information - denoted with **"F"** superscript
2) Westinghouse proprietary information - denoted with **"a,c"** superscripts

List of Acronyms and Abbreviations

BP	Burnable Poison
BOC	Beginning of Cycle
CSA	Criticality Safety Analysis
COLR	Core Operating Limits Report
DOE	Department of Energy (USA)
EALF	Energy of the Average Lethargy of a neutron causing Fission
EOL	End of Life
FA	Fuel Assembly
FRC	Fuel Rod Canister
FRSC	Fuel Rod Storage Container
FP	Fission Product
GWd/MTU	Gigawatt*day per Metric Ton (Tonne) of Uranium. A unit of burnup.
HFP	Hot Full Power
HTC	Haut Taux de Combustion. This is a set of critical experiments done in France that uses fuel that represents the uranium and plutonium content of 4.5 wt% fuel burned to 37.5 GWd/MTU
ID	Inner Diameter
IFBA	Integral Fuel Burnable Absorber which is a ZrB_2 coating placed on the outside of the fuel pellet. A Westinghouse product.
ISG	Interim Staff Guidance from the NRC
MOX	Mixed Oxide fuel. Contains both UO_2 and PuO_2.
MWd/MTU	Megawatt*day per Metric Ton (Tonne) of Uranium. A unit of burnup.
NCS	Nuclear Criticality Safety
NFSA	New Fuel Storage Area. Referring to the concrete pit and steel racks used to hold the new fuel. Sometimes used interchangeably with NSFR.
OD	Outer Diameter
pcm	0.00001 in k (acronym from percent mille)
ppm	Parts per million by weight
PWR	Pressurized Water Reactor
RCCA	Rod Cluster Control Assembly (control rod)
RCS	Reactor Coolant System
RSS	square Root of the Sum of the Squares
RTP	Rated Thermal Power
SER	Safety Evaluation Report
SFP	Spent Fuel Pool
SNF	Spent Nuclear Fuel
SPS	Surry Power Station
SS	Stainless Steel
VF	Volume Fraction

Introduction

1 A spent fuel pool (SFP) and new fuel storage area (NFSA) criticality analysis is performed for Surry Power Station to allow for increased enrichment, include gadolinium burnable poison into the licensing basis, to update computer codes and analysis methods, and to increase identified margin to k-effective (k-eff) limits.

Criticality analysis scope includes normal fuel storage, normal fuel handling, abnormal fuel storage conditions, abnormal fuel handling events, and storage of non-standard fuel-bearing components. A boron dilution analysis is provided that identifies potential SFP dilution events, dilution water source flow rates and volumes, means of detection, time required for detection and mitigation, and minimum dilution event soluble boron concentration.

Changes to the operation and administration of the SFP are summarized as follows:

- Modify the maximum enrichment in Technical Specification 5.3.1.1
- Modify Figure 5.3-1 to extend and adjust the burnup curve for Region 1.

Operations and administration of the SFP that are not changing are summarized as follows:

- The SFP two region layout described in Technical Specification 5.3.1.3 is not changing.
- SFP soluble boron requirement in Technical Specification 5.3.2 is not changing.
- The capacity of the SFP as described in Technical Specification 5.3.4 is not changing because empty cells are still not required.

Changes to the operation and administration of the NFSA are summarized as follows:

- Modify maximum enrichment to 4.35 wt% in Technical Specification 5.3.1.2 without requiring any empty cells.
- Add a requirement and figure to Technical Specification 5.3.1.2 to require empty cells at the locations specified in Figure 7-3 to store maximum enrichments up to 5.0 wt%.

Fuel burnup, when used to compare to fuel storage requirements, is the volume averaged burnup of the assembly as determined using the measured reaction rates with no reduction for measurement uncertainty. Enrichment when used to compare to fuel storage requirements is the maximum planar volume averaged as-built initial enrichment in the assembly. If the assembly has axial blankets the lower enriched fuel is not credited in determining the enrichment.

2 Acceptance Criteria and Regulatory Guidance

The Code of Federal Regulations Title 10 Part 50 Section 68 (b).4 states:

> *"If credit is taken for soluble boron, the k-effective of the spent fuel storage racks loaded with fuel of the maximum fuel assembly reactivity must not exceed 0.95, at a 95 percent probability, 95 percent confidence level, if flooded with borated water, and the k-effective must remain below 1.0 (subcritical), at a 95 percent probability, 95 percent confidence level, if flooded with unborated water. "*

This analysis shows at a 95 percent probability and 95 percent confidence level that if the fuel loaded in the SFP meets the Technical Specification requirement for enrichment and burnup, the SFP k-eff will be less than 0.95 crediting soluble boron and less than 1.0 with unborated water as specified in 10CFR50.68. [1]

Further, Title 10 Part 50 Section 68 (b) paragraphs 2 and 3 state:

> *"(2) The estimated ratio of neutron production to neutron absorption and leakage (k-effective) of the fresh fuel in the fresh fuel storage racks shall be calculated assuming the racks are loaded with fuel of the maximum fuel assembly reactivity and flooded with unborated water and must not exceed 0.95, at a 95 percent probability, 95 percent confidence level. This evaluation need not be performed if administrative controls and/or design features prevent such flooding or if fresh fuel storage racks are not used.*
>
> *(3) If optimum moderation of fresh fuel in the fresh fuel storage racks occurs when the racks are assumed to be loaded with fuel of the maximum fuel assembly reactivity and filled with low-density hydrogenous fluid, the k-effective corresponding to this optimum moderation must not exceed 0.98, at a 95 percent probability, 95 percent confidence level. This evaluation need not be performed if administrative controls and/or design features prevent such moderation or if fresh fuel storage racks are not used"*

This analysis of the fresh fuel storage racks shows that the storage racks meet the requirements of paragraphs 2 and 3 when fully loaded with fresh 5.0 wt% U-235 fuel assemblies with required empty cell locations or fresh 4.35 wt% U-235 fuel assemblies without any required empty cell locations.

Due to compliance with 10CFR50.68 paragraph (b), an exemption from the requirements of 10CFR70.24 paragraphs (a) through (c) is permitted per 10 CFR 70.24(d).

Meeting 10CFR50.68 also satisfies 10CFR50, Appendix A, General Design Criterion 62 [2] which states:

"Criticality in the fuel storage and handling system shall be prevented by physical systems or processes, preferably by use of geometrically safe configurations."

Guidance for the regulatory review is found in the Standard Review Plan, NUREG-0800 Section 9.1.1, "Criticality Safety of Fresh and Spent Fuel Storage and Handling." [3] Below are the eleven specific areas of review from this guidance with where the information is found in this report. (Note that there are actually 13 areas of review but the last two do not apply to License Amendment Requests.)

1. *Fuel assembly design to verify that appropriate fuel assembly data were used.*

   Fuel assembly design data is found in Section 3.

2. *Fuel storage rack design to verify that appropriate fuel storage rack data were used*.

   Storage rack design data is found in Section 4.

3. *Evaluation of performance effectiveness of the neutron absorbing materials in the fresh and spent fuel racks*.

   There are no neutron absorbing materials installed in the fresh fuel or spent fuel racks.[5]

4. *Computational methods and related data to verify that acceptable computational methods and data were used.*

   Computational methods are described in Sections 5 and 6.

5. *Computational method validation to verify that the validation study is thorough and uses benchmark critical experiments that are similar to the normal-conditions and abnormal conditions models and to verify that the neutron distribution coefficient (K(eff)) bias and bias uncertainty values are conservatively determined.*

   Validation is summarized in Section 6 and the details are provided in Appendix A and B.

6. *Identification of normal conditions to verify that the scope of specified normal conditions is comprehensive*.

   Range of normal conditions is identified in Section 11

7. *Normal-conditions models to verify that normal conditions are modeled conservatively and that all modeling approximations and assumptions are appropriate*.

   Normal conditions models and the tolerances and uncertainties in these models are described in Sections 7 - 11.

8. *Identification of abnormal conditions to verify that the scope of considered abnormal conditions is comprehensive*.

Abnormal conditions are described in Section 7 and 12.

9. *Abnormal-conditions models to verify that abnormal conditions are modeled conservatively and that all modeling approximations and assumptions are appropriate*.

Abnormal condition models are described in Section 9.1 and 12.

10. *Analysis of normal and credible abnormal conditions to verify that the analysis is complete and logically sound and that assumptions, limits, and controls are clearly stated*.

The analysis is contained in Sections 7 through 12. The limitations of the analysis are listed in Section 13.

11. *Analysis conclusions to verify the applicant's conclusions regarding maintaining subcriticality for all normal and credible abnormal conditions*.

The conclusion of the analysis is in Section 13.

Guidance for spent fuel pool criticality analysis is given in NEI 12-16 [32]. NEI 12-16 has been endorsed, with certain exceptions, in RG 1.240 [6].

3 Reactor and Fuel Design Description

3.1 *Fuel Description*

Surry uses a 15x15 lattice fuel with a center instrument tube and 20 guide tubes. Seven fuel designs have been used but all the designs are similar for the criticality analysis. The initial fuel design, which is designated "Standard," used all Inconel grids. The currently used fuel designs are the Westinghouse Upgrade design and Framatome Agora LTAs. Table 3-1 provides fuel dimensions on historical fuel assembly designs. Note that SIF (Surry Improved Fuel) and SIF/P+ are grouped together due to their similarities and SIF/P+Z and SIF/P+Z2 are grouped together for the same reason. Table 3-3 shows the bounding assembly design used in the KENO models. This bounding assembly is a hybrid of historical designs that bounds historical and anticipated future designs.

In addition to the typical 15x15 fuel type, four 17x17 demonstration assemblies were used at the beginning of Surry's operation (last irradiated in 1979). Their dimensions are listed in Table 3-9. These four assemblies are still in the SFP and will be handled on a case specific analysis in this analysis in Section 9.

The fuel pellet is dished and chamfered. The fuel batch stack density (density of the pellet reduced by the dishing and chamfering) has ranged from [redacted]^{a,c} of the UO_2 theoretical density. A conservative input of 95.5% will be used for this analysis.

A bounding fuel stack density is used in this analysis (as opposed to a nominal value), but an uncertainty is still evaluated in the k-eff calculations for conservatism. The density uncertainty of historical batches can be determined by calculating the standard deviation for all Surry batches (after applying the void volume correction). The resulting standard deviation is [redacted]^{a,c}. This number is artificially high because the nominal void volume has changed as fuel designs have evolved. The standard deviation of just the Upgrade fuel is [redacted]^{a,c}. For conservatism and to bound AGORA reloads, the former standard deviation will be rounded up to 0.7% for uncertainty calculations in this analysis.

The active length of the fuel is 365.76 $\pm$ [redacted]^{a,c} cm. The distance from the bottom of the fuel assembly to the bottom of the active fuel has varied by design from [redacted]^{a,c} cm.

No axial blankets are credited in this analysis. All fuel pins in an assembly have had the same enrichment except for the Agora LTA assemblies which had reduced enrichments in the fuel pins that contained gadolinia.

The assembly pitch in the core is 21.50 cm. The location of the guide tubes in the assembly is given on Figure 3-1. Table 3-3 lists the bounding assembly design used in the Spent Fuel Pool and New Fuel Storage Area analysis.

Table 3-1: Fuel Design Dimensions
(Dimensions in cm)

Dimension Description	Standard	SIF & SIF/P+	SIF/P+Z & SIF/P+Z2	Upgrade	Agora-5A LTA
Pellet Diameter	[			]a,c	[ ]F
Clad Inner Diameter	[			]a,c	[ ]F
Clad Outer Diameter	[			]a,c	[ ]F
Clad Material	[			]a,c	[ ]F
Fuel Rod Pitch	[			]a,c	[ ]F
GT & IT* Inner Diameter	[			]a,c	[ ]F
GT & IT* Outer Diameter	[			]a,c	[ ]F
Grid Volume† (cm^3)	[			]a,c	[ ]F
Grid Material	[			]a,c	[ ]F

*GT stands for Guide Tube. IT stands for Instrument Tube.
†The grid volume is the volume of the grids plus sleeves in the active fuel and conservatively ignores the bottom grid since it is made out of Inconel.
‡ [ ]F

Table 3-2: Fuel Design Tolerances

Tolerance Description	Value
Pellet Diameter	a,c
Clad Inner Diameter	]a,c
Clad Outer Diameter	[ ]a,c
Rod Pitch	]a,c
Guide Tube and Instrument Tube Inner Diameter	]a,c
Guide Tube and Instrument Tube Outer Diameter	]a,c
Fuel Stack Density	]a,c
Fuel Stack Length	]a,c

Table 3-3: Assembly Model Dimensions in SFP and NFSA

Parameter	Value
Fuel Pin Array size	15x15
Fuel Rods per Assembly	204
Guide Tubes per Assembly	20
Instrument tubes per assembly	1
Fuel Percent Theoretical Density (%)	95.5 ± 0.7
Annular Pellet I.D. (cm)	0 cm (not modeled)
Fuel Pellet O.D. (cm)	0.9335 ± 0.0026
Fuel Clad Diameter I.D. (cm)	0.9484 ± 0.0076
Fuel Clad Diameter O.D. (cm)	1.0719 ± 0.0076
Guide Tube / Instrument Tube I.D. (cm)	1.305 ± 0.010
Guide Tube / Instrument Tube O.D. (cm)	1.354 ± 0.010
Pin Pitch (cm)	1.4300 ± 0.0029
Active Fuel Length (cm)	365.76 ± 1.12
Bottom of Assembly to Bottom of Active Fuel (cm)	8.275
Clad alloy	pure zirconium
Grid Volume Fraction	Unborated SFP: 0.0083 Borated SFP: 0.0137
Guide Tube / Instrument Tube Inserts	None
Burnable Poisons	None

Figure 3-1: 15x15 Fuel Design

F	F	F	F	F	F	F	F	F	F	F	F	F	F	F
F	F	F	F	F	F	F	F	F	F	F	F	F	F	F
F	F	G	F	F	G	F	F	F	G	F	F	G	F	F
F	F	F	F	F	F	F	G	F	F	F	F	F	F	F
F	F	F	F	G	F	F	F	F	F	G	F	F	F	F
F	F	G	F	F	F	F	F	F	F	F	F	G	F	F
F	F	F	F	F	F	F	F	F	F	F	F	F	F	F
F	F	F	G	F	F	F	I	F	F	F	G	F	F	F
F	F	F	F	F	F	F	F	F	F	F	F	F	F	F
F	F	G	F	F	F	F	F	F	F	F	F	G	F	F
F	F	F	F	G	F	F	F	F	F	G	F	F	F	F
F	F	F	F	F	F	F	G	F	F	F	F	F	F	F
F	F	G	F	F	G	F	F	F	G	F	F	G	F	F
F	F	F	F	F	F	F	F	F	F	F	F	F	F	F
F	F	F	F	F	F	F	F	F	F	F	F	F	F	F

(F = Fuel, G = Guide Tube, I = Instrumentation Tube)

3.2 *Fuel Inserts Description*

3.2.1 Burnable Absorbers

Four types of burnable poison have been used at Surry. Borosilicate Glass BP and Alumina B_4C are discrete burnable poisons. IFBA and Gadolinia are integral burnable poisons. Discrete and integral burnable poisons have not been used in the same fuel assembly at Surry.

[redacted]]a,c The rods are often referred to as "fingers." There are up to 20 fingers in a Borosilicate glass or Alumina B_4C assembly. Table 3-4 provides the information needed to model Borosilicate glass and Alumina B_4C burnable absorbers.

An IFBA (Integral Fuel Burnable Absorber) rod is a fuel rod with a thin ZrB_2 coating on the surface of some of the fuel pellets. The pellets at the top and bottom 6 inches of an IFBA fuel rod are annular. Surry fuel assemblies with IFBA have contained 16 to 148 IFBA rods. A Gadolinia BP rod is a fuel rod with gadolinium oxide mixed into the fuel which displaces some uranium in the fuel. Additionally, a U-235 enrichment cutback for gadolinia BP rods is recommended by the manufacturer. Table 3-5 provides IFBA and Gadolinia modeling data.

Table 3-4: Description of Discrete Burnable Poisons

Dimension	Borosilicate Glass	Alumina B_4C
Cycles Used	S1C1 – S1C10 S2C1 – S2C10	S1C11 – S1C21 S2C11 – S2C21
Inner Annular Fill	[redacted]	[redacted]a,c
Inner Clad I.D. (cm)	[redacted]	[redacted]a,c
Inner Clad O.D. (cm)	[redacted]	[redacted]a,c
BP I.D. (cm)	[redacted]	[redacted]a,c
BP O.D. (cm)	[redacted]	[redacted]a,c
Outer Clad I.D. (cm)	[redacted]	[redacted]a,c
Outer Clad O.D. (cm)	[redacted]	[redacted]a,c
Clad Material	[redacted]	[redacted]a,c
Poison Loading (mg B-10/cm)	[redacted]	[redacted]a,c
BP Material	[redacted]	[redacted]a,c
BP Material Density (g/cc)	[redacted]	[redacted]a,c
BP Binding Material	[redacted]	[redacted]a,c

Table 3-5: Description of Integral Burnable Poisons

Dimension	IFBA	Gadolinia
Cycles Used	S1C21 – Current S2C21 – Current	S1C29 - Current
BP I.D. (cm)	[redacted]a,c	[redacted]F
BP O.D. (cm)	[redacted]a,c	[redacted]F
Poison Loading	[redacted]a,c	[redacted]F
BP Material	[redacted]a,c	[redacted]F
BP Material Density (g/cc)	[redacted]a,c	[redacted]F

3.2.2 Control Rods

Surry has only used Ag-In-Cd control rods. A control rod assembly has 20 fingers. When fully inserted, the control rod neutron absorber extends above the top of the active fuel but leaves a small amount of fuel un-poisoned at the bottom of the core. At the bottom of the control rod is a stainless steel end plug. Table 3-6 summarizes the relevant design features.

Table 3-6: Description of Control Rods

Dimension	Value
Absorber Pellet O.D. (cm)	[ ]a,c
Absorber Pellet Material	[ ]a,c
Absorber Material Density (g/cc)	[ ]a,c
Clad I.D. (cm)	[ ]a,c
Clad O.D. (cm)	[ ]a,c
End Plug Length (cm)	[ ]a,c
Clad Material	[ ]a,c
Step Size (cm/step)	[ ]a,c
Bottom of fuel to bottom of End Plug (cm)	[ ]a,c

* Material and dimensional tolerances are not provided because credit is not taken for control rods in the NFSA or SFP.

3.2.3 Sources and Other Inserts

Cycles 1-14 use primary and secondary source assemblies. Three different assembly types are used: the first has one primary and three secondary source rods, the second has four secondary source rods, and the third has one primary source rod. Starting in S1C27 and S2C26, secondary source assemblies were reintroduced with 6 secondary source rods. Because source rods do not contain a strong absorber material the impact of a source rod is less than a discrete burnable absorber rod.

The source rods had a maximum outer diameter of [ ]a,c cm. The sources are weaker absorbers and displace less water than the 20 finger Alumina B_4C BP assembly. Therefore, depletion effects of the 20 finger Alumina B_4C bound those of source rods alone. Depletion effects of source rods and integral BP in the same fuel assembly are evaluated in the determination of the bounding fuel assembly depletion conditions.

Flux suppression inserts were also used during earlier Surry cycles. The absorber in these inserts were Hafnium pellets with a pellet diameter of [ ]a,c cm and a cladding outer diameter of [ ]a,c cm. The absorber in these flux suppression inserts were never longer than 137.16 cm and were located in the bottom half of the fuel. Since these inserts displaced less water (<20 fingers per assembly) and were located in the bottom half of the fuel (neutronically less important for burned fuel), the depletion effects of the 20 finger Alumina B_4C bound those of the flux suppression inserts.

Prior to operation, thimbles for the in-core flux monitoring are inserted into the instrument tubes of about one third of the assemblies. Since these thimbles displace water, they have a small effect on fuel depletion. The dimensions of the thimbles are given in Table 3-7. Two designs have been used at Surry Power Station. A bounding design was used which is further described in Section 8.9 of this report.

Table 3-7: Dimensions of In-core Thimble

Parameter	Westinghouse	Areva
In-Core Thimble Outer Tube O.D.	[ ]a,c	[ ]F
In-Core Thimble Outer Tube I.D.	[ ]a,c	[ ]F
In-Core Thimble Inner Tube O.D.	[ ]a,c	[ ]F
In-Core Thimble Inner Tube I.D.	[ ]a,c	[ ]F

[ ]a,c

3.3 *Non-Standard Fuel in the Pool*

There are a few items in the spent fuel pool that are not standard fuel assemblies. If the item does not have fuel in it, it can be placed in any cell that is allowed to have fuel. The following items in the Surry SFP contain fuel but are not standard fuel assemblies:

- Fuel rod storage container (FRSC)
- Reconstituted fuel assemblies with SS replacement pins
- Four 17x17 demonstration assemblies
- Assembly which exceeds the standard depletion boron (assembly was discharged mid-cycle)

The key design features of the FRSC are below. Figure 3-2 is a schematic view and picture of the FRSC.

Table 3-8: Fuel Rod Storage Container

Dimension	Value
Lattice Type	Square Lattice
No. of Storage Tubes	105 tubes
Storage Tube Pitch	[redacted]F
Storage Tube O.D.	[redacted]F
Storage Tube Wall Thickness	[redacted]F

The key design features of the 17x17 demonstration assemblies are below. Figure 3-3 shows the guide tube and instrument tube layout of a 17x17 fuel assembly.

Table 3-9: 17x17 Demonstration Assemblies

Property	Value
Rod Pitch (cm)	[redacted]a,c
Pellet O.D. (cm)	[redacted]a,c
Fuel Clad O.D. (cm)	[redacted]a,c
Fuel Clad Thickness (cm)	[redacted]a,c
Active Fuel Height (cm)	[redacted]a,c
Fuel Material	[redacted]a,c
Cladding Material	[redacted]a,c
Grid Volume Fraction	[redacted]a,c

Figure 3-2: Fuel Rod Storage Container

[ ]F

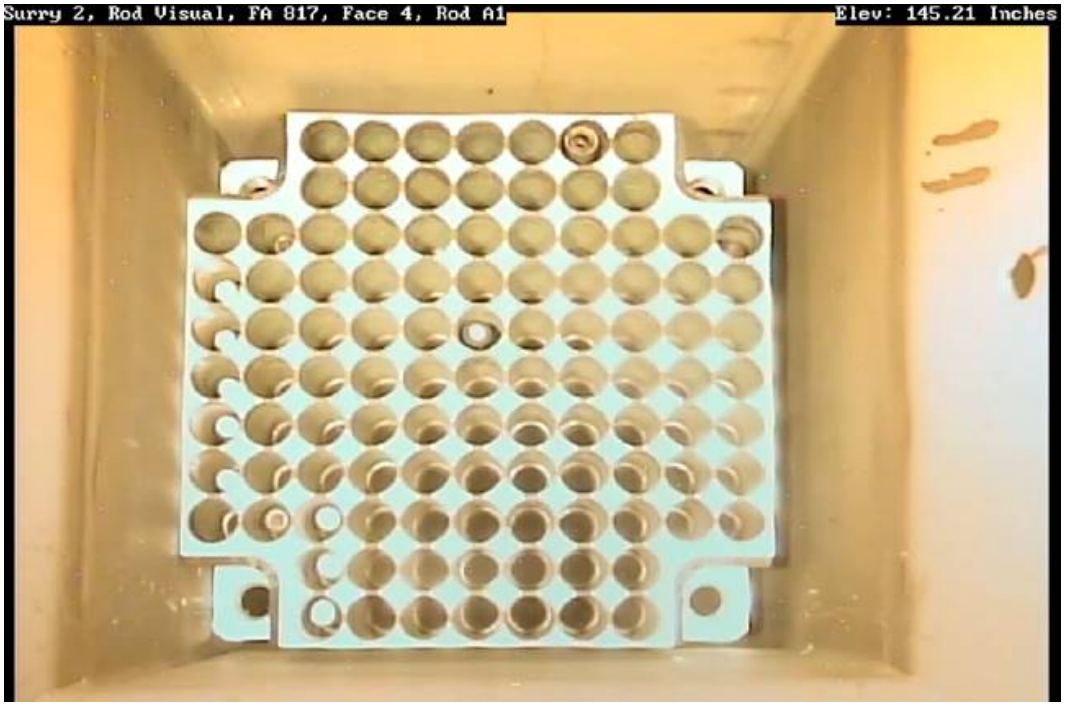

Figure 3-3: 17x17 Fuel Design

F	F	F	F	F	F	F	F	F	F	F	F	F	F	F	F	F
F	F	F	F	F	F	F	F	F	F	F	F	F	F	F	F	F
F	F	F	F	F	G	F	F	G	F	F	G	F	F	F	F	F
F	F	F	G	F	F	F	F	F	F	F	F	F	G	F	F	F
F	F	F	F	F	F	F	F	F	F	F	F	F	F	F	F	F
F	F	G	F	F	G	F	F	G	F	F	G	F	F	G	F	F
F	F	F	F	F	F	F	F	F	F	F	F	F	F	F	F	F
F	F	F	F	F	F	F	F	F	F	F	F	F	F	F	F	F
F	F	G	F	F	G	F	F	I	F	F	G	F	F	G	F	F
F	F	F	F	F	F	F	F	F	F	F	F	F	F	F	F	F
F	F	F	F	F	F	F	F	F	F	F	F	F	F	F	F	F
F	F	G	F	F	G	F	F	G	F	F	G	F	F	G	F	F
F	F	F	F	F	F	F	F	F	F	F	F	F	F	F	F	F
F	F	F	G	F	F	F	F	F	F	F	F	F	G	F	F	F
F	F	F	F	F	G	F	F	G	F	F	G	F	F	F	F	F
F	F	F	F	F	F	F	F	F	F	F	F	F	F	F	F	F
F	F	F	F	F	F	F	F	F	F	F	F	F	F	F	F	F

(F = Fuel, G = Guide Tube, I = Instrumentation Tube)

4 Storage Rack Description

4.1 *New Fuel Storage Area*

The New Fuel Storage Area (NFSA) racks are designed with two 16x2, one 16x3, and one 7x2 storage cell rack modules. Within each rack module, the pitch is the same in both directions. The spacing between the rack modules is larger than the normal cell pitch and is described in Table 4-1. There are no neutron absorbers installed in the racks. The dimensions of the NFSA racks modules are shown below in Table 4-1 and the rack positions are given in Table 4-2. Figure 4-1 and 4-2 gives an overview of the area.

Table 4-1: New Fuel Storage Area Rack Dimensions

Measurement Description	Dimension (cm)
Cell I.D.	22.86 ± 0.10
Cell Wall Thickness	0.3175 ± 0.025
Cell Pitch	53.340 ± 1.27
Cell Tube Material	Stainless Steel
SS Tube Height	420
Distance from NFSA floor to bottom of active fuel	8.593 ± 0.16
Concrete Thickness	30.48 or 91.44 ± 15.24

Table 4-2: New Fuel Storage Area Rack Positions

Location	x-coordinate* (cm)	y-coordinate* (cm)	z-coordinate* (cm)
Bottom Southwest Inside Corner of NFSA	0	0	0
Bottom Left Corner of North 16x2 Group	54.61	316.23	0
Bottom Left Corner of 16x3 Group	54.61	133.35	0
Bottom Left Corner of South 16x2 Group	54.61	3.81	0
Bottom Left Corner of 7x2 Group	427.99	483.87	0
NW Void (adjacent to 7x2 Group)	0 -> 389.89	495.3 -> 594.36	0 → 421.96

*All positions are relative to the bottom southwest corner of the NFSA (using the called North in Figure 4-1)

Figure 4-1: Surry Power Station New Fuel Storage Area (Radial View)

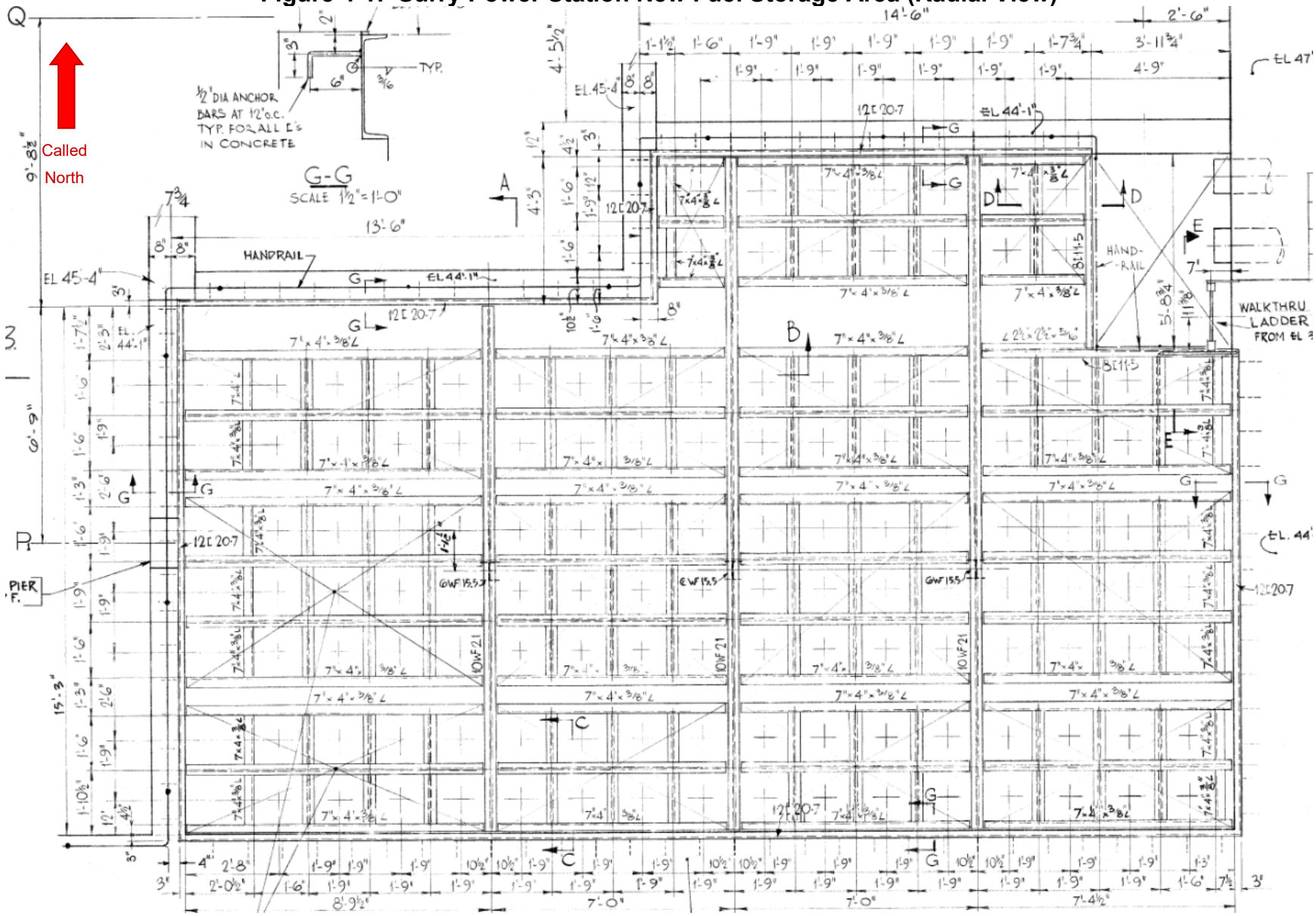

Figure 4-2: Surry Power Station New Fuel Storage Area (Axial View)

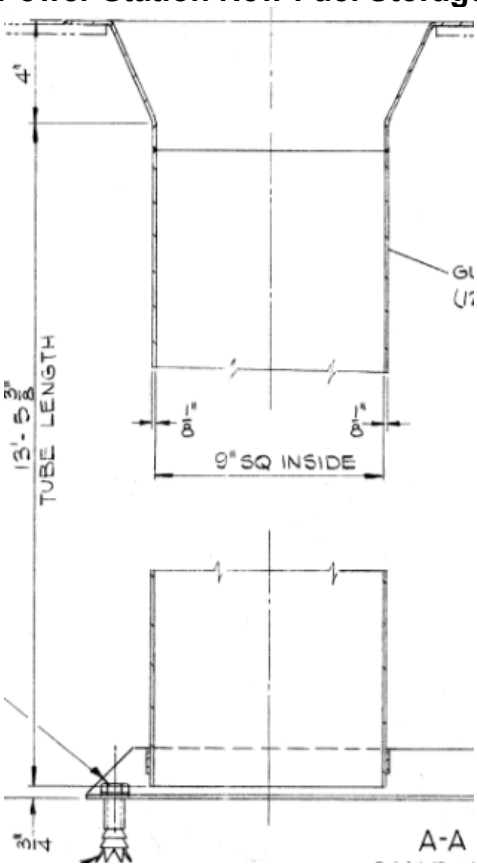

4.2 *Spent Fuel Pool*

There is only one rack design in the Surry SFP split into two regions designated Region 1 and Region 2. In total, there are twenty-nine 6x6 rack modules (nine in Region 1 and twenty in Region 2) for a total of 1044 rack cells. Region 1 includes the first three rows of fuel rack modules adjacent to the Cask Loading Area (324 storage locations) and Region 2 contains the remainder of the fuel rack cells in the fuel pool. Region 1 racks are susceptible to damage from a cask drop accident while Region 2 is not. Figure 4-3 shows the location of each Region in the SFP.

Figure 4-3: Surry SFP Rack Orientation

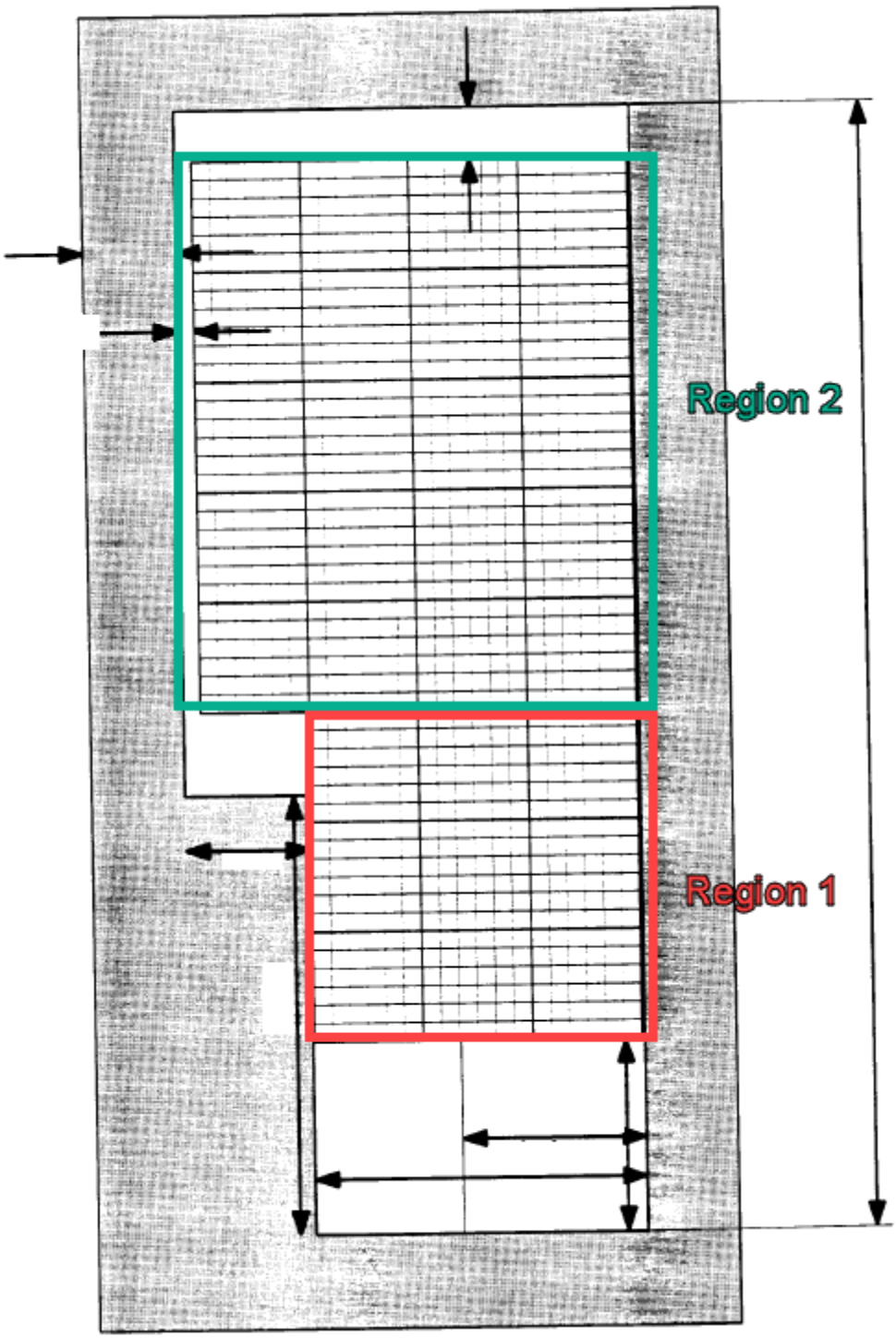

All the racks in the Surry pool consists of a 6x6 square array of stainless steel boxes with a nominal pitch of 14 inches. Each cell consists of a square stainless-steel tube. The cell pitch is the same in both X and Y directions. The rack modules are restrained to the SFP floor and cannot slide during any design-basis seismic event. Figure 4-4 shows a radial view of the rack while Figure 4-5 shows an axial view. Table 4-3 shows relevant dimensions.

Table 4-3: Surry Power Station Spent Fuel Racks

Parameter	Value
Assembly pitch (cm)	35.5600 $\pm$ 0.3175
SS Tube I.D. (cm)	22.70125 $\pm$ 0.15875
SS Tube Thickness (cm)	0.22860 $\pm$ 0.02286
Height of the Whole Rack (cm)	438.785
Rack Cell Floor Thickness (cm)	0.635
Rack Footer Height (cm)	15.24
SFP Floor Liner (cm)	0.635
Rack Proximity to the Wall (cm)	10.795
Concrete Floor Thickness (cm)	30.48
Rack Structural Material	Type 304 Stainless Steel

Figure 4-4: Surry Power Station Spent Fuel Racks (Radial View)

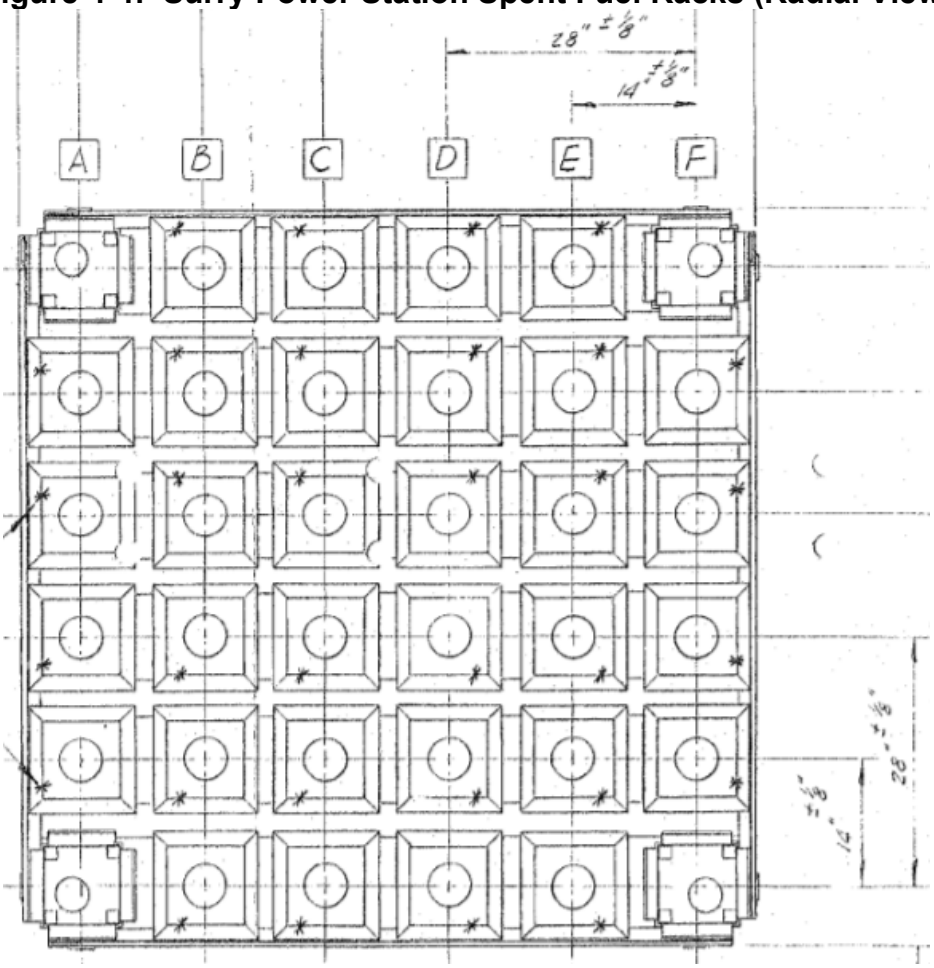

Figure 4-5: Surry Power Station Spent Fuel Racks (Axial View)

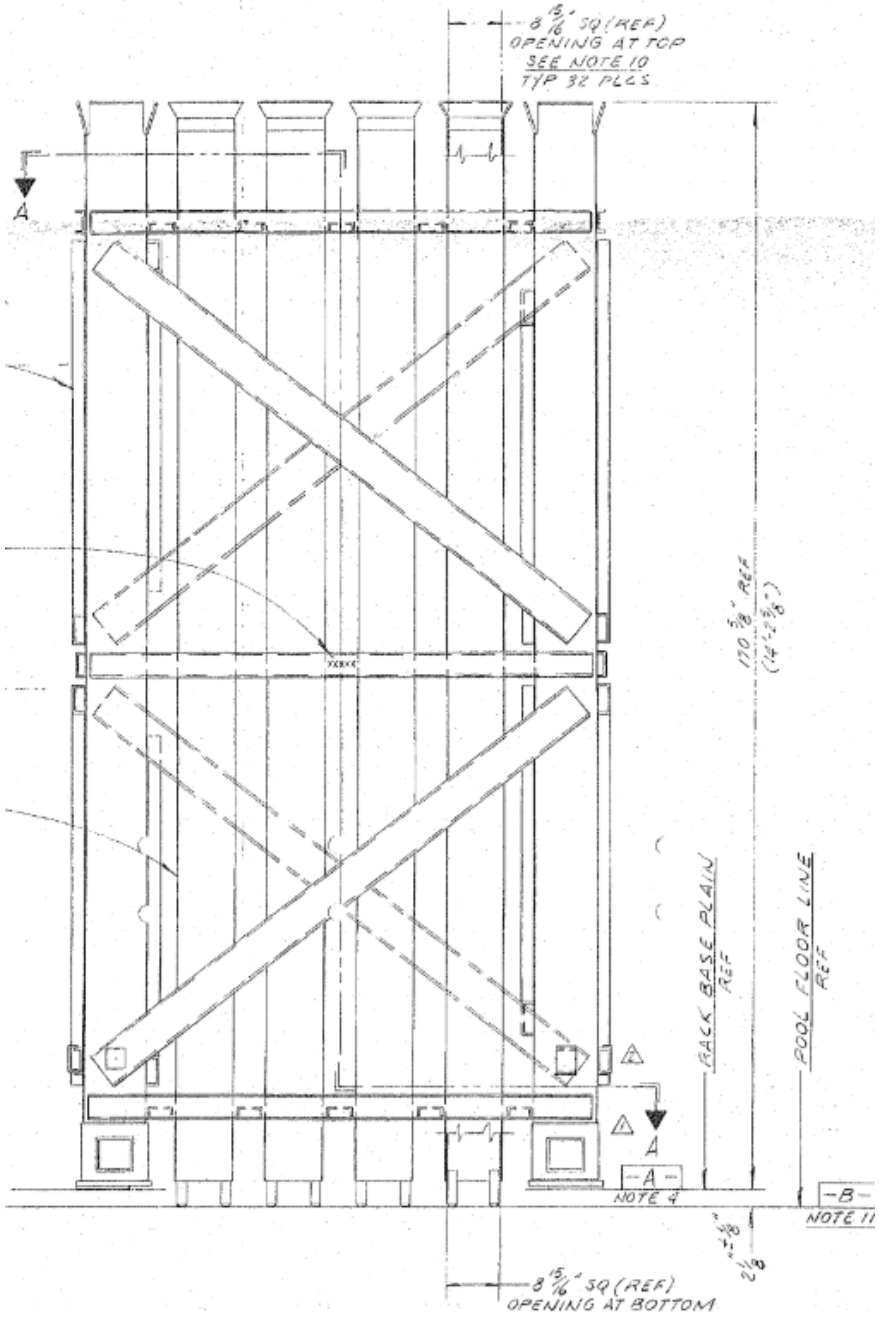

5 Overview of the Method of Analysis

5.1 *New Fuel Storage Area*

The criticality analysis of the New Fuel Storage Area (NFSA) is performed assuming two accident conditions, fully flooded with water and fully flooded with low density water (optimum moderation). Two different loading strategies for meeting the regulatory limits are proposed herein: requiring enrichments less than 4.35 wt% or requiring a minimum number of empty cells.

Table 5-1: Storage Requirements

Enrichment (wt%)	Fuel Loading Geometry Restriction
≤ 4.35%	None
≤ 5.00%	3 out of 4 See Figure 13-3

When modeling the NFSA with a minimum number of empty spaces, one out of every 2x2 storage cell matrix is an empty cell with the remaining three cells containing 5.0 wt%, un-poisoned fuel. Note that the extra space between rack modules cannot be credited as an empty cell.

The analysis considers both centered and asymmetric placement of the assemblies in the storage cells. The analysis models the full NFSA with boundaries extended sufficiently to justify use of zero flux boundary conditions. A range of moderator temperatures from 32°F to 105°F is used to cover the maximum range of temperature allowed in the Fuel Building. The concrete composition, which is important to the optimum moderation cases, is conservatively determined.

A single composite fuel design is created from the range of historical fuel design features to bound new fuel storage reactivity for current and anticipated future fuel designs.

Reduced enrichment and annular pellet axial blankets are not modeled. Using higher than actual enrichment in the blanket region is conservative. The stack fuel density (combination of UO_2 density, dishing, and chamfering) in the model conservatively bounds the highest expected stack density for Surry. New fuel is conservatively assumed to have no U-234 or U-236. To cover the variation in zirconium alloys, pure zirconium is used in the analysis since the alloying elements reduce reactivity.

The analysis uses SCALE 6.2.3 and the ENDF/B-VII cross section library [7]. Criticality calculations are done with the CSAS5 module (KENO-V.a) [8].

Determination of the 95% probability, 95% confidence (95/95) k-eff includes uncertainties for manufacturing tolerances of both the fuel and rack calculated at both the full and optimum moderation conditions.

5.2 *Spent Fuel Storage Racks*

5.2.1 Storage Requirements

Regions 1 and 2 do not require any empty cells, therefore there are no geometry restrictions. Additionally, Regions 1 and 2 do not credit any burnable absorbers, inserts, nor decay time. However, Region 1 does require a minimum amount of burnup (calculated as a function of initial U-235 enrichment). Table 5-2 shows these storage requirements

Table 5-2: Storage Restrictions

Region	Enrichment Restriction	Burnup Restriction
2	≤ 5.00 wt% U-235	None
1	≤ 5.00 wt% U-235	Burnup Curve See Figure 9-15

5.2.2 Bounding Fuel Design

A single composite fuel design is created from the range of historical fuel design features to bound SFP reactivity for historical and anticipated future fuel designs. Seven fuel designs have been used at Surry. Other than small changes in axial fuel stack position, these are the features that vary among these designs:

- Guide tube / instrument tube diameter (all similar)
- Clad alloy (all are Zr based)
- Grid material (Old designs used Inconel while modern designs all used Zr alloys)
- Grid volume (variation in grid size and number of grids)
- Fuel loading (combination of density, dish, and chamfer)
- Burnable Poison Types (Multiple forms of discrete and integral burnable poisons)

Inconel grids are stronger neutron absorbers than zirconium grids. Additionally, they were mainly used in old fuel with less limiting depletion conditions. Therefore, they do not need to be considered for the SFP rack model because it is conservative to ignore the extra neutron absorptions and less limiting depletion conditions. Clad alloys and grid materials are represented in the KENO rack model as pure zirconium, since the alloying materials are small quantities and are stronger neutron absorbers than zirconium.

Grid volume is maximized in TRITON depletions (a harder neutron spectrum produces higher reactivity depleted fuel isotopic content) and minimized in the SFP rack models.

Sensitivity cases were run to decide whether to maximize the cladding material in the fuel pin cladding, guide tubes, and instrument tubes since they have a competing effect during depletion and in the SFP (Section 8.13). The test cases show that increased moderation (less cladding material) in the SFP has a larger positive reactivity effect than the harder neutron spectrum effect (more cladding material) during depletion. Therefore, it is conservative to use the minimum clad, guide tube, and instrument tube parameters.

The test cases in Section 8.13 were run in unborated SFP conditions. However, it is still acceptable to use minimum clad parameters for borated cases because the limiting borated condition is the cask drop accident scenario which models optimum pin pitch and stacks of pellets at optimum pitch. The optimum pitch would adjust to compensate for different amounts of cladding.

Higher fuel density increases k-eff (verified in rack model tolerance cases), so a bounding high value is used. Reduced enrichment and annular pellet axial blankets are not modeled nor credited.

TRITON depletions are performed using a bounding burnable poison loading of 20 fingers of Alumina B_4C, bounding high fuel density, bounding high power and temperatures, and instrument thimble water displacement by an incore detector thimble. Nominal fuel assembly dimensions are used in the TRITON depletions. Clad creep and grid expansion with depletion are neglected in the depletion because both increase the amount of water in the fuel lattice, soften the neutron spectrum during depletion, reduce Pu production, and reduce depleted fuel reactivity in the SFP.

Clad creep and grid expansion effects are not included as a bias in the SFP k-eff calculations. This is because burnup is only required during the cask drop accident which results in deforming the racks and grids until optimal pitch. Optimal pitch occurs with decreased fuel rod pitch due to borated water conditions. Therefore, a grid expansion bias is not applicable.

5.2.3 Soluble Boron Credit

The spent fuel storage rack analysis for Regions 1 and 2 credits soluble boron. To support the use of boron credit, a boron dilution analysis is provided in an attachment to this submittal that initiates at the Technical Specifications minimum allowable soluble boron concentration of 2300 ppm. The boron dilution analysis confirms that the time needed for a dilution event to reduce the soluble boron concentration to the minimum acceptable boron level of 400 ppm (a level at which the criticality analysis normal operation k-eff remains less than 0.95) is greater than the time needed for actions to be taken to prevent further dilution. The boron dilution accident analysis confirms that operators have sufficient time to identify, diagnose and correct the cause of the inadvertent dilution, thereby preventing SFP k-eff from exceeding the regulatory limit.

5.2.4 Burnup Credit

Fuel burnup is credited in Region 1. To conservatively calculate the isotopic content of depleted fuel, these depletion variables are considered:

- Fuel and moderator temperature (density)

- Power history
- Axial burnup profile
- Radial burnup tilt
- Soluble boron history
- Burnable absorber
- Control rod insertion
- Fuel inserts

Bounding axial node depletion temperatures are determined in part by selecting a bounding high fuel assembly average power. The assembly average power selected bounds the power history (average lifetime depletion power) experienced by Surry fuel at each analyzed assembly average burnup. High assembly power results in high fuel and moderator temperatures, which hardens the neutron spectrum, increases Pu production, and increases fuel reactivity in the SFP.

Axial burnup profiles from DOE database reviewed in NUREG/CR-6801 [9] are used within their respective burnup ranges. With fuel assembly power and the axial burnup profile known, the nodal moderator temperature is determined for each of the 18 axial nodes starting from the core inlet and integrating the enthalpy added in each successive node. Data used for the axial heat balance calculation includes bounding high core power, Core Operating Limits Report (COLR) minimum Reactor Coolant System (RCS) coolant flow, conservatively high core bypass flow, and COLR Hot Full Power (HFP) RCS average temperature limit. These heat balance input values result in the TRITON depletions using bounding core average RCS outlet temperatures 2.0 °F higher than any Surry historical cycle.

Due to the margin to prior cycle RCS exit temperatures and the bounding nature of the inputs, it is unlikely that a future cycle would operate with moderator temperatures in an actual fuel assembly higher than the analyzed bounding assembly.

Fuel temperatures are determined for each node by adding to the nodal moderator temperature a value for fuel temperature increase above local moderator temperature. The fuel temperature increase value is a function of fuel burnup and nodal power. Fuel temperature data is from the SIMULATE5 model used by Dominion for its licensed fuel management analysis. [10] Fuel temperatures are pellet average and uniform for all fuel rods across the assembly plane (with the exception of the planar burnup tilt bias in Sections 8.11 and 9.1.8).

Bounding high power history is selected to maximize fuel and moderator temperature during depletion. However, depleting at low power produces less Pm-149, which has the effect of reducing Sm-149 peaking after fuel discharge, increasing fuel reactivity in the SFP. High power history combined with reduced power near end of life (EOL) is used to capture both effects.

Depletion is performed at constant high power conditions for all but the last 20 days of depletion. Depletion for 20 days at half the bounding power is performed at EOL instead of 10 days of depletion at the bounding power. Depletion of 20 days at half power bounds all actual operations because typical power coastdowns only last ~10 - 15 days and only coastdown to ~85% power. Bounding high power level fuel and moderator temperatures are retained throughout the depletion for simplicity and conservatism.

High depletion soluble boron hardens the neutron spectrum, increases Pu production, and increases fuel reactivity in the SFP. A constant soluble boron that bounds the cycle average boron for all historical cycles (with 1 assembly being an exception and justified in Section 9.3.1) and expected future cycle average boron is used in the TRITON depletions.

Depleted fuel content is determined for each of the 18 axial fuel nodes of a fuel assembly with independent TRITON depletions. All isotopes produced during depletion are used in the SFP rack k-eff calculations. With no credit for fuel decay time, isotopic content decayed for 100 hours after the at-power fuel depletion maximizes fuel reactivity. Consistent with the depletion code benchmarking analysis, isotopic changes due to decay time are calculated with ORIGAMI calculations. There is a post-TRITON and ORIGAMI reduction applied to some fission gases and volatile elements to account for the possibility of migration of these isotopes away from where they were produced.

Determination of bounding assembly depletion conditions includes consideration of neutron absorbers and fuel assembly inserts that displace water. Neutron spectrum hardening by absorbers and inserts increases Pu production during depletion and fuel reactivity in the SFP. Some inserts (discrete BP, control rods, source rods, etc) are mutually exclusive because they occupy guide tubes. The following absorbers and water displacers are evaluated:

- Borosilicate Glass discrete BP (used in cycles 1 - 10)
- Alumina B_4C discrete BP (used in cycles 11 – 21)
- IFBA integral BP (used in cycles 21 – 30 and is still currently being used)
- Gadolinia integral BP (currently being used in LTAs for cycles 29 – 30)
- Primary and secondary sources
- In-core detector thimble
- Control rod insertion (≤ 12 steps cycle average insertion)

Depletion analysis assumes all fuel assemblies are depleted with 20 Alumina B_4C rods and an in-core thimble inserted. Alumina B_4C is depleted with the fuel and is retained throughout the entire depletion. This modeling approach conservatively bounds the actual depletion history of all Surry fuel assemblies to date. In particular, discrete BP is removed after one cycle, only about a third

of the core has in-core thimbles, IFBA has annular pellets at the fuel's top and bottom which are not modeled, and the manufacturer recommends enrichment reductions for gadolinia rods which is not credited.

The analysis shows that Gadolinia reduces the depleted fuel's SFP k-eff compared to all other BP cases and a case without any BP (description of this model is in Section 8.7) which aligns with the studies cited in Section 4.2.1 of NEI 12-16 [6, 32]. The analysis also evaluates some IFBA and Alumina B_4C combinations and confirms which combinations are bounded by depletion with 20 Alumina B_4C. Depletion with maximum IFBA / maximum source rods is demonstrated to be bounded by depletion with 20 Alumina B_4C.

A bias is calculated to account for maximum horizontal burnup tilts (also referred to as radial burnup tilts) when burnup is credited (Region 1).

5.2.5 Other Credit

The cask drop accident is described in Section 5.2.7. The accident is modeled as a block of 324 cells with reduced assembly and fuel rod pitches. The block of 324 assemblies is deformed up against a mirror boundary which effectively means the model is calculating a block of 648 assemblies. Since this is not an infinite sea of assemblies, some amount of neutron leakage could be considered credited. However, 648 assemblies of the same reactivity at optimum pitch is large enough so that the amount of neutrons leaking out is small.

No other credit is taken (e.g. control rod credit, BP loading credit, decay credit, and crediting empty cells).

5.2.6 Neutron Absorbers

No neutron absorbers are installed in the Surry spent fuel pool. [5]

5.2.7 Accident Analysis

The cask drop accident is the most limiting accident scenario by a significant margin. This accident scenario simulates dropping a dry storage cask being handled in the spent fuel pool which then tips over and impacts the adjacent spent fuel pool racks. Note that a cask drop accident is credible at Surry because there is no structural barrier between the cask loading area and the spent fuel racks. The first two rows of rack modules are susceptible to be damaged by this event, but three rows will be assumed for conservatism and for continuity with the current criticality safety analysis. This accident is modeled in a bounding and conservative manner:

1. The rack cells and assemblies for all 324 Region 1 locations are deformed by reducing their respective pitches until optimum moderation occurs.
2. Stacks of fuel pellets are modeled below and between rack cells at optimum pitch to bound the scenario of fuel assembly damage.
3. All material mass is conserved in the model. For example, the rack cell wall thickness increases when the diameter decreases to conserve its mass.
4. The model is surrounded by the borated water on three sides and a mirror boundary on the fourth.

For a postulated boron dilution event, all storage racks are filled with fresh 5.0 wt% fuel assemblies with nominal pitch and the spent fuel pool soluble boron concentration is diluted to 350 ppm. It is shown that the 95/95 k-eff is significantly less than 0.95.

A multiple misload accident is not analyzed because no burnup credit is needed in the spent fuel pool for normally spaced rack cells (burnup is only needed for the cask drop accident). Therefore, the only difference between a multiple misload accident and the boron dilution accident is that the multiple misload accident can credit more soluble boron.

An assembly misplacement and drop are analyzed and are considerably less limiting than the cask drop accident. The assembly misplacement is modeled to occur outside the racks in a corner between two racks. Misplacement of an assembly inside a rack cell is non consequential because no empty cells are required and burnup is only required when the racks are damaged. An assembly drop which damages the assembly's grids is modeled by placing a fresh assembly with optimum pin pitch, surrounded by fresh assemblies with nominal pin pitch, all placed in rack cells with nominal rack pitch, and in a borated SFP.

Normal operation SFP temperatures (including the associated water density change) are included as part of the normal operation rack k-eff calculations. Analysis of loss of cooling moderator temperatures (up to and including boiling) shows that in an over-temperature accident the 95/95 k-eff is much less than 0.95.

5.2.8 Normal Operations

Analysis is performed for all normal operating conditions including movement, inspection, and reconstitution. All fuel bearing containers in the SFP are identified and analyzed to determine the limitations on location in the pool.

6 Cross Sections, Computer Codes, and Validation

6.1 *Cross Sections and Computer Codes*

This analysis uses the CSAS5 [8] module of SCALE 6.2.3 [7] to calculate SFP k-eff. Depleted fuel isotopic content is calculated using the SCALE 6.2.3 t5-depl TRITON [11] module which uses KENO-V.a for the flux calculations needed to collapse neutron cross sections spatially and in energy for the depletion. The ORIGAMI module of SCALE 6.2.3 [33] was used to decay the fuel isotopics calculated from TRITON. All analyses are performed using the 238 group ENDF/B-VII cross section library (v7-238).

Code validation for these three modules of SCALE 6.2.3 is performed in accordance with the DSS-ISG-2010 [4], NUREG/CRs 6698 [12] and 7109 [13], EPRI 3002010613 [35], and EPRI 3002016888 [36].

6.1.1 CSAS5

The CSAS5 module uses BONAMI to provide resonance corrected cross sections in the unresolved resonance range and WORKER, CENTRM, and PMC to provide resonance-corrected cross sections in the resolved resonance range. This is followed by KENO V.a which uses the processed cross sections to calculate the k-eff of three dimensional system models. All of the SFP CSAS5 computer runs use a Monte Carlo sampling of at least 9000 generations, 12000 neutrons per generation, and 500 generations skipped to achieve a converged statistical uncertainty in k-eff of less than 0.0001. Convergence was confirmed using a two sample student t test comparing the means of the first half of generations vs. the 2nd half of generations after accounting for generations skipped. If the means are not statistically unequal (null hypothesis of equal means not rejected), then this convergence test is passed. Cases which failed this screening were rerun with additional generations and/or generations skipped. Note that the code options and inputs for the SFP cases in this CSA are consistent with the validation cases.

Unless otherwise specified, all of the k-eff values reported in this document are raw calculated k-eff values with no adjustment for bias and uncertainty. The final values to be compared to the criticality criteria are the calculated values plus the total bias and uncertainty.

A uniform initial source distribution in fissile material was used for the k-eff calculations (the default option in CSAS5).

For some sensitivity cases, convergence was ensured by ensuring that the midpoint k-eff (accounting for generations skipped) is within 2 final problem standard deviations from the final problem k-eff. Cases which failed this screening were rerun with additional generations and/or generations skipped until it passed.

6.1.2 Isotopes Used

New fuel is conservatively assumed to have no U-234 or U-236. The Triton runs used parameter option 'addnux=3' which instructs Triton to follow 233 isotopes during the depletion. These isotopes are listed in Table 6-1. Note that the SCALE manual says that 'addnux=3' forces TRITON to follow 231 isotopes [7]. But inspection of the composition files show that the code follows O-17 and O-18 which are not listed in the user manual. All isotopes retained by TRITON (concentrations > 1×10^{-20}) were retained through ORIGAMI and KENO.

Table 6-1: Isotopes Used in the Criticality Analysis

Ag-107	Ag-109	Ag-111	Am-241	Am-242	Am-242m	Am-243	As-75	Au-197	B-10
B-11	Ba-134	Ba-135	Ba-136	Ba-137	Ba-138	Ba-140	Br-79	Br-81	Cd-106
Cd-108	Cd-110	Cd-111	Cd-112	Cd-113	Cd-114	Cd-115m	Cd-116	Ce-140	Ce-141
Ce-142	Ce-143	Ce-144	Cm-242	Cm-243	Cm-244	Cs-133	Cs-134	Cs-135	Cs-136
Cs-137	Dy-160	Dy-161	Dy-162	Dy-163	Dy-164	Er-166	Er-167	Eu-151	Eu-152
Eu-153	Eu-154	Eu-155	Eu-156	Eu-157	Gd-152	Gd-154	Gd-155	Gd-156	Gd-157
Gd-158	Gd-160	Ge-72	Ge-73	Ge-74	Ge-76	H-1	Ho-165	I-127	I-129
I-130	I-131	I-135	In-113	In-115	Kr-80	Kr-82	Kr-83	Kr-84	Kr-85
Kr-86	La-139	La-140	Lu-175	Lu-176	Mo-100	Mo-92	Mo-94	Mo-95	Mo-96
Mo-97	Mo-98	Mo-99	N-14	Nb-93	Nb-94	Nb-95	Nd-142	Nd-143	Nd-144
Nd-145	Nd-146	Nd-147	Nd-148	Nd-150	Np-237	O-16	O-17	O-18	Pa-231
Pa-233	Pd-102	Pd-104	Pd-105	Pd-106	Pd-107	Pd-108	Pd-110	Pm-147	Pm-148
Pm-149	Pm-151	Pr-141	Pr-142	Pr-143	Pu-238	Pu-239	Pu-240	Pu-241	Pu-242
Rb-85	Rb-86	Rb-87	Re-185	Re-187	Rh-103	Rh-105	Ru-100	Ru-101	Ru-102
Ru-103	Ru-104	Ru-105	Ru-106	Ru-96	Ru-98	Ru-99	Sb-121	Sb-123	Sb-124
Sb-125	Sb-126	Se-76	Se-77	Se-78	Se-80	Se-82	Sm-144	Sm-147	Sm-148
Sm-149	Sm-150	Sm-151	Sm-152	Sm-153	Sm-154	Sn-112	Sn-114	Sn-115	Sn-116
Sn-117	Sn-118	Sn-119	Sn-120	Sn-122	Sn-123	Sn-124	Sn-125	Sn-126	Sr-84
Sr-86	Sr-87	Sr-88	Sr-89	Sr-90	Ta-181	Tb-159	Tb-160	Tc-99	Te-120
Te-122	Te-123	Te-124	Te-125	Te-126	Te-127m	Te-128	Te-129m	Te-130	Te-132
Th-230	Th-232	U-232	U-233	U-234	U-235	U-236	U-238	W-182	W-183
W-184	W-186	Xe-124	Xe-126	Xe-128	Xe-129	Xe-130	Xe-131	Xe-132	Xe-133
Xe-134	Xe-135	Xe-136	Y-89	Y-90	Y-91	Zr-90	Zr-91	Zr-92	Zr-93
Zr-94	Zr-95	Zr-96							

The isotopic atom densities used come directly from the initial fuel content or the depletion analysis, except for an adjustment for gaseous or volatile fission products (hereafter called fission gases). Table 6-2 lists the fission gases used in the criticality analysis. The treatment of the fission gases for this criticality analysis is the same as was done for a recently approved Millstone Unit 3 criticality analysis [14] and the key elements of the position are repeated here.

Table 6-2: Fission Product Gases and Volatiles

Noble Gases	^{80}Kr, ^{82}Kr, ^{83}Kr, ^{84}Kr, ^{85}Kr, ^{86}Kr ^{126}Xe, ^{128}Xe, ^{129}Xe, ^{130}Xe, **^{131}Xe**, ^{132}Xe, ^{133}Xe, ^{134}Xe, ^{135}Xe, ^{136}Xe
Alkali Metals	^{85}Rb, ^{86}Rb, ^{87}Rb **^{133}Cs,** ^{134}Cs, ^{135}Cs, ^{136}Cs, ^{137}Cs
Halogens	^{79}Br, ^{81}Br ^{127}I, ^{129}I, ^{130}I, ^{131}I, ^{135}I

Most of the fission gases remain in the active fuel near where they were created. The mobility of fission gases is important in assessing the consequences of reactor accidents. Regulatory Guide 1.183 provides conservative release fractions for fission gases. [15]

According to RG 1.240, it is expected that RG 1.183 will be updated to reflect higher linear powers than were used in developing the current limits. PNNL-18212 Rev. 1, "Update of Gap Release Fractions for Non-LOCA Events Utilizing the Revised ANS 5.4 Standard," which was completed in June 2011, provides a new analysis. [16].

In Appendix C of PNNL-18212, Rev. 1 [16], plant specific release fractions are calculated based off a given power history. These release fractions are listed in Table 6-3. The assembly power history used in the Appendix C calculations (shown on page C.5 of PNNL-18212, Rev. 1) is ~9.7 kW/ft for the 1st cycle, ~6.8 kW/ft for the 2nd cycle, and ~4.8 kW/ft for the 3rd cycle. This power history is very similar to actual operations at Surry. The average power history at Surry is 6.7 kW/ft. The bounding relative power multiplier, calculated in Section 8.2, means that the bounding linear power history for Surry will be approximately equal to the power history in PNNL-18212, Rev. 1, App. C. For conservatism, the release fractions used in this analysis are significantly increased. The release fraction used in this analysis are shown in Table 6-3 which are generous compared to Appendix C of PNNL-18212 and is more bounding than the current RG (note that I-131 is low worth). Note that these are the same release fractions used in the recent North Anna [23] and Millstone Unit 3 [14] criticality safety analysis (CSA).

Table 6-3: Fission Gas Release Fractions

Isotopes	Current RG 1.183	Bounding Proposed in PNNL-18212	Appendix C of PNNL-18212	Implemented in MPS3 Criticality Analysis
K-85	0.10	0.38	0.13	0.20
I-131	0.08	0.08	0.02	0.05
Other Nobles Gases	0.05	0.08	0.02	0.05
Other Halogens	0.05	0.05	0.01	0.05
Alkali Metals	0.12	0.50	0.16	0.20

The release rates for PNNL-18212 assume cladding breach. For the criticality analysis the concern is for the fission products moving into the plenum and therefore no longer acting as effective absorbers. The boiling point of Cesium (951 K) is much higher than the clad temperature during normal fuel use (boiling point of water at 2250 psia is 618 K). It is unlikely that a significant amount of Cesium can migrate away from the fuel due to the clad acting as a condensing surface. This contention is supported by two observations. It is common to use Cs-137 as a measure of burnup. The agreement between Cs-137 and Nd-148 as a burnup measurement for chemical assays has been generally good [17-21]. Also, the BNFL burnup measurement device which is based on Cs-137 has agreed well with the reactor record burnup. [22] For this analysis it is assumed that 20% of the Cs-133 is lost, and Cs-133 is about a third of the worth of the fission gases. Therefore, the fission gas loss assumptions are considered conservative.

6.1.3 TRITON

The t5-depl sequence of SCALE's TRITON [11] enables depletion calculations to be performed by coordinating iterative calls between cross-section processing codes (CENTRM and BONAMI), KENO-V.a, and the ORIGEN-S point-depletion code. A 2D KENO model of the fuel assembly in the core provides the flux distribution needed to collapse the cross sections spatially and in energy for the ORIGEN-S depletion calculations. All the fuel pins are treated as a single depletion material. TRITON parameter addnux=3 is selected to obtain a reasonably large number of depletion isotopes (Table 6-1). The depleted fuel content is taken directly from the TRITON's output files.

The flux solution for each TRITON depletion step uses a KENO calculation with input requesting 2000 generations, 2000 neutrons per generation (NPG), and 100 generations skipped. It is also important that the depletion time steps are short enough to assure convergence. For this analysis time steps of 10 and 40 days are used for the first two time steps. The other burn steps are 50 days except when approaching a restart point (generally every 10,000 MWD/MTU) or approaching the target final burnup.

Case 1 of the depletion benchmarks was rerun with the number of generations, neutrons per generation, and generations skipped shown below. This resulted in an additional 72 test cases being run to ensure convergence (case 1 * 6 burnup steps * 4 decay steps * 3 neutron history combinations):

- Standard convergence (2000 generations, 2000 NPG, 100 skipped)
- More neutron histories (4500 generations, 6000 NPG, 500 skipped)
- More neutron histories (9000 generations, 12000 NPG, 1000 skipped)
- Twice as many depletion steps (2000 generations, 2000 NPG, 100 skipped)

The 72 test cases were compared to the standard convergence results. Sensitivity case differences ranged from -70 pcm to 10 pcm, but the standard deviation of the differences is one to two standard deviations. Also, the reported results are consistently high compared with the sensitivity results. Higher case kinf values are conservative (depletion has a lesser effect on k).

Based on the sensitivity results, the parameters used for the reported results are adequate for convergence of the depletion runs. In addition, note that any bias due to fewer generations will be represented in the depletion bias value from the depletion benchmarking analysis.

6.1.4 ORIGAMI

ORIGAMI computes detailed isotopic compositions for light water reactor assemblies containing UO2 fuel by using the ORIGEN transmutation code with pre-generated ORIGEN libraries, for a specified assembly power distribution [33]. This CSA used ORIGAMI to decay the fuel.

Inputs into the ORIGAMI run includes an ORIGEN library, fuel temperature, fuel density, .f71 file from TRITON, and decay times. The vast majority of cases in this CSA (other than the cases used in the depletion benchmarking analysis) used a fuel temperature of 170°F, a fuel density of 10.4668 g/cc, and a decay time of 100 hours.

6.2 *Uncertainty and Bias in Depleted Fuel Isotopic Content*

The Surry burnup credit analysis was calculated in accordance with the guidance given in Appendix A of NEI 12-16 [32]. The approach of validation using the measured flux data from PWR reactors was used. This method is further detailed in the Benchmarks EPRI Report [35] and the EPRI Utilization Report [36].

The method includes a calculated depletion Application-Specific Bias. This bias was calculated by first running the depletion benchmark cases using this analysis' code system described in Section 6.1 herein. The calculated reactivity decrement was then compared to the measured reactivity decrement in the EPRI Utilization Report [36]. The bias is then determined by summing the maximum measured-to-predicted difference for each perturbation off of case 3 as described in the EPRI Utilization Report RAI 8 and echoed in the SER [37]. See Table 6-4 for a summary of the Application-Specific Bias. This bias is not a function of burnup but is a function of decay time. See Section 9.1.11 and Appendix B herein for more details on this calculation.

In addition to the Application-Specific Bias, an additional bias and uncertainty term was used. Table 6-5 lists these values which were taken straight from the SER [37] and are not calculated by the Licensee. This term is a function of burnup but not decay time. As discussed in the SER, linear interpolation between burnup points is acceptable [37].

The worth of the EPRI Benchmarks and Utilization method was directly compared to the worth of the historical Kopp 5% uncertainty method. The maximum k-eff of the Region 1 cask drop analysis (Section 9.1) was calculated by using the EPRI bias and uncertainty method and by using the Kopp 5% uncertainty method. The results are shown in Table 6-6. For this application, the

reactivity worth produced by the EPRI method is significantly larger than the Kopp 5% method for low burnups and very slightly smaller than the Kopp 5% at the largest burnups. This relative change in magnitude between the two methods occurs because the Application-Specific Bias is calculated as an absolute reactivity difference, as opposed to a depletion worth percentage, and because it is not a function of burnup. This comparison shows that the EPRI method and the calculations in Appendix B resulted in a synonymous reactivity effect as the Kopp method for the burnup ranges of most importance (most spent fuel assemblies have burnups >30 GWD/MTU).

Table 6-4: Application-Specific Calculated Bias

Condition	Decay Time		
	< 100 hours	< 5 years	< 15 years
Base Case	0.0010	0.0040	0.0041
Rod OD < 0.95 cm	--	--	--
< 4.25% Enrichment	0.0017	0.0015	0.0017
> 4.25% Enrichment	--	--	--
Burnable Absorber	--	--	--
> 900 ppm Depletion	--	--	--
Rack T > 293 K	--	--	--
Borated Rack	--	--	--
Power > 38.1 MW/MT	--	0.0002	0.0003
Conservative Bias	0.0028	0.0057	0.0061

Table 6-5: Depletion Code Additional Bias and Uncertainty

Burnup (GWd/MTU)	10	20	30	40	50	60
Additional Bias (% of Worth)	0.0%	0.0%	0.0%	0.15%	0.35%	0.54%
Uncertainty (% of Worth)	3.05%	2.66%	2.33%	2.12%	1.95%	1.81%

Table 6-6: Maximum k-eff with Kopp Uncertainty vs EPRI Benchmarks

Burnup (GWD/MTU)	0	10	20	30	40	47	53.00
Enrichment (U-235 wt%)	1.65%	2.20%	2.85%	3.45%	4.10%	4.55%	5.00%
Maximum k-eff							
Kopp Method	0.9093	0.9377	0.9284	0.9170	0.9156	0.9301	0.9384
EPRI Benchmarks Method	0.9093	0.9403	0.9299	0.9177	0.9155	0.9300	0.9383
Difference (EPRI – Kopp)	**0.0000**	**0.0026**	**0.0016**	**0.0007**	**-0.0001**	**-0.0001**	**-0.0002**

6.3 *Validation of Criticality Analysis*

Criticality computer codes and cross sections are validated for their ability to predict k-eff. The Surry criticality validation attempts to reasonably match the Surry racks for isotopic content, neutron energy spectrum and geometry.

Due to isotopic limitations in the critical experiments the validation is done in two steps. The first step is to use laboratory critical experiments to validate the structural materials and major actinides in a variety of geometries which produce a range of neutron spectra. The second step is to validate the minor actinides and fission products. Since there is little to no use of these latter isotopes in critical experiments, this validation is based on the uncertainty in the cross section measurement.

6.3.1 Major Actinides and Structural Materials

The validation for the major actinides and structural materials follows NUREG/CR-6698 [12]. Three hundred forty nine (349) critical experiments were selected from the OECD/NEA handbook [25] and the HTC critical experiments [26] that are relevant to the conditions of the Surry new fuel storage area and spent fuel pool. These experiments were analyzed with SCALE 6.2.3 using the 238-group ENDF/B-VII cross-section library. The resulting predicted k's were then fit for trends on the key parameters influencing k. Using these trends, the most limiting bias and uncertainty in the area of applicability was determined. Although some of the trends may not be statistically significant, it is conservative to use all of the trends in determining the limiting bias and uncertainty. The Surry spent fuel pool is covered by the area of applicability of the validation. Specifically,

1. Enrichment: The benchmarks selected range from 2.35 to 4.74 wt% U-235. The fuel in the spent fuel pool currently ranges from 1.85 to 4.25 wt% U-235 and the maximum enrichment will be extended to 5.0 wt% in herein. The bias decreases with enrichment and the slope is small allowing for a small extrapolation for higher enrichments.

2. Spectrum: The benchmarks cover a wide range of spectrum by varying the pin pitch. The Energy of the Average Lethargy causing Fission (EALF) of the benchmarks ranges from 0.0605 to 0.7137 eV. This covers the range of spectrum in borated and non-borated conditions in the spent fuel pool with normal spaced rack cells and the full moderated condition in the new fuel storage area. Some extrapolation is required for the optimum moderator condition in the new fuel storage area and for the crushed

racks of the cask accident analysis. This extrapolation follows the guidance in NUREG/CR-6698 [12] and is detailed in Appendix A.

3. Fuel Pin Pitch: The fresh fuel pin pitch of the benchmarks ranges from 1.08 to 2.54 cm while the MOX benchmarks range from 1.30 to 4.32 cm. The Surry fuel pin pitch is 1.43 cm.
4. Assembly Spacing: The benchmarks include spacing between assemblies of 0 to 15.4 cm of water. The separation between assemblies in normal spaced spent fuel pool racks is 12.4 cm and the separation approaches 0 cm during the cask drop accident. The NFSA has a separation of about 30 cm. The critical experiments cover the entire relevant range since neutron transport through >15.4 cm of full density water has small effect on k. If the water has decreased density, then the separation effectively decreases. The optimum density of water in the NFSA is less than 20%. At 20% water density the effective separation is 30*0.2= 6 cm which is well within the range of experimental data; therefore, the NFSA optimum moderation cases are covered.
5. Soluble Boron: The benchmarks have soluble boron concentrations up to 5030 ppm. The soluble boron credited to meet the k less than 0.95 and credited for the accident analysis is well within the range of experiments.

Details on the area of applicability can be found in Appendix A.

For the UO_2 and MOX critical experiments, the change in the k predicted for the critical experiments as a function of a parameter is performed for four different parameters: pin diameter, pin pitch, soluble boron content, and EALF. A fifth parameter was also trended: U-235 enrichment for the UO_2 set and Pu enrichment for the MOX set. Rather than eliminate any trend, the largest bias from any of the trends is selected. The largest bias was generally from the trend as a function of EALF. Table 6-7 provides the biases and uncertainties as a function of EALF.

For the spent fuel pool, the bias and uncertainty depends on the burnup since at low burnup the dominant fissile material is U-235 and at high burnup the dominant fissile material is Pu-239. In order to avoid trying to properly weight the critical experiments for the amount of U-235 and Pu-239, two sets of bias and uncertainty are employed: one from the fresh UO_2 critical experiments and one from the MOX critical experiments. The final bias and uncertainty employed for burned fuel is that which produces the highest 95/95 k. The UO_2 critical experiments have a higher bias but lower uncertainty than the MOX experiments. Since the uncertainty is statistically combined

with other uncertainties it is not possible to determine which set is more limiting until the other uncertainties due to factors such as manufacturing tolerances are determined. For the new fuel storage area or unburned fuel in the spent fuel pool, only the UO2 set from Table 6-7 is used.

Table 6-7: Validation Code Bias and Uncertainty

(For depleted fuel, calculate with both UO2 and MOX bias and uncertainty and use the set that provides the highest 95/95 k)

UO_2 / Fresh Fuel

EALF	Bias	Uncertainty
0.00 – 0.40 eV	0.0030	0.0040
0.40 – 0.80 eV	0.0040	0.0045
0.80 – 1.10 eV	0.0055	0.0050
1.10 – 1.25 eV	0.0060	0.0050
1.25 – 1.40 eV	0.0065	0.0055

MOX / Burned Fuel

EALF	Bias	Uncertainty
0.00 – 0.40 eV	0.0015	0.0060
0.40 – 0.80 eV	0.0025	0.0095
0.80 – 1.10 eV	0.0030	0.0120
1.10 – 1.25 eV	0.0035	0.0135
1.25 – 1.40 eV	0.0035	0.0145

6.3.2 Minor Actinides and Fission Products

The minor actinides are defined as actinides not contained in the criticality validation benchmarks. Table 6-1 lists all the isotopes used in the analysis. The major actinides are U-234, U-235, U-238, Pu-238, Pu-239, Pu-240, Pu-241, Pu-242, and Am-241. U-236 is not a major actinide although it has a significant worth in spent fuel. Am-241 is treated as a major actinide because it decays from Pu-241 and is included in the MOX critical experiments.

Since there are few to no critical experiments that contain some of the isotopes used in this criticality evaluation, validation is done by estimating the maximum error in k-eff due to cross section measurement uncertainty. NUREG-7109 [13] has shown that applying a bias of 1.5% of the worth of the minor actinides and fission products conservatively accounts for both the bias and uncertainty due to the minor actinides and fission products. NUREG-7109 mainly addresses the 28 highest worth isotopes but on the last sentence of page 106 it states, “An upper value of 1.5% of the worth is also applicable for SNF isotopic compositions consisting of all nuclides in the SFP configuration.” NUREG-7109 limits the applicability to certain cross section sets but ENDF/B-VII used here is one of those sets. Note that the use of the 1.5% bias is part of the NRC’s transport division in ISG-8 Rev.3. [27]

NEI 12-16 [32], the EPRI Benchmark Report [35], and the EPRI Utilization Report [36] do not discuss any additional code bias needed for minor actinides and fission products. The depletion code used in this analysis was benchmarked against depletion measurements in accordance with the method described in the EPRI Reports. Since the depletion code was compared to measurements, the calculated bias should include any bias for minor actinides and fission products. However, due to the complexity of the EPRI method and due to the regulatory uncertainty, a bias of 1.5% of the minor actinides and fission product worth is applied in the maximum k-eff calculation in this analysis.

6.3.3 Temperature Dependence

All of the critical experiments utilized in Section 6.3 were done at room temperature. There is one set of critical experiments which were run as a function of temperature in the range of interest for spent fuel pools. There are a couple of sets of experiments with temperatures greater than 200 C [29, 30] but LEU-COMP-THERM-046 [30] is ideal for determining a bias as a function of temperature in the range of interest. LEU-COMP-THERM-046 is not used in the set of

experiments from Section 6.3 since in general they are at elevated temperatures and as such represent a unique set. The analysis of this temperature dependent set is detailed in Appendix A.

The analysis of the only set of thermal critical experiments in the International Handbook that uses elevated temperatures has shown a small increase in the bias with temperature. This increase can be conservatively handled by a bias from room temperature (293K) of 1.0 pcm/ΔK.

Note that the EPRI Depletion Benchmarks [35] contains a hot to cold branch case that models depleted fuel in the SFP at 150°F. Therefore, it could be argued that the temperature bias for depleted fuel is wholly covered by the depletion code bias and uncertainty. However, to simplify the review process, the 1.0 pcm/Δk bias is applied to all burnups.

6.3.4 Absorbers Credited

No absorbers are credited in this analysis other than soluble boron. Note that several burnable absorbers are used and tested to determine the bounding loading during depletion. The absorber in these burnable poisons were boron or gadolinium. Gad and boron as non-soluble absorbers is adequately covered in the benchmark experiments.

7 Criticality Safety Analysis of the New Fuel Storage Area

7.1 *New Fuel Storage Area Overview and KENO Model*

The New Fuel Storage Area has two storage options to meet the k-eff limits stated in 10CFR50.68:

1) All fuel assemblies in the NFSA have initial U-235 enrichments ≤4.35 wt% (does not require empty cells).
2) All fuel assemblies in the NFSA have initial U-235 enrichments ≤5.00 wt% **AND** requires empty cells in the locations that are shown in Figure 7-3.

The description of the New Fuel Storage Area (NFSA) racks is given in Section 4.1. The SCALE CSAS5 (KENO) model for the NFSA is a three dimensional model of the entire rack including the concrete walls and floor. Tables 4-1 and 4-2 provides the dimensions and tolerances.

Figure 7-1 shows the KENO model with 4.35 wt% fuel in every cell and Figure 7-3 shows where empty cells are required for storage of assemblies up to 5.00 wt%.

Figure 7-1 shows a planar view of the NFSA KENO model. This may be compared to the actual rack drawing shown in Figure 4-1. Structural components are mostly omitted, and the area above the active fuel is simplified. Cell walls are assumed to be straight rather than flared out at the top. Except for the cell wall, the area above the active fuel is assumed to be water at the same density as throughout the rack. The top and bottom nozzles are also modeled as water. Figure 7-2 shows an axial representation of the KENO model. As can be seen when comparing Figure 7-2 to Figure 4-2, the model is simplified by removing most structural components and straightening the rack cell tube.

The New Fuel Storage Vault is surrounded by concrete (other than its top). The KENO model conservatively extended the wall and floor thickness to 3 feet to account for surrounding structures that may provide additional neutron reflection. The uncertainty cases in Section 7.5.1 show that additional wall thickness beyond 3 feet does not impact the results. Uncertainty calculations in Section 7.6 validate this assumption. Nonetheless, a 6 inch tolerance will be used in uncertainty space to account for the potential for variation of k-eff with additional reflection.

As stated in Section 6.1, the library used in this calculation is ENDF/B-VII 238 group. The boundary conditions are set to void. Unless otherwise noted, each of the KENO cases run use 5000 generations, 15000 neutrons per generation, and skips at least 500 generations. The initial source distribution of neutrons is uniform in the fuel.

Figure 7-1: Planar View of the New Fuel Storage Area Model

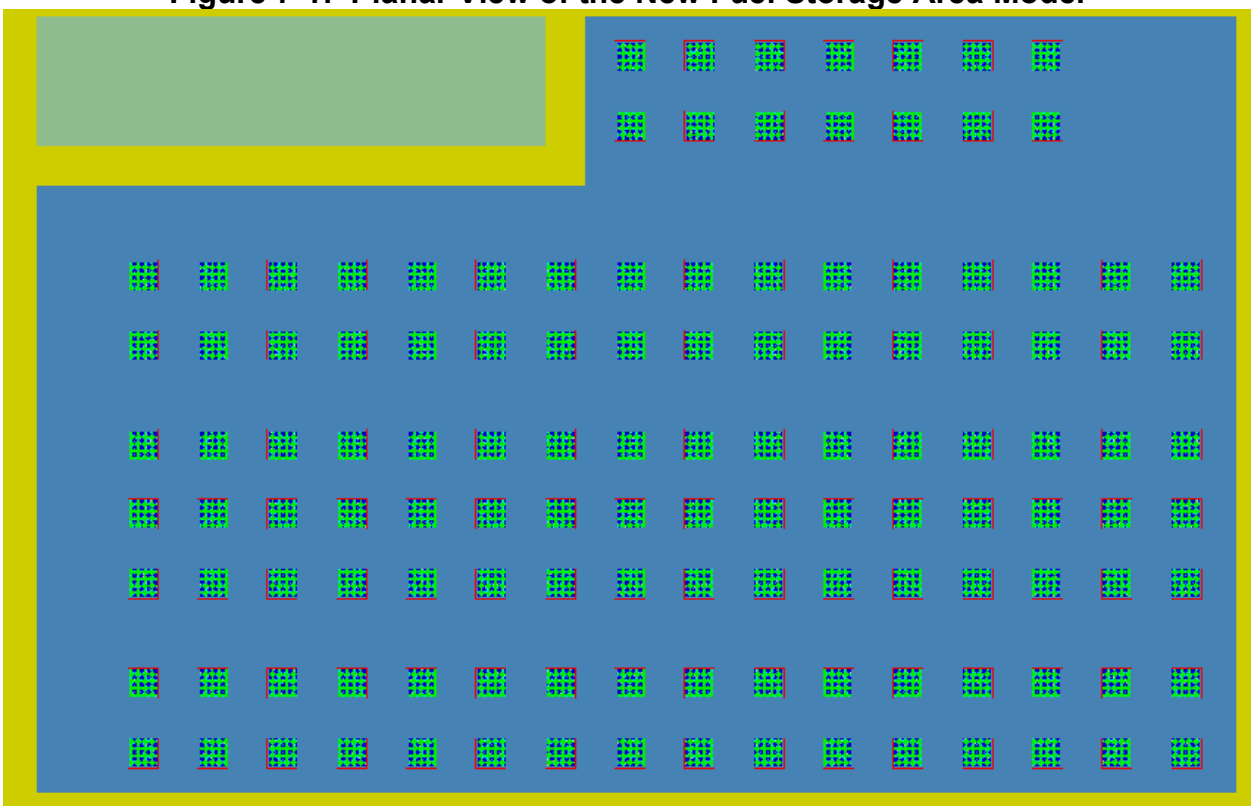

Figure 7-2: Axial Representation of the New Fuel Storage Area Model

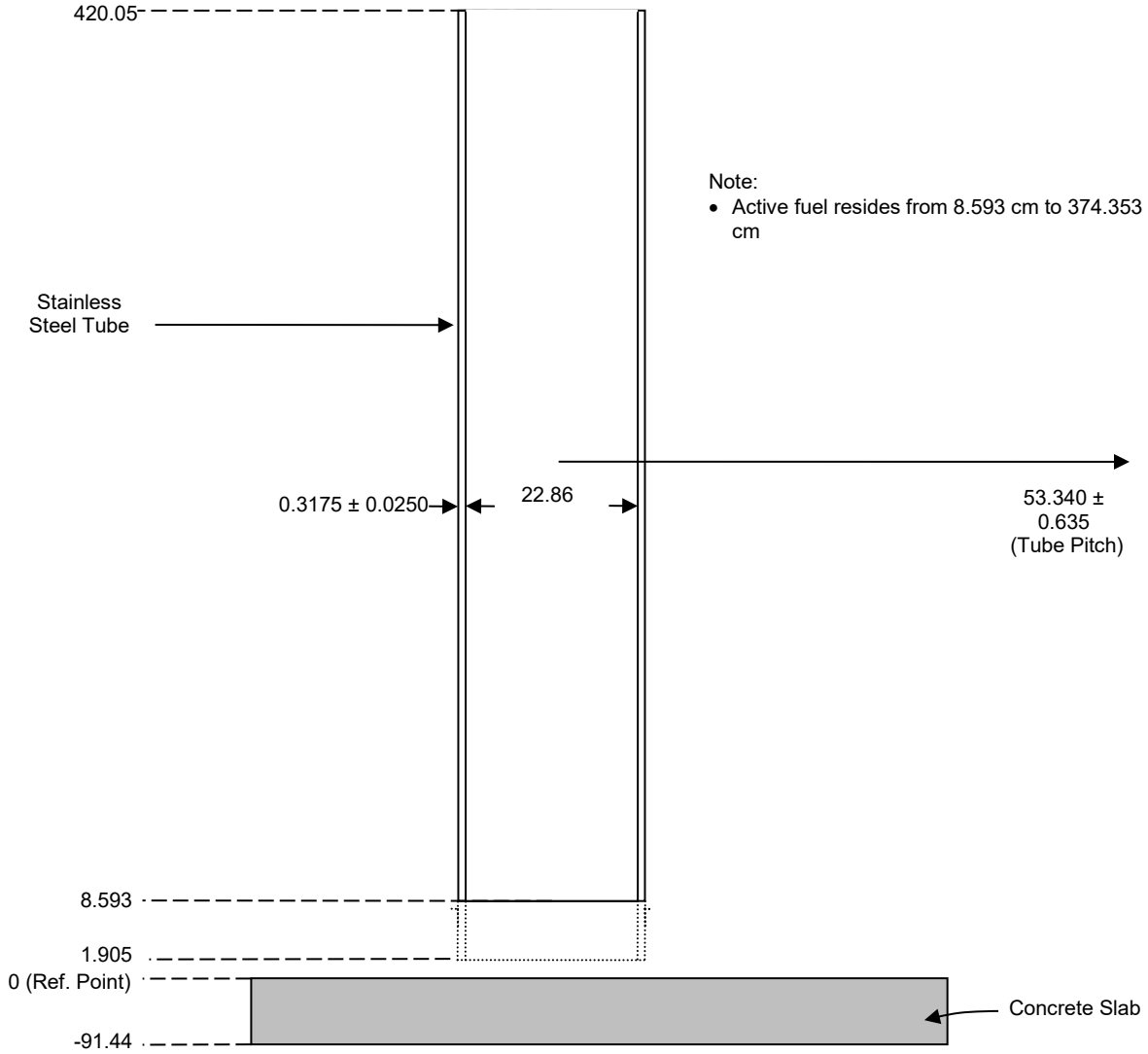

Figure 7-3: Empty Cells Required New Fuel Storage Area

*The "**X**" in the figure above signifies that the corresponding rack cell must remain empty if the NFSA contains at least one assembly with an initial enrichment that is >4.35 wt% and ≤5.00 wt%.*

7.2 *Limiting Fuel Design*

The NFSA analysis employs a composite fuel design that bounds the range of variation in Surry fuel. Variation in fuel dimensions and clad materials over the history of Surry is summarized in Table 3-1.

7.2.1 Fuel Cladding Materials

Throughout the life of Surry, there have been three zirconium alloys used in the cladding and grids: Zircaloy-4, ZIRLO, and M5 Alloy. In addition to these materials, a pure Zirconium case is included (base case). Sensitivity cases were performed to discover if there is a significant difference between the zirconium alloys with respect to the k-eff of the NFSA. Additionally, to allow for future zirconium alloy cladding changes, pure zirconium was tested to see if it is a bounding cladding type.

Tables 7-1 and 7-2 show that k-eff generally increases as the amount of zirconium increases. This result can be attributed to the small microscopic cross section of Zirconium compared with other alloy materials. Of the listed elements, only oxygen has a smaller absorption cross section than Zirconium in the thermal and epithermal energy range.

Table 7-1: k-eff of Zirconium Alloys in Optimum Moderation

Case Description	k-eff	σ	Δk	Δk/rss(σ)
M5 Alloy	0.946210	0.000083	-0.000565	-467%
Optimized ZIRLO	0.946034	0.000090	-0.000741	-589%
Zircaloy-4	0.946262	0.000085	-0.000513	-419%
Zirconium	0.946775	0.000088	N/A	N/A

Table 7-2: k-eff of Zirconium Alloys in Flooded Conditions

Case Description	k-eff	σ	Δk	Δk/rss(σ)
M5 Alloy	0.892940	0.000100	-0.000410	-290%
Optimized ZIRLO	0.892830	0.000100	-0.000520	-368%
Zircaloy-4	0.892778	0.000097	-0.000572	-411%
Zirconium	0.893350	0.000100	N/A	N/A

Tables 7-1 and 7-2 show that the pure zirconium cladding resulted in the largest k-eff in optimum moderation and flooded conditions. Therefore, the cladding in the NFSA will be modeled as pure zirconium.

7.2.2 Instrument and Guide Tubes

The Instrument and Guide Tube design varies with different fuel types. To quantify the effect that this design input has on the k-eff of the NFSA, sensitivity cases were run. Table 7-3 shows the inner and outer diameters that will be used in the sensitivity cases.

Adding more zirconium in the active fuel region generally decreases k-eff. Therefore, to bound potential future fuel types, a hypothetical thin tube design was tested (labeled "Hypothetical Thin Walled Tube" in Tables 7-3 and 7-4). This hypothetical design took the largest inner diameter and smallest outer diameter of the fuel designs to obtain a bounding tube wall. Also, a Maximum Zirconium case was run where the maximum cladding thickness and the maximum instrument/guide tube wall thickness was also run. The volume fraction of Zirconium for a single lattice (including the guide/instrument tube cladding and the fuel pin cladding) is listed in Table 7-3 for each case.

Table 7-3: Instrument and Guide Tube Inner and Outer Diameter

Fuel Type	Inner Diameter (cm)	Outer Diameter (cm)	Zr Vol. Frac.
Standard	[redacted]	[redacted]	[redacted]a,c
SIF, SIF variants, and Upgrade	[redacted]	[redacted]	[redacted]a,c
Agora-5A	[redacted]	[redacted]	[redacted]F
Hypothetical Thin Walled Tube	[redacted]	[redacted]	[redacted]a,c
Max Zirconium Vol. Frac.	[redacted]	[redacted]	[redacted]a,c

Table 7-4a: k-eff of Instrument and Guide Tubes in Optimum Moderation

Case Description	k-eff	σ	Δk	Δk/rss(σ)
Agora-5A	0.946389	0.000085	-0.000386	-315%
Max Zirconium Vol. Frac.	0.945509	0.000091	-0.001266	-1000%
Standard	0.946543	0.000089	-0.000232	-185%
SIF, SIF variants, and Upgrade	0.946588	0.000089	-0.000187	-149%
Hypothetical Thin Walled Tube	0.946775	0.000088	N/A	N/A

Table 7-4b: k-eff of Instrument and Guide Tubes in Full Density Water

Case Description	k-eff	σ	Δk	Δk/rss(σ)
Agora-5A	0.889910	0.000100	-0.003440	-2432%
Max Zirconium Vol. Frac.	0.885640	0.000100	-0.007710	-5452%
Standard	0.891213	0.000098	-0.002137	-1526%
SIF, SIF variants, and Upgrade	0.891090	0.000100	-0.002260	-1598%
Hypothetical Thin Walled Tube	0.893350	0.000100	N/A	N/A

Tables 7-4a and b show that the Hypothetical Thin Walled Tube results in the largest k-eff for both the optimum moderation and full density water scenarios. For the optimum moderation case, a range of water densities were explored to ensure that the limiting moderator density does not impact the results. The flooded and optimally moderated k-eff versus volume fraction of Zirconium in the lattice is plotted in Figure 7-4.

The results show that the lattice itself is under moderated and minimizing the Zirconium volume fraction is conservative. Furthermore, the impact of Zr volume fraction on full density water is much greater than it is for optimum moderation. Lastly, the results show that the optimum moderation cases are all limiting at nearly the same moderator density. This finding bolsters the argument that the flooded geometry cases are more highly dependent on local lattice parameters while optimum moderation cases are more dependent on global NFSA geometric parameters.

Therefore, the base case in the NFSA analysis will use the hypothetical thin Instrument and Guide Tube design to calculate the maximum k-eff of the NFSA. The calculations here also validate the use of the minimum clad thickness dimensions as they result in a lower volume fraction of Zirconium material in the fuel region.

Figure 7-4: k-eff of NFSA vs. Zirconium Volume Fraction in Lattice

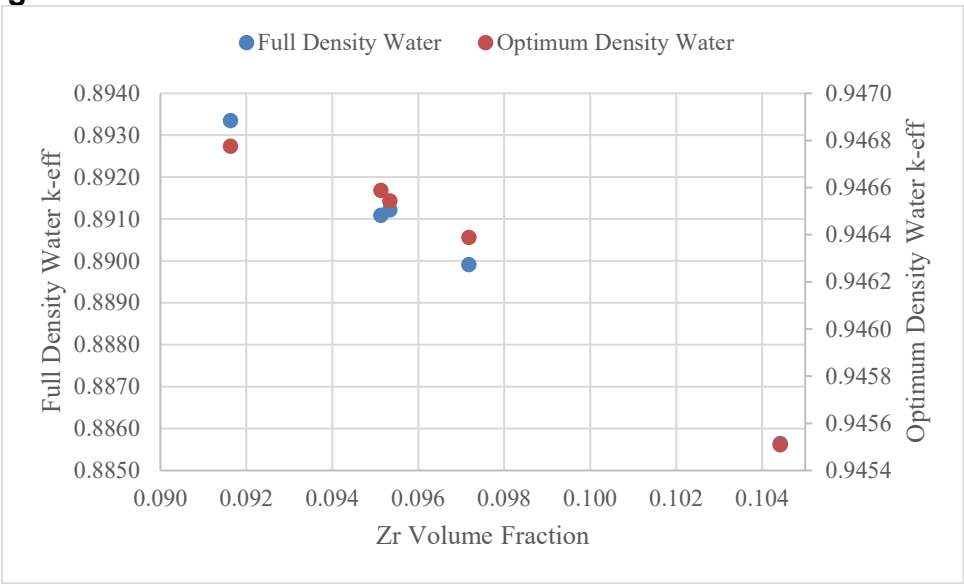

7.2.3 Top and Bottom Assembly Reflectors

The top assembly reflector is defined in this calculation as the material within the assembly radial profile that is above the active fuel and below the top of the top nozzle. The bottom assembly reflector is defined as the material within the assembly radial profile that is below the active fuel and above the bottom of the bottom nozzle. There are several fuel designs with varying reflector thickness and composition in the Surry SFP. This section proves that no reflector material and only water above and below the active fuel is bounding.

Two hypothetical reflectors for both top and bottom of the fuel are modeled based on historical assembly designs. As in Section 7.2.2, a range of moderation density was run to ensure the optimum water density is used with the updated reflector conditions. Despite the adjustment of the moderation density, Table 7-5a shows that assuming only water above and below the fuel is conservative compared with the reflector models when at optimum moderation. Removing moderation in high importance areas for the optimum moderation conditions reduces neutron thermalization giving lower reactivity.

Table 7-5b shows that adding reflector above and below the fuel is slightly non-conservative in full density water for the two calculations run. Furthermore, the difference is within two RSS standard deviations. Therefore, it is unlikely that reflector material has a significant impact on NFSA k-eff in full density water. Also, Section 7.6 shows that the margin to the NRC limit is very large for the full density scenario compared with the differences observed in this calculation.

Table 7-5a: NFSA k-eff with Varying Reflector in Optimum Moderation

Case Description	k-eff	σ	Δk	Δk/rss(σ)
Max. Reflector Material	0.937697	0.000096	-0.009078	-6971%
Min. Reflector Material	0.938048	0.000088	-0.008727	-7012%
No Reflector Material (low density water)	0.946775	0.000088	N/A	N/A

Table 7-5b: NFSA k-eff with Varying Reflector in Full Density Water

Case Description	k-eff	σ	Δk	Δk/rss(σ)
Max. Reflector Material	0.893601	0.000099	0.000251	178%
Min. Reflector Material	0.893350	0.000100	0.000000	0%
No Reflector Material (full density water)	0.893350	0.000100	N/A	N/A

The bottom nozzle height varies by fuel design. A minimum and maximum distance is evaluated in this section to determine the impact of this distance. Table 7-6 shows that the minimum distance to the floor is conservative for both optimum moderation conditions and flooded conditions.

The minimum fuel height (bottom of fuel assembly to the bottom of the active fuel) used in this analysis is 8.593 cm.

Table 7-6a: NFSA k-eff with Varying Height Above Floor in Optimum Moderation

Case Description	k-eff	σ	Δk	Δk/rss(σ)
Max. Fuel Height	0.941458	0.000087	-0.005317	-4297%
Min. Fuel Height	0.946775	0.000088	N/A	N/A

Table 7-6b: NFSA k-eff with Varying Height Above Floor in Full Density Water

Case Description	k-eff	σ	Δk	Δk/rss(σ)
Max. Fuel Height	0.893330	0.000100	-0.000020	-14%
Min. Fuel Height	0.893350	0.000100	N/A	N/A

7.2.4 Assembly Grids

The New Fuel Storage Area analysis does credit fuel assembly grids. The assembly design that had the lowest volume of grids was used in the base case. Table 7-7 shows the grid volumes and Table 7-8 shows the bounding grid volume fraction. The grids are smeared homogeneously throughout the coolant within the active fuel.

Table 7-7: Grid Volume in Active Fuel Region for Historical Fuel Designs

Fuel Type	Midspan Grids			IFM Grids			Total Volume (cc)
	Density (g/cc)	Total Mass (g)	Volume (cc)	Density (g/cc)	Total Mass (g)	Volume (cc)	
SIF	[						]a,c
SIF/P+	[						]a,c
SIF/P+Z	[						]a,c
SIF/P+Z2	[						]a,c
Upgrade	[						]a,c
Agora	[						]F

The total volume of the coolant-grid mixture (V_{lattice}) in an assembly is calculated based on the equation below. Note that the water inside the guide tubes and instrument tube is not considered in this equation because it will not be smeared with grid material. Table 7-8 shows the volumes and volume fraction of the grid - coolant mixture.

$$V_{\text{lattice}} = h_{fuel}\left[n_{rod} * \left(pitch_{\text{rod}}^2 - \frac{\pi}{4} OD_{\text{cladding}}^2\right) + n_{G\&I\ Tubes} * \left(pitch_{\text{rod}}^2 - \frac{\pi}{4} OD_{G\&I\ Tubes}\right)\right] \quad (8.6.2\text{-}1)$$

Table 7-8: Grid Volume Fractions

Fuel Type	Grid Volume (cc)	Coolant-Grid Mixture Volume (cc)	Grid Volume Fraction
Agora	[		]F

7.2.5 Fuel Density

The entire fuel stack is modeled as solid pellets even though newer designs use annular pellets in the top and the bottom of the fuel. The model is conservative because it adds fuel material compared with fuel designs that have the annular pellets.

The pellet density is a combination of sinter density and geometric density (accounting for dishing and chamfer). The void volume of historical fuel designs is approximately [ ]^{a,c} – [ ]^{F}.

Using the void volume of [ ]^{F} and historical pellet densities, the batchwise densities (in units of %TD) can be determined. The maximum stack density (factoring in void fraction) from historical batches is [ ]^{a,c}. A conservative value of 95.5% will be used for the NFSA analysis.

The uncertainty of historical batches can be determined by calculating the standard deviation over all data (after applying the void volume correction). The resulting standard deviation is [ ]^{a,c}. This number is artificially high because the nominal void volume has changed as fuel designs have evolved over time. The standard deviation of just the current fuel is [ ]^{a,c}. For conservatism and to bound future reloads, the former standard deviation will be rounded up to 0.7% for uncertainty calculations.

7.2.6 Burnable Poisons and Axial Blankets

Burnable poisons and axial blankets are not credited in this analysis. This is conservative because it removes neutron absorbers and removes fissile material from the fuel, respectively.

7.3 *Limiting Rack Model*

7.3.1 Concrete

Concrete has the capability to reflect leakage neutrons back towards the fuel increasing the k-eff of the NFSA. A review of station drawings and documents shows that they do not explicitly specify what concrete was used for the NFSA concrete, but the evidence provided points toward it being Portland concrete.

For this scenario, EPRI [30] recommended two conservative concretes, dry and wet, that were determined by maximizing the isotopic content of the positive worth isotopes and minimizing the isotopic content of negative worth isotopes based on the concrete compositions in the SCALE User Manual. In addition to the EPRI recommendation, an analysis was done for the North Anna NFSA to determine a modified EPRI Wet concrete composition justified using site specific parameters [23]. Millstone Unit 3 used the EPRI Dry concrete without any justification needed other than it produces the highest reactivity compared to the SCALE and EPRI concretes [14]. The compositions of these concretes are shown in Table 7-9.

Table 7-9: Concrete Composition

Element	EPRI Wet Concrete (wt%)	EPRI Dry Concrete (wt%)	Portland Concrete (wt%)	NAPS Concrete (wt%)
Fe	0.45	0.45	1.40	0.41
H	0.26	0.00	1.00	0.23
C	13.97	14.00	0.10	15.06
O	42.41	42.52	52.9107	44.90
Na	2.31	2.32	1.60	2.12
Mg	7.51	7.53	0.20	6.90
Al	2.71	2.72	3.3872	2.49
Si	26.87	26.94	33.7021	24.67
Ca	3.51	3.52	4.40	3.22
K	0.00	0.00	1.30	0.00
Density (g/cm^3)	2.91	2.90	2.30	3.17

Table 7-10b shows that NFSA k-eff with full density water is not sensitive to the concrete composition. Even for the nominal Portland concrete, the difference is within two standard deviations of the limiting concrete model. This makes sense because the large distances between the fuel and the concrete with the higher density water tends to isolate the fuel from the concrete. The likelihood of neutrons travelling to the concrete and scattering back to the fuel before being absorbed is very low.

Table 7-10a however, shows a strong NFSA k-eff sensitivity toward the concrete composition for optimum moderation conditions. The results show that EPRI dry concrete is far more conservative than either of the wet concrete models and the nominal Portland concrete. It should be noted here that the Portland concrete represents a best estimate model of the concrete.

Table 7-10a: k-eff of Various Concrete Types in Optimum Moderation

Case Description	k-eff	σ	Δk	Δk/rss(σ)
EPRI Wet Concrete	0.931650	0.000090	-0.01403	-10960%
EPRI Dry Concrete	0.945678	0.000091	--	--
Modified EPRI Wet (NAPS)	0.934120	0.000098	-0.01156	-8642%
Portland Nominal Concrete	0.910989	0.000091	-0.03469	-26955%

Table 7-10b: k-eff of Various Concrete Types in Full Density Water

Case Description	k-eff	σ	Δk	Δk/rss(σ)
EPRI Wet Concrete	0.893380	0.000100	0.00035	249%
EPRI Dry Concrete	0.893030	0.000099	--	--
Modified EPRI Wet (NAPS)	0.893300	0.000100	0.00027	192%
Portland Nominal Concrete	0.893321	0.000098	0.00029	209%

7.3.2 Temperature and Water Density

Due to the strong sensitivity of the NFSA k-eff with respect to system temperature and moderator density, a detailed analysis is warranted to determine what the limiting conditions for the calculations should be. For this study, a range of moderator densities are run between 0.0 and 1.0 g/cm^3. This range represents all plausible water densities at atmospheric conditions. The minimum temperature for this analysis is 273 K as frozen water is precluded. Section 9.13.3.2 of the Surry UFSAR gives the maximum permissible fuel building temperature of 105° F. This gives a maximum NFSA temperature of 314 K. The entire range of densities is run with both the minimum and maximum temperature, regardless of the physical properties of water.

Figure 7-5 shows the behavior of the NFSA k-eff as moderator density increases. The behavior is indicative of two length scales, the over moderation of the NFSA as a whole due to large assembly spacing and the under moderation of the assembly lattice. For all densities, the higher temperature, 314 K, is limiting. The higher k-eff at higher temperatures shows that the decreased absorption in the 1/v materials (i.e. hydrogen) outweighs the increase of resonance absorption in U-238 from the doppler effect.

Figure 7-5 shows that the peak reactivity occurs at a temperature of 314 K and at a water density of about 0.06 g/cc. Further, more detailed cases were run for storage configuration at 0.001 g/cc intervals. Intervals of 0.001 g/cc is sufficient since the Table 7-11 shows that the differences are within 2 RSS(σ) at the peaks and because NEI 12-16 [32] only recommends every ~0.01 g/cc. Note that these cases are run for each loading scenario since the optimum water density can change when empty cells are introduced.

Table 7-11 and Figure 7-6 shows these case results. The maximum k-eff of each loading pattern scenario will be used to calculate the NFSA maximum k-eff in Section 7.6.

Table 7-11: Water Density Sensitivity Cases for All Enrichment Combinations

Combination	Water Density (g/cc)	k-eff	σ	dk	dk/RSS(σ)
4.35 wt%, No Empty Spaces	0.052	0.942168	0.000090	-0.00134	-1059%
	0.053	0.942370	0.000089	-0.00114	-905%
	0.054	0.942842	0.000087	-0.00067	-536%
	0.055	0.943246	0.000091	-0.00026	-207%
	0.056	0.943399	0.000093	-0.00011	-85%
	0.057	0.943509	0.000089	--	--
	0.058	0.943262	0.000084	-0.00025	-202%
	0.059	0.943303	0.000096	-0.00021	-157%
	0.060	0.943100	0.000093	-0.00041	-318%
	0.061	0.942620	0.000092	-0.00089	-695%
	0.062	0.942342	0.000089	-0.00117	-927%
	1.000	0.891461	0.000098	--	--
5.00 wt%, Empty Spaces (3 Out of 4 Pattern)	0.040	0.854861	0.000086	-0.00189	-1526%
	0.041	0.855340	0.000093	-0.00141	-1095%
	0.042	0.855856	0.000094	-0.00089	-691%
	0.043	0.856488	0.000087	-0.00026	-211%
	0.044	0.856450	0.000087	-0.00030	-241%
	0.045	0.856750	0.000089	--	--
	0.046	0.856624	0.000088	-0.00013	-101%
	0.047	0.856293	0.000087	-0.00046	-367%
	0.048	0.855890	0.000091	-0.00086	-676%
	0.049	0.855505	0.000096	-0.00125	-951%
	0.050	0.855121	0.000094	-0.00163	-1258%
	1.000	0.911850	0.000100	--	--

Figure 7-5: k-eff of NFSA vs. Water Density

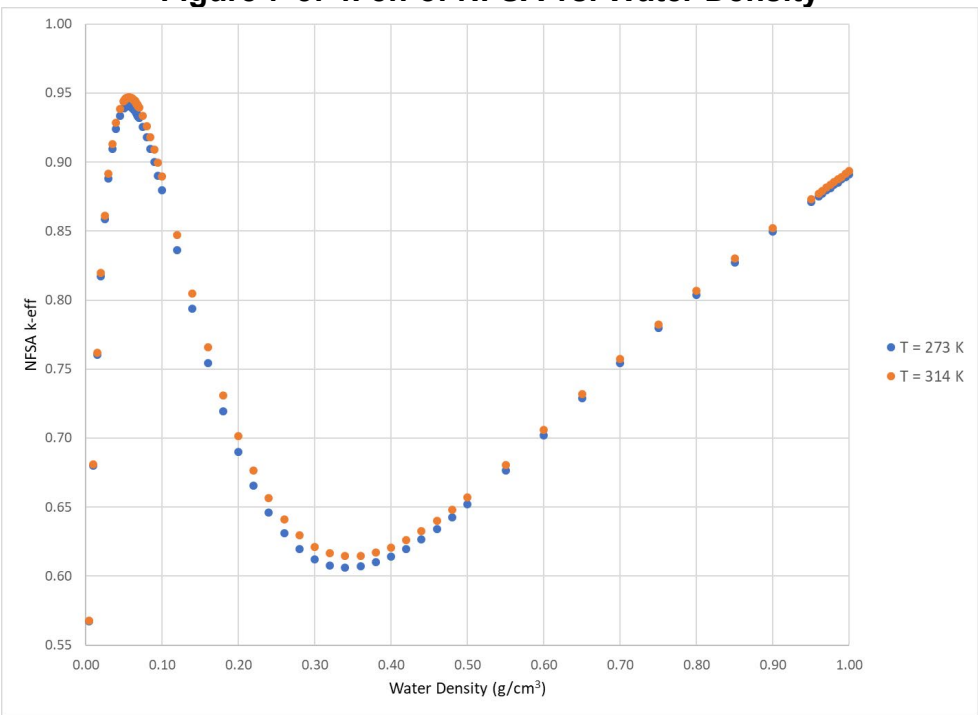

Figure 7-6: k-eff of NFSA vs. Water Density

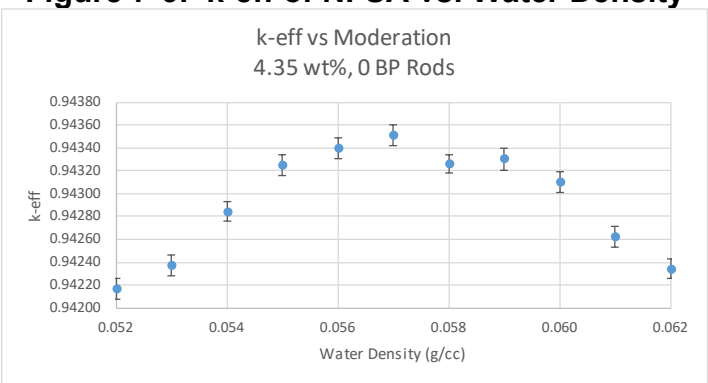

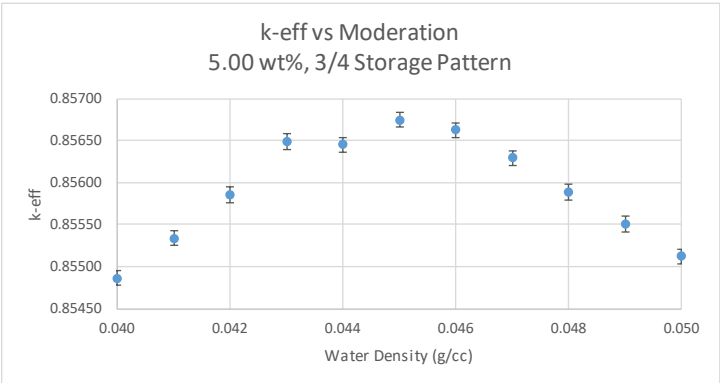

7.3.3 Asymmetric Fuel Placement

To ensure that there will be no limitations on where/how the assemblies are placed within the stainless-steel tubes, four cases were run which skewed the assembly placements towards each other to achieve the highest possible k-eff. Figure 7-7 shows how the assemblies were skewed for each case. In addition to the three cases indicated in the figure, an additional case is run where assemblies in a 2x2 group are shifted toward each other.

Table 7-12a shows that the highest k-eff in optimum moderation is achieved when the assemblies are shifted towards the center of the NFSA. This result is indicative of a system where the highest neutron importance is in the center of the NFSA for the optimum moderation scenario. Table 7-12b shows that any shift from center results in increased k-eff for full density water, but the type of shift doesn't matter. This result is best explained by considering that in full density water, nearest neighbor coupling is of primary importance for this sensitivity. Every shift will result in roughly the same decreased spacing between nearest neighbors.

Table 7-12a: k-eff of NFSA with Asymmetry in Optimum Moderation

Case Description	k-eff	σ	Δk	Δk/rss(σ)
Centered in Cell	0.945067	0.000090	-0.001708	-1357%
2x2 Cell Shift	0.943281	0.000094	-0.003494	-2714%
Shift North	0.946000	0.000095	-0.000775	-598%
Shift South	0.946697	0.000092	-0.000078	-61%
Shift Middle	0.946775	0.000088	N/A	N/A

Table 7-12b: k-eff of NFSA with Asymmetry in Full Density Water

Case Description	k-eff	σ	Δk	Δk/rss(σ)
Centered in Cell	0.891338	0.000096	-0.002012	-1451%
2x2 Cell Shift	0.893310	0.000100	-0.000040	-28%
Shift North	0.893370	0.000100	0.000020	14%
Shift South	0.893300	0.000100	-0.000050	-35%
Shift Middle	0.893350	0.000100	N/A	N/A

For simplicity, the middle shift case will be used for both optimum moderation and flooded conditions. Though all shifts are within one standard deviation of each other for the full density case, the north shift gives slightly higher k-eff for this set of calculations. The differences are within two RSS standard deviations and the full density water condition is far from limiting compared with the optimum moderation condition.

Figure 7-7: Asymmetric Skewing of Assemblies

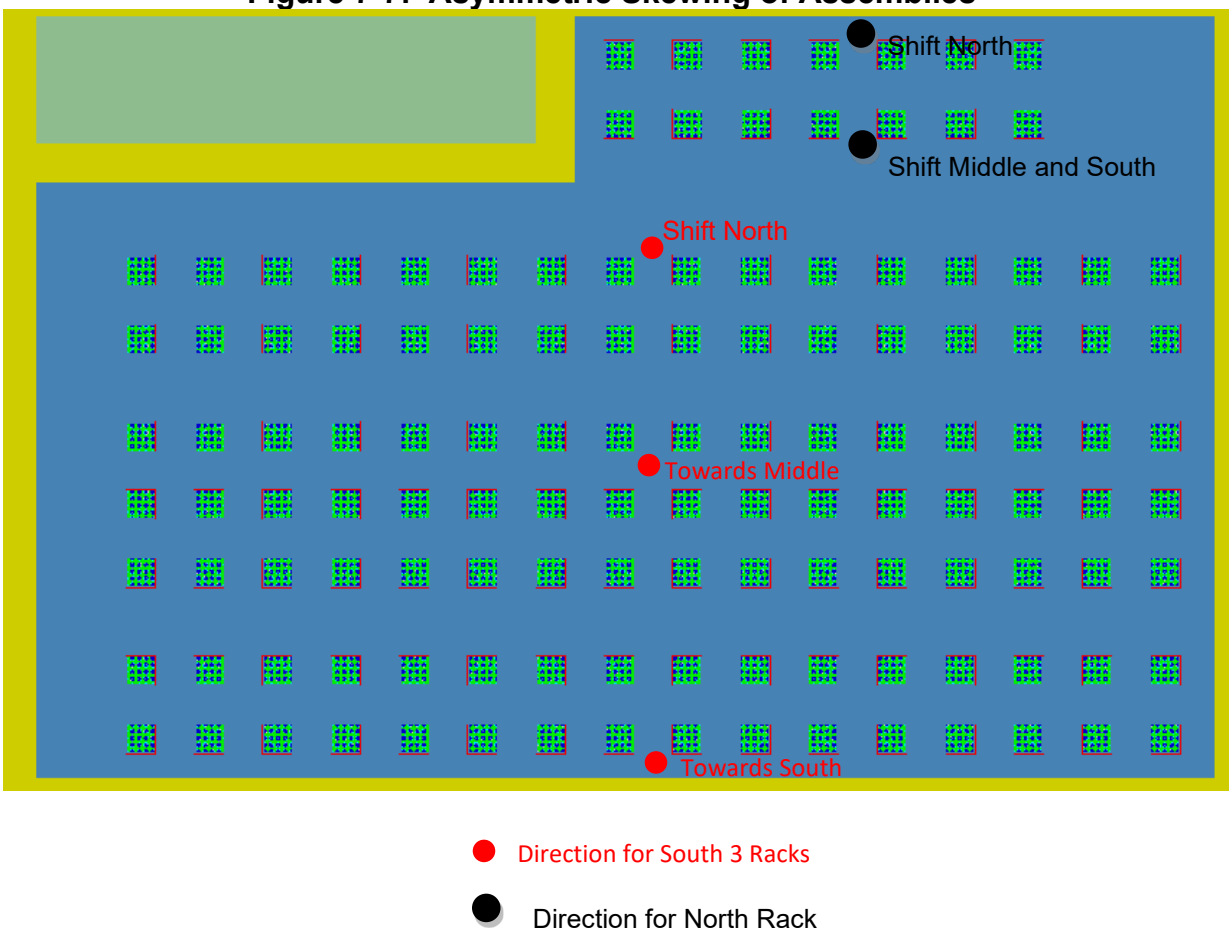

7.3.4 Credited Structural Beams

The majority of the structural beams in the New Fuel Storage Area are not modeled. Only a few beams at the bottom of the NFSA are credited. The thickness uncertainty case of the cell tubes in Section 7.5.1 shows that it is conservative to model less structural steel in the NFSA.

Figure 7-8 shows a drawing of the bottom structural beams. For each rack cell, this consists of two L-Beams fastened to the NFSA floor which brackets two sides of the rack cell. There is a flat bar welded to the insides of the L beams which brackets the remaining two sides of the rack cell.

The model only credits the beams in direct contact with the rack cell. Figure 7-9 shows the KENO model. Only a small fraction of the beams are modeled. Therefore, the dimensions are considered bounding and no uncertainty cases are run for these beams.

Figure 7-8: Drawing of NFSA Lower Structural Beams

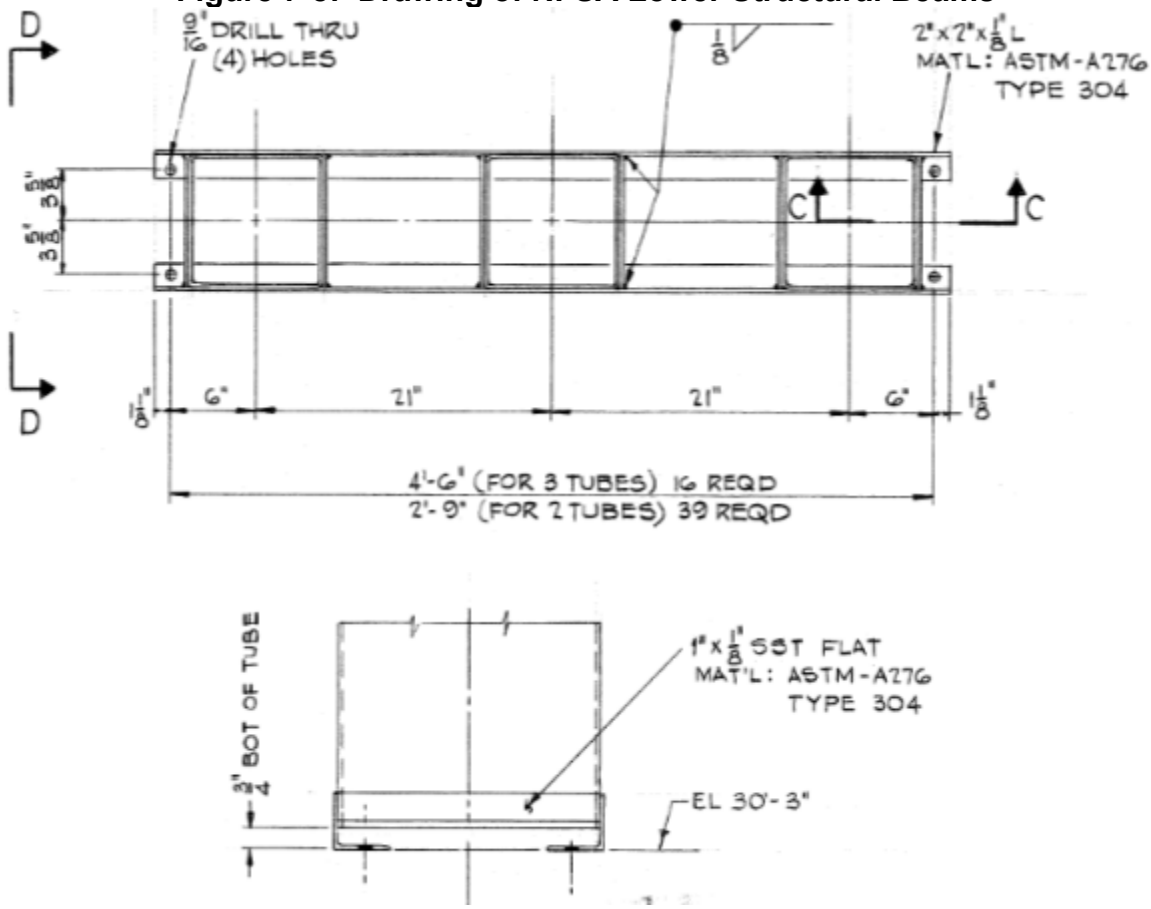

Figure 7-9: KENO Model of NFSA Lower Structural Beams

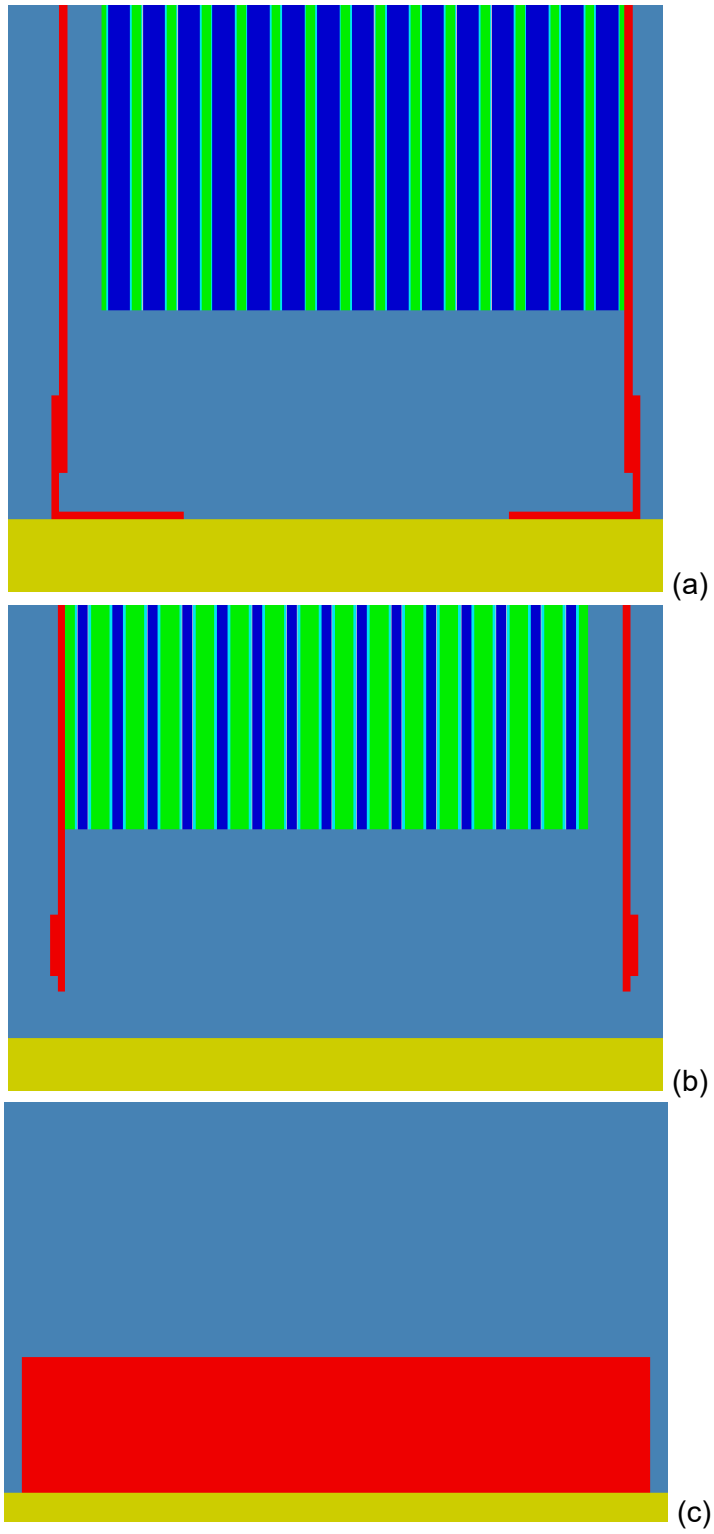

Picture (a) shows L-beams and picture (b) shows the flat beams that brace the rack tube. Picture (c) shows a side view of the L-Beam and shows that the beams are not modeled in-between assemblies, only at the rack cell.

7.4 *Summary of the Base Case for the NFSA Analysis*

Sections 7.1-7.3 describe the development of the limiting Surry NFSA model. The base case model includes these features:

1. There are two storage options:
    a. All storage cells contain a 4.35 wt% U-235 fresh fuel assembly with no burnable absorbers.
    b. 3 out of 4 storage cells contain 5.00 wt% U-235 fresh fuel assembly with no burnable absorbers. The 3 out of 4 pattern is shown in Figure 7-3.
2. The fuel contains no U-234 or U-236.
3. The fuel stack density is 95.5% of the UO2 theoretical density.
4. The fuel model includes minimum water displacement guide tubes and grids
5. The fuel clad material is modeled as zirconium.
6. Most of the rack structures are ignored. A small amount of structural beams (Section 7.3.4) and the concrete are modeled.
7. EPRI dry concrete composition is used to conservatively represent the concrete.
8. Concrete thickness is conservatively assumed to be 3 feet.
9. Fuel is asymmetrically positioned in each rack cell to maximize k-eff.
10. The fuel and moderator temperature for the fully flooded and optimum moderation conditions is 314 K.
11. The water density for the full density flooded case is set to 1.0 gm/cm^3. For the optimum moderation case, the scenario with no empty cells has a water density of 0.057 gm/cm^3 and the empty cell scenario has a water density of 0.045 gm/cm^3.
12. KENO cases are run with 5000 generations, 15,000 neutrons per generation, and 500 generations skipped.
13. There are no fixed neutron absorbers in the NFSA racks.

7.5 *Biases and Uncertainties for the New Fuel Storage Area Analysis*

7.5.1 Manufacturing Uncertainties

Tables 7-13 and 7-14 display the results of the tolerance sensitivity calculations for the Optimum Moderation case and Full Density Water case, respectively. The "Total Manufacturing Uncertainty" is calculated using the equation below and only uses the cases in which the k-eff increased. For optimum moderation tube pitch and tube thickness uncertainty, a range of moderator densities were calculated to ensure that the optimum was retained with the shifted parameter. Note that sensitivity cases were only run for the 4.35 wt% no empty cells scenario because the 5.00 wt% empty cell scenario had a very large amount of margin to the limit as shown in Section 7.6.

$$\text{Total Manufacturing Unc.} = \left[\sum\left(k_{\pm Unc.} - k_{Nominal} + 2 * \sqrt{\sigma^2_{\pm Unc.} + \sigma^2_{Nominal}}\right)^2\right]^{1/2}$$

Table 7-13: Manufacturing Tolerance in Optimum Moderation

Case Description	k-eff	σ	Max Δk	Δk/rss(σ)
Best Estimate Model - No BP	0.946775	0.000088	N/A	N/A
Bottom of Fuel Height - Decrease	0.946869	0.000090	0.000346	75%
Cladding ID-Increase	0.947380	0.000091	0.000858	478%
Cladding OD-Decrease	0.947317	0.000092	0.000797	426%
Concrete Wall Thickness - Increase	0.946882	0.000095	0.000366	83%
Fuel Stack %TD - Increase	0.947365	0.000090	0.000842	469%
Enrichment - Increase	0.948921	0.000092	0.002401	1686%
Guide Tube ID-Increase	0.946968	0.000092	0.000448	152%
Guide Tube OD-Decrease	0.946937	0.000091	0.000415	128%
Active Fuel Length - Increase	0.947069	0.000086	0.000540	239%
Fuel Pellet OD-Increase	0.947325	0.000096	0.000810	422%
Pin Pitch - Increase	0.947520	0.000093	0.001001	582%
Distance to Concrete - Decrease	0.947045	0.000092	0.000525	212%
Tube ID - Decrease	0.947742	0.000084	0.001210	795%
Tube Pitch - Decrease	0.946978	0.000097	0.000465	155%
Tube Thickness - Decrease	0.959452	0.000091	0.012930	10014%
Total Manufacturing Uncertainty (Δk) – No Empty Cells			***0.0134***	

Table 7-14: Manufacturing Tolerance in Full Density Water

Case Description	k-eff	σ	Max Δk.	Δk/rss(σ)
Best Estimate Model - No BP	0.893350	0.000100	N/A	N/A
BAF Height - Decrease	0.893400	0.000100	0.000333	35%
Cladding ID-Decrease	0.893715	0.000099	0.000646	259%
Cladding OD-Decrease	0.896170	0.000100	0.003103	1994%
Concrete Wall Thickness - Increase	0.893610	0.000100	0.000543	184%
Fuel Stack %TD - Increase	0.894180	0.000100	0.001113	587%
Enrichment - Increase	0.895250	0.000100	0.002183	1344%
Guide Tube ID-Increase	0.893930	0.000100	0.000863	410%
Guide Tube OD-Decrease	0.894007	0.000099	0.000938	467%
Active Fuel Length - Increase	0.893510	0.000100	0.000443	113%
Fuel Pellet OD-Increase	0.893950	0.000100	0.000883	424%
Pin Pitch - Increase	0.894550	0.000100	0.001483	849%
Distance to Concrete - Decrease	0.893590	0.000099	0.000521	171%
Tube ID - Increase	0.893960	0.000100	0.000893	431%
Tube Pitch - Decrease	0.893690	0.000100	0.000623	240%
Tube Thickness - Decrease	0.895150	0.000098	0.002080	1286%
Total Manufacturing Uncertainty (Δk)			***0.0052***	

7.5.2 Nominal Model Uncertainty

The sigma values for each of the nominal models is ≤ 0.0001. For simplicity, a bounding sigma of 0.0001 will be used for the total uncertainty of every enrichment/BP case. This sigma is then doubled to achieve a 95%/95% probability and confidence level. Therefore, the Nominal Model Uncertainty is **0.00020** Δk.

7.5.3 Code Benchmark Bias and Uncertainty

Validation of SCALE/KENO using ENDF/B-VII 238 group cross sections identified EALF as the primary bias and uncertainty trend. The applicable bias and uncertainty for fresh fuel and depleted fuel are shown in Table 7-15. This table is taken from Appendix A. For the NFSA, only the fresh fuel statistics are used. Table 7-16 show the code benchmark bias and uncertainty applied to this analysis.

Table 7-15: Code Benchmarking Bias and Uncertainty (Appendix A)

EALF (eV)	Bias (Δk)	Uncertainty (Δk)
Fresh UO_2 Fuel		
0.00 – 0.40	0.0030	0.0040
0.40 – 0.80	0.0040	0.0045
0.80 – 1.10	0.0055	0.0050
1.10 – 1.25	0.0060	0.0050
1.25 – 1.40	0.0065	0.0055
Burned MOX Fuel		
0.00 – 0.40	0.0015	0.0060
0.40 – 0.80	0.0025	0.0095
0.80 – 1.10	0.0030	0.0120
1.10 – 1.25	0.0035	0.0135
1.25 – 1.40	0.0035	0.0145

Table 7-16: Code Uncertainty for Nominal Cases

Enrichment/BP	Case Description	EALF (eV)	Bias (dk)	Uncertainty (dk)
4.35% / No Empty Cells	Optimum Moderation	1.01	0.0055	0.0050
	Full Density Water	0.23	0.0030	0.0040
5.00% / 3 out of 4 Storage Pattern	Optimum Moderation	1.37	0.0065	0.0055
	Full Density Water	0.25	0.0030	0.0040

7.5.4 Code Temperature Bias

Appendix A identified and calculated a temperature bias associated with the computer codes and methodology. The temperature bias is defined below where T is the temperature of the model in Kelvin.

$$Bias = 1 * 10^{-5} * (T - 293)$$

All the models are run at 314 K. This equates to a temperature Δk bias of 0.00021.

7.5.5 NRC Administrative Margin

A **0.01000** Δk bias was included in the maximum k-eff calculation for the NRC to use during their review.

7.6 *NFSA Maximum k-eff*

10CFR50.68 asserts that the maximum k-eff of the New Fuel Storage Area must not exceed 0.98 when flooded with low-density hydrogenous fluid and must not exceed 0.95 when flooded with unborated water. Tables 7-17 and 7-18 display the maximum k-eff of the NFSA for the limiting loading configurations and the margins to the limits for the optimum moderation scenario and full water density scenario, respectively. The grayed-out values in Tables 7-17 and 7-18 signify that the value is taken from the 4.35 wt% scenario. This is method is acceptable due to the excess amount of margin the empty cell scenario has compared to the 4.35 wt% scenario.

Table 7-17: Maximum k-eff of New Fuel Storage Area, Optimum Moderation Scenario

Fuel Constraints		
Maximum Enrichment (U-235 wt%)	4.35%	5.00%
Additional Restrictions	None	Empty Cells
Uncertainties		
BAF Height - Decrease	0.0003	0.0003
Cladding ID-Increase	0.0009	0.0009
Cladding OD-Decrease	0.0008	0.0008
Concrete Wall Thickness - Increase	0.0004	0.0004
Fuel Stack %TD - Increase	0.0008	0.0008
Enrichment - Increase	0.0024	0.0024
Guide Tube ID-Increase	0.0004	0.0004
Guide Tube OD-Decrease	0.0004	0.0004
Active Fuel Length - Increase	0.0005	0.0005
Fuel Pellet OD-Increase	0.0008	0.0008
Pin Pitch - Increase	0.0010	0.0010
Distance to Concrete - Decrease	0.0005	0.0005
Tube ID - Decrease	0.0012	0.0012
Tube Pitch - Decrease	0.0005	0.0005
Tube Thickness - Decrease	0.0129	0.0129
Code Uncertainty	0.0050	0.0055
KENO Base Case Uncertainty	0.0002	0.0002
RSS of Uncertainties	**0.0143**	**0.0145**
Biases		
Temperature Bias	0.0002	0.0002
Code Bias	0.0055	0.0065
Sum of Biases	**0.0057**	**0.0067**
Wrap-Up		
Base Case k-eff	0.9435	0.8568
Total Bias and Uncertainty	0.0200	0.0212
NRC Review Margin	0.0100	0.0100
Maximum k-eff	0.9735	0.8879
NRC Limit	0.9800	0.9800
DOMINION MARGIN FOR 50.59	**0.0065**	**0.0921**

Table 7-18: Maximum k-eff of New Fuel Storage Area, Full Water Density

Fuel Constraints		
Maximum Enrichment (U-235 wt%)	4.35%	5.00%
Additional Constriction	None	Empty Cells
Uncertainties		
BAF Height - Decrease	0.0003	0.0003
Cladding ID-Decrease	0.0006	0.0006
Cladding OD-Decrease	0.0031	0.0031
Concrete Wall Thickness - Increase	0.0005	0.0005
Fuel Stack %TD - Increase	0.0011	0.0011
Enrichment - Increase	0.0022	0.0022
Guide Tube ID-Increase	0.0009	0.0009
Guide Tube OD-Decrease	0.0009	0.0009
Active Fuel Length - Increase	0.0004	0.0004
Fuel Pellet OD-Increase	0.0009	0.0009
Pin Pitch - Increase	0.0015	0.0015
Distance to Concrete - Decrease	0.0005	0.0005
Tube ID - Increase	0.0009	0.0009
Tube Pitch - Decrease	0.0006	0.0006
Tube Thickness - Decrease	0.0021	0.0021
Code Uncertainty	0.0040	0.0040
KENO Base Case Uncertainty	0.0002	0.0002
RSS of Uncertainties	**0.0066**	**0.0066**
Biases		
Temperature Bias	0.0002	0.0002
Code Bias	0.0030	0.0030
Sum of Biases	**0.0032**	**0.0032**
Wrap-Up		
Base Case k-eff	0.8915	0.9119
Total Bias and Uncertainty	0.0098	0.0098
NRC Review Margin	0.0100	0.0100
Maximum k-eff	0.9112	0.9316
NRC Limit	0.9500	0.9500
DOMINION MARGIN FOR 50.59	**0.0388**	**0.0184**

7.7 *Accident Conditions*

7.7.1 Optimum Moderation

It should be noted that it is unlikely for the Surry NFSA to be flooded with low density hydrogenous moderator (foam). This is because most of the NFSA is covered. The only part that is not covered is a small opening in the northeast corner to allow personnel to climb into the vault. Regardless, both the accident scenarios of flooding the NFSA with water and optimum moderator were analyzed throughout Section 7.

7.7.2 Dropped and Misloaded Assembly

For this analysis, a multiple misload accident is credible due to empty spaces being required for higher enriched fuel. Additionally, a dropped/misplaced assembly is usually analyzed as well. However, a dropped or misloaded assembly would be analyzed in an air moderated NFSA. This is because of the double contingency principal of ANS-8.1/N16.1-1975 [31] which specifies that it shall require at least two unlikely, independent and concurrent events to produce a criticality accident. This principle precludes the necessity of considering the simultaneous occurrence of multiple accident conditions such as a fuel handling accident occurring at the same time as a flooding accident.

The Surry NFSA has a stainless-steel ceiling and stainless-steel tube covers which prohibits crushing another assembly. Additionally, fuel handling procedures would control which storage cells assemblies are placed in the NFSA. However, an assembly could be misloaded into empty cell locations or dropped in the ceiling opening in the northeastern corner. However, placing a single assembly in the corner or misloading multiple fuel assemblies in an air moderated NFSA is not a criticality safety concern since there is no moderator [32]. Therefore, neither the misloaded assemblies nor crushed assembly accidents need to be analyzed.

7.7.3 Seismic Event

A seismic event is commonly analyzed as well. During a seismic event, free standing equipment shifts around which can move fuel closer or farther apart. However, the Surry NFSA has no free-standing equipment except for the assemblies inside the stainless-steel tubes. Therefore, the fuel assemblies will shift inside the stainless-steel tubes, but that scenario is covered by Section 7.3.3 (Asymmetric Placement of Assemblies). No other components will shift around so no additional cases need to be run.

8 Depletion Modeling and Burnup Effects

This section describes the Surry SCALE 6.2.3 (TRITON) depletion models and conservative depletion conditions suitable for use in the Surry SFP criticality calculations.

8.1 *Depletion Method Overview*

TRITON depletions are used to determine the isotopic content of depleted fuel for Spent Fuel Pool criticality analysis, specifically to develop burnup curves (required minimum fuel burnup as a function of initial enrichment). Performing TRITON depletions requires a SCALE model of an axial segment of a fuel assembly that includes geometry, material content, and depletion conditions (fuel temperature, moderator temperature and density, soluble boron, presence of burnable absorbers and/or control rods, and depletion power).

Conservatism (maximizing SFP fuel reactivity) is incorporated via use of a bounding fuel assembly design and by choice of input depletion conditions that bound anticipated actual fuel depletion conditions. The methodology associated with determination of conservative models and conditions is consistent with that used for the recently accepted License Amendment Requests [14, 23] and NEI 12-16 [32].

Section 6 provides information on the depletion computer code used (TRITON), the cross section library (238 group ENDF/B-VII), decay code used (ORIGAMI), how it was run (number of neutrons followed, time step size, isotopes followed, and cooling time), and the validation.

Each fuel assembly is modeled using 18 equal size axial nodes. For each node the burnup is the product of the assembly average burnup and the relative axial burnup distribution (Section 8.6). The axial burnup distribution also provides the averaged axial power distribution which is used to determine depletion conditions for each node. The following parameters are included in the considerations for each depletion node:

- Assembly power (Section 8.2)
- Soluble boron (Section 8.3)
- Moderator temperature and density (Section 8.4)
- Fuel temperature (Section 8.5)
- Axial burnup shape (Section 8.6)
- Control rod insertion history (Section 8.8)
- Horizontal or planar burnup shape (Sections 8.11)
- Spacer grids (Section 8.12)
- Fuel density (Section 7.2.5)
- In-core thimble for flux map detectors (Section 8.9)
- Burnable absorber and history (Section 8.7)

- Reduced Power Prior to Discharge (Section 8.10)

TRITON models are conservative in the sense that fuel features and depletion conditions will be selected to accommodate past, present, and expected future fuel designs and depletion history in a way that maximizes Spent Fuel Pool (SFP) k. TRITON models are best estimate in the sense that uncertainties in fuel features (such as clad OD design tolerance) are not considered. However, the majority of inputs are conservatively bounding. The methodology associated with determination of conservative models and conditions is consistent with previous analyses. [14, 23]

Each of these features or conditions will be evaluated using fuel design information, core design history, and operating history. Justification for the conservatism of each feature or condition will be provided using first principles, prior evaluations, or TRITON depletion sensitivity cases.

Throughout Section 8, sensitivity cases were run to get a general understanding of how much each parameter affects the SFP k-eff. For sensitivity calculations, only axial node 16 is used in the calculation rather than running the full 18 axial nodes. Node 16 is near the top of the fuel which is the most reactive location in SFP applications where depleted PWR fuel is analyzed. However, Node 16 is not at the extreme edge of the fuel which loses importance because of neutron leakage. Therefore, Node 16 is appropriate to use when calculating the relative change of SFP k-eff (but not the absolute SFP k-eff).

Additionally, the Section 8 sensitivity case k-effs are run at SFP conditions. The temperature is modeled at 150°F, the SFP is unborated, and the SFP is undamaged (the rack pitch and fuel pin pitch is nominal).

8.2 *Bounding Fuel Assembly Depletion Power*

Fuel and moderator temperatures depend in part on the fuel assembly power. Depletion with higher fuel and moderator temperature increases fuel reactivity in the SFP via increased Pu production resulting from a harder depletion neutron spectrum. Therefore, a bounding high power is desired for depletion.

The assembly average power for depletion to a particular fuel burnup is chosen to bound the average power an actual assembly could sustain from initial use through the fuel burnup being analyzed (the burnup averaged assembly power). Burnup averaged nodal fuel and moderator temperatures are calculated for the depletion analysis using the highest **b**urnup **a**veraged **r**elative

assembly **p**ower (BARAP). The BARAP at the end of each cycle is the accumulated assembly burnup divided by the sum of the cycle burnups for all cycles the assembly has resided in the core.

$$\mathrm{BARAP_j} = \frac{\text{Assembly EOL Burnup}_\mathrm{j}}{\sum_{i=1}^{n} \text{Cycle Burnups}_i}$$

where,

j is the specific assembly which the BARAP is being calculated for

i is a cycle that assembly j was burned in

n is the number of cycles that assembly j was burned in.

For each assembly in Surry Unit 1 Cycles 1-29 and Surry Unit 2 Cycles 1-28, the burnup at the end of each cycle divided by the accumulated cycle burnup was calculated and plotted in Figure 8-1 versus the assembly burnup. Figure 8-1 also shows a bounding a line for the BARAP as a function of burnup. Table 8-1 shows the breakpoints and values for the bounding (high) BARAP function. This BARAP function will be used as input to calculate depletion power, fuel temperature, and moderator temperature.

Additionally, sensitivity cases were run to determine the sensitivity of the SFP k-eff to the depletion power. The TRITON inputs were calculated with a BARAP input increased by 0.05. The operating temperatures were also updated according to the increased power. Only node 16 was run to show relative differences between depletion powers. The results show depletion power only has a weak effect on reactivity. At 20 GWD/MTU, the increased power did not result in significant reactivity differences. At 40 GWD/MTU, the increased power resulted in an increase of 67 pcm which is small relative to the total depletion effect.

Figure 8-1: Bounding Burnup Averaged Relative Assembly Power

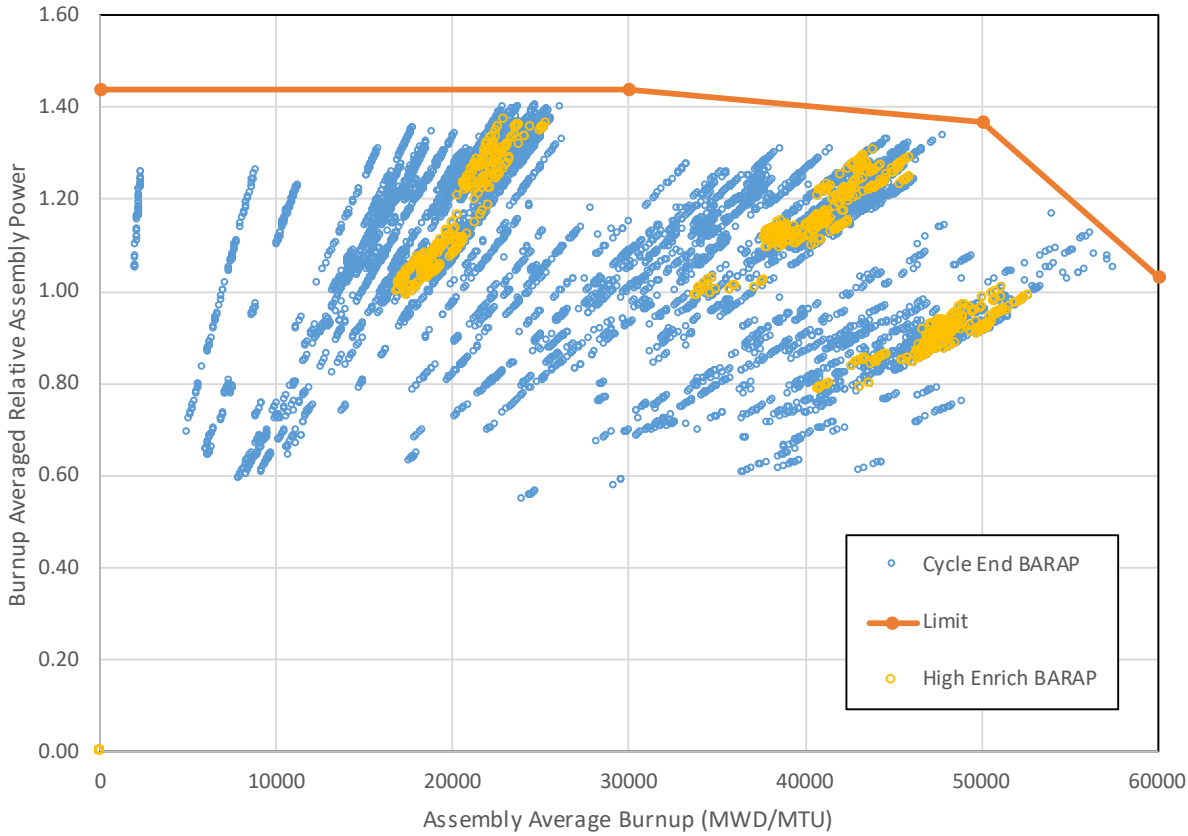

Table 8-1: Bounding BARAP versus Burnup
(Linearly interpolate for intermediate points)

Burnup (MWD/MTU)	RPD
0	1.44
30000	1.44
50000	1.37
60000	1.03

Table 8-2: Sensitivity Cases with Increased Depletion Power

Case Description	Burnup	SFP k-eff	σ	Δk	Δk/RSS(σ)	ρ (pcm)
Nominal	20 GWD/MTU	0.86849	0.00008	--	--	--
Increased Power 5%		0.86834	0.00007	-0.00014	-139%	-19
Nominal	40 GWD/MTU	0.76310	0.00007	--	--	--
Increased Power 5%		0.76349	0.00007	0.00039	390%	67

8.3 *Bounding Depletion Boron*

Spent fuel reactivity is increased by depletion at higher soluble boron. Cycle average soluble boron concentration is calculated by trapezoidal integration of boron versus cycle burnup for cycles S1C01 – S1C30 and S2C01 – S2C29. Measured average boron concentrations were calculated for cycles which data was available (S1C23/S2C23 and onwards). Predicted boron concentrations were determined from the predicted critical boron concentrations from Dominion's qualified reactor neutronics benchmarking depletion calculations.

Figure 8-2 shows that a boron concentration of 850 ppm bounds all cycle averages except for S1C10. S1C10 shut down early due to a fuel failure. The only relevant difference between S1C10 and S1C10A is that Assembly 4G7 was replaced with Assembly 2U0. Therefore, with the exception of Assembly 4G7, all the assemblies in S1C10 will be bounded by the depletion parameter of 850 ppm because the average of S1C10 and S1C10A is 749 ppm. Assembly 4G7 is dispositioned in Section 9.3.1.

Note that there is ORNL research that concludes that mid-cycle shutdowns can be non-conservative when assuming a constant depletion boron [38]. However, with the exception of the dispositioned assembly 4G7, shutdown between S1C10 and S1C10A should not be considered a "mid-cycle shutdown" for these purposes. All of the S1C10 fuel, except for 4G7, were present for the entire cycle.

Table 8-3 shows the sensitivity of the SFP k-eff to the depletion boron concentration. The TRITON depletion cases were run with 850 and 900 ppm of boron. Only node 16 was run to show relative differences between depletion boron levels. The k-eff was then calculated in a unborated spent fuel pool. The results show that depletion boron only has a minor effect on the spent fuel pool reactivity. At 20 and 40 GWD/MTU, 50 ppm of depletion boron is only worth 26 pcm and 65 pcm respectively. When compared to the Monte Carlo uncertainty and the total depletion effect, these differences are relatively small.

Extra test cases were run to see if the SFP reactivity difference would change if the SFP was borated to 2250 ppm instead of unborated. When the depletion boron was increased by 50 ppm, the Δk of the borated and unborated SFP cases were statistically equal.

Figure 8-2: Surry Bounding Cycle Average Soluble Boron

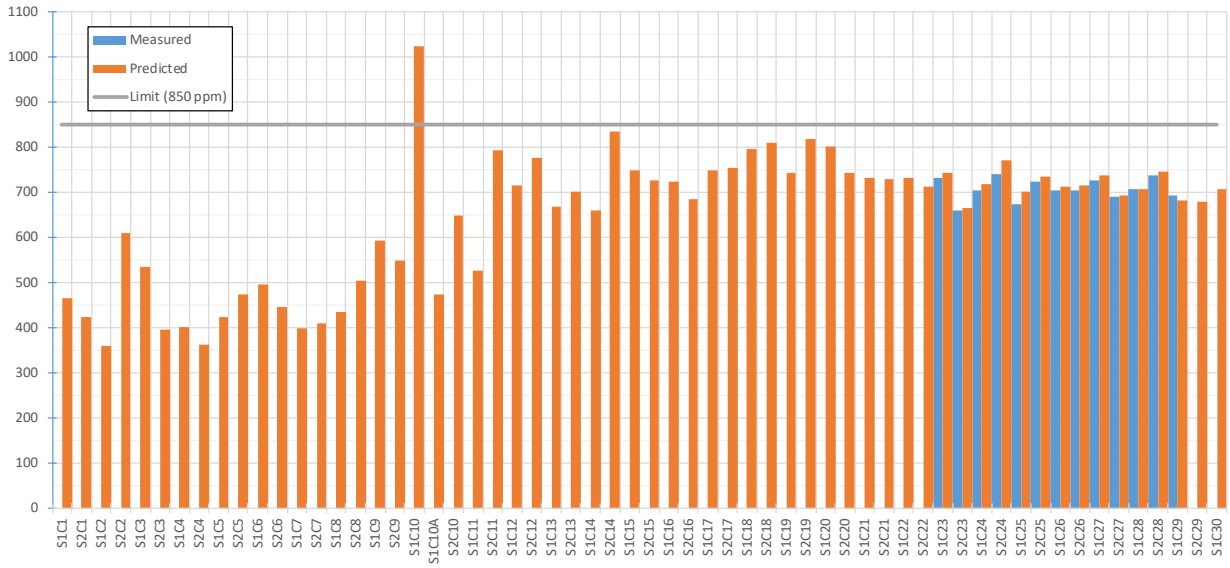

Table 8-3: Sensitivity Cases with Increased Depletion Boron

Case Description	Burnup	SFP k-eff	σ	Δk	Δk/RSS(σ)	ρ (pcm)
Nominal (850 ppm)	20 GWD/MTU	0.86849	0.00008	--	--	--
Increased Boron 50 ppm		0.86868	0.00007	0.00020	186%	26
Nominal (850 ppm)	40 GWD/MTU	0.76310	0.00007	--	--	--
Increased Boron 50 ppm		0.76348	0.00007	0.00038	387%	65

Bounding RCS Temperature

8.4 Higher depletion moderator temperature produces more plutonium and increases burned fuel k-eff in the SFP. Calculation of the bounding high Reactor Coolant System (RCS) temperature is performed using a simple heat balance with the input variables: 1) minimum RCS flow (Core Operating Limit), 2) burnup averaged relative assembly power (maximum from Figure 8-1), 3) core power (bounds all historical cycles), and 4) nominal RCS pressure (bounds all historical cycles). The RCS flow is further reduced by a high bypass flow.

Rated core power, inlet temperature, RCS flow, and bypass flow data is given on Table 8-4. Average fuel assembly moderator exit temperature is calculated via simple heat balance to determine most limiting historical T/H conditions. Table 8-4 shows the results of the exit temperature calculation. The most limiting cycle is S1C25. Exit temperature is taken as the key metric for bounding RCS temperature because the reactivity of depleted PWR fuel is dominated by the top region of the fuel. Table 8-5 shows the inputs for the bounding moderator temperature and density calculation.

Table 8-4 shows that the RCS temperature calculation inputs described in Table 8-5 produce a bounding core average moderator outlet temperature. These inputs are expected to remain bounding for future cycles.

The depletion moderator temperature of each of the 18 nodes of a fuel assembly is calculated as follows. The fuel assembly average power is BARAP times the core average assembly power. The axial power profile is the appropriate NUREG normalized burnup profile or uniform profile (Section 8.6). With the fuel assembly power and the axial power profile known, the nodal average moderator enthalpy (average of the enthalpy at the upper and lower boundaries of the node) is determined for each of the 18 axial nodes starting from the calculated core inlet and integrating the enthalpy added in each successive node. Moderator temperature and density is determined from moderator enthalpy using a pressure of 2250 psia.

Sensitivity cases were run to determine the effect of moderator temperature (with the corresponding density) during depletion on the Spent Fuel Pool reactivity. The moderator temperature was increased 5°F (or ~2.8 Kelvin absolute degrees) in the depletion cases. Since the moderator temperature affects the temperature of the other materials in the core, all other temperatures in the TRITON case were increased by 5°F. The results of the sensitivity cases are shown in Table 8-6. The results show that moderator temperature can have a significant impact at higher burnups.

Table 8-4: RCS Thermal Hydraulic History for Surry

Cycle	Inputs						Calculations									
	Power [MW]	RPD	Pressure [psia]	T_ave,vessel [°F]	Vessel Flow [gpm]	Bypass Flow [%]	ρ_ave,vessel [lbm/ft^3]	m^dot_vessel [lbm/hr]	Δh_vessel [Btu/lbm]	h_ave,vessel [Btu/lbm]	h_in [Btu/lbm]	Core Flow [gpm]	Core Flow [lbm/hr]	ΔEnthalpy [Btu/lbm]	h_out,core [Btu/lbm]	T_out,core [°F]
S1C01	2441	1	2250	564.0	285,561	4.50%	45.92	1.05E+08	79.20	564.74	525.14	272,711	1.00E+08	82.9	608.1	596.5
S1C02	2441	1	2250	565.0	278,538	4.50%	45.85	1.02E+08	81.32	566.02	525.36	266,004	9.78E+07	85.1	610.5	598.2
S1C03	2441	1	2250	566.0	271,515	4.50%	45.78	9.97E+07	83.55	567.31	525.53	259,297	9.52E+07	87.5	613.0	600.0
S1C04	2441	1	2250	566.0	264,489	4.50%	45.78	9.71E+07	85.76	567.31	524.42	252,587	9.27E+07	89.8	614.2	600.8
S1C05	2441	1	2250	566.4	257,175	4.50%	45.75	9.44E+07	88.26	567.82	523.69	245,602	9.01E+07	92.4	616.1	602.1
S1C06	2441	1	2250	574.0	285,561	4.50%	45.21	1.04E+08	80.43	577.68	537.47	272,711	9.89E+07	84.2	621.7	606.0
S1C07	2441	1	2250	574.4	285,000	4.50%	45.18	1.03E+08	80.64	578.21	537.89	272,175	9.86E+07	84.4	622.3	606.4
S1C08	2441	1	2250	574.4	283,533	4.50%	45.18	1.03E+08	81.06	578.21	537.68	270,774	9.81E+07	84.9	622.6	606.6
S1C09	2441	1	2250	574.4	284,425	4.50%	45.18	1.03E+08	80.80	578.21	537.81	271,626	9.84E+07	84.6	622.4	606.5
S1C10	2441	1	2250	574.4	286,606	4.50%	45.18	1.04E+08	80.19	578.21	538.11	273,709	9.92E+07	84.0	622.1	606.3
S1C10A	2441	1	2250	574.4	286,606	3.60%	45.18	1.04E+08	80.19	578.21	538.11	276,288	1.00E+08	83.2	621.3	605.7
S1C11	2441	1	2250	574.4	284,731	3.60%	45.18	1.03E+08	80.72	578.21	537.85	274,481	9.95E+07	83.7	621.6	605.9
S1C12	2441	1	2250	574.4	284,731	3.60%	45.18	1.03E+08	80.72	578.21	537.85	274,481	9.95E+07	83.7	621.6	605.9
S1C13	2441	1	2250	574.4	284,731	3.60%	45.18	1.03E+08	80.72	578.21	537.85	274,481	9.95E+07	83.7	621.6	605.9
S1C14	2546	1	2250	573.0	285,104	3.60%	45.28	1.04E+08	83.89	576.38	534.43	274,840	9.98E+07	87.0	621.5	605.8
S1C15	2546	1	2250	573.0	285,104	3.60%	45.28	1.04E+08	83.89	576.38	534.43	274,840	9.98E+07	87.0	621.5	605.8
S1C16	2546	1	2250	573.0	285,104	3.60%	45.28	1.04E+08	83.89	576.38	534.43	274,840	9.98E+07	87.0	621.5	605.8
S1C17	2546	1	2250	573.0	285,104	3.60%	45.28	1.04E+08	83.89	576.38	534.43	274,840	9.98E+07	87.0	621.5	605.8
S1C18	2546	1	2250	573.0	285,104	3.60%	45.28	1.04E+08	83.89	576.38	534.43	274,840	9.98E+07	87.0	621.5	605.8
S1C19	2546	1	2250	573.0	285,104	3.60%	45.28	1.04E+08	83.89	576.38	534.43	274,840	9.98E+07	87.0	621.5	605.8
S1C20	2546	1	2250	573.0	285,104	3.60%	45.28	1.04E+08	83.89	576.38	534.43	274,840	9.98E+07	87.0	621.5	605.8
S1C21	2546	1	2250	573.0	285,104	4.50%	45.28	1.04E+08	83.89	576.38	534.43	272,274	9.89E+07	87.8	622.3	606.4
S1C22	2546	1	2250	573.0	285,183	4.60%	45.28	1.04E+08	83.87	576.38	534.44	272,065	9.88E+07	87.9	622.4	606.5
S1C23	2546	1	2250	573.0	285,157	4.60%	45.28	1.04E+08	83.88	576.38	534.44	272,040	9.88E+07	87.9	622.4	606.5
S1C24	2587	1	2250	573.0	285,420	4.60%	45.28	1.04E+08	85.15	576.38	533.80	272,291	9.89E+07	89.3	623.1	606.9
S1C25	2587	1	2250	573.0	285,157	4.90%	45.28	1.04E+08	85.23	576.38	533.76	271,184	9.85E+07	89.6	623.4	607.2
S1C26	2587	1	2250	573.0	285,262	4.90%	45.28	1.04E+08	85.19	576.38	533.78	271,284	9.85E+07	89.6	623.4	607.1
S1C27	2587	1	2250	573.0	285,262	4.90%	45.28	1.04E+08	85.19	576.38	533.78	271,284	9.85E+07	89.6	623.4	607.1
S1C28	2587	1	2250	573.0	288,904	4.90%	45.28	1.05E+08	84.12	576.38	534.32	274,748	9.98E+07	88.5	622.8	606.7
S1C29	2587	1	2250	573.0	289,004	4.90%	45.28	1.05E+08	84.09	576.38	534.33	274,843	9.98E+07	88.4	622.8	606.7
Bounding	2587	1	2250	573.0	274,000	6.00%	45.28	9.95E+07	88.70	576.38	532.03	257,560	9.36E+07	94.4	626.4	609.2
Bounding	2587	1.44	2250	573.0	274,000	6.00%	45.28	9.95E+07	127.72	576.38	512.51	257,560	9.36E+07	135.9	648.4	623.6

*Note that the “Bounding” rows result in core exit temperatures which are bounding for both Surry Unit 1 and Unit 2.

Table 8-4: RCS Thermal Hydraulic History for Surry (cont.)

Cycle	Inputs						Calculations									
	Power [MW]	RPD	Pressure [psia]	T_ave,vessel [°F]	Vessel Flow [gpm]	Bypass Flow [%]	ρ_ave,vessel [lbm/ft3]	m^dot_vessel [lbm/hr]	Δh_vessel [Btu/lbm]	h_ave,vessel [Btu/lbm]	h_in [Btu/lbm]	Core Flow [gpm]	Core Flow [lbm/hr]	ΔEnthalpy [Btu/lbm]	h_out,core [Btu/lbm]	T_out,core [°F]
S2C01	2441	1	2250	564.0	298,137	4.50%	45.92	1.10E+08	75.86	564.74	526.81	284,721	1.05E+08	79.4	606.2	595.2
S2C02	2441	1	2250	566.0	287,817	4.50%	45.78	1.06E+08	78.81	567.31	527.90	274,865	1.01E+08	82.5	610.4	598.1
S2C03	2441	1	2250	564.7	277,497	4.50%	45.87	1.02E+08	81.58	565.64	524.85	265,010	9.75E+07	85.4	610.3	598.0
S2C04	2441	1	2250	564.0	268,680	4.50%	45.92	9.90E+07	84.17	564.74	522.66	256,589	9.45E+07	88.1	610.8	598.4
S2C05	2441	1	2250	564.0	299,463	4.50%	45.92	1.10E+08	75.52	564.74	526.98	285,987	1.05E+08	79.1	606.1	595.0
S2C06	2441	1	2250	574.0	299,463	4.50%	45.21	1.09E+08	76.70	577.68	539.34	285,987	1.04E+08	80.3	619.6	604.6
S2C07	2441	1	2250	574.0	296,769	4.50%	45.21	1.08E+08	77.39	577.68	538.99	283,414	1.03E+08	81.0	620.0	604.9
S2C08	2441	1	2250	574.4	298,182	4.50%	45.18	1.08E+08	77.08	578.21	539.67	284,764	1.03E+08	80.7	620.4	605.1
S2C09	2441	1	2250	574.4	296,210	4.50%	45.18	1.07E+08	77.59	578.21	539.41	282,881	1.03E+08	81.2	620.7	605.3
S2C10	2441	1	2250	574.4	296,738	4.50%	45.18	1.08E+08	77.45	578.21	539.48	283,385	1.03E+08	81.1	620.6	605.2
S2C11	2441	1	2250	574.4	296,901	3.60%	45.18	1.08E+08	77.41	578.21	539.51	286,213	1.04E+08	80.3	619.8	604.7
S2C12	2441	1	2250	574.4	296,901	3.60%	45.18	1.08E+08	77.41	578.21	539.51	286,213	1.04E+08	80.3	619.8	604.7
S2C13	2546	1	2250	574.4	296,901	3.60%	45.18	1.08E+08	80.74	578.21	537.84	286,213	1.04E+08	83.8	621.6	605.9
S2C14	2546	1	2250	574.4	297,302	3.60%	45.18	1.08E+08	80.63	578.21	537.89	286,599	1.04E+08	83.6	621.5	605.9
S2C15	2546	1	2250	573.0	297,302	3.60%	45.28	1.08E+08	80.45	576.38	536.15	286,599	1.04E+08	83.5	619.6	604.6
S2C16	2546	1	2250	573.0	292,826	3.60%	45.28	1.06E+08	81.68	576.38	535.54	282,284	1.03E+08	84.7	620.3	605.0
S2C17	2546	1	2250	573.0	292,826	3.60%	45.28	1.06E+08	81.68	576.38	535.54	282,284	1.03E+08	84.7	620.3	605.0
S2C18	2546	1	2250	573.0	292,826	3.60%	45.28	1.06E+08	81.68	576.38	535.54	282,284	1.03E+08	84.7	620.3	605.0
S2C19	2546	1	2250	573.0	292,641	3.60%	45.28	1.06E+08	81.73	576.38	535.51	282,106	1.02E+08	84.8	620.3	605.0
S2C20	2546	1	2250	573.0	292,641	3.60%	45.28	1.06E+08	81.73	576.38	535.51	282,106	1.02E+08	84.8	620.3	605.0
S2C21	2546	1	2250	573.0	292,826	4.40%	45.28	1.06E+08	81.68	576.38	535.54	279,942	1.02E+08	85.4	621.0	605.5
S2C22	2546	1	2250	573.0	292,826	4.60%	45.28	1.06E+08	81.68	576.38	535.54	279,356	1.01E+08	85.6	621.2	605.6
S2C23	2546	1	2250	573.0	292,799	4.60%	45.28	1.06E+08	81.69	576.38	535.53	279,330	1.01E+08	85.6	621.2	605.6
S2C24	2587	1	2250	573.0	293,063	4.60%	45.28	1.06E+08	82.93	576.38	534.91	279,582	1.02E+08	86.9	621.8	606.1
S2C25	2587	1	2250	573.0	293,063	4.90%	45.28	1.06E+08	82.93	576.38	534.91	278,703	1.01E+08	87.2	622.1	606.3
S2C26	2587	1	2250	573.0	293,827	4.90%	45.28	1.07E+08	82.71	576.38	535.02	279,429	1.01E+08	87.0	622.0	606.2
S2C27	2587	1	2250	573.0	293,959	4.90%	45.28	1.07E+08	82.67	576.38	535.04	279,555	1.02E+08	86.9	622.0	606.2
S2C28	2587	1	2250	573.0	288,904	4.90%	45.28	1.05E+08	84.12	576.38	534.32	274,748	9.98E+07	88.5	622.8	606.7
S2C29	2587	1	2250	573.0	289,103	4.90%	45.28	1.05E+08	84.06	576.38	534.34	274,937	9.99E+07	88.4	622.7	606.7
Bounding	2587	1	2250	573.0	274,000	6.00%	45.28	9.95E+07	88.70	576.38	532.03	257,560	9.36E+07	94.4	626.4	609.2
Bounding	2587	1.44	2250	573.0	274,000	6.00%	45.28	9.95E+07	127.72	576.38	512.51	257,560	9.36E+07	135.9	648.4	623.6

*Note that the “Bounding” rows result in core exit temperatures which are bounding for both Surry Unit 1 and Unit 2.

Table 8-5: RCS Thermal Hydraulic History for Surry

Parameter	Value	Basis
Reactor Thermal Power	2587 MW	Bounds historical data
Assembly Relative Power	Burnup (MWD/MTU) / RPD 0 / 1.44 30000 / 1.44 50000 / 1.37 60000 / 1.03	Bounds historical data
RCS Pressure	2250 psia	Bounds historical data
Vessel Flow Rate	274,000 gpm	COLR Limit
Bypass Flow Rate	6.00%	Bounds historical data
HFP Average RCS Temperature	573°F	COLR Limit

Table 8-6: Sensitivity Cases with Increased Moderator Temperature

Case Description	Burnup	SFP k-eff	σ	Δk	Δk/RSS(σ)	ρ (pcm)
Nominal	20 GWD/MTU	0.86849	0.00008	--	--	--
Increased Moderator Temperature 5F		0.86866	0.00007	0.00017	163%	22
Nominal	40 GWD/MTU	0.76310	0.00007	--	--	--
Increased Moderator Temperature 5F		0.76425	0.00007	0.00115	1179%	197

8.5 *Bounding Fuel Temperature*

Higher depletion fuel temperature increases depleted fuel reactivity in the SFP by increasing U-238 neutron capture and production of Pu. Calculation of fuel temperature is performed on a nodal basis and is dependent on local specific power, local moderator temperature, and fuel burnup.

Depletion fuel temperatures are determined for each fuel node using the nodal moderator temperature and fuel temperature difference from the moderator temperature, which is dependent on the nodal fuel power and burnup. The fuel temperature data is taken from the SIMULATE-5 model used by Dominion for its licensed fuel management analysis. [24] Fuel temperatures are pellet average. Fuel temperature data (a function of power and burnup) used for this calculation is also integrated to the burnup of interest to obtain an appropriate depletion average temperature rather than an instantaneous value at a particular burnup. Table 8-7 shows the fuel temperature calculation for an array of burnups.

Sensitivity cases were run to determine the effect of fuel temperature during depletion on the Spent Fuel Pool reactivity. The fuel temperature to moderator temperature difference was increased by 5%. The results of the sensitivity cases are shown in Table 8-8. The results show that fuel temperature only has a minor effect on the spent fuel pool reactivity. At 20 GWD/MTU, the results are not statistically different when the fuel temperature is increased. At 40 GWD/MTU, a 5% increase of the temperature difference between the fuel and moderator is only worth 53 pcm. When compared to the Monte Carlo uncertainty and the total depletion effect, this difference is relatively small.

Table 8-7: Example Calculations for Fuel Temperature

	Burnup (GWD/MTU)								
	0	5	10	15	20	30	40	50	65
Assembly Relative Power [§ 8.2]	1.44	1.44	1.44	1.44	1.44	1.44	1.405	1.37	0.86
Fuel-to-Moderator ΔTemperature (K) [§ 8.5]	505	501	497	493	489	485	476	472	298
Moderator Temperature (K) [§ 8.4]	574	574	574	574	574	574	574	574	574
Fuel Temperature (K) [Calculated]	1079	1075	1071	1066	1062	1059	1050	1046	872

Table 8-8: Sensitivity Cases with Increased Moderator Temperature

Case Description	Burnup	SFP k-eff	σ	Δk	Δk/RSS(σ)	ρ (pcm)
Nominal	20 GWD/MTU	0.86849	0.00008	--	--	--
Increased Fuel Temperature dT 5%		0.86846	0.00007	-0.00003	-26%	-4
Nominal	40 GWD/MTU	0.76310	0.00007	--	--	--
Increased Fuel Temperature dT 5%		0.76341	0.00007	0.00031	313%	53

8.6 *Bounding Axial Burnup Profiles*

A uniform axial burnup shape may not always be conservative. Often, the SFP criticality is dominated by the top portion of the fuel assembly due to less burnup due to leakage and more plutonium production due to hotter operating temperatures and control rod insertion. A bounding axial burnup shape will determine how much less burnup the top portion of the fuel receives compared to the assembly average burnup.

NEI 12-16, Section 5.1.4 [32] gives three options to modeling the axial burnup shape. Broadly speaking, the 1st option is to use industry generic axial shapes which have been shown to be bounding, the 2nd option is to take the plant specific most limiting power shape (minimum burnup in each node) without renormalization of the shape, and the 3rd option is to take the plant specific most limiting power shape (minimum burnup in each node) with renormalization of the shape. Note that for all options, uniform shapes need to also be considered and the limiting of the two options used when calculating the burnup curves. The 1st option was chosen for this analysis (industry generic axial shapes).

Consistent with NEI 12-16, site-specific verification that the NUREG/CR-6801 shapes are bounding is required. NUREG/CR-6801 [9] states that the slope of the burnup at the top of the fuel is the primary driver of the end effect in the Spent Fuel Pool.

> *Although the end effect is dependent upon many factors, it is primarily dependent on the slope of the burnup profile near the ends of the fuel, which is influenced by the fuel burnup, assembly design, and reactor operating environment.*

End of cycle axial burnups were calculated for each assembly for the past 20 Surry cycles (10 for each unit) with Simulate5. This equates to data for 3140 assemblies. There are 18 burnups for each assembly corresponding to the 18 uniformly distributed axial nodes (consistent with NUREG/CR-6801). These burnups were compared to the NUREG/CR-6801 burnup shapes. Figures 8-3 through 8-11 shows the comparison between the Surry burnup shapes and the NUREG/CR-6801 burnup shapes. In these figures, the NUREG burnup shape is displayed by a red line and the Surry specific data is displayed by a box and whisker plot. Note that the box and whisker plot will show individual data points if they are considered outliers (formally defined as 1.5 times the interquartile range). No assemblies had an end of cycle burnup of < 14 GWD/MTU.

The figures show that the burnup slope at the top of the fuel is determined by nodes 16 – 18. For all burnup bins, the NUREG burnup slope is steeper than the slope generated by the Surry data. In addition, the NUREG relative burnups for Nodes 17 and 18 are significantly less than the Surry

data which will contribute to a larger end effect. Therefore, the axial burnup shapes from NUREG/CR-6801 are conservative when compared to the site-specific Surry data.

Simulate5 predicted burnups were used instead of measured burnups so that a like to like comparison could be made. Measured burnups are calculated at four axial nodes with Dominions QA codes. It would be impossible to compare the burnup slope with only four nodes. Additionally, predicted data from Simulate5 is acceptable because the predicted axial offset matches reasonably well with measured axial offset. On average, Simulate5 will predict an axial offset ~1.2% too low at Surry. Shifting the power distribution up by 1.2% would move the Surry data in a conservative direction. Therefore, predicted data was used to compare against the NUREG/CR-6801 burnup shapes.

Figure 8-3: NUREG vs. Surry Axial Burnup Shapes, 14-18 GWD/T Burnup Bin

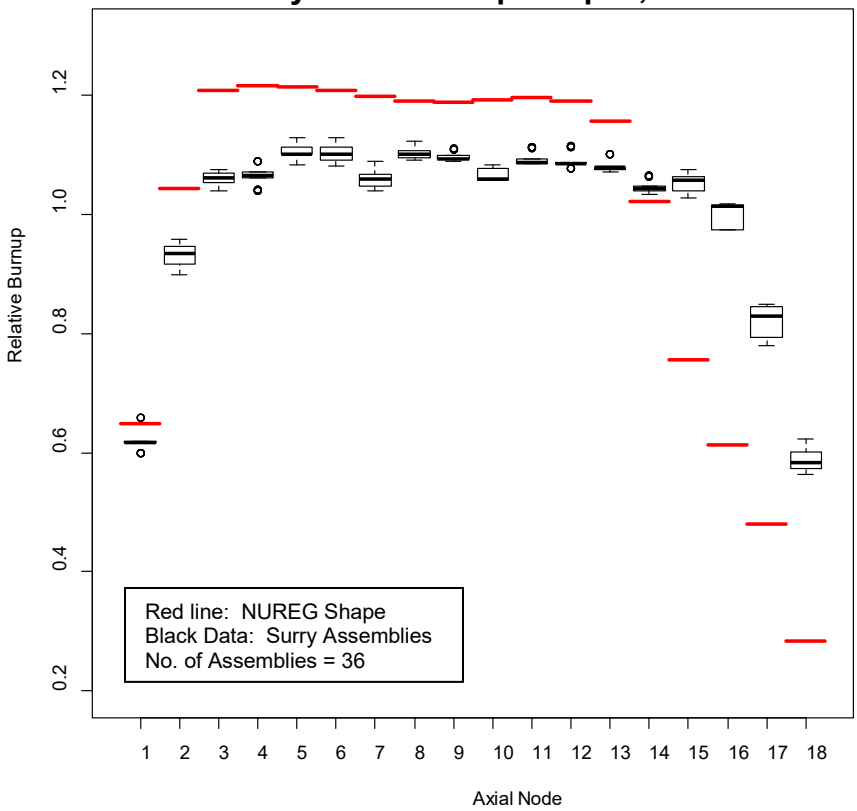

Figure 8-4: NUREG vs. Surry Axial Burnup Shapes, 18-22 GWD/T Burnup Bin

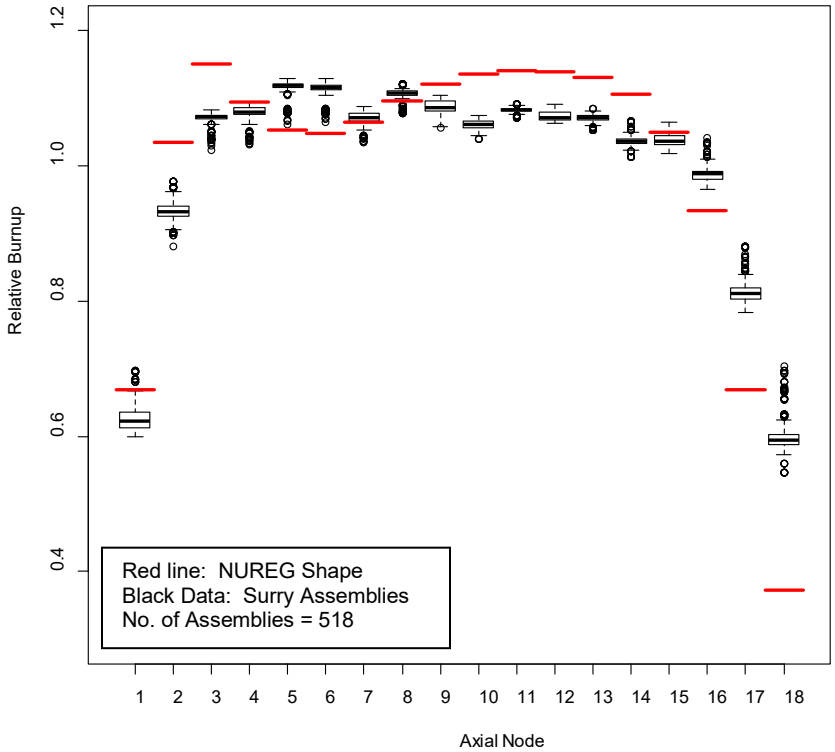

Figure 8-5: NUREG vs. Surry Axial Burnup Shapes, 22-26 GWD/T Burnup Bin

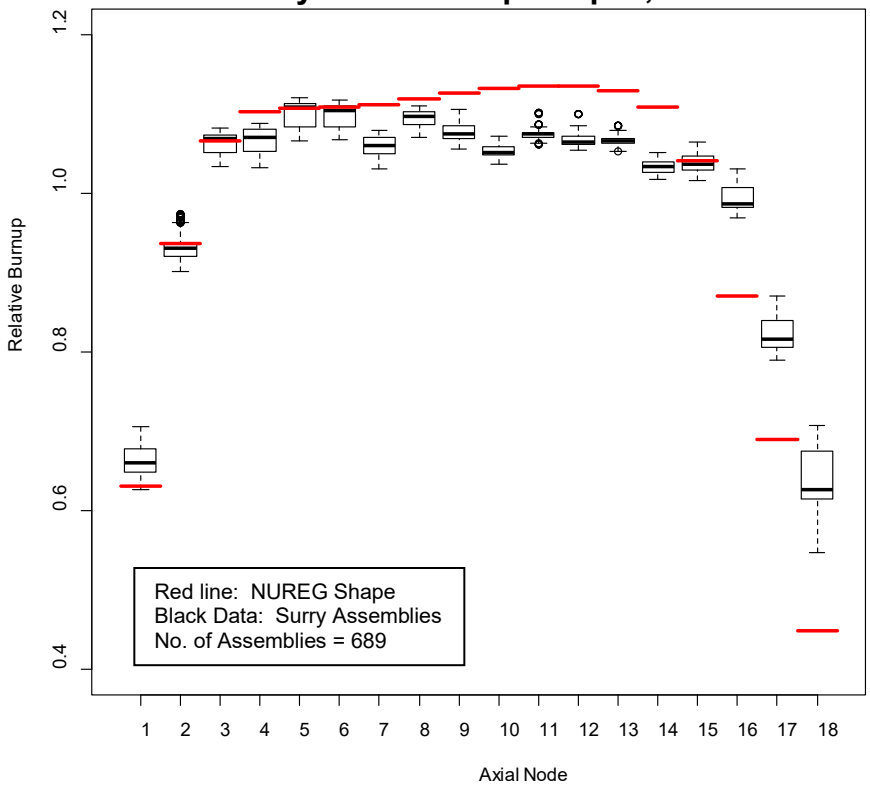

Figure 8-6: NUREG vs. Surry Axial Burnup Shapes, 26-30 GWD/T Burnup Bin

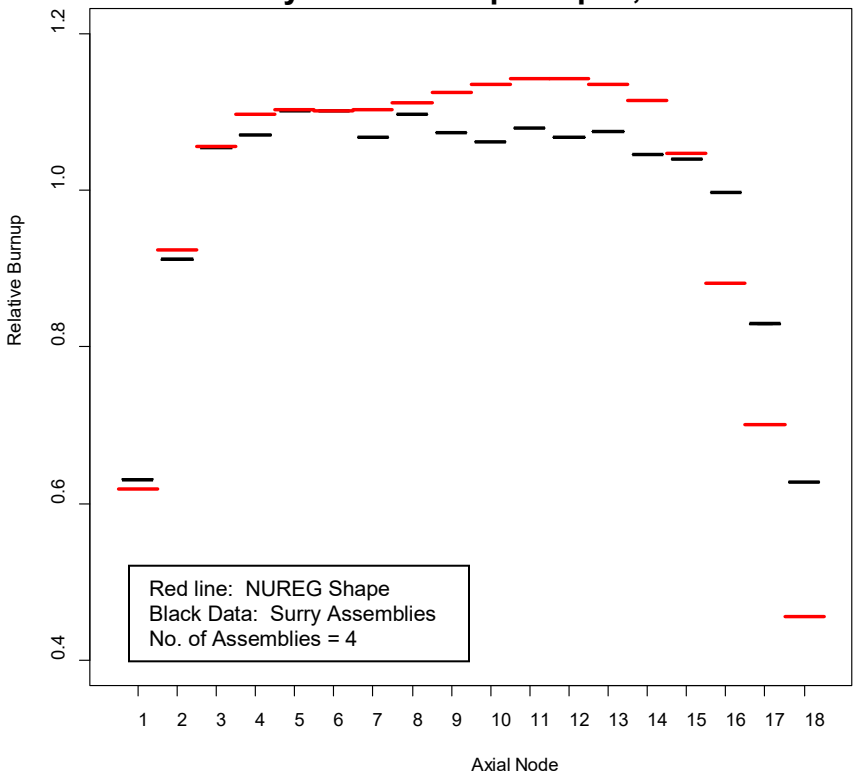

Figure 8-7: NUREG vs. Surry Axial Burnup Shapes, 30-34 GWD/T Burnup Bin

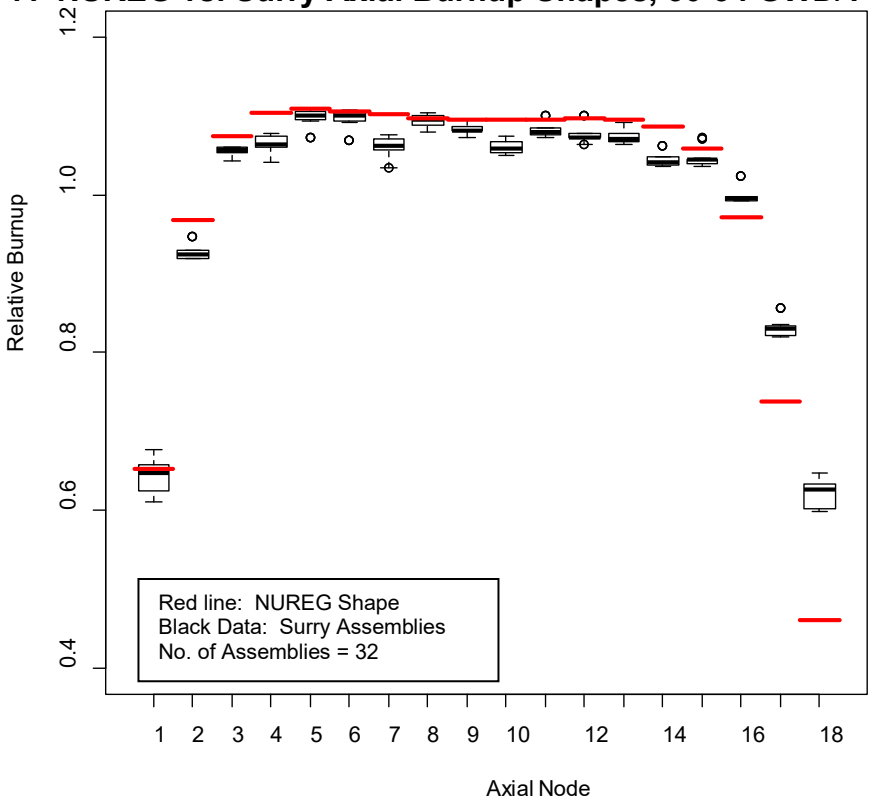

Figure 8-8: NUREG vs. Surry Axial Burnup Shapes, 34-38 GWD/T Burnup Bin

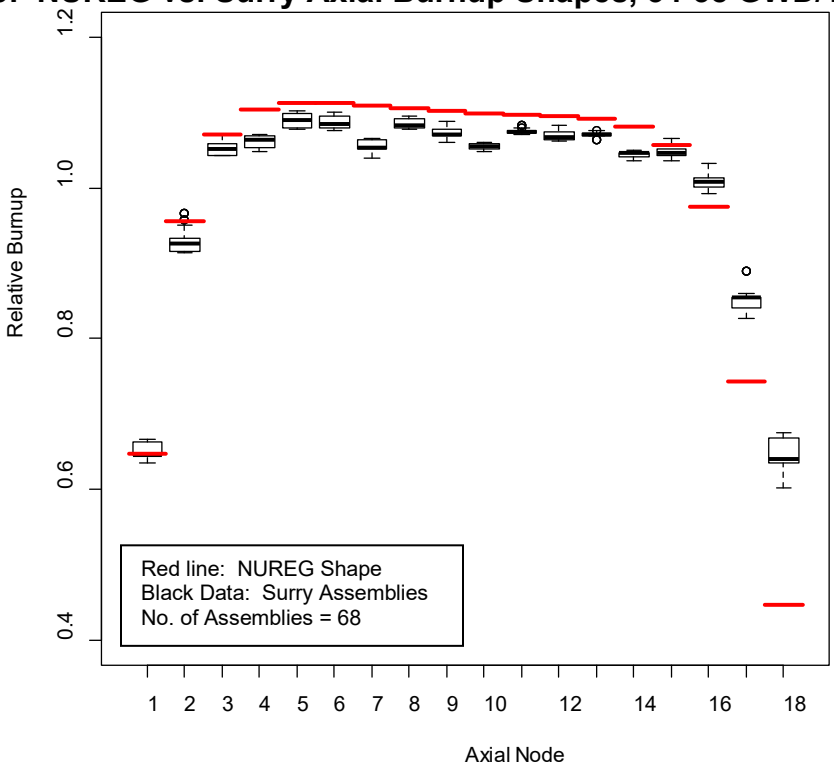

Figure 8-9: NUREG vs. Surry Axial Burnup Shapes, 38-42 GWD/T Burnup Bin

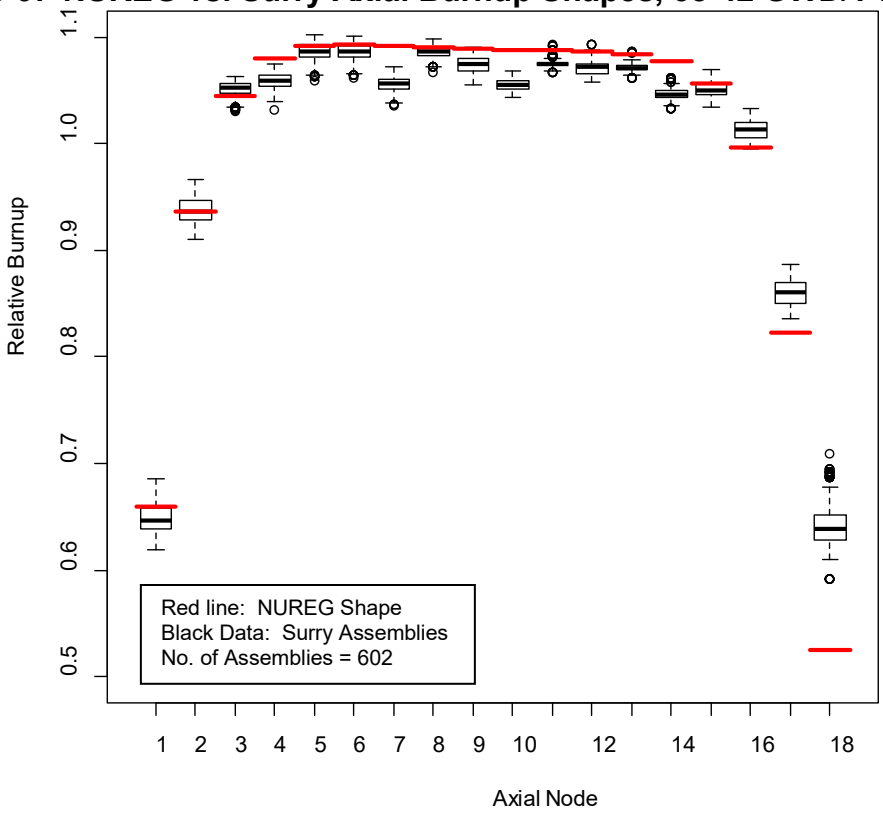

Figure 8-10: NUREG vs. Surry Axial Burnup Shapes, 42-46 GWD/T Burnup Bin

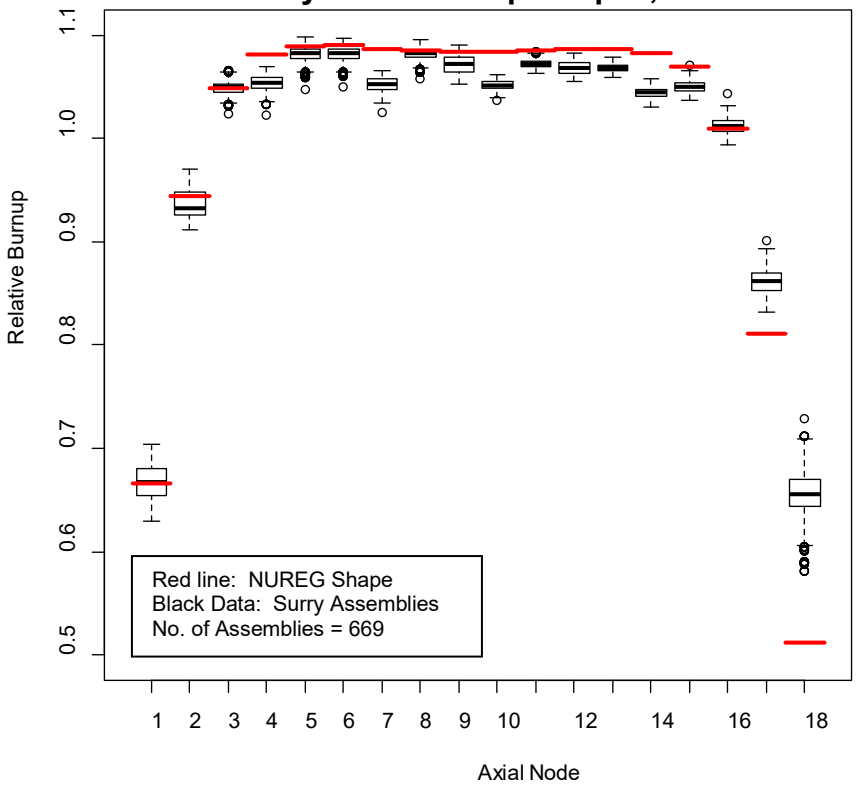

Figure 8-11: NUREG vs. Surry Axial Burnup Shapes, 46-62 GWD/T Burnup Bin

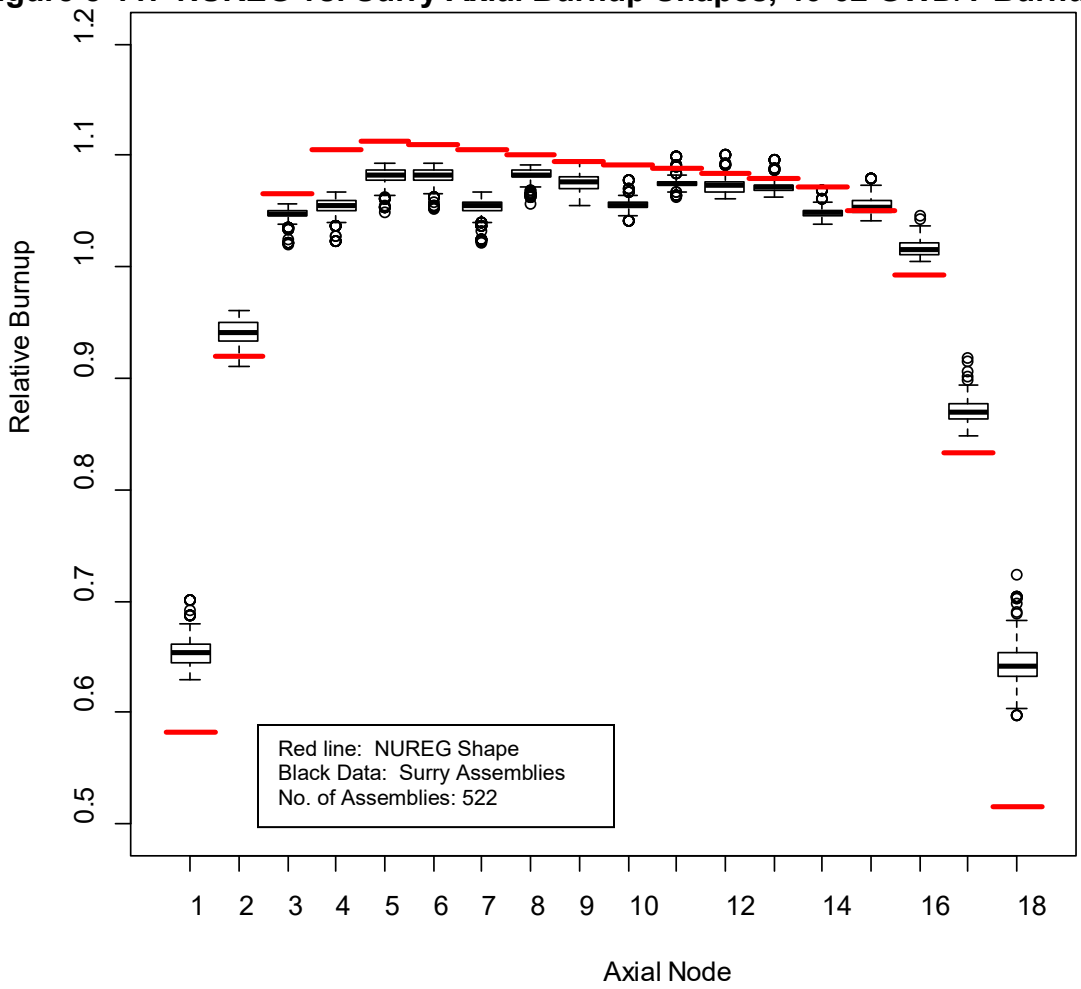

8.7 *Burnable Absorbers*

Several different types of burnable absorber have been used at Surry (detailed in Section 3.2.1). Borosilicate Glass, Alumina B_4C, IFBA, and Gadolinia were modeled for this analysis. These burnable poisons cover all historical and expected burnable poisons types.

All the burnable poisons absorb low energy neutrons and harden the depletion neutron spectrum, increasing spent fuel reactivity. Borosilicate Glass and Alumina B_4C also displace moderator in the guide tubes, which further hardens the depletion neutron spectrum.

Test cases were run to determine an appropriate bounding burnable poison loading. One case had no burnable poisons and was included just for information purposes. For Borosilicate Glass and Alumina B_4C, all 20 guide tubes were filled with discrete BP to bound all assemblies. For IFBA, 148 IFBA pins at 1.5x strength was used to bound the maximum IFBA loading at Surry.

For Gadolinia, it is not clear whether a heavy loading or light loading will be bounding since there are competing effects. More Gadolinia will create a larger isotopic effect, but more gadolinia will also displace more UO_2 fuel. Therefore, two sensitivity cases were run using Gadolinia. One had a gad loading of 8.0 wt% Gd_2O_3 (maximum) and the other had a gad loading of 2.0 wt% Gd_2O_3 (minimum). In the model, the amount of UO_2 in each fuel rod was reduced based on the Gadolinia loading. No enrichment reduction was modeled in these sensitivity cases. Note that gadolinia is the only burnable poison with residual poison in the SFP models. The other poisons are exclusively modeled in the reactor and not in the spent fuel pool.

The results of these sensitivity cases are shown in Table 8-9. The results show that Alumina B_4C is bounding. Therefore, all burnup cases used to calculate the burnup curve in Section 9.1 will be depleted with 20 fingers of Alumina B_4C.

The gad cases show that more Gadolinia decreases SFP reactivity. This is due to residual Gadolinia left in the fuel at lower burnups and the displacement of UO_2 fuel at all burnups. Therefore, any loading of Gadolinia is bounded which is consistent with the guidance in NEI 12-16.

Table 8-9: Depletion with Different Burnable Absorbers

Case Description	Burnup	SFP k-eff	σ	Δk	Δk/RSS(σ)	ρ (pcm)
Nominal (Alumina B_4C)	20 GWD/MTU	0.86849	0.00008	--	--	--
IFBA		0.86617	0.00007	-0.00232	-2219%	-309
Maximum Gad		0.78952	0.00007	-0.07897	-77491%	-11517
Minimum Gad		0.86379	0.00008	-0.00470	-4434%	-627
No BP		0.86446	0.00007	-0.00403	-3851%	-537
Borosilicate glass BP		0.86781	0.00007	-0.00067	-641%	-90
Nominal (Alumina B_4C)	40 GWD/MTU	0.76310	0.00007	--	--	--
IFBA		0.75376	0.00005	-0.00934	-11044%	-1624
Maximum Gad		0.74570	0.00007	-0.01740	-18077%	-3058
Minimum Gad		0.74929	0.00007	-0.01381	-14347%	-2415
No BP		0.75094	0.00007	-0.01216	-12369%	-2122
Borosilicate glass BP		0.76269	0.00007	-0.00041	-422%	-71

To assess the combination of discrete and integral burnable poisons, IFBA and Alumina B_4C are tested. The test cases are depleted out to 40 GWD/MTU and only used IFBA and Alumina B_4C because they are bounding for each type of poison tested.

Table 8-10 shows the results of the sensitivity cases. (Note that the '0 IFBA, 20 Alumina B4C' case in Table 8-10 was modeled slightly different than the 'Nominal' case in Table 8-9 due to the internal review process. This is acceptable since the relative difference is the important value in these cases). . The results show that depletion with 20 Alumina B_4C rods and 0 IFBA bounds 148 IFBA pins with 12 Alumina B_4C rods. Since the burnup curves are generated with 20 Alumina B_4C rods and 0 IFBA pins, the mixed BP combinations of ≤12 Alumina B_4C rods AND ≤148 IFBA rods are bounded. Any combinations with 12 Alumina B_4C rods or 148 IFBA rods must follow the same discrete BP loading pattern shown in Figure 8-12 or IFBA loading pattern shown in Figure 8-13 to be bounded.

Table 8-10: Mixed Burnable Poison Loadings During Depletion

BP Rod Description	SFP k-eff	σ	Δk	Δk/RSS(σ)	ρ (pcm)
0 IFBA, 20 Alumina B_4C	0.76077	0.00007	--	--	--
148 IFBA, 4 Alumina B_4C	0.75364	0.00007	-0.00712	-7518%	-1243
148 IFBA, 8 Alumina B_4C	0.75605	0.00007	-0.00472	-4983%	-821
148 IFBA, 12 Alumina B_4C	0.75840	0.00007	-0.00236	-2458%	-410
148 IFBA, 12 SbBe Source Rods	0.75700	0.00007	-0.00376	-3857%	-654
148 IFBA, 12 Stainless Steel Rods	0.75786	0.00007	-0.00291	-3073%	-505
148 IFBA, 20 Alumina B_4C	0.76339	0.00007	0.00262	2688%	452

Surry currently uses secondary source rods and have used primary source rods. Several different source rod design types have been used at Surry. 1, 3, or 4 finger assembly design types were used for Cycles 1 – 14 (~1972 – 1997). No secondary sources were used from Cycle 15 – Cycle 25. Since Unit 2, Cycle 25 (2014), a 6-finger secondary source design has been used. The 6-finger secondary source design is shown in Table 8-11.

Table 8-11: Secondary Sources Dimensions

Dimension	Value
Clad Material	[redacted]a,c
Source Material	Sb+Be
Tube ID (cm)	[redacted]a,c
Tube OD (cm)	[redacted]a,c

Source rods can affect the fuel isotopics by (i) displacing the moderator, (ii) absorbing thermal neutrons, and (iii) generating neutrons of their own. For the first affect, comparing the outer diameter of the Alumina B_4C rod to the outer diameter of the secondary source rod shows that each discrete BP rod displaces more moderator than each secondary source rod. For the second and third affect, Simulate benchmarking work shows that modeling the secondary source as stainless steel has approximately the same reactivity affect as modeling it as Sb+Be. This means that Sb+Be absorbs a similar number of thermal neutrons as stainless steel which is known to absorb fewer neutrons than B_4C. Modeling the secondary source as stainless-steel rods in Simulate also suggests that the neutron production in the source is negligible when compared to neutrons generated when the reactor is at power. Since each BP rod (i) displaces more moderator, (ii) absorbs more neutrons, and (iii) the neutrons generated by the secondary source are negligible for this application, Alumina B_4C BP rods bound secondary sources of equal or lesser number of rods. The SbBe and stainless steel test cases shown in Table 8-10 support this argument that Alumina B_4C rods bound both source rods and stainless steel rods of equal number. Therefore, Table 8-10 shows that 20 Alumina B_4C rods with 0 IFBA rods bounds $\leq$12 secondary source rods with 148 IFBA rods.

Bounding the secondary source with the burnable absorber is standard practice as NEI 12-16 [4] states “Normally, primary and secondary sources will be covered by the conservatism in the burnable absorber assumptions, but confirmation is necessary.” Confirmation is provided in the paragraph above.

Figure 8-12: Assembly Map with 12 Discrete BP Rods

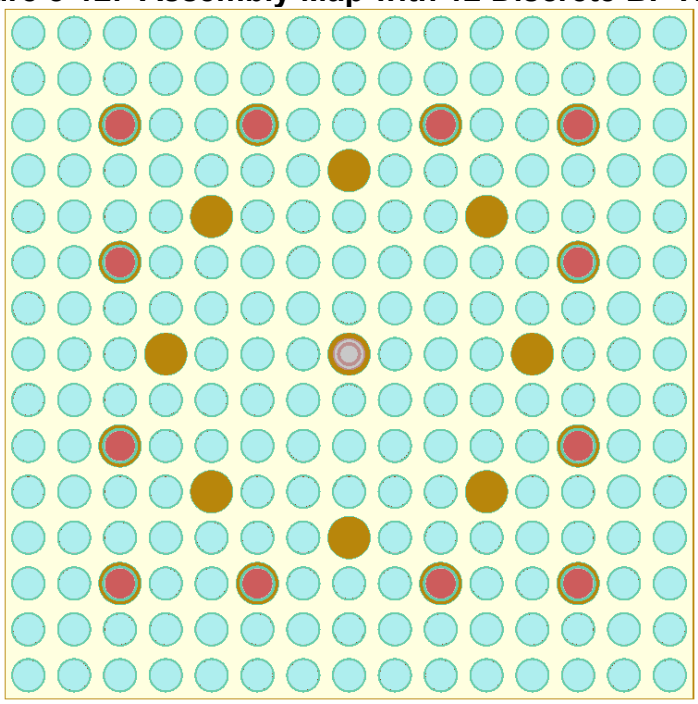

Figure 8-13: Assembly Map with 148 IFBA Rods

[redacted]a,c

C	Instrument Tube
X	IFBA Pin
P	Non-IFBA Pin
G	Guide Tube Location

Note: Diagrams are 1/8 assembly symmetric
Location 8,8 is the center of an assembly

8.8 *Control Rod History*

Depleting fuel assemblies with control rods inserted hardens the neutron spectrum and increases depleted fuel reactivity. Only fuel assemblies in lead control bank (Control Bank D) locations accumulate any significant rodded exposure. Control Bank D only has 8 control rods out of 157 core locations. Control rod insertion is mutually exclusive with any other insert component (Alumina B_4C, Borosilicate Glass, and sources). Conversely, fuel assemblies can have IFBA and control rod insertion. Control rod dimensions are listed in Table 8-12.

Table 8-12: Control Rod Model

Dimension	Value
Absorber Pellet O.D. (cm)	[ ]a,c
Absorber Pellet Material	[ ]a,c
Absorber Material Density (g/cc)	[ ]a,c
Clad I.D. (cm)	[ ]a,c
Clad O.D. (cm)	[ ]a,c
End Plug Length (cm)	[ ]a,c
Clad Material	[ ]a,c
Step Size (cm/step)	[ ]a,c
End Plug Location at 0 Steps (cm)	[ ]a,c

Assessment of the effect of rodded depletion history is performed to determine whether the standard depletion with maximum Alumina B_4C BP bounds depletion scenarios involving control rod insertion. Figure 8-14 shows the cycle burnup averaged control rod insertion of the lead control rod bank over the last 20 years of operation. 2 steps of control rod insertion bound all measured Surry cycles.

Figure 8-14: Cycle Average Control Rod Insertion

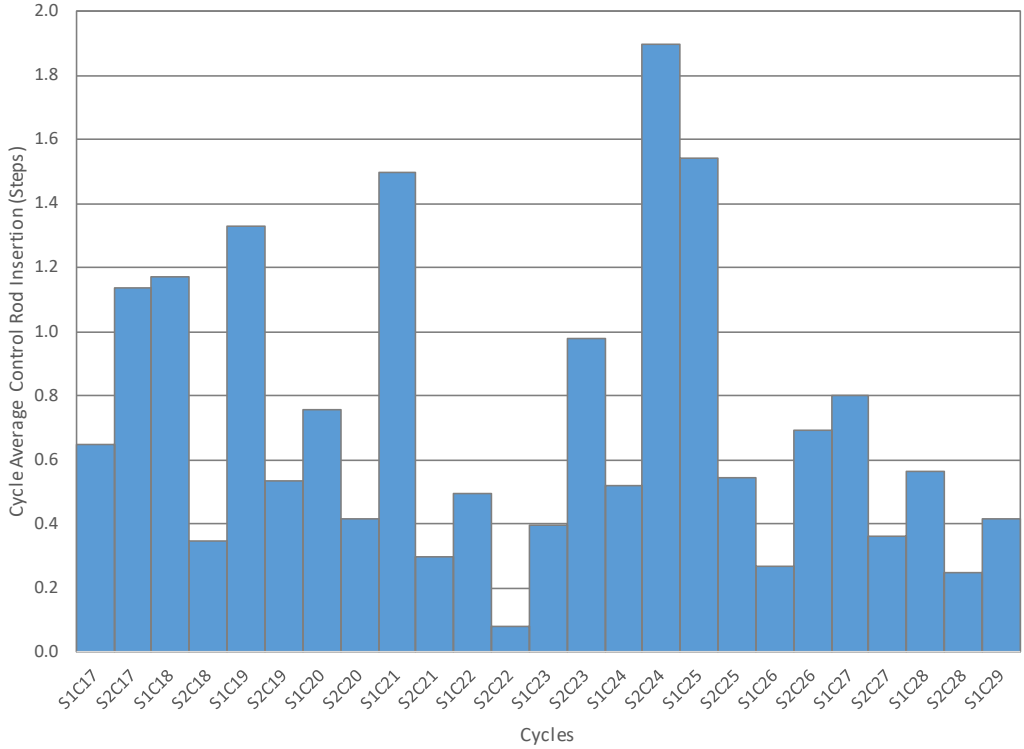

Sensitivity cases were run to determine the effect that depletion with control rods have on SFP reactivity. Full assembly cases were run with no control rods, 1 node with a control rod and 2 nodes with a control rod. Since control rods do not preclude integral burnable absorbers, full length IFBA is also modeled with all control rod cases. These will be compared to the nominal bounding case which has Alumina B_4C along the entire axial height. Discrete BP and control rods are mutually exclusive because both are inserted into the assembly's guide tubes.

Note that the control rods are conservatively not depleted though the depletion. Additionally, note that the axial burnup shape discussed in Section 8.6 will not change due to depletion with a control rod. This is appropriate because the industry generic axial burnup shapes were developed from a database which included measurements from assemblies that experienced rodded depletion [9].

Table 8-13 shows the results from these sensitivity cases. It shows that depletion with Alumina B_4C bounds control rods inserted only one node at low and high burnups, but not when the control rod is inserted two nodes. Therefore, the bounding deletion model bounds a cycle average control rod insertion of 1 node.

The control rod absorber is out of the active fuel when the control rod is at 225 steps. Each control rod step is 1.5875 cm and each node has a height of 20.32 cm (365.76 cm / 18 nodes). One

node is equivalent to 12.8 steps (20.32 cm / 1.5875 cm/step). Therefore, the bounding deletion model bounds a cycle average control rod insertion of less than or equal to 12 steps. Figure 8-14 shows that 12 steps provides adequate margin to Surry's actual operation.

Table 8-13: Control Rod Use Sensitivity Cases

Case Description	Burnup	SFP k-eff	σ	Δk	Δk/RSS(σ)	ρ
Nominal (Alumina B_4C)	20 GWD/MTU	0.86459	0.00009	N/A	N/A	N/A
No CR or BP		0.86294	0.00008	-0.00165	-1436%	-221
1 Node w/ CR depletion		0.86345	0.00008	-0.00114	-975%	-152
2 Node w/ CR depletion		0.86512	0.00007	0.00053	467%	70
Nominal (Alumina B_4C)	40 GWD/MTU	0.77772	0.00007	N/A	N/A	N/A
No CR or BP		0.77161	0.00007	-0.00611	-6004%	-1019
1 Node w/ CR depletion		0.77606	0.00007	-0.00166	-1620%	-275
2 Node w/ CR depletion		0.78674	0.00007	0.00902	8859%	1474

8.9 *In-core Thimble in the Instrument Tube*

At Surry, 50 of the 157 core locations can contain an in-core detector thimble in the assembly's instrument tube. The in-core thimble is a hollow, thin wall tube that displaces water, absorbs thermal neutrons, and has the potential to further harden the neutron spectrum during depletion and increase k_{eff} in the SFP. Table 8-14 shows the relevant dimensions of the in-core thimbles and instrument tube. [ ]^{F}. Note that all depletions in this criticality analysis conservatively assumed that every assembly in the core contained an in-core detector thimble.

Table 8-14: In-Core Thimble and Instrument Tube Dimensions

Dimension (cm)	Westinghouse	Areva	Modeled
Modeled I.T. Inner Diameter	[ ]^{a,c}	[ ]^{F}	1.305
In-Core Thimble Outer Tube O.D.	[ ]^{a,c}	[ ]^{F}	1.006
In-Core Thimble Outer Tube I.D.	[ ]^{a,c}	[ ]^{F}	0.904
In-Core Thimble Inner Tube O.D.	[ ]^{a,c}	[ ]^{F}	0.754
In-Core Thimble Inner Tube I.D.	[ ]^{a,c}	[ ]^{F}	0.538

Table 8-15: In-Core Thimble Material Parameters

Material	Area (cm^2)		Volume Fraction		
	Westinghouse	Areva	Westinghouse	Areva	Modeled
Area Inside I.T.	[ ]^{a,c}	[ ]^{F}	[ ]^{a,c}	[ ]^{F}	N/A
Inconel	[ ]^{a,c}	[ ]^{F}	[ ]^{a,c}	[ ]^{F}	0.278
Water	[ ]^{a,c}	[ ]^{F}	[ ]^{a,c}	[ ]^{F}	0.406
Air	[ ]^{a,c}	[ ]^{F}	[ ]^{a,c}	[ ]^{F}	0.316

8.10 *Reduced Power before Storage*

Bounding high power history was selected to maximize spent fuel reactivity because high fuel power maximizes fuel and moderator temperature during depletion, which hardens the neutron spectrum and increases plutonium production. However, depleting at low power produces less Pm-149, which has the effect of reducing Sm-149 peaking after fuel discharge. Reducing Sm-149 in SFP fuel increases k_{eff}. Therefore, high power history combined with reduced power near end of life (EOL) results in higher k_{eff} in the SFP. Pm-149 has a 2.2 day half life, so reduced power for at least several days at EOL is required for substantial reduction in SM-149 peaking.

There are two plausible ways to achieve low power near EOL for sufficient duration: (1) Fuel placement in a low power location during the last cycle, and (2) power coastdown. A final cycle at low power would reduce fuel assembly burnup average moderator and fuel temperature substantially, which would tend to reduce fuel reactivity. Power coastdown would have far less impact on burnup average moderator and fuel temperature because of the relatively short duration. Power coastdown below 50% power is not likely due to economic considerations. A bounding approximation for power coastdown is to deplete at high power conditions (with associated high fuel and moderator temperatures) for all but the last 20 days of depletion. Twenty days of operation is more than sufficient for PM-149 to reach a reduced equilibrium level. For the last 20 days, deplete at 50% of the prior power retaining high power fuel and moderator temperatures for simplicity and conservatism. Note that 10 days is added to the depletion time to ensure that the same burnup is achieved even though the last 20 days have half the power. Table 8-16 shows the effect that a low power EOC has on the spent fuel pool reactivity. It is conservative to model an end of cycle power coast down.

Table 8-16: Low Power EOC Effect on SFP Reactivity

Case Description	Burnup	SFP k-eff	σ	Δk	Δk/RSS(σ)	ρ (pcm)
No EOL Power Coast	20 GWD/MTU	0.86849	0.00008	N/A	N/A	N/A
Yes EOL Power Coast		0.86905	0.00007	0.00056	528%	74
No EOL Power Coast	40 GWD/MTU	0.76310	0.00007	N/A	N/A	N/A
Yes EOL Power Coast		0.76412	0.00007	0.00101	1038%	174

8.11 *Planar Burnup Tilt*

A planar tilt (synonymous with "Horizontal Tilt" or "Radial Tilt") occurs when there is a burnup gradient across the x-y plane of an assembly. Large planar tilts usually occur when an assembly is close to the edge of the core or has asymmetric burnable poisons. If multiple assemblies are stored in the SFP with the low burnup sides facing each other, then the resulting k-eff will be larger than if the assemblies had a uniform burnup distribution.

DSS-ISG-2010-01 [4] briefly mentions "radial burnup profile" as a possible result of reactor operation with control rods inserted. NUREG/CR-6800 [34] addresses the effect of horizontal burnup tilts for SFP storage in casks. NEI 12-16 does not mention a planar, radial or horizontal tilt. However, the Surry criticality safety analysis will incorporate this effect to address DSS-ISG-2010-01 and NUREG/CR-6800, to ensure this analysis is congruent with other Dominion criticality analyses, and most importantly, because the NRC believed that Dominion did not adequately account for this effect in the Millstone Unit 3 criticality safety analysis and used some of its review margin to reconcile this omission [39].

For this criticality safety analysis, the quantity of the tilt (%) is defined by the equation below. Therefore, any quadrant with a negative planar tilt means that the quadrant has a burnup below the assembly average burnup and vice versa.

$$\text{Planar Tilt (\%)} = \left(\frac{\text{Quarter Assembly Burnup}}{\text{Assembly Average Burnup}} - 1\right) * 100\%$$

End of cycle quadrant burnups were calculated for each assembly for the past 20 Surry cycles (10 for each unit) with Simulate5. This equates to data for 3140 assemblies. The cases output an EOC exposure map with assemblies broken down to 2x2 radial meshes. The Horizontal Tilt was calculated with these maps and were organized and plotted in Figure 8-15.

The figure shows that the planar tilt can be modeled by the limit defined in Table 8-17. This defined tilt encompasses >99% of the data points and is therefore sufficient to satisfy the 95% probability and 95% confidence criteria.

When modeling this effect in the SFP, the horizontal tilt will be conservatively applied to half of the assembly even though the magnitude of the tilt value was calculated using a quarter of the assembly.

Figure 8-15: Planar Tilt vs. Burnup for Surry Assemblies

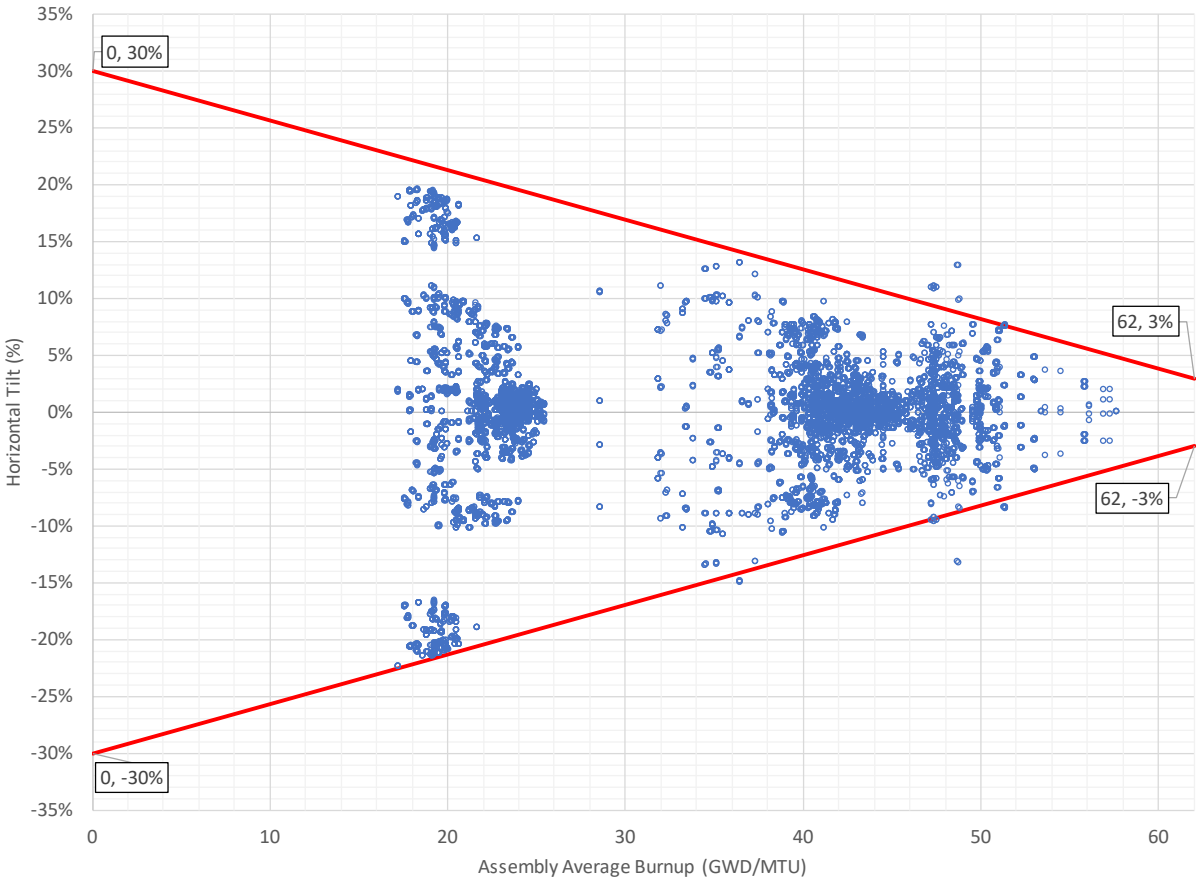

Table 8-17: Modeled Planar Burnup Tilt

Burnup [GWD/MTU]	Planar Tilt	
	Negative	Positive
0	-30%	30%
62	-3%	3%

8.12 *Grids*

NEI 12-16 [32] allows grids to be modeled as water for both the depletion and reactivity calculations. However, the Surry Criticality Safety analysis is crediting grids. This section provides the basis for this analysis to use maximum grids in the depletion and minimum grids in the SFP as inputs into the model. All current fuel in Surry's SFP are bounded by these inputs. Future fuel assembly designs will be evaluated against these design inputs.

The bottom Inconel grid may be ignored because it is a strong neutron absorber and because it is located at the bottom of the active fuel stack which is an unimportant neutronic region for depleted fuel. The grids of the original Standard Fuel can be ignored because it had Inconel mid-span grids which would significantly reduce the reactivity of the assembly in the spent fuel pool since Inconel is a very strong absorber when compared to zirconium.

Table 8-18 shows the grid volumes in the active fuel region for the Surry assemblies. Grid volume is calculated by summing the mass of grids and sleeves of the Mid-Span and IFM grids and then converting to volume by using the grid density. The largest total volume of zircaloy-based grids per assembly is in the Westinghouse Upgrade fuel. The smallest total volume of zircaloy-based grids per assembly is in Framatome Agora Fuel.

Table 8-18: Grid Volume in Active Fuel Region for Historical Fuel Designs

Fuel Type	Midspan Grids			IFM Grids			Total Volume (cc)
	Density (g/cc)	Total Mass (g)	Volume (cc)	Density (g/cc)	Total Mass (g)	Volume (cc)	
SIF	6.55	7983	1219	6.55	0	0	1219
SIF/P+	6.55	7983	1219	6.55	0	0	1219
SIF/P+Z	6.55	7961	1215	6.55	0	0	1215
SIF/P+Z2	6.55	7961	1215	6.55	0	0	1215
Upgrade	6.56	6305	961	6.56	1755	268	1229
Agora	6.6	3610	547	6.6	1215	184	731

The total volume of the coolant-grid mixture (V_{lattice}) in an assembly is calculated based on the equation below. Note that the water inside the guide tubes and instrument tube is not considered in this equation because it will not be smeared with grid material. Table 8-19 shows the volumes and volume fraction of the grid - coolant mixture.

$$V_{\text{lattice}} = h_{fuel}\left[n_{rod} * \left(pitch_{\text{rod}}^2 - \frac{\pi}{4} OD_{\text{cladding}}^2\right) + n_{G\&I\ Tubes} * \left(pitch_{\text{rod}}^2 - \frac{\pi}{4} OD_{G\&I\ Tubes}\right)\right] \qquad (8.6.2\text{-}1)$$

Table 8-19: Grid Volume Fractions

Fuel Type	Grid Volume (cc)	Coolant-Grid Mixture Volume (cc)	Grid Volume Fraction
Upgrade	1229	89886	0.0137
Agora	731	88319	0.0083

Sensitivity cases were run to determine the reactivity effect that grids have on the Spent Fuel Pool reactivity. Two sensitivity cases were run. The first case modeled no grids in both the depletion and the SPF reactivity calculations. This case determines the total effect of grids on SFP reactivity. The second case only models grids in the rack calculation. This case breaks up the total effect into the separate components. The results of the sensitivity cases are shown in Table 8-20. The results show that grids have an overall negative effect on reactivity. The moderator displacement effect resulting from grids in the SFP dominates the isotopic effect that results from grids during depletion.

While grids reduce reactivity in unborated SFP conditions, they can increase reactivity at high borated conditions. However, the sensitivity cases in Table 8-20 are only run at unborated conditions. This is because the limiting borated scenario in this CSA is the cask drop accident. The amount of grids in this accident is inconsequential because it assumes optimum rack pitch, fuel pin pitch, and fuel pellet stack pitch. The optimum pitches would readjust to account for the different grid volumes to achieve the optimum reactivity for the system. Therefore, the sensitivity cases focus on unborated SFP conditions.

Table 8-20: Varying Methods for Modeling Grids Cases

Case Description	Burnup	SFP k-eff	σ	Δk	Δk/RSS(σ)	ρ
Nominal (Grids in Depl and SFP)	20 GWD/MTU	0.86849	0.00008	N/A	N/A	N/A
No Grids in Depl and SFP		0.87046	0.00008	0.00197	1858%	261
No Grids in Depl only		0.86826	0.00007	-0.00023	-216%	-30
Nominal (Grids in Depl and SFP)	40 GWD/MTU	0.76310	0.00007	N/A	N/A	N/A
No Grids in Depl and SFP		0.76369	0.00007	0.00059	603%	101
No Grids in Depl only		0.76178	0.00007	-0.00133	-1369%	-228

8.13 *Clad Volume*

Similar to the grids, more cladding during depletion will displace water and harden the neutron spectrum and thus increases Pu production and k_{eff} in the SFP. On the other hand, more cladding in the SFP displaces water and decreases k_{eff} (assuming reasonable boron conditions). The cases below test which of these effects is dominant. One test case tests an assembly with the most cladding volume and the other tests the least cladding volume.

Table 8-21: Bounding Assembly Parameters

Parameter		**Maximum Clad**	**Minimum Clad**
Fuel clad Diameter (cm)	I.D. / I.R.	0.9484 / 0.4742	0.95 / 0.475
	O.D. / O.R.	1.077 / 0.5385	1.072 / 0.536
Guide Tube / Instrument Tube (cm)	I.D. / I.R.	1.267 / 0.6335	1.305 / 0.6525
	O.D. / O.R.	1.41 / 0.705	1.3538 / 0.6769

Table 8-22 shows the results of the test cases. Similar to the grid sensitivity cases in Section 8.12, these cases are only run at unborated SFP conditions since the cask drop accident models all pitches at optimum moderation.

The test cases below show that decreased moderation in the SFP has a larger negative reactivity effect than the positive reactivity effect of the harder neutron effect during depletion. Therefore, it is conservative to use the minimum clad parameters.

Table 8-22: Varying Clad Volume Fractions Cases

Case Description	Burnup	SFP k-eff	σ	Δk	Δk/RSS(σ)	ρ (pcm)
Nominal (Min Clad)	20 GWD/MTU	0.86849	0.00008	N/A	N/A	N/A
Max Clad		0.86195	0.00008	-0.00654	-6125%	-874
Nominal (Min Clad)	40 GWD/MTU	0.76310	0.00007	N/A	N/A	N/A
Max Clad		0.75916	0.00007	-0.00394	-4039%	-681

Common Depletion Elements Not Modeled/Credited

8.14 The following are commonly modeled or credited in criticality safety analyses which are not included in this analysis:

- Grid growth bias
- Clad creep down bias
- Decay time credit

Zircaloy based grids tend to grow with increasing fuel burnup. Grid growth increases fuel pin pitch. Because fuel pins are constrained within the grid lattice, fuel pin pitch growth is assumed to be the same relative magnitude as grid growth increasing the moderator in the fuel pin lattice. Similarly, zircaloy cladding can shrink down during depletion which can decrease the clad's diameter. This also increases the amount of moderator in the lattice. Increasing the amount of moderator in the lattice during depletion decreases reactivity, so it will not be modeled in TRITON.

However, the only scenario in this analysis that credits burnup is the cask drop accident. In this accident, the grids are damaged so that the fuel pins are moved to optimum moderation. Because the grids are damaged and the fuel lattice is already at optimum moderation, grid growth and clad creep down either is not applicable or has no effect.

Additionally, the burnup curve in Section 12 was developed with models using 100 hours of decay time. This amount of decay time is bounding. Longer lengths of decay time was not credited because a reduction to the burnup curve was not needed to accommodate expected future operations.

8.15 *TRITON Depletion Model Summary*

Tables 8-23 and 8-24 summarizes the key elements of the Surry depletion model.

Table 8-23: Depletion Inputs for TRITON Depletion Model

Parameter	Value
Assembly Relative Power	Burnup (MWD/MTU) / RPD 0 / 1.44 30000 / 1.44 50000 / 1.37 60000 / 1.03 Interpolate between burnup points
RCS Boron Concentration	850 ppm
Rated Thermal Power	2587 MW
RCS Pressure	2250 psia
HFP Vessel Average Temperature	573.0°F
Core Bypass Fraction	5.40%
Vessel Flow	274,000 gpm
Axial Burnup Shapes	NUREG/CR-6801 Shapes [9]
Planar Burnup Tilt	Burnup [GWD/MTU] / Planar Tilt: Negative / Positive 0 / -30% / 30% 62 / -3% / 3% Interpolate between burnup points
Decay Time	100 hours
Reduced Power at EOL	50% Power during the last 20 days of depletion
Geometric Changes During Depletion	None
Remove Isotopes with Low Concentrations	None
Volatile Fission Products Release Fractions	Isotopes / Release Fraction Kr-85 / 0.20 I-131 / 0.05 Kr & Xe / 0.05 Br & I / 0.05 Rb & Cs / 0.20

Table 8-24: Assembly Inputs for TRITON Models

Parameter	Value
Array size	15x15
Assembly pitch	21.50 cm
Rod pitch	1.43 cm
Active fuel length	365.76 cm
Fuel rods/assembly	204
Guide tubes/assembly	20
Instrument tubes/assembly	1
Fuel pellet O.D.	0.9335 cm (radius: 0.46675 cm)
Annular pellet I.D.	0 cm (not modeled)
Annular region length	0 cm (not modeled)
Fuel clad ID	I.D.: 0.95 cm / I.R.: 0.475 cm O.D.: 1.072 cm / O.R.: 0.536 cm
Guide tube / instrument tube	I.D.: 1.305 cm / I.R.: 0.6525 cm O.D.: 1.3538 cm / O.R.: 0.6769 cm
Clad alloy	pure zirconium
Minimum grid volume fraction for SFP criticality calculations	0.0083
Maximum grid volume fraction for depletion calculations	0.0137
Grid material	pure zirconium
Percent Theoretical Density	95.5%
Burnable Poison for depletion calculations	Alumina B4C
Average Control Rod Insertion	12 Steps
Source rods	None
In-core Detector Thimble Material	Inconel
In-core Detector Thimble Inner Tube	I.D.: 0.538 cm / I.R.: 0.269 cm O.D.: 0.754 cm / O.R.: 0.377 cm
In-core Detector Thimble Outer Tube	I.D.: 0.904 cm / I.R.: 0.452 cm O.D.: 1.006 cm / O.R.: 0.503 cm
Bottom of Assembly to Bottom of Active Fuel	8.275 cm

9 Spent Fuel Rack Analysis

The racks and fuel types are the same for both Region 1 and Region 2. The only difference is that the Region 1 racks are susceptible to rack damage due to the cask drop accident. Because of the cask drop accident, Region 1 requires a burnup curve while Region 2 does not.

This section is split up into a damaged rack pitch analysis subsection (Section 9.1) and a nominal rack pitch rack analysis subsection (Section 9.2). Section 9.1 only applies to Region 1 while Section 9.2 applies to both Region 1 and Region 2. However, Section 9.2 only discusses Region 2 because the Region 1 requirements are determined solely by the damaged rack analysis and not the nominal pitch analysis.

Both the Region 1 and Region 2 analyses use the assembly data and rack data in Tables 3-3 and 4-3, respectively.

Note that most spent fuel pools in the industry denote “Region 1” as the fresh fuel, high reactivity fuel region. This is <u>not</u> the case for this CSA. Region 1 stores depleted fuel while Region 2 can store depleted or fresh fuel. This naming convention was chosen so that the region names can stay consistent with the current Technical Specifications at Surry. This will avoid creating any human performance error precursors that switching the names can introduce.

9.1 *Damaged Rack Analysis (Cask Drop Accident) – Region 1*

9.1.1 Region 1 Fuel Storage Requirements

The following Technical Specification criticality requirements for storing a fuel assembly in Region 1 are being modified:

1) The fuel assembly has an initial U-235 enrichment ≤5.0 wt%.
2) The fuel assembly burnup and enrichment satisfy the burnup credit curve (Figure 9-15)

Criterion 1 was confirmed by analysis using an infinite lattice 6x6 rack cell model and is described in Section 9.2. Criterion 2 was developed by using a finite model described in Section 9.1.3.

There is an additional Technical Specification requirement to be stored in Region 1: fuel assemblies must have at least 150 days of cooling. This requirement is driven by the radiological consequences analysis and is not changing from the existing analysis [40]. Note that this criticality analysis conservatively assumed 100 hours of decay time.

9.1.2 Cask Drop Accident Description and Assumptions

Unlike most plants, Surry has no physical barrier that separates the cask loading area from the fuel racks and has a cask crane which is not single failure proof. Therefore, if the cask tips over in the direction of the fuel racks due to a crane accident, then it could come into contact and damage the fuel racks.

The rack damage calculation is a simple energy balance analysis. The analysis ran different cases which had different amounts of fuel assemblies loaded into the first four rows of rack modules. The analysis concluded that "The first rack will be totally damaged, i.e. first and the last row of cells will yield and the pins at the base will shear. The second rack will be partially damaged, i.e. the first row of cells will fail and the second row of cells will undergo minor deformation. The third rack will remain undamaged." This analysis was reviewed by the NRC in [40]. Previous Spent Fuel Pool criticality analysis assumed that the first 3 rows of rack modules were damaged. For conservatism, this analysis also assumes that the first 3 rows are damaged.

Since the structural analysis did not dictate how the fuel racks will be damaged, three plausible damage scenarios were analyzed. The three scenarios are: 1) all the fuel stays in the fuel cells; 2) fuel pellets fall to the SFP floor; 3) fuel pellets are between the fuel cells. These scenarios and models are further described in Sections 9.1.2.1 through 9.1.2.3. These scenarios are not meant to simulate how the SFP would actually look after a cask drop accident. Instead, it is meant to be an extremely conservative scenario which bounds what the actual configuration could be. Each of these scenarios were modeled and the resulting k-effs were compared against each other. The limiting scenario was then used to calculate the bias, uncertainties, and maximum k-eff for each analyzed burnup state point.

The double contingency principle precludes the need to analyze two independent simultaneous accidents. The structural analysis determined that the SFP walls and floor remain functional during a cask drop accident [40]. Therefore, the double contingency principle eliminates the need to model the cask drop accident in unborated conditions meaning all cases are run at borated conditions.

Additionally, the volume of structural materials is conserved in the calculation and the volume and mass of fuel was either conserved or conservatively increased. For example, the thickness of the stainless steel cell tubes is increased when the cell inner diameter decreases and the fuel assembly grid volume fraction is increased when the fuel pins are pushed closer together. Note that only the rack cell is modeled. No other structural support material is modeled.

The exact radial distance between the spent fuel racks and the wall is not modeled nor needed. This is because the distance between the fuel and wall increases when the racks are deformed. Since the water is borated, the fuel is neutronically isolated from the walls for this accident.

All boundaries of the model are reflective boundaries. As can be seen in Figure 9-1, there are significant amounts of borated water and concrete to all the boundaries except the +y boundary. Therefore, +y is the only boundary that is neutronically important. While assuming reflective boundary is not realistic since the fuel racks on the other side of the boundary are not damaged, it is conservative to assume they are. Assuming deformed racks above the boundary results in a more reactive boundary than if normal spaced racks were assumed above the boundary since the damage racks are assumed to be at optimum pitch and moderation.

Some additional modeling assumptions for all three damage scenarios are below.

a) SFP water modeled with 2250 ppm. Surry Technical Specification 5.3.2 sets the spent fuel pool boron concentration lower limit at 2300 ppm.

b) The assembly axial reflectors (plenum region, guide tubes above and below the active fuel, and top and bottom nozzles) are modeled as unborated water for the scenarios where all the fuel stays in the rack cells and when the fuel falls between the rack cell. See Section 9.1.2.2 for a description of the bottom reflector when the fuel is on the SFP floor.

c) The storage cell is modeled as its nominal length.

d) Neither reduction in fuel enrichment nor annular pellets are modeled for axial blankets. This is conservative because it increases SFP k-eff.

e) Zr-based clad materials are modeled as pure Zr.

f) Water density is determined assuming the pressure is 28 psia to simulate increased pressure at the bottom of the SFP.

g) Grids are represented by homogenizing the grid and the water in the fuel lattice over the length of the fuel. Water inside the guide tubes is modeled as pure water (not homogenized with grids). Justification of this assumption is given in Section 8.12.

h) For the Fuel Pin Clad OD uncertainty cases, the grid volume stays constant. This is acceptable for several reasons. 1) The clad OD uncertainty has a small effect on the moderator to fuel ratio. 2) The reactivity effect of the optimum moderator to fuel ratio is already accounted for in the Optimum Pitch Bias. 3) The clad OD uncertainty is small enough that it only affects the final RSS uncertainty term by less than ~10 pcm.

i) The fuel density uncertainty values are calculated by changing the density of fresh fuel instead of burned fuel for all burnup steps. This is acceptable because enrichment changes generally have a larger effect on fresh fuel rather than burned fuel. Additionally, the PTD uncertainty is small enough that it only affects the final RSS uncertainty term by less than ~10 pcm.

j) This analysis models all fuel assemblies in Region 1 with the same enrichment and burnup. This means, that the optimum pitch for all assemblies is the same. In reality, the fuel stored in Region 1 will have a variety of different burnups meaning the pitch between all the assemblies will need to be different to achieve optimum moderation.

Table 9-1: Region 1 Reactivity Under Various Cask Drop Scenarios

Scenario	Enrichment/ Burnup	k-eff	σ
Fuel Between Cells	1.65 wt%/ 0 GWD/MTU	0.861170	0.000049
Fuel on SFP Floor		0.829438	0.000032
All Fuel in Cells		0.829482	0.000047
Fuel Between Cells	2.20 wt%/ 10 GWD/MTU	0.900875	0.000052
Fuel Between Cells, Axial BU Shape Reversed		0.903734	0.000052
Fuel on SFP Floor		0.879719	0.000054
All Fuel in Cells		0.878884	0.000059
Fuel Between Cells	2.85 wt%/ 20 GWD/MTU	0.892691	0.000050
Fuel Between Cells, Axial BU Shape Reversed		0.893959	0.000035
Fuel on SFP Floor		0.877938	0.000057
All Fuel in Cells		0.886364	0.000057
Fuel Between Cells	3.45 wt%/ 30 GWD/MTU	0.877811	0.000052
Fuel Between Cells, Axial BU Shape Reversed		0.878803	0.000056
Fuel on SFP Floor		0.869988	0.000063
All Fuel in Cells		0.878406	0.000053
Fuel Between Cells	4.10 wt%/ 40 GWD/MTU	0.863261	0.000052
Fuel Between Cells, Axial BU Shape Reversed		0.873836	0.000059
Fuel on SFP Floor		0.875768	0.000054
All Fuel in Cells		0.865959	0.000054
Fuel Between Cells	4.55 wt%/ 47 GWD/MTU	0.855104	0.000050
Fuel Between Cells, Axial BU Shape Reversed		0.874092	0.000039
Fuel on SFP Floor		0.889408	0.000055
All Fuel in Cells		0.863615	0.000054
Fuel Between Cells	5.00 wt%/ 53 GWD/MTU	0.851668	0.000049
Fuel Between Cells, Axial BU Shape Reversed		0.875774	0.000058
Fuel on SFP Floor		0.895885	0.000047
All Fuel in Cells		0.863315	0.000056

The highlighted rows indicate the limiting cask drop damage scenario for each burnup step. The limiting scenario is then used to calculate the uncertainty and bias cases for each burnup step.

9.1.2.1 Fuel in Cells Scenario

This scenario bounds when the fuel cell walls stay intact. This means that the fuel from each assembly will stay contained in their respective fuel cell. This scenario is modeled by deforming the cell pitch and fuel assembly's fuel pins until they reach optimum fuel pin pitch. Deformation to optimum pin pitch is modeled for all 324 assemblies in Region 1. Details of the optimum pin pitch calculation are in Section 9.1.4.

Figures 9-1 – 9-3 show axial and radial diagrams of the KENO model. Table 9-1 shows the reactivity of Region 1 when modeled to this scenario for each burnup. For comparison purposes, the reactivity of the other two scenarios are also shown.

The biases, uncertainties, and maximum k-eff of the 30 GWD/MTU burnup state-point will be calculated using this scenario. At 30 GWD/MTU, this scenario is slightly less bounding than the "Fuel Between Cells, Axial Burnup Shape Reversed" scenario. However, the difference between the two scenarios is small (within a dk of 0.0005). Additionally, Table 9-17 shows that the 30 GWD/MTU burnup state point has significantly more margin than most other burnup points. This means that using the "Fuel in Cells" scenario rather than the "Fuel Between Cells, Axial Burnup Shape Reversed" scenario does not affect the burnup curve.

Figure 9-1: Cask Drop Accident Model (x-y Profile)

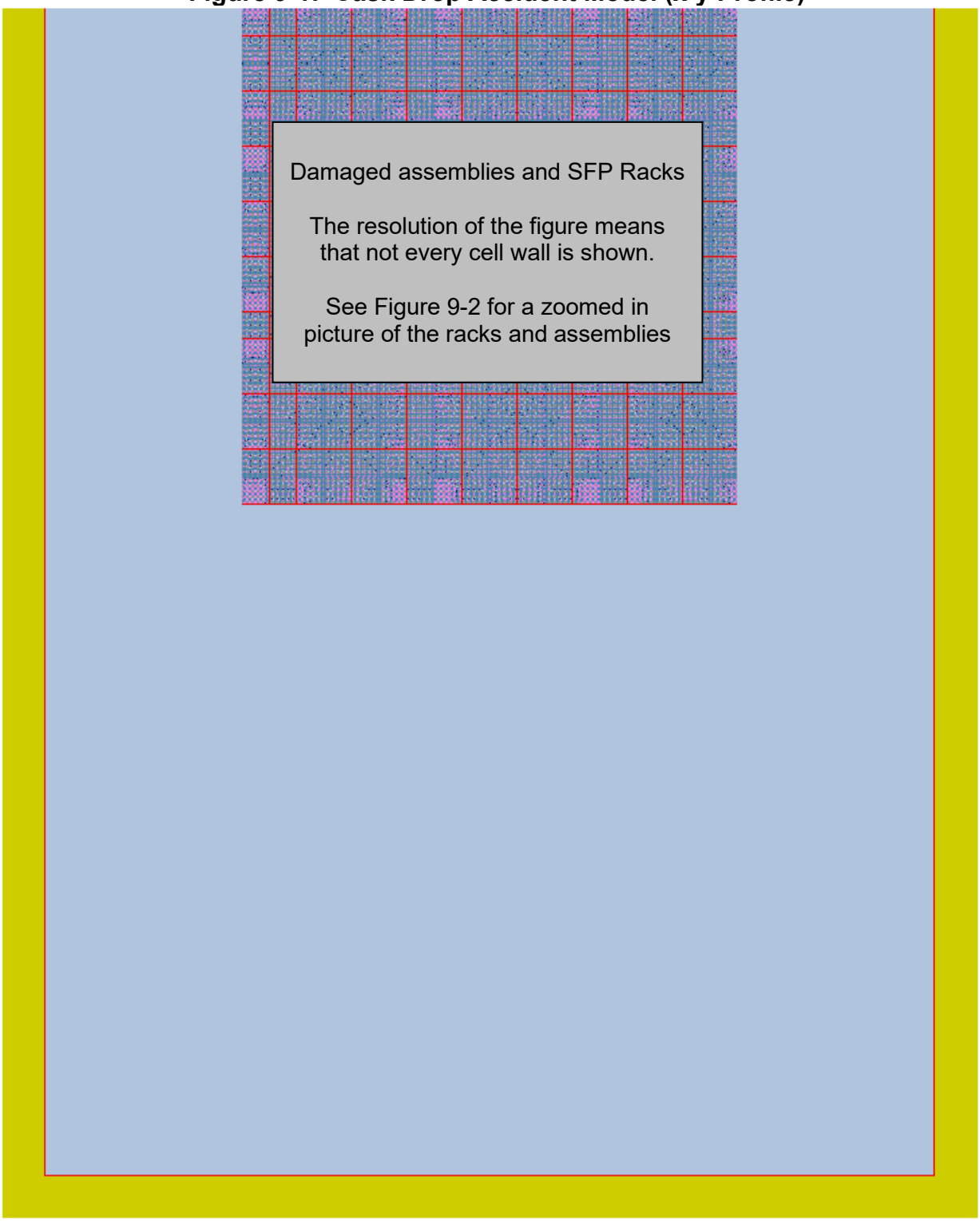

Picture of an x-y plane of the whole KENO model. See Figure 9-3 for an y-z plane and 9-2 of a zoomed in shot of the fuel. Concrete is in yellow, stainless steel is red, light blue is borated water, and the block in the sea of water are the crushed assemblies.

Figure 9-2: Cask Drop Accident Model, Zoomed In (x-y Profile)

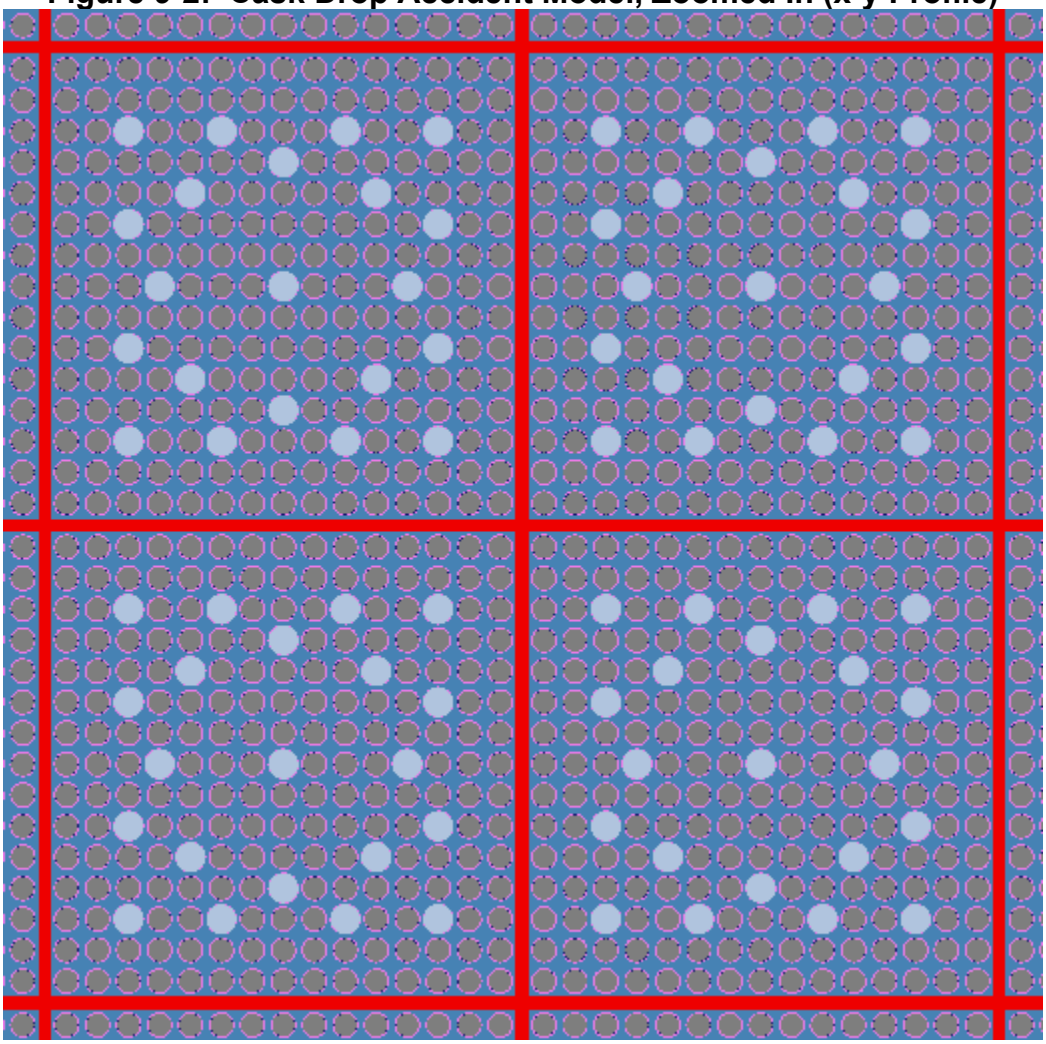

Picture of an x-y plane of the fuel in the KENO model. See Figure 9-1 for an x-y plane and 9-3 of an y-z plane. Stainless steel is red, light blue is borated water, grey is fuel, darker blue is borated water smeared with grids and purple is zirconium.

Figure 9-3: Cask Drop Accident Model (y-z Profile)

Picture of an y-z plane of the whole KENO model. See Figure 9-1 for an x-y plane and 9-2 of a zoomed in shot of the fuel. Concrete is in yellow, stainless steel is red, light blue is borated water, turquoise is unborated water and the block in the sea of water are the crushed assemblies. Note that the resolution of this photo means that many of the boundaries were not shown (including some cell walls)

9.1.2.2 Fuel on Floor Scenario

This scenario accounts for when the rack cell walls and the fuel assembly cladding rupture. This allows individual fuel pellets to fall out of the rack cell. The fuel pellets could either drop to the SFP floor or get stuck between the rack cell walls. This section analyzes when the pellets fall to the SFP floor. Section 9.1.2.3 analyzes the scenario when fuel pellets get stuck between the fuel rack cells.

This scenario is modeled by stacking fuel pellets to the height of 15.24 cm which is the distance between the SFP floor and the fuel cell floor. These pellet stacks fill the area beneath the fuel cells and are spaced at optimum pitch from each other. To conserve the total amount of fuel, the fuel assembly height is reduced to compensate for some of the fuel being moved to the bottom of the SFP. For the burned fuel cases, fuel from the top node (Node 18) was modeled underneath the fuel racks since it has the highest reactivity. Placing the highest reactive fuel at optimum pitch without any zirconium or water holes is conservative.

This model places fuel from the top of the assembly below the fuel from the bottom of the assembly separated by the assembly's bottom reflector (area between the bottom of the fuel and bottom of the assembly). The fuel from the bottom and top are more reactive than fuel from the center of assembly due to the NUREG axial burnup curves. This means that the assembly's bottom reflector is neutronically important. Therefore, the bottom reflector was modeled as a zirconium and borated water mixture. Since the dropped cask can deform the racks and assembly, the assembly bottom reflector was deformed as well. It should be noted that the bottom nozzle is a robust assembly component that would resist significant deformation. Regardless, it was conservatively modeled as only 3.174 cm in height which is over 50% shorter than the nominal reflector height. But more importantly, this crushing of the reflector displaces borated water. The model has moderator volume fraction of 0.536 which results in over 70% of the borated water being displaced when compared to all of Surry's historical fuel assembly designs.

Even though 100% of the borated water was not removed from the assembly bottom reflector, this model is still extremely conservative due to the following reasons:

- It is practically impossible for fuel pellets to fall to the bottom of the SFP and end up in stacks at optimum pellet pitch.
- If the bottom assembly reflector was reduced in height by over 50%, then the racks themselves would likely deform. This would reduce the amount of space below the racks for fuel pellets to coalesce.
- The fuel assemblies remaining within the fuel cells are still modeled at optimum pin pitch.

- The scenario is modeled for all assemblies in Region 1 (324 assemblies). Optimum assembly pitch, fuel pin pitch, and pellet stack pitch is modeled for all 324 assemblies in Region 1.

Deformation to the optimum pin and assembly pitch is detailed in Section 9.1.4. The optimum pellet pitch calculation is shown in Table 9-2. This calculation modeled 15.24 cm high fuel stacks at various pitches to determine when reactivity peaked.

Figures 9-4 – 9-6 show axial and radial diagrams of the KENO model. Table 9-1 shows the reactivity of Region 1 when modeled with fuel on the floor for each burnup. For comparison purposes, the reactivity of the other two scenarios are also shown. This scenario is limiting for the 40, 47, and 53 GWD/MTU state points. Therefore, the biases, uncertainties, and maximum k-eff for these burnups will be calculated using this scenario.

Table 9-2: Optimum Pellet Stack Pitch

Enrichment/ Burnup	Pin Pitch (cm)	k-eff	σ
1.65 wt%/ 0 GWD/MTU	1.09	0.663522	0.000060
	1.10	0.664436	0.000058
	1.11	0.665141	0.000059
	1.12	0.665771	0.000056
	1.13	0.665728	0.000057
	1.14	0.665345	0.000055
	1.15	0.664736	0.000058
2.20 wt%/ 10 GWD/MTU	1.17	0.710683	0.000063
	1.18	0.711267	0.000063
	1.19	0.711277	0.000059
	1.20	0.711296	0.000060
	1.21	0.711170	0.000059
	1.22	0.710693	0.000058
	1.23	0.709841	0.000063
2.85 wt%/ 20 GWD/MTU	1.20	0.748528	0.000061
	1.21	0.749217	0.000064
	1.22	0.749260	0.000059
	1.23	0.749121	0.000064
	1.24	0.749156	0.000060
	1.25	0.748700	0.000062
	1.26	0.748115	0.000059
3.45 wt%/ 30 GWD/MTU	1.23	0.751014	0.000062
	1.24	0.751695	0.000061
	1.25	0.751713	0.000061
	1.26	0.751895	0.000059
	1.27	0.751611	0.000064
	1.28	0.751476	0.000064
	1.29	0.750879	0.000062
4.10 wt%/ 40 GWD/MTU	1.27	0.750361	0.000063
	1.28	0.750695	0.000060
	1.29	0.750690	0.000064
	1.30	0.750500	0.000062
	1.31	0.750201	0.000065
	1.32	0.749588	0.000060
	1.33	0.749119	0.000063
4.55 wt%/ 47 GWD/MTU	1.27	0.756681	0.000062
	1.28	0.757140	0.000062
	1.29	0.757569	0.000061
	1.30	0.757433	0.000060
	1.31	0.757271	0.000060
	1.32	0.757038	0.000061
	1.33	0.756679	0.000060
5.00 wt%/ 53 GWD/MTU	1.28	0.762389	0.000061
	1.29	0.762790	0.000062
	1.30	0.763050	0.000060
	1.31	0.763123	0.000064
	1.32	0.762938	0.000066
	1.33	0.762829	0.000063
	1.34	0.762350	0.000060

Figure 9-4: Cask Drop Accident Model, Zoomed In, x-y Profile, In-Fuel Racks

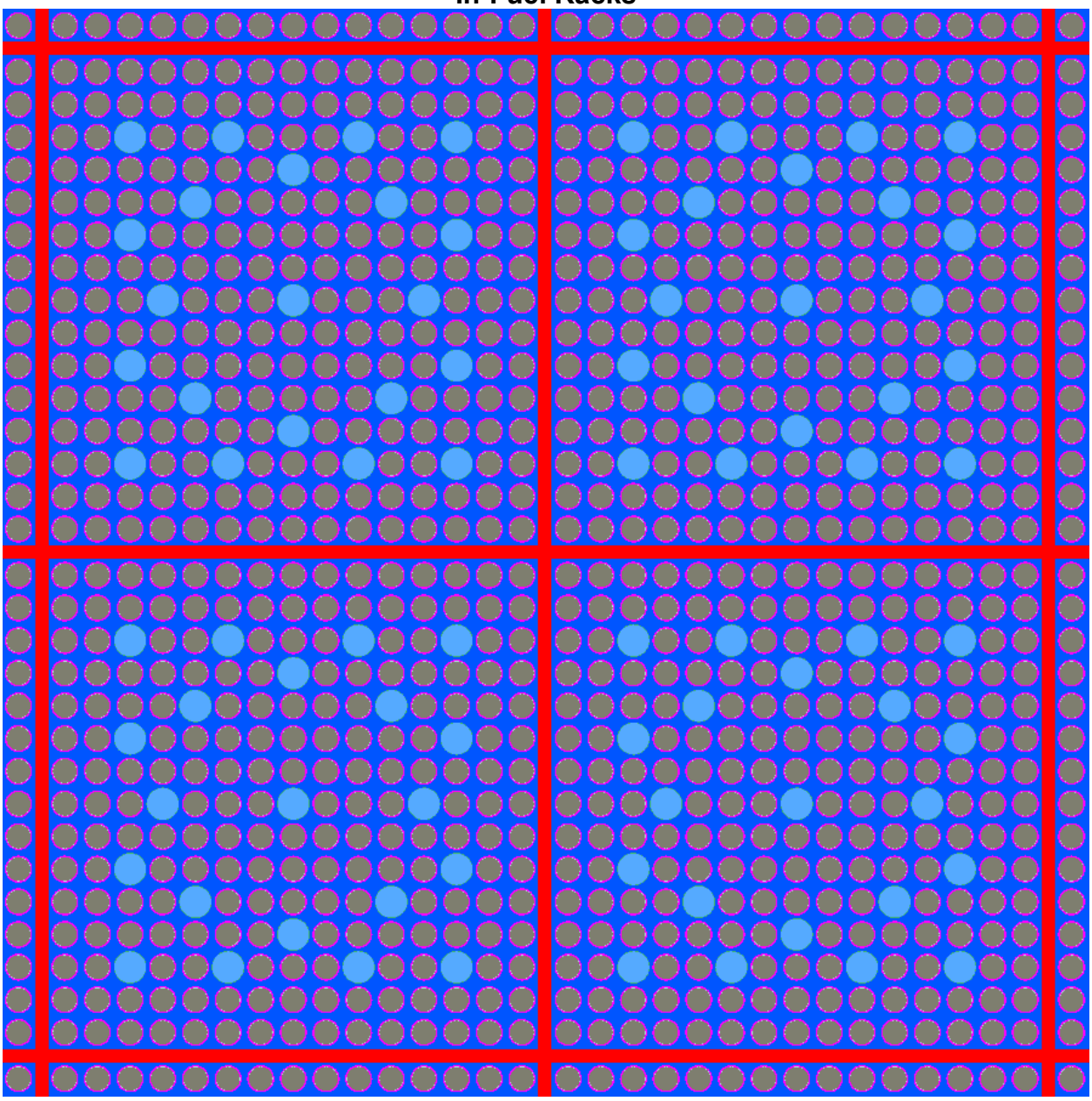

Picture of an x-y plane of the fuel assemblies in the KENO model. See Figure 9-5 for an x-y plane at the SFP floor and 9-6 of an y-z plane. Stainless steel is red, light blue is borated water, grey is fuel, darker blue is borated water smeared with grids and purple is zirconium. Comparing this figure to Figure 9-2 shows that this model is almost identical to the Fuel in Cell scenario. The only difference is that there are fuel pellet stacks on the floor and the assembly fuel stack is shorter.

Figure 9-5: Cask Drop Accident Model, Zoomed In, x-y Profile, Beneath Fuel Racks

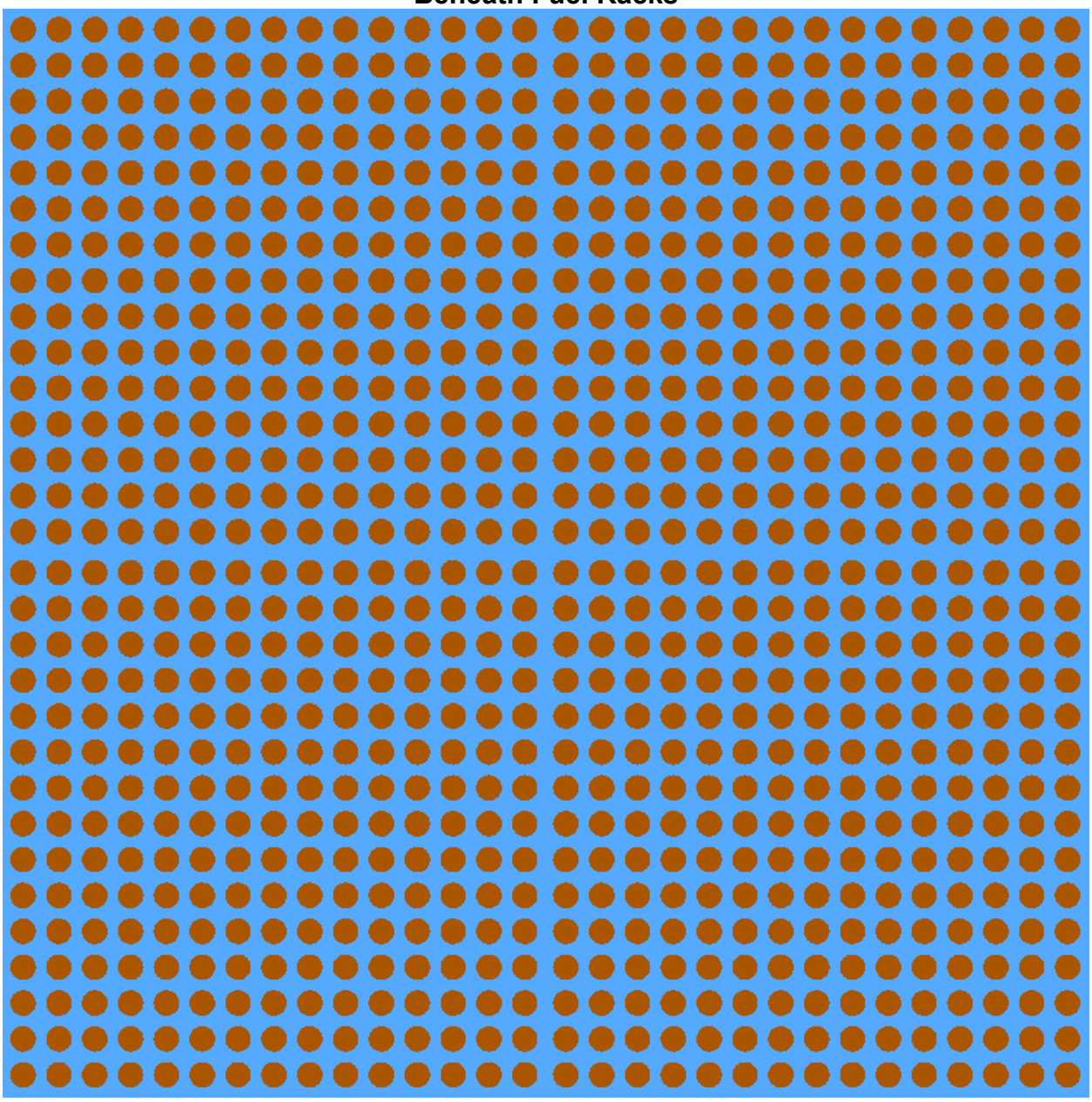

Picture of an x-y plane of the fuel in the KENO model beneath the fuel racks. See Figure 9-4 for an x-y plane in the fuel racks and 9-6 of an y-z plane. Light blue is borated water and brown is fuel (from the top axial depletion node)

Figure 9-6: Cask Drop Accident Model, Zoomed In, y-z Profile

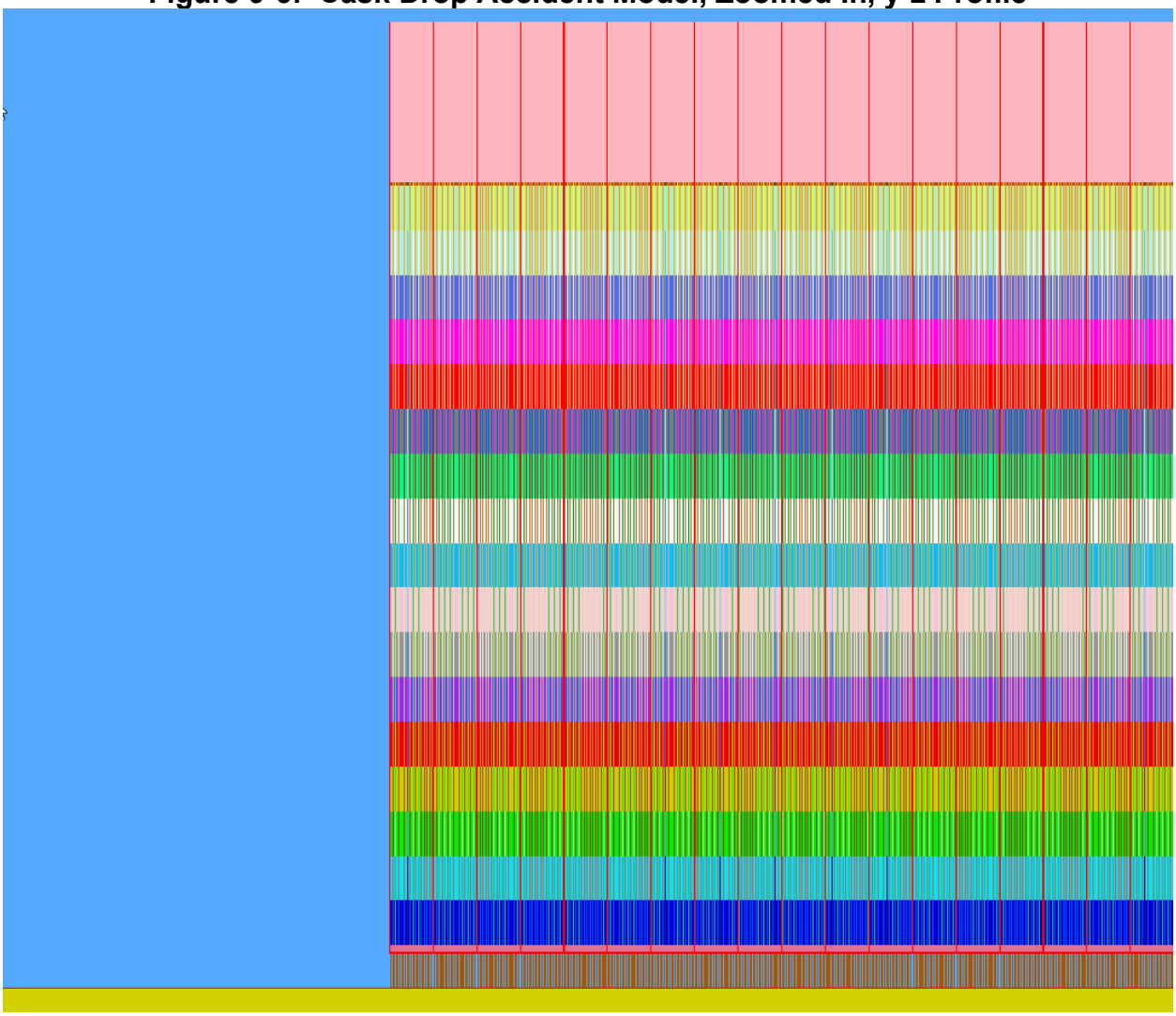

Picture of an y-z plane of the fuel in the KENO model with fuel beneath the fuel racks. See Figure 9-4 for an x-y plane in the fuel racks and 9-5 of an x-y plane below the fuel racks. Light blue is borated water, yellow at the bottom of the figure is concrete, the rainbow colored portion represents the fuel from different axial depletion nodes, light pink above the fuel is the unborated water reflector, brown on the SFP floor are the fuel pellet stacks, and the dark pink between the dark blue and brown fuel is the borated water/zirconium reflector.

9.1.2.3 Fuel Between Rack Cells Scenario

This scenario accounts for when the rack cell walls and the fuel assembly cladding rupture. This allows individual fuel pellets to fall out of the rack cell. The fuel pellets could either drop to the SFP floor or get stuck between the rack cell walls. This section analyzes when the pellets are stuck between the rack cell walls. Section 9.1.2.2 analyzes the scenario when fuel pellets fall to the SFP floor.

This scenario is modeled by stacking fuel pellets between the cell walls. The total height of these fuel pellet stacks equals the height of remaining fuel in the assemblies. Additionally, the fuel pellet stacks are spaced at optimum pitch from each other. Optimum pellet stack pitch is calculated for each burnup and is shown in Table 9-2. Figures 9-7 through 9-9 illustrate how this scenario is modeled. Only three rows of fuel pellet stacks are modeled between each rack cell. This is because the fuel pellets would likely fall to the SFP floor if the space between the cells were larger which would be bounded by Fuel on the Floor analysis in Section 9.1.2.2.

For the burned fuel cases, the fuel pellets can either be axially aligned in ascending or descending order. In other words, the top depletion node (Node 18) can be located at the bottom of the fuel pellet stack or the top. Figure 9-8 and 9.1.2.3-3 shows these different scenarios. Both scenarios are tested and the results are shown in Table 9-1. For all burnup state points, the more reactive configuration was with Node 18 located at the bottom of the fuel pellet stack.

This model is extremely conservative due to the following reasons:

- It is practically impossible for fuel pellets to fall out of its assembly and rack cell and get stuck between rack cells at optimum pitch to other fuel pellets.
- The fuel assemblies in the fuel cells are still modeled at optimum pin pitch. It would be practically impossible for this to occur because lateral loads needed to deform the assembly would mean that the cells walls would be pushed up against each other. This likely would not leave enough space for fuel pellets to coalesce in fuel pellet stacks along the entire axial length of the fuel left in the assemblies.
- The scenario is modeled for all assemblies in Region 1 (324 assemblies). Optimum assembly fuel pin pitch and pellet stack pitch is modeled for all 324 assemblies in Region 1.

Deformation to the optimum pin and assembly pitch is detailed in Section 9.1.4. The optimum pellet pitch calculation is shown in Table 9-2. Figures 9-7 – 9-9 show axial and radial diagrams of the KENO model. Table 9-1 shows the reactivity of Region 1 when modeled with this scenario for each burnup. For comparison purposes, the reactivity of the other two scenarios are also shown. This scenario is limiting for the 0, 10, and 20 GWD/MTU state points. Therefore, the biases, uncertainties, and maximum k-eff for these burnups will be calculated using this scenario.

Figure 9-7: Cask Drop Accident Model, Zoomed In, x-y Profile

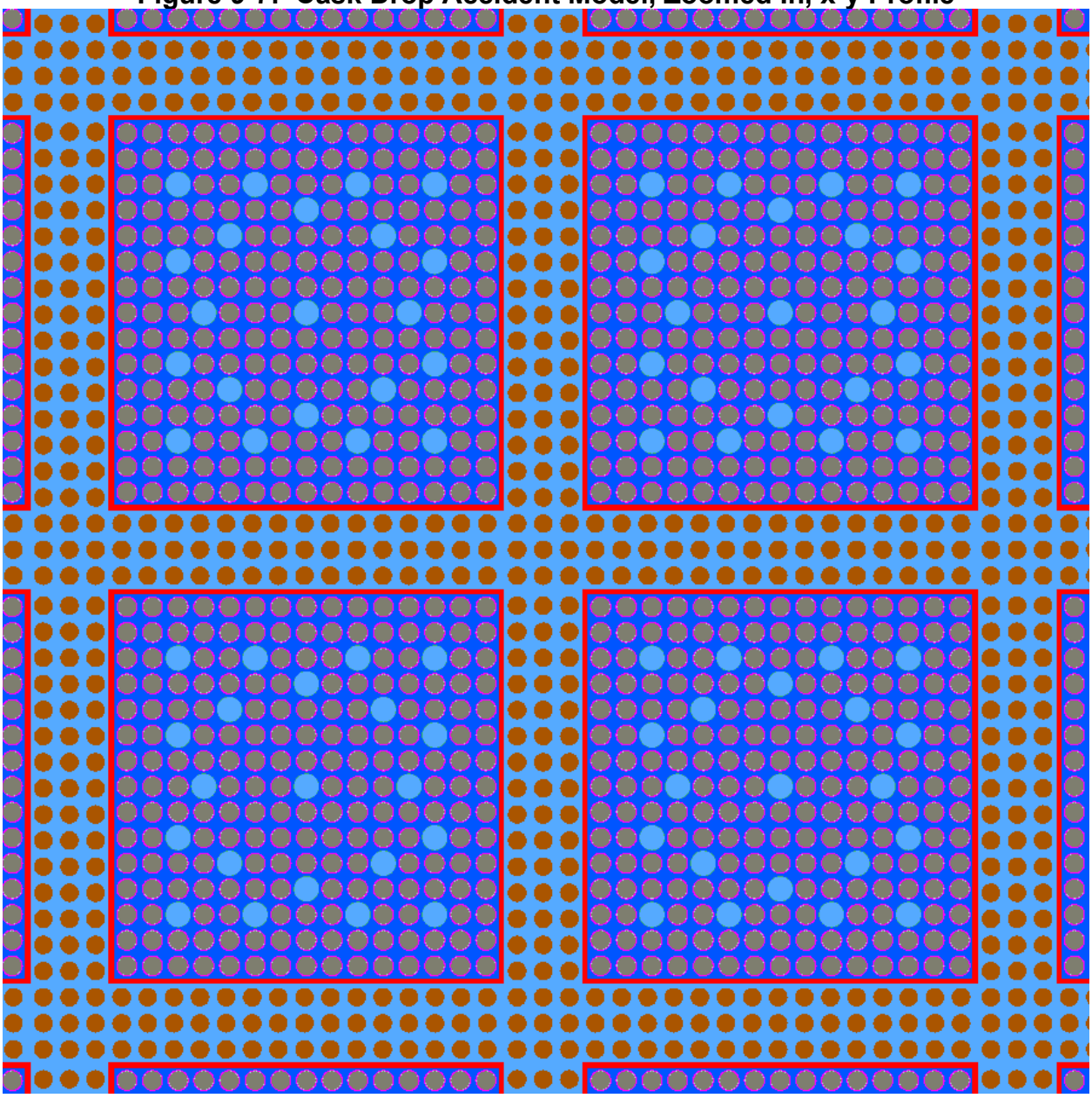

Picture of an x-y plane of the fuel in the KENO model. See Figure 9-8 and 9-9 for y-z planes. Stainless steel is red, light blue is borated water, grey is fuel, brown is fuel from a different depletion axial node, darker blue is borated water smeared with grids, and purple is zirconium.

Figure 9-8: Cask Drop Accident Model, Zoomed In, y-z Profile

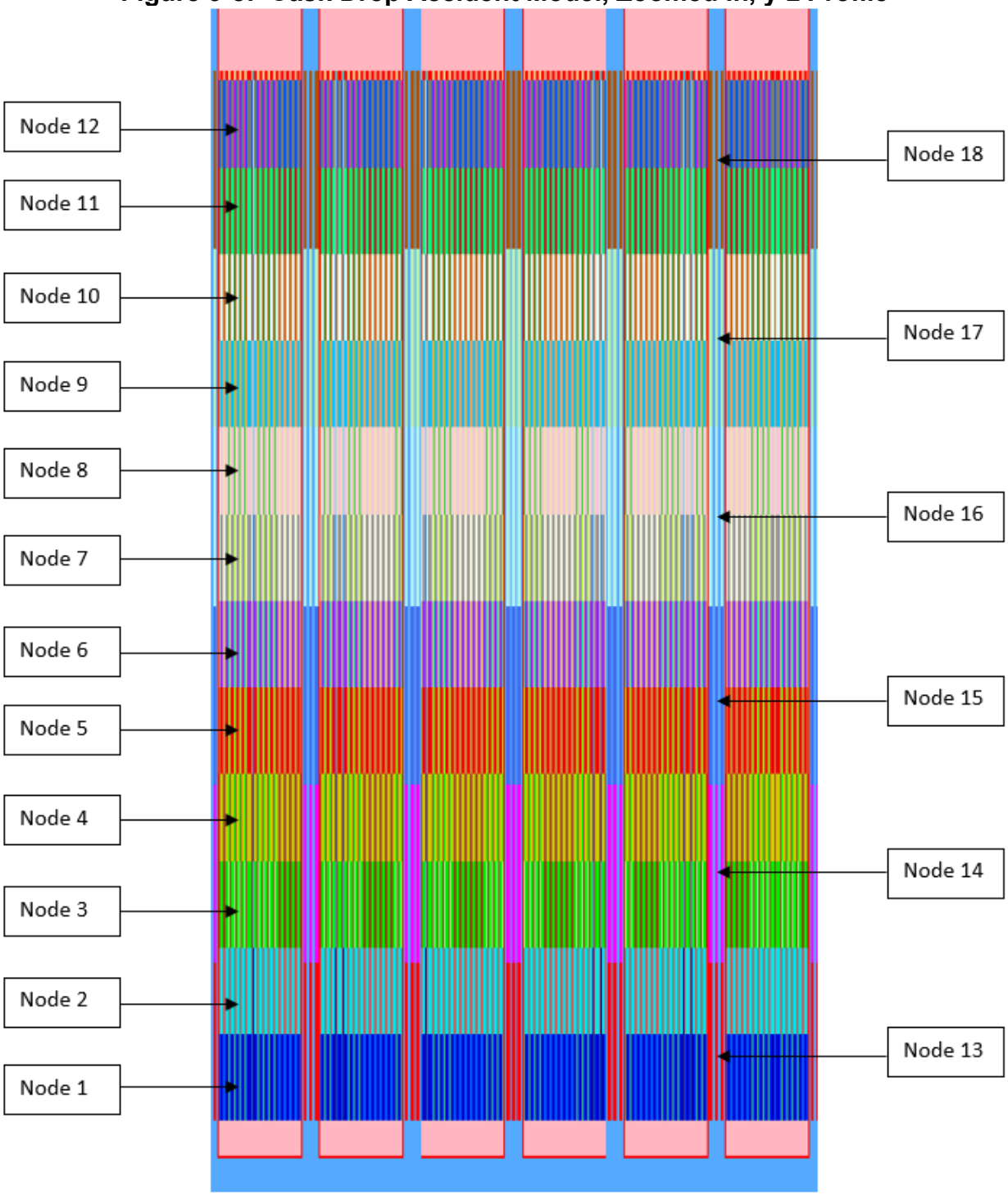

Picture of an y-z plane of the fuel in the KENO model. See Figure 9-7 for an x-y plane. Light blue is borated water, the rainbow colored portion represents the fuel from different axial depletion nodes and light pink above and below the fuel is the unborated water reflector. The dark brown is Node 18 and it is at the top of the fuel pellet stacks.

Figure 9-9: Cask Drop Accident Model, Zoomed In, y-z Profile, Pellet Stacks Reversed Axially

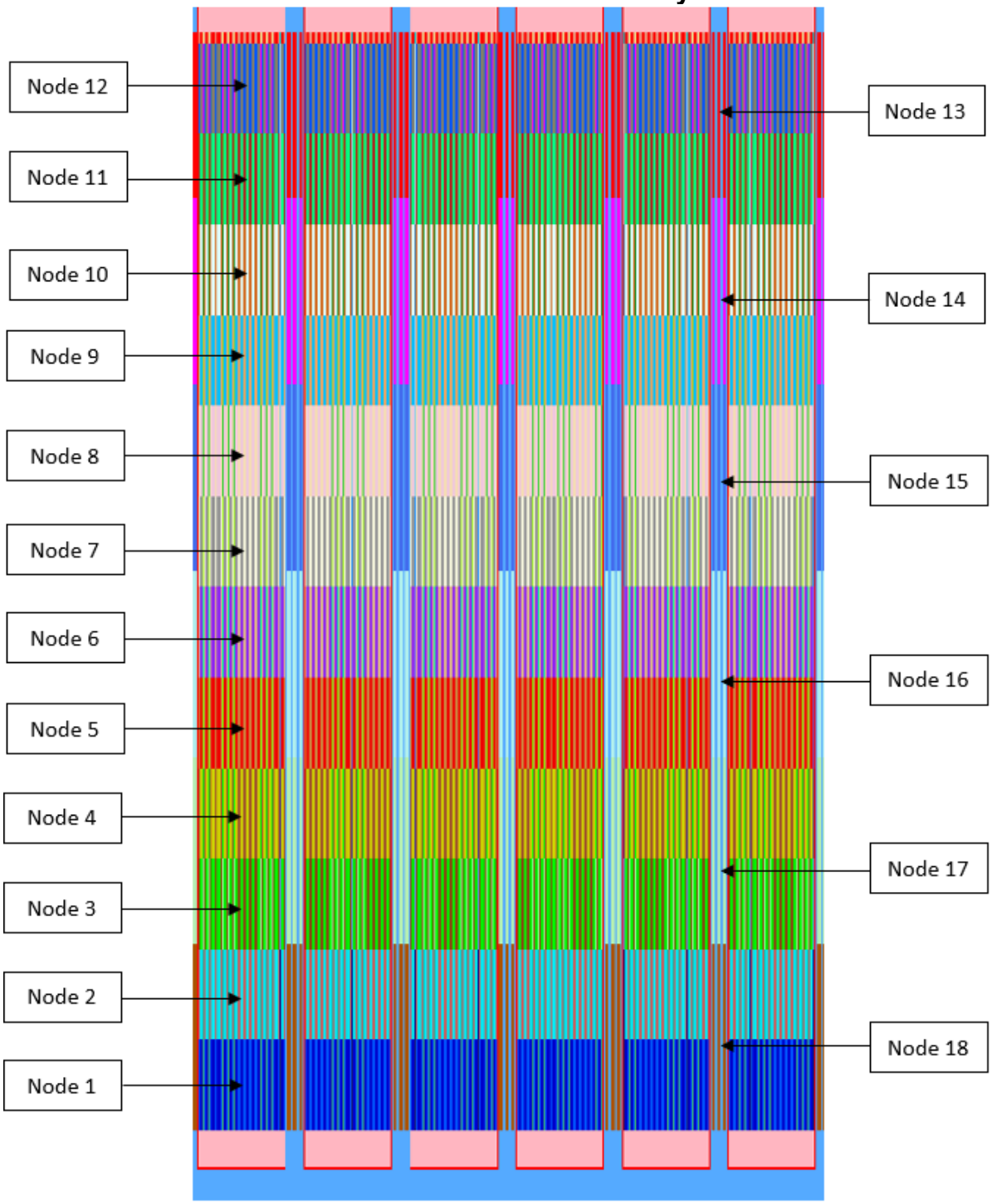

Picture of an y-z plane of the fuel in the KENO model. See Figure 9-7 for an x-y plane. Light blue is borated water, the rainbow colored portion represents the fuel from different axial depletion nodes and light pink above and below the fuel is the unborated water reflector. The dark brown is Node 18 and it is at the bottom of the fuel pellet stacks.

9.1.3 Region 1 KENO Model

Drawings and dimensions of the fuel racks are provided in Section 4.2. The primary KENO Region 1 model is a finite model with reflective boundary conditions. All assemblies in Region 1 are modeled in a 18x18 block. The initial neutron distribution source is uniform in all fissile material. Because the fuel is distributed evenly and because the convergence criterion was met, a uniform neutron source acceptable.

This analysis assumes that the Region 1 rack cells are damaged by a dropped cask. The deformation was modeled in an extreme and conservative manner. To simulate deformation, three scenarios were investigated: all fuel remains in the rack cells, fuel pellets on the SFP floor, and fuel pellets between rack cells. For each burnup state point, the most reactive scenario was used. Section 9.1.2 and its subsections go into more details about how the accident was modeled.

All figures in Sections 9.1.2.1 – 9.1.2.3 show the KENO models for the deformed racks of the cask drop accident. For comparison purposes, the normal fuel spacing can be seen in Figure 9-10. As can be seen in the figures, the amount of deformation required to reach optimum pitch in borated water is extensive.

Figure 9-10: Region 1 Model, Nominal Pitch

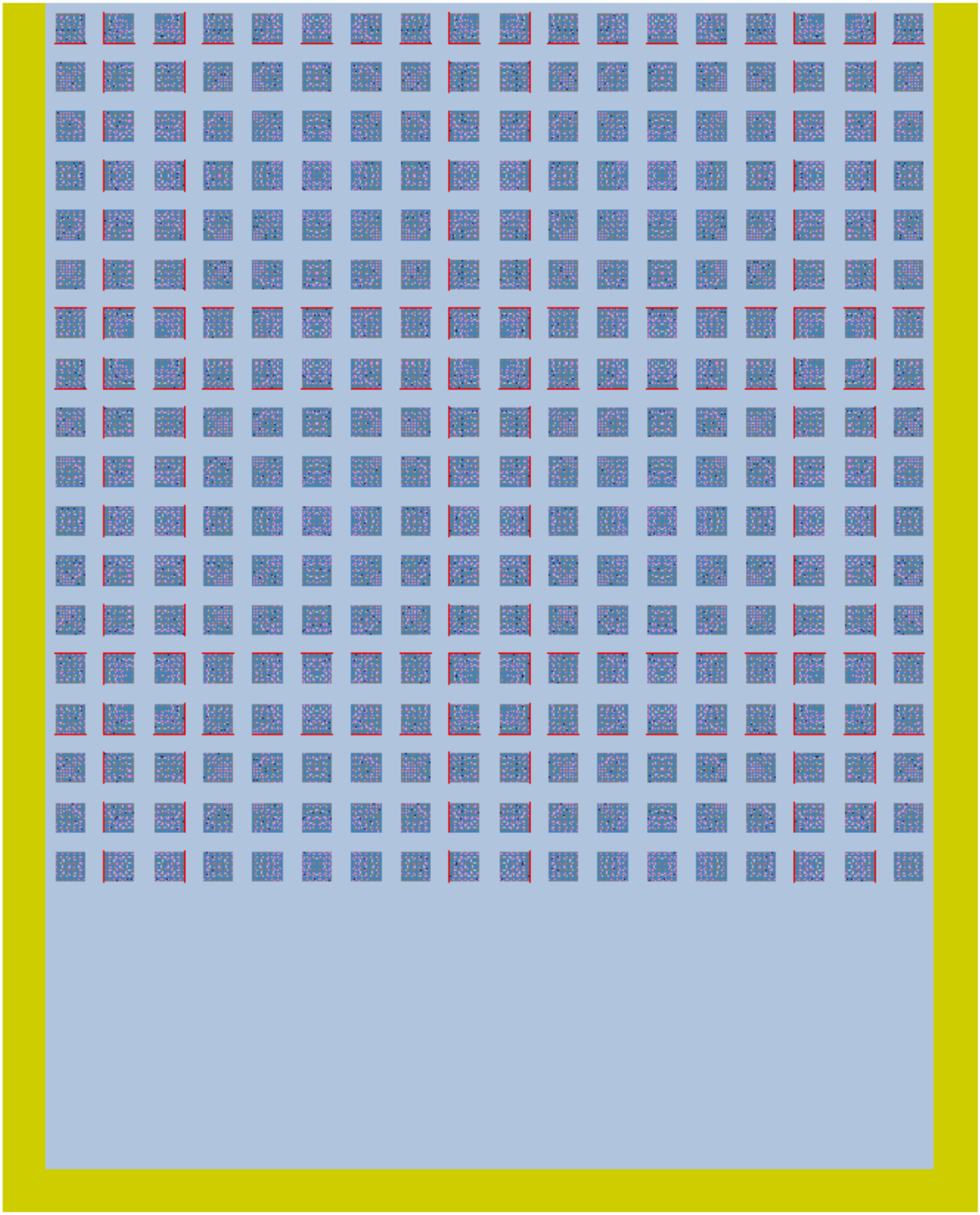

Picture of an x-y plane of the whole KENO model with nominal pitch. Concrete is in yellow, stainless steel is red, light blue is borated water, and the blocks are the assemblies. The cask loading area is at the bottom of the figure. Region 2 is north of Region 1 and starts at the figure's top boundary.

9.1.4 Optimum Pitch Calculation and Bias

The structural analysis did not determine exactly how the racks will be deformed/damaged by a cask drop accident; therefore, the racks were deformed until all the assemblies are at optimum pitch since this configuration will bound all other deformation possibilities. As discussed in Section 9.1.2, only the first 3 rack module rows are deformed by a dropped cask (all of Region 1). Table 9-3 shows test cases used to find the maximum k-eff. The 6 columns of distances in the table show how the racks and assemblies were modeled so that the optimum distance between assemblies and fuel pins could be found. Note that nominal assembly pitch is 35.56 cm and all cases in Table 9-3 were run with all the fuel in the rack cells (no loose fuel pellets on the SFP floor or between the rack cells).

The results of Table 9-3 show that the maximum k-eff for the fresh fuel occurs when there is significant rack and fuel assembly deformation. All the rack cells are pushed up against each other and the square rack tubes are crushed so that there is no additional space between the assembly and the inner cell wall. Additionally, the fuel pin pitch is reduced by 10% and the diameter of the guide and instrument tubes are decreased by ~5% due to the crushing of the fuel assembly. Figure 9-1 and 9.1.2.1-2 shows the KENO model and the layout for this scenario. For comparison purposes, Figure 9-10 shows the model and layout with the normal fuel pitch.

The optimum pitch changes depending primarily on the fuel burnup and SFP temperature. The temperature is fixed at 350K (see Section 9.1.5). The required burnup changes for each initial enrichment as shown in the burnup curve. It takes more than a trivial amount of time and effort to make new crush scenarios (each row in Table 9-3) due to the necessity to recalculate positions and conserve the volume of the solid materials. Therefore, it is not practical to find the optimum pitch for each burnup/enrichment combination. Instead, all cases are run with an assembly pitch of 19.84 cm and a quadratic regression curve of Δk vs. the assembly pitch is created for each burnup in Table 9-3 and the maximum of that curve is used as the “Optimal Pitch Bias”. This quadratic regression is shown in Figure 9-11. For each burnup, three data points are used to create the regression curve because using four data points sometimes resulted in a negative (non-conservative) bias. Note that all the cases in Section 9.1, outside of this subsection, use an assembly pitch of 19.84 cm.

While this method is not perfect due to the limited number of data points, it is still extremely conservative due to modeling the whole of Region 1 at optimum pitch. Reducing the pitch of all the cells into one cluster is an assumption that represents the maximum reactivity the fuel could conceivably attain. Finally, this accident is modeled as 6 rows of rack modules (3 rows modeled

and 3 reflected via the boundary condition) when the mechanical analysis only stated 2 rows would be damaged. Therefore, this method of calculating an optimum pitch using a regression curve is sufficient.

The calculated Optimum Pitch Bias is shown in Table 9-4. The trend of the bias is reasonable and in line with expectations.

Table 9-3: Region 1 k-eff at Varying Degrees of Rack Deformation

Burnup (GWD/T)	Assembly Pitch	Distance Between		Pin Pitch	Guide Tube/ Inst. Tube O.D.	Fuel Pin O.D.	k-eff	σ	Δk
		Adjacent Cell Walls	Assembly and Inner Cell Wall						
0	35.56	12.40	0.63	1.43	1.354	1.0719	0.495065	0.000019	-0.402587
	29.36	6.20	0.63	1.43	1.354	1.0719	0.561021	0.000052	-0.336631
	23.16	0.00	0.63	1.43	1.354	1.0719	0.819330	0.000046	-0.078322
	21.93	0.00	0.00	1.43	1.354	1.0719	0.832608	0.000048	-0.065044
	20.82	0.00	0.00	1.354	1.354	1.0719	0.869966	0.000049	-0.027686
	19.84	0.00	0.00	1.287	1.287	1.0719	0.897652	0.000019	--
	16.72	0.00	0.00	1.0719	1.0719	1.0719	0.891103	0.000059	-0.006549
10	21.93	0.00	0.00	1.43	1.354	1.0719	0.852792	0.000054	-0.043436
	20.82	0.00	0.00	1.354	1.354	1.0719	0.879296	0.00005	-0.016932
	19.84	0.00	0.00	1.287	1.287	1.0719	0.896228	0.000022	--
	16.72	0.00	0.00	1.0719	1.0719	1.0719	0.842795	0.000020	-0.053433
20	21.93	0.00	0.00	1.43	1.354	1.0719	0.870393	0.000053	-0.029074
	20.82	0.00	0.00	1.354	1.354	1.0719	0.890089	0.000059	-0.009378
	19.84	0.00	0.00	1.287	1.287	1.0719	0.899467	0.000051	--
	16.72	0.00	0.00	1.0719	1.0719	1.0719	0.823475	0.000056	-0.075992
30	21.93	0.00	0.00	1.43	1.354	1.0719	0.88112	0.000022	-0.018882
	20.82	0.00	0.00	1.354	1.354	1.0719	0.895593	0.000052	-0.004409
	19.84	0.00	0.00	1.287	1.287	1.0719	0.900002	0.000056	--
	16.72	0.00	0.00	1.0719	1.0719	1.0719	0.811321	0.000056	-0.088681
40	21.93	0.00	0.00	1.43	1.354	1.0719	0.885944	0.000054	-0.010928
	20.82	0.00	0.00	1.354	1.354	1.0719	0.896215	0.000058	-0.000657
	19.84	0.00	0.00	1.287	1.287	1.0719	0.896872	0.000022	--
	16.72	0.00	0.00	1.0719	1.0719	1.0719	0.800513	0.000056	-0.096359
47	21.93	0.00	0.00	1.43	1.354	1.0719	0.881843	0.000055	-0.007587
	20.82	0.00	0.00	1.354	1.354	1.0719	0.890397	0.000058	0.000967
	19.84	0.00	0.00	1.287	1.287	1.0719	0.889430	0.000059	--
	16.72	0.00	0.00	1.0719	1.0719	1.0719	0.790616	0.000021	-0.098814
53	21.93	0.00	0.00	1.43	1.354	1.0719	0.856384	0.000039	-0.006931
	20.82	0.00	0.00	1.354	1.354	1.0719	0.864822	0.000053	0.001507
	19.84	0.00	0.00	1.287	1.287	1.0719	0.863315	0.000056	--
	16.72	0.00	0.00	1.0719	1.0719	1.0719	0.765212	0.000061	-0.098103

*(All distances are in cm)

Table 9-4: Optimum Pitch Bias

Burnup (GWD/MTU)	Bias (Δk)
0	0.02112
10	0.00293
20	0.00015
30	0.00016
40	0.00031
47	0.00098
53	0.00193

Figure 9-11: Example of Optimum Pitch Bias Regression Curve (53 GWD/MTU)

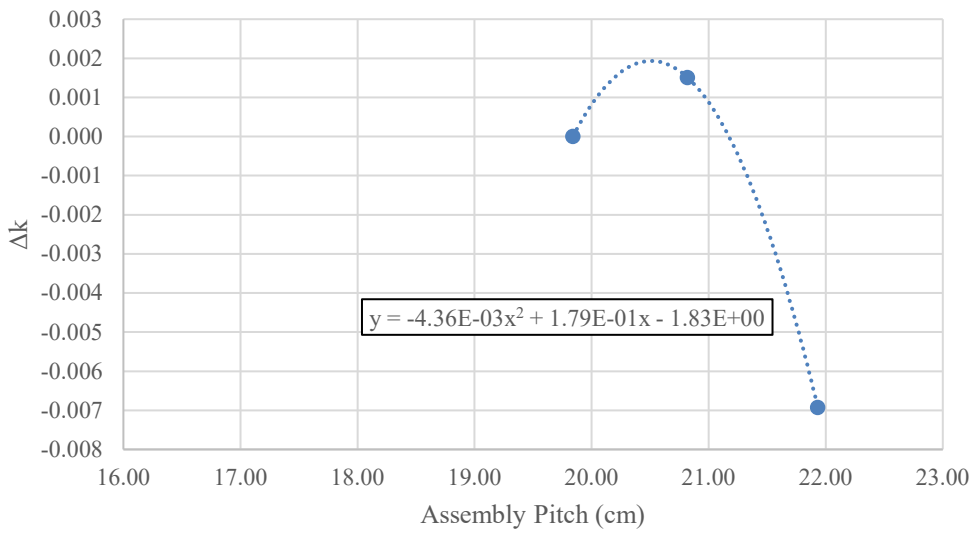

9.1.5 SFP Normal Operation Water Temperature and Density

Temperature's effect on the reactivity is largely based on its effect on the fuel to moderator ratio. The fuel to moderator ratio is mostly affected by the fuel and assembly pitch which is further discussed in Section 9.1.4.

The maximum, non-accident SFP temperature of the SFP is 350K or 170°F. The low temperature limit of the SFP is set to lower physical limit of liquid water: 273K or 32°F. Test cases were run and determined the maximum reactivity occurs at the highest operating temperature. Therefore, all cases are run at 350K. The test case results are shown in Table 9-5.

Table 9-5: Region 1 k-eff at Varying Spent Fuel Pool Temperatures

Temperature		k-eff	σ	Δk
(°F)	(K)			
32	273	0.894412	0.00005	-0.00324
100	311	0.896774	0.00005	-0.00088
170	350	0.897652	0.000019	--

9.1.6 Axial Burnup Shapes

Section 8.6 showed that the NUREG/CR-6801 [9] industry burnup shapes are applicable for Surry. However, NEI 12-16 [32] states that all burnup shapes must be compared against a uniform axial shape with the limiting shape being used in the maximum k-eff calculation.

Previous criticality analyses [14, 23] showed that uniform burnup shapes are most reactive, relative to the NUREG/CR-6801 burnup shapes, at low assembly burnups. Therefore, uniform depletion cases were run at 10 and 20 GWD/MTU for Surry.

Keno cases were run with the NUREG burnup shapes and the uniform burnup shapes. Table 9-6 shows the results of these cases. Both burnups show that the NUREG shape is conservative. As burnup increases, the NUREGs become more conservative. Therefore, the NUREG shapes will be used for all burnups.

Table 9-6: Bounding Burnup Shape Cases

Case Description	Burnup (GWD/MTU)	Enrichment (wt%)	k	σ	Δk
NUREG Shape	10	2.20%	0.903734	0.000052	--
Uniform Shape			0.898858	0.000053	-0.00488
NUREG Shape	20	2.85%	0.893959	0.000035	--
Uniform Shape			0.892009	0.000049	-0.00195

9.1.7 Manufacturing Uncertainties

A full complement of uncertainty cases was run for all burnup steps. Tables 3-3 and 4-3 shows the uncertainty values for the SFP assemblies and racks, respectively. Table 9-7 shows the uncertainty KENO cases.

The percent theoretical density uncertainty case was calculated at 0 GWD/MTU of burnup. This is acceptable because this uncertainty is worth a relatively small amount. When root sum squared with the other uncertainty worths, it is only worth ~3 pcm.

To include the Monte Carlo uncertainty in the maximum k-eff uncertainty calculations, the "Uncert." column is calculated by adding 2 times the root sum square of the case uncertainties to the Δk between cases.

Table 9-7: Uncertainty Cases

Case Description	Burnup (GWD/MTU)	Enrichment (wt%)	k	σ	Uncert. (Δk)
Base Case	0	1.65%	0.861170	0.000049	--
Fuel Stack PTD			0.86241	0.000047	0.0014
Enrichment		1.60%	0.850431	0.000053	0.0109
Pellet OD		1.65%	0.862312	0.000051	0.0013
Active Fuel Length			0.861252	0.000046	0.0002
Clad ID, +			0.861553	0.000051	0.0005
Clad ID, -			0.860755	0.000051	-0.0003
Clad OD, +			0.862065	0.000053	0.0010
Clad OD, -			0.860416	0.000051	-0.0006
GT, +			0.861731	0.000047	0.0007
GT, -			0.860725	0.000048	-0.0003
Cell Wall Thickness			0.864113	0.000051	0.0031
Base Case	10	2.20%	0.903734	0.000052	--
Enrichment		2.25%	0.909460	0.000039	0.0059
Pellet OD		2.20%	0.904290	0.000052	0.0007
Active Fuel Length			0.903857	0.000051	0.0003
Clad ID, +			0.904168	0.000053	0.0006
Clad ID, -			0.903327	0.000037	-0.0003
Clad OD, +			0.903989	0.000062	0.0004
Clad OD, -			0.903613	0.000047	0.0000
GT, +			0.903901	0.000048	0.0003
GT, -			0.903415	0.000052	-0.0002
Cell Wall Thickness			0.906193	0.000034	0.0026
Fresh Fuel Case	0		0.957522	0.000048	--
Fuel Stack PTD			0.958536	0.000052	0.0012

Table 9-7: Uncertainty Cases (cont.)

Case Description	Burnup (GWD/MTU)	Enrichment (wt%)	k	σ	Δk
Base Case	20	2.85%	0.893959	0.000035	--
Enrichment		2.80%	0.889333	0.000056	0.0048
Pellet OD		2.85%	0.894327	0.000050	0.0005
Active Fuel Length			0.894552	0.000053	0.0007
Clad ID, +			0.894301	0.000052	0.0005
Clad ID, -			0.893611	0.000034	-0.0003
Clad OD, +			0.893826	0.000034	0.0000
Clad OD, -			0.893970	0.000050	0.0001
GT, +			0.894101	0.000037	0.0002
GT, -			0.893762	0.000056	-0.0001
Cell Wall Thickness			0.896420	0.000049	0.0026
Fresh Fuel Case	0		1.044377	0.000039	--
Fuel Stack PTD			1.045328	0.000055	0.0011
Base Case	30	3.45%	0.878406	0.000053	--
Enrichment		3.40%	0.874690	0.000062	0.0039
Pellet OD		3.45%	0.878823	0.000036	0.0005
Active Fuel Length			0.880458	0.000055	0.0022
Clad ID, +			0.878712	0.000055	0.0005
Clad ID, -			0.878037	0.000052	-0.0002
Clad OD, +			0.877581	0.000059	-0.0007
Clad OD, -			0.879209	0.000063	0.0010
GT, +			0.878241	0.000056	0.0000
GT, -			0.878483	0.000039	0.0002
Cell Wall Thickness			0.880676	0.000035	0.0024
Fresh Fuel Case	0		1.080581	0.000055	--
Fuel Stack PTD			1.081402	0.000065	0.0010
Base Case	40	4.10%	0.875768	0.000054	--
Enrichment		4.05%	0.872095	0.000053	0.0038
Pellet OD		4.10%	0.876223	0.000058	0.0006
Active Fuel Length			0.875756	0.000056	0.0001
Clad ID, +			0.875820	0.000037	0.0002
Clad ID, -			0.875398	0.000056	-0.0002
Clad OD, +			0.875437	0.000063	-0.0002
Clad OD, -			0.875876	0.000053	0.0003
GT, +			0.875734	0.000037	0.0001
GT, -			0.875701	0.000056	0.0001
Cell Wall Thickness			0.876638	0.000057	0.0010
Fresh Fuel Case	0		1.132643	0.000057	--
Fuel Stack PTD			1.133640	0.000056	0.0012

Table 9-7: Uncertainty Cases (cont.)

Case Description	Burnup (GWD/MTU)	Enrichment (wt%)	k	σ	Δk
Base Case	47	4.55%	0.889408	0.000055	--
Enrichment		4.50%	0.886147	0.000060	0.0034
Pellet OD		4.55%	0.889932	0.000066	0.0007
Active Fuel Length			0.889525	0.000057	0.0003
Clad ID, +			0.889659	0.000059	0.0004
Clad ID, -			0.889197	0.000065	0.0000
Clad OD, +			0.889440	0.000057	0.0002
Clad OD, -			0.889719	0.000038	0.0004
GT, +			0.889307	0.000060	0.0001
GT, -			0.889415	0.000063	0.0002
Cell Wall Thickness			0.890350	0.000063	0.0011
Fresh Fuel Case	0		1.162918	0.000059	--
Fuel Stack PTD			1.163584	0.000038	0.0008
Base Case	53	5.00%	0.895885	0.000047	--
Enrichment		4.95%	0.893034	0.000060	0.0030
Pellet OD		5.00%	0.896326	0.000039	0.0006
Active Fuel Length			0.896004	0.000057	0.0003
Clad ID, +			0.896042	0.000057	0.0003
Clad ID, -			0.895816	0.000059	0.0001
Clad OD, +			0.895773	0.000039	0.0000
Clad OD, -			0.896105	0.000057	0.0004
GT, +			0.895912	0.000055	0.0002
GT, -			0.896030	0.000060	0.0003
Cell Wall Thickness			0.896831	0.000063	0.0011
Fresh Fuel Case	0		1.189125	0.000037	--
Fuel Stack PTD			1.189717	0.000057	0.0007

9.1.8 Planar Burnup Tilt Bias

A planar or radial burnup tilt occurs when there is a burnup gradient across the x-y plane of an assembly. This can cause reactivity increases when low burnup sides of assemblies are oriented towards each other.

The radial burnup tilt bias is calculated using Node 16. Three TRITON depletion cases are run to calculate each bias. The base TRITON case has the base burnup, the high burnup TRITON case increases the base burnup by the appropriate percentage, and the low burnup TRITON case decreases the base burnup by the appropriate percentage. The depletion powers are altered to achieve the desired burnup assuming the depletion time stays constant and a uniform axial burnup shape. Since the depletion power has changed, the depletion temperatures are accordingly updated.

Surry rack modules have 36 rack cells arranged in a 6x6 configuration. The outer row of assemblies in each rack module (20 assemblies) will be modeled with a uniform burnup profile across all fuel pins. The 16 assemblies in the middle of the rack module will be modeled with a horizontal tilt. The assemblies will be orientated so that the low burnup halves are pointed towards the center to maximize reactivity. Figures 9-12 and 9-13 shows this model for the cask drop damage scenario when all fuel is contained in the rack cells (30 GWD/MTU). For the scenarios where fuel pellets drop to the SFP floor (40, 47, and 53 GWD/MTU) or are stuck between rack cells (0, 10, and 20 GWD/MTU), the pellets are arranged in the same orientation as in Figures 9-12 and 9-13. For each of the middle 16 assemblies, pellet stacks with low burnup are stacked toward the middle of the 6x6 rack module and pellet stacks with high burnup are stacked toward the outside of the 6x6 rack module.

A separate base radial tilt KENO case is run where none of the assemblies have a radial burnup tilt. The k-eff of this uniform case is subtracted from the radial tilted case to calculate the radial burnup tilt bias.

It is adequate to only model 16 assemblies with a radial tilt rather than all 36 in the rack module because it is very unlikely for 16 assemblies to have both the assumed tilt and also be optimally positioned. Figure 8-15 shows that the fraction of the fuel population with a large radial tilt is small. The fuel shuffling and storage process does not cluster fuel assemblies with high tilt nor arrange tilted fuel in the most reactive configuration by design.

Presuming each fuel assembly has high radial tilt and the tilt orientation is one of four equally probable diagonal orientations and if assembly placement is random (there is no operational

procedure or design feature which would make this process non-random), there is a 25% chance that each assembly is correctly positioned in the 4x4 block. The probability for 16 assemblies to be simultaneously optimally orientated is 0.25^{16} = 2.3E-10. Assuming Surry operates for another 40 years and shuffles the SFP every refueling outage (1.5 years) for each unit (2 units) means that the 324 cells have a maximum of 17,280 (40 / 1.5 * 2 * 324) chances to form an optimal 4x4 block of radial tilted assemblies. Multiplying the probability of success (2.3E-10) by the number of trials (17,280) results in the SPS SFP having an expected outcome of 4.0E-6. Assuming random placement, this configuration is unlikely to occur over the lifetime of the SFP. Factoring in that the magnitude of the radial tilt is a bounding 95/95 curve, it is clear that this is a conservative method.

These cases are only run at Node 16. This is acceptable because the Δk is the only value that matters. The absolute k-eff itself does not affect maximum k-eff. However, comparing the Node 16 base case KENO k-eff in Table 9-9 to the full assembly absolute k-eff in Table 9-7 shows that the two k-effs are similar. This means that Node 16 is a good proxy for the whole assembly.

From Figure 8-15 and Table 8-17, the amount of tilt for the burnups in this calculation was determined. These tilts are displayed in Table 9-8 below. Table 9-9 shows the results of these KENO cases. The radial burnup bias is calculated by adding 2 times the root sum square of the case uncertainties to the Δk between cases. Note that this bias was calculated with the bounding cask drop scenario determined in Table 9-1.

Table 9-8: Radial Burnup Tilt Burnup

Burnup [GWD/MTU]	Planar Tilt [%]	
	Negative	Positive
10	-25.6%	25.6%
20	-21.3%	21.3%
30	-16.9%	16.9%
40	-12.6%	12.6%
47	-9.53%	9.53%
53	-6.92%	6.92%

Table 9-9: Radial Burnup Tilt Bias

Case Description	Nominal Burnup (GWD/MTU)	Enrichment (wt%)	k	σ	Δk	Bias (Δk)
Uniform Burnup	10	2.20%	0.891021	0.000052	--	0.0004
Burnup Tilt			0.891244	0.000057	0.00022	
Uniform Burnup	20	2.85%	0.901000	0.000050	--	0.0009
Burnup Tilt			0.901758	0.000053	0.00076	
Uniform Burnup	30	3.45%	0.872438	0.000053	--	0.0010
Burnup Tilt			0.873355	0.000034	0.00092	
Uniform Burnup	40	4.10%	0.857149	0.000049	--	0.0009
Burnup Tilt			0.857937	0.000051	0.00079	
Uniform Burnup	47	4.55%	0.849760	0.000048	--	0.0005
Burnup Tilt			0.850130	0.000053	0.00037	
Uniform Burnup	53	5.00%	0.843424	0.000050	--	0.0004
Burnup Tilt			0.843714	0.000034	0.00029	

Figure 9-12: Radial Tilt KENO Model (zoomed out)

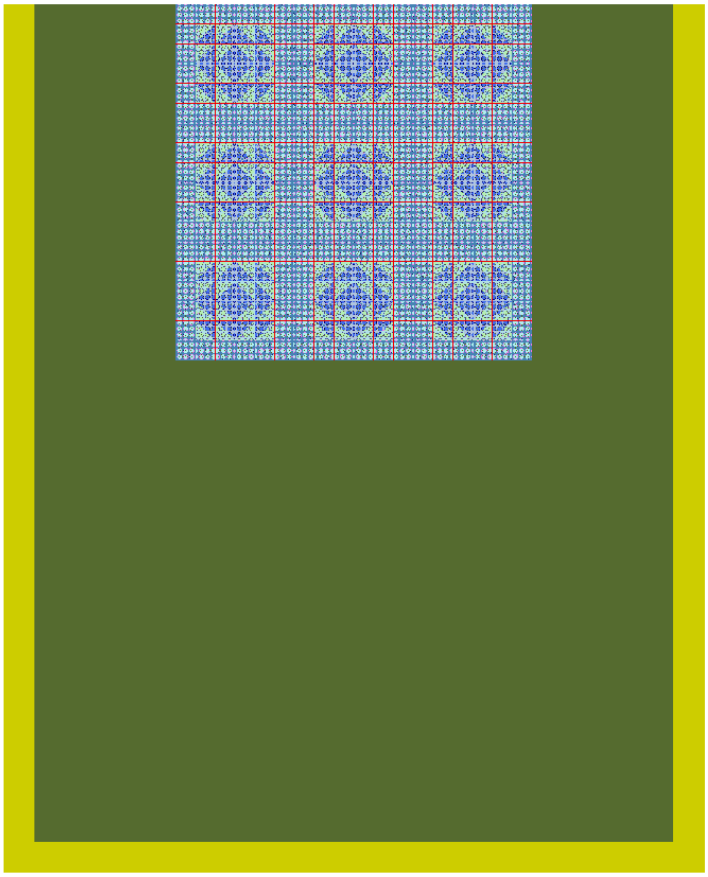

Figure 9-13: Radial Tilt KENO Model (zoomed in)

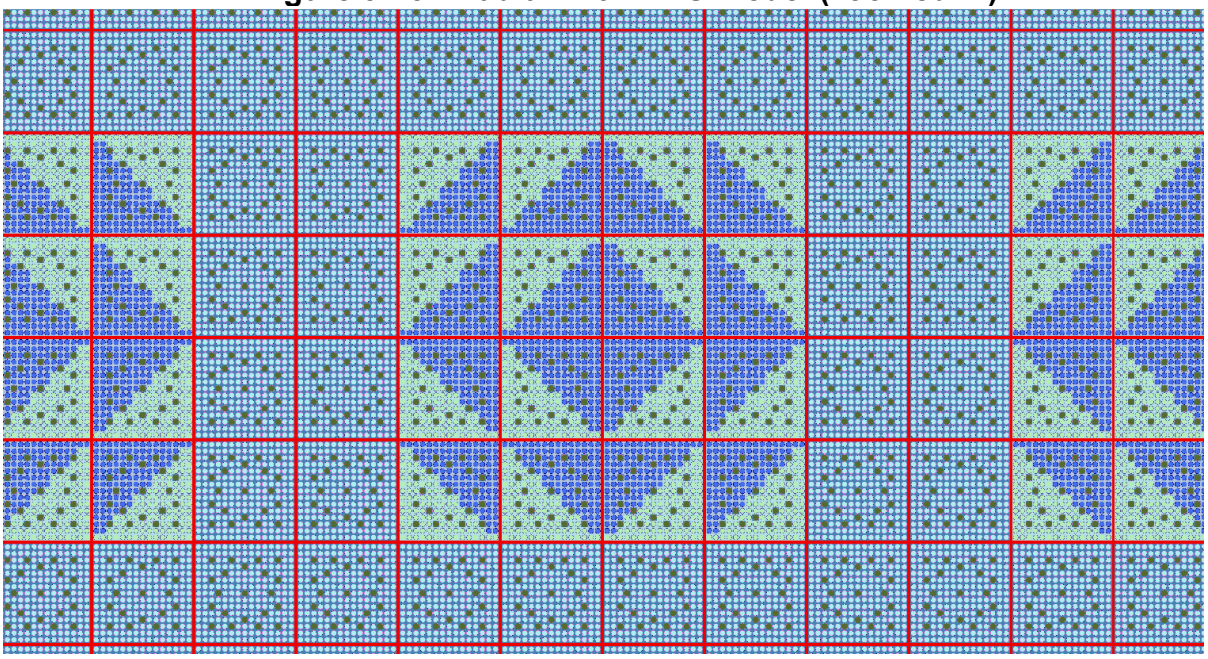

9.1.9 Reduced Power Coastdown Bias

As discussed in Section 8.10, reducing power at the end of an assembly's lifetime can have the effect of producing less PM-149 and reducing the SM-149 peak after discharge. Section 8.10 advised modeling 20 days at 50% power at the end of the depletion. This requires that 10 days is added to the depletion time to ensure the same amount of burnup. A sensitivity case with the power coastdown was run for all burnup steps. Like the Radial Burnup Bias, this bias is only calculated at Node 16. Results are shown in Table 9-10. The low power coastdown bias is calculated by adding 2 times the root sum square of the case uncertainties to the Δk between cases.

Table 9-10: Low Power Coastdown Bias

Case Description	Burnup (GWD/MTU)	Enrichment (wt%)	k	σ	Δk	Bias (Δk)
Constant Power	10	2.40%	0.891021	0.000052	--	0.0022
Low Power at EOL			0.893101	0.000051	0.00208	
Constant Power	20	3.05%	0.901000	0.000050	--	0.0017
Low Power at EOL			0.902590	0.000052	0.00159	
Constant Power	30	3.80%	0.872438	0.000053	--	0.0017
Low Power at EOL			0.873978	0.000052	0.00154	
Constant Power	40	4.65%	0.857149	0.000049	--	0.0016
Low Power at EOL			0.858598	0.000051	0.00145	
Constant Power	47	5.00%	0.849760	0.000048	--	0.0013
Low Power at EOL			0.850943	0.000048	0.00118	
Constant Power	53	5.00%	0.843424	0.000050	--	0.0011
Low Power at EOL			0.844338	0.000051	0.00091	

9.1.10 Minor Actinides and Fission Product Bias

Section 6.3.2 has further background and discussion about the applicability of this bias.

An additional bias will be added to the maximum k-eff calculation which is worth 1.5% of the minor actinides and fission product worth. To calculate the worth of the minor actinides and fission products, an extra KENO case is run with only the major actinides. The base case k-eff (containing all isotopes) is then subtracted from the k-eff which was calculated using only major actinides.

The fuel isotope composition file from the standard depletion and decay cases was used. This composition file was edited so that all isotopes were removed except for the major actinides. This calculation uses the same major actinides as were used in NUREG/CR-7109 [13]: U-234, U-235, U-238, Pu-238, Pu-239, Pu-240, Pu-241, Pu-242, and Am-241. O-16 was also included in these cases.

Table 9-11 shows the results from the Minor Actinide Bias cases. The bias is calculated by taking the difference between the major actinide case and the nominal case and then multiplying that difference by 1.5%.

Table 9-11: Minor Actinides Bias

Case Description	Burnup (GWD/MTU)	Enrichment (wt%)	k	σ	Δk	Bias (Δk)
All Isotopes	10	2.20%	0.903734	0.000052	--	0.0006
Major Actinides Only			0.946622	0.000036	0.0429	
All Isotopes	20	2.85%	0.893959	0.000035	--	0.0011
Major Actinides Only			0.966285	0.000053	0.0723	
All Isotopes	30	3.45%	0.878406	0.000053	--	0.0012
Major Actinides Only			0.960026	0.000055	0.0816	
All Isotopes	40	4.10%	0.875768	0.000054	--	0.0012
Major Actinides Only			0.957976	0.000058	0.0822	
All Isotopes	47	4.55%	0.889408	0.000055	--	0.0013
Major Actinides Only			0.974789	0.000059	0.0854	
All Isotopes	53	5.00%	0.895885	0.000047	--	0.0014
Major Actinides Only			0.986819	0.000058	0.0909	

9.1.11 Depletion Benchmark Bias and Uncertainty

Application Code Bias

Appendix B benchmarked the TRITON depletion and ORIGAMI decay method against measured depletion decrement data in EPRI 3002010613 [35]. The cask drop accident does not change the fuel's depletion characteristics. Therefore, the fuel is completely within the range of applicability of described in Appendix B. The depletion benchmark calculated the depletion Application Code Bias which is repeated Table 9-12.

Table 9-12: Depletion Application Code Bias (Δk)

Condition	Decay Time		
	< 100 hours	< 5 years	< 15 years
Base Case	0.0010	0.0040	0.0041
Rod OD < 0.95 cm	--	--	--
< 4.25% Enrichment	0.0017	0.0015	0.0017
> 4.25% Enrichment	--	--	--
Burnable Absorber	--	--	--
> 900 ppm Depletion	--	--	--
Rack T > 293 K	--	--	--
Borated Rack	--	--	--
Power > 38.1 MW/MT	--	0.0002	0.0003
Conservative Bias	0.0028	0.0057	0.0061

The decay time in this analysis is always 100 hours, so the 5 and 15 year columns will not be used. The 40 GWD/MTU and 45 GWD/MTU state points have fuel enrichments > 4.25% meaning the 0.0017 bias could be removed. However, for simplicity and conservatism, **all burnups and enrichments will use a Depletion Application Code Bias of 0.0028 Δk**.

Added EPRI Uncertainty and NRC Bias

As stated in Appendix B, there are additional bias and uncertainty terms that need to be added in compliance with the EPRI Utilization Report [36]. These terms are mandated and there are no calculations or stipulations associated with it. These terms are shown below.

Table 9-13: Additional Depletion Bias and Uncertainty Terms

Burnup (GWD/MTU)	Enrichment (wt%)	Bias (%)	Uncertainty (%)	Bias (Δk)	Uncertainty (Δk)
10	2.20%	0.00%	3.05%	0.0000	0.0016
20	2.85%	0.00%	2.66%	0.0000	0.0040
30	3.45%	0.00%	2.33%	0.0000	0.0047
40	4.10%	0.15%	2.12%	0.0004	0.0054
47	4.55%	0.29%	2.00%	0.0008	0.0055
53	5.00%	0.41%	1.91%	0.0012	0.0056

9.1.12 Code Temperature Bias

Appendix A identified and calculated a temperature bias associated with the computer codes and methodology. The temperature bias is defined below where T is the temperature of the model in Kelvin.

$$Bias = 1 * 10^{-5} * (T - 293)$$

All the models for the cask drop accident is run at 350 K. This equates to a temperature Δk bias of 0.00057 for all burnups.

9.1.13 Code Validation Bias and Uncertainty

Validation of SCALE/KENO using ENDF/B-VII 238 group cross sections in Appendix A identified EALF as the primary bias and uncertainty trend. Region 1 KENO cases have EALFs ≤ 1.25 eV. They had such high EALFs because (i) the racks and fuel pins were so close to each other due to deformation and (ii) the SFP water was borated to 2250 ppm since this is an accident scenario. The applicable bias and uncertainty for fresh fuel and depleted fuel are shown in Table 9-14. This table is taken from Appendix A.

Table 9-15 show the code benchmark bias and uncertainty applied to this analysis. Note that both the UO_2 and MOX biases and uncertainties can apply to the burned fuel in the table below. However, the MOX bias and uncertainty bounds the UO_2 bias and uncertainty.

Table 9-14: Code Benchmarking Bias and Uncertainty (Appendix A)

EALF (eV)	Bias (Δk)	Uncertainty (Δk)
Fresh UO_2 Fuel		
0.00 – 0.40	0.0030	0.0040
0.40 – 0.80	0.0040	0.0045
0.80 – 1.10	0.0055	0.0050
1.10 – 1.25	0.0060	0.0050
1.25 – 1.40	0.0065	0.0055
Burned MOX Fuel		
0.00 – 0.40	0.0015	0.0060
0.40 – 0.80	0.0025	0.0095
0.80 – 1.10	0.0030	0.0120
1.10 – 1.25	0.0035	0.0135
1.25 – 1.40	0.0035	0.0145

Table 9-15: Cask Drop Code Benchmarking Bias and Uncertainty

Burnup (GWD/MTU)	EALF (eV)	Bias (Δk)	Uncertainty (Δk)
0	0.69	0.0040	0.0045
10	0.91	0.0030	0.0120
20	1.06	0.0030	0.0120
30	1.11	0.0035	0.0135
40	0.97	0.0030	0.0120
47	0.99	0.0030	0.0120
53	1.03	0.0030	0.0120

9.1.14 Measured Burnup Uncertainty

This analysis uses a measured burnup uncertainty of 5%. This value is an industry generic value discussed in NEI 12-16 [32]. The following exercise confirms that this value is applicable and bounding for Surry.

The uncertainty of the measured burnup consists of five measurement uncertainties. These uncertainties are root sum squared together to determine the final measured burnup uncertainty.

1) Assembly relative power uncertainty
   - Monitored location uncertainty:
     The CMS5 benchmarking analysis for Surry determined that the integral pin reaction rate measurement uncertainty is **2.37%**. This value is going to be used for the power measurement uncertainty of monitored locations.
   - Unmonitored location uncertainty:
     This term accounts for the increased uncertainty that occurs when the power of an assembly without a direct measurement needs to be inferred from a neighboring assembly which are directly measured. An analysis was performed for Millstone Unit 3 which removed a monitored assembly from a flux map and then compared the RPDs from that particular location with and without the direct measurement [14]. This was done for all locations of 12 flux maps. The 95/95 tolerance limit percent difference was +2.69% and -1.99%. For this Surry analysis, a conservative value of **3.00%** is used which bounds the data from the Millstone Unit 3 analysis. Applying this Millstone Unit 3 value to Surry is acceptable because this analysis is only used to confirm the industry generic 5% reactor record burnup uncertainty. The unmonitored location uncertainty term will be root sum squared with the other four terms so any small differences between Millstone Unit 3 and Surry will have a small effect on the combined uncertainty compared to the industry generic 5% uncertainty.
2) Calorimetric power uncertainty
   The bounding calorimetric power uncertainty for Surry is **2.00%**.
3) Fuel assembly uranium loading uncertainty
   The Surry new fuel storage area calculation determined that the fuel density standard deviation of the Upgrade fuel is 0.17%. This will be multiplied by 2 to generate a 95% confidence uncertainty. Therefore, the fuel assembly uranium loading uncertainty is **0.34%**. Note that this uncertainty is needed for the calculation of burnup (Energy / Uranium Mass).

4) Monthly time integration of power uncertainty
   This uncertainty term accounts for the amount of power drift that an assembly experiences between measurements. An excel hand calculation was performed for the last 4 Surry cycles where assembly burnups were calculated using 1000 MWD/MTU measurement intervals and constant RPDs over the whole interval. For example, an assembly's burnup between a cycle burnup of 11 – 12 GWD/MTU is the assembly's RPD at 11 GWD/MTU multiplied by 1 GWD/MTU. This method represents a no-drift burnup. This no-drift burnup is then compared to SIMULATE calculated burnups at end of cycle. The results have a standard deviation of 0.56%. This value is doubled to generate a 95% confidence uncertainty of **1.12%**.

Root sum squaring the 5 components results in a Burnup Measurement Uncertainty of RSS(2.37%, 3.00%, 2.00%, 0.34%, 1.12%) = 4.47%.

Since some engineering judgment was used for the RPD uncertainty associated with unmonitored locations, an industry standard value of **5%** will be used for the Burnup Measurement Uncertainty instead of the Surry specific value of 4.47%. 5% has typically been assumed in criticality analyses according to NEI 12-16 [32]. The analysis above shows that an uncertainty of 5% is conservative for Surry since it is greater than the site specific value. Table 9-16 shows the Δk worth of the burnup measurement uncertainty for each burnup state point (5% * depletion worth).

Table 9-16: Measured Burnup Uncertainty

Burnup (GWD/MTU)	Burnup Worth (Δk)	Uncertainty (Δk)
10	0.0538	0.0027
20	0.1504	0.0075
30	0.2022	0.0101
40	0.2569	0.0128
47	0.2735	0.0137
53	0.2932	0.0147

9.1.15 Common Depletion Biases Not Applicable for Surry

The following three biases are usually included for SFP criticality safety analyses which credit burnup. However, these are not applicable for Surry's analysis.

- Asymmetric / eccentric fuel placement
- Grid growth bias
- Clad creep down bias

The reason these are not applicable is because the cask drop accident prohibits these scenarios from happening. The fuel racks are damaged by the dropped cask and optimum fuel assembly pitch is assumed. In the borated environment of the spent fuel pool, optimum moderation occurs when the assemblies are very close to each other. The racks are crushed until there is no space between the assembly and the rack cell wall. This means that eccentric fuel positioning cannot happen since there is no space to move an assembly within the cell. Additionally, the fuel assembly is damaged so that the fuel pins are pushed closer together to an optimal distance. Since optimal pin pitch occurs when the fuel pins are moved closer together, a grid growth bias and clad creep down bias is not applicable.

9.1.16 Region 1 Damaged Rack Analysis Results

The preceding subsections of Section 9.1 all feed into the calculation of the 95/95 maximum k-eff. Table 9-17 shows the calculation of the maximum k-eff, the NRC's review margin (0.01 Δk), the NRC limit (0.95 for borated scenarios in accordance with 10 CFR 50.68), and the margin to the limit which belongs to Dominion for any potential 10CFR50.59 evaluations in the future. Note that decay time is not credited in this analysis.

Figure 9-14 shows the new burnup curve compared to the burnup curve currently in the Technical Specifications. As can be seen, the new burnup curve requires significantly more burnup than the current Technical Specifications. However, it adequately supports the current inventory of fuel in the SFP and anticipated future loadings.

Figure 9-15 shows the burnup curve that is included in the proposed Technical Specifications. The equation for the burnup curve bounds all analyzed points.

Table 9-17: Cask Drop Accident Maximum k-eff and Margin to the Limit

Burnup (GWD/MTU)	0	10	20	30	40	47	53
Enrichment (U-235 wt%)	1.65%	2.20%	2.85%	3.45%	4.10%	4.55%	5.00%
Worths							
Burnup Worth	--	0.0538	0.1504	0.2022	0.2569	0.2735	0.2932
Minor Actinides and Fission Product Worth	--	0.0429	0.0723	0.0816	0.0822	0.0854	0.0909
Uncertainties							
Fuel Stack PTD	0.0014	0.0012	0.0011	0.0010	0.0012	0.0008	0.0007
Enrichment	0.0109	0.0059	0.0048	0.0039	0.0038	0.0034	0.0030
Pellet OD	0.0013	0.0007	0.0005	0.0005	0.0006	0.0007	0.0006
Active Fuel Length	0.0002	0.0003	0.0007	0.0022	0.0001	0.0003	0.0003
Clad ID	0.0005	0.0006	0.0005	0.0005	0.0002	0.0004	0.0003
Clad OD	0.0010	0.0004	0.0001	0.0010	0.0003	0.0004	0.0004
Guide Tube	0.0007	0.0003	0.0002	0.0002	0.0001	0.0002	0.0003
Cell Wall Thickness	0.0031	0.0026	0.0026	0.0024	0.0010	0.0011	0.0011
Depletion NRC Unc.	--	0.0016	0.0040	0.0047	0.0054	0.0055	0.0056
Burnup Measurement	--	0.0027	0.0075	0.0101	0.0128	0.0137	0.0147
Code Benchmarking	0.0045	0.0120	0.0120	0.0135	0.0120	0.0120	0.0120
KENO Base Case	0.0001	0.0001	0.0001	0.0001	0.0001	0.0001	0.0001
RSS of Uncertainties	**0.0124**	**0.0141**	**0.0158**	**0.0183**	**0.0189**	**0.0194**	**0.0200**
Biases							
Radial Burnup Tilt	--	0.0004	0.0009	0.0010	0.0009	0.0005	0.0004
Low Power Coastdown	--	0.0022	0.0017	0.0017	0.0016	0.0013	0.0011
Optimum Pitch Bias	0.0211	0.0029	0.0001	0.0002	0.0003	0.0010	0.0019
Minor Actinides and Fission Product Worth	--	0.0006	0.0011	0.0012	0.0012	0.0013	0.0014
Depletion Application Bias	--	0.0028	0.0028	0.0028	0.0028	0.0028	0.0028
Depletion NRC Bias	--	0.0000	0.0000	0.0000	0.0004	0.0008	0.0012
Code Temperature Bias	0.0006	0.0006	0.0006	0.0006	0.0006	0.0006	0.0006
Code Benchmarking Bias	0.0040	0.0030	0.0030	0.0035	0.0030	0.0030	0.0030
Sum of Biases	**0.0257**	**0.0125**	**0.0102**	**0.0110**	**0.0108**	**0.0113**	**0.0123**
Wrap-Up							
Base Case k-eff	0.8612	0.9037	0.8940	0.8784	0.8758	0.8894	0.8959
Total Bias and Uncertainty	0.0381	0.0266	0.0260	0.0293	0.0297	0.0306	0.0324
NRC Review Margin	0.01	0.01	0.01	0.01	0.01	0.01	0.01
Maximum k-eff	0.9093	0.9403	0.9299	0.9177	0.9155	0.9300	0.9383
NRC Limit	0.95	0.9500	0.95	0.95	0.95	0.95	0.95
DOMINION MARGIN FOR 50.59	**0.0407**	**0.0097**	**0.0201**	**0.0323**	**0.0345**	**0.0200**	**0.0117**

Figure 9-14: Region 1 Burnup Curve and Relevant Data

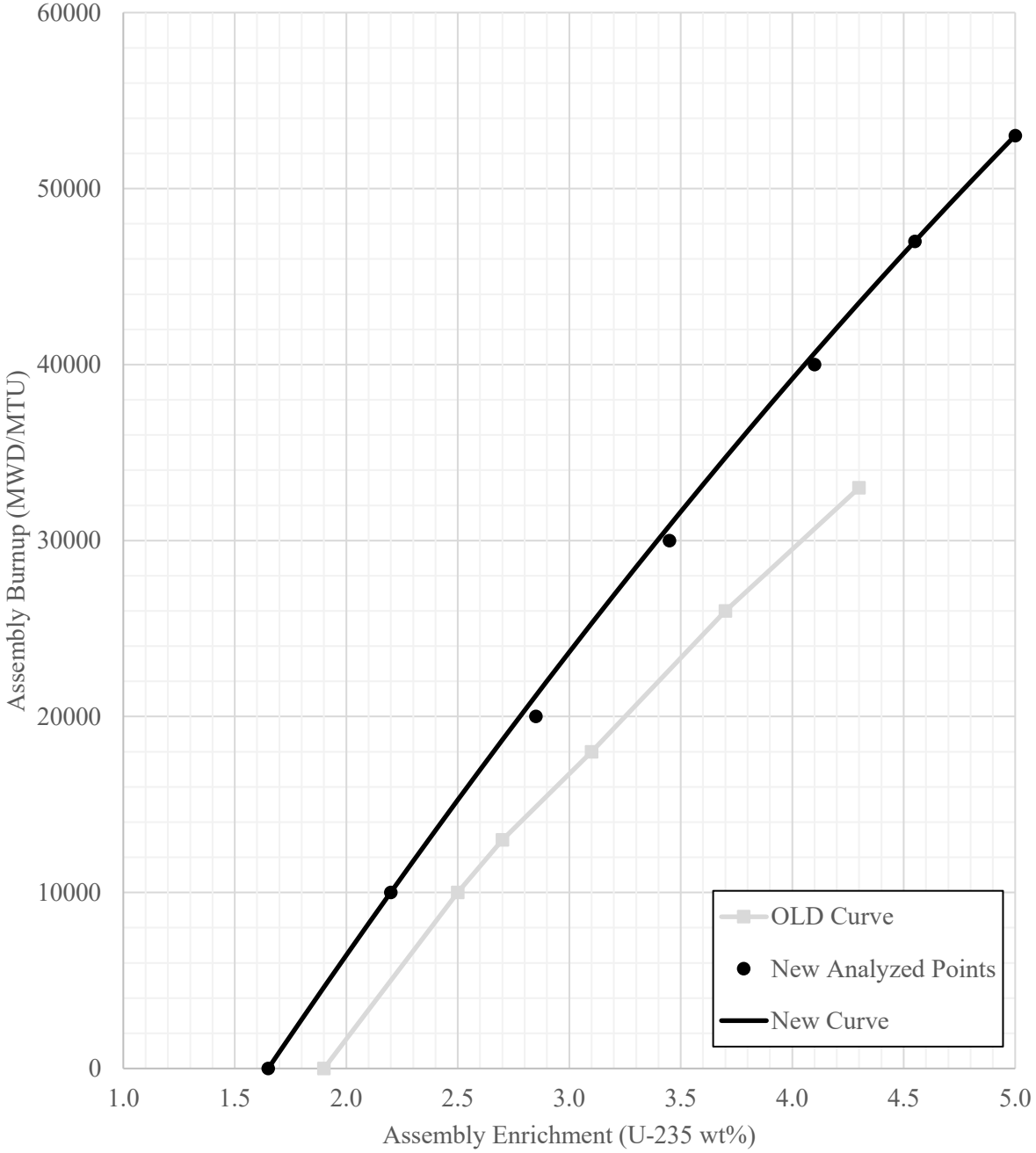

$$New\ Curve\ Required\ Burnup\ (MWD/MTU) = -849x^2 + 21470x - 33110$$

Figure 9-15: Burnup Curve for Region 1

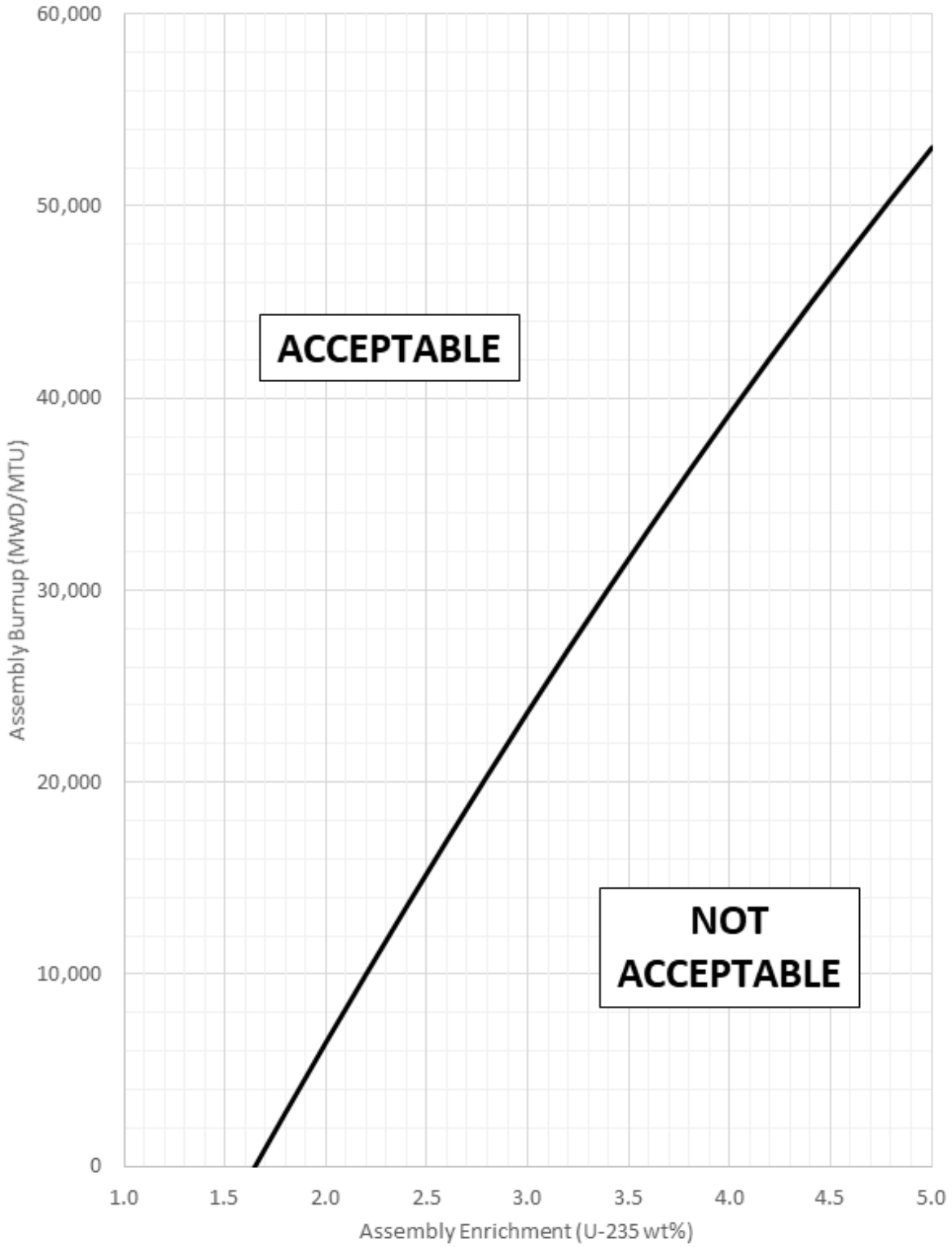

$$Required\ Burnup\ (MWD/MTU) = -849x^2 + 21470x - 33110$$

9.2 *Nominal Rack Analysis (Unborated) – Region 2*

9.2.1 Region 2 Fuel Storage Requirements

A fuel assembly may be placed in Region 2 at all times if it meets all of the following criteria:

1) The fuel assembly has an initial U-235 enrichment ≤5.0 wt%.

Criteria 1 is confirmed in Section 9.2 by use of an infinite rack model.

9.2.2 Region 2 Modeling Assumptions

These modeling simplifications and assumptions are used in the Region 2 analysis:

a) SFP water modeled with 0 ppm. This analysis satisfies the 10 CFR 50.68 k-eff limit of 1.0 in unborated water.

b) The assembly axial reflectors (plenum region, guide tubes above and below the active fuel, and top and bottom nozzles) are modeled as unborated water.

c) The storage cell is modeled as its nominal length. The rack structure below the bottom of the storage cell tube is modeled as water.

d) Neither reduction in fuel enrichment nor annular pellets are modeled for axial blankets. This is conservative because it increases SFP k-eff.

e) Zr-based clad materials are modeled as pure Zr.

f) The water density was calculated using a pressure of 15 psia. It is acknowledged that the pressure near the bottom of the SFP is greater than atmospheric pressure, but water density is much more sensitive to temperature than pressure. In addition, the 32°F test case conservatively assumed a density of 1.0 g/cc which is the maximum density for water.

g) Grids are represented by homogenizing the grid and the water in the fuel lattice over the length of the fuel. Water inside the guide tubes are modeled as pure water. Justification of this assumption is given in Section 8.12.

h) For the Fuel Pin Clad OD uncertainty cases, the grid volume stays constant. This is acceptable for several reasons. 1) The clad OD uncertainty has a small effect on the moderator to fuel ratio. 2) The clad OD uncertainty is small enough that it only affects the final RSS uncertainty term by less than ~10 pcm.

i) The analysis uses an infinite lattice model. The model repeats a 6x6 block of rack cells by mirror boundaries. The minimum gap between a rack and the wall is less than the inter rack cell gap. Therefore, reactivity effects of the wall proximity will be analyzed in Section 9.2.6. The gap between rack modules are greater than or equal to the assembly pitch distance. Therefore, an inter-rack module gap does not need to be analyzed.

j) The corner cells of the 6x6 rack modules have thicker tube walls to structurally reinforce the rack. The thicker rack cell tubes on the corners will be conservatively ignored and modeled as a standard cell tube instead. It is conservative to model them as the standard cell tubes because the thicker cell wall thickness decreases reactivity (see Section 9.2.7).

k) The asymmetric or eccentric fuel placement bias is built into the base model. More discussion of this bias is in Section 9.2.5.

9.2.3 Region 2 Infinite Lattice Model

Drawings and dimensions of Region 2 fuel racks are provided in Section 4.2. The KENO Region 2 model is an infinite 6x6 model with reflective boundary conditions. The rack module to module spacing is ignored since the inter-rack module spacing is at least the cell pitch distance. Fuel is stored in all cells of the infinite lattice model. The initial neutron distribution source is uniform in all fissile material. Because the fuel is distributed evenly and because the convergence criteria is met, a uniform neutron source acceptable. Figure 9-16 shows a planar view of the Region 2 model.

Figure 9-16: Planar View of the Region 2 KENO Model

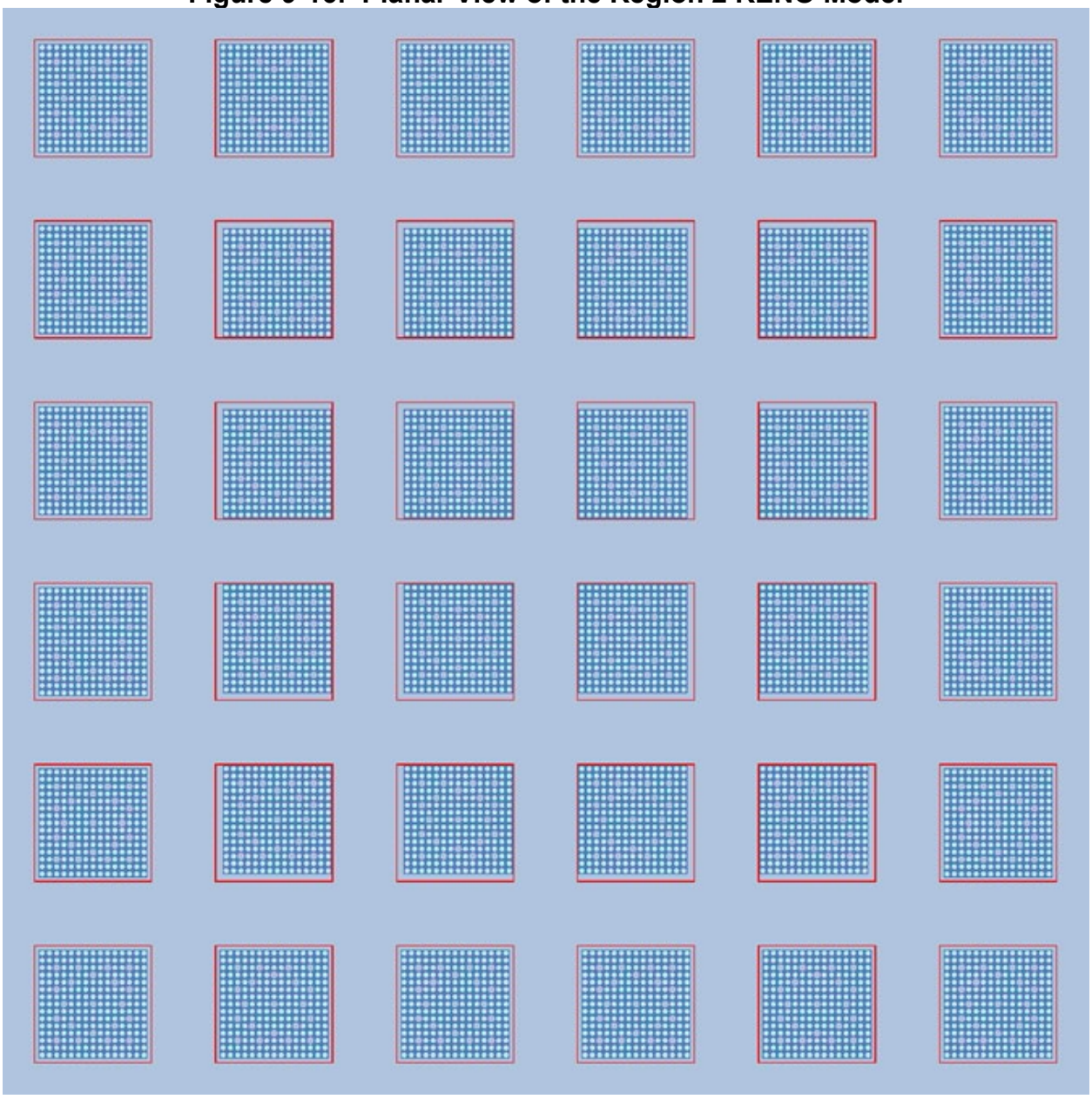

9.2.4 SFP Normal Operation Water Temperature and Density

The maximum, non-accident SFP temperature of the SFP is 350K or 170°F. The low temperature limit of the SFP is set to lower physical limit of liquid water: 273K or 32°F. The water density was calculated using a pressure of 14.7 psia. Test cases were run and determined the maximum reactivity occurs at the highest operating temperature. Therefore, all cases are run at 350K. The test case results are shown in Table 9-18.

Table 9-18: Region 2 k-eff at Varying Spent Fuel Pool Temperatures

Case Description	Burnup (GWD/MTU)	Enrich. (wt%)	k-eff	σ	Δk
Base Case (170°F)	0	5.000	0.968636	0.000085	-
Temperature - 32°F	0	5.000	0.963641	0.000084	-0.004995
Temperature - 68°F	0	5.000	0.963204	0.000088	-0.005432

9.2.5 Asymmetric or Eccentric Fuel Positioning

Asymmetric placement of fuel in the storage cell is evaluated by co-locating fuel in the center 4x4 group of storage cells into the corner of each cell toward the center of the 6x6 model. The remaining storage locations have fuel centered in each cell. The justification for this model is the same probabilistic argument that was discussed in Section 9.1.8.

Test cases for Region 2 confirm that asymmetric placement increases rack k-eff (~0.003 dk). The Region 2 KENO base model includes the 4x4 group of asymmetrically placed fuel.

Table 9-19: Region 2 k-eff at with Varying Fuel Placements

Case Description	Burnup (GWD/MTU)	Enrich. (wt%)	k-eff	σ	Δk
Base Case (Asymmetric Positioning)	0	5.000	0.968636	0.000085	-
Centered Positioning	0	5.000	0.965447	0.000083	-0.003189

9.2.6 Wall Boundary and Wall-to-Rack Gap

The model repeats a 6x6 block of rack cells by mirror boundaries. The minimum gap between a rack and the wall is less than the inter rack cell gap. Therefore, reactivity effects of the wall proximity was analyzed by running a test case.

The rack wall proximity case (added an 18" concrete wall, ¼" stainless steel liner, and 10.795 cm of water to the rack model consistent with Table 4-3) indicates reduced reactivity compared to the infinite rack model. Therefore, the reactivity effect of the rack wall may be ignored.

Table 9-20: Rack Wall Proximity Case

Case Description	Burnup (GWD/MTU)	Enrich. (wt%)	k-eff	σ	Δk
Centered Positioning, Infinite Lattice	0	5.000	0.965447	0.000083	-
Rack Wall Proximity	0	5.000	0.964788	0.000081	-0.000659

Figure 9-17: Rack Wall Proximity Case

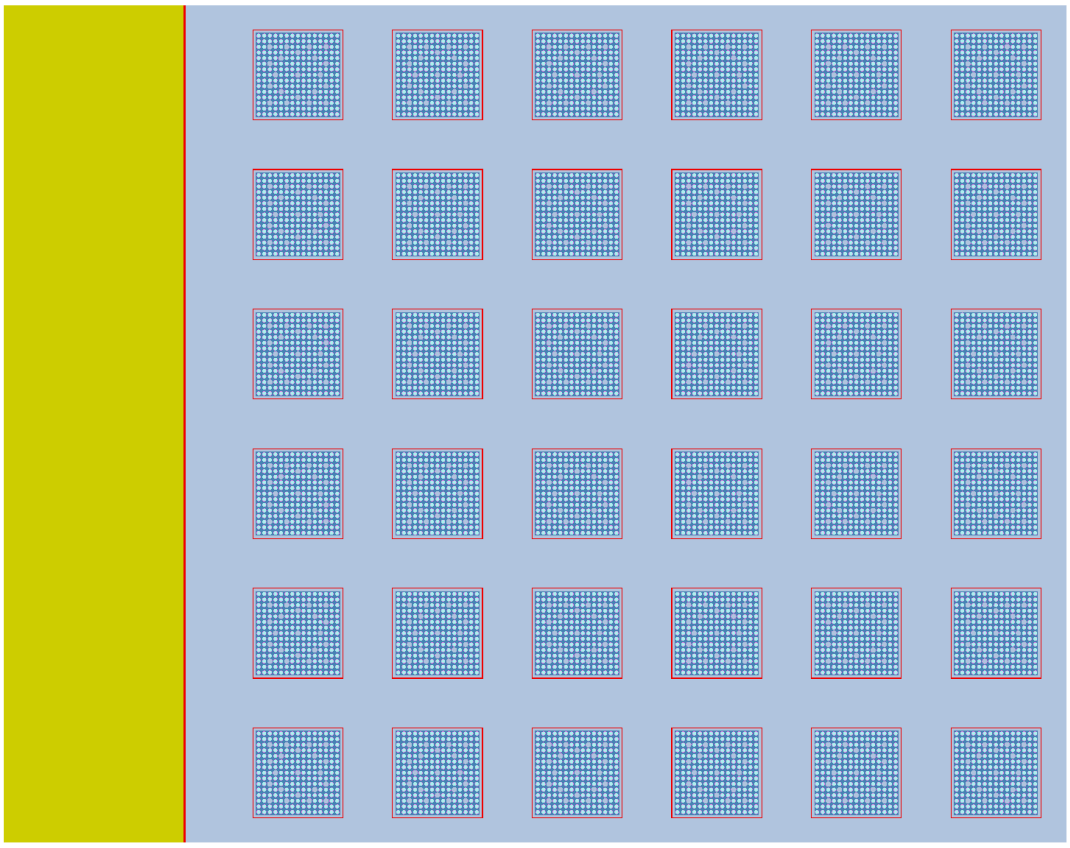

9.2.7 Manufacturing Uncertainties

A full complement of uncertainty cases was run. Tables 3-3 and 4-3 shows the uncertainty values for the SFP assemblies and racks, respectively. Table 9-21 shows the uncertainty KENO cases.

To include the Monte Carlo uncertainty in the maximum k-eff uncertainty calculations, the "Uncert." column is calculated by adding 2 times the root sum square of the case uncertainties to the Δk between cases.

Table 9-21: Region 2 Manufacturing Uncertainty Cases

Case Description	Burnup (GWD/MTU)	Enrich. (wt%)	k-eff	σ	Δk	Uncert. (Δk+2σ)
Base Case	0	5.000	0.968636	0.000085	-	-
Cell ID -	0	5.000	0.967976	0.000082	-0.000660	-0.000424
Cell ID +	0	5.000	0.969800	0.000081	0.001164	0.001399
Cell Pitch -	0	5.000	0.972722	0.000078	0.004086	0.004317
Cell Wall Thickness -	0	5.000	0.972033	0.000081	0.003397	0.003632
Cell Wall Thickness +	0	5.000	0.965689	0.000081	-0.002947	-0.002712
Clad ID -	0	5.000	0.969009	0.000079	0.000373	0.000605
Clad ID +	0	5.000	0.968398	0.000085	-0.000238	0.000002
Clad OD -	0	5.000	0.971237	0.000079	0.002601	0.002833
Enrichment +	0	5.050	0.970249	0.000082	0.001613	0.001849
Active Fuel Length +	0	5.000	0.968721	0.000082	0.000085	0.000321
Pellet OD +	0	5.000	0.969349	0.000092	0.000713	0.000964
Pin Pitch +	0	5.000	0.970448	0.000079	0.001812	0.002044
Fuel Stack PTD +	0	5.000	0.969599	0.000080	0.000963	0.001196
Tube OD -	0	5.000	0.969453	0.000079	0.000817	0.001049
Tube ID +	0	5.000	0.969238	0.000079	0.000602	0.000834
Tube ID -	0	5.000	0.968265	0.000084	-0.000371	-0.000132
Tube OD +	0	5.000	0.968191	0.000078	-0.000445	-0.000214

9.2.8 Code Temperature Bias

Appendix A identified and calculated a temperature bias associated with the computer codes and methodology. The temperature bias is defined below where T is the temperature of the model in Kelvin.

$$Bias = 1 * 10^{-5} * (T - 293)$$

All the models for the cask drop accident is run at 350 K. This equates to a temperature Δk bias of **0.00057** for all burnups.

9.2.9 Code Validation Bias and Uncertainty

Validation of SCALE/KENO using ENDF/B-VII 238 group cross sections in Appendix A identified EALF as the primary bias and uncertainty trend. Region 2 KENO cases have EALFs ≤ 0.40 eV. The applicable bias and uncertainty for fresh fuel and depleted fuel are shown in Table 9-22. This table is taken from Appendix A.

Table 9-23 show the code benchmark bias and uncertainty applied to this analysis. Note that only the UO_2 biases and uncertainties apply to Region 2 since burnup credit is not used.

Table 9-22: Code Benchmarking Bias and Uncertainty (Appendix A)

EALF (eV)	Bias (Δk)	Uncertainty (Δk)
Fresh UO_2 Fuel		
0.00 – 0.40	0.0030	0.0040
0.40 – 0.80	0.0040	0.0045
0.80 – 1.10	0.0055	0.0050
1.10 – 1.25	0.0060	0.0050
1.25 – 1.40	0.0065	0.0055
Burned MOX Fuel		
0.00 – 0.40	0.0015	0.0060
0.40 – 0.80	0.0025	0.0095
0.80 – 1.10	0.0030	0.0120
1.10 – 1.25	0.0035	0.0135
1.25 – 1.40	0.0035	0.0145

Table 9-23: Cask Drop Code Benchmarking Bias and Uncertainty

Enrichment (wt%)	Burnup (GWD/MTU)	EALF (eV)	Bias (Δk)	Uncertainty (Δk)
5.00	0	0.24	0.0030	0.0040

9.2.10 Region 2 Nominal Rack Analysis Results

The preceding subsections of Section 9.2 all feed into the calculation of the 95/95 maximum k-eff. Table 9-24 shows the calculation of the maximum k-eff, the NRC's review margin (0.01 Δk), the NRC limit, and the margin to the limit which belongs to Dominion for any potential 10 CFR 50.59 evaluations in the future. Note that the KENO Case Uncertainty is the σ of the base case multiplied by 2.

Table 9-24 shows that Region 2 meets the 10 CFR 50.68 limit of 1.00 under unborated conditions when taking boron credit. Region 2 meets the limit without crediting burnup or decay time.

This means that Region 1 also meets this limit. The rack and fuel design of Region 1 and Region 2 are the same. The only differences are that Region 1 is susceptible to a cask drop accident and that Region 1 requires fuel burnup (depending on initial enrichment). This means that under normal storage conditions, Region 1 and Region 2 are identical except that Region 1 has lower reactive fuel. Therefore, Region 1 meets the normal storage, unborated k-eff limit of 1.00 since Region 2 does.

Table 9-24: Region 2 Summary of Biases, Uncertainties and Margins

Burnup	**0**
Enrichment	**5.000**
Uncertainties	
Fuel Stack PTD	0.0012
Enrichment, +0.05	0.0018
Pellet OD	0.0010
Active Fuel Length	0.0003
Clad ID	0.0006
Clad OD	0.0028
GT ID	0.0008
GT OD	0.0010
Pin Pitch	0.0020
Cell Wall Thickness	0.0036
Cell I.D.	0.0014
Cell Pitch	0.0043
Code Benchmarking Unc.	0.0040
KENO Case Uncertainty	0.0002
RSS OF UNCERTAINTIES	**0.0083**
Biases	
Code Temperature Bias	0.0006
Code Benchmarking Bias	0.0030
SUM OF BIASES	**0.0036**
Wrap-Up	
Base Case k-eff	**0.9686**
Total Bias and Uncertainty	**0.0119**
NRC Review Margin	**0.0100**
Maximum k-eff	**0.9905**
NRC Limit	**1.0000**
DOMINION MARGIN FOR 50.59	**0.0095**

9.3 *Unbounded Fuel Assemblies*

There are five assemblies which Sections 9.1 and 9.2 do not apply to. Assembly 4G6 had a depletion boron which was higher than the boron concentration modeled in the TRITON depletion cases. The other four assemblies are 17x17 demonstration assemblies. This differs from the cases run in Sections 9.1 and 9.2 because they used 15x15 assemblies.

9.3.1 Unbounded Depletion Boron (Assembly 4G7)

Assembly 4G7 is in a dry storage cask and is not planned to ever be in the SFP again. However, this assembly will be evaluated for completeness and to remain consistent with the previous analysis.

S1C10 was shutdown early to remove Assembly 4G7 before continuing with the cycle. It was the only assembly removed. This caused the average depletion boron for Assembly 4G7 to be 1024 ppm for S1C10. This is higher than the standard boron depletion value of 850 ppm by 174 ppm.

While Assembly 4G7 exceeded the average depletion boron limit for S1C10, it was also in a previous cycle. S1C9 had an average depletion boron level of 593 ppm. Averaging S1C9 and S1C10 results in an average boron concentration of 809 ppm which is below the limit of 850 ppm. Averaging the two cycles is conservative because S1C10 was a very short cycle, so the burnup weighted average of boron would be less than 809 ppm.

An additional argument is that the excess burnup worth of Assembly 4G7 covers this non-compliance. Assembly 4G7 has an enrichment of 3.9914 wt% and a burnup of 42914 MWD/MTU. From the burnup curve in Section 9.1.16, a 3.9914 wt% assembly requires a burnup of 39060 MWD/MTU meaning Assembly 4G7 has 3854 MWD/MTU in excess of the burnup curve. According to Section 9.1.16, the burnup worth of 40 GWD/MTU is worth ~0.257 Δk. This means that the 3854 MWD/MTU of excess burnup is worth about 0.025 Δk. Depletion boron sensitivity cases were run in Section 8.3 and repeated in Table 9-25. Table 9-25 suggests that 175 ppm of additional depletion boron is worth about 0.00133 Δk. Additionally, Wagner's ORNL research paper [38] only predicts a maximum non-conservatism with a mid-cycle shutdown to be ~0.002 Δk/k. These terms add up to be worth ~0.004 Δk which is still about an order of magnitude less than the excess burnup worth. Therefore, Assembly 4G7 can be stored as normal fuel.

Table 9-25: Depletion Boron Effect on SFP Reactivity
(Repeated here for convenience)

Case Description	Burnup	SFP k-eff	σ	Δk	Δk/RSS(σ)	ρ (pcm)	EALF (eV)
Nominal (850 ppm)	20 GWD/MTU	0.86849	0.00008	N/A	N/A	N/A	0.26
Increased Boron 50 ppm		0.86868	0.00007	0.00020	186%	26	0.26
Nominal (850 ppm)	40 GWD/MTU	0.76310	0.00007	N/A	N/A	N/A	0.29
Increased Boron 50 ppm		0.76348	0.00007	0.00038	387%	65	0.29

9.3.2 17x17 Fuel Assemblies

Surry used four 17 x 17 demonstration assemblies during its early cycles. Two assemblies were enriched to a nominal enrichment of 1.85 wt% and were irradiated in S1C02 and S1C03 to a burnup of 16032 and 16223 MWD/MTU. The other two assemblies were enriched to a nominal enrichment of 3.10 wt% and were both irradiated in S2C02, S2C03, and S2C04 while one was also irradiated in S2C05 to a burnup of 28022 and 42511 MWD/MTU. Table 9-26 shows the relevant dimensions of the 17x17 assemblies.

Table 9-26: 17 x 17 Demonstration Assemblies

Property	Value
Rod Pitch (cm)	1.26
Pellet O.D. (cm)	0.8192
Fuel Clad O.D. (cm)	0.9500
Fuel Clad Thickness (cm)	0.0572
Active Fuel Height (cm)	365.76
Fuel Material	UO_2
Cladding Material	Zirconium
Grid Volume Fraction	Same as 15x15 Assembly
Burnable Poisons	None

Table 9-27 shows the initial enrichment and burnup for all four 17x17 assemblies. They have more burnup than the burnup curve in Section 9.1.16.

Table 9-27: 17 x 17 Assembly Enrichment and Burnup

Assembly ID	Initial Enrichment (wt% U-235)	Measured Burnup (MWD/MTU)
ND1	1.860	16,032
RD1	1.860	16,223
ND2	3.088	28,022
RD2	3.088	42,511

To verify that the 17x17 assemblies are not limiting, a new depletion and SFP model was created to compare to the standard 15x15 cases for Node 16. The 5.0 wt%, standard depletion case was modified to (i) change the assembly to a 17x17 configuration and (ii) remove the burnable poisons. The fuel isotopics were carried to the KENO model through the standard process and a 17x17, nominal pitch k-eff was calculated to compare with a standard 15x15, Node 16 case. Table 9-28 compares the 15x15 and 17x17 depletion worth. It shows that the 17x17 depletion worth is larger than the 15x15 depletion worth; mostly because the 17x17 depletion had no burnable poisons.

Note that the 17x17, Node 16 depletion can not be directly compared to the 15x15 No BP depletion in Table 8-11 due to slightly different modeling conditions.

Table 9-28: Depletion Worth Comparison of 15x15 and 17x17 Fuel, Node 16

Case Description	Burnup	SFP k-eff	σ	Δk	Δk/RSS(σ)
Nominal 15x15 Assembly	20 GWD/MTU	0.85330	0.00008	--	--
17x17 Assembly (No BP)		0.84151	0.00007	-0.01179	-11090%
Nominal 15x15 Assembly	40 GWD/MTU	0.76077	0.00007	--	--
17x17 Assembly (No BP)		0.74547	0.00004	-0.01530	-19553%

The actual depletion of the 17x17 assemblies were conservative when compared to the bounding depletion in the following ways:

- Excess burnup over the burnup curve
- >40 years of decay
- Lower core power. Table 8-4 shows that Cycles 2 – 5 had a lower core power level.
- Lower depletion boron. Figure 8-2 shows that Cycles 2-5 had lower boron levels.
- Lower Fuel UO2 PTD. Cycles 2-5 had lower fuel densities than the fuel density used in the bounding model.

In summary, the 17x17 assembly is significantly less reactive than the bounding 15x15 assembly and can therefore be stored as normal fuel.

Interface Analysis

10 Region 1 and Region 2 have the same rack type. Therefore, there are no interfaces between dissimilar rack types in the Surry SFP. Additionally, both Region 1 and Region 2 have the same fuel requirements for all fuel within the region. Therefore, there is not any interface between dissimilar fuel within a region. However, Region 1 stores burned fuel and is susceptible to a cask drop accident. Therefore, an analysis is performed for the Region 1 – Region 2 interface.

The interface between Region 1 and 2 is analyzed to determine how the interface affects the reactivity of the Spent Fuel Pool. If the interface is more reactive than the regions modeled alone then the interface is “adverse”.

If Region 1 is modeled with normal racks, then Region 1 is the same as Region 2 except it has less reactive fuel due to required burnup. Region 1 meets all limits with an infinite model. Replacing part of that infinite model with the same rack but lower reactive fuel would decrease reactivity. Therefore, the interface analysis will focus on if there is a cask drop in Region 1. Since the cask drop is an accident condition, 2250 ppm of boron will be credited in the SFP water.

In Section 9.1, Region 1 was modeled as an 18 x 18 block of assemblies (324 assemblies in total). The KENO model had reflective boundaries on all sides. However, all but one side were too far away from the KENO boundary to reflect any appreciable amount of neutrons. Since only one side of the model was reflected, the Region 1 model was effectively a finite model of 648 assemblies in a 36 x 18 block orientation. Region 1 has a burnup curve that requires fuel with 0 GWD/MTU to have an enrichment ≤ ~1.65 wt% and fuel with 5.00 wt% to have a burnup ≥ 53 GWD/MTU.

In Section 9.2, Region 2 was modeled as a 6 x 6 block of assemblies (36 assemblies in total). The KENO model had reflective boundaries on all sides. The KENO boundaries were located in a position so that the reflective boundary condition simulates an infinite sea of assemblies. Region 2 has no burnup curve, so it can store fresh fuel with enrichments ≤ 5.00 wt%.

Figure 4-3 shows the Surry SFP regions and the interface. The interface between Region 1 and 2 is 18 assemblies wide. The interface will be analyzed two different ways.

1) Develop a full pool KENO model. The location of the initial neutron source is moved to different locations around the interface. Then the trend of the k-eff is examined to determine which part of the pool is most reactive.
2) Develop an interface only KENO model. Run cases to determine if the reactivity of the interface is less than i) both regions, ii) one of the regions, or iii) neither of the regions.

i. If the interface is less reactive than both regions, then it is benign and no other work needs to be done.
ii. If the interface is more reactive than one region but less reactive than the other, then an appropriate bias and uncertainty term needs to be applied to the interface k-eff to determine if it is bounded by the infinite region model.
iii. If the interface is more reactive than both regions, then the interface is adverse. It either needs to be modified (such as adding empty cells at the interface) or calculated so that the max 95/95 k-eff of the interface is less than the regulatory limit.

Figure 4-3: Surry SFP Rack Orientation
(Repeated here for convenience)

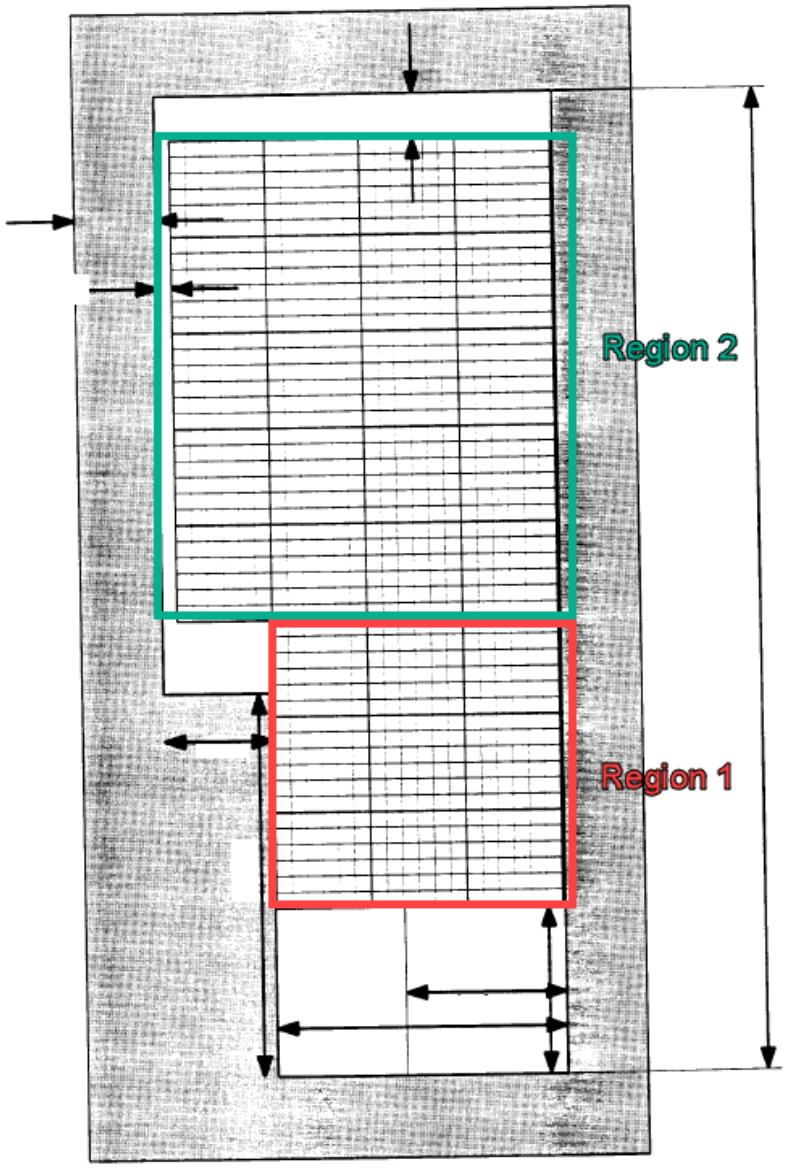

10.1 *Interface Analysis – Average k-eff vs. Generation Trend*

As stated above, the first way that the region interface will be analyzed is by placing the initial neutron source in different locations of a full pool model. The different locations are in Region 1, then around the boundary, and then in Region 2. Figure 10-1 shows where the initial neutron sources were located for each case. Figure 10-2 shows the whole pool model.

Figure 10-3 shows the average k-eff vs. generation trend. It shows that the case which started the neutrons in Region 1 starts at a higher reactivity than both the Interface and Region 2 cases. This means that interface between the two regions does not produce a reactivity higher than the reactivity of Region 1. Therefore, Region 1 bounds the interface.

Note that all 3 graphs converge to approximately the same average k-eff because the neutrons that the code tracks tend to migrate over time to the Region 1 area since that area has the highest probability of producing neutrons for the next generation. Additionally, the Region 1 burned fuel case (Figure 10-3b) takes longer to converge than the Region 1 fresh fuel case (Figure 10-3a) because the reactivity of the burned fuel is so concentrated at the top of the fuel rather than the middle axial height.

Figure 10-1: Initial Neutron Source Location

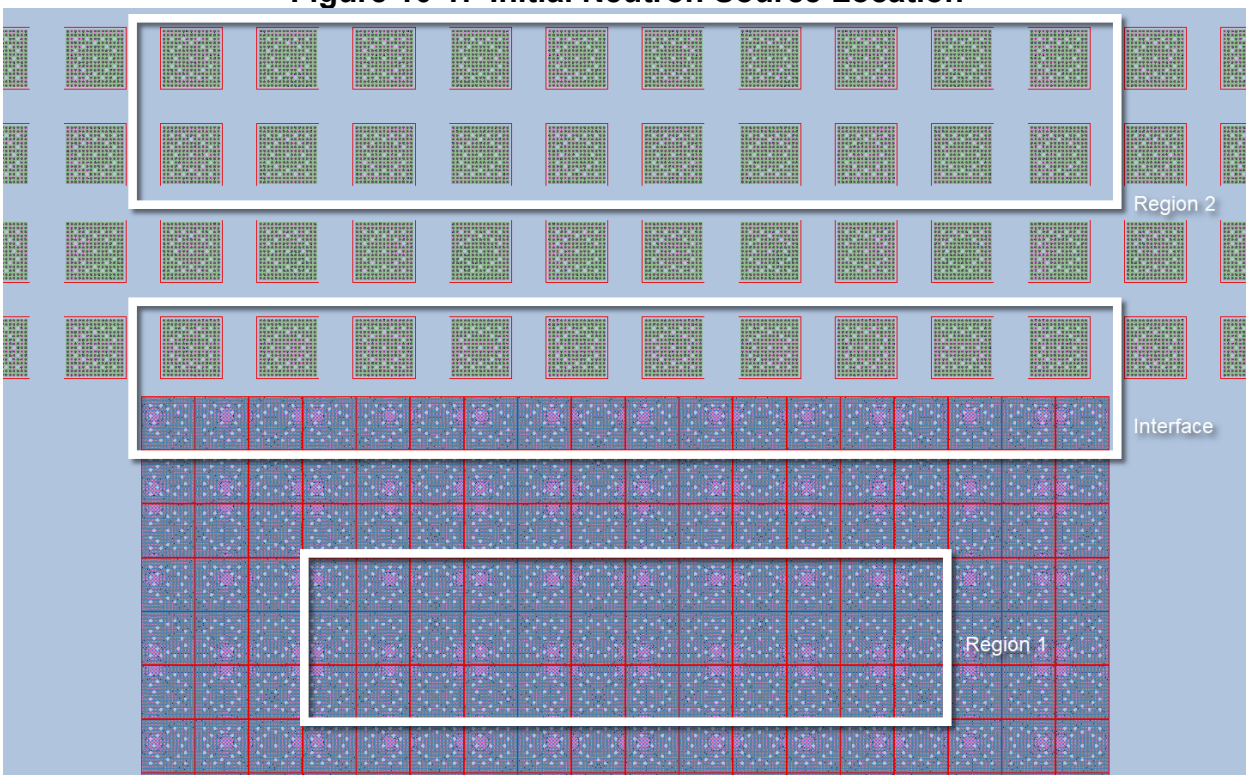

Figure 10-2: Full Pool Model

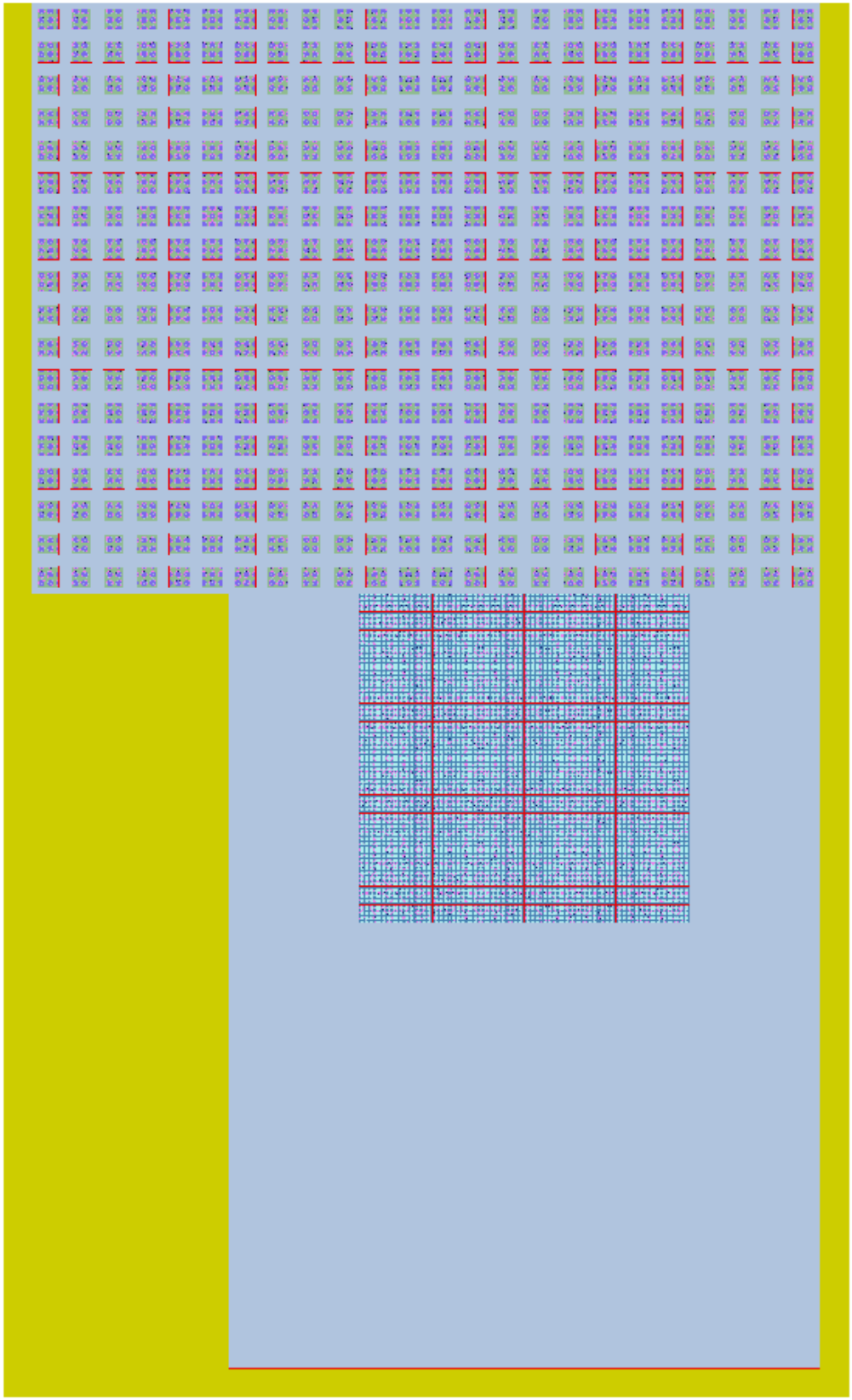

Figure 10-3a: Generation Average k-eff, Fresh Fuel in Regions 1 & 2

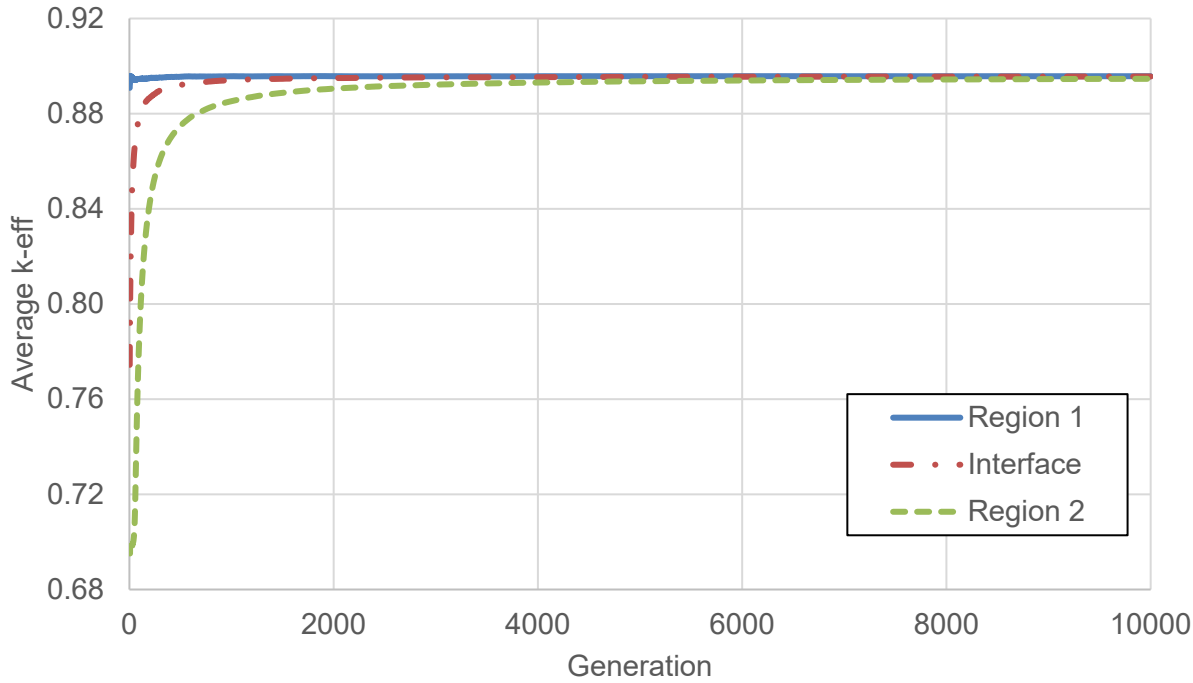

Figure 10-3b: Generation Average k-eff, Burned in Region 1 – Fresh in Region 2

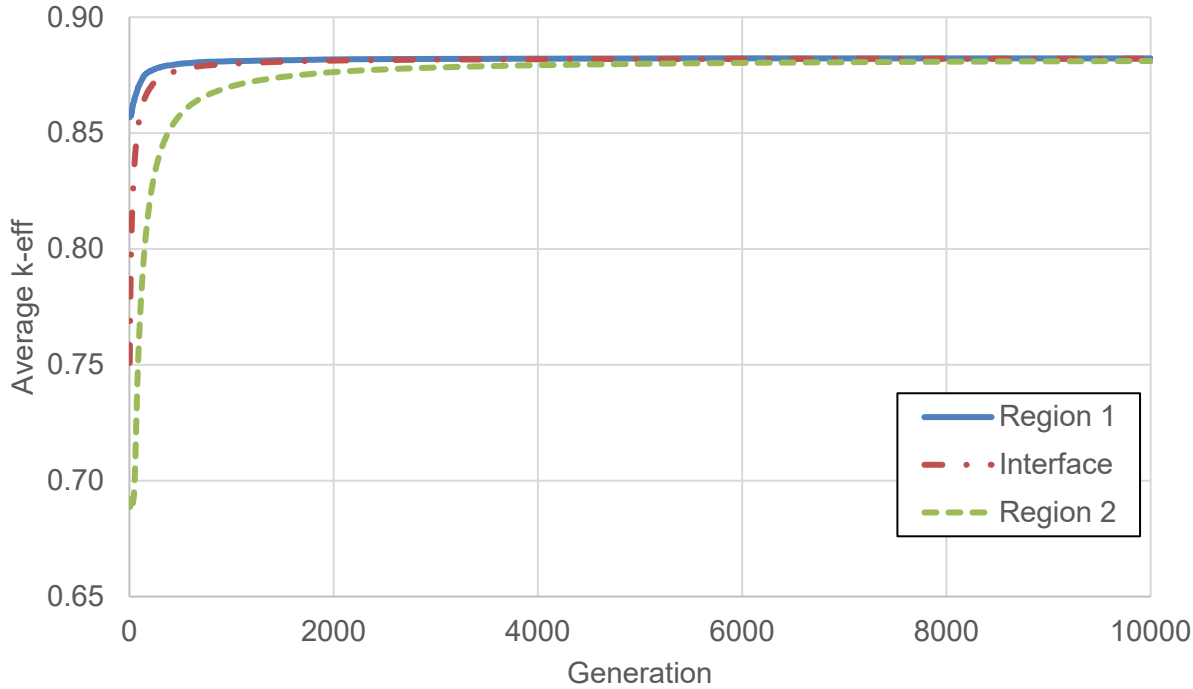

10.2 *Interface Analysis – Interface Only Models*

Another way to analyze the interface is to make models that include only the interface. The entirety of the interface model is shown below in Figure 10-4. The problem with the model in Section 10.1 is that neutrons will migrate to the middle of the most reactive region if the interface is not adverse. That would make the model insensitive to the interface since there are no neutrons at the interface to measure differences. This model restricts the neutrons from migrating to the middle of the regions so that a truer interface reactivity can be calculated.

This KENO model, shown in Figure 10-4, has periodic boundaries for the x and y coordinates meaning the interface is infinitely wide and a repeating interface of between the two regions of three rows.

Figure 10-4: Interface Only Model

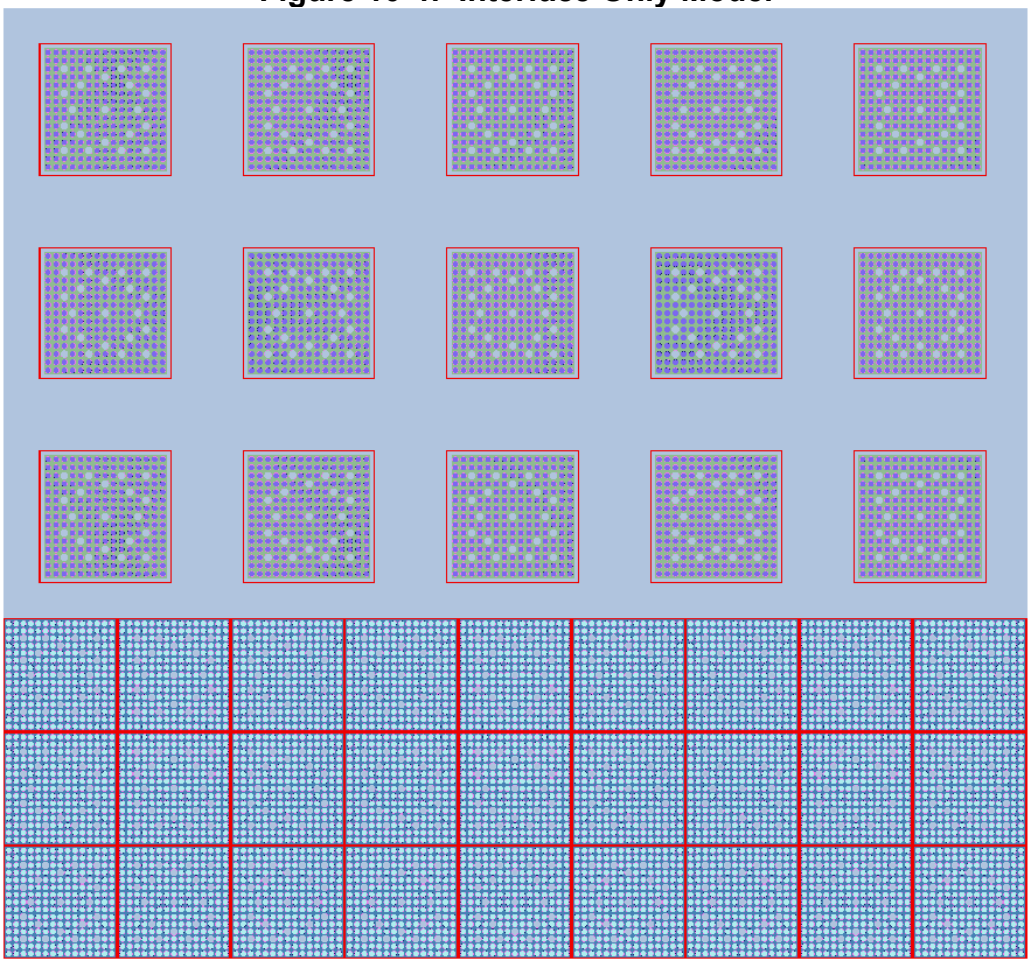

Table 10-1 shows the reactivity of the finite Region 1 model and the infinite Region 2 model. Under borated conditions, Region 1 is most reactive at 170°F while Region 2 is most reactive at 100°F. Therefore, the interface model was run at both 100°F and 170°F.

Table 10-1: Interface-Only Model Results

Model Description	Temperature °F	Enrichment (wt%)		Burnup (GWD/MTU)		k-eff	σ	Δk
		Region 1	Region 2	Region 1	Region 2			
Region 1	170	2.00	N/A	0	N/A	0.897621	0.000020	--
Region 2	100	N/A	5.00	N/A	0	0.694611	0.000070	-0.20301
Interface	100	2.00	5.00	0	0	0.834104	0.000045	-0.06352
Interface	170	2.00	5.00	0	0	0.835369	0.000043	-0.06225
Region 1	170	5.00	N/A	47	N/A	0.889430	0.000059	--
Region 2	100	N/A	5.00	N/A	0	0.694611	0.000070	-0.19482
Interface	100	5.00	5.00	47	0	0.828695	0.000045	-0.06074
Interface	170	5.00	5.00	47	0	0.826970	0.000048	-0.06246

As can be seen in Table 10-1, the reactivity of Region 1 is vastly more reactive than Region 2. The interface reactivity is also less reactive than the Region 1 reactivity because the Region 1 reactivity is being negatively impacted by the interface and Region 2. The interface models are at least 0.06 Δk less reactive than the Region 1 model. As seen in Section 9.1.16, the largest uncertainty terms are only applicable to burned fuel. If a total bias and uncertainty worth were to be calculated for the interface model, it would most likely be very similar to the Region 1 total bias and uncertainty since Region 2 does not have burned fuel. Therefore, if the Region 1 total bias and uncertainty were to be added to the interface model k-eff, there would be margin to the limit. Additionally, even if some of the interface uncertainty or bias terms increase slightly, it needs to increase 0.06 Δk until it exceeds the Region 1 maximum k-eff which is unrealistic. This means that the interface is bounded by the Region 1 analysis.

Interface Analysis Summary

10.3 The only interface in the Surry SFP is between the burned fuel in Region 1 and the fresh fuel in Region 2. This interface needs to be considered in two different ways: (i) normal conditions in an unborated SFP and (ii) accident conditions in a borated SFP.

By using first principles, it can be determined that the Region 1 – Region 2 interface will not challenge the reactivity limits under normal conditions. If Region 1 is modeled with normal racks, then Region 1 is the same as Region 2 except it has less reactive fuel due to required burnup. Region 1 meets all limits with an infinite model. Replacing part of that infinite model with lower reactive fuel in the same rack would decrease reactivity. Therefore, the Region 1-2 interface does not challenge any limits under normal conditions.

Sections 10.1 and 10.2 analyze the Region 1 – Region 2 interface under accident conditions. The first method was to build a whole pool model, initializing the neutron source at different locations and then tracking where those neutrons migrated to. Under both burned and fresh conditions, the neutrons migrated to Region 1 meaning that Region 1 is more reactive than both Region 2 and the interface. The second method was to build an interface-only model. This model showed that the interface had >0.06 Δk margin to the limit after adding Region 1's bias and uncertainty term. Therefore, the Region 1-2 interface does not challenge any limits under accident conditions.

11 Normal Conditions

11.1 *Fuel Inserts*

The SFP contains inserts that are stored in the guide tubes of the fuel assemblies. Example of these inserts are control rods, discrete burnable poison assemblies, flux suppression assemblies, source rods, etc. Conservatively ignoring any absorbing properties of the inserts means that the principal reactivity effect that inserts have is increasing the fuel to moderator ratio (removing moderator).

Three scenarios need to be considered to determine the acceptability of storing these inserts in fuel assemblies: 1) storage with normal pitch in unborated water, 2) storage with normal pitch in borated water, and 3) storage with optimum pitch in borated water due to the cask drop accident.

1. Under normal pitch and unborated conditions, the fuel lattice is under moderated. This can be seen in the Clad OD uncertainty case in Section 9.2.7. Introducing an insert will displace more moderator decreasing reactivity.
2. Under normal pitch and borated conditions, the fuel lattice might be over moderated if at high boron concentrations. However, any small increases in reactivity from the insert displacing moderator will be offset by the high boron concentrations.
3. Under optimum pitch and borated conditions, introducing an insert would displace moderator and change the moderator to fuel ratio. The optimum pitch would adjust to reach the optimum reactivity again. This means that the insert's effect on the fuel to moderator ratio would have a negligible impact on the optimum pitch scenario while any neutron absorptions would have a negative reactivity effect. Test cases were run as a proof of concept. The results are shown in Table 11-1 and Figure 11-1. They show that inserts slightly decrease reactivity.

All three scenarios either resulted in a lower reactivity or had no impact on reactivity. Therefore, fuel assembly inserts are allowed in any assembly.

Table 11-1 shows the optimum pitch test cases for assemblies with inserts and without. The inserts are modeled as a full length, solid zirconium rod with a diameter of 1.0 cm (guide tubes have an inner diameter of 1.305 cm) and are placed in every guide tube in the model. The exact dimensions of the insert is not important because these cases are a proof of concept.

The k-eff's are then fit with a binomial regression curve to calculate the optimum pitch and maximum k-eff. The maximum k-effs can be seen in Figure 11-1. The maximum k-effs without inserts are larger than the maximum k-effs with inserts. Therefore, inserts reduce reactivity.

Table 11-1: Optimum Pitch k-eff for Assemblies With and Without Inserts

Insert Status	Enrichment (wt%)	Burnup (MWD/MTU)	Assembly Pitch (cm)	Distance Between (cm)		Pin Pitch (cm)	k-eff	σ
				Adjacent Cell Walls	Assembly and Inner Cell Wall			
Empty Guide Tubes	2.00	0	35.56	12.40	0.63	1.43	0.495065	0.000019
			29.36	6.20	0.63	1.43	0.561021	0.000052
			23.16	0.00	0.63	1.43	0.819330	0.000046
			21.93	0.00	0.00	1.43	0.832608	0.000048
			20.82	0.00	0.00	1.354	0.869966	0.000049
			19.84	0.00	0.00	1.287	0.897652	0.000019
			16.72	0.00	0.00	1.0719	0.891103	0.000059
	5.00	47	21.93	0.00	0.00	1.43	0.881843	0.000055
			20.82	0.00	0.00	1.354	0.890397	0.000058
			19.84	0.00	0.00	1.287	0.889430	0.000059
			16.72	0.00	0.00	1.0719	0.790616	0.000021
Inserts in Guide Tubes	2.00	0	35.56	12.40	0.63	1.43	0.492439	0.000052
			29.36	6.20	0.63	1.43	0.560948	0.000051
			23.16	0.00	0.63	1.43	0.830615	0.000047
			21.93	0.00	0.00	1.43	0.845409	0.000048
			20.82	0.00	0.00	1.354	0.881036	0.000048
			19.84	0.00	0.00	1.287	0.905341	0.000053
			16.72	0.00	0.00	1.0719	0.839183	0.000053
	5.00	47	21.93	0.00	0.00	1.43	0.884999	0.000053
			20.82	0.00	0.00	1.354	0.889102	0.000055
			19.84	0.00	0.00	1.287	0.881751	0.000056
			16.72	0.00	0.00	1.0719	0.734193	0.000058

Figure 11-1: Optimum Pitch k-eff for Assemblies With and Without Inserts

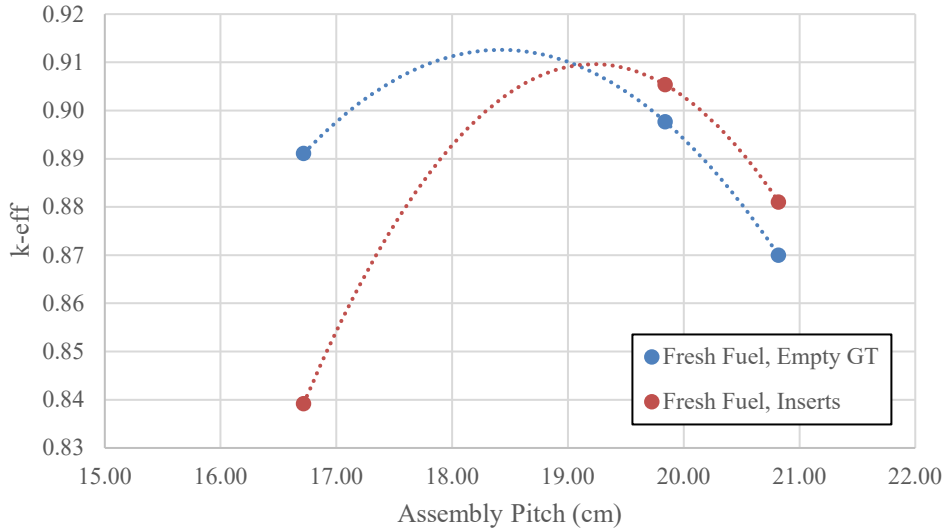

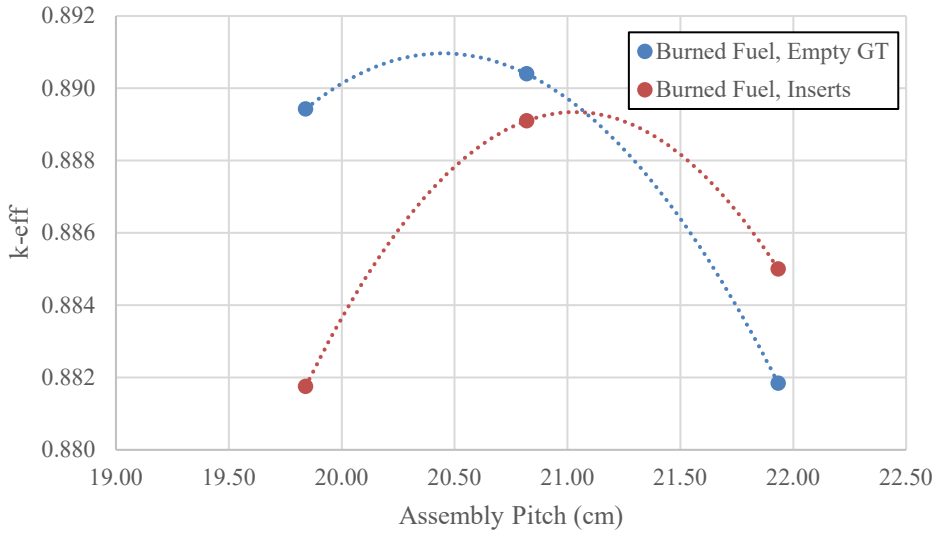

11.2 *Fuel Handling*

Surry fuel handling procedures for fresh and spent fuel place the following limits (among others) on fuel movement:

1) Only one fuel assembly at a time is allowed in the transfer canal
2) Fuel may only be moved into a location approved by procedure

A fuel handling accident can occur when two assemblies are simultaneously being moved. Since the assemblies are being moved, they are outside the rack cell and do not have the physical barrier of the racks separating them. This might occur when one assembly is being moved by the SFP crane while another assembly is being lowered into the pool by the new fuel elevator.

The model used to analyze this has two fresh, 5.00 wt% assemblies in the middle of a sea of unborated water at the same axial height. Note that unborated water is used since this is under normal conditions (Accident scenario is analyzed in Section 12.6). The two assemblies are then moved to create different spacing between them. This model is shown in Figure 11-2.

The resulting reactivity is shown in Table 11-2 and Figure 11-3. The results show that requiring 12 inches of separation is enough to practically neutronically isolate the assemblies meaning that this scenario is bounded by the normal conditions criticality analysis. Note that 12 inches of separation is the same amount as required for North Anna [23] and Millstone Unit 3 [14].

Therefore, Surry commits to updating fuel handling procedures the following way:

- At least 12 inches of separation is maintained between any two fuel assemblies outside of the storage racks

Table 11-2: Fresh Water Separation Cases

Separation Between Assemblies (inch)	k-eff	σ	dk	EALF
0	1.072524	0.000082	--	0.25
3	1.005612	0.000083	-0.066912	0.22
6	0.953244	0.000084	-0.119280	0.23
9	0.942999	0.000083	-0.129525	0.24
12	0.940737	0.000083	-0.131787	0.24
15	0.940157	0.000080	-0.132367	0.24
18	0.939900	0.000087	-0.132624	0.24
21	0.939837	0.000085	-0.132687	0.24
24	0.939909	0.000084	-0.132615	0.24

Figure 11-2: Fuel Handling Model

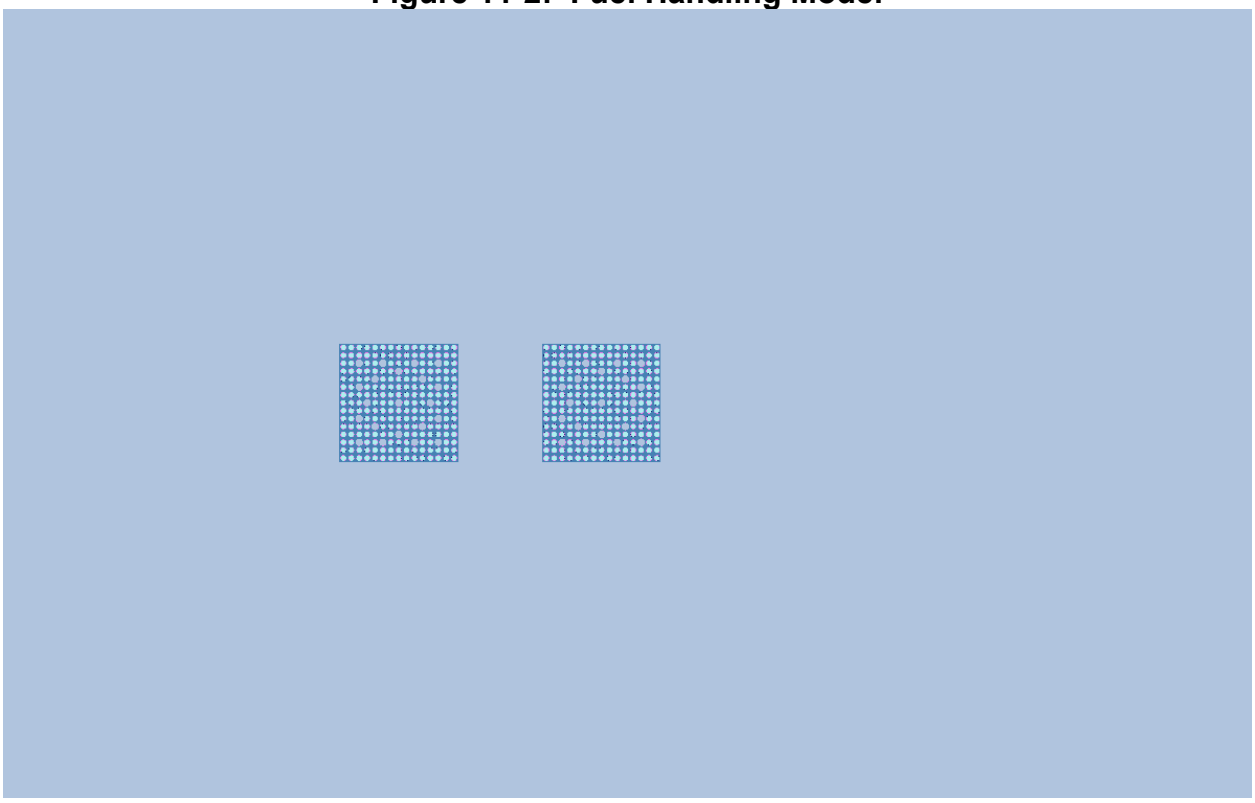

*The assemblies in the picture have 6 inches of separation.

Figure 11-3: Reactivity of Two Assemblies in Fresh Water

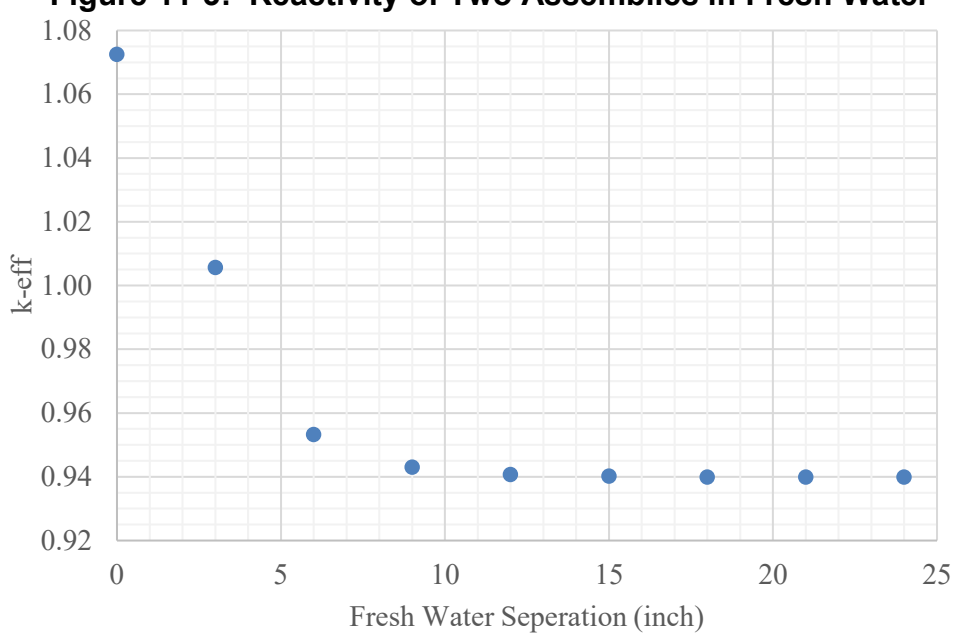

11.3 *Fuel Inspection*

Fuel inspections can be performed at any rack cell location that the assembly is qualified for. Note that there are no empty cells required in Surry's Spent Fuel Pool. If the fuel inspection is to occur outside of the racks, then it must maintain 12 inches of separation from other assemblies outside the racks (detailed in Section 11.2).

11.4 *Non-standard Fuel*

11.4.1 Fuel Rod Storage Canister

Failed fuel rods removed when reconstituting fuel assemblies are stored in a Fuel Rod Storage Canister, FRSC, (also known as fuel rod canisters, FRC) which is stored in one cell of the spent fuel storage racks. Each Fuel Rod Canister is manufactured to approximately the same exterior dimensions as a fuel assembly with a top nozzle similar to the fuel assembly. This will permit handling of the canister using normal fuel handling equipment and storage in the rack. Each canister contains tubes for the storage of individual fuel rods. The Fuel Rod Canister holds less than 204 fuel rods which is the number of fuel rods that a normal 15x15 assembly holds.

Figure 11-4 shows a drawing of the Fuel Rod Storage Canisters and Figure 11-5 shows a picture of it in a SFP rack cell. They can hold 105 fuel pins compared to the 204 fuel pins of a fuel assembly. [redacted]]F

Table 11-3 shows the relevant dimensions of the Fuel Rod Storage Canisters and Figure 11-6 shows it modeled in SCALE. Table 11-4 shows the SCALE results in both borated and unborated water. The Fuel Rod Canister is significantly less reactive than a normal Region 2 fuel assembly (5.00 wt%, 0 GWD/MTU). However, it is more reactive than a Region 1 fuel assembly (5.00 wt%, 47 GWD/MTU). Crediting burnup for the FRSCs is complicated because each fuel rod will come from different assemblies which have different burnups. Additionally, determining the FRSC optimum deformation/pitch is not straight forward. Therefore, the Fuel Rod Canister can be stored in any Region 2 cell but cannot be stored in Region 1. Both FRSCs are currently located in Region 2.

Table 11-3: Fuel Rod Canister Dimensions

Dimension	Value
No. of Fuel Tubes	105
Tube O.D.	[redacted]F
Tube Thickness	[redacted]F
Modeled Grid Volume	0 cc

Table 11-4: Reactivity of the Fuel Rod Canister

Fuel Element	Enrichment (wt%)	Burnup (GWD/MTU)	Boron	Temperature	k-eff	σ	Δk
Assembly	5.00	0	0 ppm	32°F	0.960523	0.000083	0.13274
FRC	5.00	0			0.827784	0.000080	--
Assembly	5.00	0	0 ppm	170°F	0.965739	0.000079	0.13520
Assembly	5.00	47			0.803698	0.000079	-0.02684
FRC	5.00	0			0.830540	0.000081	--
Assembly	5.00	0	2250 ppm	32°F	0.694445	0.000066	0.15216
FRC	5.00	0			0.542283	0.000062	--
Assembly	5.00	0	2250 ppm	170°F	0.693835	0.000071	0.15177
FRC	5.00	0			0.542064	0.000063	--

Figure 11-4: Drawing of Fuel Rod Storage Canister

[ ]F

Figure 11-5: Picture of Fuel Rod Storage Canister

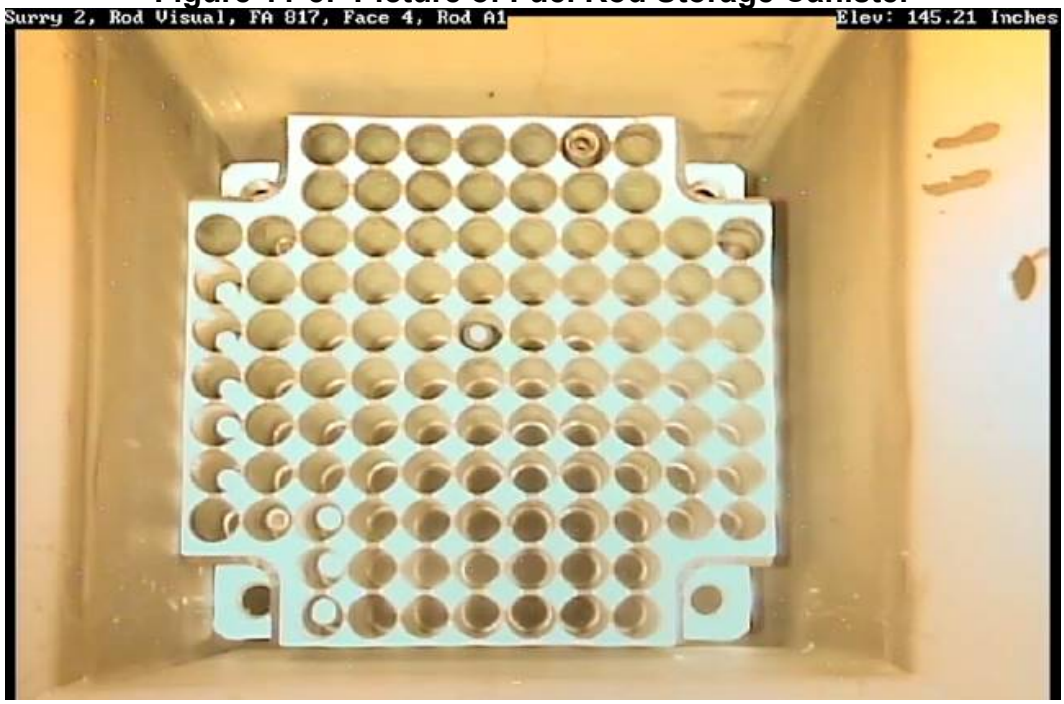

Figure 11-6: SCALE Model of Fuel Rod Storage Canister

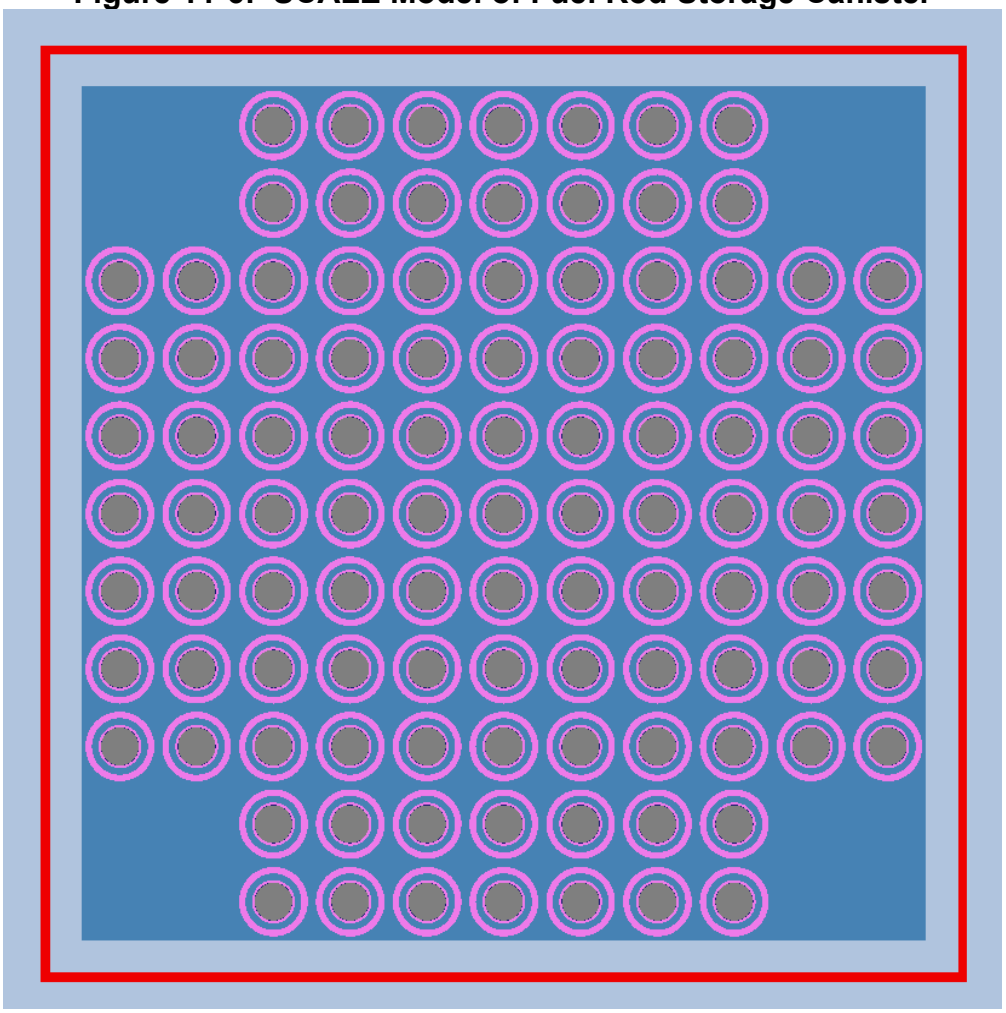

11.4.2 Reconstituted Fuel

Fuel pins in assemblies are sometimes removed and replaced to create reconstituted assemblies. There are two reconstitution scenarios evaluated:

- Remove a fuel pin(s) and replace it with an inert pin(s) (stainless steel or naturally enriched uranium).
- Remove a fuel pin(s) and do not replace the missing fuel pin(s) with anything. This scenario leaves an open water hole in the fuel lattice.

Reconstituted fuel with an open water hole can be an issue because the fuel pin lattice is under moderated when in unborated water. This means that removing a fuel assembly pin can decrease the fuel to moderator ratio which increases the reactivity of the fuel assembly. However, an inert pin is often inserted into the empty location. This has the effect of reducing the reactivity because it replaces fissionable material while keeping the fuel to moderator ratio constant.

The following rules will be enacted with regard to reconstituted assemblies:

- Assemblies with an open hole in the fuel pin lattice cannot be stored in Region 1 when a dry storage cask is in the spent fuel pool.
- Assemblies with an inert fuel pin (a stainless steel pin or naturally enriched uranium) can be stored as if it were a normal fuel assembly.
- Fuel pins cannot be pulled from fresh assemblies unless all the adjacent rack cells are empty.

This means that fuel assemblies with open water holes in the fuel pin lattices do not need to be analyzed in a cask drop accident. However, it needs to be analyzed to determine if the normal storage configuration of the spent fuel pool is bounding.

Table 11-5 shows how much reactivity is added to the SFP with an open water hole. This model uses nominal dimensions, asymmetric assembly placement in the cell, 5.00 wt% fuel, 0 GWD/MTU, 0 ppm of boron, and an infinite lattice. Nominal dimensions are acceptable because this calculation is determining whether the normal conditions analysis in Section 9.2 is bounding. Figure 11-7 shows the location of the pulled pin for each case.

Table 11-5: Reactivity Change from Removing One Fuel Pin

Case Scenario	k-eff	σ	dk	dk/RSS(σ)
Base Case	0.968636	0.000085	--	--
Exterior Pin	0.967861	0.000081	-0.00078	-660%
Interior Pin, far from GT	0.970322	0.000079	0.00169	1453%
Interior Pin, close to GT	0.969395	0.000079	0.00076	654%

Pulling a single fuel pin can increase the reactivity by 0.0017 Δk. Each time another pin is pulled, the reactivity increases by a lesser amount since the fuel to moderator ratio is already getting closer to the optimal ratio. The North Anna criticality LAR [23] ran an analysis and determined that open water holes can result in a maximum reactivity increase of ~0.015 Δk. That was for a 17x17 fuel assembly, but ~0.015 Δk seems reasonable given that one pin for Surry is worth 0.0017 Δk and Surry's 15x15 assemblies have fewer but fatter pins.

Reconstitution of a fuel assembly only occurs to burned fuel because fresh fuel does not have failed fuel pins. Section 9.1 showed that 10 GWD/MTU decreases reactivity by ~0.06 Δk. A fuel assembly generally receives ~20 GWD/MTU during the first cycle. Therefore, a fuel assembly with missing fuel pins will be bounded by the normal condition's analysis due to the assembly's burnup worth.

If for some reason, fuel pins need to be pulled from a fresh assembly, then the assembly must be isolated by emptying all adjacent fuel assembly cells. Table 4-3 of this calculation shows that the rack pitch is 14 inches (35.56 cm) which means that there will be at least this much distance between the reconstituted assembly and any other assembly if the adjacent cells are empty. Figure 11-3 shows that 14 inches is adequate to neutronically isolate the reconstituted assembly.

Figure 11-7: Location of Open Water Hole

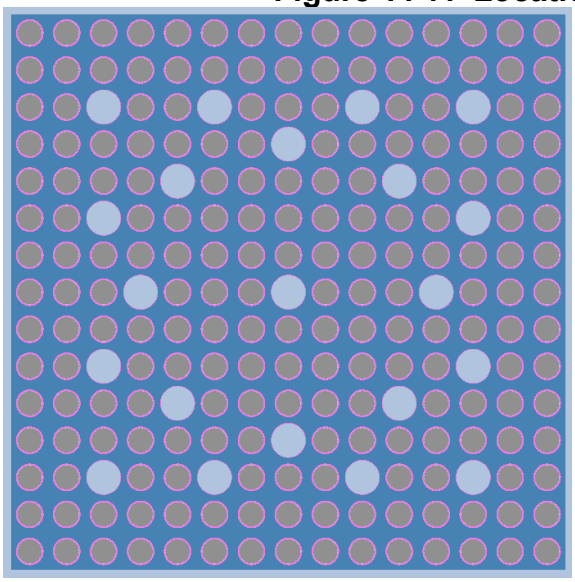

Base Model

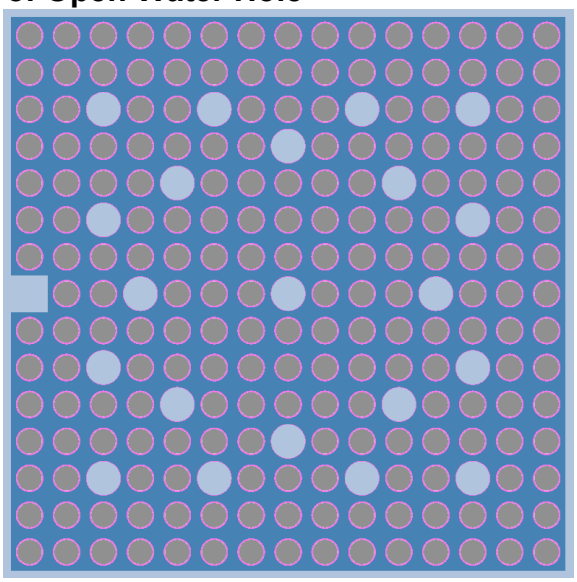

Exterior Pin

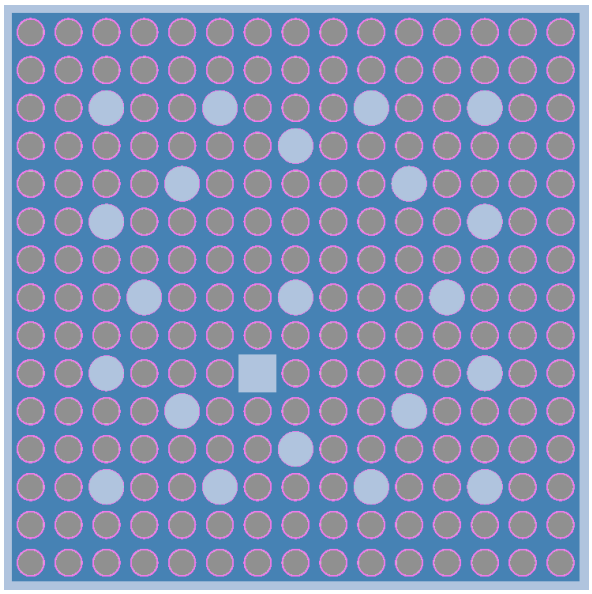

Interior Pin, far from GT

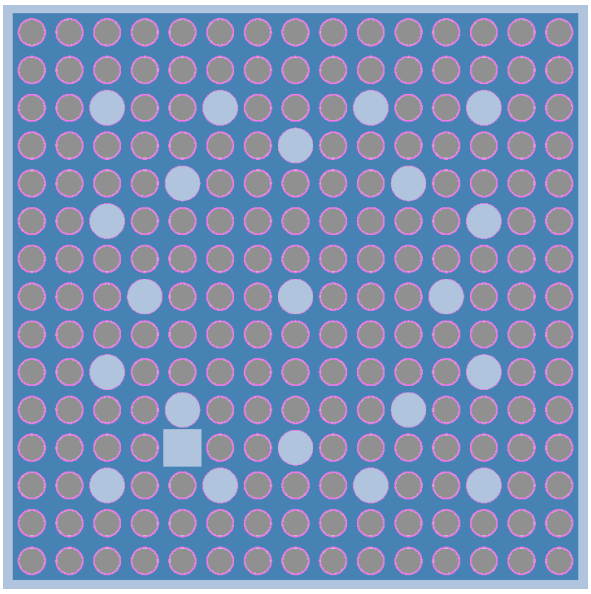

Interior Pin, close to GT

11.5 *Trash Cans*

Some rack cells in the Surry SFP are used as trash cans which store miscellaneous non-fuel material. Since there are no required empty rack cells in the SFP, trash cans cannot displace water which is credited for negative reactivity (neutron absorption). Instead, they are only replacing fuel with non-fuel material. This means trash cans only extend the distance between fuel assemblies decreasing the neutronic coupling compared to the analyzed condition in Section 9. Therefore, trash cans are allowed in any rack cell.

12 Accident Analysis

Accident scenarios include boron dilution to a minimum boron with normal storage, single fuel assembly mis-load in the fuel racks, multiple fuel assembly mis-load, loss of cooling (including partial voiding), dropped assembly into the racks with grid damage (optimum fuel pin pitch), fuel handling error (two fresh fuel assemblies out of rack in close proximity), mis-placement of an assembly between fuel racks, seismic event, and a cask drop accident. An evaluation of boron dilution time and mitigation is included as an attachment to this submittal.

The cask drop accident is the bounding accident scenario. Region 1 is susceptible to a cask drop accident while Region 2 is not. A full set of tolerance and bias cases are calculated for the cask drop accident with 2250 ppm of soluble boron. This analysis determined the burnup curve for Region 1. This analysis is performed in Section 9.1 of this report.

12.1 *Boron Dilution Accident*

The Code of Federal Regulations Title 10 Part 50 Section 68 (b).4 states:

> *"If credit is taken for soluble boron, the k-effective of the spent fuel storage racks loaded with fuel of the maximum fuel assembly reactivity must not exceed 0.95, at a 95 percent probability, 95 percent confidence level, if flooded with borated water, and the k-effective must remain below 1.0 (subcritical), at a 95 percent probability, 95 percent confidence level, if flooded with unborated water. "*

The Surry SFP criticality analysis credits soluble boron. Rather than searching for the soluble boron required for k<0.95 for all normal configurations, KENO model calculations are performed with 350 ppm soluble boron, which is shown to be more than sufficient to meet the criticality requirement.

A Surry dilution analysis determined that the lowest boron concentration that the SFP would reach is 400 ppm. Therefore, a case was run at nominal dimensions, infinite sea of assemblies (no radial leakage credited), initial U235 enrichment of 5.00 wt%, burnup of 0 GWD/MTU, temperature of 68°F, water density of 1.00 g/cc, and 350 ppm of boron which is 50 ppm below the bounding value calculated in the dilution accident. Note that the upper and bottom nozzles were modeled as fresh water (no soluble boron) since they displace a significant amount of borated water. Table 12-1 shows the results of this k-eff. Note that the Surry dilution analysis is included as an attachment to this submittal.

Table 12-1: k-eff of Boron Dilution Accident

Boron Concentration (ppm)	k-eff	σ
350	0.888251	0.000081

Table 9-17 and Table 9-24 shows that the maximum fresh fuel bias and uncertainty is <0.017 Δk (after removing the optimum pitch bias which is not applicable since the cask drop accident and dilution accident are not analyzed together due to the double contingency principle). Table 12-2 shows that there is ~3.5% Δk margin to the limit. This margin, along with the fact that the bias and uncertainty term is conservative (maximum of borated and unborated conditions), means that there is reasonable assurance that the boron dilution accident k-eff will be less than the limit even without running bias and uncertainty cases for this specific scenario.

Table 12-2: k-eff of Boron Dilution Accident

Description	k	Source
Base Case k-eff	0.88825	Table 11.5-1
Total Bias and Uncertainty	0.01600	Maximum from unborated and borated fresh fuel scenarios
NRC Review Margin	0.01000	Recommended Amount
Maximum k-eff	0.91425	Sum of Previous 3 terms
NRC Limit	0.95000	10 CFR 50.68
DOMINION MARGIN FOR 50.59	**0.03575**	**Maximum k-eff – Limit**

12.2 *Loss of Cooling*

If the spent fuel pool cooling system fails, the temperature of the SFP could increase above 170°F. Cases were run to determine the severity of this accident scenario. The cases were run at nominal dimensions, infinite sea of assemblies (no radial leakage credited), initial U235 enrichment of 5.00 wt%, burnup of 0 GWD/MTU, and 2250 ppm of soluble boron which is 50 ppm below the Technical Specification limit.

Boiling was simulated for when the temperature was modeled at 212°F. Boiling was modeled by reducing the volume fraction of the water inside the cell tubes. Reducing the volume fraction of the water is the same as modeling a homogenous void fraction. The volume fraction was not reduced for the water outside of the rack tubes because there is no heating element other than the fuel assemblies. Boiling will create vapor bubbles on the assembly fuel cladding and they will rise up out of the rack tubes and then to the surface of the pool. There is no physical mechanism for the vapor bubbles to move from the fuel assemblies to in between the fuel cells. The model of this accident is shown in Figure 12-1 and Figure 12-2.

Table 12-3 shows that the optimal temperature is about 100°F. However, the more important conclusion is that this accident results in k-effs ~0.2 Δk less than the cask drop analysis. The void fraction values of 0.15 and 0.30 were chosen to show the direction of reactivity as boiling increases (or as density decreases). If boiling intensity is lower than 0.15 or moderately greater than 0.30, then it can be deduced from the trend that reactivity is lower than the 100°F statepoint. A full bias and uncertainty analysis was performed for the cask drop scenario which has a base case k-eff much higher than this accident scenario. Since the cask drop scenario met the regulatory limit of 0.95, it can be reasonably deduced that this accident will also meet the limit without running the bias and uncertainty cases.

Table 12-3: Temperature Increase Accident Cases

Temperature		Boiling Void Fraction	Water Density (g/cc)	k-eff	σ	Δk
°F	K					
32	273	0	1.0000	0.69436	0.00007	-0.00025
100	311	0	0.9931	0.69461	0.00007	--
120	322	0	0.9886	0.69447	0.00008	-0.00014
170	350	0	0.9739	0.69391	0.00007	-0.00070
212	373	0	0.9584	0.69296	0.00007	-0.00165
212	373	0.15	0.8146	0.66367	0.00007	-0.03094
212	373	0.30	0.6709	0.62643	0.00007	-0.06818

Figure 12-1: Temperature Increase Model with Boiling

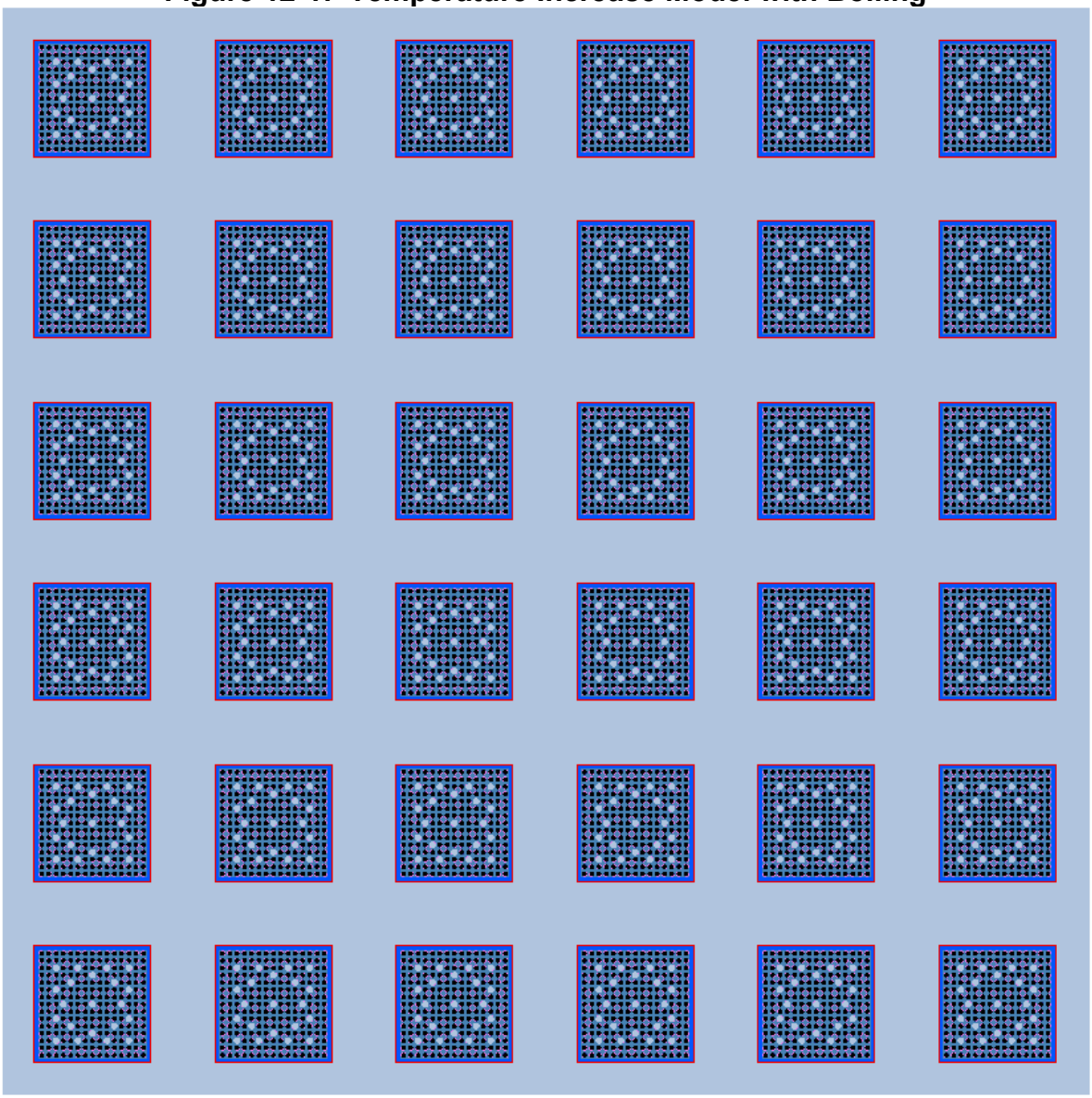

Figure 12-2: Temperature Increase Model with Boiling (zoomed in)

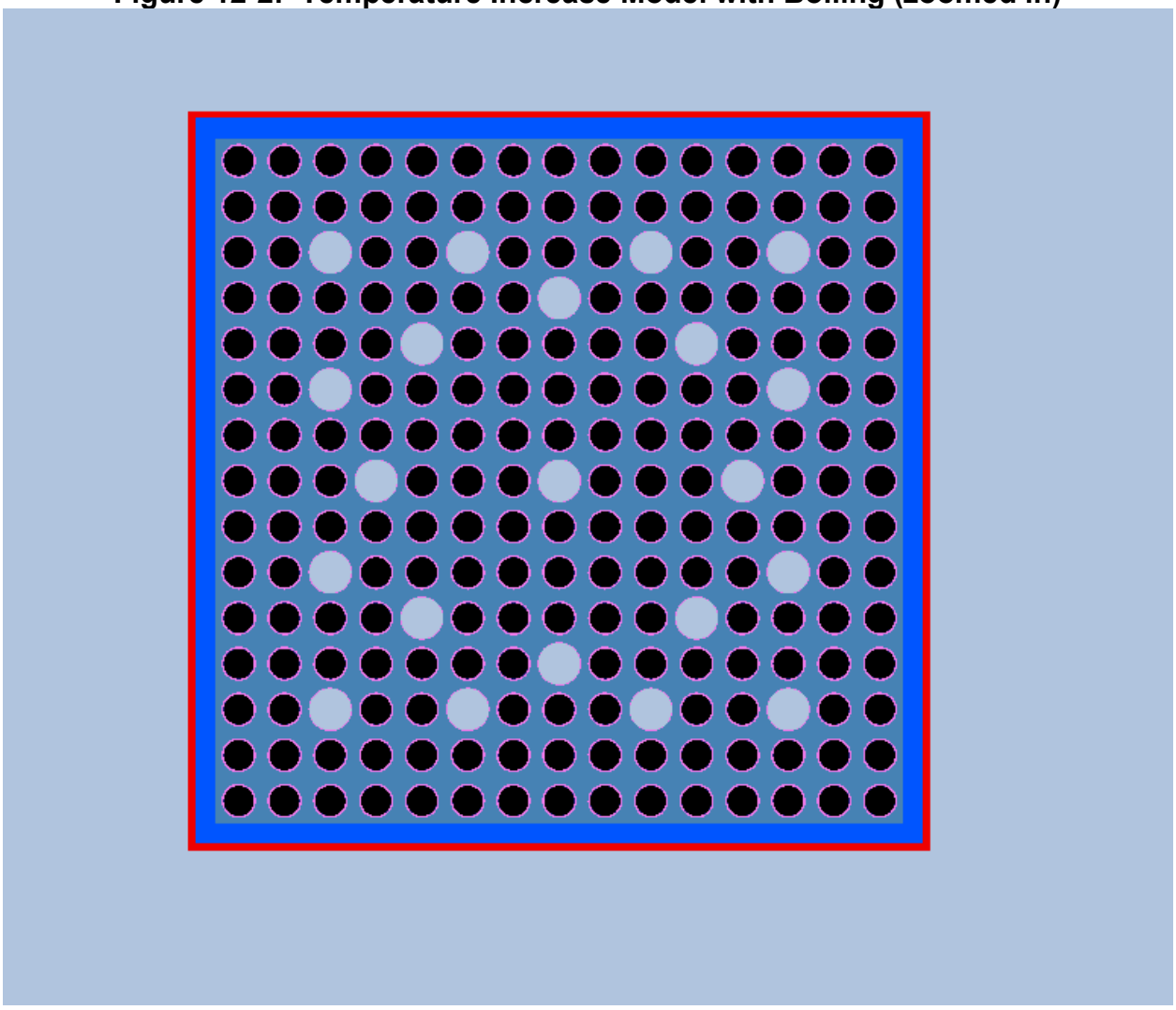

The darker blue materials within the stainless steel tube have reduced volume fractions to simulate vapor bubbles. The light blue material outside the stainless steel tube and inside the assembly guide tubes is water with no density reduction.

12.3 *Single Assembly Mis-placement*

An assembly can be misplaced inside or outside a rack cell. Misplacing an assembly inside a rack cell is covered by the Misload Accident detailed in Section 12.4.

Misplacing an assembly outside of a rack cell is possible. This will increase the coupling of the fuel. To test this scenario, a fresh 5.0 wt% fuel assembly will be dropped in a corner between Region 1 and Region 2. This is the most reactive location to drop a fuel assembly because there will be fuel adjacent to two faces of this assembly rather than just one. Figure 12-3 shows the layout of the SFP Rack Modules and the location of the simulated misplaced assembly.

Figure 12-3: Location of Misplaced Assembly
(Misplaced assembly indicated by red box)

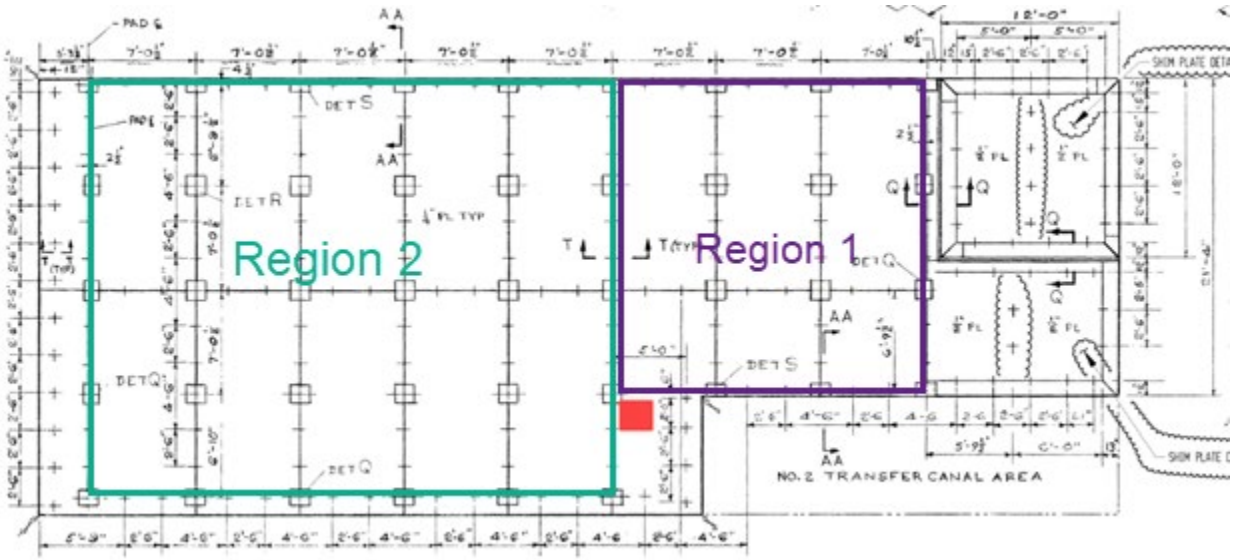

Each rack cell has a flare at the top to aid insertion of the fuel assembly. These flares restrict fuel assemblies from being misplaced right up against the outside of a rack cell. The flares stick out 1.5 inches (3.81 cm) from the inside of the cell wall. Therefore, the misplaced assembly was modeled 3.81 cm away from the inside face of the neighboring cell wall (note that the flares are not modeled in SCALE).

The SCALE model consisted of 3 6x6 rack modules to create the corner shown in Figure 12-3. One rack module contained Region 1 fuel and two rack modules contained Region 2 fuel. This model is neutronically dominated by Region 2 because Region 1 is the same rack type as Region 2 but contains less reactive fuel (either lower enrichment or more burnup). Figure 12-4 shows this model with a misplaced fuel assembly. This model contained borated water because this is an accident scenario. Also, the model had reflective boundaries.

Eight test cases were run in total. All eight had fresh, 5.0 wt% fuel in Region 2. Four had fresh fuel in Region 1 while the other four with burned fuel in Region 1. The enrichment and burnup of the Region 1 fuel assemblies are below the burnup curve in Figure 9-15 meaning they are conservatively more reactive. These four cases are shown in Table 12-4 and are described below.

- "Nominal": Does not have a misplaced assembly and has the same assembly asymmetric placement as described in Section 9.2.5. This model was only used to ensure that the model was correctly made by comparing it to the Region 2 only model. Since the model is dominated by Region 2, it should have a k-eff very similar to the Region 2 only model.
- "Asymmetry to corner": Does not have a misplaced assembly but all assemblies are asymmetrically placed toward the corner. This was done to increase the neutronic coupling of the misplaced assembly
- "Drop in corner": Assembly is misplaced as far into the corner as possible (1.5 inches away from both cell walls). This is the case shown in Figure 12-4. Initial neutron sources was started at the misplaced assembly corner.
- "Drop next to Region 2 assembly face": Assembly is misplaced in line with the assembly in the Region 2 cell. The only difference between this case and the corner case is that the misplaced assembly is shifted 9.05 cm to the right. This was tested since the Region 2 assembly is more reactive than the Region 1 assembly. Initial neutron sources was started at the misplaced assembly corner.

The maximum k-eff from Table 12-4 is 0.74. This is ~0.16 dk less reactive than the largest nominal k-eff of the cask drop accident (see Section 9.1.16). Therefore, the cask drop accident bounds the misplaced assembly accident.

Table 12-4: Misplaced Assembly Case Results

Scenario	Region 1 Fuel		k-eff	σ	Δk
	Enrichment (wt%)	Burnup (GWD/T)			
Region 2 only	N/A	N/A	0.693911	0.00007	--
Nominal	2.00%	0	0.693643	0.000067	-0.000268
Asymmetry to corner (no drop)	2.00%	0	0.692849	0.000036	--
Drop in Corner	2.00%	0	0.729440	0.000038	0.036591
Drop next to Region 2 assembly face	2.00%	0	0.739970	0.000037	0.047121
Region 2 only	N/A	N/A	0.693911	0.000072	--
Nominal	5.00%	47	0.693644	0.000069	-0.000267
Asymmetry to corner (no drop)	5.00%	47	0.692935	0.000035	--
Drop in Corner	5.00%	47	0.730114	0.000037	0.037179
Drop next to Region 2 assembly face	5.00%	47	0.739994	0.000036	0.047059

Figure 12-4: Misplaced Assembly SCALE Model

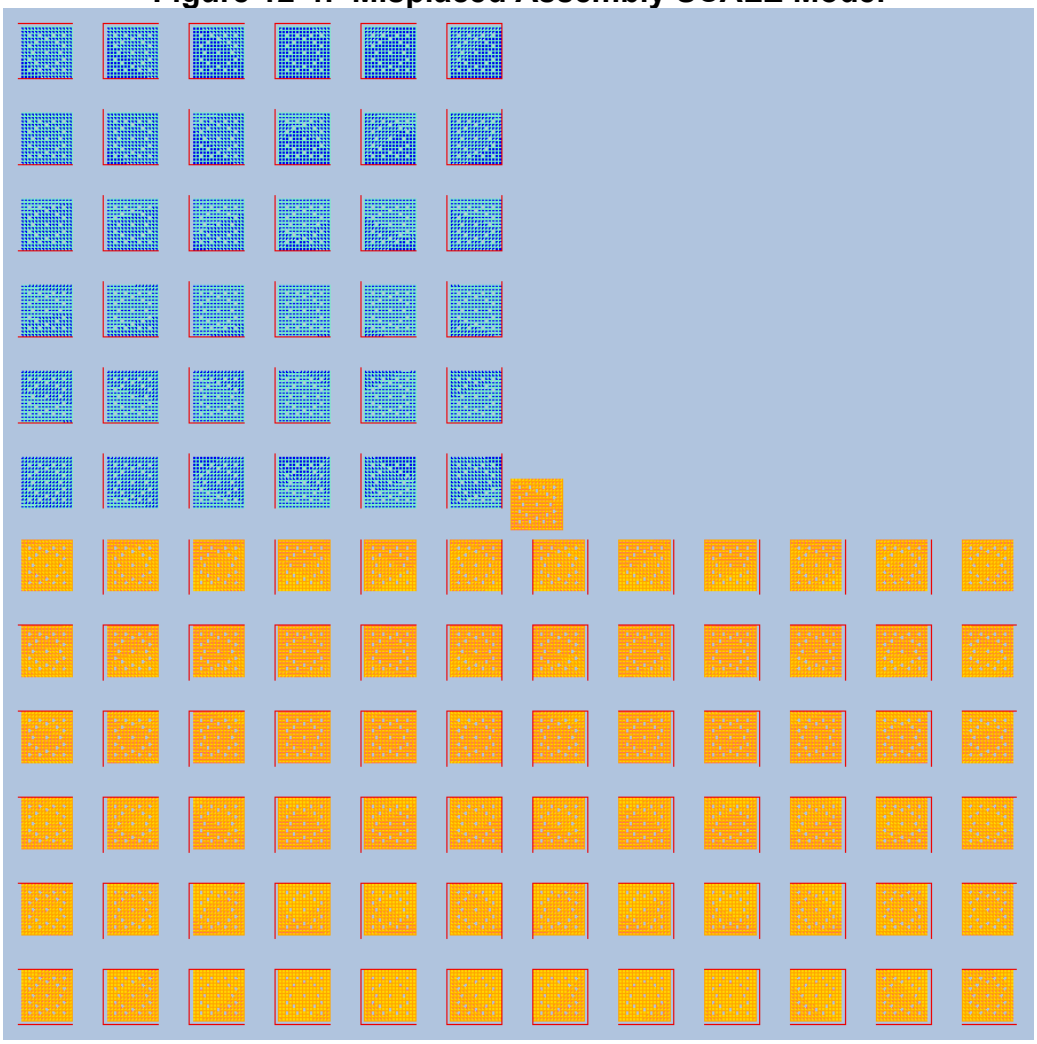

12.4 *Assembly Misload*

Region 2 of the SFP has no burnup requirement on fuel assemblies while Region 1 has a burnup curve. However, both regions have the same rack type. The only difference is that Region 1 is susceptible to the cask drop accident.

A fuel assembly misload is very unlikely to happen due to Shuffleworks, mapping the core each cycle (reading the physical fuel assembly IDs on the top nozzles of reuse assemblies), the fuel handling procedures and the Human Performance Tools in place. These strategies mitigate the chances of a misload occurring in the first place. Fuel handlers are also trained to stop if any fuel assemblies are out of place. The training of stopping when unsure separates the assembly misload accident from the cask drop accident and makes them two independent accidents. Therefore, due to the double contingency principle, Region 1 and Region 2 of the SFP can both be analyzed by modeling fresh, 5.00 wt% fuel in all cells under borated conditions. This scenario is modeled in Section 12.2, Loss of Cooling. The case results are repeated in Table 12-5 (without the high temperature cases).

Table 12-5: Fresh 5.00 wt% Fuel in All Cells with 2250 ppm

Temperature		Boiling Void Fraction	Water Density (g/cc)	k-eff	σ	Δk
°F	K					
32	273	0	1.0000	0.69436	0.00007	-0.00025
100	311	0	0.9931	0.69461	0.00007	--
120	322	0	0.9886	0.69447	0.00008	-0.00014
170	350	0	0.9739	0.69391	0.00007	-0.00070

The table above shows that loading 5.00 wt%, fresh fuel in all cells under borated conditions is much less than the limit. Therefore, this accident scenario is bounded by the Cask Drop Analysis.

12.5 *Dropped Assembly*

A dropped assembly can land on top of the fuel racks vertically or horizontally. However, the neutronic coupling of the dropped assembly and the assembly(ies) it lands on is negligible due to the geometry of the assemblies and racks separating active fuel regions by at least 12 inches. Therefore, the neutronic coupling of dropped fuel assembly is not a major concern for a dropped fuel assembly accident.

However, a dropped assembly could damage the grids of the assembly it hits. This could change the pin pitch of that particular assembly since the grids determine the pin pitch. Therefore, test cases were run where the fuel pins of one fresh, 5.0 wt% assembly are adjusted to optimum pin pitch. This configuration will bound any real configuration that a damaged fuel assembly could result in. In the model, the optimum pin pitch assembly was surrounded by fresh, 5.0 wt% assemblies with nominal pin pitch and rack pitch. The SFP is borated to 2250 ppm and is at 100°F since Section 12.2 showed that this temperature is the most reactive temperature when the SFP is borated and at nominal spacing.

The results of the SCALE cases are shown in Table 12-6. The results show that the SFP's k-eff is less than 0.70 with one damaged assembly. This shows that the dropped assembly accident is bounded by the cask drop accident. Therefore, uncertainty and bias cases do not need to be run for this scenario.

Table 12-6: Dropped Assembly Case Results

Pin Pitch (cm)	k-eff	σ	dk
1.39	0.694258	0.00007	-0.000353
1.41	0.694377	0.000071	-0.000234
1.43 (Nominal Pitch)	0.694611	0.000070	0.000000
1.45	0.694514	0.000069	-0.000097
1.47	0.694729	0.000070	0.000118
1.49	0.694971	0.000071	0.000360
1.512	0.694914	0.000068	0.000303

12.6 *Fuel Handling Error*

Section 11.2 established that 12 inches of separation will be maintained for assemblies outside of the fuel racks. An accident can occur when the required 12 inches of separation is violated. Since this is an accident scenario, 2250 ppm of borated water can be used due to the double contingency principle.

The same model was used as in Section 11.2 (two fresh assemblies, 5.00 wt%) except the assemblies are in a sea of borated water. Note that blocks of unborated water are located above and below the assemblies to conservatively deal with the fact that the assembly nozzles displace borated water. Table 12-7 and Figure 12-5 shows the spacing where the reactivity was calculated. Smaller spacing increments were used for these cases than the unborated cases because the optimum pitch peak might be missed if large 3 inch increments were used (which is likely what happened in Table 11-2). Additionally, cases were only run with the assemblies close together (≤ 3 inches) since that's where the peak reactivity occurs.

The results shown in Table 12-7 and Figure 12-5 show that the peak reactivity of two assemblies is significantly less than the reactivity of the base cases from the cask drop accident analysis (Table 9-17). This means that the fuel handling accident is bounded by the cask drop accident.

Table 12-7: Borated Water Separation Cases

Separation Between Assemblies (inch)	k-eff	σ	dk	EALF
0.00	0.793982	0.000071	--	0.52
0.25	0.792386	0.000069	-0.001596	0.50
0.50	0.785766	0.000070	-0.008216	0.48
1.00	0.764029	0.000067	-0.029953	0.48
1.50	0.740422	0.000070	-0.053560	0.49
2.00	0.721050	0.000066	-0.072932	0.50
2.50	0.706576	0.000068	-0.087406	0.51
3.00	0.69637	0.000067	-0.097612	0.52

Figure 12-5: Reactivity of Two Assemblies in Fresh Water

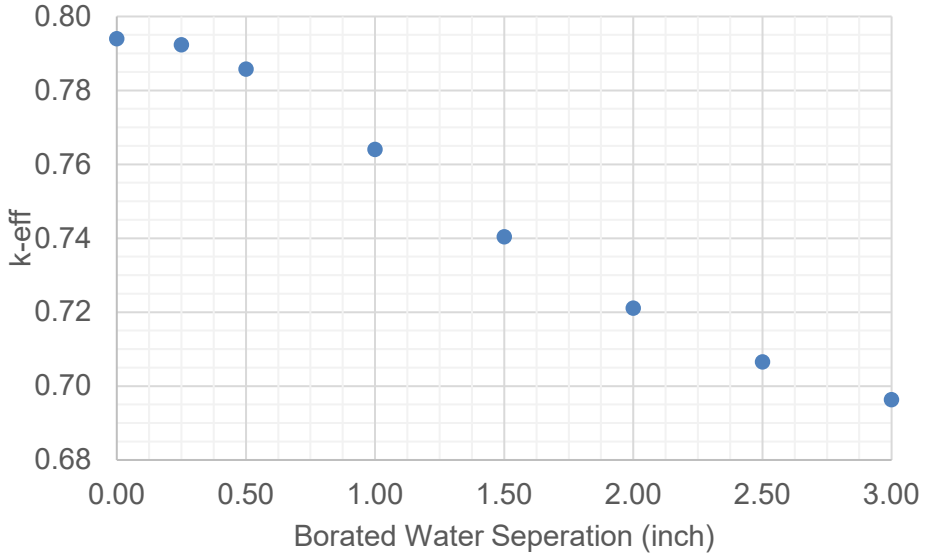

12.7 *Seismic Event*

The fuel racks and the spent fuel pool are Seismic Class I structures meaning they will be able to withstand the loadings encountered during operating-basis and safe-shutdown earthquakes. Additionally, the racks cannot slide during any design-basis seismic event. This means that during a seismic event the distance between cells and the fuel to moderator ratio will remain constant. The placement of assemblies within the cell may change, but asymmetric placement is already accounted for in the base models of the rack analysis (Section 9.2.5). Since the amount of moderator between fuel assemblies stay constant during a seismic event, this event is bounded by the Cask Drop Accident analyzed in Section 9.1 of this calculation.

12.8 *Accident Analysis Summary*

Evaluation of accident scenarios including single fuel assembly mis-load in the fuel racks, fuel assembly mis-load in the fuel racks, loss of cooling including partial voiding, dropped assembly into the racks with grid damage (optimum fuel pin pitch), mis-placement of an assembly between fuel racks, and a fuel handling error. All of these accidents are bounded by the cask drop accident. Section 9.1 confirms that 2250 ppm is more than sufficient to ensure k-eff < 0.95 for the cask drop accident. Therefore, all accident scenarios will meet the k-eff limit of 0.95.

13 Summary and Conclusions

A SFP criticality analysis is presented for Surry to allow for increased enrichment, introduce gadolinia into the licensing basis (specifically for the burnup credit), to update computer codes and analysis methods, and to increase identified margin to k-eff limits. A new fuel storage area (NFSA) criticality analysis is performed for Surry to allow for increased enrichment, update computer codes and analysis methods and to increase identified margin to k-eff limits.

As part of the criticality analyses, computer code validation is described in Appendix A and B. In support of the use of boron credit in the SFP criticality analysis, a boron dilution analysis is provided in an attachment to this submittal that identifies potential SFP dilution events, dilution water source flow rates and volumes, means of detection, time required for detection and mitigation, and minimum dilution event soluble boron concentration. A summary of this analysis is included in the attached NEI 12-16 Checklist.

13.1 *New Fuel Storage Area*

The criticality analysis demonstrates adequate margin to the k-eff limits with the NFSA fully loaded either with fresh 4.35 wt% fuel assemblies in every storage cell or with fresh 5.00 wt% fuel assemblies in a 3-out-of-4 storage configuration (Figure 13-3). A composite bounding fuel assembly design is used (Table 13-1).

13.2 *Spent Fuel Pool*

The Surry SFP contains only one unique storage rack design which does not have any fixed neutron absorber materials. The rack cells in Region 1 are susceptible to damage from a cask drop accident while the Region 2 rack cells are not. Therefore, Region 1 requires a minimum amount of burnup while Region 2 does not credit any burnup. The criticality analysis demonstrates adequate margin to the k-eff limits in each of the two SFP Regions without any required empty cells. A composite bounding fuel assembly design is used (Table 13-1).

13.3 *Bounding Fuel Design Inputs*

Table 13-1 summarizes the bounding fuel design inputs used for this SFP and NFSA analysis. All future fuel assembly designs will be evaluated against these design inputs.

Table 13-1: Bounding Fuel Design Inputs

Parameter	Value
Enrichment	≤ 5.0 wt% U-235
Pellet Diameter	≤ 0.9335 cm
Clad Outer Diameter	≥ 1.0719 cm
Clad Material	Zirconium alloy
Rod Pitch	≤ 1.4300 cm
Grid Volume Fraction	0.0083 - 0.0137 cm^3
Grid Material	Zirconium alloy
Pellet Stack Net Density	≤ 95.5% of theoretical
Fuel Pin Array size	15x15
Fuel Rods per Assembly	204
Active Fuel Length	≤ 365.76 cm

Axial blankets are not credited in the analysis and are permitted as well as annular pellets. Burnable absorbers are not credited in this analysis. Depletion related limits for burnable absorbers follow in the next section.

13.4 *Bounding Depletion Condition Inputs*

Depletion parameters were selected to cover past and anticipated future operation. Table 13-2 lists key depletion condition input selected to bound actual fuel depletion conditions. Exceptions to these parameters for existing inventory are justified in Section 9.3. Future Surry operation conditions will be evaluated against these inputs.

Table 13-2: Bounding Depletion Conditions for Burnup Credit

Parameter	Value	Notes
Maximum Burnup Averaged Soluble Boron	≤ 850 ppm	This is a cycle average
Maximum Core Average Moderator Exit Temperature	≤ 609.2 °F	This is not a value used directly in the analysis but is a proxy for the nodal moderator and fuel temperatures.
Maximum Burnup Averaged Relative Assembly Power	Burnup (MWD/MTU) / RPD 0 / ≤ 1.44 30000 / ≤ 1.44 50000 / ≤ 1.37 60000 / ≤ 1.03	Interpolate between burnup points
Maximum Removable Burnable Absorbers with IFBA	≤ 12 fingered WABA with up to 148 IFBA, ≤ 20 fingers of Alumina B_4C with no IFBA	Analysis assumed 20 Alumina B_4C as well as some combinations of IFBA and Alumina B_4C .

13.5 *Summary of Loading Constraints*

Storage geometries for each Region of the SFP are listed in Table 13-3. Region 1 credits burnup. The Region 1 burnup curve shown in Figure 13-2 with the corresponding regression fit equation. Figure 13-1 shows where Region 1 and Region 2 are in the Surry SFP.

Satisfaction of the burnup curve requirement shall use fuel assembly characteristics as follows:

1) The fuel enrichment is the maximum planar averaged as-built initial enrichment in the assembly. (Blanket enrichment is not credited by averaging with the higher enrichment central zone).
2) The fuel burnup is the volume averaged burnup of the assembly as determined using the measured reaction rates with no reduction for measurement uncertainty.

The NFSA has two storage configurations listed below:

1) All fuel assemblies in the NFSA have initial U-235 enrichments ≤4.35 wt% (does not require empty cells).
2) All fuel assemblies in the NFSA have initial U-235 enrichments ≤5.00 wt% **AND** requires empty cells in the locations that are shown in Figure 13.5-3.

Table 13-3: Surry SFP Storage Constraint Summary

Region	Geometry	Credits	Description
1	4 out of 4	Burnup	Figure 13-2
2	4 out of 4	None	≤5.00 U-235 wt%

Note that several new restrictions are committed to so that non-standard fuel will comply with these loading constraints. These new restrictions are repeated below:

- Reconstituted depleted assemblies with an open hole in the fuel pin lattice will be restricted from being stored in Region 1 when a dry storage cask is in the spent fuel pool.
- Reconstituted fresh assemblies with an open hole in the fuel pin lattice must be stored in a location with all adjacent rack cells empty.
- Fuel assemblies must be at least 12 inches apart when being handled outside of the storage racks or core.
- Fuel Rod Storage Cannisters can only be stored in Region 2.

Figure 13-1: Surry SFP Region Orientation

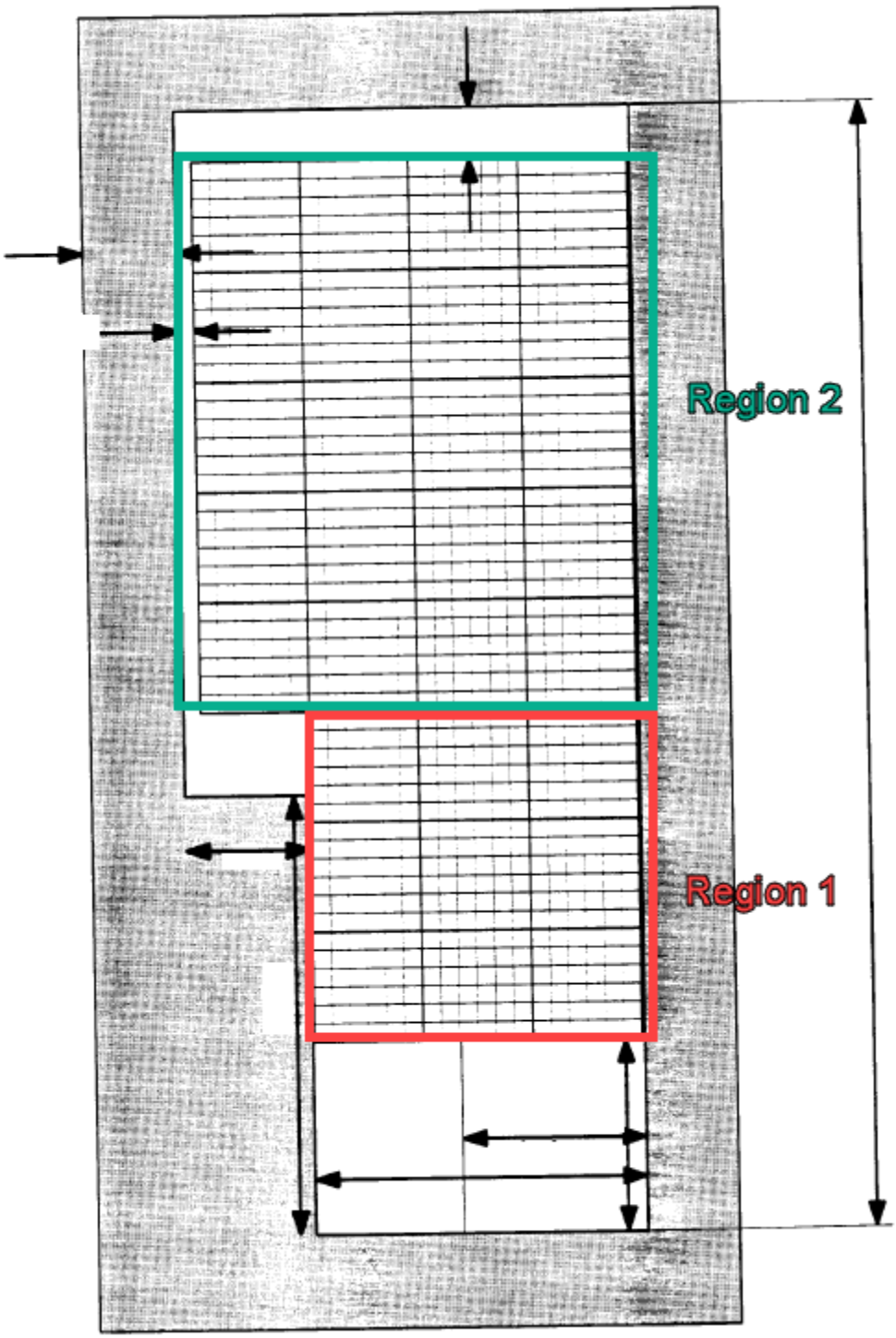

Figure 13-2: Region 1 Burnup Credit Curve

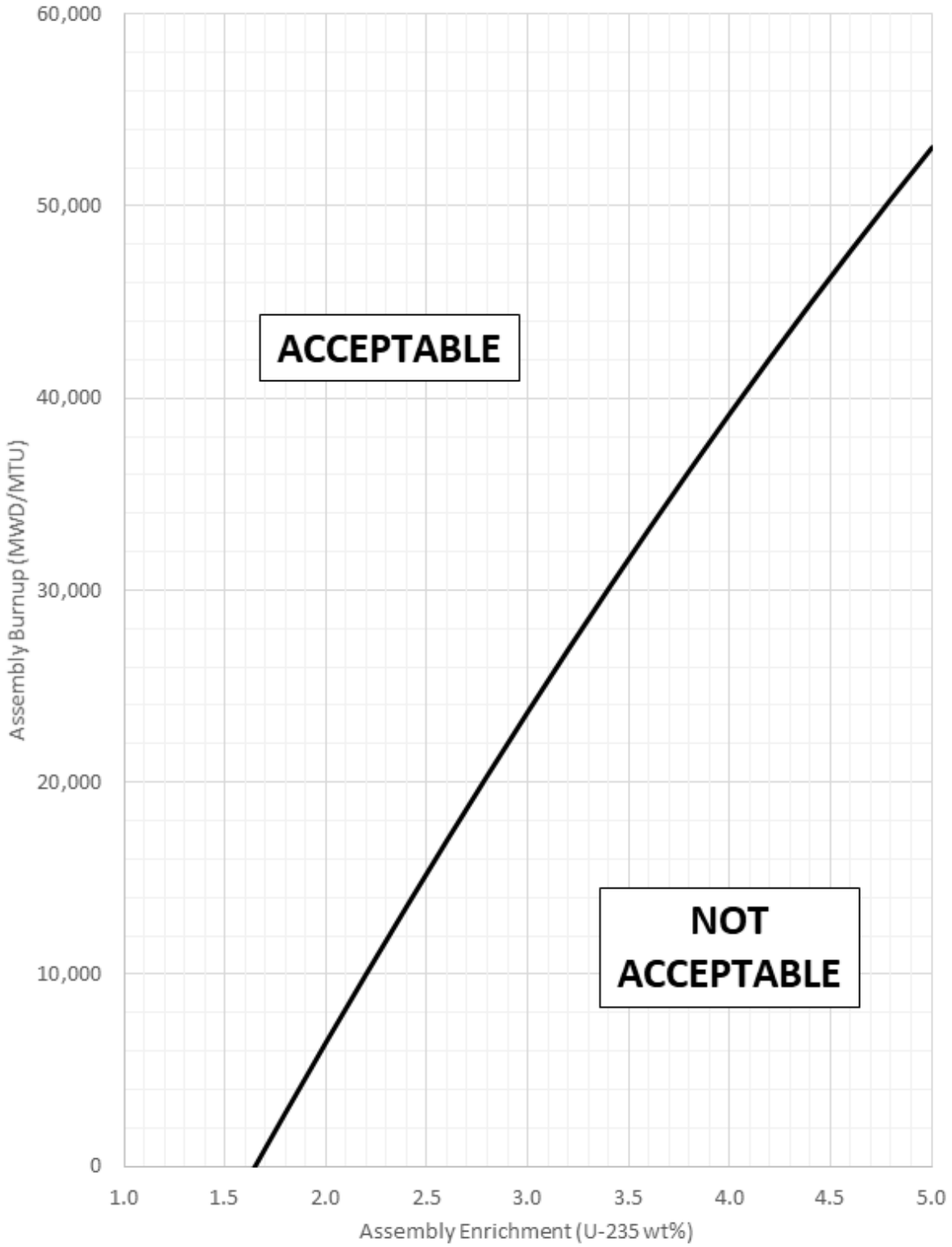

$$Required\ Burnup\ (MWD/MTU) = -849x^2 + 21470x - 33110$$

Figure 13-3: Empty Cells Required New Fuel Storage Area

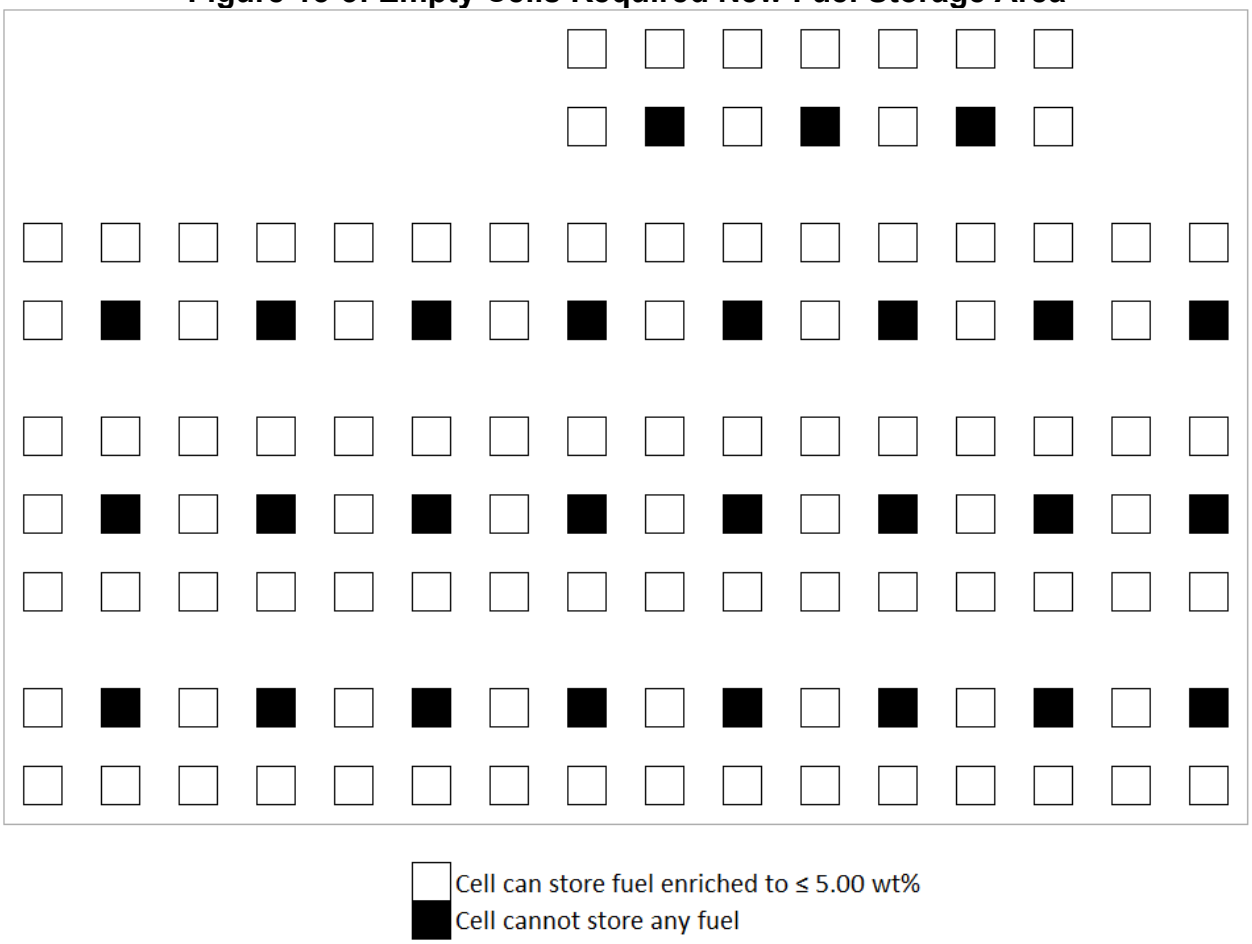

References

14

[1] Code of Federal Regulations, Title 10, Part 50, Section 68, "*Criticality Accident Requirements*."

[2] Code of Federal Regulations, Title 10, Part 50, Appendix A, "*General Design Criteria for Nuclear Power Plants*," Criterion 62, "Prevention of Criticality in Fuel Storage and Handling."

[3] NUREG-0800, *Standard Review Plan for the Review of Safety Analysis Reports for Nuclear Power Plants*, Section 9.1.1 Revision 3 (Criticality Safety of Fresh and Spent Fuel Storage and Handling), U.S. Nuclear Regulatory Commission, Washington, DC, March 2007.

[4] *Final Division of Safety Systems Interim Staff Guidance, DSS-ISG-2010-01 Revision 0, Staff Guidance Regarding the Nuclear Criticality Safety Analysis for Spent Fuel Pools*," Nuclear Regulatory Commission, October 2011. (ADAMS Accession Number ML110620086.)

[5] Dominion Resources Services, Inc. Letter to NRC, "Response to Generic Letter (GL) 2016-01, Monitoring of Neutron-Absorbing Materials in Spent Fuel Pools," 11/1/2016 (Serial No. 16-161).

[6] Regulatory Guide RG 1.240, "Fresh and Spent Fuel Pool Criticality Analyses," 03/2021 (Accession Number: ML20356A127).

[7] "*SCALE: A Modular Code System for Performing Standardized Computer Analyses for Licensing Evaluation*," ORNL/TM-2005/39, Version 6, Volumes 1-3, Oak Ridge National Laboratory, Oak Ridge, Tennessee, USA, January 2009.

[8] S. Goluoglu, N. F. Landers, L. M. Petrie, and D. F. Hollenbach,"*CSAS5: Control Module For Enhanced Criticality Safety Analysis Sequences with KENO V.A*," ORNL/TM-2005/39, Version 6, Vol. 1, Section C5, Oak Ridge National Laboratory, Oak Ridge, Tennessee, USA, January 2009.

[9] J. C. Wagner, M. D. DeHart, and C. V. Parks, "*Recommendations for Addressing Axial Burnup in PWR Burnup Credit Analyses*," US Nuclear Regulatory Commission, NUREG/CR-6801 Oak Ridge National Laboratory, Oak Ridge, Tenn. (2003).

[10] Letter from U.S.N.R.C (Richard Guzman) to Dominion (D. Heacock), "Millstone Power Station, Unit No. 3 – Issuance of Amendment Adopting Dominion Core Design And Safety Analysis Methods and Addressing The Issues Identified in Three Westinghouse Communication Documents (CAC NO. MF6251).", July 28, 2016. Dominion Energy Nuclear Licensing Serial Number 16-317 (Received August 2, 2016). NRC Accession Number: ML16131A728

[11] M. A. Jessee, and M. D. DeHart, "*TRITON: A Two-Dimensional Transport and Depletion Module for Characterization of Spent Nuclear Fuel*," ORNL/TM-2005/39, Version 6 Vol. 1, Section T1, Oak Ridge National Laboratory, Oak Ridge, Tennessee, USA, January 2009.

[12] J.C. Dean and R.W. Tayloe, Jr., *Guide for Validation of Nuclear Criticality Safety Calculational Methodology*, NUREG/CR-6698, Nuclear Regulatory Commission, Washington, DC January 2001

[13] J. M. Scaglione, D. E. Mueller, J.C. Wagner and W. J. Marshall, *An Approach for Validating*. *Actinide and Fission Product Burnup Credit Criticality Safety Analyses—Criticality (keff) Predictions*, US Nuclear Regulatory Commission, NUREG/CR-7109, Oak Ridge National Laboratory, Oak Ridge, Tenn. (2012).

[14] Letter from Dominion (M. Sartain) to U.S.N.R.C, "Millstone, Unit 3, License Amendment Request Regarding Proposed Technical Specifications Changes for Spent Fuel Storage and New Fuel Storage.", May 03, 2018. NRC ADAMS Accession Number: ML16003A008

[15] USNRC Reg. Guide 1.183, "*Alternative Radiological Source Terms for Evaluating Design Basis Accidents at Nuclear Power Reactors*", US Nuclear Regulatory Commission, Washington, DC, July 2000.

[16] C. E. Beyer, and P. M. Clifford, "*Update of Gap Release Fractions for Non-LOCA Events Utilizing the Revised ANS 5.4 Standard*", PNNL-18212 Rev. 1, Pacific Northwest National Laboratory, Richland, Washington, June 2011. ADAMS Accession Number ML112070118.

[17] J. O. Barner, "*Characterization Of LWR Spent Fuel MCC - Approved Testing Material--ATM-101*," PNL-5109 Rev. 1, Pacific Northwest National Laboratory, Richland, Washington (1985).

[18] R. J. Guenther, et al, "*Characterization Of Spent Fuel Approved Testing Material--ATM-103*," PNL-5109-103, Pacific Northwest National Laboratory, Richland, Washington (1988).

[19] R. J. Guenther, et al, "*Characterization Of Spent Fuel Approved Testing Material--ATM-104*," PNL-5109-104, Pacific Northwest National Laboratory, Richland, Washington (1991).

[20] R. J. Guenther, et al, "*Characterization Of Spent Fuel Approved Testing Material--ATM-105*," PNL-5109-105, Pacific Northwest National Laboratory, Richland, Washington (1991).

[21] R. J. Guenther, et al, "*Characterization Of Spent Fuel Approved Testing Material--ATM-106*," PNL-5109-106, Pacific Northwest National Laboratory, Richland, Washington (1988).

[22] A. Simpson, T. Marlow, J. Franco, M. Clapham and A. Chesterman, "Operational Experience in Radiometric Instrumentation for Spent Fuel Monitoring," Proceedings of the Institute of Nuclear Materials Management: INMM 44th Annual Meeting, Phoenix, Arizona, July 13-17, 2003, Institute of Nuclear Materials Management, Oakbrook Terrace, IL (2003).

[23] Letter from Dominion (M. Sartain) to U.S.N.R.C, "Virginia Electric and Power Company (DOMINION) North Anna Power Station Units 1 and 2 Proposed Licensing Amendment

Request for Spent Fuel Storage and New Fuel Storage (Serial No. 16-383)", May 2, 2017. NRC ADAMS Accession Number: ML17128A451

[24] "Studsvik Scandpower Inc. Approved Version Submittal for TOPICAL REPORT SSP-14-P01/028-TR, "GENERIC APPLICATION OF THE STUDSVIK SCANDPOWER CORE MANAGEMENT SYSTEM TO PRESSURIZED WATER REACTORS" (CAC NO. MF7273)", October 6, 2017. NRC ADAMS Accession Number: ML17279A983

[25] *International Handbook of Evaluated Criticality Safety Benchmark Experiments*, NEA/NSC/DOC(95)3, Volumes IV and VI, Nuclear Energy Agency, OECD, Paris, September, 2014.

[26] D. E. Mueller, K. R. Elam, and P. B. Fox, *Evaluation of the French Haut Taux de Combustion (HTC) Critical Experiment Data*, NUREG/CR-6979 (ORNL/TM-2007/083), prepared for the US Nuclear Regulatory Commission by Oak Ridge National Laboratory, Oak Ridge, Tenn., September 2008

[27] U.S. Nuclear Regulatory Commission, *Spent Fuel Project Office Interim Staff Guidance – 8, Rev. 3 – Burnup Credit in the Criticality Safety Analyses of PWR Spent Fuel in Transport and Storage Casks*, U.S. Nuclear Regulatory Commission, April, 2012.

[28] A. Tsiboulia, et al., "Water-Moderated U(4.92)O_2 Fuel Rods in 1.29, 1.09, and 1.01 cm Pitch Hexagonal Lattices at Different Temperatures," LEU-COMP-THERM-026, *International Handbook of Evaluated Criticality Safety Benchmark Experiments*, NEA/NSC/DOC(95)3, Volume IV, Nuclear Energy Agency, OECD, Paris, September, 2014.

[29] A. D. Santos, et al., "Critical Loading Configurations of the IPEN/MB-01 Reactor Considering Temperature Variation From 14º C to 85º C," LEU-COMP-THERM-046, *International Handbook of Evaluated Criticality Safety Benchmark Experiments*, NEA/NSC/DOC(95)3, Volume IV, Nuclear Energy Agency, OECD, Paris, September, 2014.

[30] D. Lancaster, *Sensitivity Analyses for Spent Fuel Pool Criticality*, Technical Report EPRI Doc No. 3002003073,December 2014.

[31] ANS-8.1/N16.1-1975, "Criticality safety in operations with fissionable material".

[32] NEI 12-16, Revision 4, "Guidance for Performing Criticality Analyses of Fuel Storage at LightWater Reactor Power Plants", 09/2019 (Accession Number: ML19269E069).

[33] M. L. Williams, S. E. Skutnik, Et. Al., "ORIGAMI: A CODE FOR COMPUTING ASSEMBLY ISOTOPICS WITH ORIGEN", *SCALE Code System*, ORNL/TM-2005/39.

[34] NUREG/CR-6800, "Assessment of Reactivity Margins and Loading Curves for PWR Burnup-Credit Cask Designs", March 2003.

[35] EPRI 3002010613, Revision 1, "Benchmarks for Quantifying Fuel Reactivity Depletion Uncertainty", October 2017.

[36] EPRI 3002016888, Revision 2, "Utilization of the EPRI Depletion Benchmarks for Burnup Credit Validation", August 2019.

[37] NRC Accession Number ML19168A097, Final Safety Evaluation by The Office of Nuclear Reactor Regulation Topical Report 3002010613, “Benchmarks for Quantifying Fuel Reactivity Depletion Uncertainity – Revision 1” and Topical Report 3002010614, “Utilization of the EPRI Depletion Benchmarks for Burnup Credit Validation – Revision 1”, July 2019.

[38] John Wagner, “Impact of Soluble Boron Modeling for PWR Burnup Credit Criticality Safety Analyses”, Oak Ridge National Laboratory, Submitted to the American Nuclear Society: International ANS/ENS (European Nuclear Society) 2003 Winter Meeting, November 2003.

[39] USNRC (Guzman) to Dominion (Stoddard), “Millstone Power Station, Unit No. 3 - Issuance of Amendment No. 273 Regarding Technical Specification Changes for Spent Fuel Storage and New Fuel Storage (EPID L-2018-LLA-0126)”, 05/28/2019, Accession Number ML19126A000.

[40] NRC Accession Number ML012470157, Letter from J D. Neighbors to W. L. Stewart, “Surry Power Station Units 1 and 2, Amendment 84, Revise the Technical Specifications to Remove a Restriction on Moving a Spent Fuel Case into the Fuel Building.” 03/04/1983

Appendix A: Code Validation for Criticality Analysis Using Laboratory Critical Experiments

A.1. Overview

This appendix determines the computer code and cross-section library bias and uncertainty for the calculated k's when using the CSAS5 module of SCALE 6.2.3 [A.1]. The 238 Group ENDF/B-VII.0 cross section library is used for all SCALE calculations. The calculated k bias and uncertainties determined in this Appendix covers the major actinides plus structural and absorber materials. All the benchmarking computer runs use a large Monte Carlo sampling to ensure convergence: a minimum of 9000 generations and 12000 neutrons per generation was used for the calculated k's.

The analysis to determine the calculated k bias and uncertainty follows the direction of NUREG/CR-6698, "Guide for Validation of Nuclear Criticality Safety Calculational Methodology" [A.2]. The guide establishes the following steps for performing the validation:

1. Define operation/process to identify the range of parameters to be validated
2. Select critical experiment data
3. Model the experiments
4. Analyze the data
5. Define the area of applicability of the validation and limitations

It further defines the steps of "Analyze the data" as:

1. Determine the Bias and Bias Uncertainty
2. Identify Trends in Data, Including Discussion of Methods for Establishing Bias Trends
3. Test for Normal or Other Distributions
4. Select the Statistical Method for Treatment of Data
5. Identify and Support Subcritical Margin
6. Calculate the Upper Safety Limit

The validation consists of modeling 238 UO_2 and 111 MOX critical experiments for the determination of the bias and the uncertainty in the calculation of k for fresh fuel and spent fuel. In addition, 17 critical experiments are modeled to determine a temperature bias.

A.2. Definition of the Range of Parameters to Be Validated

The validation guidance document [A.2] states:

> *"Prior to the initiation of the validation activity, the operating conditions and parameters for which the validation is to apply must be identified. The fissile isotope, enrichment of fissile isotope, fuel density, fuel chemical form, types of neutron moderators and reflectors, range of moderator to fissile isotope, neutron absorbers, and physical configurations are among the parameters to specify. These parameters will come to define the area of applicability for the validation effort."*

The fuel is low enriched uranium dioxide (less than or equal to 5.0 wt% U-235). The range of UO_2 density between 91.9% and 96.2%. The minimum historical enrichment is 1.85%. The fuel rods are arranged in 15 by 15 arrays in a square pitch. Fuel assemblies used at Surry comprise of Westinghouse assembly designs. The current reload batches for Surry consist of Westinghouse 15x15 upgrade fuel and future full fuel batches may include AGORA-5A fuel. The 15x15 assembly design at Surry has a fuel rod pitch of 1.43 cm and fuel rod clad outer diameter ranges from 1.072 cm to 1.077 cm. The fuel burnable absorber materials include IFBA (ZrB_2), Borosilicate Glass (B_2O_3, aka BPRA), Aluminum B_4C (aka WABA), and Hafnium inserts (aka Flux Suppression Inserts). Future full fuel batches may utilize Gadolinia (Gd_2O_3) as an additional absorber material. Control rods contain Ag-In-Cd absorber material. These parameters will be covered by the criticality benchmark analysis due to the sensitivity cases run in the CSA which contained these materials.

The high-density spent-fuel storage rack design is described in Appendix 9A of the Surry Power Station UFSAR. The following design features must be covered by the criticality benchmark analysis.

- Reinforced concrete structure (concrete reflector)
- Steel superstructure and fuel storage cells (steel reflector)
- Soluble boron of at least 2300 ppm
- Steel racks: steel boxes with a 14-inch pitch and 8.875 inch square cells (over-moderated assembly configurations).
- Assemblies: 8.5-inch width with 0.563-inch pin pitch (under-moderated assembly fuel pin configurations).

Note that absorber plates are not present in the pool and not credited in the spent fuel pool criticality safety analysis. Therefore, it is not appropriate to include absorber panel cases in the benchmark database.

A.3. Selection of the Critical Benchmark Experiments

The UO2 benchmarks that were selected met the following criteria:

- Low enriched (5 wt% U-235 or less) UO2 to cover the principle isotopes of concern.
- Fuel in rods to assure that the heterogeneous analysis used in SCALE also is applied in the benchmark analysis.
- Square lattices to assure the lattice features of SCALE used in the rack analysis are also modeled in the critical benchmarks selected.
- Presence of soluble boron, boron bearing rods or plates, gadolinium and Cd to cover most of the burnable poison and control rod absorption.
- No emphasis on a feature or material not of importance to the rack analysis such as lead or copper.

There are two primary sources of critical benchmark experiment data used for this analysis, the OECD/NEA *International Handbook of Evaluated Criticality Safety Benchmark Experiments* [A.3] and the HTC program [A.4 – A.8]. The HTC program was specifically designed to collect criticality benchmark data for spent fuel configurations (i.e. MOX fuel). The International Handbook contains a very large number of experiments, most of which are not applicable to this analysis. The low enriched uranium subset at thermal energies (LEU-COMP-THERM) from the handbook are listed in the Table A.3-1 where each of the experiments are explicitly identified. The HTC program benchmark cases are listed in Table A.3-2. Reasons for exclusion are given for each excluded case. In cases where a material or geometric feature is specifically benchmarked, it is added in the last column of the table. Note that all selected cases use UO_2 rod clusters in square arrays and most cases contain common structural materials like concrete, steel and aluminum. Also, flux traps are a common feature in the benchmarks. Only notable items beyond these features will be identified in the last column of the table.

To supplement the LEU database, the International Handbook was used to identify 8 additional experiments from the MOX database. These experiments consist of low enriched Uranium Oxide (<0.71 wt% U-235) and Plutonium Oxide in mixed oxide fuel rods like the composition found in spent fuel. Note that some cases have hexagonal lattices and should be excluded. However, lattice geometry is related to Energy of Average Lethargy to cause Fission (EALF)

which is trended as part of the benchmark. Due to the need for additional criticality benchmarks for MOX fuel, some of these cases will be retained for the Surry SFP benchmark analysis. The list of additional MOX Benchmarks are listed in Table A.3-3.

A later section will evaluate the area of applicability provided by this selection of critical benchmarks.

Table A.3-1: Selection Review of OECD/NEA Criticality Benchmarks
(All Experiments Start With LEU-COMP-THERM-)

Benchmark Number	Description	Lab	Selected
1	WATER-MODERATED U(2.35)O_2 FUEL RODS IN 2.032-CM SQUARE-PITCHED ARRAYS	PNL	All 8
2	WATER-MODERATED U(4.31)O_2 FUEL RODS IN 2.54-CM SQUARE-PITCHED ARRAYS	PNL	All 5
3	WATER-MODERATED U(2.35)O_2 FUEL RODS IN 1.684-CM SQUARE-PITCHED ARRAYS (GADOLINIUM WATER IMPURITY)	PNL	None. Gd impurity not well known. Not benchmark quality.
4	WATER-MODERATED U(4.31)O_2 FUEL RODS IN 1.892-CM SQUARE-PITCHED ARRAYS (GADOLINIUM WATER IMPURITY)	PNL	None. Gd impurity not well known. Not benchmark quality.
5	CRITICAL EXPERIMENTS WITH LOW-ENRICHED URANIUM DIOXIDE FUEL RODS IN WATER CONTAINING DISSOLVED GADOLINIUM	PNL	None. Soluble Gd not used in pools.
6	CRITICAL ARRAYS OF LOW-ENRICHED UO_2 FUEL RODS WITH WATER-TO-FUEL VOLUME RATIOS RANGING FROM 1.5 TO 3.0	JAEA	All 18
7	WATER-REFLECTED 4.738-WT.%-ENRICHED URANIUM DIOXIDE FUEL-ROD ARRAYS	Valduc	Only 4 cases used rest are in hexagonal arrays.
8	CRITICAL LATTICES OF UO_2 FUEL RODS AND PERTURBING RODS IN BORATED WATER	B&W	All 17 ***B_2O_3 Rods*** ***Soluble B 779 ppm-1511 ppm***
9	WATER-MODERATED RECTANGULAR CLUSTERS OF U(4.31)O_2 FUEL RODS (2.54-CM PITCH) SEPARATED BY STEEL, BORAL, COPPER, CADMIUM, ALUMINUM, OR ZIRCALOY-4 PLATES	PNL	16 cases used. Did not include Copper or borated panel cases. ***Cadmium, Zr-4***
10	WATER-MODERATED U(4.31)O_2 FUEL RODS REFLECTED BY TWO LEAD, URANIUM, OR STEEL WALLS	PNL	22 cases used. Did not use lead cases since no lead in pool. ***Depleted U***
11	CRITICAL EXPERIMENTS SUPPORTING CLOSE PROXIMITY WATER STORAGE OF POWER REACTOR FUEL (PART I - ABSORBER RODS)	B&W	All 15 ***Soluble B 0 ppm-1037 ppm and B_4C rods***

Benchmark Number	Description	Lab	Selected
12	WATER-MODERATED RECTANGULAR CLUSTERS OF U(2.35)O_2 FUEL RODS(1.684-CM PITCH) SEPARATED BY STEEL, BORAL, BOROFLEX, CADMIUM,OR COPPER PLATES (GADOLINIUM WATER IMPURITY)	PNL	None. Gd impurity not well known. Not benchmark quality.
13	WATER-MODERATED RECTANGULAR CLUSTERS OF U(4.31)O_2 FUEL RODS (1.892-CM PITCH) SEPARATED BY STEEL, BORAL, BOROFLEX, CADMIUM, OR COPPER PLATES, WITH STEEL REFLECTING WALLS	PNL	2 cases used. Did not use the cases with copper or borated panels. Borated panel cases (2, 3, and 4) not used in Surry analysis. ***Cadmium***
14	WATER-REFLECTED ARRAYS OF U(4.31)O_2 FUEL RODS (1.890-CM AND 1.715-CM SQUARE PITCH) IN BORATED WATER	PNL	None used. High boron content uncertainty. Not benchmark quality.
15	THE VVER EXPERIMENTS: REGULAR AND PERTURBED HEXAGONAL LATTICES OF LOW-ENRICHED UO_2 FUEL RODS IN LIGHT WATER	KFKI	None used due to hex arrays.
16	WATER-MODERATED RECTANGULAR CLUSTERS OF U(2.35)O_2 FUEL RODS (2.032-CM PITCH) SEPARATED BY STEEL, BORAL, COPPER, CADMIUM, ALUMINUM, OR ZIRCALOY-4 PLATES	PNL	19 cases used. Did not use the copper or borated panel cases. Borated panel cases (8 through 14) not used in Surry analysis. ***Cadmium***
17	WATER-MODERATED U(2.35)O_2 FUEL RODS REFLECTED BY TWO LEAD, URANIUM, OR STEEL WALLS	PNL	23 cases used. Did not use the 6 cases with a lead reflector. ***Depleted U***
18	LIGHT WATER MODERATED AND REFLECTED LOW ENRICHED URANIUM DIOXIDE (7 WT.%) ROD LATTICE	Winfrith	None used. Only 1 case with no SCALE sample deck. Complex system.
19	WATER-MODERATED HEXAGONALLY PITCHED LATTICES OF U(5%)O_2 STAINLESS STEEL CLAD FUEL RODS	Kurchatov Institute	None used due to hex arrays.
20	WATER-MODERATED HEXAGONALLY PITCHED PARTIALLY FLOODED LATTICES OF U(5%)O_2 ZIRCONIUM CLAD FUEL RODS, 1.3-CM PITCH	Kurchatov Institute	None used due to hex arrays.
21	HEXAGONALLY PITCHED PARTIALLY FLOODED LATTICES OF U(5%)O_2 ZIRCONIUM CLAD FUEL RODS MODERATED BY WATER WITH BORIC ACID	Kurchatov Institute	None used due to hex arrays.

Benchmark Number	Description	Lab	Selected
22	UNIFORM WATER-MODERATED HEXAGONALLY PITCHED LATTICES OF RODS WITH U(10%)O_2 FUEL	Kurchatov Institute	None used due to hex arrays.
23	PARTIALLY FLOODED UNIFORM LATTICES OF RODS WITH U(10%)O_2 FUEL	Kurchatov Institute	None used due to hex arrays.
24	WATER-MODERATED SQUARE-PITCHED UNIFORM LATTICES OF RODS WITH U(10%)O_2 FUEL	Kurchatov Institute	Did not use either case due to 10 wt% U-235 enrichment
25	WATER-MODERATED HEXAGONALLY PITCHED LATTICES OF U(7.5%)O_2 STAINLESS-STEEL-CLAD FUEL RODS	Kurchatov Institute	None used due to hex arrays.
26	WATER-MODERATED U(4.92)O_2 FUEL RODS IN 1.29, 1.09, AND 1.01 CM PITCH HEXAGONAL LATTICES AT DIFFERENT TEMPERATURES	IPPE	None used due to hex arrays.
27	WATER-MODERATED AND LEAD-REFLECTED 4.738% ENRICHED URANIUM DIOXIDE ROD ARRAYS	Valduc	None used due to lead reflector.
28	WATER-MODERATED U(4.31)O_2 FUEL RODS IN TRIANGULAR LATTICES WITH BORON, CADMIUM AND GADOLINIUM AS SOLUBLE POISONS	PNL	None used due to hex arrays.
29	WATER MODERATED AND WATER REFLECTED 4.74% ENRICHED URANIUM DIOXIDE ROD ARRAYS SURROUNDED BY HAFNIUM PLATES	Valduc	None used. No SCALE sample decks. hf plates cases without hf have the same pitch and pin as benchmark 7 above. No significant additional value
30	VVER PHYSICS EXPERIMENTS: REGULAR HEXAGONAL (1.27-CM PITCH) LATTICES OF LOW-ENRICHED U(3.5 WT.% 235U)O_2 FUEL RODS IN LIGHT WATER AT DIFFERENT CORE CRITICAL DIMENSIONS	Kurchatov Institute	None used due to hex arrays.
31	WATER-MODERATED HEXAGONALLY PITCHED PARTIALLY FLOODED LATTICES OF U(5%)O_2 ZIRCONIUM-CLAD FUEL RODS, 0.8-CM PITCH	Kurchatov Institute	None used due to hex arrays.
32	UNIFORM WATER-MODERATED LATTICES OF RODS WITH U(10%)O_2 FUEL IN RANGE FROM 20°C TO 274°C	Kurchatov Institute	None used due to hex arrays.
33	REFLECTED AND UNREFLECTED ASSEMBLIES OF 2 AND 3%-ENRICHED URANIUM FLUORIDE IN PARAFFIN	ORNL	None used. Not UO_2

Benchmark Number	Description	Lab	Selected
34	FOUR 4.738-WT.%-ENRICHED URANIUM DIOXIDE ROD ASSEMBLIES CONTAINED IN CADMIUM, BORATED STAINLESS STEEL, OR BORAL SQUARE CANISTERS, WATER-MODERATED AND -REFLECTED	Valduc	None used due to borated plates and high uncertainties with Cd panel cases. Borated plates (cases 4 through 8 and 15) not used in Surry analysis
35	CRITICAL ARRAYS OF LOW-ENRICHED UO_2 FUEL RODS IN WATER WITH SOLUBLE GADOLINIUM OR BORON POISON	JAEA	Used 2 cases. Did not use the case with dissolved Gd. (not like pool). ***Soluble B 70 ppm-147.7 ppm***
36	THE VVER EXPERIMENTS: REGULAR AND PERTURBED HEXAGONAL LATTICES OF LOW-ENRICHED UO_2 FUEL RODS IN LIGHT WATER - Part 2	KFKI	None used due to hex arrays.
37	WATER-MODERATED AND PARTIALLY CONCRETE-REFLECTED 4.738-WT.%-ENRICHED URANIUM DIOXIDE ROD ARRAYS	Valduc	None used. No SCALE sample decks.
38	WATER-MODERATED 4.738-WT.%-ENRICHED URANIUM DIOXIDE ROD ARRAYS NEXT TO A BORATED CONCRETE SCREEN	Valduc	None used. No SCALE sample decks. Used a borated concrete reflector (not like pool).
39	INCOMPLETE ARRAYS OF WATER-REFLECTED 4.738-WT.%-ENRICHED URANIUM DIOXIDE FUEL-ROD ARRAYS	Valduc	Used all 17 cases.
40	FOUR 4.738-WT.%-ENRICHED URANIUM DIOXIDE ROD ASSEMBLIES CONTAINED IN BORATED STAINLESS STEEL OR BORAL SQUARE CANISTERS, WATER MODERATED AND REFLECTED BY LEAD OR STEEL	Valduc	None used due to borated panels. Borated panel cases with no lead reflector (1, 5, 9, and 10) not used in Surry analysis.
41	STORAGE ARRAYS OF 3%-ENRICHED LWR ASSEMBLIES: THE CRISTO II EXPERIMENT IN THE EOLE REACTOR	Cadarache	Did not use the 5 cases due to complex geometry and no SCALE sample deck.
42	WATER-MODERATED RECTANGULAR CLUSTERS OF $U(2.35)O_2$ FUEL RODS (1.684-CM PITCH) SEPARATED BY STEEL, BORAL, BOROFLEX, CADMIUM, OR COPPER PLATES, WITH STEEL REFLECTING WALLS	PNL	Used 2 cases. Did not use copper or borated panel cases. Borated panel cases (2 through 4) not used in Surry analysis. ***Cadmium***
43	CRITICAL LOADING CONFIGURATIONS OF THE IPEN/MB-01 REACTOR WITH A HEAVY SS-304 REFLECTOR	IPEN	9 cases used. ***Gadolinia and Ag-In-Cd***

Benchmark Number	Description	Lab	Selected
44	CRITICAL LOADING CONFIGURATIONS OF THE IPEN/MB-01 REACTOR WITH UO_2, STAINLESS STEEL AND COPPER RODS	IPEN	None used due to copper rods.
45	PLEXIGLAS OR CONCRETE-REFLECTED $U(4.46)_3O_8$ WITH H/U=0.77 AND INTERSTITIAL MODERATION	Rocky Flats	None used since not pin geometry.
46	CRITICAL LOADING CONFIGURATIONS OF THE IPEN/MB-01 REACTOR CONSIDERING TEMPERATURE VARIATION FROM 14°C TO 85°C	IPEN	Used only for temperature bias.
47	FUEL TRANSPORT FLASK CRITICAL BENCHMARK EXPERIMENTS WITH LOW-ENRICHED URANIUM DIOXIDE FUEL	Winfrith	None used. 3 complex cases. No SCALE sample decks.
48	LIGHT WATER MODERATED AND REFLECTED LOW-ENRICHED (3 WT.% 235U) URANIUM DIOXIDE ROD LATTICES	Winfrith	All 5 cases used
49	MARACAS PROGRAMME: POLYTHENE-REFLECTED CRITICAL CONFIGURATIONS WITH LOW-ENRICHED AND LOW-MODERATED URANIUM DIOXIDE POWDER, $U(5)O_2$	Valduc	None used. Powder rather than pellets. Not similar to pools.
50	149SM SOLUTION TANK IN THE MIDDLE OF WATER-MODERATED 4.738-WT.%-ENRICHED URANIUM DIOXIDE ROD ARRAYS	Valduc	7 cases used. Did not use cases with dissolved Sm. This is not typical of pools. ***Soluble B 0/822/5030 ppm***
51	CRITICAL EXPERIMENTS SUPPORTING CLOSE PROXIMITY WATER STORAGE OF POWER REACTOR FUEL (PART II - ISOLATING PLATES)	B&W	9 cases used. Did not use cases with the borated Al plates. ***Soluble B 217 ppm-514 ppm***
52	URANIUM DIOXIDE (4.738-WT.%-ENRICHED) FUEL ROD ARRAYS MODERATED AND REFLECTED BY GADOLINIUM NITRATE SOLUTION	Valduc	None used due to hex arrays.
53	VVER PHYSICS EXPERIMENTS: REGULAR HEXAGONAL (1.27 CM PITCH) LATTICES OF LOW-ENRICHED $U(4.4\ WT.\%\ 235U)O_2$ FUEL RODS IN LIGHT WATER AT DIFFERENT CORE CRITICAL DIMENSIONS	Kurchatov Institute	None used due to hex arrays.
54	CRITICAL LOADING CONFIGURATIONS OF THE IPEN/MB-01 REACTOR WITH UO_2, AND UO_2-Gd_2O_3 RODS	IPEN	8 cases used. ***UO_2-Gd_2O_3 and Ag-In-Cd***

Benchmark Number	Description	Lab	Selected
55	LIGHT-WATER MODERATED AND REFLECTED LOW-ENRICHED URANIUM (3 wt.% 235U) DIOXIDE ROD LATTICES	Winfrith	Neither case used. Complex geometry no KENO-V.a sample deck
56	CRITICAL EXPERIMENT WITH BORAX-V BOILING WATER REACTOR TYPE FUEL ASSEMBLIES	INL	None used. No sample SCALE decks. Complex BWR geometry.
57	4.738-WT.%-ENRICHED URANIUM DIOXIDE FUEL ROD ARRAYS REFLECTED BY WATER IN A DRY STORAGE CONFIGURATION	Valduc	None used. No sample SCALE decks.
58	CRITICAL LOADING CONFIGURATIONS OF THE IPEN/MB-01 REACTOR WITH LARGE VOID IN THE REFLECTOR	IPEN	9 cases used. ***UO_2-Gd_2O_3 and Ag-In-Cd***
59	Not included in Handbook		
60	RBMK GRAPHITE REACTOR: UNIFORM CONFIGURATIONS OF U(1.8, 2.0, or 2.4% 235U)O_2 FUEL ASSEMBLIES, AND CONFIGURATIONS OF U(2.0% 235U)O_2 ASSEMBLIES WITH EMPTY CHANNELS, WATER COLUMNS, AND BORON OR THORIUM ABSORBERS, WITH OR WITHOUT WATER IN CHANNELS	Kurchatov Institute	None used. RBMK – not typical of LWRs
61	VVER PHYSICS EXPERIMENTS: HEXAGONAL (1.27-CM PITCH) LATTICES OF U(4.4 WT.% 235U)O_2 FUEL RODS IN LIGHT WATER, PERTURBED BY BORON, HAFNIUM, OR DYSPROSIUM ABSORBER RODS, OR BY WATER GAP WITH/WITHOUT EMPTY ALUMINIUM TUBES	Kurchatov Institute	None used due to hex arrays.
62	2.6%-ENRICHED UO_2 RODS IN LIGHT-WATER MODERATOR WITH BORATED STAINLESS STEEL PLATE: SINGLE ARRAYS	JAEA	None used. No SCALE sample decks.
63	LIGHT-WATER MODERATED AND REFLECTED LOW-ENRICHED URANIUM (3 wt.% 235U) DIOXIDE ROD LATTICES WITH DISCRETE POISON-ROD ARRAYS	Winfrith	None used. No SCALE sample decks.
64	VVER PHYSICS EXPERIMENTS: REGULAR HEXAGONAL (1.27 CM PITCH) LATTICES OF LOW-ENRICHED U(2.4 WT.% 235U)O2 FUEL RODS IN LIGHT WATER AT DIFFERENT CORE CRITICAL DIMENSIONS	Kurchatov Institute	None used since hex geometry.

Benchmark Number	Description	Lab	Selected
65	CRITICAL CONFIGURATIONS OF 2.6%-ENRICHED UO_2 ROD ARRAYS IN LIGHT-WATER MODERATOR WITH BORATED STAINLESS STEEL PLATE: COUPLED ARRAYS	JAEA	None used. No SCALE sample decks.
66	PLEXIGLAS-REFLECTED, CONCRETE-REFLECTED, OR THIN STEEL-REFLECTED $U(4.46)_3O_8$ WITH H/U=0.77 AND HEU DRIVERS	Rocky Flats	None used. Not an array of rods.
67	IPEN/MB-01 REACTOR W/ FUEL AND MOLYBDENUM RODS	IPEN	None used. Molybdenum not in pool.
68	PLEXIGLAS-REFLECTED, CONCRETE-REFLECTED, OR THIN STEEL-REFLECTED $U(4.48)_3O_8$ WITH H/U=1.25 OR H/U=2.03 AND HEU DRIVERS	Rocky Flats	None used. Not an array of rods.
69	PLEXIGLAS-REFLECTED $U(4.48)_3O_8$ WITH H/U=1.25 OR H/U=2.03 AND INTERSTITIAL MODERATION	Rocky Flats	None used. Not an array of rods.
70	VVER PHYSICS EXPERIMENTS: REGULAR HEXAGONAL (1.10-CM PITCH) LATTICES OF LOW-ENRICHED U(6.5 WT.% 235U)O_2 FUEL RODS IN LIGHT WATER AT DIFFERENT CORE CRITICAL DIMENSIONS	Kurchatov Institute	None used due to hex arrays.
71	LOW MODERATED 4.738-WT.%-ENRICHED URANIUM DIOXIDE FUEL ROD ARRAYS	Valduc	All 4 cases used.
72	UNDER-MODERATED 4.738-WT.%-ENRICHED URANIUM DIOXIDE FUEL ROD ARRAYS REFLECTED BY WATER OR POLYETHYLENE	Valduc	Used 3 cases. Did not use Polyethylene reflector cases.
73	UNDER-MODERATED 4.738-WT.%-ENRICHED URANIUM DIOXIDE FUEL ROD ARRAYS REFLECTED BY WATER WITH HETEROGENEITIES	Valduc	None used. No SCALE sample decks.
74	MIRTE PROGRAM FOUR 4.738-WT.%-ENRICHED URANIUM-DIOXIDE FUEL-ROD ARRAYS IN WATER SEPARATED BY A CROSS-SHAPED SCREEN OF TITANIUM (5 MM AND 10 MM THICK)	Valduc	Not used due to Titanium screens
75	VVER PHYSICS EXPERIMENTS: HEXAGONAL (1.10 CM PITCH) LATTICES OF LOW-ENRICHED U(6.5 WT.% 235U)O_2 FUEL RODS IN LIGHT WATER, PERTURBED BY BORON ABSORBER RODS AND WATER HOLES	Kurchatov Institute	None used due to hex arrays.

Benchmark Number	Description	Lab	Selected
76	LIGHT WATER MODERATED AND REFLECTED LOW ENRICHED URANIUM (3 WT.% 235U) DIOXIDE ROD LATTICES WITH EX-CORE DETECTOR FEATURE	Winfrith	None used. No KENO Va sample decks.
77	CRITICAL LOADING CONFIGURATIONS OF THE IPEN/MB-01 REACTOR	IPEN	Only one case used. Rest of cases same materials with small modification of arrays. Not sufficiently independent.
78	WATER-MODERATED SQUARE-PITCHED U(6.90)O2 FUEL ROD LATTICES WITH 0.52 FUEL-TO-WATER VOLUME RATIO (0.855 CM PITCH)	SNL	Not used due to high enrichment.
79	WATER-MODERATED U(4.31)O_2 FUEL ROD LATTICES CONTAINING RHODIUM FOILS	SNL	None used due to hex arrays.
80	WATER-MODERATED SQUARE-PITCHED U(6.90)O2 FUEL ROD LATTICES WITH 0.67 FUEL TO WATER VOLUME RATIO	SNL	Not used due to high enrichment.
81	PWR TYPE UO_2 FUEL RODS WITH ENRICHMENTS OF 3.5 AND 6.6 WT.% WITH BURNABLE ABSORBER ("OTTO HAHN" NUCLEAR SHIP PROGRAM, SECOND CORE)	ANEX	Single case not used. No sample SCALE deck. Unusual case.
82	CRITICAL LOADING CONFIGURATIONS OF THE IPEN/MB-01 REACTOR WITH LOW ENRICHED FUEL AND BURNABLE POISON RODS	IPEN	Used only one case. Rest of cases were not significantly different. ***Al-B_4C and Ag-In-Cd***
83	CRITICAL LOADING CONFIGURATIONS OF THE IPEN/MB-01 REACTOR WITH A BIG CENTRAL VOID	IPEN	Used only one case. Rest of cases were not significantly different. ***Ag-In-Cd***
84	CRITICAL LOADING CONFIGURATIONS OF THE IPEN/MB-01 REACTOR WITH A CENTRAL CRUCIFORM ROD	IPEN	Used the single case. ***Ag-In-Cd***
85	VVER PHYSICS EXPERIMENTS: REGULAR HEXAGONAL (1.27 CM PITCH) LATTICES OF LOW-ENRICHED U(6.5 WT.% 235U)O_2 FUEL RODS IN LIGHT WATER AT DIFFERENT CORE CRITICAL DIMENSIONS	Kurchatov Institute	None used due to hex arrays.
86	VVER PHYSICS EXPERIMENTS: HEXAGONAL LATTICES (1.275 CM PITCH) OF LOW ENRICHED U(3.6, 4.4 WT.% 235U)O_2 FUEL ASSEMBLIES IN LIGHT WATER WITH H3BO3	NRI	None used due to hex arrays.

Benchmark Number	Description	Lab	Selected
87	VVER PHYSICS EXPERIMENTS: HEXAGONAL LATTICES (1.22-CM PITCH) OF LOW-ENRICHED U(3.6, 4.4 WT.% U235)O_2 FUEL ASSEMBLIES IN LIGHT WATER WITH VARIABLE FUEL-ASSEMBLY PITCH	NRI	None used due to hex arrays.
88	CRITICAL LOADING CONFIGURATIONS OF THE IPEN/MB-01 REACTOR WITH HEAVY REFLECTORS COMPOSED OF CARBON STEEL AND NICKEL	IPEN	Not used due to no sample SCALE decks.
89	CRITICAL LOADING CONFIGURATIONS OF THE IPEN/MB-01 REACTOR WITH UO_2 AND BORATED STAINLESS STEEL PLATES	IPEN	None used due to borated plates. Case 1 not used in Surry analysis.
90	CRITICAL LOADING CONFIGURATIONS OF THE IPEN/MB-01 REACTOR WITH UO_2 AND STAINLESS STEEL RODS	IPEN	Used only one case. Rest of cases were not significantly different. ***Ag-In-Cd***
91	CRITICAL LOADING CONFIGURATIONS OF THE IPEN/MB-01 REACTOR WITH UO_2, STAINLESS STEEL AND GD2O3 RODS	IPEN	9 cases used. ***Gd_2O_3 and Ag-In-Cd***
92	CRITICAL LOADING CONFIGURATIONS OF THE IPEN/MB-01 REACTOR WITH SOLUBLE BORON	IPEN	Not used due to sufficient boron cases already and no SCALE sample input.
93	DEUTERIUM CRITICAL ASSEMBLY WITH 1.2% ENRICHED URANIUM VARYING COOLANT VOID FRACTION AND LATTICE PITCH	PNC	Not used since cases use D_2O rather than H_2O
94	VVER PHYSICS EXPERIMENTS: REGULAR HEXAGONAL (1.10 CM PITCH) TWO-REGION LATTICES OF LOW-ENRICHED U(6.5 AND 4.4 WT.% 235U)O_2 FUEL RODS IN LIGHT WATER AT DIFFERENT CORE CRITICAL DIMENSIONS	Kurchatov Institute	None used due to hex arrays.
96	PARTIALLY-REFLECTED WATER-MODERATED SQUARE-PITCHED U(6.90)O2 FUEL ROD LATTICES WITH 0.67 FUEL TO WATER VOLUME RATIO (0.800 CM PITCH)	Sandia	None. High enrichment.

Benchmark Number	Description	Lab	Selected
97	TITANIUM AND/OR ALUMINUM ROD-REPLACEMENT EXPERIMENTS IN FULLY-REFLECTED WATER-MODERATED SQUARE-PITCHED U(6.90)O2 FUEL ROD LATTICES WITH 0.67 FUEL TO WATER VOLUME RATIO (0.800 CM PITCH)	Sandia	None. High enrichment and titanium rods.

Table A.3-2: Selection Review of HTC Criticality Benchmarks

Phase	Description	Lab	Selected
1	WATER-MODERATED AND REFLECTED SIMPLE ARRAYS	Valduc	17 cases used. Case 18 excluded due to the model being inconsistent with a SFP environment.
2	REFLECTED SIMPLE ARRAYS MODERATED BY POISONED WATER WITH GADOLINIUM OR BORON	Valduc	21 cases used. No soluble gadolinia cases used. ***Soluble B 89 ppm-595 ppm***
3	POOL STORAGE	Valduc	20 cases used. Borated plate cases excluded. Borated plate cases (1 through 6) not used in Surry analysis. ***Cadmium***
4	SHIPPING CASK	Valduc	20 cases used. All lead screen cases discarded. Of the steel screen cases, no Boral or borated steel cases used. Boral and borated steel cases (1 through 13) not used in Surry analysis. ***Cadmium***

Table A.3-3: Selection Review of Additional OECD/NEA Criticality Benchmarks
(All Experiments Start With MIX-COMP-THERM-)

Benchmark Number	Description	Lab	Selected
1	WATER-REFLECTED MIXED PLUTONIUM-URANIUM OXIDE (20 wt% Pu) PINS	INL	None used due to high plutonium content
2	RECTANGULAR ARRAYS OF WATER-MODERATED UO2-2 Wt.% PuO2 (8% 240Pu) FUEL RODS	PNL	All 6 cases used. ***Soluble B 1 ppm to 1090 ppm***
3	RECTANGULAR ARRAYS OF WATER-MODERATED UO2-6.6 Wt.% PuO2 FUEL RODS	WREC	All 6 cases used.
4	CRITICAL ARRAYS OF MIXED PLUTONIUM-URANIUM FUEL RODS WITH WATER-TO-FUEL VOLUME RATIOS RANGING FROM 2.4 TO 5.6	JAERI	All 11 cases included.
5	WATER-MODERATED MIXED PLUTONIUM-URANIUM OXIDE PINS, 4.0 WT.% PuO2, 18% 240Pu, NATURAL URANIUM	PNL	All 7 cases included.
6	WATER-MODERATED MIXED OXIDE HEXAGONAL LATTICES - 2.0 WT.% PuO2, 8% 240Pu, NATURAL URANIUM	PNL	All 6 cases excluded due to hexagonal geometry. Cases run for future reference
7	HEXAGONAL LATTICES OF MIXED OXIDE FUEL PINS UO2 − 2 Wt.% PuO2 (16% 240Pu), NATURAL URANIUM	PNL	10 cases included. ***Hafnium and Boron absorber rods.***
8	HEXAGONAL LATTICES OF MIXED OXIDE FUEL PINS UO2 – 2.0 WT.% PuO2, 24% 240Pu, NATURAL URANIUM	PNL	All 11 cases included. ***Hafnium and Boron absorber rods with and without Cadmium***
9	MIXED-OXIDE FUEL-PIN LATTICE – 1.5 WT.% PuO2, 8% 240Pu, DEPLETED URANIUM	PNL	All 6 cases used. ***Depleted U***

A.4. Modeling and Calculating k of the Critical Experiments

Most of the inputs used for the KENO benchmark calculations originally came from the OECD/NEA handbook [A.3]. It was confirmed that the input decks matched the isotopic content given in the handbook. The geometric modeling in the decks also matched the descriptions in the handbook. In short, although there was considerable help by starting with the input files given in the handbook, the ownership of the files was taken, as required by NUREG/CR-6698 [A.2] and as stated in section 2.3:

For specific critical experiments, the facility or site may choose to use input files generated elsewhere to expedite the validation process. The site has the responsibility for ensuring that input files and the options selected are appropriate for use. Regardless of the source of the input file, the site must have reviewed the description of each critical experiment and determined that the representation of the experiment, including simplifying assumptions and options, are consistent with the intended use. In other words, the site must assume ownership of the input file.

The input files are modified for all cases to include an appropriate parameters block. The npg, gen, nsk, and rnd parameters are all set explicitly. All values are set for a target standard deviation less than or equal to 10 pcm. Calculations are cut off at 3 pcm using the sig parameter. Several cases did not have converged sources with the parameters used initially. In these cases, the gen and npg were modified and the case was rerun until the source had converged. Convergence is discussed in Section A.4.1.

In some special cases, the original input files did not run using SCALE 6.2.3. The following changes were made as needed in the input files.

- Void is specified as the gap material using ‘0’ in the latticecell input (i.e. gapd=1.283 0). Previously the code did not require the ‘0’ and set the gap to void by default.
- String delimiters were changed from * to single quotes.
- dan2pitch array-like input was changed (i.e. ‘centrm data dan2pitch(14)=0.15142 end centrm’ changed to ‘centrm data dan2pitch=0.15142 end centrm’. Note that the material number is not required as input to the given dancoff factor because each centrmdata specification is specific to the adjacent latticecell input.

The results and important experimental parameters for each of the cases run are given in Table A.4-1. Rows with a gray background were not included in the Surry benchmark database but

are left for future reference. Note that the "Analysis k-eff" is equal to the calculated k-eff divided by the experiment k-eff. In most but not all cases, the experiment k-eff is exactly 1.0.

Table A.4-1: Parameters and Results for Modelled Experiments

Experiment	Analysis k_{eff}	σ_{calc}	σ_{exp}	EALF (eV)	U-235 w/o	Pu w/o	Pitch (cm)	Pin (cm)	Boron (ppm)
HTC-P1-C01	0.99939	0.00007	0.00061	0.0693	1.57%	1.10%	2.300	0.950	0
HTC-P1-C02	0.99941	0.00006	0.00061	0.0664	1.57%	1.10%	2.300	0.950	0
HTC-P1-C03	0.99938	0.00006	0.00061	0.0663	1.57%	1.10%	2.300	0.950	0
HTC-P1-C04	0.99981	0.00008	0.00061	0.0848	1.57%	1.10%	1.900	0.950	0
HTC-P1-C05	0.99970	0.00007	0.00061	0.0827	1.57%	1.10%	1.900	0.950	0
HTC-P1-C06	0.99951	0.00008	0.00061	0.0820	1.57%	1.10%	1.900	0.950	0
HTC-P1-C07	0.99993	0.00008	0.00061	0.1021	1.57%	1.10%	1.700	0.950	0
HTC-P1-C08	0.99957	0.00008	0.00061	0.1006	1.57%	1.10%	1.700	0.950	0
HTC-P1-C09	0.99948	0.00007	0.00061	0.0995	1.57%	1.10%	1.700	0.950	0
HTC-P1-C10	1.00008	0.00007	0.00061	0.1403	1.57%	1.10%	1.500	0.950	0
HTC-P1-C11	0.99935	0.00008	0.00061	0.1356	1.57%	1.10%	1.500	0.950	0
HTC-P1-C12	0.99927	0.00008	0.00061	0.1337	1.57%	1.10%	1.500	0.950	0
HTC-P1-C13	0.99912	0.00008	0.00061	0.2557	1.57%	1.10%	1.300	0.950	0
HTC-P1-C14	0.99866	0.00008	0.00061	0.2335	1.57%	1.10%	1.300	0.950	0
HTC-P1-C15	0.99854	0.00008	0.00061	0.2298	1.57%	1.10%	1.300	0.950	0
HTC-P1-C16	0.99974	0.00008	0.00061	0.1013	1.57%	1.10%	1.700	0.950	0
HTC-P1-C17	0.99953	0.00007	0.00061	0.0992	1.57%	1.10%	1.700	0.950	0
HTC-P2-BOR-C01	0.99947	0.00008	0.00082	0.2467	1.57%	1.10%	1.300	0.950	100
HTC-P2-BOR-C02	0.99831	0.00007	0.00082	0.2441	1.57%	1.10%	1.300	0.950	106
HTC-P2-BOR-C03	0.99866	0.00008	0.00082	0.2547	1.57%	1.10%	1.300	0.950	205
HTC-P2-BOR-C04	0.99967	0.00008	0.00082	0.2629	1.57%	1.10%	1.300	0.950	299
HTC-P2-BOR-C05	0.99935	0.00008	0.00082	0.2738	1.57%	1.10%	1.300	0.950	400
HTC-P2-BOR-C06	0.99917	0.00008	0.00082	0.2705	1.57%	1.10%	1.300	0.950	399
HTC-P2-BOR-C07	1.00027	0.00008	0.00082	0.2790	1.57%	1.10%	1.300	0.950	486
HTC-P2-BOR-C08	0.99938	0.00007	0.00082	0.2865	1.57%	1.10%	1.300	0.950	587
HTC-P2-BOR-C09	0.99982	0.00007	0.00082	0.1661	1.57%	1.10%	1.500	0.950	595
HTC-P2-BOR-C10	0.99844	0.00007	0.00082	0.1608	1.57%	1.10%	1.500	0.950	499
HTC-P2-BOR-C11	1.00010	0.00007	0.00082	0.1564	1.57%	1.10%	1.500	0.950	393
HTC-P2-BOR-C12	1.00038	0.00007	0.00082	0.1500	1.57%	1.10%	1.500	0.950	295
HTC-P2-BOR-C13	0.99961	0.00008	0.00082	0.1453	1.57%	1.10%	1.500	0.950	200
HTC-P2-BOR-C14	1.00234	0.00008	0.00082	0.1399	1.57%	1.10%	1.500	0.950	89
HTC-P2-BOR-C15	1.00326	0.00007	0.00082	0.1030	1.57%	1.10%	1.700	0.950	90
HTC-P2-BOR-C16	1.00167	0.00007	0.00082	0.1070	1.57%	1.10%	1.700	0.950	194
HTC-P2-BOR-C17	1.00324	0.00007	0.00082	0.1103	1.57%	1.10%	1.700	0.950	286
HTC-P2-BOR-C18	0.99410	0.00007	0.00082	0.1157	1.57%	1.10%	1.700	0.950	415
HTC-P2-BOR-C19	1.00032	0.00008	0.00082	0.1046	1.57%	1.10%	1.700	0.950	100
HTC-P2-BOR-C20	0.99261	0.00006	0.00082	0.0895	1.57%	1.10%	1.900	0.950	220

Experiment	Analysis k_{eff}	σ_{calc}	σ_{exp}	EALF (eV)	U-235 w/o	Pu w/o	Pitch (cm)	Pin (cm)	Boron (ppm)
HTC-P2-BOR-C21	0.99653	0.00007	0.00082	0.0860	1.57%	1.10%	1.900	0.950	110
HTC-P3-C07	0.99633	0.00008	0.00107	0.1284	1.57%	1.10%	1.600	0.950	0
HTC-P3-C08	1.00371	0.00007	0.00145	0.1385	1.57%	1.10%	1.600	0.950	0
HTC-P3-C09	0.99659	0.00007	0.00107	0.1331	1.57%	1.10%	1.600	0.950	0
HTC-P3-C10	0.99682	0.00007	0.00107	0.1293	1.57%	1.10%	1.600	0.950	0
HTC-P3-C11	0.99624	0.00008	0.00107	0.1369	1.57%	1.10%	1.600	0.950	0
HTC-P3-C12	0.99953	0.00004	0.00085	0.1125	1.57%	1.10%	1.600	0.950	0
HTC-P3-C13	0.99945	0.00005	0.00085	0.1114	1.57%	1.10%	1.600	0.950	0
HTC-P3-C14	0.99982	0.00007	0.00085	0.1115	1.57%	1.10%	1.600	0.950	0
HTC-P3-C15	0.99941	0.00008	0.00085	0.1108	1.57%	1.10%	1.600	0.950	0
HTC-P3-C16	0.99964	0.00008	0.00085	0.1102	1.57%	1.10%	1.600	0.950	0
HTC-P3-C17	0.99952	0.00007	0.00085	0.1083	1.57%	1.10%	1.600	0.950	0
HTC-P3-C18	0.99945	0.00007	0.00085	0.1064	1.57%	1.10%	1.600	0.950	0
HTC-P3-C19	0.99984	0.00007	0.00085	0.1041	1.57%	1.10%	1.600	0.950	0
HTC-P3-C20	0.99998	0.00007	0.00085	0.1020	1.57%	1.10%	1.600	0.950	0
HTC-P3-C21	1.00003	0.00007	0.00085	0.1045	1.57%	1.10%	1.600	0.950	0
HTC-P3-C22	1.00067	0.00008	0.00085	0.1069	1.57%	1.10%	1.600	0.950	0
HTC-P3-C23	0.99996	0.00008	0.00085	0.1146	1.57%	1.10%	1.600	0.950	0
HTC-P3-C24	0.99971	0.00008	0.00085	0.1501	1.57%	1.10%	1.600	0.950	0
HTC-P3-C25	0.99978	0.00007	0.00085	0.1265	1.57%	1.10%	1.600	0.950	0
HTC-P3-C26	0.99937	0.00007	0.00085	0.1152	1.57%	1.10%	1.600	0.950	0
HTC-P4-ST-C14	1.00482	0.00007	0.00205	0.1491	1.57%	1.10%	1.600	0.950	0
HTC-P4-ST-C15	0.99827	0.00008	0.00135	0.1429	1.57%	1.10%	1.600	0.950	0
HTC-P4-ST-C16	0.99787	0.00007	0.00063	0.1365	1.57%	1.10%	1.600	0.950	0
HTC-P4-ST-C17	0.99594	0.00007	0.00063	0.1354	1.57%	1.10%	1.600	0.950	0
HTC-P4-ST-C18	0.99558	0.00007	0.00063	0.1339	1.57%	1.10%	1.600	0.950	0
HTC-P4-ST-C19	0.99529	0.00007	0.00063	0.1328	1.57%	1.10%	1.600	0.950	0
HTC-P4-ST-C20	0.99484	0.00007	0.00063	0.1320	1.57%	1.10%	1.600	0.950	0
HTC-P4-ST-C21	0.99848	0.00007	0.00079	0.1336	1.57%	1.10%	1.600	0.950	0
HTC-P4-ST-C22	1.00062	0.00007	0.00144	0.1732	1.57%	1.10%	1.600	0.950	0
HTC-P4-ST-C23	1.00046	0.00007	0.00144	0.1657	1.57%	1.10%	1.600	0.950	0
HTC-P4-ST-C24	0.99943	0.00007	0.00157	0.1578	1.57%	1.10%	1.600	0.950	0
HTC-P4-ST-C25	0.99959	0.00007	0.00157	0.1563	1.57%	1.10%	1.600	0.950	0
HTC-P4-ST-C26	0.99925	0.00007	0.00157	0.1550	1.57%	1.10%	1.600	0.950	0
HTC-P4-ST-C27	0.99897	0.00008	0.00157	0.1539	1.57%	1.10%	1.600	0.950	0
HTC-P4-ST-C28	0.99908	0.00007	0.00157	0.1527	1.57%	1.10%	1.600	0.950	0
HTC-P4-ST-C29	0.99928	0.00007	0.00157	0.1437	1.57%	1.10%	1.600	0.950	0
HTC-P4-ST-C30	0.99972	0.00007	0.00030	0.1340	1.57%	1.10%	1.600	0.950	0
HTC-P4-ST-C31	0.99948	0.00007	0.00030	0.1283	1.57%	1.10%	1.600	0.950	0
HTC-P4-ST-C32	0.99962	0.00008	0.00030	0.1249	1.57%	1.10%	1.600	0.950	0
HTC-P4-ST-C33	0.99956	0.00008	0.00030	0.1230	1.57%	1.10%	1.600	0.950	0
LEU-COMP-THERM-01-01	0.99856	0.00008	0.00300	0.0964	2.35%	0.00%	2.032	1.270	0
LEU-COMP-THERM-01-02	0.99780	0.00005	0.00300	0.0957	2.35%	0.00%	2.032	1.270	0

Experiment	Analysis k_{eff}	σ_{calc}	σ_{exp}	EALF (eV)	U-235 w/o	Pu w/o	Pitch (cm)	Pin (cm)	Boron (ppm)
LEU-COMP-THERM-01-03	0.99741	0.00006	0.00300	0.0949	2.35%	0.00%	2.032	1.270	0
LEU-COMP-THERM-01-04	0.99799	0.00008	0.00300	0.0955	2.35%	0.00%	2.032	1.270	0
LEU-COMP-THERM-01-05	0.99581	0.00007	0.00300	0.0941	2.35%	0.00%	2.032	1.270	0
LEU-COMP-THERM-01-06	0.99769	0.00007	0.00300	0.0951	2.35%	0.00%	2.032	1.270	0
LEU-COMP-THERM-01-07	0.99701	0.00008	0.00310	0.0934	2.35%	0.00%	2.032	1.270	0
LEU-COMP-THERM-01-08	0.99620	0.00006	0.00300	0.0945	2.35%	0.00%	2.032	1.270	0
LEU-COMP-THERM-02-01	0.99749	0.00008	0.00200	0.1132	4.31%	0.00%	2.540	1.415	0
LEU-COMP-THERM-02-02	0.99884	0.00009	0.00200	0.1130	4.31%	0.00%	2.540	1.415	0
LEU-COMP-THERM-02-03	0.99827	0.00008	0.00200	0.1128	4.31%	0.00%	2.540	1.415	0
LEU-COMP-THERM-02-04	0.99789	0.00006	0.00180	0.1119	4.31%	0.00%	2.540	1.415	0
LEU-COMP-THERM-02-05	0.99661	0.00008	0.00190	0.1103	4.31%	0.00%	2.540	1.415	0
LEU-COMP-THERM-06-01	0.99890	0.00008	0.00200	0.2356	2.60%	0.00%	1.849	1.417	0
LEU-COMP-THERM-06-02	0.99942	0.00008	0.00200	0.2421	2.60%	0.00%	1.849	1.417	0
LEU-COMP-THERM-06-03	0.99930	0.00008	0.00200	0.2488	2.60%	0.00%	1.849	1.417	0
LEU-COMP-THERM-06-04	0.99882	0.00008	0.00200	0.1818	2.60%	0.00%	1.956	1.417	0
LEU-COMP-THERM-06-05	0.99879	0.00008	0.00200	0.1870	2.60%	0.00%	1.956	1.417	0
LEU-COMP-THERM-06-06	0.99919	0.00008	0.00200	0.1918	2.60%	0.00%	1.956	1.417	0
LEU-COMP-THERM-06-07	0.99923	0.00008	0.00200	0.1969	2.60%	0.00%	1.956	1.417	0
LEU-COMP-THERM-06-08	0.99906	0.00008	0.00200	0.2019	2.60%	0.00%	1.956	1.417	0
LEU-COMP-THERM-06-09	0.99904	0.00008	0.00200	0.1357	2.60%	0.00%	2.150	1.417	0
LEU-COMP-THERM-06-10	0.99904	0.00008	0.00200	0.1390	2.60%	0.00%	2.150	1.417	0
LEU-COMP-THERM-06-11	0.99890	0.00008	0.00200	0.1424	2.60%	0.00%	2.150	1.417	0
LEU-COMP-THERM-06-12	0.99877	0.00008	0.00200	0.1456	2.60%	0.00%	2.150	1.417	0
LEU-COMP-THERM-06-13	0.99872	0.00008	0.00200	0.1491	2.60%	0.00%	2.150	1.417	0
LEU-COMP-THERM-06-14	0.99892	0.00008	0.00200	0.1146	2.60%	0.00%	2.293	1.417	0
LEU-COMP-THERM-06-15	0.99878	0.00008	0.00200	0.1173	2.60%	0.00%	2.293	1.417	0
LEU-COMP-THERM-06-16	0.99889	0.00008	0.00200	0.1199	2.60%	0.00%	2.293	1.417	0
LEU-COMP-THERM-06-17	0.99886	0.00008	0.00200	0.1224	2.60%	0.00%	2.293	1.417	0
LEU-COMP-THERM-06-18	0.99885	0.00008	0.00200	0.1251	2.60%	0.00%	2.293	1.417	0
LEU-COMP-THERM-07-01	0.99651	0.00008	0.00140	0.2407	4.74%	0.00%	1.260	0.940	0
LEU-COMP-THERM-07-02	0.99811	0.00009	0.00080	0.1089	4.74%	0.00%	1.600	0.940	0
LEU-COMP-THERM-07-03	0.99735	0.00008	0.00070	0.0709	4.74%	0.00%	2.100	0.940	0
LEU-COMP-THERM-07-04	0.99824	0.00007	0.00080	0.0605	4.74%	0.00%	2.520	0.940	0
LEU-COMP-THERM-08-01	0.99766	0.00006	0.00060	0.2760	2.46%	0.00%	1.636	1.206	1511
LEU-COMP-THERM-08-02	0.99822	0.00006	0.00060	0.2432	2.46%	0.00%	1.636	1.206	1334
LEU-COMP-THERM-08-03	0.99864	0.00006	0.00060	0.2431	2.46%	0.00%	1.636	1.206	1337
LEU-COMP-THERM-08-04	0.99826	0.00006	0.00060	0.2433	2.46%	0.00%	1.636	1.206	1183
LEU-COMP-THERM-08-05	0.99792	0.00006	0.00060	0.2433	2.46%	0.00%	1.636	1.206	1181
LEU-COMP-THERM-08-06	0.99842	0.00006	0.00060	0.2427	2.46%	0.00%	1.636	1.206	1034
LEU-COMP-THERM-08-07	0.99766	0.00006	0.00060	0.2429	2.46%	0.00%	1.636	1.206	1031
LEU-COMP-THERM-08-08	0.99749	0.00005	0.00060	0.2408	2.46%	0.00%	1.636	1.206	794
LEU-COMP-THERM-08-09	0.99783	0.00005	0.00060	0.2402	2.46%	0.00%	1.636	1.206	779
LEU-COMP-THERM-08-10	0.99776	0.00007	0.00060	0.2462	2.46%	0.00%	1.636	1.206	1245

Experiment	Analysis k_{eff}	σ_{calc}	σ_{exp}	EALF (eV)	U-235 w/o	Pu w/o	Pitch (cm)	Pin (cm)	Boron (ppm)
LEU-COMP-THERM-08-11	0.99854	0.00006	0.00060	0.2513	2.46%	0.00%	1.636	1.206	1384
LEU-COMP-THERM-08-12	0.99818	0.00007	0.00060	0.2452	2.46%	0.00%	1.636	1.206	1348
LEU-COMP-THERM-08-13	0.99815	0.00007	0.00060	0.2453	2.46%	0.00%	1.636	1.206	1348
LEU-COMP-THERM-08-14	0.99790	0.00006	0.00060	0.2475	2.46%	0.00%	1.636	1.206	1363
LEU-COMP-THERM-08-15	0.99770	0.00006	0.00060	0.2474	2.46%	0.00%	1.636	1.206	1362
LEU-COMP-THERM-08-16	0.99785	0.00006	0.00060	0.2252	2.46%	0.00%	1.636	1.206	1158
LEU-COMP-THERM-08-17	0.99707	0.00006	0.00060	0.1968	2.46%	0.00%	1.636	1.206	921
LEU-COMP-THERM-09-01	0.99833	0.00009	0.00210	0.1127	4.31%	0.00%	2.540	1.415	0
LEU-COMP-THERM-09-02	0.99808	0.00006	0.00210	0.1122	4.31%	0.00%	2.540	1.415	0
LEU-COMP-THERM-09-03	0.99747	0.00008	0.00210	0.1125	4.31%	0.00%	2.540	1.415	0
LEU-COMP-THERM-09-04	0.99816	0.00006	0.00210	0.1121	4.31%	0.00%	2.540	1.415	0
LEU-COMP-THERM-09-16	0.99831	0.00008	0.00210	0.1137	4.31%	0.00%	2.540	1.415	0
LEU-COMP-THERM-09-17	0.99881	0.00008	0.00210	0.1129	4.31%	0.00%	2.540	1.415	0
LEU-COMP-THERM-09-18	0.99778	0.00008	0.00210	0.1137	4.31%	0.00%	2.540	1.415	0
LEU-COMP-THERM-09-19	0.99891	0.00007	0.00210	0.1129	4.31%	0.00%	2.540	1.415	0
LEU-COMP-THERM-09-20	0.99815	0.00008	0.00210	0.1137	4.31%	0.00%	2.540	1.415	0
LEU-COMP-THERM-09-21	0.99890	0.00007	0.00210	0.1129	4.31%	0.00%	2.540	1.415	0
LEU-COMP-THERM-09-22	0.99842	0.00008	0.00210	0.1138	4.31%	0.00%	2.540	1.415	0
LEU-COMP-THERM-09-23	0.99925	0.00007	0.00210	0.1129	4.31%	0.00%	2.540	1.415	0
LEU-COMP-THERM-09-24	0.99782	0.00006	0.00210	0.1121	4.31%	0.00%	2.540	1.415	0
LEU-COMP-THERM-09-25	0.99826	0.00006	0.00210	0.1119	4.31%	0.00%	2.540	1.415	0
LEU-COMP-THERM-09-26	0.99857	0.00005	0.00210	0.1120	4.31%	0.00%	2.540	1.415	0
LEU-COMP-THERM-09-27	0.99840	0.00005	0.00210	0.1119	4.31%	0.00%	2.540	1.415	0
LEU-COMP-THERM-10-05	0.99961	0.00008	0.00210	0.3493	4.31%	0.00%	2.540	1.415	0
LEU-COMP-THERM-10-06	0.99988	0.00009	0.00210	0.2582	4.31%	0.00%	2.540	1.415	0
LEU-COMP-THERM-10-07	1.00054	0.00006	0.00210	0.2063	4.31%	0.00%	2.540	1.415	0
LEU-COMP-THERM-10-08	0.99713	0.00009	0.00210	0.1823	4.31%	0.00%	2.540	1.415	0
LEU-COMP-THERM-10-09	1.00060	0.00008	0.00210	0.1220	4.31%	0.00%	2.540	1.415	0
LEU-COMP-THERM-10-10	1.00066	0.00008	0.00210	0.1182	4.31%	0.00%	2.540	1.415	0
LEU-COMP-THERM-10-11	1.00060	0.00008	0.00210	0.1155	4.31%	0.00%	2.540	1.415	0
LEU-COMP-THERM-10-12	0.99967	0.00009	0.00210	0.1123	4.31%	0.00%	2.540	1.415	0
LEU-COMP-THERM-10-13	0.99700	0.00008	0.00210	0.1104	4.31%	0.00%	2.540	1.415	0
LEU-COMP-THERM-10-14	1.00175	0.00008	0.00280	0.3067	4.31%	0.00%	1.892	1.415	0
LEU-COMP-THERM-10-15	1.00209	0.00009	0.00280	0.2942	4.31%	0.00%	1.892	1.415	0
LEU-COMP-THERM-10-16	1.00250	0.00008	0.00280	0.2848	4.31%	0.00%	1.892	1.415	0
LEU-COMP-THERM-10-17	1.00205	0.00009	0.00280	0.2787	4.31%	0.00%	1.892	1.415	0
LEU-COMP-THERM-10-18	1.00174	0.00008	0.00280	0.2741	4.31%	0.00%	1.892	1.415	0
LEU-COMP-THERM-10-19	1.00139	0.00008	0.00280	0.2673	4.31%	0.00%	1.892	1.415	0
LEU-COMP-THERM-10-24	0.99964	0.00009	0.00280	0.5906	4.31%	0.00%	1.892	1.415	0
LEU-COMP-THERM-10-25	1.00108	0.00009	0.00280	0.5451	4.31%	0.00%	1.892	1.415	0
LEU-COMP-THERM-10-26	1.00154	0.00008	0.00280	0.5056	4.31%	0.00%	1.892	1.415	0
LEU-COMP-THERM-10-27	1.00169	0.00009	0.00280	0.4721	4.31%	0.00%	1.892	1.415	0
LEU-COMP-THERM-10-28	1.00198	0.00008	0.00280	0.4424	4.31%	0.00%	1.892	1.415	0

Experiment	Analysis k_{eff}	σ_{calc}	σ_{exp}	EALF (eV)	U-235 w/o	Pu w/o	Pitch (cm)	Pin (cm)	Boron (ppm)
LEU-COMP-THERM-10-29	1.00184	0.00008	0.00280	0.4180	4.31%	0.00%	1.892	1.415	0
LEU-COMP-THERM-10-30	0.99980	0.00009	0.00280	0.3637	4.31%	0.00%	1.892	1.415	0
LEU-COMP-THERM-11-01	0.99691	0.00008	0.00180	0.1682	2.46%	0.00%	1.636	1.206	0
LEU-COMP-THERM-11-02	0.99735	0.00007	0.00320	0.2443	2.46%	0.00%	1.636	1.206	1037
LEU-COMP-THERM-11-03	0.99769	0.00007	0.00320	0.1918	2.46%	0.00%	1.636	1.206	769
LEU-COMP-THERM-11-04	0.99800	0.00007	0.00320	0.1923	2.46%	0.00%	1.636	1.206	764
LEU-COMP-THERM-11-05	0.99769	0.00007	0.00320	0.1932	2.46%	0.00%	1.636	1.206	762
LEU-COMP-THERM-11-06	0.99767	0.00007	0.00320	0.1944	2.46%	0.00%	1.636	1.206	753
LEU-COMP-THERM-11-07	0.99776	0.00007	0.00320	0.1955	2.46%	0.00%	1.636	1.206	739
LEU-COMP-THERM-11-08	0.99791	0.00008	0.00320	0.1965	2.46%	0.00%	1.636	1.206	721
LEU-COMP-THERM-11-09	0.99783	0.00007	0.00320	0.1975	2.46%	0.00%	1.636	1.206	702
LEU-COMP-THERM-11-10	0.99502	0.00008	0.00170	0.1861	2.46%	0.00%	1.636	1.206	0
LEU-COMP-THERM-11-11	0.99442	0.00008	0.00170	0.1627	2.46%	0.00%	1.636	1.206	0
LEU-COMP-THERM-11-12	0.99490	0.00008	0.00170	0.1669	2.46%	0.00%	1.636	1.206	0
LEU-COMP-THERM-11-13	0.99530	0.00008	0.00170	0.1471	2.46%	0.00%	1.636	1.206	0
LEU-COMP-THERM-11-14	0.99503	0.00008	0.00170	0.1504	2.46%	0.00%	1.636	1.206	0
LEU-COMP-THERM-11-15	0.99589	0.00007	0.00180	0.1386	2.46%	0.00%	1.636	1.206	0
LEU-COMP-THERM-13-01	1.00046	0.00008	0.00180	0.2838	4.31%	0.00%	1.892	1.415	0
LEU-COMP-THERM-13-05	1.00010	0.00009	0.00320	0.2928	4.31%	0.00%	1.892	1.415	0
LEU-COMP-THERM-16-01	0.99758	0.00008	0.00310	0.0953	2.35%	0.00%	2.032	1.270	0
LEU-COMP-THERM-16-02	0.99625	0.00006	0.00310	0.0951	2.35%	0.00%	2.032	1.270	0
LEU-COMP-THERM-16-03	0.99728	0.00006	0.00310	0.0950	2.35%	0.00%	2.032	1.270	0
LEU-COMP-THERM-16-04	0.99627	0.00007	0.00310	0.0952	2.35%	0.00%	2.032	1.270	0
LEU-COMP-THERM-16-05	0.99719	0.00006	0.00310	0.0949	2.35%	0.00%	2.032	1.270	0
LEU-COMP-THERM-16-06	0.99712	0.00008	0.00310	0.0958	2.35%	0.00%	2.032	1.270	0
LEU-COMP-THERM-16-07	0.99735	0.00006	0.00310	0.0956	2.35%	0.00%	2.032	1.270	0
LEU-COMP-THERM-16-21	0.99803	0.00008	0.00310	0.0970	2.35%	0.00%	2.032	1.270	0
LEU-COMP-THERM-16-22	0.99780	0.00008	0.00310	0.0967	2.35%	0.00%	2.032	1.270	0
LEU-COMP-THERM-16-23	0.99783	0.00006	0.00310	0.0962	2.35%	0.00%	2.032	1.270	0
LEU-COMP-THERM-16-24	0.99737	0.00008	0.00310	0.0967	2.35%	0.00%	2.032	1.270	0
LEU-COMP-THERM-16-25	0.99763	0.00006	0.00310	0.0963	2.35%	0.00%	2.032	1.270	0
LEU-COMP-THERM-16-26	0.99802	0.00007	0.00310	0.0967	2.35%	0.00%	2.032	1.270	0
LEU-COMP-THERM-16-27	0.99768	0.00007	0.00310	0.0962	2.35%	0.00%	2.032	1.270	0
LEU-COMP-THERM-16-28	0.99728	0.00006	0.00310	0.0947	2.35%	0.00%	2.032	1.270	0
LEU-COMP-THERM-16-29	0.99699	0.00007	0.00310	0.0946	2.35%	0.00%	2.032	1.270	0
LEU-COMP-THERM-16-30	0.99684	0.00007	0.00310	0.0946	2.35%	0.00%	2.032	1.270	0
LEU-COMP-THERM-16-31	0.99763	0.00006	0.00310	0.0946	2.35%	0.00%	2.032	1.270	0
LEU-COMP-THERM-16-32	0.99745	0.00007	0.00310	0.0945	2.35%	0.00%	2.032	1.270	0
LEU-COMP-THERM-17-04	0.99797	0.00008	0.00310	0.1995	2.35%	0.00%	2.032	1.270	0
LEU-COMP-THERM-17-05	0.99933	0.00006	0.00310	0.1756	2.35%	0.00%	2.032	1.270	0
LEU-COMP-THERM-17-06	0.99939	0.00006	0.00310	0.1663	2.35%	0.00%	2.032	1.270	0
LEU-COMP-THERM-17-07	0.99929	0.00006	0.00310	0.1578	2.35%	0.00%	2.032	1.270	0
LEU-COMP-THERM-17-08	0.99725	0.00008	0.00310	0.1320	2.35%	0.00%	2.032	1.270	0

Experiment	Analysis k_{eff}	σ_{calc}	σ_{exp}	EALF (eV)	U-235 w/o	Pu w/o	Pitch (cm)	Pin (cm)	Boron (ppm)
LEU-COMP-THERM-17-09	0.99714	0.00007	0.00310	0.1085	2.35%	0.00%	2.032	1.270	0
LEU-COMP-THERM-17-10	0.99801	0.00006	0.00310	0.0997	2.35%	0.00%	2.032	1.270	0
LEU-COMP-THERM-17-11	0.99808	0.00006	0.00310	0.0979	2.35%	0.00%	2.032	1.270	0
LEU-COMP-THERM-17-12	0.99790	0.00006	0.00310	0.0967	2.35%	0.00%	2.032	1.270	0
LEU-COMP-THERM-17-13	0.99805	0.00008	0.00310	0.0952	2.35%	0.00%	2.032	1.270	0
LEU-COMP-THERM-17-14	0.99833	0.00007	0.00310	0.0946	2.35%	0.00%	2.032	1.270	0
LEU-COMP-THERM-17-15	0.99745	0.00007	0.00280	0.1772	2.35%	0.00%	1.684	1.270	0
LEU-COMP-THERM-17-16	0.99828	0.00006	0.00280	0.1710	2.35%	0.00%	1.684	1.270	0
LEU-COMP-THERM-17-17	0.99964	0.00006	0.00280	0.1662	2.35%	0.00%	1.684	1.270	0
LEU-COMP-THERM-17-18	0.99820	0.00006	0.00280	0.1647	2.35%	0.00%	1.684	1.270	0
LEU-COMP-THERM-17-19	0.99836	0.00008	0.00280	0.1620	2.35%	0.00%	1.684	1.270	0
LEU-COMP-THERM-17-20	0.99726	0.00006	0.00280	0.1605	2.35%	0.00%	1.684	1.270	0
LEU-COMP-THERM-17-21	0.99725	0.00007	0.00280	0.1591	2.35%	0.00%	1.684	1.270	0
LEU-COMP-THERM-17-22	0.99645	0.00008	0.00280	0.1580	2.35%	0.00%	1.684	1.270	0
LEU-COMP-THERM-17-26	0.99621	0.00008	0.00280	0.3679	2.35%	0.00%	1.684	1.270	0
LEU-COMP-THERM-17-27	0.99782	0.00009	0.00280	0.3157	2.35%	0.00%	1.684	1.270	0
LEU-COMP-THERM-17-28	0.99832	0.00008	0.00280	0.2769	2.35%	0.00%	1.684	1.270	0
LEU-COMP-THERM-17-29	0.99880	0.00009	0.00280	0.2476	2.35%	0.00%	1.684	1.270	0
LEU-COMP-THERM-35-01	0.99910	0.00008	0.00180	0.2076	2.60%	0.00%	1.956	1.417	70
LEU-COMP-THERM-35-02	0.99818	0.00008	0.00190	0.2113	2.60%	0.00%	1.956	1.417	148
LEU-COMP-THERM-39-01	0.99643	0.00008	0.00140	0.2218	4.74%	0.00%	1.260	0.940	0
LEU-COMP-THERM-39-02	0.99732	0.00008	0.00140	0.2115	4.74%	0.00%	1.260	0.940	0
LEU-COMP-THERM-39-03	0.99708	0.00009	0.00140	0.1920	4.74%	0.00%	1.260	0.940	0
LEU-COMP-THERM-39-04	0.99617	0.00009	0.00140	0.1837	4.74%	0.00%	1.260	0.940	0
LEU-COMP-THERM-39-05	0.99809	0.00009	0.00090	0.1392	4.74%	0.00%	1.260	0.940	0
LEU-COMP-THERM-39-06	0.99790	0.00009	0.00090	0.1453	4.74%	0.00%	1.260	0.940	0
LEU-COMP-THERM-39-07	0.99653	0.00009	0.00120	0.2127	4.74%	0.00%	1.260	0.940	0
LEU-COMP-THERM-39-08	0.99684	0.00009	0.00120	0.2028	4.74%	0.00%	1.260	0.940	0
LEU-COMP-THERM-39-09	0.99711	0.00008	0.00120	0.1975	4.74%	0.00%	1.260	0.940	0
LEU-COMP-THERM-39-10	0.99767	0.00009	0.00120	0.1728	4.74%	0.00%	1.260	0.940	0
LEU-COMP-THERM-39-11	0.99535	0.00008	0.00130	0.2216	4.74%	0.00%	1.260	0.940	0
LEU-COMP-THERM-39-12	0.99565	0.00008	0.00130	0.2164	4.74%	0.00%	1.260	0.940	0
LEU-COMP-THERM-39-13	0.99585	0.00008	0.00130	0.2139	4.74%	0.00%	1.260	0.940	0
LEU-COMP-THERM-39-14	0.99639	0.00009	0.00130	0.2122	4.74%	0.00%	1.260	0.940	0
LEU-COMP-THERM-39-15	0.99653	0.00009	0.00130	0.2109	4.74%	0.00%	1.260	0.940	0
LEU-COMP-THERM-39-16	0.99674	0.00009	0.00130	0.2100	4.74%	0.00%	1.260	0.940	0
LEU-COMP-THERM-39-17	0.99654	0.00009	0.00130	0.2097	4.74%	0.00%	1.260	0.940	0
LEU-COMP-THERM-42-01	0.99761	0.00008	0.00160	0.1688	2.35%	0.00%	1.684	1.270	0
LEU-COMP-THERM-42-05	0.99892	0.00008	0.00330	0.1769	2.35%	0.00%	1.684	1.270	0
LEU-COMP-THERM-43-01	1.00031	0.00008	0.00100	0.1521	4.35%	0.00%	1.500	0.981	0
LEU-COMP-THERM-43-02	1.00040	0.00008	0.00100	0.1552	4.35%	0.00%	1.500	0.981	0
LEU-COMP-THERM-43-03	0.99996	0.00008	0.00100	0.1551	4.35%	0.00%	1.500	0.981	0
LEU-COMP-THERM-43-04	1.00001	0.00008	0.00100	0.1524	4.35%	0.00%	1.500	0.981	0

Experiment	Analysis k_{eff}	σ_{calc}	σ_{exp}	EALF (eV)	U-235 w/o	Pu w/o	Pitch (cm)	Pin (cm)	Boron (ppm)
LEU-COMP-THERM-43-05	0.99996	0.00008	0.00100	0.1546	4.35%	0.00%	1.500	0.981	0
LEU-COMP-THERM-43-06	0.99995	0.00008	0.00100	0.1547	4.35%	0.00%	1.500	0.981	0
LEU-COMP-THERM-43-07	0.99975	0.00008	0.00100	0.1544	4.35%	0.00%	1.500	0.981	0
LEU-COMP-THERM-43-08	0.99978	0.00008	0.00100	0.1542	4.35%	0.00%	1.500	0.981	0
LEU-COMP-THERM-43-09	0.99984	0.00008	0.00100	0.1525	4.35%	0.00%	1.500	0.981	0
LEU-COMP-THERM-48-01	1.00033	0.00008	0.00250	0.6679	3.00%	0.00%	1.320	1.094	0
LEU-COMP-THERM-48-02	1.00034	0.00008	0.00250	0.6422	3.00%	0.00%	1.320	1.094	0
LEU-COMP-THERM-48-03	1.00027	0.00008	0.00250	0.6725	3.00%	0.00%	1.320	1.094	0
LEU-COMP-THERM-48-04	1.00031	0.00008	0.00250	0.6742	3.00%	0.00%	1.320	1.094	0
LEU-COMP-THERM-48-05	1.00042	0.00008	0.00250	0.6640	3.00%	0.00%	1.320	1.094	0
LEU-COMP-THERM-50-01	0.99817	0.00009	0.00100	0.1994	4.74%	0.00%	1.300	0.940	0
LEU-COMP-THERM-50-02	0.99795	0.00009	0.00100	0.1905	4.74%	0.00%	1.300	0.940	0
LEU-COMP-THERM-50-03	0.99854	0.00008	0.00100	0.2070	4.74%	0.00%	1.300	0.940	822
LEU-COMP-THERM-50-04	0.99783	0.00009	0.00100	0.1976	4.74%	0.00%	1.300	0.940	822
LEU-COMP-THERM-50-05	0.99923	0.00009	0.00100	0.2222	4.74%	0.00%	1.300	0.940	5030
LEU-COMP-THERM-50-06	0.99928	0.00008	0.00100	0.2138	4.74%	0.00%	1.300	0.940	5030
LEU-COMP-THERM-50-07	0.99926	0.00009	0.00100	0.2093	4.74%	0.00%	1.300	0.940	5030
LEU-COMP-THERM-51-01	0.99743	0.00007	0.00200	0.1471	2.46%	0.00%	1.636	1.206	143
LEU-COMP-THERM-51-02	0.99862	0.00008	0.00240	0.1964	2.46%	0.00%	1.636	1.206	510
LEU-COMP-THERM-51-03	0.99852	0.00007	0.00240	0.1961	2.46%	0.00%	1.636	1.206	514
LEU-COMP-THERM-51-04	0.99834	0.00007	0.00240	0.1976	2.46%	0.00%	1.636	1.206	501
LEU-COMP-THERM-51-05	0.99841	0.00008	0.00240	0.1982	2.46%	0.00%	1.636	1.206	493
LEU-COMP-THERM-51-06	0.99833	0.00007	0.00240	0.1995	2.46%	0.00%	1.636	1.206	474
LEU-COMP-THERM-51-07	0.99776	0.00007	0.00240	0.2000	2.46%	0.00%	1.636	1.206	462
LEU-COMP-THERM-51-08	0.99829	0.00008	0.00240	0.2008	2.46%	0.00%	1.636	1.206	432
LEU-COMP-THERM-51-09	0.99765	0.00008	0.00190	0.1668	2.46%	0.00%	1.636	1.206	217
LEU-COMP-THERM-54-01	0.99971	0.00008	0.00050	0.1509	4.35%	0.00%	1.500	0.981	0
LEU-COMP-THERM-54-02	0.99961	0.00008	0.00050	0.1505	4.35%	0.00%	1.500	0.981	0
LEU-COMP-THERM-54-03	0.99960	0.00007	0.00050	0.1507	4.35%	0.00%	1.500	0.981	0
LEU-COMP-THERM-54-04	0.99933	0.00009	0.00050	0.1508	4.35%	0.00%	1.500	0.981	0
LEU-COMP-THERM-54-05	0.99940	0.00008	0.00050	0.1517	4.35%	0.00%	1.500	0.981	0
LEU-COMP-THERM-54-06	0.99949	0.00008	0.00050	0.1515	4.35%	0.00%	1.500	0.981	0
LEU-COMP-THERM-54-07	0.99924	0.00008	0.00050	0.1517	4.35%	0.00%	1.500	0.981	0
LEU-COMP-THERM-54-08	0.99934	0.00008	0.00050	0.1517	4.35%	0.00%	1.500	0.981	0
LEU-COMP-THERM-58-01	0.99941	0.00008	0.00050	0.1523	4.35%	0.00%	1.500	0.981	0
LEU-COMP-THERM-58-02	0.99909	0.00008	0.00050	0.1523	4.35%	0.00%	1.500	0.981	0
LEU-COMP-THERM-58-03	0.99917	0.00008	0.00050	0.1525	4.35%	0.00%	1.500	0.981	0
LEU-COMP-THERM-58-04	0.99921	0.00008	0.00050	0.1528	4.35%	0.00%	1.500	0.981	0
LEU-COMP-THERM-58-05	0.99913	0.00008	0.00050	0.1534	4.35%	0.00%	1.500	0.981	0
LEU-COMP-THERM-58-06	0.99919	0.00008	0.00050	0.1537	4.35%	0.00%	1.500	0.981	0
LEU-COMP-THERM-58-07	0.99951	0.00008	0.00050	0.1491	4.35%	0.00%	1.500	0.981	0
LEU-COMP-THERM-58-08	0.99899	0.00008	0.00050	0.1500	4.35%	0.00%	1.500	0.981	0
LEU-COMP-THERM-58-09	0.99933	0.00008	0.00050	0.1504	4.35%	0.00%	1.500	0.981	0

Experiment	Analysis k_{eff}	σ_{calc}	σ_{exp}	EALF (eV)	U-235 w/o	Pu w/o	Pitch (cm)	Pin (cm)	Boron (ppm)
LEU-COMP-THERM-71-01	0.99660	0.00009	0.00070	0.7515	4.74%	0.00%	1.100	0.949	0
LEU-COMP-THERM-71-02	0.99632	0.00008	0.00070	0.6904	4.74%	0.00%	1.100	0.949	0
LEU-COMP-THERM-71-03	0.99577	0.00008	0.00070	0.6550	4.74%	0.00%	1.100	0.949	0
LEU-COMP-THERM-71-04	0.99561	0.00008	0.00060	0.8419	4.74%	0.00%	1.075	0.949	0
LEU-COMP-THERM-72-01	0.99824	0.00009	0.00120	0.1101	4.74%	0.00%	1.600	0.949	0
LEU-COMP-THERM-72-02	0.99763	0.00009	0.00120	0.1062	4.74%	0.00%	1.600	0.949	0
LEU-COMP-THERM-72-03	0.99814	0.00009	0.00120	0.1085	4.74%	0.00%	1.600	0.949	0
LEU-COMP-THERM-77-03	1.00125	0.00008	0.00100	0.1620	4.35%	0.00%	1.500	0.980	0
LEU-COMP-THERM-82-03	1.00090	0.00008	0.00100	0.1497	4.35%	0.00%	1.500	0.980	0
LEU-COMP-THERM-83-01	1.00066	0.00008	0.00100	0.1514	4.35%	0.00%	1.500	0.980	0
LEU-COMP-THERM-84-01	1.00061	0.00008	0.00100	0.1541	4.35%	0.00%	1.500	0.980	0
LEU-COMP-THERM-90-01	0.99972	0.00008	0.00100	0.1461	4.35%	0.00%	1.500	0.980	0
LEU-COMP-THERM-91-01	0.99968	0.00008	0.00100	0.1487	4.35%	0.00%	1.500	0.981	0
LEU-COMP-THERM-91-02	0.99982	0.00008	0.00100	0.1518	4.35%	0.00%	1.500	0.981	0
LEU-COMP-THERM-91-03	1.00013	0.00008	0.00100	0.1505	4.35%	0.00%	1.500	0.981	0
LEU-COMP-THERM-91-04	0.99947	0.00008	0.00100	0.1508	4.35%	0.00%	1.500	0.981	0
LEU-COMP-THERM-91-05	0.99954	0.00008	0.00100	0.1501	4.35%	0.00%	1.500	0.981	0
LEU-COMP-THERM-91-06	0.99947	0.00008	0.00100	0.1318	4.35%	0.00%	1.500	0.981	0
LEU-COMP-THERM-91-07	0.99623	0.00008	0.00100	0.1323	4.35%	0.00%	1.500	0.981	0
LEU-COMP-THERM-91-08	0.99689	0.00008	0.00100	0.1313	4.35%	0.00%	1.500	0.981	0
LEU-COMP-THERM-91-09	0.99683	0.00008	0.00100	0.1309	4.35%	0.00%	1.500	0.981	0
MIX-COMP-THERM-02-02	1.00088	0.00008	0.00590	0.7137	0.71%	2.00%	1.778	1.435	2
MIX-COMP-THERM-02-01	1.00093	0.00008	0.00450	0.5373	0.71%	2.00%	1.778	1.435	688
MIX-COMP-THERM-02-04	1.00453	0.00007	0.00287	0.2699	0.71%	2.00%	2.210	1.435	1
MIX-COMP-THERM-02-03	1.00274	0.00008	0.00206	0.1847	0.71%	2.00%	2.210	1.435	1090
MIX-COMP-THERM-02-06	1.00321	0.00007	0.00224	0.1765	0.71%	2.00%	2.515	1.435	2
MIX-COMP-THERM-02-05	1.00484	0.00008	0.00241	0.1331	0.71%	2.00%	2.515	1.435	767
MIX-COMP-THERM-07-01	1.00353	0.00008	0.00350	0.1898	0.72%	2.00%	2.362	1.283	0
MIX-COMP-THERM-07-06	0.99686	0.00008	0.00390	0.1364	0.72%	2.00%	2.667	1.283	0
MIX-COMP-THERM-07-02	0.99893	0.00008	0.00390	0.1374	0.72%	2.00%	2.667	1.283	0
MIX-COMP-THERM-07-07	0.99400	0.00008	0.00390	0.1377	0.72%	2.00%	2.667	1.283	0
MIX-COMP-THERM-07-08	0.99506	0.00008	0.00390	0.1376	0.72%	2.00%	2.667	1.283	0
MIX-COMP-THERM-07-09	0.99564	0.00008	0.00390	0.1372	0.72%	2.00%	2.667	1.283	0
MIX-COMP-THERM-07-10	0.99638	0.00008	0.00390	0.1368	0.72%	2.00%	2.667	1.283	0
MIX-COMP-THERM-07-03	1.00107	0.00008	0.00460	0.1164	0.72%	2.00%	2.903	1.283	0
MIX-COMP-THERM-07-04	1.00023	0.00007	0.00570	0.0952	0.72%	2.00%	3.353	1.283	0
MIX-COMP-THERM-07-05	0.99867	0.00007	0.00610	0.0904	0.72%	2.00%	3.520	1.283	0
MIX-COMP-THERM-08-01	0.99767	0.00008	0.00320	0.3761	0.72%	2.00%	2.032	1.435	0
MIX-COMP-THERM-08-02	0.99878	0.00008	0.00300	0.1917	0.72%	2.00%	2.362	1.435	0
MIX-COMP-THERM-08-03	0.99873	0.00008	0.00380	0.1381	0.72%	2.00%	2.667	1.435	0
MIX-COMP-THERM-08-04	1.00183	0.00007	0.00470	0.1169	0.72%	2.00%	2.903	1.435	0
MIX-COMP-THERM-08-05	1.00234	0.00007	0.00560	0.0954	0.72%	2.00%	3.353	1.435	0
MIX-COMP-THERM-08-06	1.00208	0.00007	0.00650	0.0904	0.72%	2.00%	3.520	1.435	0

Experiment	Analysis k_{eff}	σ_{calc}	σ_{exp}	EALF (eV)	U-235 w/o	Pu w/o	Pitch (cm)	Pin (cm)	Boron (ppm)
MIX-COMP-THERM-08-07	0.99902	0.00007	0.00390	0.1373	0.72%	2.00%	2.667	1.435	0
MIX-COMP-THERM-08-08	0.99507	0.00008	0.00390	0.1383	0.72%	2.00%	2.667	1.435	0
MIX-COMP-THERM-08-10	0.99637	0.00007	0.00390	0.1379	0.72%	2.00%	2.667	1.435	0
MIX-COMP-THERM-08-09	0.99613	0.00007	0.00390	0.1381	0.72%	2.00%	2.667	1.435	0
MIX-COMP-THERM-08-11	0.99632	0.00007	0.00390	0.1375	0.72%	2.00%	2.667	1.435	0
MIX-COMP-THERM-09-01	0.99946	0.00008	0.00540	0.5135	0.16%	1.50%	1.397	1.077	0
MIX-COMP-THERM-09-02	0.99600	0.00008	0.00490	0.2931	0.16%	1.50%	1.524	1.077	0
MIX-COMP-THERM-09-03	0.99700	0.00007	0.00500	0.1526	0.16%	1.50%	1.803	1.077	0
MIX-COMP-THERM-09-04	0.99649	0.00008	0.00620	0.1152	0.16%	1.50%	2.032	1.077	0
MIX-COMP-THERM-09-05	0.99828	0.00007	0.00740	0.0947	0.16%	1.50%	2.286	1.077	0
MIX-COMP-THERM-09-06	1.00011	0.00007	0.00800	0.0904	0.16%	1.50%	2.362	1.077	0

A.4.1 Convergence Criteria

As with any Monte Carlo methodology, the determination of convergence is dependent on the code user and is typically done by experience. SCALE 6.2.3 includes new features compared with previous code versions to aide in the determination of convergence. Ultimately, convergence is determined in this analysis by three factors:

1. The calculated standard deviation should be comparable to or smaller than the experimental uncertainty. In the calculations generated for this analysis, the Monte Carlo standard deviation is 10 pcm or less. In most experiments the referenced experimental uncertainty exceeds 200 pcm. No experimental uncertainty is less than 30 pcm. By trial and error, it was found that 9000 generations and 12000 particles per generation, at a minimum, will achieve this standard deviation for the criticality benchmark experiments.
2. The generated k-eff distribution, within a given KENO calculation, satisfies the chi squared test for normality at the 95% level. By the central limit theorem, the sampled mean of a data set will tend toward a normal distribution after a sufficient number of samples. Failure of the chi square test would indicate that the mean and standard deviation are generated from some off-normal distribution and may change with further samples.
3. The three internal SCALE fission source convergence checks pass. For more information on these tests, see Section 8.1.6.7 of the SCALE manual.

In Monte Carlo cases, there is the potential for rare events that are under sampled but of high importance to exist within the problem (i.e. k-eff of the world problem). The convergence criteria above would not necessarily identify this issue. However, the k-eff plots can be inspected for anomalous events in the k-eff by generation (or alternatively the k-eff by generations skipped) edits in the KENO output. All KENO cases will be inspected for the following anomalous changes that occur in the last half of the generations:

1. Standard deviation change in a single generation compared with the previous 20 that is greater than the final problem standard deviation
2. Change in average k-eff in a single generation that exceeds the average k-eff over previous 20 generations by more than two standard deviations
3. Change in average k-eff from one generation to the next that exceeds two standard deviations
4. The midpoint k-eff (accounting for generations skipped) is within 2 final problem standard deviations from the final problem k-eff

Failing one of these criteria will trigger further evaluation of the output for anomalous under-sampled events and potentially require a revised source distribution.

A.5. Statistical Analysis of the Data

The statistical treatment used follows the guidance provided in NUREG/CR-6698 [A.2]. The NUREG approach weights the calculated k's by the experimental uncertainty. This approach means the higher quality experiments (i.e.: lower uncertainty) affect the results more than the low quality experiments. The uncertainty weighting is used for the analysis of the set of experiments as a whole, as well as for the analysis for trends.

Spent fuel goes from having little plutonium to having about 1.5 wt% plutonium at discharge burnups. Since the bias is not the same for plutonium critical experiments as it is for uranium critical experiments, the bias would be expected to be a function of burnup. Rather than attempt to make the bias a function of burnup, analysis of the UO2 and MOX critical experiments are separated and the most limiting bias and uncertainty from the two sets will be used in the analysis of the spent fuel pool. The fresh fuel storage uses only the UO2 critical experiments.

A.5.1 Statistical Analysis of the UO2 Critical Experiments

This section follows closely NUREG/CR-6698 so in order to help matching with the NUREG the equation numbers from the NUREG are given in parentheses.

The first step of the analysis is force all the experiments to be critical so the analysis is consistent over the entire set. This is done by converting supercritical experiments to critical experiments using the following equation (9). This was already done in Table A.4-1.

$$k_{norm} = k_{calc} / k_{exp}$$

Normality Tests

To meet NUREG/CR-6698 normality testing requirements, the QQ plots and histogram distributions can be inspected for obvious departures from normality. However, several numerical tests also exist. The Shapiro-Wilk test is suggested in NUREG/CR-6698. However, the Anderson-Darling test is also commonly used. A third test is the Jarque-Bera test. Each of these tests were applied to the UO2 data set.

The Anderson-Darling test and the Jarque-Bera test are described in [A.9]. The Royston Method was used for the Shapiro-Wilk test because NUREG/CR-6698's method was only applicable for sample sizes below 50 ($n \leq 50$). These three tests are described in [A.10], [A.11], and [A.12].

The UO_2-only database passes all three normality tests described above at the 95% confidence level. (Note that the null hypothesis for all normality tests is that the data is normal. So the failure to reject the null hypothesis means that there is not enough evidence to say that the data is not normal.) The results of the tests are given in Table A.5.1-1. Additionally, a qualitative visual examination of the histogram (Figure A.5.1-1) and the Q-Q plot (Figure A.5.1-2) does not show any obvious indication of non-normal behavior, trend, or skewness. Given no obvious non-normal behavior with the histogram and Q-Q plot and passing the normal distribution tests, a normal distribution assumption is acceptable. Notice that the calculated k's are a little closer to the mean and a little higher (conservative) than expected in a normal distribution. This means assuming a normal distribution may be conservative for this data.

Table A.5.1-1: Normality Tests, UO2 Only Database

Shapiro-Wilk (Royston Method)		**Jarque-Bera**	
		Skew	0.178323
n	238	Excess Kurtosis	0.175553
u	0.065	JB	1.567
m	234.464	p-value	**0.45681**
e	237.358	alpha	**0.05**
asq	1	reject	**no**
Test Statistic			
W	0.992		
mean	-5.157	**Anderson-Darling**	
stdev	0.431	A^2	0.580
z	0.678	A*^2	0.589
p-value	**0.24901**	p-value	**0.12445**
alpha	**0.05**	alpha	**0.05**
reject	**no**	reject	**no**

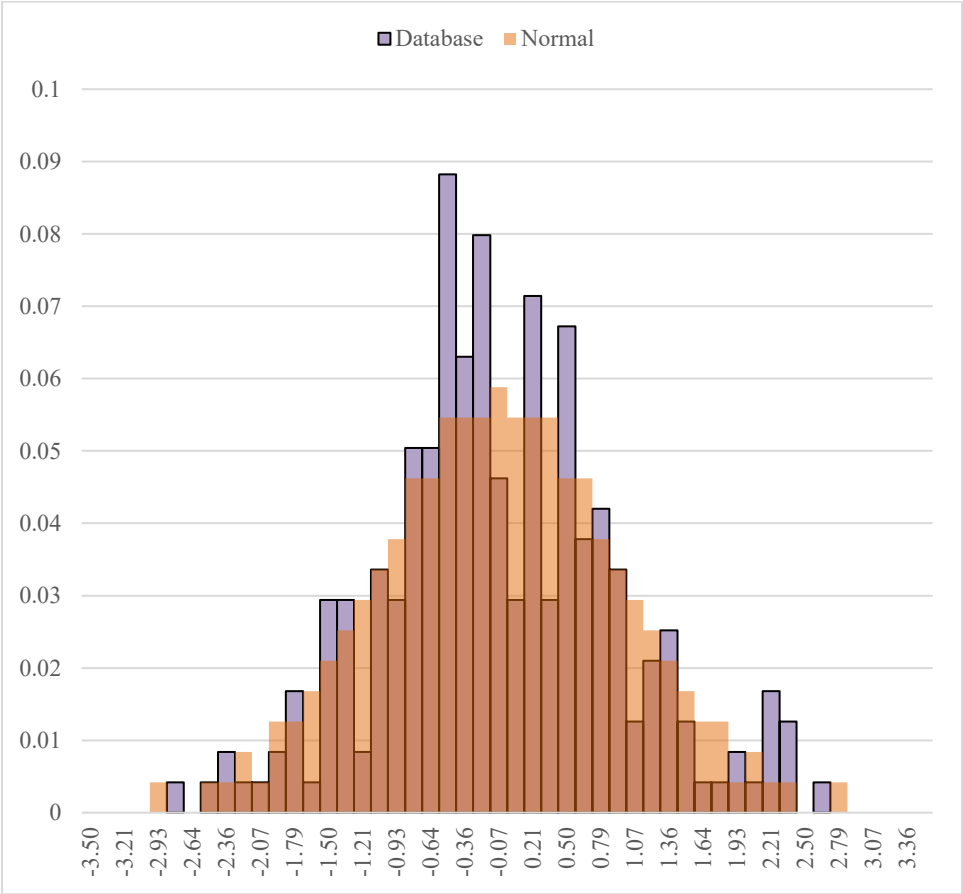

Figure A.5.1-1: Histogram of the Calculated k's, UO2 Only Benchmarks

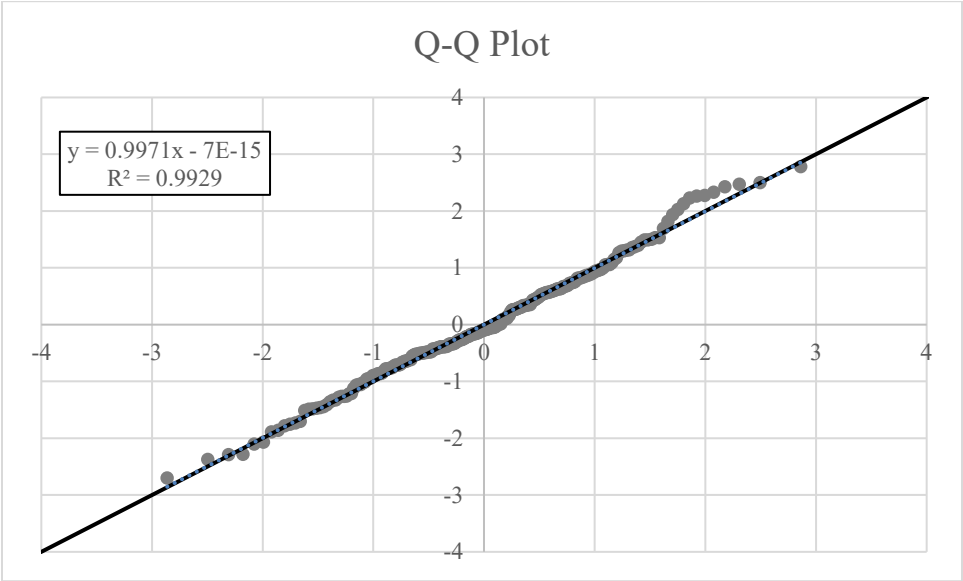

Figure A.5.1-2: Q-Q Normality Plot, UO2 Only Benchmarks

Weighted Uncertainty Analysis

NUREG/CR-6698 recommends weighting the data by its uncertainty (NUREG/CR-6698 equations shown in parentheses). The combined error for each experimented is calculated (3):

$$\sigma_t = \sqrt{\sigma_{calc}^2 + \sigma_{exp}^2}$$

The weighted mean keff (6):

$$\bar{k}_{eff} = \frac{\sum \frac{1}{\sigma_i^2} k_{eff,i}}{\sum \frac{1}{\sigma_i^2}}$$

The bias is calculated as follows (8):

$Bias = \bar{k}_{eff} - 1$; the bias is set to zero if calculated to be greater than zero.

The variance about the mean (4):

$$s^2 = \frac{\frac{1}{n-1} \sum \left\{ \frac{1}{\sigma_i^2} \left[k_{eff,i} - \bar{k}_{eff} \right]^2 \right\}}{\frac{1}{n} \sum \frac{1}{\sigma_i^2}}$$

The average total uncertainty (5):

$$\bar{\sigma}^2 = \frac{n}{\sum \frac{1}{\sigma_i^2}}$$

The square root of the pooled variance (7):

$$S_p = \sqrt{s^2 + \bar{\sigma}^2}$$

The uncertainty is calculated by multiplying the square root of the pooled variance by the one-sided lower tolerance factor. Since the analysis has a sample size greater than 50, 2.065 is used as the single-sided lower tolerance factor. This analysis is summarized in Table A.5.1-2.

Table A.5.1-2: One-Sided Tolerance Limit Analysis, UO_2 Only Database

Sample Size	238
$\bar{k}_{eff}$	0.998536
Bias	**0.001464**
s^2	1.517×10^{-6}
$\bar{\sigma}^2$	1.211×10^{-6}
U	2.065
S_P	0.001652
Uncertainty	**0.003411**

Trend Analysis

The next step in the analysis is to look for trends in the data. In the past it was assumed that unless there is a high confidence level (95%) that the slope was non-zero, the analysis would assume a zero slope (no trend) on the given parameter. The analysis will include consideration of the data as non-trended, however it is more conservative to assume there is a trend. Inverting the statistical test to requiring a high confidence that the slope is zero will result in all cases having a trend. At this time, although a test on the confidence of the trend is performed, the analysis assumes all calculated trends are real.

Trends can be established using the tolerance band described in NUREG/CR-6698 [A.2]. An evaluation of the dependence of the data on EALF and enrichment is required per industry guidance. In addition, pin pitch, pin diameter (D_{pin}), and soluble boron concentration are also evaluated for this data set. A summary of these calculations is given in Table A.5.1-3.

Table A.5.1-3: Trend Analysis, UO_2 Database Only

p	0.95
$F_a^{(fit,n-2)}$	3.034
Z_{2p-1}	1.645
γ	0.025
$\chi^2_{1-\gamma,n-2}$	195.3

	EALF <0.40 eV	EALF <0.80 eV	EALF <1.10 eV	EALF <1.25 eV	EALF <1.40 eV	U_{235} wt%	Pitch (cm)	D_{pin} (cm)	Boron (ppm)
Δ	6.72E+14	6.72E+14	6.72E+14	6.72E+14	6.72E+14	3.40E+12	3.02E+15	8.17E+14	2.33E+22
a	0.99937	0.99937	0.99937	0.99937	0.99937	0.997330	0.997734	0.999653	0.998603
b	-0.0041	-0.0041	-0.0041	-0.0041	-0.0041	0.03168	0.00051	-0.00104	-1.79E-07
xbar	0.2057	0.2057	0.2057	0.2057	0.2057	0.0381	1.580	1.074	375.7
r^2	0.190	0.190	0.190	0.190	0.190	5.85E-02	0.0134	0.0152	0.0128
x_{min}	**0.00**	**0.40**	**0.80**	**1.10**	**1.25**	**1.85%**	**1.43**	**1.072**	**0**
x_{max}	**0.40**	**0.80**	**1.10**	**1.25**	**1.40**	**5.00%**	**1.43**	**1.077**	**2300**
$k_{fit}(x_{min})$	0.9994	0.9977	0.9961	0.9949	0.9943	0.99792	0.99846	0.99854	0.99860
$k_{fit}(x_{max})$	0.9977	0.9961	0.9949	0.9943	0.9937	0.99891	0.99846	0.99853	0.99819
s^2-fit	1.23E-06	1.23E-06	1.23E-06	1.23E-06	1.23E-06	1.60E-06	1.57E-06	1.55E-06	1.56E-06
$S_{p,fit}$-fit	0.00156	0.00156	0.00156	0.00156	0.00156	0.00168	0.00167	0.00166	0.00167
Uncert.(x_{min})	0.0033	0.0033	0.0040	0.0045	0.0048	0.0035	0.0033	0.0033	0.0033
Uncert.(x_{max})	0.0033	0.0040	0.0045	0.0048	0.0051	0.0034	0.0033	0.0033	0.0037
Bias	**0.0023**	**0.0039**	**0.0051**	**0.0057**	**0.0063**	**0.0021**	**0.0015**	**0.0015**	**0.0018**
Uncertainty	**0.0033**	**0.0040**	**0.0045**	**0.0048**	**0.0051**	**0.0035**	**0.0033**	**0.0033**	**0.0037**

The width of the tolerance band is a function of the trending parameter. When the value for the independent variable is known, it is used in the calculation of the uncertainty. For simplicity sometimes the maximum width of the tolerance band over the range of data is taken as the uncertainty.

In the final analysis, the calculated k of the system must be less than the minimum of k(x) minus the uncertainty minus the administrative safety margin. The uncertainty in k from other independent uncertainties, such as the manufacturing tolerances, burnup, and depletion uncertainties can be statistically combined with the uncertainty in the criticality validation.

Neutron Spectrum Trend

From Table A.5.1-3, it's clear that the most limiting and significant trend is EALF. The data from the EALF trend analysis has been further analyzed using truncated upper limits on the EALF of 0.4 eV, 0.8 eV, 1.1 eV, 1.25 eV, and 1.40 eV. The overall bias and uncertainty will be a function of the EALF for the case. Table A.5.1-4 summarizes the bias and uncertainty as a function of EALF for the fresh fuel database.

Table A.5.1-4: Bias and Uncertainty versus EALF, UO_2 Database Only

EALF	Bias	Uncertainty
0.00 – 0.40 eV	0.0030	0.0040
0.40 – 0.80 eV	0.0040	0.0045
0.80 – 1.10 eV	0.0055	0.0050
1.10 – 1.25 eV	0.0060	0.0050
1.25 – 1.40 eV	0.0065	0.0055

Note that the primary EALF trend analysis in Table A.5.1-3 is extrapolated past the upper bound listed in Table A.5.1-5 from 0.84 eV to 1.40 eV to encompass the optimum moderation scenario of the New Fuel Storage Area (NFSA) analysis. NUREG/CR-6698 Section 5 is a short discussion about extending the area of applicability. Its recommendations are (1) run more experiments to cover the range of applicability, or (2) justify an extension to the area of applicability. For commercial power plant applications, the high EALF is needed for the UO_2-only analysis because of the NFSA optimum moderation accident. There are no UO_2, fresh water moderated experiments which result in EALF's this high. Therefore, the first option from NUREG/CR-6698 is non-viable. However, analytically extending the area of applicability can be justified.

Two graphs were examined to determine the acceptability of this extrapolation. Figure A.5.1-3 shows a scatter plot of the Analysis k-eff's with Excel's best estimate regression line (dotted line) and NUREG/CR-6698's conservative regression line (solid line). The slope of the conservative regression line is much more negative than the BE line which means that the bias will become larger as EALF is extrapolated. Similarly, uncertainty increases as EALF is extrapolated. Figure A.5.1-4 shows this bias and uncertainty trend as EALF increases. NUREG/CR-6698, Section 5 [2] states "… the margin due to extension of the area of applicability may already be accounted for in the determination of bias. For example, use of the tolerance band (described in Section 2.4.4) and confidence band techniques accounts for uncertainty in extrapolation of the quantified parameters." Figure's A.5.1-3 and A.5.1-4 show that the method in which these values were calculated adequately cover the extrapolation up to 1.40 eV.

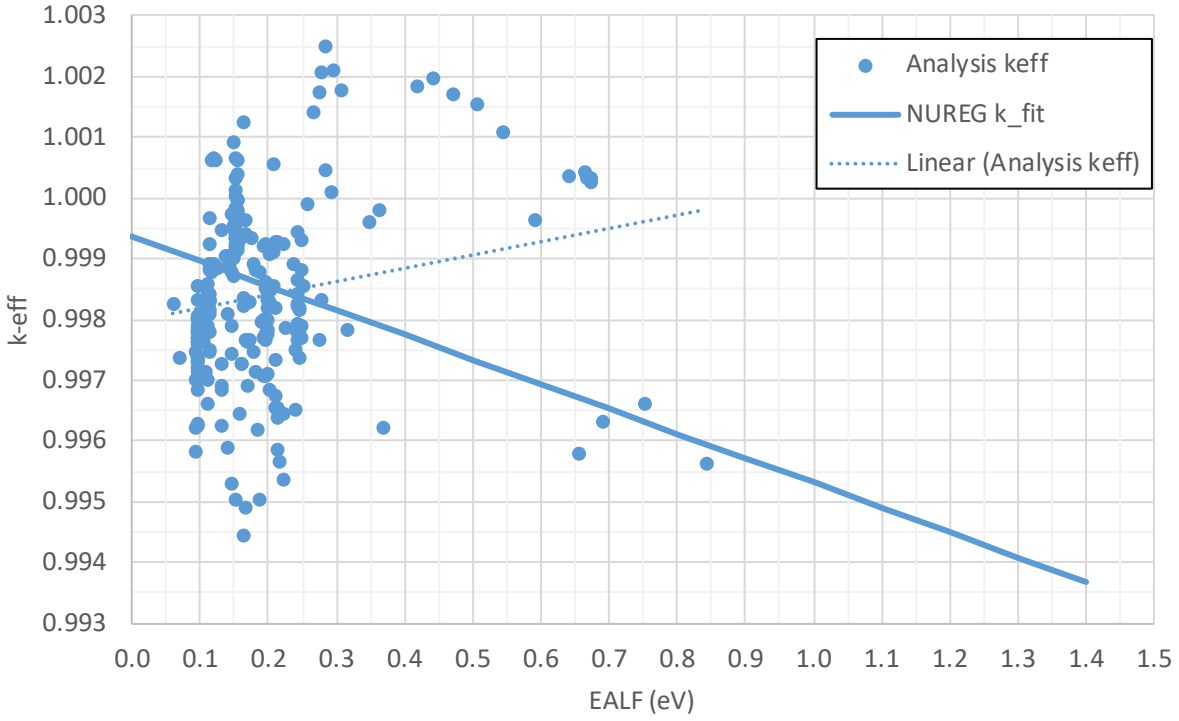

Figure A.5.1-3: Regression Analysis of Analysis k-eff's – UO_2 Database Only

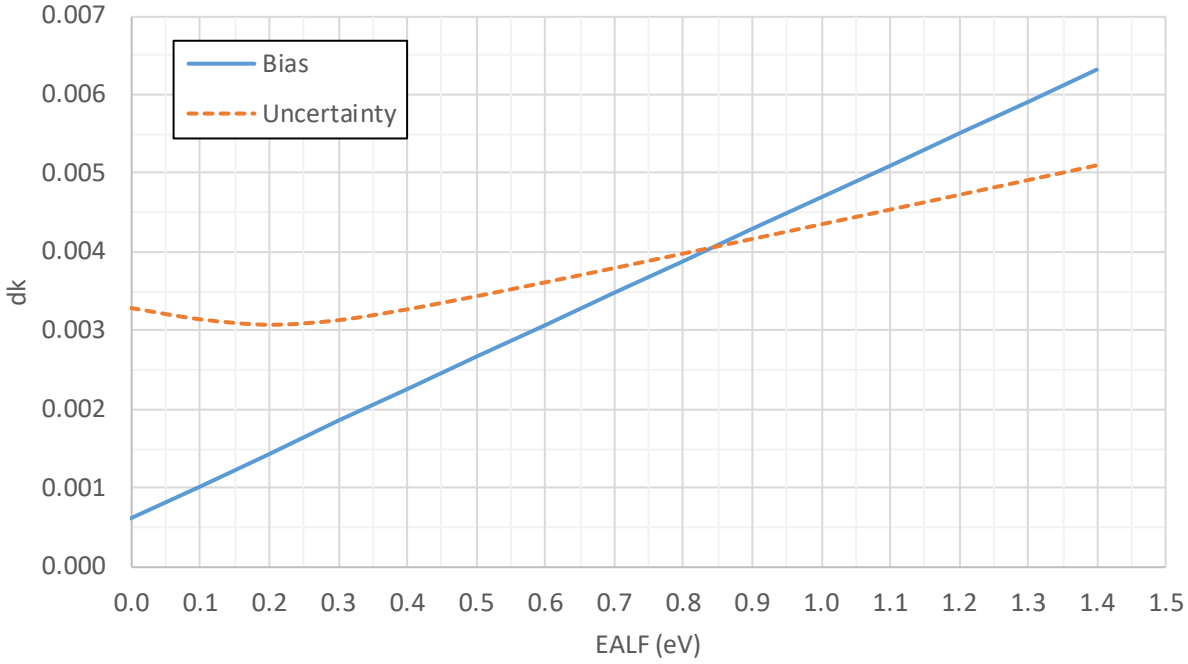

Figure A.5.1-4: Bias and Uncertainty Trend with EALF – UO_2 Database Only

Geometry, Enrichment, and Soluble Boron Trends

The other trends displayed in Table A.5.1-3 (U-235 wt%, pitch, pin diameter, and soluble boron) will not be used to determine the bias and uncertainty because they are statistically less significant and because they are less conservative than the EALF trend.

Table A.5.1-3 shows that the r^2 value for the EALF trend is 0.19 while the r^2 values for the other trend parameters are all <0.02. This means that EALF is more strongly correlated with the code bias and uncertainty.

Additionally, the large and negative slope of the EALF trend means that the resulting code bias will be larger than the other parameters. The bias is calculated by subtracting the trend line value from a value of 1.00. A bigger slope means the beginning or end of the trend line will be further below 1 which results in a larger bias. Table A.5.1-3 shows the calculated bias and uncertainty for each trend. The U-235 wt%, pitch, pin diameter, and soluble boron trends all result in lower biases and uncertainties that are roughly equal to the lowest EALF uncertainty.

Previous SCALE benchmarking analyses support only using the EALF trend to calculate the bias and uncertainty. Millstone Unit 3 had a very similar benchmarking analysis [A.13] that used the same codes and cross section library: CSAS5 of SCALE and ENDF/B-VII.0. The only difference is a code version change where the Millstone Unit 3 analysis used SCALE 6.0 and this analysis is using SCALE 6.2.3. The trend statistics and trend figures for EALF, U-235 wt%, pitch, pin diameter, and soluble boron in [A.13] shows that the EALF trend should be used to calculate the bias and uncertainty.

Establishing the Bias and the Uncertainty

Table A.5.1-4 summarizes the bias and uncertainty as a function of EALF for the fresh fuel database. As stated above, EALF has the most statistically significant trend and results in the largest bias and uncertainties. This bias and uncertainty is conservative for the entire parameter space.

Table A.5.1-4: Bias and Uncertainty versus EALF, UO_2 Database Only (Repeated from above)

EALF	Bias	Uncertainty
0.00 – 0.40 eV	0.0030	0.0040
0.40 – 0.80 eV	0.0040	0.0045
0.80 – 1.10 eV	0.0055	0.0050
1.10 – 1.25 eV	0.0060	0.0050
1.25 – 1.40 eV	0.0065	0.0055

Note also that there is no data between boron concentrations of 1511 ppm and 5030 ppm. This makes it suspect to extend the bounds of the database to 5030 ppm. However due to the strong trend in EALF, it is not expected that extension of the Boron past 1511 ppm to 2300 ppm would impact the results. This is because increased boron increases the EALF which trends with higher bias and uncertainty values. Note also that the data point at 5030 ppm shows low bias indicating that extrapolating the trend with increased boron is conservative. All other parameter ranges in Table A.5.1-3 are bounded by the ranges in Table A.5-1-5.

Table A.5.1-5: Database Bounds for Trended Parameters, UO_2 Database Only

Parameter	Min	Max
EALF	0.0605	0.8419
U235 wt%	2.35%	4.74%
Pitch (cm)	1.075	2.540
Diam. (cm)	0.940	1.417
Boron (ppm)	0	2300

A.5.2 Statistical Analysis of MOX Critical Experiments

The same process as in Section A.5.1 will be used except the MOX database will be used instead of the UO_2 only database.

Normality Tests

The three normality tests were run on using the MOX-only database. Details for these tests can be found in the equivalent subsection in Section A.5.1. The MOX-only database does not pass two of the tests at the 95% confidence level. (Note that the null hypothesis for all normality tests is that the data is normal. So, the failure to reject the null hypothesis means that there is not enough evidence to say that the data is not normal.) The results of the tests are given in Table A.5.2-1.

A qualitative visual examination of the histogram (Figure A.5.2-1) and the Q-Q plot (Figure A.5.2-2) shows a strong tendency for data to cluster toward the mean. For this reason, it is conservative to assume a normal distribution for this analysis because the normal distribution will give larger confidence intervals. Note that this was how the MOX-only database was handled for the SCALE 6.0 benchmarking analysis for Millstone Unit 3 [A.13].

Table A.5.2-1: Normality Tests, MOX Only Database

Shapiro-Wilk (Royston Method)		**Jarque-Bera**	
n	111	Skew	-0.103
u	0.095	Excess Kurtosis	0.681
m	107.826	JB	2.342
e	109.565	p-value	**0.310**
asq	1	alpha	**0.05**
		reject	**no**
Test Statistic			
W	0.947		
mean	-4.501	**Anderson-Darling**	
stdev	0.448	A^2	3.011
z	3.471	A*^2	3.113
p-value	**0.00026**	p-value	**<0.0001**
alpha	**0.05**	alpha	**0.05**
reject	**yes**	reject	**yes**

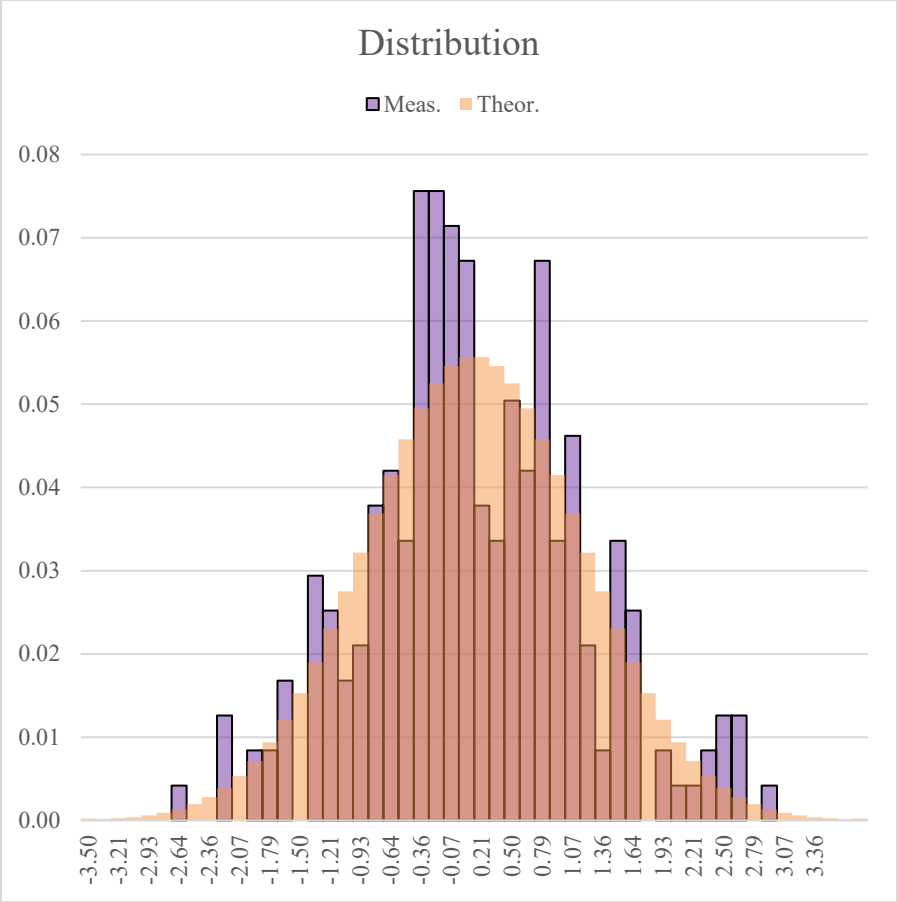

Figure A.5.2-1: Histogram of the Calculated k's, MOX Only Benchmarks

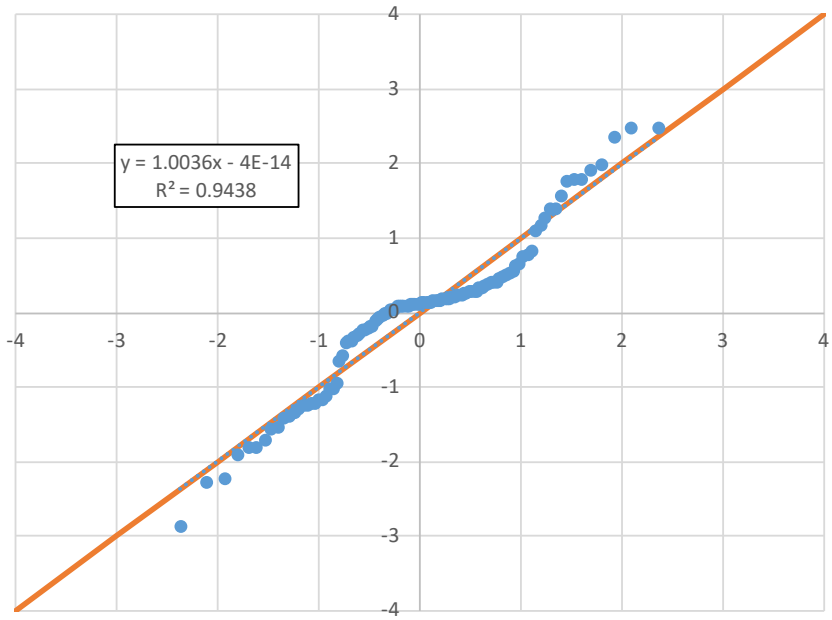

Figure A.5.2-2: Q-Q Normality Plot, MOX Only Benchmarks

Weighted Uncertainty Analysis

NUREG/CR-6698 recommends weighting the data by its uncertainty (NUREG/CR-6698 equations shown in parentheses). Details for these method can be found in the equivalent subsection in Section A.5.1.

A one-sided tolerance limit was calculated for the MOX only database. The uncertainty is calculated by multiplying the square root of the pooled variance by the one-sided lower tolerance factor. Since the analysis has a sample size greater than 50, 2.065 is used as the single-sided lower tolerance factor. This analysis is summarized in Table A.5.2-2.

Table A.5.2-2: One-Sided Tolerance Limit Analysis, MOX Only Database

Sample Size	111
$\overline{k}_{eff}$	0.99919
Bias	**0.000812**
s^2	2.734E-06
$\overline{\sigma}^2$	6.816E-07
U	2.065
S_P	0.00185
Uncertainty	**0.003816**

Trend Analysis

The next step in the analysis is to look for trends in the data. In the past it was assumed that unless there is a high confidence level (95%) that the slope was non-zero, the analysis would assume a zero slope (no trend) on the given parameter. The analysis will include consideration of the data as non-trended, however it is more conservative to assume there is a trend. Inverting the statistical test to requiring a high confidence that the slope is zero will result in all cases having a trend. At this time, although a test on the confidence of the trend is performed, the analysis assumes all calculated trends are real.

Trends can be established using the tolerance band described in NUREG/CR-6698 [A.2]. An evaluation of the dependence of the data on EALF and enrichment is required per industry guidance. In addition, pin pitch, pin diameter (D_{pin}), Total Plutonium wt%, and soluble boron concentration are also evaluated for this data set. A summary of these calculations is given in Table A.5.2-3.

Table A.5.2-3: Trend Analysis, MOX Database Only

p	0.95
$F_a^{(fit,n-2)}$	3.064
Z_{2p-1}	1.645
γ	0.025
$\chi^2_{1-\gamma,n-2}$	103.0

	EALF <0.40 eV	EALF <0.80 eV	EALF <1.10 eV	EALF <1.25 eV	EALF <1.40 eV	Pu wt%	Pitch (cm)	D_{pin} (cm)	Boron (ppm)
Δ	6.99E+13	6.99E+13	6.99E+13	6.99E+13	6.99E+13	2.77E+10	1.45E+15	6.80E+13	5.34E+20
a	0.99928	0.99928	0.99928	0.99928	0.99928	0.99817	0.99912	0.99695	0.99916
b	-0.0019*	-0.0019*	-0.0019*	-0.0019*	-0.0019*	0.0918	0.0000	0.0023	0.0000
xbar	0.1362	0.1362	0.1362	0.1362	0.1362	0.0111	1.6324	0.9558	57.5678
r^2	0.000	0.000	0.000	0.000	0.000	0.003	0.000	0.005	0.002
x_{min}	0.00	0.40	0.80	1.10	1.25	0.00%	1.30	1.072	0
x_{max}	0.40	0.80	1.10	1.25	1.40	2.00%	1.43	1.077	2300
$k_{fit}(x_{min})$	0.9993	0.9985	0.9977	0.9972	0.9969	0.9982	0.9992	0.9995	0.9992
$k_{fit}(x_{max})$	0.9985	0.9977	0.9972	0.9969	0.9966	1.0000	0.9992	0.9995	1.0004
s^2-fit	2.76E-06	2.76E-06	2.76E-06	2.76E-06	2.76E-06	2.75E-06	2.76E-06	2.74E-06	2.75E-06
$S_{p,fit}$-fit	0.00185	0.00185	0.00185	0.00185	0.00185	0.00185	0.00185	0.00185	0.00185
Uncert.(x_{min})	0.0048	0.0058	0.0092	0.0117	0.0130	0.0083	0.0043	0.0046	0.0040
Uncert.(x_{max})	0.0058	0.0092	0.0117	0.0130	0.0143	0.0073	0.0041	0.0046	0.0104
Bias	**0.0015**	**0.0023**	**0.0028**	**0.0031**	**0.0034**	**0.0018**	**0.0008**	**0.0005**	**0.0008**
Uncertainty	**0.0058**	**0.0092**	**0.0117**	**0.0130**	**0.0143**	**0.0083**	**0.0043**	**0.0046**	**0.0104**

*The slope of the EALF columns were conservatively tripled. See below for a justification.

Note that U-235 is not part of the trend analysis in Table A.5.2-3. A U-235 trend analysis would be based on a small range of enrichments that is far below the enrichments that will be used in the downstream analyses. The small enrichment range would lead to extrapolation errors when applied to high enrichments.

The width of the tolerance band is a function of the trending parameter. When the value for the independent variable is known, it is used in the calculation of the uncertainty. For simplicity sometimes the maximum width of the tolerance band over the range of data is taken as the uncertainty.

In the final analysis, the calculated k of the system must be less than the minimum of k(x) minus the uncertainty minus the administrative safety margin. The uncertainty in k from other independent uncertainties, such as the manufacturing tolerances, burnup, and depletion uncertainties can be statistically combined with the uncertainty in the criticality validation.

Neutron Spectrum Trend

From Table A.5.2-3, it's clear that the most limiting and significant trend is EALF. The bias and uncertainty dependence on EALF bounds the dependence of the other variables. The data from the EALF trend analysis has been further analyzed using truncated upper limits on the EALF of 0.4 eV, 0.8 eV, 1.1 eV, 1.25 eV and 1.40 eV. The overall bias and uncertainty will be a function of the EALF for the case. Table A.5.2-4 summarizes the bias and uncertainty as a function of EALF for the MOX fuel database.

Table A.5.2-4: Bias and Uncertainty versus EALF, MOX Database Only

EALF	Bias	Uncertainty
0.00 – 0.40 eV	0.0015	0.0060
0.40 – 0.80 eV	0.0025	0.0095
0.80 – 1.10 eV	0.0030	0.0120
1.10 – 1.25 eV	0.0035	0.0135
1.25 – 1.40 eV	0.0035	0.0145

Note that the EALF range from the experimental database had a maximum of 0.71 eV. However, the cask drop accident analysis requires biases and uncertainties for EALFs up to 1.40 eV due to the high burnup, high soluble boron, and small pin pitch. Therefore, the bias and uncertainty must be extrapolated from the experimental range.

NUREG/CR-6698 Section 5 is a short discussion about extending the area of applicability. Its recommendations are (1) run more experiments to cover the range of applicability, or (2) justify an extension to the area of applicability. For Surry's applications, the extremely high EALF is needed for the MOX only analysis because of the cask drop accident where the assembly and pin pitches are reduced to optimal distances using burned fuel and borated water. There are no MOX experiments which are water moderated, representative of commercial power plant burned fuel, and results in EALFs this high. Therefore, the first option from NUREG/CR-6698 is non-viable. However, analytically extending the area of applicability can be justified.

Figure A.5.2-3 shows difference between the conservative nature of NUREG/CR-6698's regression line (solid line) verses Excel's best estimate regression line (dotted line). Like the UO_2 only analysis, the slope of the conservative NUREG regression line is less than the best estimate line. However, the MOX analysis needs to extrapolate a larger range than the UO_2 analysis. In addition, the optimum pin pitch in the cask drop accident analysis (~1.29 cm) is right around the lower limit of the database bounds (1.30 cm). Therefore, the slope of the line

will be tripled to ensure that the bias is conservative (shown as the dashed line in Figure A.5.2-3).

Figure A.5.2-4 shows the bias trend relative to EALF. It also shows that the uncertainty of the bias increases as EALF is extrapolated away from the center of the data. As stated in the previous UO_2 only sub-section, NUREG/CR-6698 states that this conservative method of calculation can be enough to justify the extrapolation. Therefore, since the bias is being increased, no further adjustment to the uncertainty is needed for the extrapolation.

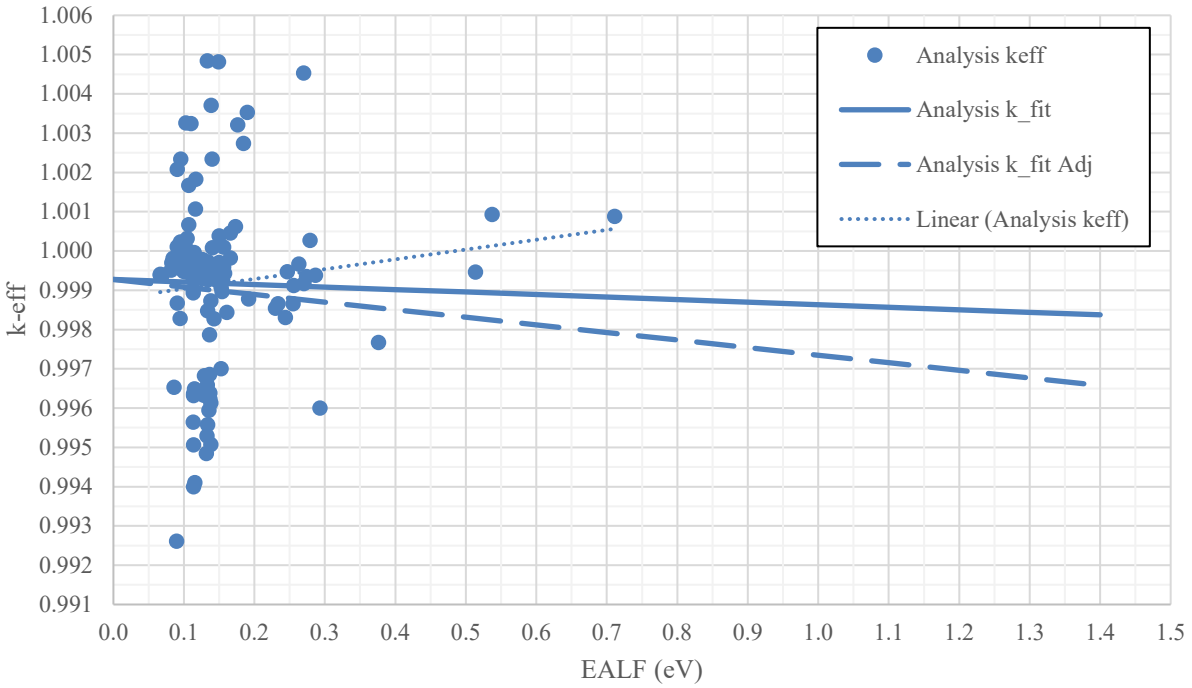

Figure A.5.2-3: Regression Analysis of Analysis k-eff's – MOX Database Only

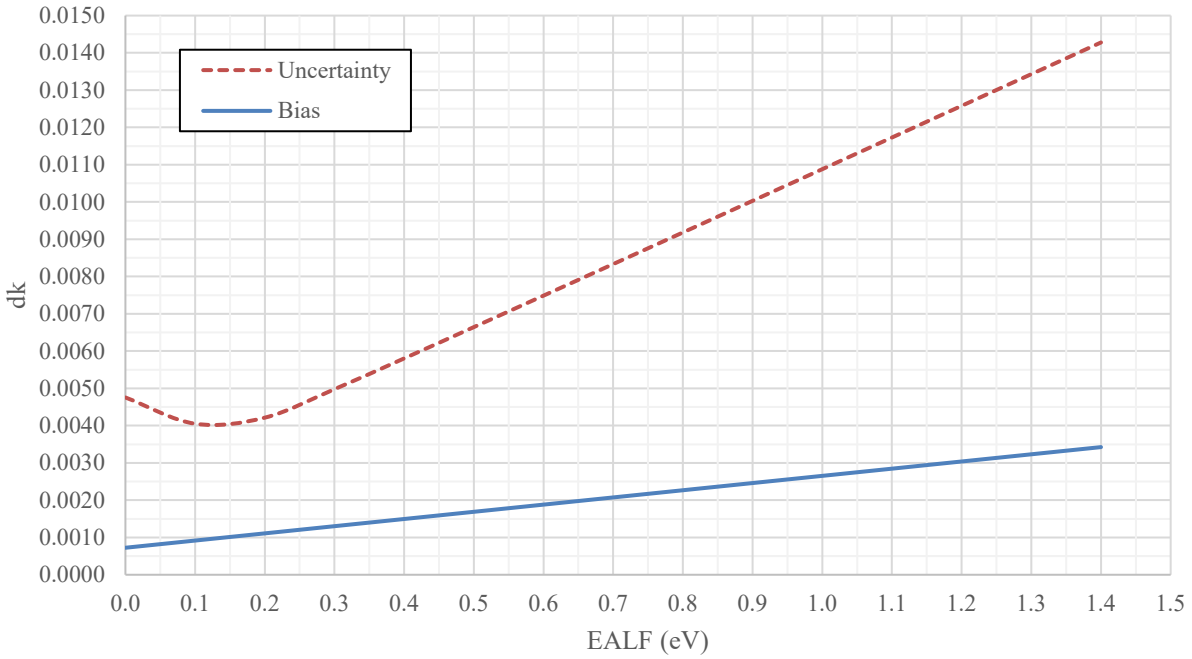

Figure A.5.1-4: Bias and Uncertainty Trend with EALF – MOX Database Only

Plutonium, Geometry, and Soluble Boron Trends

The other trends displayed in Table A.5.2-3 (Pu wt%, pitch, pin diameter, and soluble boron) will not be used to determine the bias and uncertainty because they are less conservative than the EALF trend.

The large and negative slope of the EALF trend means that the resulting code bias will be larger than the other parameters. The bias is calculated by subtracting the trend line value from a value of 1.00. A bigger slope means the beginning or end of the trend line will be further below 1 which results in a larger bias. Table A.5.2-3 shows the calculated bias and uncertainty for each trend. The Pu wt%, pitch, pin diameter, and soluble boron trends all result in lower biases and uncertainties that are roughly equal to the lowest EALF bias and uncertainty.

Previous SCALE benchmarking analyses support only using the EALF trend to calculate the bias and uncertainty for the MOX only database. Millstone Unit 3 had a very similar benchmarking analysis [A.13] that used the same codes and cross section library: CSAS5 of SCALE and ENDF/B-VII.0. The only difference is a code version change where the Millstone Unit 3 analysis used SCALE 6.0 and this analysis is using SCALE 6.2.3. The trend statistics and trend figures for EALF, U-235 wt%, pitch, pin diameter, and soluble boron in [A.13] shows that the EALF trend should be used to calculate the bias and uncertainty.

Establishing the Bias and the Uncertainty

Table A.5.2-4 summarizes the bias and uncertainty as a function of EALF for the MOX fuel database. As stated above, EALF results in the largest bias and uncertainties. This bias and uncertainty are conservative for the entire parameter space.

Table A.5.2-4: Bias and Uncertainty versus EALF, MOX Database Only (Repeated from above)

EALF	Bias	Uncertainty
0.00 – 0.40 eV	0.0015	0.0060
0.40 – 0.80 eV	0.0025	0.0095
0.80 – 1.10 eV	0.0030	0.0120
1.10 – 1.25 eV	0.0035	0.0135
1.25 – 1.40 eV	0.0035	0.0145

Table A.5.2-5 gives the database bounds for each of the trended parameters. As discussed in the previous subsection, the EALF trend was extrapolated from the data. Also, the Boron concentration is extrapolated from 1090 ppm to 2300 ppm. All other parameter ranges in Table A.5.2-3 are bounded by the ranges in Table A.5.2-5. The Plutonium concentration for spent fuel pool calculations is not expected to exceed 1.5%. Extrapolation for this parameter would however be conservative based on the positive trend in the bias. Due to the larger and more conservative trend in EALF, it is not expected that extrapolation of the boron past the database range has impacted the overall bias and uncertainty.

Table A.5.2-5: Database Bounds for Trended Parameters, MOX Database Only

Parameter	Min	Max
EALF	0.0663	0.7113
Pitch (cm)	1.300	3.52
Diam. (cm)	0.950	1.435
Boron (ppm)	0	1090
Pu wt%	1.10%	2.00%

A.5.3 Subcritical Margin

In the USA, the NRC has established subcritical margins for rack analysis. The subcritical margin for borated spent fuel pools, casks, and fully flooded dry storage racks is 0 when the analysis is performed with unborated water. This is actually saying the subcritical margin is contained in the uncredited soluble boron. To make sure there is sufficient soluble boron, analysis is also performed with soluble boron and a subcritical margin of 5% in k is required. For dry storage racks analyzed with optimum moderation, the subcritical margin is 2% and 5% with optimum and full moderation, respectively. In the analysis of 238 critical UO_2 experiments, which generously cover the range of expected conditions, the lowest calculated k was 0.9944. The additional 111 MOX experiments also support this subcritical margin since the lowest calculated k is 0.9926. The subcritical margin is more than sufficient.

A.6. Temperature Bias

All of the critical experiments used thus far have been at room temperature. There could be a bias in k in the temperature range of interest to spent fuel pools and dry storage racks (0 to 100 C). There is one critical benchmark evaluation in the OECD/NEA handbook [A.3] that performed measurements with elevated temperatures in this range, LEU-COMP-THERM-046 (shortened to LCT-046). LCT-046 consists of 22 experiments but the last 5 experiments contain copper rods. Since copper is not in North Anna's spent fuel pool only the first 17 experiments are analyzed.

Two sets of LCT-46 cases were run. A set that used best-estimate thermal expansion for the fuel and structural materials and a set that only applied a density change to the moderator. Both sets were rerun. The cases were run and are confirmed to have converged based on the criteria discussed in Section A.4.1.

Table A.6-1 presents the resulting raw k-eff values calculated from the two sets of cases. The results of the two sets are within two standard deviations of each other for all except case 14. All cases are within three standard deviations. Therefore, as in the previous benchmarking analyses [A.13], ignoring thermal expansion is negligible compared with the statistical uncertainty of the methodology. However, It is appropriate to model thermal expansion for the determination of temperature bias as this most accurately represents the experimental configurations. Therefore, all analyses for calculating temperature bias will include the effect of thermal expansion of the structural and fuel materials.

Table A.6-1: SCALE Results for LCT-46 Temperature Dependence Benchmark Calculations

Case	Temperature (K)	Thermal Expansion SCALE k-eff	No Thermal Expansion SCALE k-eff	Uncertainty (pcm)	Absolute Difference k-eff (pcm)
1	297.05	0.999679	0.999725	8.1	4.6
2	310.41	0.999857	0.999758	7.8	9.9
3	315.43	0.999696	0.999635	7.9	6.1
4	319.96	0.999785	0.999796	7.9	1.1
5	324.93	0.999589	0.999524	7.6	6.5
6	332.53	0.999750	0.999794	7.6	4.4
7	287.22	1.000069	1.000069	7.8	0.0
8	315.91	0.999755	0.999624	7.5	13.1
9	330.27	0.999763	0.999690	7.8	7.3
10	337.44	0.999574	0.999600	7.9	2.6
11	351.99	0.999749	0.999648	7.7	10.1
12	303.6	0.999559	0.999558	7.9	0.1
13	312.95	0.999606	0.999487	7.8	11.9
14	321.16	0.999616	0.999414	7.8	20.2
15	328.24	0.999527	0.999370	7.7	15.7
16	338.26	0.999363	0.999344	7.9	1.9
17	358.31	0.999354	0.999232	8.0	12.2

The k-eff values from Table A.6-1 are corrected for high experimental k-eff (k_{calc}/k_{exp}) and regression is applied to the corrected data set. The results are plotted in Figure A.6-1. The least-squares linear fit is given in the figure. The slope is -0.528 pcm/K and the intercept is 1.00098. Note that all cases have a very similar total uncertainty (combination of experimental and calculated uncertainty). Therefore, the regression analysis does not need to be weighted for uncertainty like the cases in Section A.5.

As stated above, Table A.6-1 shows that the difference between modeling high temperature cases with and without thermal expansion is relatively small with a dk of ~0.0001. Therefore, downstream high temperature analyses do not need to model thermal expansion.

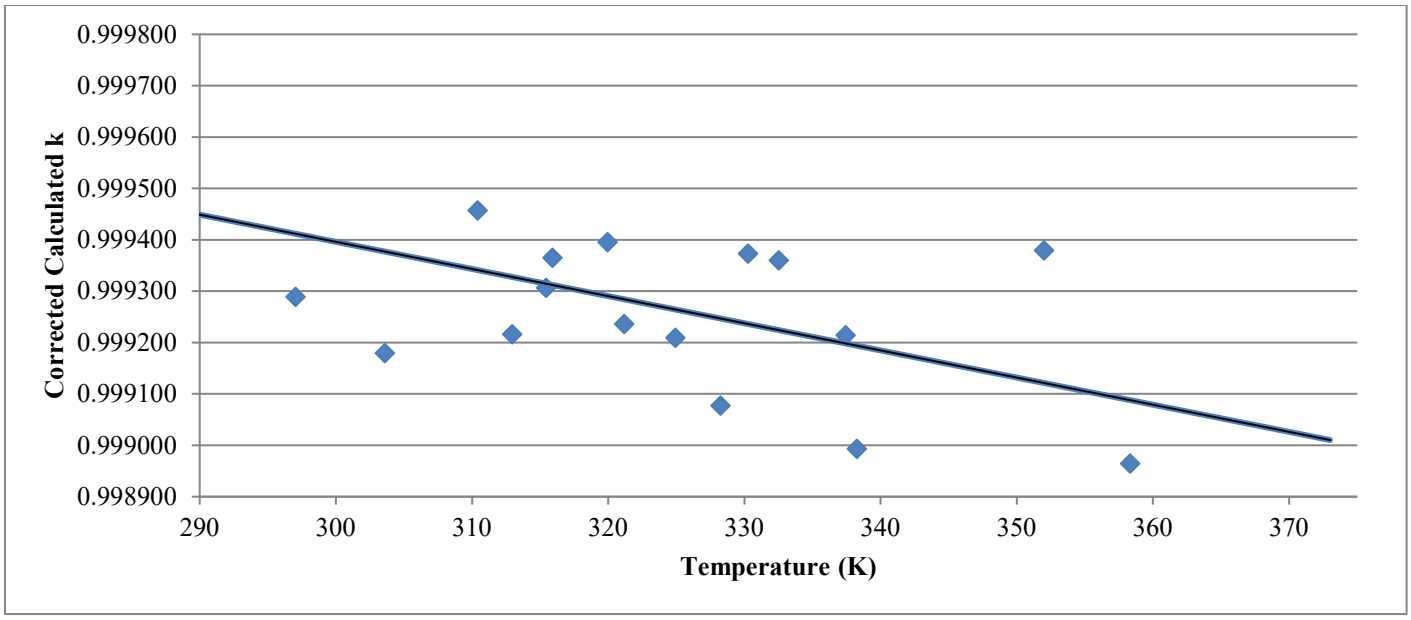

Figure A.6-1: LCT-46 k-eff versus Temperature with Least Squares Fit

The slope is of interest in downstream analyses. Since the criticality database is entirely comprised of cases at cold temperatures (nominally 293 K), the temperature bias is calculated as the slope times the maximum deviation at in-rack conditions from 293 K. To obtain this slope with 95% confidence, the uncertainty is calculated using an unweighted confidence band analysis. The resulting slope is -0.961 pcm/K. This is conservatively round to -1.0 pcm/K for downstream analyses.

A.7. Area of Applicability (Benchmark Applicability)

The critical benchmarks selected cover both the new fuel storage area and the spent fuel pool of Surry. To summarize the range of the benchmark applicability (or area of applicability), Table A.7-1 is provided below.

Table A.7-1: Area of Applicability (Benchmark Applicability)

Parameter	Range	Comments
Fissionable Material/Physical Form	UO_2 – fresh fuel MOX – burned fuel	The fuel material is the same as in the benchmark experiments
Isotopic Composition (wt%)	Fresh UO_2 – **1.35% - 5.0%** Burned UO_2 - **<5.0% initial enrichment**	*See Discussion points 1 and 2, next page*
Spectrum - EALF (eV)	Fresh UO_2 – 0.0605 eV to 1.25 eV Burned UO_2 – 0.0663 eV to 1.25 eV	Experiments cover an EALF of 0.06 – 0.85 eV. This range covers the expected range in spent fuel pool applications of 0.1 to 0.8 eV except for the optimum moderation accident in new fuel racks. The EALF of this scenario may be as high as 1.25 eV. Some extrapolation of the data is performed in a conservative manner.
Lattice Characteristics Type Pin Pitch (cm) Rod Diameter (cm)	 Square MOX - 1.30 to 4.32 UO_2 - 1.08 to 2.54 MOX - 0.95 to 1.43 UO_2 - 0.94 to 1.41	Hex lattices have been excluded except for some MOX cases. Surry 15x15 pin pitch is 1.43. Surry rod diameter varies from 1.072 cm to 1.077 cm.
Assembly Spacing in Racks Distance between Assemblies (cm)	0 to 15.4	*See Discussion point 3.*
Soluble Absorbers Concentration	≤ 2300 ppm	*See Discussion point 4.*
Non-Soluble Absorbers Materials	Discrete Cd Absorber Gad Abosrber Boron Absorber	Gad and Boron non-soluble absorbers is adequately covered in the benchmarks
Reflectors Materials	Water Concrete Steel	Most racks are reflected by water, steel, and concrete which was covered in the set of experiments.
Fuel Storage Racks Materials	Steel	Steel racks were adequately covered in the benchmarks
Temperature	273 K to 408 K	Most experiments are done at room temperature (293K). LCT 46 covers temperatures up to 358 K. NRC allows up to ±50 K extrapolation for temperatures in this range (Ref. 13). The lower bound is set to 273 since no ice experiments were analyzed.
Moderating material	Water	The moderator in all benchmark experiments is water, therefore water as a moderating material is covered

The following discussion points supplement Table A.6-1

1. Table 2.3 of NUREG/CR-6698 [A.2] provides for experimental ranges for enrichment applicatiblity for fissile materials. For weight fractions between 0% to 2%, an experimental

range of ±1% is allowed while for weight fractions of 2% to 5%, an experimental range of ±1.5% is allowed. Experiments in Table A.5.1-3 range in enrichment from 2.35 wt% to 4.74 wt% U-235. Intermediate enrichments include 2.6 wt%, 3.0 wt%, and 4.4 wt% among others. This shows that, within the tolerances specified by the NRC, enrichments between 1.35% and 6.24% are allowed. The upper range is truncated at 5.0 wt% U-235. Also, there are no significant gaps between enrichments.

2. Burned fuel is comprised of mixed oxide fuel. For burned fuel, the Surry depletion results from Appendix B were used as a basis for the foregoing discussion. The isotopics was retrieved from the Benchmark runs and were inspected. By NRC guidelines, fissile materials below 0.5 wt% may be neglected for the purposes of AOA analysis [A.2]. Pu-240 and Pu-241 never exceed this threshold. However, total Plutonium content does reach 0.5 wt% at a burnup of approximately 10 GWd/MT. At this point, the total Plutonium increases to at most 1.5 wt% of total fissionable material. The uranium content in this fuel varies between 0.25 wt% to 3.10 wt%.
3. The U-235 concentration for MOX fuel extends down to 0.16 wt% for this fuel type up to 1.57 wt%. With an NRC allowed range of ±1.5 wt%, the database range extends between 0 wt% to 3.07 wt% U-235. The total Plutonium content ranges from 1.5 wt% to 6.6 wt%. With an NRC allowed range of ±1 wt%, the database range extends between 0.5 wt% PU to well beyond 2.0 wt%. Since below 0.5 wt% is considered negligible, all anticipated ranges of Plutonium are covered by the database. Also, the expected U-235 concentration at depletion levels where Plutonium is considered non-negligible for fuel initially loaded up to 5.0 wt% U-235 is also covered by the database with a negligible amount of extrapolation.
4. The 0 to 15.4 cm spacing range covers all spacing for racks. Neutron transport through larger than 15.4 cm has a small effect on k. Note that the spacing is assumed to be filled with full density water. If the water density is lower, this separation effectively decreases. Therefore, optimum moderation cases of wide spaced racks are covered.
5. The range of boron values in the benchmarking experiments was 0 – 5030 ppm. An upper limit of 2300 was used because of the large interpolation between 1511 ppm and 5030 ppm (discussed in Section A.5.1). It was determined that the bias for higher Boron concentrations would not challenge the bias based on EALF. Note that increased Boron also results in increased EALF. Therefore, the impact of higher Boron on the bias is already captured by the increased bias with higher EALF.

A.8. Summary and Recommendations

238 UO2 and 111 MOX critical experiments were analyzed with SCALE 6.2.3 and the 238 group ENFD/B-VII.0 cross section set. The calculated k's were analyzed for trends using the statistical approach recommended in NUREG/CR-6698. The criticality code bias and uncertainty for cold (293 K) configurations at Surry for fresh fuel and burned fuel was calculated. The bias and uncertainty for calculating critical configurations of fresh fuel and burned fuel are summarized in Tables A.8-1 and A.8-2. The bias is a function of the calculated EALF where larger EALF results in higher bias and uncertainty.

For the spent fuel pool, the bias and uncertainty depends on the burnup since at low burnup the dominant fissile material is U-235 and at high burnup the dominant fissile material is Pu-239. In order to avoid trying to properly weight the critical experiments for the amount of U-235 and Pu-239, it is recommended to use two sets of bias and uncertainty , one from the fresh UO2 critical experiments and one from the MOX critical experiments. The final bias and uncertainty to be used will be that which produces the highest 95/95 k. The UO2 critical experiments have a higher bias but lower uncertainty than the MOX experiments. Since the uncertainty is statistically combined with other uncertainties it is not possible to determine which set is more limiting until the other uncertainties due to factors such as manufacturing tolerances are determined.

There is also an additional bias of 1.0 pcm/K for temperatures above 293 K which is calculated in Section A.6.

Table A.8-1: Critical Configuration Bias and Uncertainty Versus EALF – Fresh Fuel

EALF	Bias	Uncertainty
0.00 – 0.40 eV	0.0030	0.0040
0.40 – 0.80 eV	0.0040	0.0045
0.80 – 1.10 eV	0.0055	0.0050
1.10 – 1.25 eV	0.0060	0.0050
1.25 – 1.40 eV	0.0065	0.0055

Table A.8-2: Critical Configuration Bias and Uncertainty Versus EALF – MOX Fuel

EALF	Bias	Uncertainty
0.00 – 0.40 eV	0.0015	0.0060
0.40 – 0.80 eV	0.0025	0.0095
0.80 – 1.10 eV	0.0030	0.0120
1.10 – 1.25 eV	0.0035	0.0135
1.25 – 1.40 eV	0.0035	0.0145

A.9. Appendix References

[A.1] ORNL/TM-2005/39, Version 6.2.3, "SCALE Code System", March 2018.

[A.2] NUREG/CR-6698, "Guide for Validation of Nuclear Criticality Safety Calculational Methodology," U.S. Nuclear Regulatory Commission, Washington DC, January 2001.

[A.3] NEA/NSC/DOC(95)03, "International Handbook of Evaluated Criticality Safety Benchmark Experiments," Nuclear Energy Agency, September 2016 Edition.

[A.4] D. E. Mueller, K. R. Elam, and P. B. Fox, *Evaluation of the French Haut Taux de Combustion (HTC) Critical Experiment Data*, NUREG/CR-6979 (ORNL/TM-2007/083), prepared for the US Nuclear Regulatory Commission by Oak Ridge National Laboratory, Oak Ridge, Tenn., September 2008.

[A.5] F. Fernex, "Programme HTC – Phase 1 : Réseaux de crayons dans l'eau pure (Water-moderated and reflected simple arrays) Réévaluation des expériences," DSU/SEC/T/2005-33/D.R., Institut de Radioprotection et de Sûreté Nucléaire, 2008.

[A.6] F. Fernex, *ProgrammeHTC – Phase 2 : Réseaux simples en eau empoisonnée (bore et gadolinium) (Reflected simple arrays moderated by poisoned water with gadolinium or boron) Réévaluation des expériences*, DSU/SEC/T/2005-38/D.R., Institut de Radioprotection et de Sûreté Nucléaire, 2008.

[A.7] F. Fernex, *Programme HTC – Phase 3 : Configurations "stockage en piscine" (Pool storage) Réévaluation des expériences*, DSU/SEC/T/2005-37/D.R., Institut de Radioprotection et de Sûreté Nucléaire, 2008.

[A.8] F. Fernex, *Programme HTC – Phase 4 : Configurations "chateaux de transport" Réévaluation des expériences*, DSU/SEC/T/2005-36/D.R., Institut de Radioprotection et de Sûreté Nucléaire, 2008.

[A.9] J. P. Royston, "Approximating the Shapiro-Wilk W-test for non-normality ", Statistics and Computing, Vol. 2,, September 1992.

[A.10] Kleinbaum, Kupper, and Muller, Applied Regression Analysis and Other Multivariable Methods, Second Edition, page 48, PWS-KENT Publishing Company, Boston, MA 1988.

[A.11] "PROPHET StatGuide: Examining normality test results," http://www.basic.northwestern.edu/statguidefiles/n-dist_exam_res.html, located on 6/8/09.

[A.12] R. Mark Sirkin, Statistics for the Social Sciences, Third Edition, 2005, page 245, Sage Publications, Thousand Oaks, CA.

[A.13] NRC Accession Number ML18128A049, "Millstone, Unit 3, License Amendment Request Regarding Proposed Technical Specifications Changes for Spent Fuel Storage and New Fuel Storage", 05/03/2018.

Appendix B: Fuel Depletion Code Validation for Criticality Analysis Using the EPRI Benchmarks

B.1. Introduction

Methods for treating burnup credit in spent fuel pool criticality analysis commonly made use of the Nuclear Regulatory Commission (NRC) 1998 "Kopp Memo," [1] which allows analysts to use 5% of the computed fuel depletion Δk to compensate for reactivity decrement uncertainties which might arise from uncertainties in computed nuclide number densities and/or neutron cross sections. The guidance in the "Kopp Memo" provided regulatory clarity and stability for many years. Starting in 2005, regulatory staff positions on acceptable criticality analysis methods evolved through interactions with licensees, and the basis for the guidance in the Kopp Memo was portrayed as being insufficient in light of operational/licensing changes being sought by utilities. [2]

Due to this regulatory guidance, the EPRI Benchmarks Report [2] and the EPRI Utilization Report [3] were developed to provide experimental quantification of pressurized water reactor (PWR) fuel reactivity burnup decrement biases and uncertainties obtained through extensive analysis of in-core flux map data from operating power. [2]

This Surry submittal utilizes the method developed in these two EPRI Reports to determine the depletion bias and uncertainty. The depleted fuel isotopic content is calculated using the t5-depl TRITON [4] module in SCALE 6.2.3 [5] which uses KENO-V.a [6] for the flux calculations needed to collapse neutron cross sections spatially and in energy for the depletion. The ORIGAMI [7] module of SCALE 6.2.3 was used to decay the fuel isotopics calculated from TRITON. All analyses are performed using the 238 group ENDF/B-VII.0 cross section library (v7-238).

B.2. Methodology

The results of the depletion benchmark will be analyzed using guidance in EPRI Utilization Report [3] with certain clarifications and exceptions identified in the NRC safety evaluation [8]. The uncertainty is quantified in EPRI Benchmarks Report [2] as part of the generation of the measured depletion reactivity worth database and does not need to be re-evaluated as part of this analysis.

The code specific bias is generated by running the benchmark cases from the EPRI Benchmarks Report [2]. The bias is calculated by evaluating the difference between measured reactivity decrement (from the EPRI Reports) and calculated reactivity decrement (calculated in this analysis) versus case number, burnup, and decay time.

The design inputs for the depletion benchmark calculations can be found in Appendix B of EPRI Benchmarks Report [2]. The use of these inputs is justified based on the NRC safety evaluation for the benchmark that references the EPRI report [8]. The input for the base depletion will be summarized here. The other cases follow these steps with minor changes to the input. See Chapter 3.1 of the SCALE 6.2.3 User's Manual as a general reference for the inputs described in this section.

All depletion benchmark calculations are performed using three separate SCALE runs.

1) t5-depl calculation to produce standard composition files of depleted fuel for the zero-hour decay interval.
2) An ORIGEN/ORIGAMI stacked case to produce standard composition files for the other decay intervals.
3) A KENO calculation with the appropriate standard composition input for the case/depletion energy/decay interval combination.

This approach was chosen due to a couple factors. First, through informal contact with Oak Ridge National Laboratory code developers, this is considered the preferred way of doing depletion followed by decay calculations. Second, this is the most computationally efficient way to produce several standard composition files for a given depletion/decay matrix.

The depletion case inputs are given in Appendix B of the EPRI Benchmarks Report [2]. This includes the number densities and temperatures for each case. The gap is modeled as void because the gap material is not specified. This is a negligible approximation since typically the gap is filled with Helium which has a negligible absorption cross section and a very low scattering cross section. The low interaction rate is also compounded by the low density of the fill gas.

The burndata block can be prepared in two different ways depending on how one wants to do the depletion calculation. The primary approach to the depletion, for this benchmark, is to run on depletion for the entire 60 GWd/MT interval and use downstream codes to process the decay time impacts prior to running the final KENO case. The power density is 38.1 MW/MT per page B-1 of the EPRI Benchmarks Report [2] for all cases except 11 (150% * 38.1 = 57.15 MW/MT). The burn input is in days. The first two timesteps are 10 and 40 days respectively. Other burn steps

are 50 days except when approaching a restart point. This was found to be adequate for achieving convergence as discussed later. Since t5-depl uses the midpoint of the burn step to KENO runs for flux updates (library runs), a small step is used at each of the six depletion steps (10, 20, 30, 40, 50, and 60 GWD/T).

The number of neutron histories is set similar to the criticality benchmark cases. Notably, the gen, npg, and nsk inputs are reduced in order to run depletions efficiently while still obtaining adequate flux solutions and stable isotopics. Therefore, the goal of low KENO variance is not considered important for the depletion. Each step runs 2000 generations, 2000 neutrons per generation, and 100 generations skipped. These inputs were found to result in adequate convergence for the depletion run. See Section B.4 for more discussion. Also note that any bias and uncertainty due to fewer generations will be compiled into the depletion bias values.

The geometry input is straightforward from the design inputs from the EPRI Benchmarks Report [2] . A full assembly model is used despite the overall assembly symmetry due to KENO-V.a limitations. All boundaries are modeled as reflected. This option models an infinite lattice of assemblies much like a CASMO-5 calculation.

Though some of these options can be changed, doing so would invalidate the code bias evaluated in this calculation. Therefore, the specific inputs will be listed in Section B.6 as a limitation on the use of the results from this evaluation.

This benchmark requires an additional calculation to get the isotopics for varying decay intervals. A stacked ORIGEN and ORIGAMI case is used for this process. ORIGAMI is a module that automates ORIGEN calculations and creates standard composition files. In order for ORIGAMI to work, a specific binary file format is required (an f71 file). To accomplish this for our purposes, an ORIGEN run is generated to pull the depletion energy data that is needed from the TRITON 0-hour decay standard composition file to create the ORIGAMI ready binary file. The ORIGAMI input was chosen to produce a standard composition file that will match the TRITON parameter addnux=3.

The ORIGEN and ORIGAMI inputs are chained to create standard composition files for the entire depletion/decay matrix. For this benchmarking analysis, each ORIGEN/ORIGAMI case outputs standard composition files at each of the six restart burnups (10, 20, 30, 40, 50, and 60 GWD/MTU) and for each of the three decay times (100 hours, 5 years, and 15 years) used in the EPRI Reports (resulting in 18 standard compositions files for each ORIGAMI file).

The output must be post processed to change the material number from ORIGAMI's default numbering back to the original depletion numbering. The standard composition files were also postprocessed to remove isotopes of negligible density. Isotopes that are below a number density of 1e-20 atoms/b-cm are removed from the standard composition file to save computer resources on downstream KENO cases.

The model for the final KENO calculation using the generated standard compositions is identical to the model used for the depletion. The temperature is set to 293 K for all materials. Also, the KENO convergence parameters are increased to 4500 generations, 6000 particles per generation, and 500 skipped generations. These parameters were found to give adequately converged k-eff results.

Previous criticality analyses [9] used a different method for performing depletion. This was to deplete up to the depletion energy of interest (using the same depletion time steps) and use the down input to specify the decay interval instead of a separate ORIGAMI case. This approach has the advantage that it is simpler since only one input deck is needed instead of two. However, this process was not used because it is less efficient since the depletion needs to be run multiple times and a zero power/zero time burn step is required in order to avoid a code nuance in which short-lived absorbers could appear in long decay time standard composition outputs. A sensitivity case was run to ensure that this method gives equivalent results to the primary method for all burn steps and decay intervals. The results of the sensitivity case show that this is indeed true.

B.3. Depletion Source Convergence

The convergence of the depletion code has the potential to impact the depletion code bias. New to SCALE 6.2.3 are source convergence monitors using three tests on the entropy of the source distribution. All cases were run with adequate particles per generation, skipped generations, and total generations so that the source convergence criteria internal to SCALE 6.2.3 are met. Note that this is a more conservative approach to previous convergence checks because the source convergence is typically much slower than the k-eff convergence.

The SCALE depletion calculations were run and checked for adequate source distribution convergence. It was noted that the first SCALE default source convergence test routinely failed for all KENO calculations that are performed for the depletion benchmark. The first source convergence test would fail no matter how many particles and generations were set (up to 8,000/16,000 gen/npg). The highest level of gen/npg inputs resulted in prohibitive computational time and were unpractical. From the SCALE manual, there is discussion but not direct confirmation that the first test may perform poorly for a nearly uniform source distribution (i.e. infinite lattice calculations with no buckling correction). Therefore, the first source convergence test can be disregarded for the infinite lattice cases run for the depletion benchmark analysis. Also, since k-eff isn't particularly important for the depletion calculation, k-eff convergence statistics are ignored. However, all other source convergence tests were confirmed to pass for the depletion.

To confirm the main user inputs that can affect convergence, test cases were run. The two most important parameters for depletion code convergence are the number of particles simulated in the intermediate KENO calculations (combination of NPG, GEN, and NSK in the parameters block) and the time step size. Case 1 was re-run using changes to these parameters to assess the impact of the increased level of convergence. For the reported results, 2000 particles per generation, 2000 generations, and 100 skipped generations were used for the depletion KENO calculations. In the first additional case, these parameters are changed to 4500 generations, 6000 particles per generation, and 500 generations skipped. In the second additional case, the parameters are changed to 9000 generations, 12000 particles per generation, and 1000 generations skipped. A third additional case uses times steps that are half that of the reported results.

The additional cases were run to ensure convergence based upon the criteria discussed above. Overall, the difference of the final case matrix k_{inf} values is within the statistical uncertainty of the

overall methodology. Note that the cold case results are converged with a standard deviation of approximately 10 pcm. Sensitivity case differences ranged from -70 pcm to 10 pcm. The standard deviation of the difference between reported and sensitivity k_{inf} values is one to two standard deviations. Also, the reported results are consistently high compared with the sensitivity results. Higher case k_{inf} values are conservative (depletion has a lesser effect on k).

Based on the sensitivity results, the parameters used for the reported results are adequate for convergence of the depletion runs. Use of different time steps or particles in the KENO calculations (including shorter time steps and/or more particles) was not used in the downstream analyses because the calculated bias is specific to these inputs.

B.4. Depletion Benchmark – Calculations

The depletion benchmark cases were run in accordance to the methodology discussed in Section B.2 and convergence was verified in accordance with Section B.3. The procedure for evaluating a depletion code bias is given in Section 4 of the EPRI Utilization Report [3]. Reactivity decrements (Δk) are defined as the difference between the zero depletion k_{inf} and the k_{inf} from the specific depletion/decay interval for each case. To generate a depletion code bias, the measured reactivity decrements from Appendix C of the EPRI Benchmarks Report [2] are subtracted from the calculated results of each case/depletion/decay (Δk_{calc} - Δk_{EPRI}). A negative value indicates that the calculated reactivity decrement is conservative (calculates a smaller burnup decrement than the measured EPRI decrement).

Tables B.4-1 through B.4-4 give the bias values for all burnups and decay intervals for each case. Similar tables are given in Section 3 of EPRI 3002016888 [3]. These tables in the EPRI report were generated using SCALE 6.1.2 t5-depl with ENDF/B-VII 238 group cross section libraries. The EPRI report example calculation tracked more isotopes than this analysis. The overall magnitude of the bias is similar between the reference and this analysis but had a different trend with burnup.

Table B.4-1: Code Bias Cases/Burnup Matrix, No Cooling

Case	Burnup (GWD/MTU)					
	10	20	30	40	50	60
1	-0.0010	-0.0012	-0.0009	-0.0002	0.0006	0.0018
2	-0.0007	-0.0009	-0.0012	-0.0014	-0.0011	-0.0010
3	-0.0006	-0.0009	-0.0008	-0.0009	-0.0005	0.0003
4	-0.0018	-0.0021	-0.0022	-0.0021	-0.0016	-0.0005
5	-0.0011	-0.0011	-0.0008	-0.0008	-0.0005	0.0000
6	0.0001	0.0000	-0.0005	-0.0010	-0.0011	-0.0009
7	-0.0005	-0.0001	-0.0002	-0.0007	-0.0009	-0.0006
8	-0.0007	-0.0010	-0.0011	-0.0007	-0.0005	0.0001
9	-0.0009	-0.0014	-0.0011	-0.0010	-0.0007	0.0002
10	-0.0008	-0.0012	-0.0011	-0.0008	-0.0010	-0.0003
11	-0.0013	-0.0019	-0.0015	-0.0016	-0.0010	-0.0001

Table B.4-2: Code Bias Cases/Burnup Matrix, 100 Hour Cooling

Case	Burnup (GWD/MTU)					
	10	20	30	40	50	60
1	-0.0002	-0.0003	0.0000	0.0007	0.0015	0.0028
2	0.0001	-0.0002	-0.0004	-0.0002	-0.0005	0.0001
3	0.0000	-0.0002	0.0001	-0.0002	0.0004	0.0010
4	-0.0002	-0.0007	-0.0007	-0.0007	-0.0003	0.0007
5	-0.0004	0.0000	-0.0001	0.0003	0.0004	0.0010
6	0.0009	0.0007	0.0004	0.0000	-0.0003	-0.0002
7	0.0002	0.0008	0.0006	0.0003	0.0001	0.0000
8	-0.0002	-0.0002	-0.0001	-0.0002	0.0004	0.0010
9	-0.0028	-0.0030	-0.0029	-0.0026	-0.0024	-0.0014
10	-0.0002	-0.0004	-0.0002	-0.0005	-0.0003	0.0003
11	-0.0003	-0.0007	-0.0005	-0.0005	0.0001	0.0009

Table B.4-3: Code Bias Cases/Burnup Matrix, 5 Year Cooling

Case	Burnup (GWD/MTU)					
	10	20	30	40	50	60
1	0.0014	0.0020	0.0023	0.0030	0.0040	0.0055
2	0.0015	0.0019	0.0022	0.0023	0.0025	0.0029
3	0.0016	0.0020	0.0023	0.0024	0.0031	0.0040
4	0.0013	0.0013	0.0016	0.0019	0.0023	0.0033
5	0.0011	0.0022	0.0026	0.0028	0.0031	0.0036
6	0.0022	0.0030	0.0030	0.0027	0.0027	0.0027
7	0.0017	0.0031	0.0033	0.0031	0.0029	0.0031
8	0.0017	0.0020	0.0025	0.0027	0.0029	0.0038
9	-0.0014	-0.0009	-0.0004	0.0002	0.0007	0.0015
10	0.0012	0.0014	0.0014	0.0014	0.0014	0.0023
11	0.0015	0.0020	0.0023	0.0027	0.0034	0.0043

Table B.4-4: Code Bias Cases/Burnup Matrix, 15 Year Cooling

Case	Burnup (GWD/MTU)					
	10	20	30	40	50	60
1	0.0017	0.0021	0.0024	0.0032	0.0041	0.0058
2	0.0022	0.0025	0.0024	0.0025	0.0026	0.0028
3	0.0021	0.0023	0.0025	0.0027	0.0029	0.0041
4	0.0015	0.0017	0.0019	0.0017	0.0025	0.0034
5	0.0015	0.0024	0.0027	0.0031	0.0032	0.0040
6	0.0026	0.0034	0.0031	0.0031	0.0029	0.0030
7	0.0019	0.0036	0.0037	0.0035	0.0033	0.0036
8	0.0020	0.0023	0.0026	0.0027	0.0031	0.0040
9	-0.0008	-0.0006	-0.0001	0.0001	0.0009	0.0019
10	0.0014	0.0014	0.0014	0.0013	0.0014	0.0020
11	0.0018	0.0020	0.0025	0.0029	0.0034	0.0044

It was determined by EPRI during NRC approval of the benchmark that depletion code bias would not be a function of burnup (page 20 of SER, [8]). However, RAI 2a response (echoed in the SER) indicates that the bias can be broken up by decay time.

On page 21 of the final safety evaluation [8] the procedure for determining the depletion code bias with the full case matrix results is discussed. From the SER, the following guidance is given.

The most limiting bias is not merely the largest of the calculated biases but could include perturbations off of case 3 when a number of these perturbations simultaneously exist in the application. For example, the application could be 5 wt% enriched fuel run at 150% power. For this example, the application bias would be the case 3 bias (4.25% ^{235}U, 100% power) plus the difference between case 3 and case 2 (5 wt% ^{235}U, 100% power) plus the difference between case 3 and case 11 (4.25 wt% ^{235}U, 150% power). If any of the differences were negative (i.e., non-conservative), then that difference would be set to zero. This example was chosen to provide a clear explanation; however, for the actual implementation, it is recommended to start with case 3 and then conservatively add all the biases from all the deltas off of case 3 to determine a single bounding bias for the range of benchmarks.

The description of the cases run is given in Table B.4-5 as reproduced from Table A-1 of EPRI 3002016888 Revision 2 [3]. Additional biases are possible due to higher or lower enrichment (>4.25% enrichment in case 2 and <4.25% in case 1), presence of burnable absorber in the fuel (cases 5, 6, and 7), high boron depletion (>900 ppm exposure averaged, case 8), high temperature rack conditions (>293 K, case 9), presence of soluble Boron in rack (>0 ppm, case 10), and high power depletion (>38.1 MW/MT, case 11). The base bias and perturbation biases are summarized for these cases in Table B.4-6. Based upon the depletion and fuel parameters, sums of these biases make up the total depletion code bias. The criticality analysis used the conservative bias in the last row may be used for all depletion calculations.

Table B.4-5: Benchmark Lattice Cases

Case	Description
1	3.25% Enrichment
2	5.00% Enrichment
3	4.25% Enrichment
4	Off-nominal pin diameter
5	20 WABA depletion
6	104 IFBA depletion
7	104 IFBA plus 20 WABA depletion
8	High boron depletion - 1500 ppm
9	Branch to hot rack (150F coolant/fuel) -338.7 K
10	Branch to high rack boron - 1500 ppm
11	High power depletion (power, coolant/fuel temp)

Table B.4-6: Aggregate Depletion Code Bias

Condition	Decay Time		
	< 100 hours	< 5 years	< 15 years
Base Case	0.0010	0.0040	0.0041
Rod OD < 0.95 cm	--	--	--
< 4.25% Enrichment	0.0017	0.0015	0.0017
> 4.25% Enrichment	--	--	--
Burnable Absorber	--	--	--
> 900 ppm Depletion	--	--	--
Rack T > 293 K	--	--	--
Borated Rack	--	--	--
Power > 38.1 MW/MT	--	0.0002	0.0003
Conservative Bias	0.0028	0.0057	0.0061

B.5. Depletion Benchmark – Applicability

The benchmark data generated by EPRI [2] used only two fuel types, both from 17x17 plants. Furthermore, the benchmark analysis included Gadolinia bearing fuel types in the data population but did not explicitly include Gadolinia rod cases in the benchmark set. The applicability of Gadolinia bearing fuel types are specifically addressed in the limitations and conditions of the final safety evaluation for the benchmark [8].

Section 2.3 of the EPRI utilization report [3] details the similarity analysis used to justify applicability of the benchmark to other fuel types. The geometric parameter of interest is the water to pellet volume ratio. Surry has used Westinghouse 15x15 fuel and could possibly use Framatome AGORA fuel in the future. Table 2-6 of the EPRI report shows Westinghouse 15x15 fuel is geometrically within the bounds of the measured database which can also be verified with Dominion data. AGORA fuel is slightly outside the bounds of the measured fuel types with a ratio of 1.656, but well within the full tabulated bounds in Table 2-6 of the report. In the EPRI report, the argument for applicability of the benchmark to other fuel types rest primarily on the similarity of the burnup average EALF of the different fuel types.

Depletions for Surry fuel types were generated to compare with the EALF data from the report. These depletions used identical inputs as described in Section B.2 with the following exceptions.

- The geometric parameters for Surry Westinghouse Upgrade and Framatome Agora fuel are used to construct celldata and geom block inputs.
- A nominal power of 35 MW/MT is used in the depletion block with corresponding changes to the burn days. A low power of 33 MW/MT is used for the low depletion power case. The power densities are representative of rated power and core loadings for all Surry cycles.
- UO2 enrichments of low, nominal, and high correspond to number densities in EPRI cases 1, 3, and 2 respectively. Nominal enrichments were used for the Gad cases and the low power case.
- Gadolinia fuel composition is generated for 2% and 8% Gad loadings.
- For gad rod cases, a low-density helium composition is added for the gap. This is required by the code when multiple rod types are used.
- A 16 gad rod layout is used. This strategy matches the choices made in the benchmark where the number of IFBA rods was neither extremely high nor extremely low.

The depletion cases for a high and low Gad AGORA fuel type are run. Also, a high and low enrichment at nominal power, and a nominal enrichment at low power using Westinghouse Upgrade fuel type are run.

The burnup average calculated EALF for the 11 benchmark cases and the five Surry depletions are given in Table B.5-1. The benchmark case burnup averaged EALF can be compared with the reported values in Table 2-8 of the EPRI Utilization report [3].

Table B.5-1: Burnup Average EALF for Calculated Benchmark and Select Surry Cases

Case	Sub-batch Burnup (GWd/T)					
	10	20	30	40	50	60
1	0.664	0.734	0.796	0.854	0.91	0.965
2	0.891	0.943	0.984	1.017	1.048	1.079
3	0.781	0.839	0.887	0.929	0.97	1.011
4	0.608	0.646	0.678	0.706	0.734	0.765
5	1.084	1.081	1.086	1.103	1.129	1.16
6	1.006	0.987	0.994	1.013	1.038	1.069
7	1.381	1.276	1.226	1.212	1.217	1.235
8	0.876	0.943	1.001	1.052	1.1	1.148
9	0.877	0.951	1.013	1.066	1.116	1.166
10	0.664	0.734	0.796	0.854	0.91	0.965
11	0.891	0.943	0.984	1.017	1.048	1.079
Surry High Gad	1.136	1.071	1.043	1.044	1.058	1.081
Surry Low Gad	0.906	0.904	0.926	0.953	0.984	1.018
Surry High Enr	0.863	0.907	0.937	0.963	0.987	1.013
Surry Low Enr	0.657	0.720	0.773	0.825	0.876	0.928
Surry Low Pow	0.761	0.811	0.849	0.884	0.919	0.956

Generally, the calculation and reported burnup average EALF values agree well. The difference between the calculated and reported values are in the range of approximately -0.05 to 0.01 eV and the differences are distributed near evenly around zero. Note that the 238 group library energy bounds in the range of 0.5 to 1.5 eV are spaced at least 0.025 eV apart (see Table 10.1.8 in the SCALE 6.2.3 manual [5]).

Benchmark cases 1 through 4 are considered nominal cases and are appropriate for comparing to the Surry high and low enrichment cases. Also, the low power depletion is compared with the first four cases since, for some cycles, the low power would be considered the nominal depletion power. The results are given in Figure B.5-1. The figure shows that the Surry non-Gad results are bounded between the small pellet (high hydrogen to uranium ratio) benchmark, case 4, and the high enrichment benchmark, case 2. Therefore, the Surry Upgrade fuel type is bounded by the depletion benchmark database. Also, since all depletion power densities for Surry fuel types fall between 33 MW/MT and the benchmark value of 38.1 MW/MT, the depletion powers used in the Surry depletion analyses are also bounded by the depletion benchmark database.

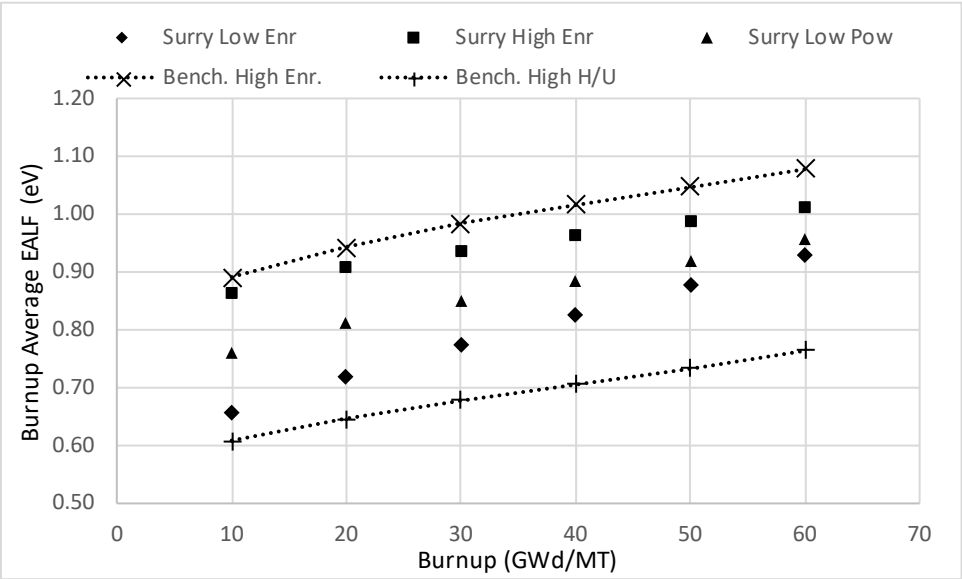

Figure B.5-1: Burnup Average EALF for Surry Nominal and Low Power Cases

Gadolinia bearing fuel should be compared with benchmark cases 5, 6, and 7 where IFBA and WABA are used. These results are given in Figure B.5-2. The high Gad wt% case is bounded by the IFBA and the IFBA+WABA benchmark cases. However, the low Gad wt% case falls below the IFBA benchmark case, but above the small pin nominal enrichment benchmark case. This is expected because lowering the burnable poison to near zero concentration would approach fuel without any burnable poison (i.e. nominal benchmark cases). The low wt% Gadolinia fuel is above the minimum EALF for nominal fuel range and near the range of burnable poison benchmark cases; it has burnup average EALF consistent with the benchmark results. Since the benchmark database contains a large range of IFBA and WABA fuel types, and the benchmark cases that are run are representative of average fuel in the database, it would be expected that burnable absorber cases exist within the full database that span the gap between the benchmark IFBA case and the corresponding non-burnable absorber bearing fuel type (i.e. between benchmark cases 3 and 6). Therefore, the low and high wt% gadolinia cases burnup average EALF are considered bounded by the entire benchmark database despite the low case not being bounded by the burnable poison cases in the benchmark set

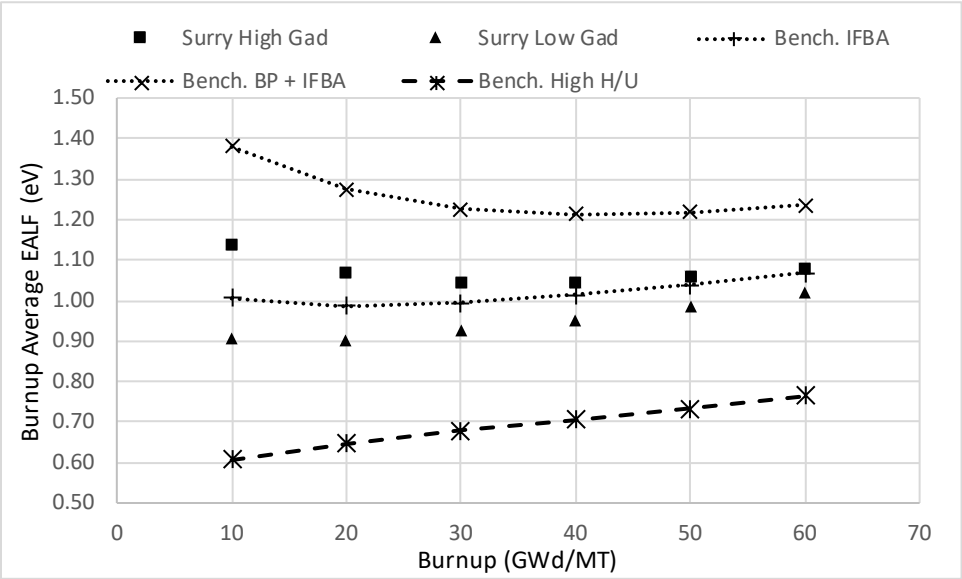

Figure B.5-2: Burnup Average EALF for Surry AGORA Fuel Cases

B.6. Depletion Benchmark – Conclusion

The depletion code bias was calculated herein. Table B.6-1 summarizes the calculated biases to be used for the downstream depletion analyses. The first row applies to all depletion analyses. All other rows apply as described in the first column of the table. However, the downstream calculations of Surry's criticality analysis uses the Conservative Bias for all calculations. Table B.6-2 gives an additional NRC mandated bias and the depletion code uncertainty as a function of burnup. The values can be found in Tables 4-1 and 4-2 of the EPRI Utilization report. Linear interpolation can be used for specific assembly burnups between the listed burnups in Table B.6-2 [3]. Additionally, Table B.6-3 lists code parameters that are covered by this analysis

Table B.6-1: Depletion Code Bias (% of Depletion Worth)

Condition	Decay Time		
	< 100 hours	< 5 years	< 15 years
Base Case	0.0010	0.0040	0.0041
Rod OD < 0.95 cm	--	--	--
< 4.25% Enrichment	0.0017	0.0015	0.0017
> 4.25% Enrichment	--	--	--
Burnable Absorber	--	--	--
> 900 ppm Depletion	--	--	--
Rack T > 293 K	--	--	--
Borated Rack	--	--	--
Power > 38.1 MW/MT	--	0.0002	0.0003
Conservative Bias	0.0028	0.0057	0.0061

Table B.6-2: Depletion Code Additional Bias and Uncertainty Versus Burnup

Burnup (GWd/MTU)	10	20	30	40	50	60
Additional Bias (% of Worth)	0.0%	0.0%	0.0%	0.15%	0.35%	0.54%
Uncertainty (% of Worth)	3.05%	2.66%	2.33%	2.12%	1.95%	1.81%

Table B.6-3: SCALE 6.2.3 Code Parameters Covered by Benchmark Calculations

Parameter	Depletion Bias and Uncertainty
Module	t5-depl
Library	v7_238g
Self-sheilding	latticecell (centrm)
Depletion NPG/GEN/NSK	2000/2000/100
Depletion step size	(1,10 d) (1,40 d) (n, 50 d)

B.7. Comparison with the Kopp 5% Depletion Uncertainty

The worth of the EPRI Benchmarks and Utilization method was directly compared to the worth of the historical Kopp 5% uncertainty method. The maximum k-eff of the Region 1 cask drop analysis (Section 9.1) was calculated by using the EPRI bias and uncertainty method and by using the Kopp 5% uncertainty method. The results are shown in Table B.7-1. For this application, the reactivity worth produced by the EPRI method is significantly larger than the Kopp 5% method for low burnups and very slightly smaller than the Kopp 5% at the largest burnups. This relative change in magnitude between the two methods occurs because the Application-Specific Bias is calculated as an absolute reactivity difference, as opposed to a depletion worth percentage, and because it is not a function of burnup. This comparison shows that the EPRI method and the calculations in Appendix B resulted in a synonymous reactivity effect as the Kopp method for the burnup ranges of most importance (most spent fuel assemblies have burnups >30 GWD/MTU).

Table B.7-1: Maximum k-eff with Kopp Uncertainty vs EPRI Benchmarks

Burnup (GWD/MTU)	0	10	20	30	40	47	53.00
Enrichment (U-235 wt%)	1.65%	2.20%	2.85%	3.45%	4.10%	4.55%	5.00%
Maximum k-eff							
Kopp Method	0.9093	0.9377	0.9284	0.9170	0.9156	0.9301	0.9384
EPRI Benchmarks Method	0.9093	0.9403	0.9299	0.9177	0.9155	0.9300	0.9383
Difference (EPRI – Kopp)	**0.0000**	**0.0026**	**0.0016**	**0.0007**	**-0.0001**	**-0.0001**	**-0.0002**

B.8. References

1. L. Kopp, NRC memorandum from L. Kopp to T. Collins, "Guidance on the Regulatory Requirements for Criticality Analysis of Fuel Storage at Light-Water Reactor Power Plants," dated August 19, 1998 (ADAMS Accession No. ML003728001).
2. EPRI Report 3002010613. "Benchmarks for Quantifying Fuel Reactivity Depletion Uncertainty – Revision 1". EPRI, Palo Alto, CA: 2017.
3. EPRI Report 3002016888. "Utilization of the EPRI Depletion Benchmarks for Burnup Credit Validation – Revision 2". EPRI, Palo Alto, CA: 2019.
4. M. A. Jessee, and M. D. DeHart, "*TRITON: A Two-Dimensional Transport and Depletion Module for Characterization of Spent Nuclear Fuel*," ORNL/TM-2005/39, Version 6 Vol. 1, Section T1, Oak Ridge National Laboratory, Oak Ridge, Tennessee, USA, January 2009.
5. "*SCALE: A Modular Code System for Performing Standardized Computer Analyses for Licensing Evaluation*," ORNL/TM-2005/39, Version 6, Volumes 1-3, Oak Ridge National Laboratory, Oak Ridge, Tennessee, USA, January 2009.
6. S. Goluoglu, N. F. Landers, L. M. Petrie, and D. F. Hollenbach,"*CSAS5: Control Module For Enhanced Criticality Safety Analysis Sequences with KENO V.A*," ORNL/TM-2005/39, Version 6, Vol. 1, Section C5, Oak Ridge National Laboratory, Oak Ridge, Tennessee, USA, January 2009.
7. M. L. Williams, S. E. Skutnik, Et. Al., "ORIGAMI: A CODE FOR COMPUTING ASSEMBLY ISOTOPICS WITH ORIGEN", *SCALE Code System*, ORNL/TM-2005/39.
8. NRC Accession Number ML19168A097, Final Safety Evaluation by The Office of Nuclear Reactor Regulation Topical Report 3002010613, "Benchmarks for Quantifying Fuel Reactivity Depletion Uncertainity – Revision 1" and Topical Report 3002010614, "Utilization of the EPRI Depletion Benchmarks for Burnup Credit Validation – Revision 1", July 2019.
9. NRC Accession Number ML18128A049, "Millstone, Unit 3, License Amendment Request Regarding Proposed Technical Specifications Changes for Spent Fuel Storage and New Fuel Storage", 05/03/2018.

Attachment 7

SPENT FUEL POOL BORON DILUTION ANALYSIS

VIRGINIA ELECTRIC AND POWER COMPANY
(DOMINION ENERGY VIRGINIA)
SURRY POWER STATION UNITS 1 AND 2

1 Introduction

A Spent Fuel Pool (SFP) criticality reanalysis has been completed for crediting soluble boron in the Surry Power Station (SPS) SFP under both normal and accident conditions. As a result of the soluble boron credit, a boron dilution analysis is required and is presented herein. This analysis includes the following plant specific features and potential events:

- Administrative procedures
- Dilution sources
- Dilution flow rates
- Boron dilution initiating events
- Boron dilution times and volumes
- Boron dilution mitigation actions

The boron dilution analysis, along with the criticality reanalysis, ensures that sufficient time is available to detect and mitigate the dilution before the design basis limit on the effective multiplication factor (keff = 0.95) is reached.

The current Technical Specifications minimum SFP boron concentration of 2300 ppm will be maintained. This dilution analysis will assume the dilution event starts at a boron concentration of 2300 ppm and the lower boron concentration limit is 400 ppm. The ending boron concentration of 400 ppm was conservatively chosen to be 50 ppm higher than the concentration required to maintain k-eff < 0.95 in the criticality analysis (350 ppm).

2 Spent Fuel Pool and Related System Features

This section provides background information on the SFP and related systems.

2.1 Spent Fuel Pool

The spent fuel pool structure located in the fuel building. The cask loading area is immediately adjacent to the SFP racks and cannot be isolated from the SFP water. The transfer canal is connected to the SFP but has gates which can isolate the SFP water from the water in the transfer canal.

The spent fuel pool is designed to accommodate fuel racks that store new and spent fuel assemblies. The storage racks are located under water in the spent fuel pool.

There is a 1’-6” curb bordering the South edge of the pool. The curb is formed by the wall of the pool and the adjacent walkway. The top edge of the pool wall is at elevation 47’-4” and the walkway is at elevation 45’–10”. There are no drains in the walkway. Any liquid on the walkway would be diverted to the stairway at the South-West corner of the building where it would drain to the lower levels of the fuel building and eventually to the building sump. The new fuel storage area forms the West edge of the pool. The new fuel storage elevation is 44’-1”. Embedded in the wall between the new fuel storage area and the SFP is the fire protection emergency SFP makeup pipe discharge. Since the FP piping is either below the surface of the SFP or embedded in concrete (other than the discharge which is open to air), pipe breaks are not a concern. The North edge of the SFP is bordered by a walkway at elevation 47’-4”. There is not a curb. Rather, there is a grated pipe trench through which the SFP cooling system return piping runs from the SFP cooling heat exchangers back to the East end of the SFP. This pipe trench is open to the lower elevations of the Fuel Building. Any liquid on the walkway will drain through the grating, fall to the lower elevations, and eventually collect in the building sump. The pipe chase continues around the North-East corner of the SFP and partially along the East edge of the pool. The SFP cooling return pipe, pool skimmer return lines, and purification system return line are located in the pipe chase along the East edge of the SFP. Near the South-East corner of the pool, on the East edge is the transition step from the South walkway elevation (45’-10”) to the North-East corner walkway elevation (47’-4”).

2.2 Spent Fuel Pool Storage Racks

There is only one type of fuel storage rack type in the spent fuel pool. The spent fuel storage pool contains a total of 1044 total fuel storage locations. All storage locations can store fuel assemblies.

The fuel storage racks are made up of 6x6 rack modules. Each rack module is fastened to the floor and have a nominal 14 inch pitch between adjacent fuel storage locations. The racks are not a flux trap design and they have no neutron absorbing material.

(Appendix 9A of UFSAR; Ref. 1)

2.3 Spent Fuel Pool Instrumentation

Wide range level instrumentation provides indication of spent fuel pit level in the cable spreading room. The instrumentation measures spent fuel pit water level from 7 inches above the top of the fuel racks to 10 inches above normal water level. (Section 9.5.1 of UFSAR; Ref. 1). Additionally, the fuel pool has low level alarm indicators which alarm when the SFP is 5 inches below the normal water level.

As discussed in Section 2.1, any liquid on the walkway would be diverted to the stairway at the South-West corner of the fuel building where it would drain to the lower levels of the fuel building and eventually to the building sump. The sump pumps sounds an alarm on high sump level (UFSAR Section 9.7.3). This analysis assumes that these automatic safety systems failed, and the only way operations can discover a dilution event is during operator rounds.

2.4 Spent Fuel Pool Administrative Procedure

Currently, Technical Specifications (TS) requires the soluble boron concentration in the SFP to always be greater than or equal to 2300 ppm (TS 5.3.2; Ref. 2). The spent fuel pool boron concentration must be measured every month in accordance with the Technical Specification Surveillance Test Interval List.

Additionally, operator rounds plant procedures state a log entry for the Spent Fuel Pool Local Level is required once per day at 20:00. However, other procedure Sequences require log entries twice per day at 08:00 and 20:00. Two additional Sequences are checks on the “A” and “B” Spent Fuel Pool Cooling Pumps. These pump checks cannot be accessed without passing by the top of the SFP at elevation. It is not credible to assume that an Operator would not notice if the SFP were overflowing and fail to report the situation to the Main Control Room. Hence, the SFP level is observed every 12 hours with a log entry recording the actual level every 24 hours. A 15 hour undetected dilution interval allows for reasonable variation in the time at which the rounds are made and for securing of the dilution source in accordance with Annunciator Response Procedures. The SFP High Level Annunciator Response Procedure would be entered upon notification of a high spent fuel pit level even with the alarm not present. For reference, this time interval value is consistent with the value used in the Millstone Unit 3 boron dilution analysis (Ref. 3).

2.5 Dilution Sources

Potential dilution sources from system interfaces and from pipe cracks were identified by review of plant documentation such as the UFSAR, drawings, Design Basis Documents (DBDs), and Nuclear Control Room Operator Development Program Modules (NCRODPs). A walkdown was performed to confirm the findings of the documentation research.

Based on the pre-walkdown preparation, insights from the walkdown, and subsequent document and drawing review post-walkdown, the identified potential dilution sources are discussed below.

2.5.1 Spent Fuel Pool Cooling System Subsystem

The SFP cooling system consists of three subsystems: SFP cooling, SFP purification, and the SFP skimmers. Each of these three subsystems pull borated water from the SFP; pass it through heat exchangers, filters, or ion exchangers; and return it back to the SFP. All system piping is below the elevation of the top edge of the SFP (47’-4”).

The SFP Cooling Heat Exchangers are cooled by Component Cooling water. Failure of a heat exchanger tube or tubes would result in unborated water being returned to the SFP.

2.5.2 SFP Purification Subsystem

The SFP Purification subsystem interfaces with the Primary Grade water system and the RWST. The RWST interface allows for borated water addition to the SFP and purification of RWST contents. The PG system interface allows for SFP makeup for water lost to evaporation. Mispositioning of PG system valve would result in addition of unborated water to the SFP.

2.5.3 SFP Skimmer Subsystem

The skimmers do not interface with other systems. They do not represent a credible potential dilution source.

2.5.4 Emergency Makeup System

The emergency make up flow paths are through the Fire Protection (FP) system and the External Beyond Design Basis (BDB) connection. These systems interface with the SFP in that they

discharge unborated water directly onto the surface of the SFP through a 6” discharge pipe that is open to the Fuel Building atmosphere. The Fire Protection system is capable of providing 2500 gpm of SFP emergency make up. The BDB emergency make up system will deliver a minimum of 500 gpm. These flow paths are not considered credible dilution sources as discussed below in Section 4.4.

2.5.5 Fire Protection

There were no fire stations (hoses) on or above the 47’-4” elevation (the elevation of the SFP wall). There are two below this elevation. Piping to these stations comes from below. Although these elevations are below the elevation of the SFP surface it could be speculated that breaks in piping could result in unborated water being sprayed up onto the surface of the SFP.

2.5.6 Primary Grade Water

The PG system interfaces with the SFP Purification system as mentioned above. There is also a PG water pipe/valve near the SFP at elevation 47’-4” that locally branches to two valved connections. A break in this pipe could result in unborated water being sprayed onto the surface of the SFP.

2.5.7 Clean Water Hose Connection

There is a clean water hose connection on the East end of the SFP serving the 47’-4” elevation. A break in this hose connection could result in unborated water being sprayed onto the surface of the SFP.

2.5.8 Building Heating

There are three heating steam (HS) units in the SFP vicinity. The HS units provide localized heating. Steam to the HS units is routed at elevations that are above the surface of the SFP along the outer walls of the Fuel Building. It is reasonable to assume that steam from pipe cracks would migrate to or rise above the surface of the SFP and condense into the pool providing a potential dilution source.

The Fuel Building Ventilation System is located in the Aux Building and supplies air (heated or cooled, as needed) to the Fuel Building via a large duct on the South wall. There is no open air

communication between the Aux building and the Fuel Building. There is a single security door on the South wall connecting the two buildings. A failure of HS steam piping supplying the ventilation system heat exchanger would result in steam release and condensation within the Aux building. If any condensate were to flow through the duct or the door into the Fuel building it would be directed by the South edge curb, walkway, and South-West stairway to lower elevations of the Fuel building and eventually to the sump. However, it will be conservatively assumed that a crack in the steam line to the heating coil in the Aux Building results in steam being transferred to the Fuel Building via the Fuel Building Supply Fan.

2.5.9 Roof Drains or Penetrations

There are not any roof drain downspouts inside the Fuel Building. However, there is a penetration or hatch in the roof of the Fuel Building. Post walkdown searches of construction drawings indicate that there may have been plans for a cooler of some sort on the roof of the Fuel Building that was either never installed or removed in the past. The drawing also indicates that the roof of the Fuel Building is sufficiently sloped such that buildup of rain water and challenge of the opening lip/seal is not a concern. The elevation of the centerline of the roof is 75’-0” and the elevation of the side walls is 74’-9⅝” providing a 2⅜” slope over a 19’-4¼” distance for runoff.

3 Spent Fuel Pool Dilution Event

3.1 Calculation of SFP Volume and Dilution Volume

The borated volume of the SFP is calculated using Eq. (1). It is assumed that the SFP fuel transfer canal gates are installed and that the SFP level is at the low level alarm. This is conservative in that it minimizes the SFP dilution volume.

$$V_{sfp} = V_{low\ level\ alarm} - V_{fuel\ racks} - N_{FA}(V_{FA} + V_{RCCA}) \qquad \text{Eq. (1)}$$

$$V_{sfp} = 70111.91 - 619.15 - 1044(2.65 + 0.329341) = 66{,}382.33\ ft^3$$

OR

$$66{,}382.33\ ft^3\ x\ \frac{7.4805\ gal}{ft^3} = 496{,}574\ gal$$

where :

V_{sfp} = volume of borated water in the SFP

$V_{low\ level\ alarm}$ = volume of pool when level is at the low level alarm; 70111.91 ft^3

$V_{fuel\ racks}$ = volume of empty fuel racks; 619.15 ft^3

N_{FA} = number of fuel assemblies; 1,044 assemblies

V_{FA} = volume of fuel assemblies; 2.65 ft^3

V_{RCCA} = volume of RCCAs; 0.329341 ft^3

3.2 Plant Equipment Operator Response

As discussed in Section 2.4, the automatic safety systems that could detect a dilution event are assumed to have failed leaving operator rounds as the only method to discover the event. Operator rounds plant procedures state a log entry for the Spent Fuel Pool Local Level is required once per day at 20:00. However, other procedure Sequences require log entries twice per day at 08:00 and 20:00. Two additional Sequences are checks on the “A” and “B” Spent Fuel Pool Cooling Pumps. These pump checks cannot be accessed without passing by the top of the SFP at elevation. It is not credible to assume that an Operator would not notice if the SFP were overflowing and fail to report the situation to the Main Control Room. Hence, the SFP level is observed every 12 hours with a log entry recording the actual level every 24 hours. A 15 hour undetected dilution interval allows for reasonable variation in the time at which the rounds are made and for securing of the dilution source in accordance with Annunciator Response

Procedures. The SFP High Level Annunciator Response Procedure would be entered upon notification of a high spent fuel pit level even with the alarm not present. For reference, this time interval value is consistent with the value used in the Millstone Unit 3 boron dilution analysis (Ref. 3).

3.3 Calculation of SFP Boron Dilution Water Flow Rate

The total amount of unborated water that can be added to the SFP to reduce the boron concentration from 2300 ppm to 400 ppm is determined using continuous dilution methodology (Ref. 4 - 7) consistent with the approach employed by Millstone Unit 3 SFP dilution calculation (Ref. 3). The continuous dilution method models unborated water being added at a constant rate with an equally constant rate of removal of a homogenous mixture of borated water. From a SFP criticality perspective, perfect mixing is acceptable since the criticality analysis ensures that k_{eff} is less than 1 when the SFP is filled with unborated water. Therefore, stratification (or slugs) of unborated water are not a concern. For conservatism, the SFP volume used excludes areas outside the SFP liner envelope (see Section 3.1 for further detail).

The amount of water that must be added to the pool to reduce the boron concentration from *2300 ppm* to *400 ppm* can be derived from Eq. (2) by solving for for *t* Eq. (3), substituting *t* for V_{add}/Q, and solving for V_{add} resulting in Eq. (4).

$$V_{sfp}\frac{dC}{dt} = -QC \qquad \text{Eq. (2)}$$

$$t_{end} = \frac{V_{sfp}}{Q}\ln\left(\frac{C_{(0)}}{C_{(end)}}\right) \qquad \text{Eq. (3)}$$

$$V_{add} = V_{sfp} * \ln\left(\frac{C_{(0)}}{C_{(end)}}\right) \qquad \text{Eq. (4)}$$

$$V_{add} = 496,574\ gal * \ln\left(\frac{2300\ ppmB}{400\ ppmB}\right) = 868,607\ gallons$$

where :

V_{add} = volume of water added to the pool

V_{sfp} = volume of borated water in the SFP; 496,574 gal

$C_{(0)}$ = SFP boron concentration, initial; 2300 ppmB

$C_{(end)}$ = SFP boron concentration, final; 400 ppmB

The maximum allowable dilution flow rate is determined by dividing the required unborated water volume to dilute the SFP by the maximum response time by a Plant Equipment Operator (PEO) which is 15 hours (discussed in Section 2.4).

$$Q_{dilution} = \frac{V_{add}}{t_{PEO}} * \frac{1\ hr}{60\ min} \qquad \text{Eq. (5)}$$

$$\frac{868{,}607\ gal}{15\ hrs} x \frac{1\ hr}{60\ min} = 965\ gpm$$

where :

$Q_{dilution}$ = Minimum flow rate to dilute the SFP below 400 ppm in 15 hours

V_{add} = volume of water added to the pool; 868,607 gal

t_{PEO} = maximum response time by a Plant Equipment Operator; 15 hours

<u>Therefore, the minimum flow rate that could dilute the SFP from 2300 ppm to 400 ppm in 15 hours is 965 gpm</u>**.** Note that the SFP would need to fill to overflowing prior to applying the feed and bleed methodology, however, the outlined approach is conservative since it results in boron exiting the SFP immediately.

4 Dilution Source Path Evaluation

This section evaluates the potential for dilution of the SFP from systems that interface with the SFP. These sources were identified in Sections 2.5.1 – 2.5.4.

4.1 Spent Fuel Pool Cooling Subsystem

The Fuel Pit Coolers are cooled by component cooling water. The design flow rate of the component cooling water through the heat exchanger is 1322 gpm. For a highly unlikely catastrophic failure of all tubes, the dilution flow rate would be the full flow rate of the component cooling water. Using Eq. (3), the SFP would dilute to 400 ppmB in slightly under 11 hours.

$$t_{end} = \frac{496{,}574}{1{,}322} \ln\left(\frac{2300}{400}\right) = 657\ minutes\ or\ 10.95\ hours$$

This catastrophic failure is not considered credible.

A more likely scenario is that a percentage of tubes crack. This scenario is analyzed in Section 5.5.

4.2 Spent Fuel Pool Purification Subsystem

Inadvertent opening of a Primary Grade valve will result in a flow path from the Primary Supply Water Pumps to the SFP. If a pump is running, 350 gpm of primary grade water will be delivered to the SFP. This is well below the flow rate of 965 gpm required to dilute the pool to 400 ppmB between operator rounds.

4.3 Chemical and Volume Control System

The Makeup Subsystem of the CVCS System can be aligned such that PG water is routed to the blender and then to the SFP. If the Chemical Mixing Tank were isolated from the blender, then the PG water would be unborated. This could allow transfer of unborated PG water directly to the SFP if a valve was open and a Primary Supply Water Pump were running. In this case, 350 gpm of primary grade water will be delivered to the SFP. This is well below the flow rate of 965 gpm required to dilute the pool to 400 ppmB between operator rounds.

4.4 Spent Fuel Pool Emergency Makeup System(s)

As stated in Section 2.5.4, the emergency makeup system is supplied by the Fire Protection (FP) emergency makeup flow path and the External Beyond Design Basis (BDB) emergency make up connection. These systems interface with the SFP in that they discharge unborated water directly onto the surface of the SFP through a 6" discharge pipe that is open to the Fuel Building atmosphere. The Fire Protection system is capable of providing 2500 gpm of SFP emergency make up. The BDB emergency make up system will deliver a minimum of 500 gpm. These flow paths are not considered credible dilution sources as discussed below:

4.4.1 Fire Protection System

To prevent building flooding the FP system is normally isolated from the fuel building. Per procedure, makeup from the fire main requires 3 manual actions: (1) start the Motor-Driven (1-FP-P-1) or Diesel Driven (1-FP-P-2) fire pump, (2) locally open Post-Indicator Valve, and (3) locally pull one of three deluge stations. Because deliberate manual actions are required to establish this flowpath it is not considered a credible undetected dilution source.

If it were established the SFP would dilute to 400 ppmB in 5.79 hours assuming the minimum flow rate of 2500 gpm.

$$\frac{868{,}607\ gal}{2500\ \frac{gal}{min}} x\ \frac{1\ hr}{60\ min} = 5.79\ hr$$

4.4.2 External BDB Connection

This is a BDB FLEX connection. Manual action is required to physically connect a water source. Because this is a BDB system and deliberate manual actions are required to establish this flowpath it is not considered a credible undetected dilution source.

If it were established the SFP would dilute to 400 ppmB in less than 28.9 hours assuming the minimum flow rate of 500 gpm.

$$\frac{868{,}607\ gal}{500\ \frac{gal}{min}} x\ \frac{1\ hr}{60\ min} = 28.9\ hr$$

5 Dilution from Pipe Cracks

This section evaluates potential pipe breaks that are in close proximity to the SFP. These dilution sources are identified in Sections 2.5.5 – 2.5.9.

Per UFSAR Section 14B.2.2.1 (Ref. 1), "Design-basis pipe breaks are postulated in piping for which the maximum operating pressure exceeds 275 psig and the maximum operating temperature equals or exceeds 200°F. The critical crack size is taken to be one-half the pipe diameter in length (d/2) and one-half the wall thickness in width (t/2). Pipe cracks (d/2 x t/2) are postulated in piping for which either the operating pressure exceeds 275 psig or the operating temperature equals or exceeds 200°F. If both operating pressure and temperature are below these values, breaks and cracks are not postulated." None of the identified pipes have pressures exceeding 275 psig <u>and</u> temperatures exceeding 200°F. Therefore, none of the tubes are analyzed as tube breaks. However, even if both the operating pressure is less than 275 psig and the operating temperature is less than 200 °F, pipe cracks are assumed in this analysis for conservatism.

The liquid flow rate from pipe cracks is calculated using equation 3-19 of Crane (Ref. 8):

$$Q = 236 * d^2 * \sqrt{\frac{\Delta P}{K * \rho}} \qquad \text{Eq. (6)}$$

where :

Q = flow rate through the opening (gpm)

ΔP = pressure differential across the opening (psi)

d = equivalent hydraulic diameter of round break (in)

K = loss coefficient of the pipe exit, in this analysis a value of 1.5 is used which is the summation of exit (K=1.0) and flush entrance (K=0.5 for r/d = 0.0) loss coefficients given in Crane (Ref. 8).

ρ= density of water before the pipe exit (lb/ft^3)

The hydraulic diameter is defined below. For a rectangular crack of length "a" and width "b":

$$d = \frac{2ab}{(a+b)} \qquad \text{Eq. (7)}$$

where :

a = 0.5 * pipe diameter

b = 0.5 * wall thickness

For pipe cracks with steam, the steam flow rate from pipe breaks is calculated assuming choked flow. From Refs. 9 and 10, the stream mass discharge rate from a steam break is given by:

$$W_{crit} = f\ P\ A \qquad \text{Eq. (8)}$$

where :

W_{crit} = the steam mass discharge rate; *lbm/hr*

P = pipe pressure, *psi*

A = break area, in^2

f = critical mass flow rate, in *lbm/(hr * in² * psi)*, obtained from the steam tables (Ref. 10).

This is converted to gpm as follows:

$$Q_{crit} = W_{crit} \left[\frac{7.48 \frac{gal}{ft^3}}{60 \frac{min}{hr} * \rho \frac{lbm}{ft^3}} \right] \qquad \text{Eq. (9)}$$

where :

Q_{crit} = steam condensation rate, *gpm*

W_{crit} = the steam mass discharge rate; *lbm/hr*

ρ = density of water at SFP temperature and atmospheric pressure.

5.1 Fire Protection Piping (except SFP emergency makeup)

Review of drawings indicates that a 6” FP header enters the Fuel Building where it transitions to a 2 ½” horizontal line that transitions to 2” vertical lines that go to the Fire Hose Racks at the 6’-10” and 27’-6” elevations. The hose racks connect to the 2” line with a 1 ½” line. The fire hose is 75’ x 1 ½” and is hung, loosely gathered, on the rack. Based on the physical location of the piping and hose racks relative to the top of the pool (El. 47’-4”) it is unlikely that water from a crack in the piping would reach the pool. Nevertheless, for the dilution evaluation a crack in the 6” header is considered.

Drawings do not indicate the class or schedule of this pipe but do show that the 6” piping is schedule 40. Design pressure and temperature conditions are conservatively assumed to be those of the Fire Protection Pumps, 175 psig and 95 °F.

Using this information and Eq. (6) and Eq. (7), dilution flow through a crack is calculated to be 23.34 gpm. This is well below the flow rate of 965 gpm required to dilute the pool to 400 ppmB between operator rounds.

5.2 Primary Grade Water Piping

There are several varieties of PG piping around the vicinity of the SFP. There are ¾", 1", and 2" lines. A crack is analyzed in the bounding 2" line.

The 2" Class 152 piping is schedule 10s. This portion of the PG piping has design conditions of 150 psig and 120°F.

Using this information and Eq. (6) and Eq. (7), dilution flow through a crack is calculated to be 3.3 gpm. This is well below the flow rate of 965 gpm required to dilute the pool to 400 ppmB between operator rounds.

5.3 Clean Water Hose Connection Piping

The clean water valve is on a 1" line. Since this piping serves a purpose similar to the PG piping discussed above (hose connections), it is assumed that design conditions for the PG piping are applicable to the clean water line. Since water is incompressible, water density is not significantly sensitive to pressure and temperature.

Using this information and Eq. (6) and Eq. (7), dilution flow through a crack is calculated to be 23.34 gpm. This is well below the flow rate of 965 gpm required to dilute the pool to 400 ppmB between operator rounds.

5.4 Building Heating Piping

A HS unit is on a 1½" line that extends down from a 4" pipe. Similarly, other HS units are on a 1½" line that extends down from a 2½" line that comes off a 4" pipe. Therefore, for the dilution evaluation, two 4" pipes are assumed to crack.

Per the Pipe Design Standard, 4" Class 121 piping is schedule 40 (Standard) and a maximum operating pressure of 125 psig for saturated steam.

Using this information and Eq. (8) and Eq. (9), dilution flow through a crack in a 4" line is calculated to be 4.00 gpm or for 2 lines, 8.00 gpm.

For conservatism, it is assumed that a crack in the steam line to the heating coil in the Aux Building results in steam being transferred to the Fuel Building via the Fuel Building Supply Fan. This is a 6" line. This dilution flow is calculated to be 6.95 gpm for this line.

Therefore, the total dilution flow from the building heating piping is 14.95 gpm. This is well below the flow rate of 965 gpm required to dilute the pool to 400 ppmB between operator rounds.

5.5 SFP Cooler Tube Rupture

The Fuel Pit Coolers are cooled by component cooling water. The cooler specification provides the following information:

Table 4-1 SFP Cooler Information

Parameter	Shell Side	Tube Side
Fluid	Component Cooling	Fuel Pit
Design Flow Rate	1,322 gpm	4,200 gpm
Design Pressure	150 psig	100 psig
Operating Pressure	60 psig	40 psig
Tube Outer Diameter	--	0.75 in
Tube Wall Thickness	--	0.058 in
No. of Tubes	1484	--
Temperature	200°F	--

Using this information and Eq. (6) and Eq. (7), dilution flow through a crack in one heat exchanger tube is calculated to be 0.88 gpm for a 150 psig pressure drop.

For a highly unlikely catastrophic break of all tubes the dilution flow rate would be the shell side flow rate of 1,322 gpm. This catastrophic failure is not considered credible.

A more likely scenario is that a percentage of tubes fail. Assuming 15% tube failure, the dilution flow rate is 196.35 gpm. This flow rate is well below the flow rate of 965 gpm required to dilute the pool to 400 ppmB between operator rounds.

6 Securing the Dilution Source

Two activities are needed to cease a dilution event: the dilution needs to be discovered, and then the dilution source needs to be secured. Sections 4 and 5 address the possible dilution sources and their associated flow rates. A summary of the potential dilution sources, flow rates, ppmB at 15 hours, and the time to dilute to 400 ppmB is presented in Table 6-1. This table reports the results conservatively; the dilution flow rate is rounded up, and the ppmB at 15 hours and time to dilute to 400 ppmB are rounded down.

Table 6-1: Summary of Dilution Sources, ppmB at 15 hrs, and time to Dilute to 400 ppmB

Dilution Source	Dilution Flow (gpm)	Boron Concentration at 15 hrs (ppmB)	Time (hrs) to dilute to 400 ppmB	Section Calculated
SFP Cooler Heat Exchanger (1)	197	1611	73	5.5
SFP Purification (PG water)	350	1219	41	4.2
Chemical and Volume Control System (PG water)	350	1219	41	4.3
Liquid pipe cracks (FP, PG, Clean Water)	>30	2179	488	5.1 - 5.3
Steam pipe cracks (HS)	15	2238	968	5.4

(1) Assumes 15% of the SFP Cooler heat exchanger tubes have cracked.

Table 6-1 shows that unintentionally diluting the SFP from the PG water system is the bounding scenario. Using the assumptions from Sections 2.4 and 3.2, the Spent Fuel Pool is observed at least every 12 hours meaning that operators must secure the dilution in 3 hours to satisfy the 15 hour assumption used in this analysis. The Spent Fuel Pit High Level Annunciator Response Procedure would be entered upon notification of a high spent fuel pit level even with the alarm not present. While there is no formal time requirement on these procedural actions, discussions with Operations confirmed that 3 hours to go through the procedure and isolate PG to the spent fuel pit is a conservative assumption. Note that an operator will already be at the SFP since the event was assumed to be discovered via operator rounds.

Table 6-1 shows that there is a large amount of margin in this analysis since it takes at least 41 hours to dilute the SFP to 400 ppm. This is 26 hours longer than the time assumed to secure the dilution (15 hours). The other dilution scenarios have much more time to determine and secure the source of the dilution; therefore they are bounded by the dilution scenario from the PG Water System.

7 Conclusions

This engineering analysis of potential scenarios which could dilute the boron concentration in the SFP demonstrates that sufficient time is available to detect and mitigate a boron dilution from 2300 ppm prior to reaching 400 ppm.

The systems which could dilute the spent fuel pool, either by direct connection to the spent fuel pool or by a potential pipe crack/break, have been analyzed via a bleed and feed methodology. However, in reality, the addition of unborated water to the SFP will lead to increased SFP water level and, if not controlled, an overflow of the SFP.

The volume of the SFP at the low-level alarm is 496,574 gal. To dilute the SFP from an initial boron concentration of 2300 ppm to a final concentration of 400 ppm requires the addition of 868,607 gallons of unborated water. All dilution scenarios evaluated here will eventually cause SFP high water level alarms either detected directly by control room alarm, by the plant operators detecting high SFP water levels or SFP overflow.

Using the conservative assumption that operator rounds identify and secure the dilution source within 15 hours, a maximum dilution rate of 965 gpm is acceptable. A summary of the potential dilution sources, flow rates, ppmB at 15 hours, and the time to dilute to 400 ppmB is presented in Table 6-1 in the preceding section. All flow rates are well below the acceptable value of 965 gpm, the minimum boron concentration is well above 400 ppmB, and the time to dilute to 400 ppmB is 2.7 times the operator rounds interval of 15 hours for the most limiting dilution rate.

The major conservatisms of this evaluation are as follows:

- The SFP is assumed to contain the least amount of borated water possible when the dilution event initiates
    - Water level at the low level alarm set point
    - Maximum amount of assemblies in the SFP and each assembly has an RCCA are stored in them.
    - The SFP transfer canal gates are installed which isolates the transfer canal from the SFP.
- Water level alarms do not detect the dilution event. It is assumed that this occurs if either the level indicators fail or the Bleed and Feed methodology keeps the water level constant.
- Operators are not notified of the dilution event via the Fuel Building Sump Pump auto start up.

- Operator rounds are the only way to detect a dilution event. It is assumed that no other workers or operators can discover an 868,607 gallon dilution event.
- The maximum time interval to secure the dilution is 15 hours (12 hours between operator rounds to detect the dilution and 3 hours to secure the dilution). The minimum time to dilute the pool from 2300 ppm to 400 ppm is 41 hours which is 26 hours more than the maximum response time.
- The ending boron concentration of 400 ppm is 50 ppm higher than the concentration required to maintain k-eff < 0.95 in the criticality analysis (350 ppm).

8 References

1) Surry Power Station Updated Final Safety Analysis Report, Rev. 52.03, 03/31/21.

2) Surry Units 1 and 2 Technical Specifications, Change 64, Amendment Nos. 301 and 301.

3) ML18128A049, “Millstone, Unit 3, License Amendment Request Regarding Proposed Technical Specifications Changes for Spent Fuel Storage and New Fuel Storage”, Attachment 7, 05/03/2018.

4) “Air Contaminants and Industrial Hygiene Ventilation – A Handbook of Practical Calculations, Problems, and Solutions, Roger L. Wabeke”, 1998 by CRC Press.

5) ML17309A917, “St. Lucie Unit 2 Spent Fuel Pool Dilution Analysis”, 11/26/97.

6) ML003760090, “Comanche Peak Steam Electric Station Spent Fuel Pool Boron Dilution Analysis”, August 2000.

7) ML003758403, Appendix A, “North Anna Units 1 and 2 Spent Fuel Pool Boron Dilution Analysis”, submitted September 2000.

8) Crane Technical Paper No. 410, Flow of Fluids through Valves, Fittings, and Pipe, 1988.

9) ML12142A162, Fundamentals of Nuclear Engineering, "Module 13: Critical Flow Phenomenon", Joseph S. Miller, P.E.

10) ASME Steam Tables, Fifth Edition, 1983.

Attachment 8

PLANNED UFSAR CHANGES (MARK-UP)

VIRGINIA ELECTRIC AND POWER COMPANY
(DOMINION ENERGY VIRGINIA)
SURRY POWER STATION UNITS 1 AND 2

FOR INFORMATION ONLY

extend upward to the same elevation as the refueling cavity. The floor of the canal is at a lower elevation than the refueling cavity, to provide the greater depth required for the fuel transfer system upending device and the control rod assembly change fixture.

9.12.3.3 Spent Fuel Pool

The spent fuel pool is designed for the underwater storage of spent fuel assemblies and control rod assemblies after their removal from the reactor. It is designed to accommodate a total of approximately 1044 fuel assemblies. The nominal size of a full core is 157 assemblies.

The spent fuel pool is constructed of reinforced concrete. The entire interior of the pool is lined with 0.25-inch type 304 stainless steel.

High-density storage racks erected on the pool floor are provided to hold the spent fuel assemblies. Fuel assemblies are placed in vertical cells, grouped in parallel rows with a minimum center-to-center spacing of 14 inches. The racks ensure the necessary spacing between assemblies to prevent criticality even if the pool were inadvertently filled with unborated water. Control rod assemblies and other non-fuel inserts/components may be stored in the fuel assemblies. Storage rack design details are given in Appendix 9A.

Failed fuel rods removed when reconstituting fuel assemblies will be stored in a fuel rod canister which will be stored in one cell of the spent fuel storage racks. Each fuel rod canister is manufactured to the same exterior dimensions as a fuel assembly with a top nozzle similar to the fuel assembly. This will permit handling of the canister using normal fuel handling equipment and storage in the rack. Each canister contains tubes for the storage of individual fuel rods. The accidental dropping of a fully loaded fuel rod canister in the spent fuel pool is conservatively bounded by the Fuel Handling Accident in the Spent Fuel Pool described in Section 14.4.1.3, since that accident assumes all 204 rods of the highest power assembly are failed. The fuel rod canisters hold less than 204 rods.

Radiation monitors for the spent fuel pool area are provided as described in Section 11.3.4.

9.12.3.4 New-Fuel Storage

New fuel assemblies and control rod assemblies are stored in a separate area of the fuel building, where they are unloaded from trucks. This storage area is designed to hold 126 new fuel assemblies in vertical racks, and is used primarily for the storage of the one-third replacement core plus 10% for each of the two units. The new fuel assemblies are stored in racks in parallel rows having a minimum center-to-center distance of 21 inches.

Change 1

Radiation monitoring for the new fuel storage area is discussed in Section 11.3.4.

New paragraph
Insert 1

Insert 1:

The normally dry new fuel storage racks are designed to ensure keff will not exceed 0.95 when fully loaded with fuel of the highest licensed enrichment and flooded with unborated water. Additionally, for the new fuel storage racks, keff will not exceed 0.98 with fuel of the highest licensed enrichment in place and assuming optimum moderation (e.g., aqueous foam). No criterion is given for the refueling operation; however, the margin resulting from the above referenced limits provided for the storage of the fuel is adequate for the controlled and continuously monitored operations involved.

In the analysis for the storage facilities, fuel of the highest licensed enrichment must be considered. No credit is taken for neutron poisons (such as BPRA, WABA, IFBA, etc.). Assemblies cannot be closer together than the design separation provided by the storage facility except in special cases such as in fuel-shipping containers, where analyses are carried out to establish the acceptability of the design. The mechanical integrity of the fuel assembly is assumed. All fuel designs and relevant historical operating parameters at Surry were considered in the criticality analysis, and the most reactive characteristics used.

The criticality analysis of the new fuel storage racks is based on KENO-V Monte Carlo code calculations (Reference 3). Both normal and postulated accidents in new fuel storage rack conditions were considered. In order to accommodate the increased reactivity of fuel enriched up to 5.0 weight percent U-235 with no burnable poisons, the placement of fuel assemblies was limited to 3-out-of-4 spacing, as shown in Figure 9.12-2. The cells shown are required to be empty whenever any fuel stored in the new fuel storage area has an enrichment greater than 4.35 weight percent U-235. An additional analysis was conducted to demonstrate that if the maximum fuel enrichment for any stored fuel is 4.35 weight percent U-235 or less, than the empty cells are not required and assemblies may be stored in 4-out-of-4 configuration.

The results of the analysis of 3-out-of-4 spacing demonstrate that keff will remain ≤ 0.95 if flooded with unborated water, and ≤ 0.98 for any potential aqueous moderator density for fresh fuel enrichments of 5.0 weight percent U-235 or less. The results of a detailed parametric study of keff versus water density for 5.0 weight percent initial enrichment fuel showed a peak keff of 0.8879 (including calculational biases and uncertainties) at a moderator density of 0.045 gm/cc. A keff of 0.9316 (including calculational biases and uncertainties) was found at a moderator density of 1.0 gm/cc.

The results of the analysis of 4-out-of-4 spacing demonstrate that keff will remain ≤ 0.95 if flooded with unborated water, and ≤ 0.98 for any potential aqueous moderator density for fresh fuel enrichments of 4.35 weight percent U-235 or less. The results of a detailed parametric study of keff versus water density for 4.35 weight percent initial enrichment fuel showed a peak keff of 0.9735 (including calculational biases and uncertainties) at an optimum moderator density of about 0.057 gm/cc. A keff of 0.9112 (including calculational biases and uncertainties) was found at a moderator density of 1.0 gm/cc.

FOR INFORMATION ONLY

9.12 REFERENCES

1. *Dry Cask Independent Spent Fuel Storage Installation (ISFSI) Safety Analysis Report.*
2. *Final Safety Analysis Report, Horizontal Modular Storage System for Irradiated Nuclear Fuel (NUHOMS).*

Change 2

New Reference
3. NRC Submittal

9.12 REFERENCE DRAWINGS

The list of Station Drawings below is provided for information only. The referenced drawings are not part of the UFSAR. This is not intended to be a complete listing of all Station Drawings referenced from this section of the UFSAR. The contents of Station Drawings are controlled by station procedure.

	Drawing Number	Description
1.	11448-FM-1B	Machine Location: Reactor Containment, Elevation 18'- 4"
2.	11448-FM-1E	Machine Location: Reactor Containment; Sections “A-A”, “E-E”, & “Z-Z”
3.	11448-FM-9B	Arrangement: Fuel Building, Sheet 2, Unit 1

FOR INFORMATION ONLY

Change 3:
Insert Figure 9.12-2

Intentionally Blank

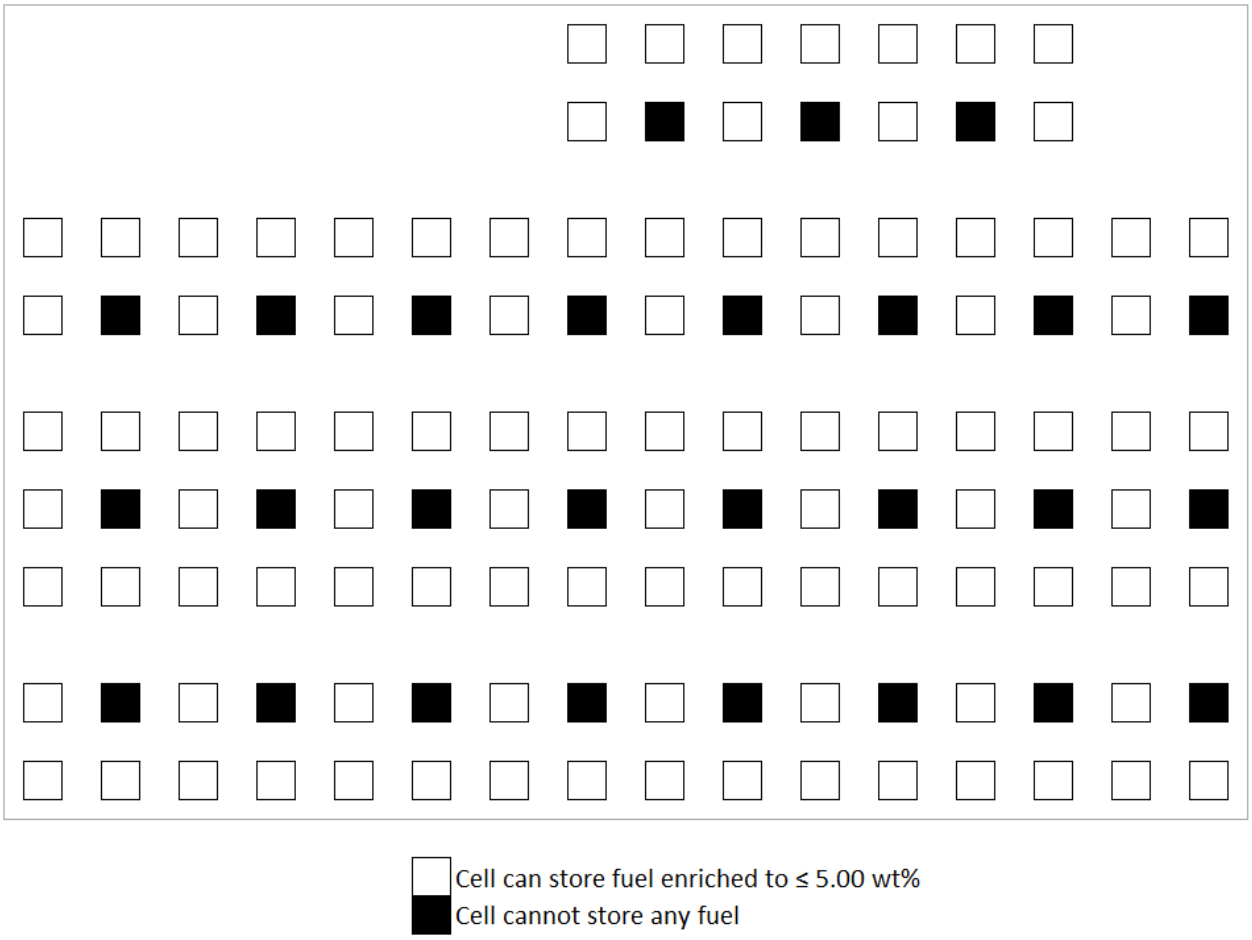

Figure 9.12-2
REQUIRED EMPTY CELLS WHEN ANY STORED FUEL IS > 4.35 WT% U-235

FOR INFORMATION ONLY

APPENDIX 9A HIGH-DENSITY SPENT-FUEL STORAGE RACK DESIGN

The storage of fuel in the new fuel storage area is described in UFSAR Section 9.12.3.4.

9A.1 DESIGN BASES

The high-density spent-fuel storage racks are designed to provide vertical storage locations for up to 1044 irradiated fuel assemblies, including insert components, in a borated water pool (with a boron concentration not less than 2300 ppm). The racks are designed to maintain the stored fuel, having maximum initial uranium enrichment of ~~4.3~~ 5.0 weight percent U-235 in UO_2, in a safe, coolable, and subcritical configuration under all conditions.

Change 4

The reinforced concrete structure and steel superstructure of the Fuel Building and spent fuel storage racks are designed to withstand Design Basis Earthquake loadings as Class 1 structures. The spent fuel pool has a stainless steel liner to protect against loss of water.

The spent fuel pool is divided into a two-region storage pool. Region 1 includes the first three rows of fuel racks (324 storage locations) adjacent to the Fuel Building Trolley Load Block. Region 2 contains the remainder of the fuel racks in the fuel pool. During spent fuel cask handling, Region 1 is limited to storage of spent fuel assemblies which have decayed at least 150 days after discharge and will be restricted to those assemblies in the “acceptable” domain as described in Technical Specification 5.4.

9A.2 STORAGE RACK DESCRIPTION

The spent fuel pool is a seismic Category I structure. Its primary function is to store spent fuel assemblies. The spent fuel pool is a 72 ft. 6 in. long, 29 ft. 3 in. wide and 40 ft. 6 in. deep reinforced concrete structure resting on a pile foundation. The floor and walls of the pool are nominally 6 feet thick. The pool is lined with 0.25-inch thick stainless steel liner plate. The spent fuel cask loading area (12 ft x 12 ft) is located at the northeast end of the pool. The floor of the cask loading area is 2 ft. 6 in. lower than the pool floor. The cask pad sits in this area.

Each fuel storage rack consists of a 6 x 6 array of fuel storage cells, which are square stainless steel boxes spaced nominally 14 inches on centers. The rack is shown on the general arrangement drawing, Figure 9A-1.

The fuel storage rack has two basic components: the support structure and the fuel storage cell. The support structure consists primarily of the four corner storage cells, which interface with the spent-fuel pool floor pads, and two horizontal grid members, which are supported by the four corner cells and which maintain the horizontal position and vertical alignment of the remaining 32 (inner) storage cells. The inner storage cells rest directly on the spent-fuel pool floor. Diagonal bracing is provided on the structure to accommodate the loads imposed by rack installation, by fuel handling, and by seismic events.

FOR INFORMATION ONLY

The maximum stress values are given in Table 9A-1 for load combinations 1 through 4.

A summary of stresses of the supporting pool structure is provided in Table 9A-2.

The following load combinations were considered:

1. Hydrostatic + dead load + live load.
2. Hydrostatic + dead load + live load + operating-basis earthquake.
3. Hydrostatic + dead load + live load + safe-shutdown earthquake.
4. Hydrostatic + dead load + live load + high-density racks.

The allowable stresses are based on the minimum sampled coupon strength of 43,600 psi and the acceptance criteria stated in ACI 318-63. It should be noted that with the new high-density fuel storage racks, the mat loadings are lower than those originally calculated. This is due to the different analytical model used. For the high-density fuel storage rack loadings, the model accounted for the detailed location of both the pilings and the fuel rack embedments in the mat. This resulted in a significant portion of the load due to spent fuel being transmitted to the pilings without inducing mat bending. In the analysis for the original loading, the rack loads were spread uniformly over the mat, and the pilings were lumped at discrete locations that were further apart than the actual pile spacing. The method used to calculate the mat loadings from the new high-density fuel storage racks represents the as-built condition at Surry.

As given in Section 9.5, the spent-fuel pool temperature will be maintained at or below the original limits of 140°F (normal case) and 170°F (abnormal case). Therefore, the maximum temperature of the thermal gradient in the pool walls and the base slab as originally designed will not be exceeded.

Change 5

9A.3.2 Nuclear Analysis

Insert 2

~~A detailed nuclear analysis was performed to demonstrate that for all anticipated normal and abnormal configurations of fuel assemblies within the fuel storage racks, the k_{eff} of the system is substantially subcritical ($k_{eff} < 0.95$).~~ Certain conservative assumptions about the fuel assemblies and racks were used in the calculations. These assumptions are described in Section 9A.3.2.1.

The reference configuration which is the basis of the criticality calculations consists of an array of square stainless steel boxes (9.12 inches o.d. with a wall thickness of 0.090 inch) spaced 14.0 inches on centers with fuel assemblies centrally located within the boxes. Variations from this reference configuration were also studied and included the effects of dimensional and spacing variations, fuel enrichment changes, water temperature increases and mislocations of fuel assemblies and boxes. A description of the calculational method and codes is presented in Section 9A.3.2.3, and the results of the criticality analysis are presented in Section 9A.3.2.4.

Insert 2:

A detailed nuclear analysis was performed to demonstrate that for all anticipated normal and abnormal configurations of fuel assemblies within the fuel storage racks, the keff of the system is substantially subcritical ($k_{eff} \leq 0.95$) when credit is taken for soluble boron, and subcritical ($k_{eff} < 1.0$) when no credit is taken for soluble boron.

FOR INFORMATION ONLY

The analysis of the Surry spent fuel racks followed the methodology described in Reference 9 and approved by the NRC in Reference 10. ~~Differences between this approved methodology and the Surry analysis are described in Section 9A.3.2.3.1.~~ Criticality calculations were performed using BONAMI and ~~NITAWL-II~~ CENTRM codes for cross section generation, and the KENO-V.a Monte Carlo code for reactivity determination. Sensitivity calculations for normal and abnormal conditions were performed using ~~the Westinghouse PHOENIX-P code~~ a statistical analysis.

Change 6

9A.3.2.1 Design Criteria and Assumptions

Change 7

~~The criticality design criterion established for the Surry Power Station spent fuel racks is that the multiplication constant (k_{eff}) shall be less than 0.95 for all normal and abnormal configurations, as confirmed by transport theory.~~

Insert 3

The following conservative assumptions were used in the criticality calculations performed to verify the adequacy of the rack design with respect to the rack design criteria:

Change 8

1. ~~The pool water has no soluble poison.~~

Insert 4

2. The fuel assemblies have no burnable poison.
3. The fuel is fresh and of a specified nominal enrichment as high or higher than that of any fuel available.
4. No credit is taken for structural material other than the fuel can.
5. All fuel cans are assumed to be 0.090 inches thick, the minimum allowable thickness.

9A.3.2.2 Configurations Analyzed

The various configurations of fuel within racks that are possible are classed as either normal or abnormal configurations. Normal configurations result from the placement of fuel within racks and the variation in rack dimensions permitted in fabrication. Abnormal configurations are typically the results of accidents or malfunctions such as seismic events, malfunction of the fuel pool cooling system, etc.

9A.3.2.2.1 Normal Configurations

Change 9

The normal configuration~~s~~ analyzed ~~were~~ was: a reference configuration ~~consists~~ consisting of an infinite array of storage cells having 5.00 nal dime asymmetrically ining a 15 x 15 ~~Westinghouse~~ fuel assembly of nominal ~~4.25~~ weight percent enrichment positioned ~~centrally~~ within the cell. ~~The 15 x 15 designed fuel assemblies were selected for reference configuration because racks with the 15 x 15 fuel assemblies are slightly more reactive than the rack with the 17 x 17 designed fuel assemblies with equal enrichment.~~ The storage cells are 9.12 inches in outside dimensions, have 0.090-inch walls, and are spaced 14.0 inches on centers. The spent fuel pool water is assumed to be 170°F, which is the upper bound of normal operating temperatures. The effects of variations in material characteristics and physical dimensions are statistically incorporated into the keff for the spent fuel storage racks.

Insert 3:

The criticality design criterion established for the Surry Power Station spent-fuel racks is that the multiplication constant (k_{eff}) shall be less than or equal to 0.95 when credit is taken for soluble boron, and less than 1.0 when no credit is taken for soluble boron, for all normal and abnormal configurations, as confirmed by transport theory.

Insert 4:

1. When credit is taken for burnup, the fuel assemblies are assumed to have been depleted in bounding conditions which result in a conservative estimate of the burnup reactivity worth.

FOR INFORMATION ONLY

9A.3.2.2.2 Abnormal Configurations

~~Two types of accidents can typically occur in the spent fuel rack which can cause reactivity to increase. The first accident type involves a pool water temperature change, which involves an increase or decrease in the spent fuel pool water temperature and density. The second accident type involves a fuel assembly misplacement, where restrictions on location, enrichment, or burnup are not satisfied. Fuel assembly misplacement accidents include a fuel assembly drop on top of a rack, and a fuel assembly drop between rack modules or between a rack module and the spent fuel pool wall. It is also possible for a dropped fuel assembly to enter a box cleanly and impact directly on the fuel stored in the box. The effect of this type of fuel drop incident was considered from a criticality viewpoint in the initial evaluation for the high density fuel racks (Reference 3) by assuming that the stored assembly would be compressed axially. A calculation based on axial compression of 2 feet yielded a 0.06 decrease in k_{inf} of the fuel cell. Therefore, this type of fuel misplacement accident would reduce k_{eff} and was not considered further.~~

Change 10

Insert 5

~~For Surry, a fuel storage cask handling accident was also evaluated. This accident scenario assumes a fuel storage cask rotates and falls against the fuel storage racks next to the cask loading area. To evaluate this accident, the spent fuel pool is divided into two regions. Region 1 comprises the first three rows of fuel storage racks (324 locations) adjacent to the fuel building trolley load block, which is susceptible to the storage cask handling accident. The remainder of the Surry spent fuel pool (Region 2) is unaffected by this accident.~~

~~The seismic impact on criticality calculations was also considered in the initial evaluation for the high density fuel racks. These analyses indicated that the maximum rack structure deflections will be very small (less than 0.120 inches). These deflections have a negligible effect on k_{eff} since they do not change the center-to-center spacing between the storage cells or boxes significantly. The maximum deflection of the storage cells or boxes due to a seismic event occurs at the middle of the box and is less than 0.050 inches. The effect of box deflections on k_{eff} is negligible since the average center-to-center spacing between cells or boxes will not change appreciably if the boxes deflect independently in random directions or act together in a single direction. As the seismic contributions were determined to be negligible, the effect of this type of abnormal condition on the criticality calculations was not considered further.~~

9A.3.2.3 **Calculational Methods**

9A.3.2.3.1 Analytical Methods

Change 11

Insert 6

~~The design method which insures that a subcritical condition is maintained in the spent fuel storage racks is similar to the NRC-approved Westinghouse Owners Group (WOG) methodology, which is described in References 9 and 10. The analysis of the Surry spent fuel pool incorporated the following exceptions to the WOG methodology:~~

1. ~~The WOG methodology assumed a nominal UO_2 density of 95.0% T.D. The Surry spent fuel pool analysis used a nominal UO_2 density of 95.5% T.D., based on actual as-built fuel assembly uranium-loading information for Surry~~

Insert 5:

Accident scenarios resulting in abnormal configurations include: boron dilution to a minimum boron with normal storage, single fuel assembly mis-load in the fuel racks, multiple fuel assembly mis-load, loss of cooling (including partial voiding), dropped assembly into the racks with grid damage (optimum fuel pin pitch), mis-placement of an assembly between fuel racks, seismic event, and a fuel storage cask handling accident. An evaluation of boron dilution time and mitigation is included Reference 9.

The fuel storage cask handling accident is the bounding abnormal configuration. This accident scenario assumes a fuel storage cask rotates and falls against the fuel storage racks next to the cask loading area. To evaluate this accident, the spent fuel pool is divided into two regions. Region 1 comprises the first three rows of fuel storage racks (324 locations) adjacent to the fuel building trolley load block, which is susceptible to the storage cask handling accident. The remainder of the Surry spent fuel pool (Region 2) is unaffected by this accident. A full set of tolerance and bias cases are calculated for the fuel storage cask handling accident with 2250 ppm of soluble boron. This analysis determined the burnup curve for Region 1. This analysis is included in Reference 9.

FOR INFORMATION ONLY

2. ~~The WOG methodology assumed a UO_2 density variation of ±2.0% T.D. about the nominal reference density, and variation in the fuel pellet dishing fraction from 0% to twice the nominal pellet dishing fraction. The analysis for the Surry spent fuel pool assumed a ±1.5% T.D. variation in fuel pellet density, based on the fuel manufacturing specifications and as-built fuel assembly uranium-loading information.~~

3. ~~The WOG methodology used 227 group ENDF/B-V cross sections. These cross sections have not been made available to Virginia Power by Oak Ridge National Laboratory. Therefore, the Surry spent fuel pool analysis used 238 group ENDF/B-V cross sections, which have been extensively benchmarked.~~

4. ~~The Surry spent fuel pool analysis does not require any boron credit. Therefore, the WOG boron credit methodology is not applicable.~~

5. ~~The WOG methodology uses a nominal temperature of 68°F and pressure of 14.7 psia. In the analysis for the Surry spent fuel pool, the nominal temperature was set to the most conservative value over the typical temperature range, which was determined to be 170°F. The nominal pressure was set to 28 psia to account for the effects of the spent fuel pool water depth.~~

Change 11 (continued)

6. ~~Although the NRC-approved WOG methodology does not require consideration of the effect of the axial burnup distribution on fuel assembly reactivity, an axial burnup gradient reactivity bias was applied to the evaluation of the Surry spent fuel pool.~~

7. ~~The WOG methodology includes B^{10} self-shielding bias for spent fuel pools with poison panels. The Surry spent fuel storage cells do not include any poison panels, so this bias is not necessary in the Surry analysis. In addition, the Surry reactivity and tolerance calculations do not account for any poison panels~~

~~The design method uses the BONAMI and NITAWL-II codes for cross section generation, and the KENO-V.a code for reactivity determination. The 238-group ENDF/B-V cross section library is the starting point for all cross sections used for the KENO-V.a calculations. BONAMI (Reference 4) performs a resonance self-shielding calculation based on the Bondarenko method, and produces problem dependent master data sets. NITAWL-II (Reference 5) performs problem dependent resonance shielding calculations by applying the Nordheim Integral Treatment. These multigroup cross section sets are then used as input to KENO-V.a, which is a three dimensional Monte Carlo theory program designed for reactivity calculations (Reference 8). KENO-V.a calculations are always performed with sufficient neutron histories to assure convergence.~~

~~Two different KENO-V.a models were used. One model represented an infinitely reflected single spent fuel storage cell, while the other model represented the entire Surry spent fuel storage pool. The storage cells in the full pool model are placed in arrays to model each fuel storage rack, which are placed in their appropriate fuel pool location along with the fuel transfer canal and concrete buttress. This configuration is then surrounded with the stainless steel liner and concrete walls and floor.~~

Insert 6:

The design method used which insures that a subcritical condition is maintained in the spent fuel storage racks is Regulatory Guide RG 1.240 (Reference 11). This document provides acceptable approaches for performing criticality analyses for light-water nuclear reactor spent fuel pool storage racks.

This analysis uses the BONAMI and CENTRM for cross section generation, TRITON/ORIGEN for reactivity depletion using t5-depl, ORIGAMI for nuclide decay and concentration, and KENO-V.a for reactivity determination. These codes are all included in the SCALE 6.2.3 code package. The 238-group ENDF/B-VII cross section library is used for all calculations. These codes are described in detail in Reference 9.

The methodology consists of the following analyses:

1. Computer code validation
2. Determination of bounding assembly design and depletion conditions
3. Normal conditions analysis of fresh fuel with no credit for boron
4. Accident conditions analysis of fuel with credit for burnup and boron
5. Analysis of interface effects and non-standard fuel configurations

FOR INFORMATION ONLY

9A.3.2.4 **Analysis Results**

~~9A.3.2.3.2 Benchmark Calculations~~

~~In order to establish the accuracy of the computer codes used for this analysis, the KENO-V.a code and cross sections were compared to critical experiment data for fuel assemblies similar to those for which the Surry spent fuel racks were designed. These benchmarking data, which represents fifty-nine validation criticality test cases for UO_2 lattices, are sufficiently diverse to establish that the method bias and uncertainty will apply to the rack conditions covered by this analysis.~~

~~The benchmark critical experiments resulted in an average KENO-V.a k_{eff} of 0.99643, which compared to a critical k_{eff} of 1.0 gives a KENO-V.a model bias of 0.00357 Δk. On a 95% confidence level, there is a 95% probability that the uncertainty in reactivity due to the method is not greater than 0.00099 Δk.~~

Change 12

Insert 7

~~Reactivity equivalencing and tolerance calculations were performed using the Westinghouse PHOENIX-P code. The benchmarking performed for the WOG methodology covers a range of lattice parameters and configurations encompassing present fuel storage configurations. Based on the NRC acceptance of PHOENIX-P and their approval of the WOG methodology described in Reference 9, further benchmarking was not performed for the Surry spent fuel pool analysis.~~

~~9A.3.2.4 **Analysis Results**~~

~~9A.3.2.4.1 Normal Configurations~~

~~KENO-V.a calculations were performed for the reference configuration using both the infinitely reflected single storage cell model and the full spent fuel pool model. It was determined that use of the single storage cell KENO-V.a model is slightly conservative for this analysis. The k_{eff} for the single storage cell model was. 0.92950.~~

~~The effects of possible variations in material characteristics and mechanical/construction dimensions on spent fuel pool reactivity were performed using Westinghouse's PHOENIX-P code. These calculations included the effects of:~~

1. ~~Fuel enrichment tolerance.~~
2. ~~Variation in UO_2 density.~~
3. ~~Variation of the fuel pellet dishing fraction.~~
4. ~~Tolerance about the nominal reference storage cell inner dimension.~~
5. ~~Tolerance about the nominal storage cell center-to-center pitch.~~
6. ~~Tolerance about the nominal reference storage cell material thickness.~~
7. ~~Asymmetric positioning of fuel assemblies within the storage cells.~~

FOR INFORMATION ONLY

~~The impact of each of these factors on the calculated k_{eff} is given in Table 9A-3. The total uncertainty associated with material characteristics, mechanical construction, and the KENO-V.a methodology is determined by statistically combining the effects of these tolerances with the calculational uncertainty. The combined uncertainty is 0.01064, as shown in Table 9A-3.~~

~~The 95/95 k_{eff} for the Surry spent fuel storage racks was then derived from:~~

$$k_{eff} = k_{nominal} + B_{method} + B_{temp} + B_{uncert}$$

~~where:~~

~~$k_{nominal}$ = nominal conditions KENO-V.a k_{eff} (0.92950)~~

~~B_{method} = method bias determined from benchmark critical comparisons (0.00357)~~

Change 12 (continued)

~~B_{temp} = temperature bias (0.0)~~

~~B_{uncert} = uncertainty associated with material characteristics, mechanical construction, and KENO-V.a method (0.01064)~~

~~The resulting spent fuel pool k_{eff} is 0.94371.~~

~~9A.3.2.4.2 Abnormal Configurations~~

~~As discussed in Section 9A.3.2.2, one type of accident which can cause reactivity to increase in the spent fuel rack involves an increase or decrease in the spent fuel pool water temperature and density. The normal conditions analysis, which covered a normal temperature range from 50°F to 170°F, showed that k_{eff} is less than 0.95 with no boron present in the spent fuel pool. The double contingency principle of ANSI/ANS 8.1-1983 states that protection against a criticality accident does not require assumption of two unlikely, independent, concurrent events. The presence of soluble boron in the spent fuel pool storage water can therefore be assumed as a realistic initial condition, since the lack of boron in the pool would be the result of a second unlikely event (i.e., a boron dilution accident). It was determined that an increase in pool temperature from 170°F to 246.4°F, the temperature at which boiling would be expected to occur in the spent fuel pool, increases the spent fuel pool k_{eff} less than the worth of the boron normally present in the spent fuel pool. Therefore, the 0.95 k_{eff} limit will be met for a pool water temperature increase.~~

~~The second type of accident which can affect reactivity in the spent fuel pool involves the placement of a fuel assembly into a position for which any restrictions on location, enrichment, or burnup are not satisfied. The normal conditions evaluation assumed a spent fuel storage rack configuration containing all fresh fuel at the maximum permissible proposed Surry fuel enrichment, with no restrictions on assembly location. Therefore, fuel assembly misplacement under normal handling conditions is already bounded by the reference non-accident analysis.~~

FOR INFORMATION ONLY

~~Two additional fuel assembly misplacement accidents that were considered were determined to have no impact on reactivity. These accidents include a fuel assembly drop on top of a rack, and a fuel assembly drop between rack modules or between a rack module and the spent fuel pool wall. A fuel assembly which drops onto the top of the fuel racks will impact the flared tops of the fuel storage rack cells. While minor deformation of the flared tops may occur, the close proximity of the upper grid structure to the impact point will preclude significant lateral displacement of the storage cells, so the rack structure pertinent for criticality control is not excessively deformed by the fuel assembly. KENO-V.a sensitivity cases confirmed that a dropped assembly which comes to rest either horizontally or vertically on top of the rack has sufficient water separating it from the active fuel height of stored assemblies to preclude neutron interaction, so the effect on k_{eff} is negligible. For the second scenario, PHOENIX-P sensitivity cases showed that placing an assembly outside of the racks per the second accident scenario is bounded by the normal conditions analysis.~~

Change 12 (continued)

~~To ensure that the spent fuel pool k_{eff} remains less than or equal to 0.95 during a fuel storage cask handling accident, limitations must be placed on the initial enrichment and burnup of the fuel assemblies which may be stored in Region 1 of the Surry spent fuel pool.~~

~~To evaluate the impact of a storage cask handling accident on spent fuel pool criticality, the deformed fuel and the associated storage racks were assumed to be at the optimum pitch. KENO-V.a calculations were run to determine the maximum fresh fuel enrichment that meets the 0.95 k_{eff} limit, including all applicable uncertainties and tolerances. The same methodology employed for the 95/95 k_{eff} calculations for the normal configurations was used for these calculations. It was determined that any fuel with an initial U^{235} enrichment less or equal to 1.9 weight percent may be loaded into Region 1 of the Surry spent fuel pool.~~

~~To allow the loading of fuel with higher initial enrichments in Region 1 of the Surry spent fuel pool, credit must be taken for the fuel burnup. A series of reactivity calculations were performed using the PHOENIX-P code and following the methodology outlined in Reference 9 to identify fuel assembly initial enrichment-discharge burnup pairs, which all yield equivalent k_{eff} values for the Surry spent fuel storage racks. These burnup credit cases incorporated the following conservatisms and uncertainties:~~

1. ~~Fuel depletions were performed at a conservatively high boron concentration to enhance the predicted buildup of plutonium.~~
2. ~~Burnup credit cases assumed no xenon.~~
3. ~~A PHOENIX-P code uncertainty was applied.~~
4. ~~An axial burnup gradient reactivity bias was applied.~~
5. ~~A reactivity bias was applied to account for changes in optimum pitch due to burnup and enrichment changes.~~

Insert 7:

9A.3.2.4 **Analysis Results**

9A.3.2.4.1 Computer Code Validation

The methodology for performing Computer Code Validation is described in NUREG/CR-6698, Guide for Validation of Nuclear Criticality Safety Calculational Methodology (Reference 8). The validation of SCALE 6.2.3 for the purposes of fuel storage rack analyses is based on the analysis of selected critical experiments from two experimental programs. The first program is the OECD/NEA International Handbook of Evaluated Criticality Safety Benchmarks Experiments (Reference 4), which includes a variety of low-enriched UO_2 core configurations. The second program is the French Haut Taux de Combustion critical experiments (Reference 5), which utilize fuel rods with a mixture of low-enriched UO_2 and PuO_2 designed to simulate light water reactor fuel with initial 4.5% UO_2 burned to 37,500 MWD/MTU.

From these two groups of experiments, a total of 238 were selected to represent analyses using fresh fuel, and 111 experiments for burned fuel. The experiments were chosen based on having similar characteristics to the Surry SFP. The experiments were modelled in SCALE 6.2.3, and a bias and uncertainty was determined to be applied to criticality analysis results. The bias and uncertainty were determined to have a linear trend dependent on the neutron spectrum of the system. Therefore, the bias and uncertainty used for the analysis is calculated based on the specific system analyzed.

9A.3.2.4.2 Determination of Bounding Assembly Design and Depletion Conditions

In order to conservatively model fuel assemblies in the spent fuel pool, bounding fuel assembly dimensions were determined. Surry plant specific input was determined using historical plant data and proposed fuel and cycle designs. The effects of cladding material, fuel assembly dimensions, fuel density, and burnable absorbers were considered. Sensitivity study results were utilized to determine the conservative inputs for the KENO model.

In order to conservatively model burned fuel in the spent fuel pool, bounding conditions for burnup credit calculations were determined. Surry plant specific input was determined using guidance documents, historical plant data, and proposed fuel and cycle designs. The effects of control rods, fuel temperature, moderator temperature, moderator density, soluble boron, operating history, specific power, burnable absorbers were considered. Sensitivity study results were utilized to set the appropriate TRITON depletion step size, KENO variables important for adequate convergence (neutrons per generation, number of generations, number of generations skipped), and number of decay days for converged and conservative depleted fuel SFP k-effective.

Insert 7 (continued):

9A.3.2.4.3 Normal Conditions Analysis of Fresh Fuel with No Credit for Boron

The Normal Conditions Analysis uses the methodology described in RG 1.240 (Reference 11) in order to determine the maximum k-effective of the spent fuel pool, including conservatisms, uncertainties, and biases. The analysis modeled the spent fuel pool in normal conditions (non-accident conditions), with unborated water, assuming the maximum loading of the highest reactivity fresh fuel. The analysis determined the maximum k-effective was 0.9905 for fresh fuel with 5.0 weight percent U235, including uncertainties and biases. This satisfies the requirement for k-effective < 1.0 for normal storage conditions with no credit for soluble boron.

9A.3.2.4.4 Accident Conditions Analysis of Fuel with Credit for Burnup and Boron

The accident analysis uses the methodology described in RG 1.240 (Reference 11) in order to determine the maximum k-effective of the spent fuel pool, including conservatisms, uncertainties, and biases in accident conditions with borated water, assuming the maximum loading of the highest reactive fuel in each region. The results of this analysis show that the cask drop event is the bounding accident. The other accidents were analyzed to show that they are significantly less bounding than the cask drop accident.

The Surry SFP is separated into two regions. Region 1 consists of the three rows of rack modules adjacent to the cask loading area. Region 2 consists of the remaining cells of the SFP. Region 1 is susceptible to the cask drop accident while Region 2 is not.

To ensure that the spent fuel pool k-effective remains less than or equal to 0.95 during a fuel storage cask handling accident, limitations are placed on the enrichment and burnup of the fuel assemblies which may be stored in Region 1 of the Surry spent fuel pool.

To evaluate the impact of a storage cask handling accident on spent fuel pool criticality, the deformed fuel and the associated storage racks were assumed to be at the optimum pitch. SCALE calculations were run, using the bounding assembly design and depletion conditions, to determine the maximum fresh fuel enrichment that meets the 0.95 k-effective limit, including all applicable uncertainties and biases, at various burnup intervals. The combination of these enrichments and burnups were used to create a burnup curve which determines what fuel assemblies may be stored in Region 1.

Insert 7 (continued):

9A.3.2.4.5 Analysis of Interface Effects and Non-Standard Fuel Configurations

The interface between Region 1 and 2 was analyzed to determine how the interface affects the reactivity of the Spent Fuel Pool using KENO models. The results of the analysis showed that the interface region was less reactive than the Region 1 configuration.

Non-standard fuel configurations were directly dispositioned in Reference 9. These include fuel assemblies with unusual operational history as well as 17x17 lead test assemblies. An analysis of these special cases determined they were suitable to be stored as normal fuel assemblies.

Failed fuel rods removed when reconstituting fuel assemblies are stored in a Fuel Rod Storage Canister, FRSC, which is stored in one cell of the spent fuel storage racks. An analysis of the maximum reactivity of the FSRC determined that it is less reactive than a normal Region 2 assembly but could be more reactive than a Region 1 assembly. Therefore, the FSRC is limited to being stored in Region 2.

Reconstituted fuel was also analyzed. It was determined that in certain circumstances, the removal of a fuel rod can increase reactivity compared to a standard assembly. Assemblies with an inert fuel pin (often a stainless steel or naturally enriched uranium pin) can be stored as if it were a normal fuel assembly. However, the following limitations were established in regards to assemblies with removed fuel pins:

1) Assemblies with an open hole in the fuel pin lattice will be restricted from being stored in Region 1 when a dry storage cask is within the spent fuel pool.

2) Fuel pins cannot be pulled from a fresh assembly unless all the adjacent rack cells are empty.

FOR INFORMATION ONLY

Change 12 (continued)

6. ~~An uncertainty was also applied to assembly burnup to reflect uncertainties in burnup measurements.~~

~~The results of these burnup credit reactivity equivalencing calculations were used to define a curve of assembly burnup versus initial fuel enrichment, which is included in the Surry Technical Specifications as Figure 5.4-1. Use of fuel with a burnup and enrichment combination which falls above this curve in Region 1 of the Surry spent fuel pool ensures that the spent fuel pool keff remains less than or equal to 0.95 during a fuel storage handling accident.~~

9A REFERENCES

1. Letter from C. M. Stallings (Vepco) to E. G. Case (NRC), *Request for Technical Specification Change No. 53, Surry Power Station Units 1 and 2*, dated May 1977
2. Letter from J. D. Neighbors (NRC) to W. L. Stewart (Virginia Power), Approval of Technical Specifications 84 and 85, dated March 1983.
3. Nuclear Energy Services, Inc., *Nuclear Design Analysis Report For The Surry Nuclear Power Station High Density Fuel Storage Racks*, NES-81A0494, dated March 1980.
4. ~~N. M. Greene, *BONAMI: Resonance Self-Shielding by the Bondarenko Method,* ORNL/NUREG/CSD-2/V2/R5, Section F1, March 1997.~~
5. ~~N. M. Greene, et al., *NITAWL-II: SCALE System Module for Performing Resonance Shielding and Working Library Production,* ORNL/NUREG/CSD-2/V2/R5, Section F2, March 1997.~~

Change 13

Insert 8

6. Report No. 320-3254, ISB/GGC3, IBM Scientific Center, Palo Alto, California.
7. R. J. Weader, NES 81A0260, *Criticality Analysis of the Atcor Vendenburgh Cask*, February 1975.
8. ~~L. M. Petrie and N. F. Landers, *KENO-V.a: An Improved Monte Carlo Criticality Program with Supergrouping,* ORNL/NUREG/CSD-2/V1/R2, Section F11, March 1997.~~
9. ~~W. D. Newmyer, *Westinghouse Spent Fuel Rack Criticality Analysis Methodology,* WCAP-14416-P, June 1995.~~
10. ~~Letter from T. E. Collins (NRC) to Tom Greene (Westinghouse), *Acceptance for Referencing of Licensing Topical Report WCAP-14416-P, "*Westinghouse Spent Fuel Rack Criticality Analysis Methodology*",* TAC No. M93254, October 25, 1996.~~

Insert 8:

4. International Handbook of Evaluated Criticality Safety Benchmark Experiments, NEA/NSC/DOC(95)3, Volumes IV and VI, Nuclear Energy Agency, OECD, Paris, September, 2014.

5. D. E. Mueller, K. R. Elam, and P. B. Fox, Evaluation of the French Haut Taux de Combustion (HTC) Critical Experiment Data, NUREG/CR-6979 (ORNL/TM-2007/083), prepared for the US Nuclear Regulatory Commission by Oak Ridge National Laboratory, Oak Ridge, Tenn., September 2008.

8. J.C. Dean and R.W. Tayloe, Jr., Guide for Validation of Nuclear Criticality Safety Calculational Methodology, NUREG/CR-6698, Nuclear Regulatory Commission, Washington, DC January 2001.

9. THIS SUBMITTAL

10. THE NRC SER FOR THIS SUBMITTAL

11. Regulatory Guide RG 1.240, “Fresh and Spent Fuel Pool Criticality Analyses,” 03/2021 (Accession Number: ML20356A127).

FOR INFORMATION ONLY

Change 14

Table 9A-3
RESULTS OF TOLERANCE CALCULATIONS
FOR NORMAL SPENT FUEL RACK CONFIGURATION

Tolerance	Δk
Enrichment (+0.05 wt.%)	0.00247
Density (+1.5% TD)	0.00284
Dishing Fraction (0%)	0.00234
Cell Pitch (-1/4 in.)	0.00823
Cell Wall Thickness (-0.005 in.)	0.00196
Cell i.d. (-1/16 in.)	0.00005
Assembly Position	0.00439
Calculational Uncertainty	0.00130
Methodology Uncertainty	0.00099
Total Uncertainty (B_{uncert})	0.01064

The total uncertainty (B_{uncert}) was determined by statistically summing each uncertainty component.

$$B_{uncert} = \sqrt{\sum_i Unc_i^2}$$

FOR INFORMATION ONLY

The area radiation monitoring system reads out and records the radiation levels in selected areas throughout the station and activates alarms (audible and visible) if these levels exceed a preset value or if the detector malfunctions. With the exception of the containment gas and particulate monitors, each detector reads out and activates alarms, both in the control room and at its station location. Each channel is equipped with a check source remotely operated from the control room. The recorders provide a continuous permanent record of radiation levels while the detectors are functioning. Detectors monitoring Unit 1 are supplied with power from the emergency bus for Unit 1. Detectors monitoring Unit 2 are supplied with power from the emergency bus for Unit 2. Detectors monitoring areas common to both units have the capability of being supplied with power from the emergency bus for either Unit 1 or Unit 2.

Additions subsequent to the original station area radiation monitoring system include the spent resin handling area, laundry, and radwaste facilities. These systems are powered from reliable power supplies and are indicated and source tested locally.

The alarm setpoint of each area monitor is variable and is set at a level slightly above the normal background radiation level in the respective area.

The area radiation monitoring system consists of the detectors listed in Table 11.3-7, plus each unit's containment particulate and gas monitors, described below.

Change 15

Insert 9

~~Criticality monitors are not required in the spent fuel and new fuel storage and handling areas. An exemption from the criticality monitoring requirements specified in 10 CFR 70.24(a) was received from the NRC for the storage and handling of fuel assemblies enriched up to 4.3 weight percent U-235 (Reference 8).~~ The exemption was based on station design features and procedural controls that are in place to preclude an inadvertent criticality. Area radiation monitors are provided in these areas which would alert personnel to excessive radiation levels and would initiate appropriate response actions.

11.3.4.2 Containment Particulate Monitors

This channel continuously withdraws a sample from the containment atmosphere into a closed, shielded system exterior to the containment. The sample is passed through a moving filter paper with a collection efficiency of 99% for particle sizes greater than 1.0 micron. The amount of deposited activity is continuously scanned by a lead-shielded beta scintillation detector with a sensitivity of 1×10^{-11} μCi/cm^3 for particulates in a background of 2.5 mR/hr. The sample system, which is common to both the particulate and gas monitors, includes a pump with a 0.75-hp motor, a flow meter, automatic pressure protecting valves, a flow regulating valve, and isolation valves. The pump and motor are located outside the containment. A sample point is available for taking a sample of the containment atmosphere after an incident for spectrum analysis in the laboratory. During refueling a high-activity alarm automatically trips the containment purge air supply fans and closes the purge system butterfly valves, thus isolating the purge system. This automatic function is not credited in the fuel handling accident nor is it required to be functional. The operability of the containment particulate monitor is relied upon in

Insert 9:

Area radiation monitors are provided in the spent fuel and new fuel storage and handling areas which would alert personnel to excessive radiation levels and would initiate appropriate response actions. An exemption from the criticality monitoring requirements specified in 10 CFR 70.24 is granted because Surry's criticality analysis is approved under 10 CFR 50.68(b) in lieu of 10 CFR 70.24 (Reference 8).

FOR INFORMATION ONLY

5. Regulatory Guide 1.100, *Seismic Qualification of Electric Equipment for Nuclear Power Plants*, 1977.

6. Regulatory Guide 1.89, *Qualification of Class 1E Equipment for Nuclear Power Plants*, 1974.

7. G. Wortley, *Contamination of Milk with Radionuclides Dispersed into the Biosphere*, a report submitted to the Joint FAO/WHO Expert Committee on Milk Hygiene, WHO Headquarters, Geneva, Switzerland, 1969.

8. ~~Letter from G. Edison of the USNRC to J.P. O'Hanlon of Virginia Electric and Power Company dated July 15, 1998 (Serial No. 98-427), *Issuance of Revised Exemption from the Requirements of 10 CFR 70.24(a) - Surry Power Station, Units 1 and 2 (TAC Nos. MA0657 and MA0658).*~~

Change 16

The NRC SER for this Submittal

9. Letter from NRC to Vepco, *Subject: Steam Generator Program*, Surry Power Station, Units 1 and 2 dated August 17, 1977, Ser. No. 351.

Attachment 9

FRAMATOME INC. APPLICATION FOR WITHHOLDING PROPRIETARY INFORMATION FROM PUBLIC DISCLOSURE

VIRGINIA ELECTRIC AND POWER COMPANY
(DOMINION ENERGY VIRGINIA)
SURRY POWER STATION UNITS 1 AND 2

A F F I D A V I T

1. My name is Morris Byram. I am Product Manager, Licensing & Regulatory Affairs for Framatome Inc. (Framatome) and as such I am authorized to execute this Affidavit.

2. I am familiar with the criteria applied by Framatome to determine whether certain Framatome information is proprietary. I am familiar with the policies established by Framatome to ensure the proper application of these criteria.

3. I am familiar with the Framatome information contained in Attachment 5 (Criticality Safety Analysis Report) to the Virginia Electric and Power Company letter 22-018, Rev 0, entitled "Surry Power Station Units 1 and 2 License Amendment Request – Proposed Technical Specifications Change for New Fuel and Spent Fuel Storage Areas," and referred to herein as "Document." Information contained in this Document has been classified by Framatome as proprietary in accordance with the policies established by Framatome for the control and protection of proprietary and confidential information.

4. This Document contains information of a proprietary and confidential nature and is of the type customarily held in confidence by Framatome and not made available to the public. Based on my experience, I am aware that other companies regard information of the kind contained in this Document as proprietary and confidential.

5. This Document has been made available to the U.S. Nuclear Regulatory Commission in confidence with the request that the information contained in this Document be withheld from public disclosure. The request for withholding of proprietary information is made in accordance with 10 CFR 2.390. The information for which withholding from disclosure is

requested qualifies under 10 CFR 2.390(a)(4) “Trade secrets and commercial or financial information.”

6. The following criteria are customarily applied by Framatome to determine whether information should be classified as proprietary:

(a) The information reveals details of Framatome’s research and development plans and programs or their results.

(b) Use of the information by a competitor would permit the competitor to significantly reduce its expenditures, in time or resources, to design, produce, or market a similar product or service.

(c) The information includes test data or analytical techniques concerning a process, methodology, or component, the application of which results in a competitive advantage for Framatome.

(d) The information reveals certain distinguishing aspects of a process, methodology, or component, the exclusive use of which provides a competitive advantage for Framatome in product optimization or marketability.

(e) The information is vital to a competitive advantage held by Framatome, would be helpful to competitors to Framatome, and would likely cause substantial harm to the competitive position of Framatome.

The information in this Document is considered proprietary for the reasons set forth in paragraphs 6(d), and 6(e) above.

7. In accordance with Framatome’s policies governing the protection and control of information, proprietary information contained in this Document has been made available, on a limited basis, to others outside Framatome only as required and under suitable agreement providing for nondisclosure and limited use of the information.

8. Framatome policy requires that proprietary information be kept in a secured file or area and distributed on a need-to-know basis.

9. The foregoing statements are true and correct to the best of my knowledge, information, and belief.

I declare under penalty of perjury that the foregoing is true and correct.

Executed on: (7/7/2022)

BYRAM Morris Digitally signed by BYRAM Morris
Date: 2022.07.07 16:31:18 -07'00'

(NAME)

morris.byram@framatome.com

Attachment 10

WESTINGHOUSE ELECTRIC COMPANY LLC APPLICATION FOR WITHHOLDING PROPRIETARY INFORMATION FROM PUBLIC DISCLOSURE

VIRGINIA ELECTRIC AND POWER COMPANY
(DOMINION ENERGY VIRGINIA)
SURRY POWER STATION UNITS 1 AND 2

Commonwealth of Pennsylvania:
County of Butler:

(1) I, Zachary Harper, Manager, Licensing Engineering, have been specifically delegated and authorized to apply for withholding and execute this Affidavit on behalf of Westinghouse Electric Company LLC (Westinghouse).

(2) I am requesting the proprietary portions of Letter from Dominion Energy Virginia to the NRC (Serial No. 22-018) be withheld from public disclosure under 10 CFR 2.390.

(3) I have personal knowledge of the criteria and procedures utilized by Westinghouse in designating information as a trade secret, privileged, or as confidential commercial or financial information.

(4) Pursuant to 10 CFR 2.390, the following is furnished for consideration by the Commission in determining whether the information sought to be withheld from public disclosure should be withheld.

(i) The information sought to be withheld from public disclosure is owned and has been held in confidence by Westinghouse and is not customarily disclosed to the public.

(ii) The information sought to be withheld is being transmitted to the Commission in confidence and, to Westinghouse's knowledge, is not available in public sources.

(iii) Westinghouse notes that a showing of substantial harm is no longer an applicable criterion for analyzing whether a document should be withheld from public disclosure. Nevertheless, public disclosure of this proprietary information is likely to cause substantial harm to the competitive position of Westinghouse because it would enhance the ability of competitors to provide similar technical evaluation justifications and licensing defense services for commercial power reactors without commensurate expenses. Also, public disclosure of the information would enable others to use the information to meet NRC requirements for licensing documentation without purchasing the right to use the information.

(5) Westinghouse has policies in place to identify proprietary information. Under that system, information is held in confidence if it falls in one or more of several types, the release of which might result in the loss of an existing or potential competitive advantage, as follows:

(a) The information reveals the distinguishing aspects of a process (or component, structure, tool, method, etc.) where prevention of its use by any of Westinghouse's competitors without license from Westinghouse constitutes a competitive economic advantage over other companies.

(b) It consists of supporting data, including test data, relative to a process (or component, structure, tool, method, etc.), the application of which data secures a competitive economic advantage (e.g., by optimization or improved marketability).

(c) Its use by a competitor would reduce his expenditure of resources or improve his competitive position in the design, manufacture, shipment, installation, assurance of quality, or licensing a similar product.

(d) It reveals cost or price information, production capacities, budget levels, or commercial strategies of Westinghouse, its customers or suppliers.

(e) It reveals aspects of past, present, or future Westinghouse or customer funded development plans and programs of potential commercial value to Westinghouse.

(f) It contains patentable ideas, for which patent protection may be desirable.

(6) The attached documents are bracketed and marked to indicate the bases for withholding. The justification for withholding is indicated in both versions by means of lower-case letters (a) through (f) located as a superscript immediately following the brackets enclosing each item of information being identified as proprietary or in the margin opposite such information. These lower-case letters refer to the types of information Westinghouse customarily holds in confidence identified in Sections (5)(a) through (f) of this Affidavit.

I declare that the averments of fact set forth in this Affidavit are true and correct to the best of my knowledge, information, and belief. I declare under penalty of perjury that the foregoing is true and correct.

Executed on: 7/13/2022

Signed electronically by
Zachary Harper